Declassified in Part - Sanitized Copy Approved for Release 2011/12/08 : CIA-RDP80T00246A016600420001-1
50X1-HUM

Page Denied

Next 6 Page(s) In Document Denied

Declassified in Part - Sanitized Copy Approved for Release 2011/12/08 : CIA-RDP80T00246A016600420001-1

Declassified in Part - Sanitized Copy Approved for Release 2011/12/08 : CIA-RDP80T00246A016600420001-1

TO THE RESULTS OF THE CHARGED PARTICLE THREE-ELECTRODE TRAP EXPERIMENTS IN THE SECOND RADIATION BELT AND IN THE OUTERMOST BELT OF CHARGED PARTICLES

by K.I.Gringauz, S.M.Balandina, G.A.Bordovsky, N.M.Shutte

Abstract

Results are presented of the laboratory experiments with charged particle traps identical with those installed on Soviet space probes. It is shown that the traps highly efficiently record fluxes of electrons with energies on the order of tens of kevs.

The data presented confirm the conclusion about the absence of considerable soft electron fluxes in the outer radiation belt.

In the papers by S.N.Vernov, A.E.Chudakov and others (1), (2) and by J.A.Van Allen, J.A.Simpson, R.L.Arnoldy and others (3)-(6) published in 1959-1961 and devoted to descriptions of the outer radiation belt investigations the electron flux values determined by the authors were estimated as 10^{10}-10^{11} $cm^{-2}sec^{-1}$. These estimates contradicted to the results of measurements of the currents produced by the fluxes of charged particles getting into three-electrode traps mounted on the same space probes as the instruments used by S.N.Vernov and others (2). In the papers by K.I.Gringauz, V.G.Kurt, V.I. Moroz and I.S.Shklovsky published in April-July 1960 (7), (8), it was pointed out that the upper boundary of electron fluxes in the outer radiation

Declassified in Part - Sanitized Copy Approved for Release 2011/12/08 : CIA-RDP80T00246A016600420001-1

Declassified in Part - Sanitized Copy Approved for Release 2011/12/08 : CIA-RDP80T00246A016600420001-1

belt did not exceed $(2 \div 3)\ 10^7 cm^{-2}\ sec^{-1}$ during the experiments (1)-(6). It was pointed out that the counting rates observed in experiments with cosmic ray counters (1)-(6) should be accounted for not by the influence of soft electrons with the maximum energy distribution lying in the region of ~30 Kev, as it was done in (1)-(6), but by the action of electron fluxes which are not less than by 10^3 times lower than those given in the papers by J.Van Allen, S.N.Vernov et al. and with much greater energies.

In Fig.1 a diagram is presented of the spatial distribution of the charged particle belts around the Earth from the paper (7). On this figure there are also indicated the estimates of the fluxes in the second belt and in the outermost belt of charged particles which was discovered during the same three-electrode trap experiments.

In the outermost belt which was not detected by the cosmic ray counters the electron fluxes were recorded with energies more than 200 ev and lower than ~ 20 kev which exceeded the electron fluxes in the second belt by an order of magnitude.

The authors of the present report subjected the traps identical in their design to those used on Lunik II to the irradiation by electron fluxes with energies which were ascribed to soft electrons in the second and outermost belts. The aim of the experiment was to get convinced that the absence of considerable negative currents in the traps during the space rockets passage through the second

Declassified in Part - Sanitized Copy Approved for Release 2011/12/08 : CIA-RDP80T00246A016600420001-1

Declassified in Part - Sanitized Copy Approved for Release 2011/12/08 : CIA-RDP80T00246A016600420001-1

radiation belt is not due to some spurious effects (of the type of the considerable secondary electron emission from the collector under the action of soft electron fluxes in the radiation belt). At the same time it was necessary to estimate errors in the determination of electron fluxes in the outermost belt due to the same reasons. The results of these experiments were mentioned in the report by K.I.Gringauz at the Second International Space Science Symposium in Florence in 1961 (9). At present we are going to give more detailed data.

The diagram of the experiment is presented in Fig.2.

The electron flux produced by an electron gun (1) was focussed by means of a cylinder (2). The voltage variation on the cylinder with respect to the anode (3) has made it possible to change the energy of electrons from 150 ev to 40 kev. Control measurements of the value of the total current were carried out by means of a special probe (4) which was put on the way of the stream and whose design ensured the possibility of conducting absolute measurements. After each control measurement the probe was removed. The degree of the focussing of the electron beam was checked up by means of a removable luminescent screen (5). The trap (6) could be turned relative to the direction of the electron flux. The voltages on its outer and inner grids could vary during the experiment.

Fig.3 gives the dependencies of the current in the circuit of the trap collector from the inner grid potential at different energies of the electrons of the incident stream

Declassified in Part - Sanitized Copy Approved for Release 2011/12/08 : CIA-RDP80T00246A016600420001-1

Declassified in Part - Sanitized Copy Approved for Release 2011/12/08 : CIA-RDP80T00246A016600420001-1

and at its constant value ($I_0 = 5.10^{-9}$ amperes).

The upper scale of the abscissa shows the change of the inner grid potential φ_{g_1} with respect to the zero level which corresponds to the potential of the body of the instrumentation container. The lower scale shows the variation of the inner grid potential $\varphi_{g_1 c}$ with respect to the collector. From the curves of Fig.3 one can see the well known effect of the decrease of the secondary electron emission coefficient with the increase of the energy of primary electrons (10). The measured negative collector current also decreases with the increase of the energy of the incident stream. For each value of the energy of the incident stream the φ_{g_1} change in the interval from - 150 to - 200 volts does not cause any change in the collector current. The collector current decrease is accounted for chiefly by the fact that with the increase of the primary flux energy the portion increases of electrons leaving the collector surface with high velocity (inelastically scattered or reflected electrons) which correspondingly cannot be retarded by the inner grid ($\varphi_{g_1} = -200$ volts) (11), (12).

Fig.4 gives the dependences of the ratio of the collector current I_c to the value of the current I_0, which corresponds to the incident electron flux measured by means of a control probe, on the energy of the incident electron fluxes different in the magnitude (I_0 varied from 10^{-10} amp. to $5\text{-}10^{-9}$ amp.) In the inner grid the constant potential $\varphi_{g_1} = -200$ volts was kept, and the outer grid potential φ_{g_2} varied from 0 to + 50 volts. From the curves of Fig.4 is evident that the I_c/I_0 ratio in the investigated energy

Declassified in Part - Sanitized Copy Approved for Release 2011/12/08 : CIA-RDP80T00246A016600420001-1

Declassified in Part - Sanitized Copy Approved for Release 2011/12/08 : CIA-RDP80T00246A016600420001-1

range does not practically vary at considerable variations of the incident electron current. Thus it is evident that the values of the fluxes of electrons with energies up to 40 Kev determined by means of three-electrode traps of the type installed on Lunik II have turned to be not more than by 2÷3 times lower than the actual values. From this it follows that the estimate of the order of magnitude of electron currents with the above indicated energies by means of such traps is correct.

It should be noted that the recorded collector currents of the traps of the type considered can be determined generally speaking by the difference of the electron fluxes with energies exceeding $e\varphi_{g_1}$ (φ_{g_1} is the negative potential of the inner grid) and the fluxes of protons with energies more than $e\varphi_{g_2}$ (φ_{g_2} is the positive potential of the outer grid).

However, the probability that at the registration of the electron flux there is considerable compensation of the electron current by the proton one is small. If we assume that the concentration of energetic protons is equal to that of energetic electrons, the energy of protons which would be able to compensate for the current produced by electrons should be by three orders of magnitude higher than the energy of electrons. This means that the fluxes of electrons with energies of the order of tens of kevs would be able to be compensated by the fluxes of protons with energies of the order of mevs. As follows from (13), such protons at the trap nickel collector 0.3 mm thick could be recorded only with very low efficiency.

Declassified in Part - Sanitized Copy Approved for Release 2011/12/08 : CIA-RDP80T00246A016600420001-1

Declassified in Part - Sanitized Copy Approved for Release 2011/12/08 : CIA-RDP80T00246A016600420001-1

Let us note that as it follows from (14) electrons with energies up to tens of kevs should be retarded by such a collector effectively, which ensures their effective recording by the traps.

Thus the experiments confirmed the correctness of the conclusion drawn in (7) and (8) (1960) that in the second radiation belt the fluxes of soft electrons do not exceed unities per $10^7 cm^{-2}$ sec^{-1} and the counting rate in the charged particle counters observed in the second belt is not due to large fluxes of electrons with energies of the order of tens of kevs, but due to fluxes of much more energetic particles.

In conclusion we shall consider the remark by Winckler and Kellogg (15) referring to the results of measurements made by means of the traps in the outermost belt of charged particles. According to calculations carried out by the authors (15) the electron currents in the outermost belt should be on the order of 10^9 el/cm^2 sec.

The traps experiments (16) have given the value of the flux equal to 2.10^8 el/cm^2 sec. Winckler and Kellogg have pointed out that during the above mentioned measurements the amplifiers of the traps were close to saturation and would not be able to measure electron currents of the order of 10^9 el/cm^2 sec which should have taken place according to their calculations. This remark is correct. One should, however, bear in mind that the measured currents quite definitely have not reached the amplifier saturation level. On the other hand, since the traps could not record fluxes

Declassified in Part - Sanitized Copy Approved for Release 2011/12/08 : CIA-RDP80T00246A016600420001-1

Declassified in Part - Sanitized Copy Approved for Release 2011/12/08 : CIA-RDP80T00246A016600420001-1

of electrons with energies lower than 200 ev, it is quite probable that the total flux can reach the value of 10^9 el/cm·sec precisely due to the electrons with energies E<200 ev.

Electrons with energies of 10 kev recorded by L.R.Davis (17) in the region of the outermost belt on the Explorer XII satellite have apparently belonged to the energetic portion of the electron spectrum of this belt.

Declassified in Part - Sanitized Copy Approved for Release 2011/12/08 : CIA-RDP80T00246A016600420001-1

Declassified in Part - Sanitized Copy Approved for Release 2011/12/08 : CIA-RDP80T00246A016600420001-1

REFERENCES

1. S.N.Vernov, A.E.Chudakov, P.V. Vakulov, Yu.I.Logachev, Dokl.Akad.Nauk SSSR. 125, 304, 1959.

2. S.N.Vernov, A.E.Chudakov, P.V.Vakulov, Yu.I.Logachev, A.T.Nikolayev, Dokl.Akad. Nauk SSSR, 130, 517, 1960.

3. J.A.Van Allen, L.A.Frank, Nature, 183, 430, 1959.

4. J.A.Van Allen, L.A.Frank, Nature, 184, 219, 1959.

5. R.L.Arnoldy, R.A.Hoffman, J.R.Winckler, J.Geophys.Res.,65, 1361-1375, 1960.

6. C.J.Fan, P.Meyer, J.A.Simpson, J.Geophys.Res., 66, 2607-2640, 1961.

7. K.I.Gringauz, V.G.Kurt, V.I.Moroz, I.S.Shklovsky, Dokl. Akad.Nauk. SSSR, 132, 1062, 1960.

8. K.I.Gringauz, V.G.Kurt, V.I.Moroz, I.S.Shklovsky, Astronom. Zhurnal, 34, 4, 1960.

9. K.I.Gringauz, Space Research II edited by H.C. van de Hulst C. de Jager, A.F.Moor, 539, Amsterdam, 1961.

1/. Trump, van de Graaf, J. of Applied Physics, 18, 327, 1947.

11. H.Massey and E.Burhop, Electronic and Ionic Impact Phenomena, Russian translation, Moscow, 1958.

12. N.D.Morgulis, Proceedings of the Conference on the Catnode Electronics, Kiev, 1951.

13. H.Smith, Physical Review, 71, 32, 1947.

14. L.Spencer, Physical Review, 98, 1597, 1955.

Declassified in Part - Sanitized Copy Approved for Release 2011/12/08 : CIA-RDP80T00246A016600420001-1

Declassified in Part - Sanitized Copy Approved for Release 2011/12/08 : CIA-RDP80T00246A016600420001-1

15. P.J.Kellogg, J.R.Winckler, J.Geophys. Res.,66,12,1961.

16. K.I.Gringauz, V.V.Bezrukikh, V.D.Ozerov, R.E.Rybchinsky, Dokl.Akad.Nauk SSSR, 1301, 1960; "Artificial Earth Satellites", Vol.6, 101, The Publishing House of the USSR Academy of Sciences, 1961.

17. W.Beller, Missiles and Rockets, January 29, 1962.

Declassified in Part - Sanitized Copy Approved for Release 2011/12/08 : CIA-RDP80T00246A016600420001-1

Declassified in Part - Sanitized Copy Approved for Release 2011/12/08 : CIA-RDP80T00246A016600420001-1

второго радиационного пояса $N_e \leqslant 2 \cdot 10^7$ *см*$^{-2} \cdot$ *сек*$^{-1}$, мы приходим к представлению о наличии третьего, самого внешнего пояса (или оболочки),

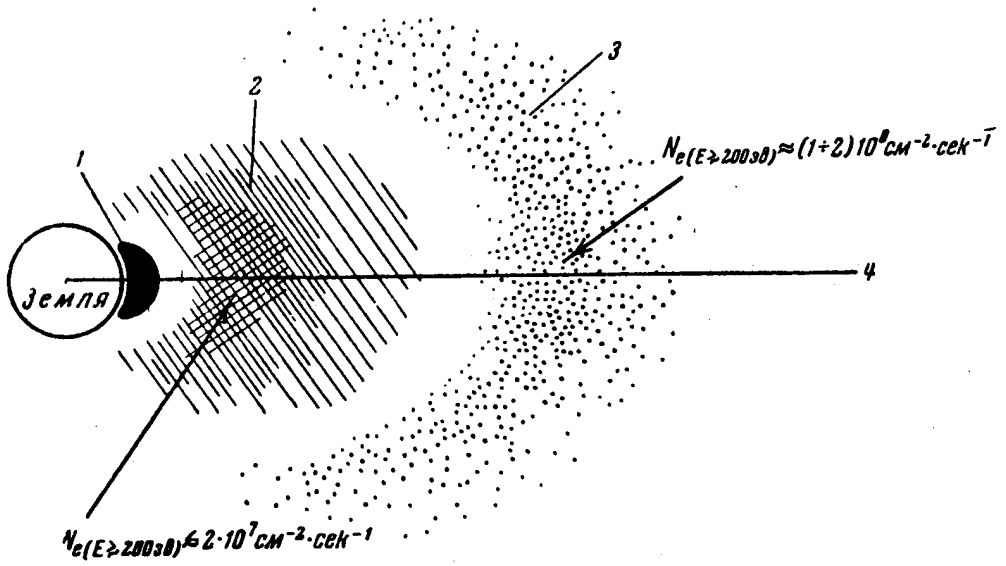

Рис. 2. Схема расположения радиационных поясов.

1 — «внутренний» пояс; *2* — «внешний» пояс; *3* — третий пояс; *4* — геомагнитный экватор

состоящего из электронов сравнительно небольших энергий. То обстоятельство, что предыдущие эксперименты не обнаружили этого самого

Declassified in Part - Sanitized Copy Approved for Release 2011/12/08 : CIA-RDP80T00246A016600420001-1

Declassified in Part - Sanitized Copy Approved for Release 2011/12/08 : CIA-RDP80T00246A016600420001-1

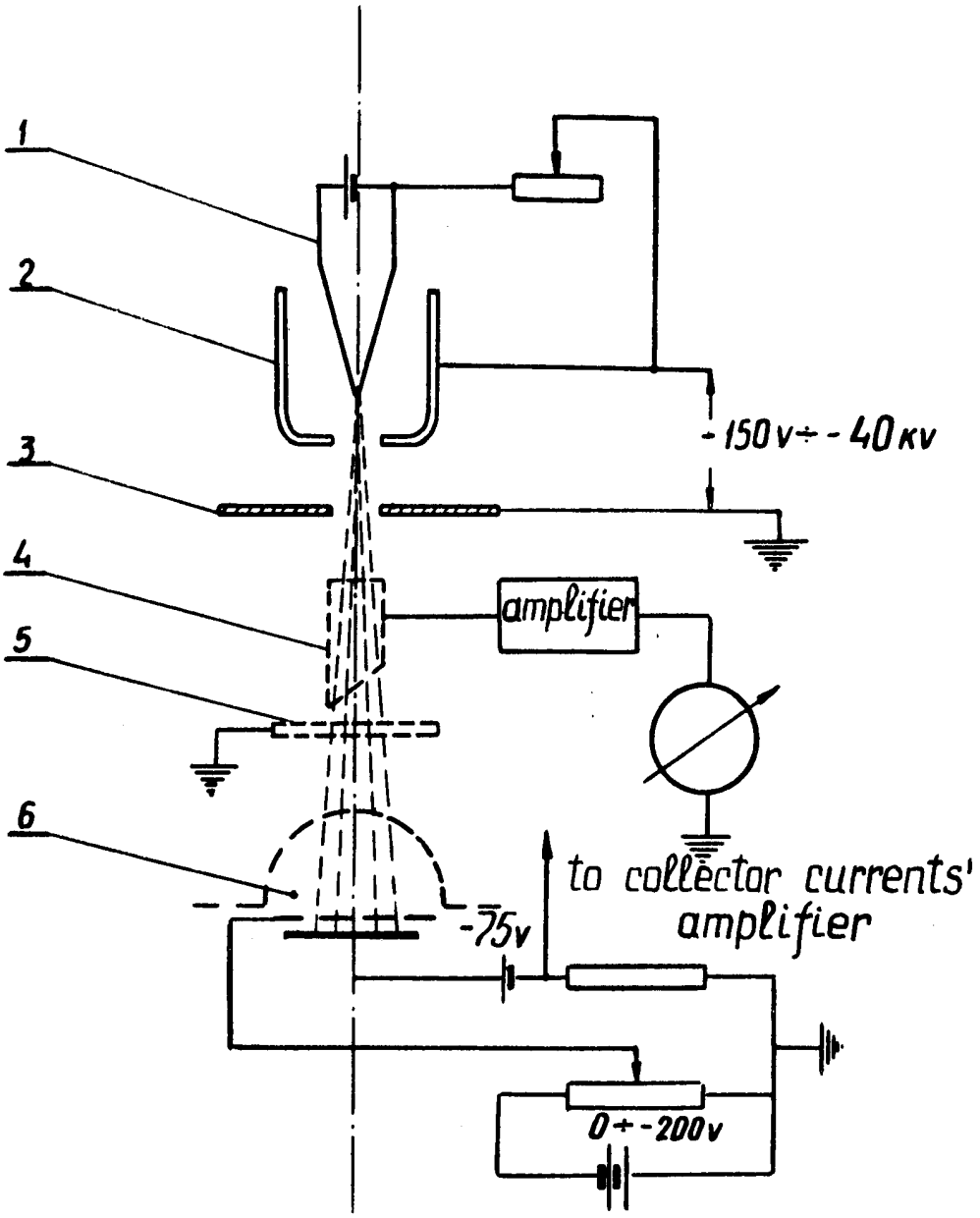

Declassified in Part - Sanitized Copy Approved for Release 2011/12/08 : CIA-RDP80T00246A016600420001-1

Declassified in Part - Sanitized Copy Approved for Release 2011/12/08 : CIA-RDP80T00246A016600420001-1

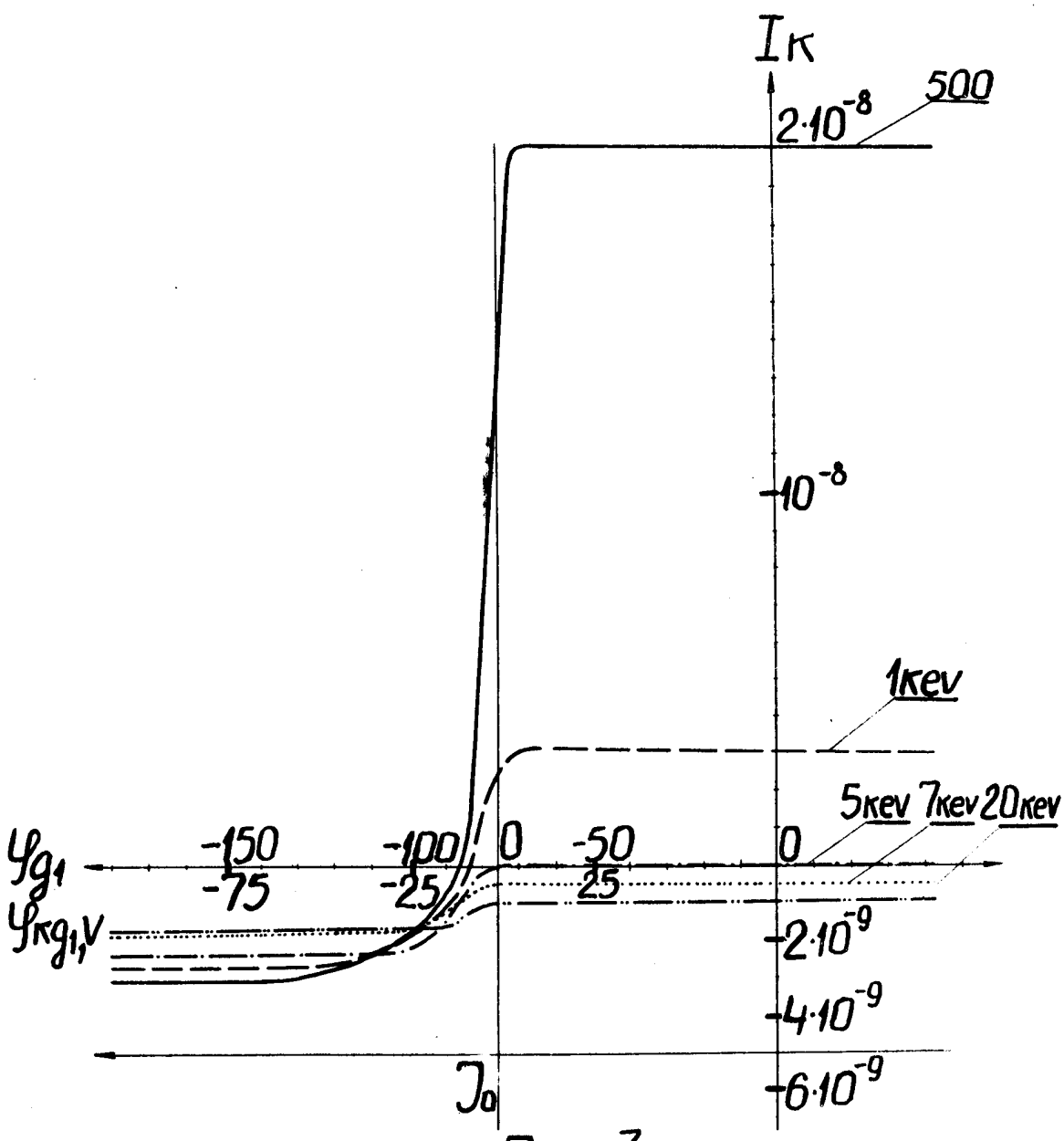

Fig. 3

Declassified in Part - Sanitized Copy Approved for Release 2011/12/08 : CIA-RDP80T00246A016600420001-1

Declassified in Part - Sanitized Copy Approved for Release 2011/12/08 : CIA-RDP80T00246A016600420001-1

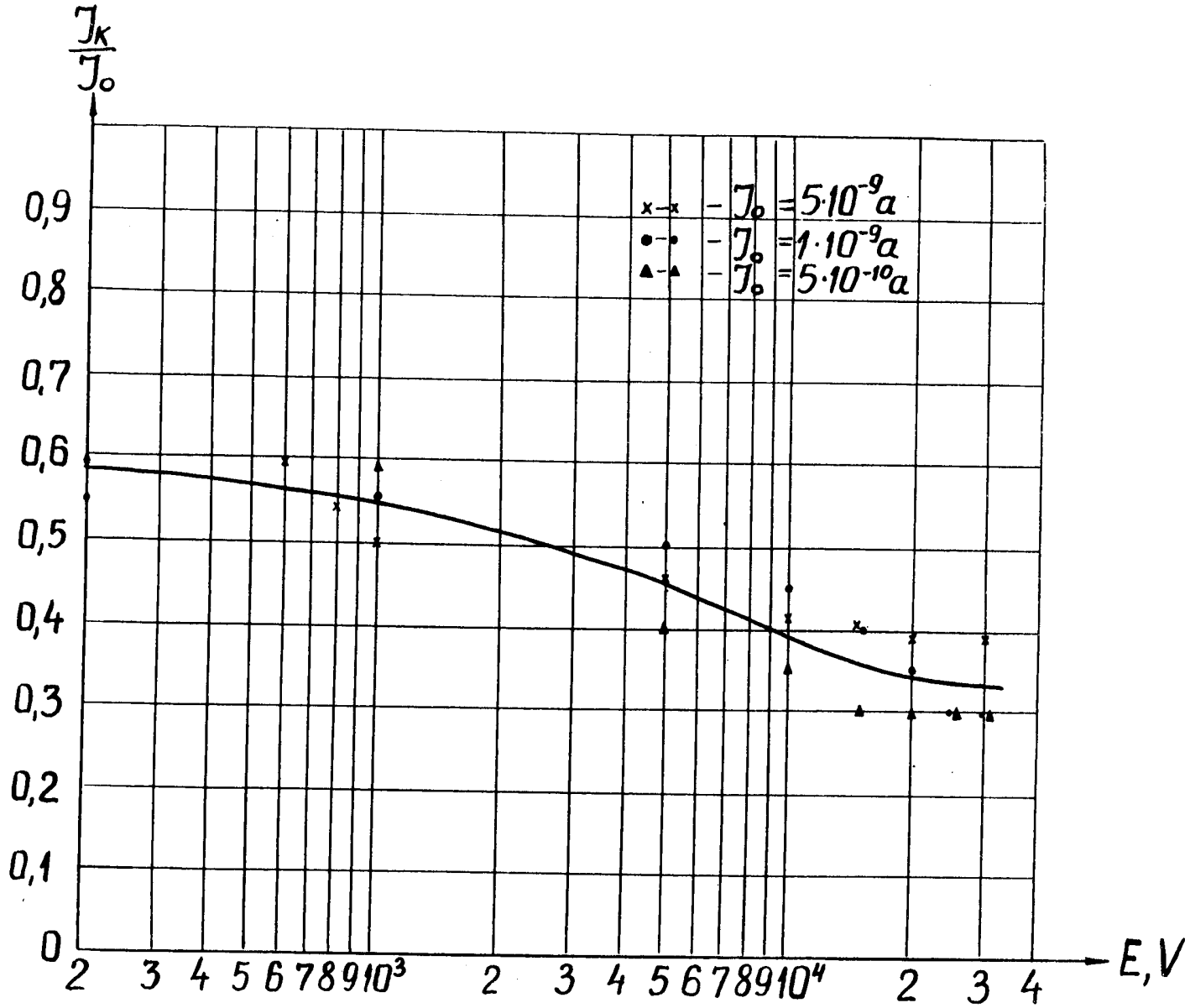

Declassified in Part - Sanitized Copy Approved for Release 2011/12/08 : CIA-RDP80T00246A016600420001-1

Declassified in Part - Sanitized Copy Approved for Release 2011/12/08 : CIA-RDP80T00246A016600420001-1

/. "NATIONAL REPORT OF THE USSR ACADEMY OF SCIENCES ON THE INVESTIGATIONS OF OUTER SPACE CARRIED OUT IN THE SOVIET UNION IN 1961."

by ~~Academician~~ A. A. Blagonravov (English) (14 pp)

High Atmosphere and Outer Space

1. Rocket Investigations

In 1961, 113 sounding rockets were launched in the Soviet Union (see the table).

During almost all the launchings the temperature and pressure measurements were performed and the wind velocities and directions were determined.

The rocket launchings were used for studies of the regime of the stratosphere over the mainland and the Pacific Ocean. The annual temperature, pressure and density variations were investigated.

As a result of the investigations of the regime of the stratosphere over the Pacific Ocean the conclusions have been drawn on the retention of the continental thermal influences in the stratosphere, on the retention of the warm Aleutian anticyclone up to heights of about 40 km and the stratosphere temperature field horizontal inhomogeneity. In the stratosphere the existence of the constant easterly winds in an extensive tropical zone and also of the easterly wind anomalous band has been revealed in the stratosphere in winter. The scheme of the seasonal reconstruction of the circulation regime has been investigated.

The investigations of the total solar eclipse on February 15, 1961, have been made by means of two sounding rockets. The program of observations envisaged the studies of the outer solar corona and also of the state of the upper atmosphere during the total eclipse and the moments close to the total phase. The data have been obtained on the passage of the outer corona radiations through the Earth's atmosphere.

In 1961 data were obtained for the first time on the neutral composition of the atmosphere up to heights exceeding 300 km. During these investigations helium was detected in the upper atmosphere at altitudes higher than 300 km. The investigations of the ionic composition have led to the discovery of ions of extraatmospheric origin at heights of about 100 km. Interesting data were obtained on the intensity and heights of glowing layers in the upper atmosphere.

Declassified in Part - Sanitized Copy Approved for Release 2011/12/08 : CIA-RDP80T00246A016600420001-1

Declassified in Part - Sanitized Copy Approved for Release 2011/12/08 : CIA-RDP80T00246A016600420001-1

II. The Venus Probe

On February 12, 1961, the Venus probe was launched in the Soviet Union. A new principle of placing a space vehicle in an interplanetary orbit was used, namely, the launching of a guided space rocket from a heavy artificial earth satellite. Such method of launching has opened up new possibilities for interplanetary flights since the necessity is excluded of choosing the definite time spans for flights to the Moon. At the same time the possibility is opened of launching heavier space vehicles to Venus and other planets, limitations are removed connected with the fact that not all launching points on the Earth are favourable for the realization of flight.

The satellite with a space rocket aboard was placed in a nearly circular orbit with the perigee 222 km and the apogee 280 km.

The space rocket was launched from the satellite in the precalculated point of the orbit. When this rocket flight velocity relative to the Earth became greater than the escape velocity and the rocket entered the precalculated point in space its motor was switched off and an automatic interplanetary station separated from it.

The creation of a powerful rocket carrier in the Soviet Union and the use of the take-off from a heavy satellite have made it possible to place the automatic interplanetary station with the weight of 643.5 kg in an interplanetary path.

The automatic interplanetary station left the sphere of the Earth's action and entered the elliptic orbit around the Sun.

This orbit is characterized by the following values: the maximum distance from the Sun is 151 million kilometres, the minimum distance from the Sun (the distance in the perihelion) is 106 million kilometres.

The automatic interplanetary station represented a unique space vehicle and was equipped with the following apparatus: a complex of radiotechnical and scientific instrumentation, the orientation and control systems, program devices, the thermal regime regulation system, the power supply system including solar batteries.

The radiotechnical complex of the Venus probe performed the following functions:

Measurements of the parameters of the station motion with respect to the Earth;

transmitting to Earth the results of measurements made by means of the probe scientific instrumentation;

transmitting to Earth the information on the work of the probe instrumentation, on the pressure and the temperature inside the probe and on its body;

reception of radio commands of the Venus probe operation control from the Earth.

Declassified in Part - Sanitized Copy Approved for Release 2011/12/08 : CIA-RDP80T00246A016600420001-1

Declassified in Part - Sanitized Copy Approved for Release 2011/12/08 : CIA-RDP80T00246A016600420001-1

The control of the work of the instrumentation aboard the probe was carried out by means of command transmissions through the radioline from the ground points and also by means of self-contained programming devices aboard the probe.

The probe orientation system performed the following functions during the flight:

the removal of the arbitrary rotation caused by the separation from the space rocket launched from the heavy satellite;

the Sun seeking from any position of the station and the orientation of solar batteries to the Sun during the whole period of the flight;

the ensuring of any necessary spatial turn and stabilization;

the orientation close to Venus of the sharply directed (parabolical) antenna in the direction towards the Earth to get higher speed of the transmission of scientific information and data on the work of the Venus probe instrumentation to Earth.

The automatic interplanetary station was equipped with scientific instrumentation to conduct physical measurements on the Earth-Venus path among them:

measurements of cosmic rays;

measurements of magnetic fields in the range from a few gammas to several tens of gammas;

measurements of the charged particles of interplanetary gas and solar corpuscular streams.

The processing of the results of trajectory measurements obtained during radio contacts with the Venus probe has shown that the probe control system ensured high accuracies of the placing of the automatic interplanetary station in a flight trajectory to Venus. The calculated errors lay within the limits of calculated tolerances of the control system errors. Without the correction of the trajectory the Venus probe passed at a distance of about 100,000 kilometres from the surface of Venus.

The data obtained during the radiocontacts testified to the normal work of the instrumentation and equipment installed aboard the Venus probe. The orientation and thermoregulation systems operated normally. The temperature and pressure inside the probe was within prescribed limits. The solar battery charged current corresponded to the calculated one.

The scientific instrumentation during the radio contacts functioned normally. New data have been obtained on the physics of outer space.

On the Venus probe traps were installed oriented to the Sun, one of which was designed for recording the solar corpuscular radiation ionic component. During the radio contact on February 17 it was recorded that the Venus probe passed through a considerable corpuscular stream with the density of the order of 10^9 particles per cm^2 per second. This observation coincided with the observations of a geomagnetic storm. Such experiments pave the way for establishing quantitative relationships between geomagnetic disturbances and the intensity of solar corpuscular streams.

Laboratory experiments with the irradiation of three-electrode charged

Declassified in Part - Sanitized Copy Approved for Release 2011/12/08 : CIA-RDP80T00246A016600420001-1

Declassified in Part - Sanitized Copy Approved for Release 2011/12/08 : CIA-RDP80T00246A016600420001-1

particle traps by electron fluxes have shown that such traps record electrons with energies on the order of tens of Kevs very efficiently. These experiments confirmed the correctness of the conclusion drawn at the beginning of 1960 by the Soviet investigators that the estimates of electron fluxes in the outer radiation belt which had been made on the basis of the cosmic ray counter indications exceeded the actual value by three orders of magnitude.

The Venus probe traps did not record considerable negative currents during the passage of the Venus probe through the outer radiation belt which confirmed once more the above-mentioned conclusion on the values of electron fluxes in the outer radiation belt.

The Venus probe was equipped with more sensitive magnetometers than those used on Soviet Luniks.

Information has been obtained during the two radio contacts with the Venus probe: on February 12 on the magnetically quiet day and on February 17 when magnetic disturbances took place.

The data of observations made on February 12 on the Earth and outside the Earth's magnetic field at a distance of 165,000-175,000 km. have shown in the main coordinated magnetic field variations relative to the average level within the limits of 4 gammas.

During the radio contact on February 17, whose duration was about 15 minutes the invariable value of the magnetic field was obtained. At the same time terrestrial observations recorded the magnetic field variations within the limits of 20-25 gammas.

One could not expect the close similarity of the curves, but in this case one reveals the complete absence of simultaneity in the magnetic activity on the Earth and in outer space.

The First Manned Flights Into Space

April 12, 1961, witnessed the great event. For the first time in history man realized space flight. The space ship "Vostok 1" piloted by the cosmonaut Yuri A. Gagarin was placed in earth satellite orbit.

The design of the spaceship Vostok 1 was based on the experience gained in the launchings of the first Soviet spaceship satellites which made it possible to work out the design of the spaceship-satellite and all its systems aboard. The first three spaceship-satellites were launched in 1960, and spaceship IV and V on March 9 and 25, 1961. At these space-ship-satellites medico-biological experiments with animals were performed.

The program of the first manned space flight was designed for one Earth circuit. However, the design and the equipment of the ship have made it possible to realize more prolonged flights.

Declassified in Part - Sanitized Copy Approved for Release 2011/12/08 : CIA-RDP80T00246A016600420001-1

Declassified in Part - Sanitized Copy Approved for Release 2011/12/08 : CIA-RDP80T00246A016600420001-1

After the completion of the program of the flight before landing the ship orientation in the definite direction was carried out by a special system. Then in the prescribed point of the orbit the retro-engine was switched. After reduction of the ship orbital velocity by the value required according to the calculation, the ship was transferred to the descent trajectory.

From the moment when the retro-engine was switched on to the moment of landing the ship covered about 8,000 km. The duration of the flight on the descent portion of the trajectory was about 30 minutes.

Since the equipment contained in the cabin was published in the press, I mention the equipment only briefly.

The cosmonaut occupied an ejector seat in which he remained during the whole flight and which enabled him to leave the vehicle if necessary.

The pilot cosmonaut wore a protective space suit which ensured preservation of his life and working capacity even in the case of the depressurization of the capsule in flight.

Vostok 1 was equipped with the following systems:

a landing system,
radio apparatus for communications with the Earth,
an autonomous system recording the work of instruments, radiotelemetry systems and various sensors,
a television system for observing the astronaut from the Earth,
instruments for recording the physiological functions of the body,
the retro-engine,
an orientation system,
a flight control system,
radio systems for measuring orbital elements,
a temperature control system,
electric supply sources.

The control of the apparatus operation was carried out automatically by means of program devices aboard the ship and, if necessary, by the pilot himself.

Control units, orientation elements, shutters of the temperature control system, and the aerials of radio systems were mounted on the outside surface of the vehicle.

The pilot's capsule is much roomier than the cockpit at an aircraft. The capsule instrumentation ensured the greatest convenience for the pilot in flight. From his chair the spaceman can perform all the necessary operations connected with observation, communication with the Earth, flight control and the ship control.

Declassified in Part - Sanitized Copy Approved for Release 2011/12/08 : CIA-RDP80T00246A016600420001-1

Declassified in Part - Sanitized Copy Approved for Release 2011/12/08 : CIA-RDP80T00246A016600420001-1

The space pilot can land in the ship capsule. Such method of landing was tested in Soviet satellite spaceship IV and V which carried test animals in their capsules. A variant was also provided for in which the pilot is catapulted with the seat from the capsule at a height of about 7 km. and is landed by parachute. This variant was also tested in descents of satellite spaceships with test animals.

For measuring the spaceship orbit parameters and checking the work of its apparatus radio measuring and radio telemetry instrumentation were installed on it. The measurements of the ship motion parameters and the reception of the telemetry information during the flight were carried out by the ground stations located in the territory of the USSR. The data of measurements were transmitted automatically through the communication lines into computing centers where their processing was carried out on electronic computers. As a result of this in the course of the flight information was obtained on the main orbital elements and further motion of the ship was predicted.

The radio system "Signal" aboard the ship served for the ship direction finding and the transmission of the part of the telemetry information.

The television system carried out the transmission of the spaceman's image to Earth which made it possible to conduct visual observations of the pilot.

The two-way communication of the space pilot with the Earth was carried out by a radiotelephone system which worked in the short wave ranges (9.019 and 20.006 megacycles) and at ultrashort waves (143.625 megacycles).

The ultrashort channel was used for communications with the ground points at distances up to 1,500-2,000 km. The communication through the short wave channel with the ground points which were located on the territory of the USSR as the experience has shown can be ensured on the largest part of the orbit.

For the ship orientation in the case of manual control the cosmonaut used the optical orientator which enabled him to determine the ship's position relative to the Earth.

The globe mounted on the instrument panel provided the opportunity of predetermining alongside the ship's current position the place of descent after switching on the retroengine at the given time moment.

The stores of food, water, regeneration substances and the capacity of the electric supply sources were designed for the flight of the 10 day duration.

Measures were envisaged in the design of the ship which prevented the increase of the temperature inside the capsule beyond the definite limit at the durable heating of its surface.

Declassified in Part - Sanitized Copy Approved for Release 2011/12/08 : CIA-RDP80T00246A016600420001-1

Declassified in Part - Sanitized Copy Approved for Release 2011/12/08 : CIA-RDP80T00246A016600420001-1

After successful orbit around the Earth the spaceship landed in the prescribed locality in the vicinity of the Smelooke village of the Pernov district of the Saratov region at 10 hours 55 minutes Moscow time (7 hours 55 minutes Universal time).

After his return from the space flight Y. A. Gagarin feels well. No deviations in his health were detected.

Gagarin's flight has made it possible to draw the conclusion of a paramount scientific significance on the practical possibility of the manned space flights. It has shown that man can normally undergo the space flight conditions, the conditions of placing in orbit and re-entry to Earth. This historic flight has proved that under weightlessness man fully preserves his working capacity, the coordination of movements, the clearness of thinking.

On August 6, 1961, at 9 hours Moscow time (6 hours Universal time) the second successful launching of the spaceship-satellite Vostok 2 piloted by Major Herman Stepanovich Titov was realized.

According to corrected data the minimum distance of the ship from the Earth's surface (the perigee) was 183 km, and the maximum distance (the apogee) was 244 km.

On August 7, 1961, at 10 hours 18 minutes Moscow time (7 hours 18 minutes Universal time) the ship Vostok 2 successfully landed in the prescribed locality over the territory of the Soviet Union near the little town Krasny Kut of the Saratov region.

For 25 hours 18 minutes of this historic flight the space ship covered more than 700,000 km and orbited the Earth more than 17 times.

The design of the spaceship Vostok 2 was in the main similar to that of Vostok 1. But on Vostok 2 a new more perfect regeneration plant was installed which differed from that of the ship Vostok 1 by the composition of blocks and chemical reagents.

The flight was planned for 17 circuits around the Earth. However, the ship design, the store of food, water, reagents of regeneration system, electricity supply sources enabled Titov to realize a more protracted flight.

After the placing in orbit the ship separated from the rocket-carrier. During the orbital flight the apparatus aboard the ship worked according to a program.

The description of the flight will be presented by Titov himself at this Symposium.

The main and most important outcome of H.S. Titov's flight proved the possibility of the complete retention of man's working capability during the 25-hour state in outer space.

The results of medical-biological investigations during the flights of spaceship-satellites Vostok 1 and Vostok 2 will be presented in other papers by Soviet scientists.

Declassified in Part - Sanitized Copy Approved for Release 2011/12/08 : CIA-RDP80T00246A016600420001-1

Declassified in Part - Sanitized Copy Approved for Release 2011/12/08 : CIA-RDP80T00246A016600420001-1

SOME ADDITIONAL RESULTS OF SCIENTIFIC INVESTIGATIONS MADE BY MEANS OF SPACESHIPS-SATELLITES

By means of the series of instruments aboard spaceship satellites I and III the energy spectra of various groups of nuclei, the chemical composition of cosmic rays, the nuclear component variations and some radiation effects were investigated. New data were obtained on the nuclear component flux short time increases connected with the solar activity. For the first time such increases in the nuclear component were recorded during Lunik II flight. This phenomenon is characterized by a sharp short time increase of the flux of nuclei which practically takes place simultaneously with the observed solar flares and radio emission outbursts.

The energy spectra were obtained of various nuclear groups on the basis of the measurements of the latitude effect. The nuclear spectrum was determined from the charges in the range from alpha-particles to oxygen. At heights 200-300 km the enhanced radiation intensity was recorded over the whole surface of the globe as compared with the intensity of the primary flux of cosmic rays and data were obtained on the spatial distribution of the radiation intensity at these heights. The fact of the existence of the increased intensity at heights of 200-300 km agrees with the data obtained by the other group of Soviet investigators and also with the data obtained in the U.S.A. and Japan, by means of the Explorer 1 satellite about the increase of the radiation intensity in a height range of 300-500 km as compared with the level of the cosmic ray intensity.

The detected gigantic anomaly of the radiation intensity at a height of 340 km over the southern part of the Atlantic Ocean called the South Atlantic anomaly and the radiation intensity anomaly at heights of 190-340 km near the shore of Antarctic Continent called the South anomaly are connected with the geomagnetic field anomalies and apparently represent specific sinks of the particles from the radiation belts.

Declassified in Part - Sanitized Copy Approved for Release 2011/12/08 : CIA-RDP80T00246A016600420001-1

Declassified in Part - Sanitized Copy Approved for Release 2011/12/08 : CIA-RDP80T00246A016600420001-1

All these measurements enabled us to make more precise our conceptions on the behaviour of the radiation belts near the Earth and to enlarge our knowledge of the Sun as a source of multiply-charged particles of cosmic rays.

SATELLITE OPTICAL TRACKING

In 1961 observations of satellites were conducted by 84 Soviet visual tracking stations and by 23 photographic tracking stations. In total 37 objects were observed with the brightness up to +9 stellar magnitude, among them many Soviet satellites: Sputniks 1960 ε_2, 1960 ε_3 (Sputnik IV and its capsule), 1961 β_1, 1961 β_2, 1961 β_3 (Sputnik VII and rocket carrier), 1961 λ_1 (Sputnik VIII - Automatic Interplanetary Station); American satellites, 1960 ζ_1 (Echo 1), 1959 ζ, 1960 ξ, 1961 δ (Explorer VII, VIII, IX), 1961 ε, 1961 ζ, 1961 λ, 1961 ξ, 1961 π, 1961 $\alpha\varepsilon$ (Discoverer XX, XXI, XXIII, XXIV, XXVI, XXXIV), 1960 β_2, 1960 π, 1961 ρ (Tiros I, II, III), 1960 γ, 1960 ζ, 1961 O (Transit IB, IIA, IV A), 1961 α (Samos II), 1961 σ, 1961 $\alpha\delta$ (Midas III, IV).

The main methods of observations were visual by means of tubes AT-1 and TZK, and photographic with the camera NATA- 3 c/25. The accuracies of visual observations were $0^{\circ}.1$ in position and 0.1 sec in time. The accuracies of photographic observations were 4"-6" and 0.005 sec respectively.

In 1961 the amount of accurate photographic tracking increased. Cameras were installed with movable film which made it possible to take pictures of fainter satellites with the brightness up to 5-6 star magnitudes. The calculations of accurate positions of artificial earth satellites in 1961 were carried out on the computers in Moscow and Leningrad.

10,200 passages of artificial Earth satellites were observed. About 47.5 thousands of visual positions were determined, about 7,000 negatives were obtained for the determination of accurate positions.

The main work on bettering the technique of observations was aimed at the automatization of observations and the enhancement of the tracking accuracy.

Declassified in Part - Sanitized Copy Approved for Release 2011/12/08 : CIA-RDP80T00246A016600420001-1

Declassified in Part - Sanitized Copy Approved for Release 2011/12/08 : CIA-RDP80T00246A016600420001-1

The processing of observations and the calculation of the orbital elements were carried out by the Institute for Theoretical Astronomy of the USSR Academy of Sciences. In 1961 systems of elements for some of the satellites 1958 δ_2, 1960 ε_1, 1960 ε_2, 1960 ε_3, were published.

The evaluation of the quality of visual observations of tracking stations is made by the Astronomical Council of the USSR Academy of Sciences from these elements.

Photometric observations were organised at a number of stations. A correlation is established between solar flares and the changes of the satellite photometric period.

In 1961 the Astronomical Council continued cooperation with foreign satellite tracking stations. About 200 stations located in 17 countries regularly sent the results of the observations of Soviet and American satellites.

In 1961 the following data were obtained from foreign states:

	The Number of Passages	The Number of Observations
Soviet Sputniks	2,600*	9,300
American satellites	4,400	15,600
The Echo satellite and its details	6,800	38,400
TOTAL	13,800	63,300

With a view of exchanging the experience of the work of stations the Astronomical Council publishes "The Bulletin of Satellite Optical Tracking Stations" in which articles are published on the problems of the techniques of observations and the results of the processing of observations. The results of the precise photographic observations are also published in this bulletin. In 1961 the precise photographic positions were published for the satellites:

Declassified in Part - Sanitized Copy Approved for Release 2011/12/08 : CIA-RDP80T00246A016600420001-1

Declassified in Part - Sanitized Copy Approved for Release 2011/12/08 : CIA-RDP80T00246A016600420001-1

Name of the Satellite	Number of Observations
1958 δ_1	26
1958 δ_2	20
1960 ε_1	30
1960 ε_2	6
1960 ε_3	40
1960 ζ_1	45
1960 λ_1	10

During 1961, the results of the researches were published in several magazines. The list of 156 publications will be handed over to the Secretariat of COSPAR.

THE PLANS OF SCIENTIFIC INVESTIGATIONS FOR 1962

The program of investigating the upper atmosphere and outer space will be continued. In the course of 1962, a series of launchings of artificial earth satellites will be carried out.

The following phenomena will be investigated according to this scientific program:

the charged particle concentration in the ionosphere, which is important for studies of radio wave propagation;
corpuscular streams and low-energy particles;
the Earth's radiation belts composition;
the geomagnetic field;
shortwave radiation of the Sun and other space bodies;
the upper atmosphere;
the influence of meteoritic matter on the elements of the design of space objects;
the distribution and production of cloud systems in the Earth's atmosphere.

The four satellites of this series "Cosmos" were launched early in 1962. Medico-biological investigations will be continued during the next manned space flights.

Declassified in Part - Sanitized Copy Approved for Release 2011/12/08 : CIA-RDP80T00246A016600420001-1

Declassified in Part - Sanitized Copy Approved for Release 2011/12/08 : CIA-RDP80T00246A016600420001-1

APPENDIX I

Research Rocket Launchings in 1961

Place of Launching

	The High Latitude Observatory on Franz-Josef Land	Middle Latitudes of the European Part of USSR	Expedition Ships in the Pacific	The Total Number of Launchings
January	8	-	18	26
February	11	14*	-	25*
March	-	3	-	3
April	-	-	4	4
May	1	-	8	9
June	9	-	13	22
July	11	-	-	11
August	-	-	-	-
September	-	1**	-	1**
October	4	-	-	4
November	-	1**	-	1
December	9	-	-	9
TOTAL	53	19	43	115

*Among them two rockets were launched in the period of the total solar eclipse on February 15, 1961.

**Research rockets for complex investigations of the upper atmosphere on September 23, 1961, to a height of 100 km and on November 15, 1961, to a height of 430 km.

Declassified in Part - Sanitized Copy Approved for Release 2011/12/08 : CIA-RDP80T00246A016600420001-1

Declassified in Part - Sanitized Copy Approved for Release 2011/12/08 : CIA-RDP80T00246A016600420001-1

APPENDIX 2

SOVIET SPACESHIPS-SATELLITES, SPACE PROBES AND EARTH SATELLITES

LAUNCHED IN 1961

Artificial Earth Satellites

Date of Launching	The Lifetime of the Satellite	Weight	The Perigee, the Apogee, the Period, the Inclination	Scientific Experiments
(1)	(2)	(3)	(4)	(5)
February 4, 1961	to February 26	6,483 kg	223 km 328 km 89.8 min 64.6°	The test of the systems of launching and the precise trajectory check.
February 12, 1961	to February 25	--	222 km 280 km 89.5 min 65°	The launching of an automatic interplanetary station to Venus from the satellite.
March 9, 1961 (the lift-off and landing)	--	4,700 kg	183.5 km 248.8 km 88.6 min 64° 56'	The testing of the ship design and its systems aboard to prepare the manned space flight. Medico-biological experiment (the dog Chernushka). Successful descent and landing.
March 25, 1961 (the lift-off and landing)	--	4,695 kg	178.1 km 247 km 88.42 min 64° 54'	Testing of the ship and its systems aboard to prepare the manned space flight. Medico-biological experiment (the dog Zvyozdochka). Successful descent and landing.
April 12, 1961 (the lift-off at 9h.07 min, the landing at 10 h.55 min)	--	4,725 kg	181 km 327 km 89.1 min 64° 57'	The first manned space flight in the world and successful landing at a prescribed area. Pilot cosmonaut Y. A. Gagarin. Radio communication on frequencies 19.995 Mc, 9.019 Mc, 20.006 Mc, 143.625 Mc.

Declassified in Part - Sanitized Copy Approved for Release 2011/12/08 : CIA-RDP80T00246A016600420001-1

Declassified in Part - Sanitized Copy Approved for Release 2011/12/08 : CIA-RDP80T00246A016600420001-1

APPENDIX 2 (Concluded)

1	2	3	4	5
August 6, 1961 9h.00 min--the lift-off; August 7, 1961, 10h.18 min--the touch down	--	4,731 kg	185 km 244 km 88.46 min 64° 56'	The second Soviet manned space flight and successful landing in a prescribed area. Pilot cosmonaut H. S. Titov. Radio communication on frequencies 15.765 Mc, 19.995 Mc, 20.006 Mc, 143.625 Mc.
February 12, 1961	--	643.5 kg—the weight of the Automatic Interplanetary Station	Towards Venus. Reached Venus at the second half of May, 1961. The minimum distance to Venus was 100,000 km and the distance covered 280 million km.	Investigation of interplanetary ionized gas and of solar corpuscular radiation. Investigation of the radiation belts and of space radiation. Magnetic measurements. Investigations of Meteoritic Dust. Radiocommunication on 922.8 Mc.

Declassified in Part - Sanitized Copy Approved for Release 2011/12/08 : CIA-RDP80T00246A016600420001-1

Declassified in Part - Sanitized Copy Approved for Release 2011/12/08 : CIA-RDP80T00246A016600420001-1

2. by G.I.GOLYSHEV, A.M.BOROVICOV, G.A.KOKIN (English)(12pp)

"SOME CHARACTERISTICS OF ATMOSPHERE STRUCTURE OF THE SOUTHEN HEMISPHERE"

Free atmosphere studies in the third antarctic expedition were carried out in accordance with the IGY Programme. The following kinds of investigation work were stipulated:

- measurements of vertical temperature distribution, Pressure, air density and wind velocity and direction in different regions of the Southern Hemisphere (the antractic region and the region of southern temperate latitudes) in summer and in autumn;
- studies of Atlantic equatorial and tropical troposphere and stratosphere structure.

The investigation Programme was ensured by meteorological rokkets firings and daily radiosonde observations, regular wind measurements at altitudes including. It should be emphasized, that such a complex of aerometeorological investigations in Antarctica and in a number of regions in the Pacific and Atlantic oceans was carried out for the first time.

This report presents some observational results for two geographical regions.

The first meridional cross section was fulfilled from April 23 through May 7, 1959 on the way from the Amundsen sea ($65^{\circ}41'S$, $109^{\circ}46'W$) to Easter Island ($27^{\circ}37'S$, $109^{\circ}25'W$) $109^{\circ}W$ meridian. During this period 8 rockets were fired

Declassified in Part - Sanitized Copy Approved for Release 2011/12/08 : CIA-RDP80T00246A016600420001-1

Declassified in Part - Sanitized Copy Approved for Release 2011/12/08 : CIA-RDP80T00246A016600420001-1

(approximately, every 5° of latitude) and 15 radiosonde ascents made, approximately, every 3° of latitude.

Space-time cross section, built with aid of these radiosonde data, is shown in Fig.1. It covers a great latitudinal zone of the Southern Hemisphere - from polar regions to the subtropical zone and characterizes the troposphere and stratosphere above the south-western part of the Pacific ocean in late fall.

Let us consider the main features and peculiarities of the atmosphere structure in this region at hand of the cross section data.

In the troposphere the horizontal temperature lapse-rate is directed from the equator to the pole. At all levels the temperature rises from the South to the North.

The tropopause, observed at height about 9 km over polar regions, also rises in this direction, reaching the 11 km altitude at 50°S. Further, in the temperate latitudes it remains nearly horizontal. In latitude 35°S there is a strongly pronounced break of the tropopause - from low (10,5 km) and warm (-54°) polar tropopause to high (15 km) and cold (-67°) tropical one. In the subtropical zone tropical tropopause rises up to 17 km and its temperature drops to about -70°.

At the heights from 12 to 21 km, i.e. in the lower stratosphere, the horizontal temperature lapse- rate changes its sign and is directed from the South to the North. A strongly pronounced closed cold area (t° down to -70°) is situated in this layer above the subtropical zone, but above

Declassified in Part - Sanitized Copy Approved for Release 2011/12/08 : CIA-RDP80T00246A016600420001-1

Declassified in Part - Sanitized Copy Approved for Release 2011/12/08 : CIA-RDP80T00246A016600420001-1

the polar regions one can observe though much less, but still marked warm area (t -50°). Thus, it should be noted, that in the southern lower stratosphere even in late fall (the end of April) there still remain some features of summer thermal conditions.

In the 21 to 38 km layer, i.e. in the upper atmosphere, the meridional temperature lapse-rate once more changes its direction. Here, above polar regions there exists a strongly pronounced and, evidently, closed cold area (with t -60°), but towards the equator the temperature begins to rise, at first (in temperate latitudes) quicker, then slower. Hence, in these fall months the upper stratosphere thermal conditions are the winter ones.

At altitudes above 30-38 km, i.e. in the stratospheric inversion area the temperature field is characterized by rather great variability.

In different latitudinal zones substantial differences in the atmosphere vertical stratification are revealed. Thus, in the subtropical lower stratosphere there is a strong inversion up to the 20 to 22 km altitude, then the temperature rise slows down and, beginning from 35-36 km altitude it rises again, now within the stratospheric inversion layer.

In the broad belt of temperate latitudes and neighbouring polar regions (approximately from 37° to $62\text{-}63^{\circ}$S) in the stratosphere up to the altitude of 34 to 35 km there is a weak

Declassified in Part - Sanitized Copy Approved for Release 2011/12/08 : CIA-RDP80T00246A016600420001-1

Declassified in Part - Sanitized Copy Approved for Release 2011/12/08 : CIA-RDP80T00246A016600420001-1

inversion or almost isothermal layer. from 18 to 35 km temperature rises only by 11°, i.e. the average lapse-rate is only 0.06/100 m. Above, the inversion becomes stronger, increasing with height.

The stratosphere structure above polar regions at this time is rater complicated. Very strong inversion can be observed beginning immediately above the tropopause and up to 15 km altitude. Then it gives place to the temperature fall with height, which goes on up to 30 km, where there exists a closed area. At this level there begins a stratospheric inversion, marked here much stronger, than at lower latitudes.

These data point to the fact, that in the polar stratosphere temperature fall must begin at higher levels. and then it gradually descends.

Wind field. Easterlies prevail in the whole layer of the polar troposphere. These must be the winds of the outskirts of antarctic tropospheric anticyclon. Thus, its influence, evidently, stretches to appreciable distance from the Antarctic coast. Westerlies prevail in the temperate latitudes. But they are, however, variable and sometimes are changed for easterlies. This happens as a result of cyclone formation. Further, steady westerlies, caused by the sub-tropical high pressure belt influence, set in throughout the subtropical zone.

There are 3 jet stream zones in wind velocity field in the troposphere. All of them are caused by high horisontal temperature contrasts in these areas, the value of the

Declassified in Part - Sanitized Copy Approved for Release 2011/12/08 : CIA-RDP80T00246A016600420001-1

Declassified in Part - Sanitized Copy Approved for Release 2011/12/08 : CIA-RDP80T00246A016600420001-1

contrast determining the jet stream intensity. The most intensive jet stream, connected with the zone of the tropical and polar tropopause break, with velocities above 70 km/sec, covers a vast area of more than 7 degrees of latitude. Its vertical extent is also very great - the area of wind velocities above 100 km/hour stretches from 6 to 19 km. The second jet stream, much slower and smaller in the area covered, was observed in polar regions near 65°S. The third, also rather a weak jet was found in the temperate latitudes at 52°S.

The following interesting features were revealed in the stratosphere wind field: First - the immense steadiness of westerlies in the whole stratosphere throughout the cross section, with the exception of its lowest layer in polar regions, where the winds have a significant southern component. This feature is most pronounced in the temperate latitudes and in the subtropical zone, where the winds are almost net westerlies.

Hence, it follows, that in late fall months one can observe a winter type of stratospheric circulation, the fact being characteristic not only in average for the whole season, but for separate days as well.

The existence of relatively weak winds belt (about 50 km/hour), vast both in latitude - from polar circle to 40°S - and in height - from the tropopause to the 24 to 26 km altitude - is the second important feature. It is characteristic that it coincides with small horizontal temperature lapse-rates area. This weak winds belt is somehow disturbed in two

Declassified in Part - Sanitized Copy Approved for Release 2011/12/08 : CIA-RDP80T00246A016600420001-1

Declassified in Part - Sanitized Copy Approved for Release 2011/12/08 : CIA-RDP80T00246A016600420001-1

places by small areas of stronger winds. It is remarkable, that these areas are situated just above the zones of tropospheric jet streams. Jet streams, originating from the troposphere, evidently, influence the above layers, making the stratospheric wind strengthen.

Above the 24-26 km level the wind strengthens with height. But in meridional direction, however, the wind velocity distribution becomes more variable in accordance with temperature variability increase at these levels. Within the 24-34 km layer over the southern polar circle at the border of the closed cold area one can observe a clearly marked stratospheric jet stream with the velocities in the center of more than 200 km/hour. As is known /1/, in winter over Antarctic coast stratospheric jet stream is found at much lower levels, beginning with 14-16 km. This allows us to draw the conclusion, that the stratospheric jet stream gradually descends as fall changes for winter, in accordance with the spread of cold. Further to the North, up to about 55°S, the winds weaken, but still have the velocity of more than 100 km/hour.

The wind velocities in this layer above the temperate latitudes are considerably less, what corresponds to very weak horizontal temperature contrast in this area. Here it is as if the rise of the upper border of the weak winds belt takes place.

However, this weak winds area over 30-32°S is broken off by a narrow zone of sharp wind strengthening. The reasons for

Declassified in Part - Sanitized Copy Approved for Release 2011/12/08 : CIA-RDP80T00246A016600420001-1

Declassified in Part - Sanitized Copy Approved for Release 2011/12/08 : CIA-RDP80T00246A016600420001-1

this strengthening are not yet clear, but, at any rate, their cause is not thermal, no lapse-rate increase is observed.

Above the 34-36 km level in the stratospheric inversion zone throughout the latitudinal belt, covered by the cross section, wind velocities are rather high - above 100 km/hour. However, even here, against the strong winds background in the region between 45 and 35°S, there exists a jet stream with the velocities above 230 km/hour, the fact being pointed to by the data of rocket firing on May 3. It is, evidently, caused by thermal variations, as it coincides with the area of sharp variations of isotherms height.

The second meridional cross section was drawn for the period July 10-26,1959 for the way from Montevideo to Europe (Fig.2). It stretches from 32°S to 40°N and covers the subtropical and tropical belts of the Southern Hemisphere, the equatorial region, the tropical zone, and part of the temperate latitudes of the Northern Hemisphere. The plane of the cross section is not strictly meridional, the cross section began at 46°W and ended at 18°W.

Thus, the cross section data characterize the atmosphere structure above the central part of the Atlantic ocean in middle winter of the Southern Hemisphere and in middle summer of the Northern Hemisphere.

During the cross section period there were 9 rocket firings altogether (on the average every 8 degrees of latitude) and 16 radiosonde ascents (roughly every 4.5° of latitude).

In the troposphere above the Southern Hemisphere in

Declassified in Part - Sanitized Copy Approved for Release 2011/12/08 : CIA-RDP80T00246A016600420001-1

Declassified in Part - Sanitized Copy Approved for Release 2011/12/08 : CIA-RDP80T00246A016600420001-1

about 12 km layer at all altitudes slight temperature rise is observed in the direction of the equator. Above the subtropical zone there exists a double tropopause - polar tropopause at the altitude about 11 km, temperatures in it being -57°, and tropical tropopause - at the altitude about 16 km with $t^{\circ} = -65^{\circ}$. The break between the tropopauses is 5 km. In this layer (12-16 km) the thermal lapse-rate has the opposite direction - at altitudes near the equator the temperature is lower.

In the Northern Hemisphere the thermal field throughout the troposphere becomes rather homogenious - the isotherms pass almost horizontally, suffering only slight fluctuations from day to day. The typical tropical tropopause is also situated, approximately, at one and the same level, between 16 and 17 km. The lowest temperatures in it are observed immediately above the equator and reach -77°.

Throughout all our Northern Hemisphere cross section there are neither break, nor double tropopause, and the isotherm pattern gives no grounds for expecting the break somewhere nearby. Thus, if there was the tropopause break, it was appreciably displaced to the North, at any rate, higher than 40°N.

The stratosphere thermal field is characterized by a very interesting feature: the invasion of warm summer stratosphere of the Northern Hemisphere into the winter Southern one. And indeed, as is clear from the cross section, thermal conditions of the tropical and equatorial belts of the summer Northern Hemisphere reach 15°S. The zone between 15° and 25°S

Declassified in Part - Sanitized Copy Approved for Release 2011/12/08 : CIA-RDP80T00246A016600420001-1

Declassified in Part - Sanitized Copy Approved for Release 2011/12/08 : CIA-RDP80T00246A016600420001-1

is a transition area, where temperatures at all heights fall in the direction of the South (on the average by 10° in the latitudinal interval) and only more to the South than 25°S winter conditions set in in the stratosphere.

Considerable differences are observed in the vertical stratification of the stratosphere in this zone too. If above the areas with "summer" stratosphere there is an inversion lapse-rate, uniform throughout its body, (on the average about -0,3°/100 m), above the regions with "winter" stratosphere in the 20-30 km layer there are almost isothermal conditions ($\gamma \leq -0.1°$/100 m), but stratospheric inversion above 30 km is pronounced much stronger.

The fact of invasion of the stratosphere of the summer hemisphere into the winter hemisphere is confirmed by the character of wind distribution in the stratosphere. Apparently, in the whole layer of the stratosphere throughout our cross section up to 15°S, at the altitude above 20 km there can be observed only easterly winds. Only more south of 20-25°S stratospheric winds become westerlies.

This means, that anticyclonic summer type of the stratosphere circulation covers not only the whole of the summer hemisphere, but also rather a vast (about 15-20° of latitude) area of winter hemisphere. One can suppose, that the given invasion process can be one of the air exchange mechanisms between the hemispheres in the stratosphere.

The other peculiarity of the stratosphere wind field is a very powerful both in width (from 5°S to 32°N) and in

Declassified in Part - Sanitized Copy Approved for Release 2011/12/08 : CIA-RDP80T00246A016600420001-1

Declassified in Part - Sanitized Copy Approved for Release 2011/12/08 : CIA-RDP80T00246A016600420001-1

vertical extent (from 23 km to above 38 km) eastern jet stream. Maximum wind velocities are observed at the altitude 38 km - 250 km/hour, but higher they, perhaps, can be greater.

This jet stream coincides, generally speaking, with the so-called subtropic maximum of easterlies, marked by other authors, but its velocities, observed by us, prevail the velocities shown on the average cross sections of Kochanski /2/, Dubentsov/3/, Murgatroyd/4/ and others.

In the Southern Hemisphere near 25°S at the altitude 34 km and more there also exists a jet stream, but here it is western. Its area is much less, than that of the eastern one in the Northern Hemisphere. It is notable, that as well as in the previous cross section, the latitudinal position of its axis is very close to the position of the tropospheric jet axis.

In the Southern Hemisphere troposphere up to the equator there is observed general western flow, with the exception of the lowest one-km-thick layer, in which easterlies, evidently, more or less strongly pronounced trade-winds, prevail.

As well as in the previous cross section, in the region of the tropopause break there exists a jet stream, its velocities being about 250 km/hour. However, in comparison with the previous cross section it is a bit displaced to the North (from 32° to 27°S). This means, that while fall changes for winter the subtropical jet displaces to lower latitudes.

Declassified in Part - Sanitized Copy Approved for Release 2011/12/08 : CIA-RDP80T00246A016600420001-1

Declassified in Part - Sanitized Copy Approved for Release 2011/12/08 : CIA-RDP80T00246A016600420001-1

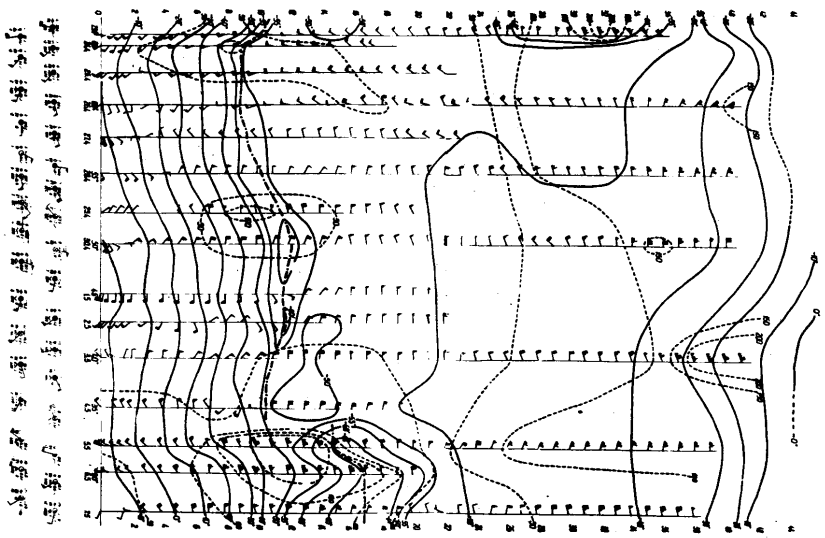

Declassified in Part - Sanitized Copy Approved for Release 2011/12/08 : CIA-RDP80T00246A016600420001-1

Declassified in Part - Sanitized Copy Approved for Release 2011/12/08 : CIA-RDP80T00246A016600420001-1

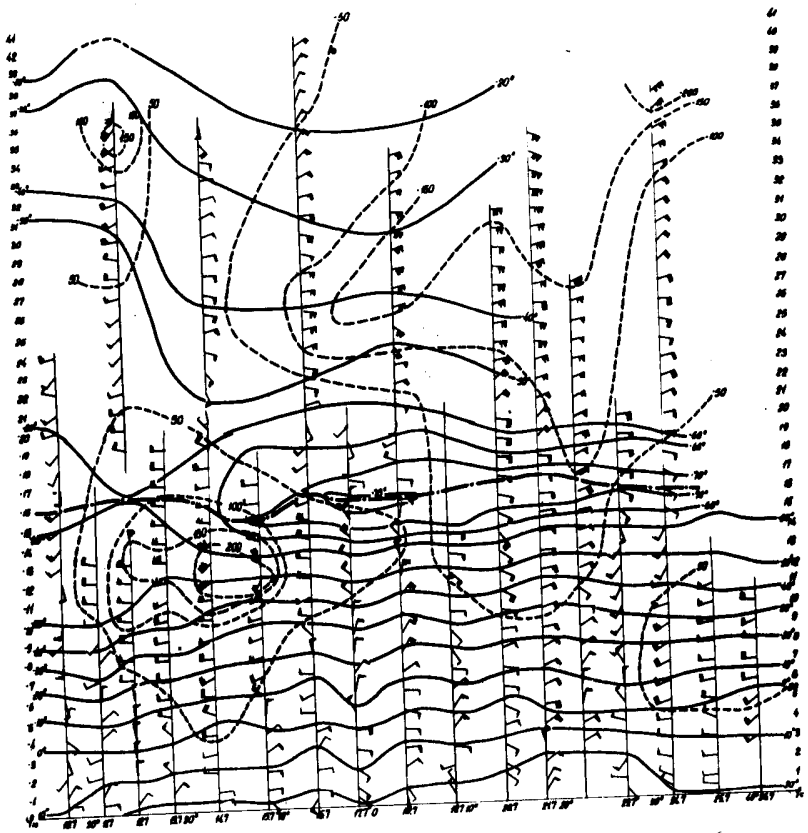

Declassified in Part - Sanitized Copy Approved for Release 2011/12/08 : CIA-RDP80T00246A016600420001-1

Declassified in Part - Sanitized Copy Approved for Release 2011/12/08 : CIA-RDP80T00246A016600420001-1

1.6

by V.G.Istomin, A.A.Pokhunkov. (English) (27pp)

3. " MASS-SPECTROMETER MEASUREMENTS OF THE ATMOSPHERE COMPOSITION IN THE USSR."

Abstract

The given paper is a brief piece of information of the state of mass-spectrometer methods used for atmosphere studies in the USSR. Consideration is given to certain main results achieved in this field. In this light possible problems of further investigations of the neutral atmosphere composition and ionized Earth atmosphere component are discussed.

The main ionosphere components, according to rocket soundings, are NO^+, O_2^+, O^+, N_2^+, and N^+ ions. The first three components were found to have diurnal effects at the 100-210 km height. According to the satellite measurements data the main component up to 1000 km is ionized atomic oxygen O^+. Absolute concentrations of various ions for the altitude range 100-210 km, measured during three experiments, are given. N^+ ion absolute concentration constancy in the altitude range 300-500 km is explained by a possible high temperature which these ions may have during their formation in the process of dissociative ionization: ($N_2 + e \rightarrow N^+ + N + 2e$) by low energy electrons.

Declassified in Part - Sanitized Copy Approved for Release 2011/12/08 : CIA-RDP80T00246A016600420001-1

Declassified in Part - Sanitized Copy Approved for Release 2011/12/08 : CIA-RDP80T00246A016600420001-1

The main components of the neutral atmosphere up to the 300 km altitude are molecular nitrogen N_2, atomic oxygen O, and molecular oxygen O_2. The O/N_2 relative concentration increase with height is observed. At the heights of about 200 km considerable quantity of non-dissociated oxygen O_2 is observed, what indicates the importance of diffusion processes. Above 110 km the stability of Ar and N_2 gravitational separation is observed. Alongside Mg^+, Ca^+, Fe^+, and Si^+ inns neutral magnesium oxide MgO of meteor origin is found. Difficulties of chemically active atmosphere atomic gases measurements are pointed out and the ways of their overcoming are indicated.

Declassified in Part - Sanitized Copy Approved for Release 2011/12/08 : CIA-RDP80T00246A016600420001-1

Declassified in Part - Sanitized Copy Approved for Release 2011/12/08 : CIA-RDP80T00246A016600420001-1

I. Introduction

Everybody who deals with problems connected with ionosphere physics and chemistry is aware of the fact that it was characteristic of the works carried out in this field more than 2-3 years ago to have abudance of suggested conceivable and possible chemical and photo-chemical reactions, this resulted in great uncertainty in the conclusions concerning the ionosphere formation and processes occurring in the latter. This resulted mainly from uncerntainty of the chemical composition of the atmosphere neutral component above 100 km and almost entire lack of knowledge of the chemical composition and nature of its ionized component (positive ions). In connection with successful fulfilment of direct mass-spectrometer measurements of the ionosphere composition (the first convinc ing results were obtained in the USA in 1956 (1) and in the USSR in 1957 (2)) there appeared a possibility to form more precise and concrete ideas concerning the main reactions occurring in the ionosphere.

Old ideas concerning atmosphere ionization sources suffered considerable changes. For example, it became apparent that recombination processes (and consequently ionization ones) are much more intensive in the ionosphere than it was supposed earlier. A.D.Danilov's (3), G.S.Ivanov-Kholodney and L.A.Antonova's (4,5) and some other works were devoted to considering such questions on the bases of the obtained experimental data.

Declassified in Part - Sanitized Copy Approved for Release 2011/12/08 : CIA-RDP80T00246A016600420001-1

Declassified in Part - Sanitized Copy Approved for Release 2011/12/08 : CIA-RDP80T00246A016600420001-1

2.-Methods

The Table presented below gives a list of soundings, in which atmosphere composition analyses were carried out.

Table I

	Date	Height of the Sun	Time of the day	Carrier	Mass-spectrometer	Height range, km	Sort of measurements
I	7.9.I957	-6°	evening	container	PMC-I	I05-206	ion composition
2	I5.5.I958	0°	-	the third	PMC-I	225-980	ion composition
3	2.8.I958	36°	morning	container	PMC-I	I00-2I0	ion composition
4	I3.8.I958	0°	morning	container	PMC-I	I00-2II	ion composition
5	I4.7.I959	30°		container	MX-640I	98-203	neutral composition
6	22.7.I959	0°	morning	container	MX-640I	9I -2II	neutral composition
					MX-640I		ion composition
7	I5.6.I960	I5°	morning	container	MX-6403	92-206	ion composition
8	23.9.I960	-	midnight	container	MX-6403		neutral composition
9	I5.II.6I	+5°	evening	sounding rocket	MX-640I	I30-430	neutral and ion composition

In the listed soundings there were used radio-frequency mass-spectrometer PMC-I (6), MX-640I (7) and MX-6403. These instruments are non-magnetic, and for ion separation according to their masses they use axial electric fields. Bennett (8) was the first to suggest and use this principle in I950. Radiofrequen-

Declassified in Part - Sanitized Copy Approved for Release 2011/12/08 : CIA-RDP80T00246A016600420001-1

Declassified in Part - Sanitized Copy Approved for Release 2011/12/08 : CIA-RDP80T00246A016600420001-1

cy mass-spectrometers of Bennett type turned out to be rather useful for such investigations. The main characteristics of the used instruments are given in Table 2.

As can be seen from the above Table at present we have at our disposal rather perfect mass-spectrometers; these instruments came into practice of geophysical atmosphere investigations.

Mass-spectrometer measurements at the 100-210 km altitude are carried out according to the method of separated container, which is widely spread in the USSR(9).

We believe that the use of this method is of great advantage as the influence of gas release of a comparatively small container upon measuring instruments as well as upon its surface may be made small if necessary precautions are taken. A rocket, the principle source of the atmosphere pollution, along the considerable parts of its trajectory produces no hinderances, as at the ascent the container with neutral and ionic mass--spectrometer is ahead of the rocket at the distance of many mean free paths of a molecule from it. This fact guarantees complete lack of rocket pollutions and measurements being taken at the appreciable part of the trajectory in the undisturbed atmosphere. Ions rocket pollutions were recorded by the ionic-mass-spectrometer mainly at the descending part of the container trajectory; variations analysis in the atmosphere ion spectra obtained for this part of the trajectory surely indicates ionization of pollution molecules by means of intercharging with ions O^+ /10/.

Declassified in Part - Sanitized Copy Approved for Release 2011/12/08 : CIA-RDP80T00246A016600420001-1

Declassified in Part - Sanitized Copy Approved for Release 2011/12/08 : CIA-RDP80T00246A016600420001-1

Due to the indicated methodical peculiarities and also due to comparatively high instrument sensitivity it appeared possible to detect the atmosphere distribution of not only the main ion components - nitrogen oxide, molecular and atomic oxygen, - but also minor ion components such as molecular and atomic nitrogen, metals ions and some other ones.

In the sounding rocket firing on November I5, I96I up to the height of 430 km the mass-spectrometer was not separated from the rocket, but was in a special container in the head. This fact and connected with it possibility of recording the rocket pollutions and also the fact that the mass-spectrometer in this case simultaneously recorded neutral as well as ionic atmosphere components, makes it difficult to give a simple interpretation of the obtained results. Nevertheless, according to these experimental results one can come to definite conclusions concerning the neutral /II/ as well as ionic composotion.

For the first time the ionosphere composition at the 225--980 km heights was studied by mass-spectrometer, installed in the Third Soviet Satellite. As you remember, at the time previous to the First Soviet Satellite launching any possibility of direct structual atmosphere parameters measurement was not obvious. So, many American scientists considered that it was not expedient to carry out experiments connected with investigation of the upper atmosphere composition on a satellite owing to a continuous strong gas release from its surface and resulting from it pollution of the neighbouring atmosphere regions /I2/.

Declassified in Part - Sanitized Copy Approved for Release 2011/12/08 : CIA-RDP80T00246A016600420001-1

Declassified in Part - Sanitized Copy Approved for Release 2011/12/08 : CIA-RDP80T00246A016600420001-1

The problem of gasious medium disturbances caused by a satellite was considered by B.A.Mirtov /9/. He showed in particular, additional ionization produced by the satellite in its flight would not considerably influence the recording of instruments installed in it. The ions mass spectrum measurements made by the Third Satellite supported this supposition.

Mass peaks of the atmosphere ions were clearly distinguished from pollution ions peaks. The latter were recorded only for several hours after the satellite came out into the orbit /2/, as it was shown /23/, (H_2O^+) pollution ions were probably formed as a result of interchange processes of pollution molecules with atomic oxygen ions: $H_2O + O^+ \rightarrow H_2O^+ + O$.

3. Ion Composition

The main rsults concerning atmosphere positive ions mass spectrum at the heights of 100-210 km were obtained in five rocket soundings in moderate latitudes of the European Part of the USSR. All the soundings were fulfilled during summer months, in the years of the maximum solar activity (see Table I).

The result of fundamental importance was achieved in the very first soundings on September 9, 1957: in the investigated atmosphere region there predominated ions with mass number M=30, the ions of nitrogen oxide NO^+ /2/. The following soundings backed this conclusion; there were also obtained assentially new geophysical results. The following ions obtained in rocket

Declassified in Part - Sanitized Copy Approved for Release 2011/12/08 : CIA-RDP80T00246A016600420001-1

Declassified in Part - Sanitized Copy Approved for Release 2011/12/08 : CIA-RDP80T00246A016600420001-1

experiments were detected and identified with atmosphere components: nitrogen oxide NO^+, molecular oxide O_2^+, atomic oxygen O^+, molecular nitrogen N_2^+, atomic nitrogen N^+ /I0,I3/. Note, that the last two ions are a small ionosphere component at I00 - 200 km height; they could be surely recorded in our measurements (contrary to the results of investigators in the USA /I4/) only due to a peculiar method and high sensitivity of the used mass--spectrometer.

The main ionosphere components (NO^+, O_2^+, and O^+) show effects which may be connected with diurnal atmosphere variations (Fig.I). According to the measurement results for the heights of the Sun -6^o, 0^o, $I5^o$, and 36^o it is clear, that relative atomic oxygen ions concentration at all the heights from I40 to 200 km increases with the Sun height increase, most quickly and directly responding to variations of atmosphere illumination conditions. On the contrary, molecular oxygen ions relative concentration probably responds to the duration of the atmosphere illumination by the Sun.decreasing during daytime. The maximum relative concentration of O_2^+ shifts during the time of the day from about I60 km (morning) up to the I40 km height (daytime) and lower (evening).

For three rocket experiments due to simultaneous electron concentration measurements made from the rocket at the same heights /I5, I6/ not only relative, but also absolute positive ions concentrations values were obtained. These results are given in Tables 3-5.

Absolute ions concentrations calculations were made according to the ratio: $[M_1^+] = i_{M_1^+} \cdot n_e / \sum i_{M^+}$, which may be true,

Declassified in Part - Sanitized Copy Approved for Release 2011/12/08 : CIA-RDP80T00246A016600420001-1

Declassified in Part - Sanitized Copy Approved for Release 2011/12/08 : CIA-RDP80T00246A016600420001-1

when following the below assumptions:

I) Positive ions concentrations sum is equal to electron concentration, i.e. there are no negative ions in the atmosphere: $\sum [M^+] = n_e$. For the daytime ionosphere this assumption may be considered true /I7/.

2) Ion peaks amplitudes sum on mass-spectrogramme is proportianal to the summary positive ions concentration: $\sum i_{M^+} = K \sum [M^+]$. This means, that ions which are not in the mass range of the instrument (I-4 and IO-56 atomic units) are supposed to be not existing, and this also does not seem doubtfull.

3) Ion peaks amplitudes ratio in the spectrum is equal to concentrations ratio of the corresponding ions in the atmosphere

$$i_{M_1^+} / i_{M_2^+} = [M_1^+] / [M_2^+]$$

The latter is equivalent to the assumption that discrimination of ions of various masses in the mass-spectrometer is lacking. Actually it is quite true, as there is probably certain discrimination in radiofrequency analyser. A serious quantitative account of this phenomenon is of some difficulty nowadays therefore discrimination is not accounted in the Tables of ion concentrations presented below. This may mostly affect the values of atomic oxygen ions O^+ concentrations and atomic nitrogen N^+ concentrations, which are probably somewhat lowered, and may be considered correct only with accuracy within a factor of 2. Actual concentrations of N_2^+, NO^+, and O_2^+ molecular ions cannot differ much from those presented in the Tables, as their masses are analogous, and there

Declassified in Part - Sanitized Copy Approved for Release 2011/12/08 : CIA-RDP80T00246A016600420001-1

Declassified in Part - Sanitized Copy Approved for Release 2011/12/08 : CIA-RDP80T00246A016600420001-1

must be practically no discrimination effects.

Alongside ions of nitrogen-oxygen composition during some rocket experiments there were recorded ions of the following metals: iron, magnesium, calcium and probably silicon. These ions were detected at the I00-I20 km height, their extra-terrestrial (meteor origin) is doubtless. These results were presented in special report /I8/, therefore these problems would not be dicussed here.

It is of importance to note that ion mass-spectrometers in no soundings recorded hydrogen and helium ions though corresponding mass-numbers were in the limits of the apparatus working range. Possible estimations of the upper limit of absolute H^+ and He ions concentrations at the height of I00-2I0 km $[H^+, He^+] < I6o:200$ ions/cm^3 are presented in Tables 3 and 4.

According to the data, obtained by means of the Third Artificial Satellite up to the heights of the order of I000 km ions of H^+ and He^+ do not become predominant earth ionosphere components those remain to be the ions of atomic oxygen O^+ /I9/.

Let us consider the above mentioned results concerning molecular and atomic nitrogen atmosphere ion distribution in detail. These results are given in Fig. 2. It is seen that N_2^+ ions are concentrated mainly in the ionosphere regions in the height range 200 - 350 km, with the maximum concentration of $I.I0^4$ cm^{-3} at the 250 km height. Distribution peculiarities of ions with M=28 - thin layers at the heights of I00-2I0 km are discussed in detail in paper /I8/.

The character of atomic nitrogen ions is quite different. They appear in appreciable quantities (more than I00 ions cm^{-3})

Declassified in Part - Sanitized Copy Approved for Release 2011/12/08 : CIA-RDP80T00246A016600420001-1

Declassified in Part - Sanitized Copy Approved for Release 2011/12/08 : CIA-RDP80T00246A016600420001-1

above 160 km, at first their absolute concentration increases rapidly, its maximum about 3.10^4 cm^{-3} is achieved in the region of F_2 maximum at the 300 km height, but further with height increase N^+ concentration remains constant or slightly decreases, what is not observed for all other ions occurring at these heights /O^+, O_2^+, N_2^+, and NO^+/.

We believe, that N^+ absolute concentration constancy in a large height range (300-500) in other words very high values of the scale height $H=kT/Mg$ for $M=14^+$ may and must serve as an indication to the fact that atomic nitrogen ions are not in thermodynamical equillibrium with the neutral atmosphere components for which isothermal condintions with $T=1600+1300^oK$ /17/ are established, but they have higher thermal velocities, or essentially higher temperature, if Maxwellian distribution according to velocities could be assumed for them. This point of view is qualitatively backed by the N^+ and O^+ ion currents components dependences on the angle between the mass-spectrometer tube and the satellite velocity vector: when the angle varies from 0^o to 60^o N^+ ion current decreases considerably slower than O^+ ion current, what indicates higher thermal velocities of N^+. Naturally to make the final conclusion it is necessary to have a detailed quantitative analysis of the dependences available.

The hypothesis of high ion temperature for N^+ is in accordance with the corpuscular hypothesis of ionosphere ionization by electrons of comparatively low energy, presented by L.A. Antonova and G.S.Ivanov-Kholodny /5/.

As it is known, while electrons interact with two-atomic

Declassified in Part - Sanitized Copy Approved for Release 2011/12/08 : CIA-RDP80T00246A016600420001-1

Declassified in Part - Sanitized Copy Approved for Release 2011/12/08 : CIA-RDP80T00246A016600420001-1

molecules, e.i., while electron [redacted] transitions with dissociation, the dissociation products (atoms and ions) may have great relative kinetic energies. So, O^+ ions from CO or NO, and also C^+ ions from CO do not have Maxwellian distribution in the energy range of $\Delta E \sim 10$ ev /(20, p.214/.

For nitrogen $N_2+e \rightarrow N^+ + N + 2e$ reaction gives zero relative energy of atoms only when electrons energy is 24,5 ev. /(20), p.225/ There are reasons to consider, that at least a part of atomic nitrogen ions may be formed in such a way, as nitrogen is the main earth atmosphere neutral molecular component up to the high altitudes. As electron energies are supposed to be of the order of hundreds of ev, atomic nitrogen ions should be "hotter" than other atmosphere components.

These "hot" ions will go up to higher altitudes, than "ordinary" ions and they should have high scale height value. "Hot" ions must also exist in the earth exosphere.

Let us briefly indicate possible problems of further ion composition investigation, which, we believe, deserve attention.

The prime task is to investigate the night ionosphere composition at the 100-700 km height, as only such investigations will give an opportunity of further developing ionosphere chemistry problems. In particular, they probably give additional information concerning the nature of the agent of the producing night ionization in F region.

Accurate measurements of isotopic ion composition of nitrogen and oxigen at the 100-700 km heights (such increase

Declassified in Part - Sanitized Copy Approved for Release 2011/12/08 : CIA-RDP80T00246A016600420001-1

Declassified in Part - Sanitized Copy Approved for Release 2011/12/08 : CIA-RDP80T00246A016600420001-1

of accuracy is quite real) will help to determine gravitational separation of oxigen and nitrogen isotopes separately and independently of other gases. And this is considered to be important, as now there are direct data concerning the existance of the gravitational separation of argon and molecular nitrogen (II), and inderectly obtained information contradicting to this information concerning stable nitrogen-oxigen atmosphere composition for the heights of about 400 km /2I/. While studying isotope composition of oxigen and nitrogen ions there may be revealed a possible role of chemical processes in establishing the principle atmosphere component equillibrium, and also a possible role of the principle atmosphere components transport (oxigen, nitrogen) from the interplenitary space.

4. Neutral Composition.

Parallel to ionic measurements there were carried out the earth atmosphere muetral gaseous composition measurements. The results obtained in this important field of investigations in the last two rocket soundings are discussed in detail in special information presented at the symposium /II/. Therefore they are given little attention in this survey article. The latter mainly presents generalizing conclusions concerning neutral atmosphere composition above I00 km according to all four soundings /23,24/.

The most important result, which defines the upper atmosphere conditions is the detection of gravitational separation of argon and molecular nitrogen. This separation was surely recorded above I00 km in all experiments carried out at different time (see Table I) what points to the stability of the atmosphere, where

Declassified in Part - Sanitized Copy Approved for Release 2011/12/08 : CIA-RDP80T00246A016600420001-1

Declassified in Part - Sanitized Copy Approved for Release 2011/12/08 : CIA-RDP80T00246A016600420001-1

gravitational separation conditions are established.

According to investigation data the separation level is near the height of I05-II0 km. It is important to note that these results are obtained for moderate latitudes, and being added by analogous results of American scientists /25/ obtained in polar latitudes (Fort Churchill) we can come to the conclusion of stable existance of argon and molecular nitrogen gravitational separation in the earth atmosphere at least in moderate and polar latitudes of the Northern hemisphere at the heights exceeding I05-II0 km .

From our point of view it was extremely interesting to detect neutral particles with mass number 42 in the height range I00-I20 km which were identified with magnesium oxide and evidently were of meteor origin. This circumstance alongside the facts of Ca^+, Fe^+, and probably Si^+ ions detection at the same heights indicates that meteor substance in the earth atmosphere at the mentioned heights is of fair importance. According to variation of magnesium oxide relative concentration one can estimate the size of trnsition layer, dividing the atmosphere with established gravitational separation conditions from the turbulent atmosphere. The maximum height this layer reaches is II7-II8 km, if the separation begins near II0.

As far as the main atmosphere components definding the atmosphere density and its molecular weight are concerned, the presented measurements show that nitrogen-oxigen atmosphere composition exists at least up to the height of 300 km. Light gases - hydrogen and helium - atmosphere content up to

Declassified in Part - Sanitized Copy Approved for Release 2011/12/08 : CIA-RDP80T00246A016600420001-1

Declassified in Part - Sanitized Copy Approved for Release 2011/12/08 : CIA-RDP80T00246A016600420001-1

the 300 km height is so small, that its effect on the density and mean molecular weight variations is nigligible.

Molecular nitrogen remains a dominating component defining the atmosphere density up to the 280 km height, where the equallity of densities $\rho(N_2) = \rho(O_2)$ is esfablished. It is also important to note, that molecular nitrogen dissociation turned out to be unessential up to the height of 2I0 km, as a result of which the atomic nitrogen concentration remains no more than I-2 per cent of the molecular nitrogen concentration up to the mentioned heights.

It was supported experimentally that at the heights exceeding I00 km there is atomic oxigen, relative concentration of which relative to molecular nitrogen increases with height. According to one of the last experiments (night) atomic oxigen concentration at the 2I0 km height was 65 ± 20 per cent of molecular nitrogen concentration. At the same time molecular oxigen relative concentration being approximately equal to the surface one at the I00 km level decreases with height increase and it is $I4\pm6$ per cent of molecular nitrogen concentration and at the 2I0 km height. Table 4 presented below gives per cent values of dissiciated molecular oxigen in the night atmosphere, calculated according to the formulae of per cent dissociation $O_2 = \left[1 - \frac{n(O_2)}{0{,}21\, n(M)}\right] \cdot 100\ \%$ where $n(O_2)/n(M)$ O_2 - relative concentration relative to the total concentration of the main atmosphere components.

Declassified in Part - Sanitized Copy Approved for Release 2011/12/08 : CIA-RDP80T00246A016600420001-1

Declassified in Part - Sanitized Copy Approved for Release 2011/12/08 : CIA-RDP80T00246A016600420001-1

h km	I00	II0	I20	I30	I40	I50	I60	I70	I80
per cent diss. O_2	I4±II	I9±II	24±II	27±II	3I±II	36±I2	40±I2	45±I3	49±I4

h km	I90	200	2I0
per cent diss. D_2	54±I4	59±I5	63±I6

It is seen from the Table that one can observe per cent increase of dissociated oxigen. Nevertheless, There is a considerable amount of non-dissociated oxigen at the 2I0 km height, which indicates essential importance of diffusion in restoring the molecular oxigen height distribution disturbed by photochemical reactions. With calibrated plots showing the dependence of the separate atmosphere components ion currents upon partial pressures ~~at Rand~~ it becomes possible to measure absolute concentrations, and consequently the total atmosphere density at various heights. For the heights exceeding the gravitational separation layer it becomes possible to estimate atmosphere neutral particles temperature by computing another neutral component by means of the barometric formulae according to the scale height.

Avoiding the results discussed in special detailed information /II/, we shall point out, that temperature estimation by means of mass-spectrometer, is carried out more accurately than that according to monometric data, which need ~~demanding~~ a serious account on mean molecular weight variation with height.

In spite of achievements, it should be noted the problem of atmosphere neutral gasious composition above I00 km comes

Declassified in Part - Sanitized Copy Approved for Release 2011/12/08 : CIA-RDP80T00246A016600420001-1

Declassified in Part - Sanitized Copy Approved for Release 2011/12/08 : CIA-RDP80T00246A016600420001-1

across fair difficulties in its solving. As it was mentioned in work /22/, neutral mass-spectrometer in rocket measurements equally records both the direct flux of undisturbed atmosphere particles coming into the instrument and the particle flux coming out of the instrument after mumerous impingements with its electrods and walls. Due to the atoms recombination on the walls surfaces and electrods, and also because of other possible reactions on the surfaces (metal hydrides, nitrides and oxides formations) the inverse flow would be fairly rapped of atomic components. Therefore without the mentioned reactions taken into account the data concerning atomic component concentrations will be underestimated, but molecular gases values and the mean molecular weight value will be overestimated.

In work /26/ there was made an attemp to overcome the mentioned difficulties by introducing a correction factor, that takes into account atomic oxigen concentration variations, and concequently molecular oxigen inside the analyser. There was made a comparison of atomic component concentrations measured by two different analysers, which deliberately have different coefficient values, characterising atomic oxigen concentration variations both in direct fluxes and inverse ones. Taking sertain simplafying assumptions there was obtained the correction factor value, which takes into consideration gas content variations inside the analyser and allows to pass from measured concentrations to atmosphere atomic and molecular component concentrations. All the abovemention ed data as well as mean molecular weight values up to the heights of 2I0 km /II/ were obtained taking into account this coefficient.

Declassified in Part - Sanitized Copy Approved for Release 2011/12/08 : CIA-RDP80T00246A016600420001-1

Declassified in Part - Sanitized Copy Approved for Release 2011/12/08 : CIA-RDP80T00246A016600420001-1

While the neutral atmosphere content satellite measurements, considerable difference in the rates of direct and inverse fluxes particles makes them possible to be distinquished, and the selection of the corresponding mass-spectrometer regime allows to avoid the inverse flux record in order to obtain only undisturbed atmosphere particles content data /22/. It should be also noted that in this case the mass-apectrometer would be insensitive to the cathode electrode and the instrument walls gas release background as well as to the pollution of the satellite. Due to this, the radio-frequency mass-spectrometer may be the only instrument on a satellite, which in case the orientation of its inlet relative to the velocity vector is known gives total information about undisturbed atmosphere structural parameters - neutral paricles densities, pressures and temperatures. At the same time this mass spectrometer in the ionic analysis regime will give corresponding information about ionic temperature component as the satellite potential can be estimated according to the difference of the recorded mass numbers values of neutral and ionic components of identitive composition /22/.

Declassified in Part - Sanitized Copy Approved for Release 2011/12/08 : CIA-RDP80T00246A016600420001-1

Declassified in Part - Sanitized Copy Approved for Release 2011/12/08 : CIA-RDP80T00246A016600420001-1

TABLE 2

the name of the instrument		PMC-I	MX-6401	MX-6403
the number of cycles in the analyser drifts		5 - 7	5-9-4-7	5-9-4-7
weight of the instrument without feeding	kg	6.5	3.3	2.0
feeding		from special block	battery of accumulators 27v I0 per cent	
power demand	watt	30	5.3	3.2
period scanning of mass	sec.	I.7	3.0	3.0
mass-scale	a.m.u	6-48 8-63	I.4/I2-56 (2 mass-subscales)	I.4/I2-56
resolution R=M/ΔM /according to the peak base/ a)maximum		30	50	50
b)in the used operating conditions /in M=20 region according to laboratory spectrum of analyser filling/		20	20	20
sensitivity in the ion ion analysis operating conditions /I% the telemetric scale/ a)rocket	ions/cm^3	$4.2 \cdot 10^2$	5.10^2	$I.10^2$
b)satellite	"	80	- /were not used in satellites/	-
sensitivity in the neutral analysis operating conditions /according to argon/	particles/cm^3	-	$I.6 \cdot 10^8$	$I.6 \cdot 10^7$

Declassified in Part - Sanitized Copy Approved for Release 2011/12/08 : CIA-RDP80T00246A016600420001-1

Declassified in Part - Sanitized Copy Approved for Release 2011/12/08 : CIA-RDP80T00246A016600420001-1

REFERENCES

I. Johnson C.Y. et al., Ann.Géophys., I4, 475, I958

2. Istomin V.G. Sb."Iskusstvennye cputniki Zemli", vyp.2, izd-vo AN SSSR, I958, str.32.

3. Danilov A.D. DAN SSSR, t.I3I, N 5, I098 (I96I)
Danilov A.D. Doklad na 3- simposium COSPAR

4 Ivanov-Kholodny G.S. DAN SSSR, t.I37, N 2,327 (I96I)
Ivanov-Kholodny G.S. Report on the third symposium COSPAR

5. Antonova L.A. and Ivanov-Kholodny G.S. Geomagnetizm i aeronomya, I,N 2, I64, (I96I)

6. Istomin V.G. sb. "Iskusstvennye sputniki Zemli", byp.3, izd-vo AN SSSR, I959., str.98.

7. Pavlenko V.A., Rafalson A.E., slutsky M.E., Tsveiman G.A., Stchutov M.D. Pribory i tekhnika experimenta N 6, 89, I960

8. Bennett W.H. J. of App. Phys., 2I, No.2, I43 (I950)

9. Mirtov B.A. Gazovyi sostav atmosfery Zemli i metody ego analiza. Izd. AN SSSR, Moskva, I96I.

I0. Istomin V.G. Sb."Iskusstvennye sputniki Zemli", vyp.7. Izd-vo AN SSSR, I96I, str. 64.

II. Pokhunkov A.A. Report on the third symposium COSPAR

I2. Newell H.E. Jr. Jet Propulsion, 25, No.2, 73 (I955).

I3. Istomin V.G. Dokl. AN SSSR, t.I37, N 5, II02, I96I

I4. Johnson C.Y., Holmes J.C. Proc. I st sym. COSPAR, Ed.H.Kallmann Bijl North-Holland Publish. Comp., p.4I7 (I960)

Johnson C.Y. Ann. Géophys., I7, I00 (I960)

I5. Gringauz K.I. Dokl. AN SSSR, t.I20, I234, I958; Sb."Iskusstvennie sputniki Zemli" vyp. I, izd-vo AN SSSR, I958, p.6.

I6. Rudakov V.A. "Iskusstvennie sputniki Zemli" sb., vyp.I0 izd-vo AN SSSR? I96I.

I7. Nicolet M. Aeronomy (preprint), I96I

I8. Istomin V.G. Report on the third symposium COSPAR

I9. Istomin V.G. sb. "Iskusstvennye sputniki Zemli", vyp.6, izd-vo ANSSSR, I96I., p.I27.

20. Messi H. Barkhop E. -Elektronnye i ionnye ctolknovenija, IL,I958

2I. Danilov A.D. Sb."Iskustvennye sputniki Zemli", Izd-vo AN SSSR, vyp.I0,98(I96I)

22. Istomin V.G. Geomagnetizm i aeronomija I N 3, 359 (I96I)

23. Pokhunkov A.A. Izv. AN SSSR, ser, geofiz. N II,I649, I960

24. Pokhunkov A.A. Iskusstvennye sputniki Zemli, vyp.7, Izd. AN SSSR, I96I, p.89.

25. Meadows E.B. and Townsend Proc. of the first Internat. Space Science Symposium, Nice, I75, I960

Declassified in Part - Sanitized Copy Approved for Release 2011/12/08 : CIA-RDP80T00246A016600420001-1

Declassified in Part - Sanitized Copy Approved for Release 2011/12/08 : CIA-RDP80T00246A016600420001-1

26. Pokhunkov A.A. Iskusstvennye sputniki Zemli, vyp. I2, Izd. AN SSSR, I962 (in print).

27. Jatsenko S.P. Sb."Iskusstvennye sputniki Zemli", v.7,p.60 /I96I/.

Declassified in Part - Sanitized Copy Approved for Release 2011/12/08 : CIA-RDP80T00246A016600420001-1

Declassified in Part - Sanitized Copy Approved for Release 2011/12/08 : CIA-RDP80T00246A016600420001-1

TABLE_3

Positive ion concentrations in the atmosphere in the morning on June I5, I960. ~~The height of the Sun~~ $h_\odot = 15^\circ$

Maximal height /the container trajectory peak/ - 208 km

Height km	I00	I05	II0	I20	I30	I40	I50	I60	I70	I80	I90	200
N_e	40	95	80	90	85	90	I00	I20	I65	I90	2I0	245 (extrapolation)
$[Fe^+]$		I5 /approximately/										
$[Ca^+]$	-	0.5	-	-	-	-	-	-	-	-	-	-
$[O_2^+]$	5.0	-	I9	30	35	39	40	42	52	46	45	49
$[NO^+]$	35	-	6I	60	50	56	56	65	87	9I	94	92
$[N_2^+]$	-	-	-	I.7[x/]	-	-	-	0.5	0.7	I.I	I.7	2.7
$[Mg^+]$	-	I4	I.0	0.4	-	-	-	-	-	-	-	-
$[O^+]$	-	-	-	-	-	I.0	4.0	I2.0	25	46	75	I25
$[N^+]$	-	-	-	-	-	-	-	0.I	0.2	0.26	0.32	0.36

Concentrations $I0^3$ cm^{-3}

Hydrogen and helium ions concentrations in all the heights range and also corresponding ions concentrations at the heights, marked by the sign - do not excced the following magnitudes

0.4 0.34 0.I6 0.2 0.2 0.2 0.I8 0.I8 0.24 0.22 0.26 0.3

---

x/ -probably

Declassified in Part - Sanitized Copy Approved for Release 2011/12/08 : CIA-RDP80T00246A016600420001-1

Declassified in Part - Sanitized Copy Approved for Release 2011/12/08 : CIA-RDP80T00246A016600420001-1

TABLE 4

Positive ions concentrations in the atmosphere in the morning on June 22,1959

~~Height of the Sun~~ / $h_\odot$ = 0°/

Maximal height - 2II km

Height km	95	Ioo	II0	I20	I30	I40	I50	I60	I70	I80	I90	200	2Io
n_e	20	23	I9	30	42	4I	42	45	46	52	60	70	80
													(extrapolation)
$[O_2^+]$	-	-	-	3.5	8.0	I0	II	I3	I4	I6	I8	20	2I
$[NO^+]$	-	23	I9	26.5	34	3I	3I	3I	30	32	36.5	40	56
$[O^+]$	-	-	-	-	-	-	-	I.0	2.0	4.0	6.5	I0	I2

Concentration $10^3/cm^3$

Hydrogen and helium ions concentrations in the whole heights range, and also corresponding ions concentrations at the heights marked by the signs - do not exceed the following magnitudes

	0.5	23	I.3	0.6	0.4	0.7	I.4	0.5	0.5	0.8	0.5	0.5	0.6

Declassified in Part - Sanitized Copy Approved for Release 2011/12/08 : CIA-RDP80T00246A016600420001-1

Declassified in Part - Sanitized Copy Approved for Release 2011/12/08 : CIA-RDP80T00246A016600420001-1

TABLE 5

Positive ions concentrations in the atmosphere in the evening on September 9, I957.

~~of the Sun~~ / $h_\odot$ =-6°/

Maximal height - 206 km

Height km	I05	I40	I90	200	205
n_e	~ I0	~ I0	~ 20	~ 40	~ 40
$[NO^+]$	I0	9	I6	33	29
$[O_2^+]$	< I.5	~ I	I.5	< 4	~ I
$[O^+]$	< I.5	< I.5	3	7	I0

Concentration $I0^3 cm^{-3}$

Declassified in Part - Sanitized Copy Approved for Release 2011/12/08 : CIA-RDP80T00246A016600420001-1

Declassified in Part - Sanitized Copy Approved for Release 2011/12/08 : CIA-RDP80T00246A016600420001-1

Fig.I - Diagram, showing the ionosphere composition variation with height of the Sun and diurnal variation. The segments of the horizontal straight lines in the three regions into which the diagram is divided by curves, are proportinal to relative concentrations of the corresponding components.

Fig.2 - Atomic and molecular nitrogen positive ions distribution in the earth atmosphere according to the data obtained during rocket launching on August 9, I958, rocket launching on June I5, I960, and of the Third Soviet Artifial, May, I958.

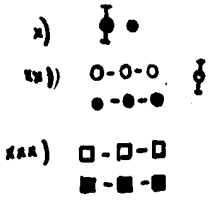

Declassified in Part - Sanitized Copy Approved for Release 2011/12/08 : CIA-RDP80T00246A016600420001-1

Declassified in Part - Sanitized Copy Approved for Release 2011/12/08 : CIA-RDP80T00246A016600420001-1

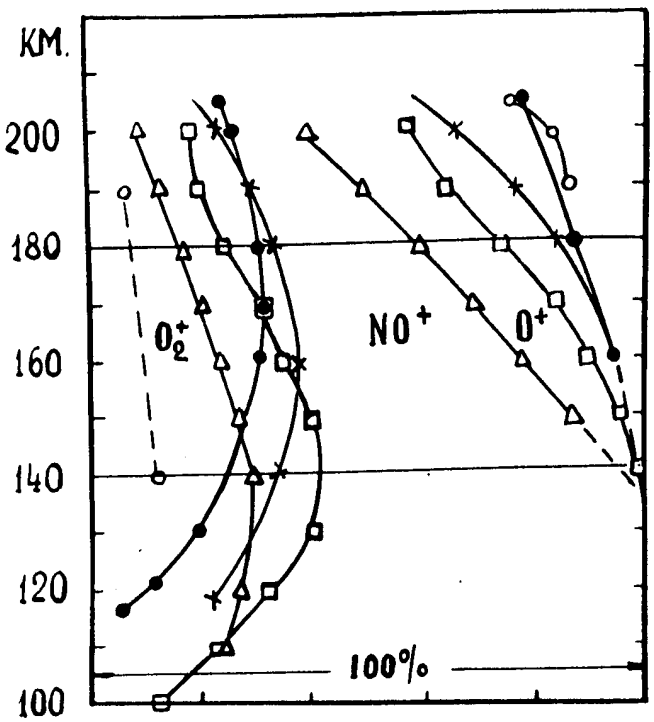

ooo - 9. IX. 1957 г., $h_\odot = -6°$, вечер.
ΔΔΔ - 2. VIII. 1958 г., $h_\odot = 36°$, утро.
××× - 13. VIII. 1958 г., $h_\odot = 0°$, утро.
●●● - 22. VII. 1959 г., $h_\odot = 0°$, утро.
□□□ - 15. VI 1960 г., $h_\odot = 15°$, утро.

Declassified in Part - Sanitized Copy Approved for Release 2011/12/08 : CIA-RDP80T00246A016600420001-1

Declassified in Part - Sanitized Copy Approved for Release 2011/12/08 : CIA-RDP80T00246A016600420001-1

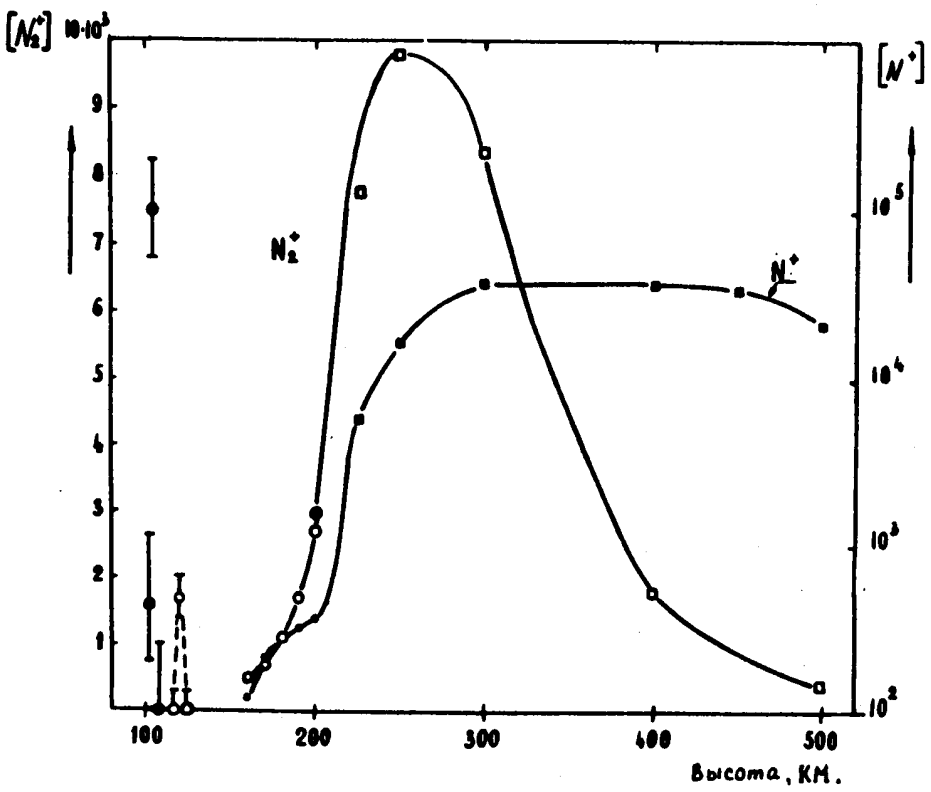

Declassified in Part - Sanitized Copy Approved for Release 2011/12/08 : CIA-RDP80T00246A016600420001-1

Declassified in Part - Sanitized Copy Approved for Release 2011/12/08 : CIA-RDP80T00246A016600420001-1

1.9

by V.G.ISTOMIN (English) (20pp)

4. "IONS OF EXTRA-TERRESTRIAL ORIGIN IN THE EARTH IONOSPHERE."

The measurements of the Mass spectrum of positive ions by sounding rockets and the 3rd artificial Earth satellite were made to define chemical composition of the main ion components, which are responsible for the existence of the Earth ionosphere in the day time, and to study the change of these main components composition with height in E, F-1 and F-2 regions. Nowadays, the necessary experimental data can be considered as obtained /1 - 3/. Considerable advances are also gained in their interpretation, namely, the selection of possible, photochemical and ion-exchange reactions, which can explain the observed ion composition /4,5/.

Some rocket measurements, however, detected ions, whose existence in the oxigen-nitrogen earth ionosphere needs further explanation as for their origin and the nature of possible ionising agents. These results, which up till now were published only partially /6/ are presented below.

The method of measurements.

The method of ion composition measurements by mass-spectrometer, installed in rockets /1,3/ as well as radio-frequency mass-spectrometer in its various forms /7,8/ are well-known and do not need detailed description, and here

Declassified in Part - Sanitized Copy Approved for Release 2011/12/08 : CIA-RDP80T00246A016600420001-1

Declassified in Part - Sanitized Copy Approved for Release 2011/12/08 : CIA-RDP80T00246A016600420001-1

only the main peculiarities are worth mentioning.

To gain maximum-possible precision of the experiment the equipment for measurements was installed in the container, separated from the rocket.

As the container escapes at the 65-70 km altitude, its velocity relative to the rocket being of the order of 1 m/sec, in the measurable altitude range /100 km and above/ at the ascent the container almost all the time is in the uncontaminated region of the atmosphere at the distance equal to many mean free paths from the rocket.

This is illustrated in the following Table:

Altitude km	100	120	140	160	180	200	210
The distance between the container and the rocket in the units of the mean free path	> 30	11	8	5	3.7	3	2.7

Radio-frequency mass- spectrometer analyzer consists of a tube, opened at one end, with a set of flat parallel grids inside

It operates according to the principle of separation of these ions in axial electric fields; one of the first devices of such a kind was proposed by Bennett /9/. Alternating and fixed potentials feed the tube grids; the analyzer is installed on the container surface, as is shown in Fig.1. Fig.2 shows the outward appearance and sizes of a recent model of radio-frequency mass-spectrometer.

Ionic current of the mass-spectrometer collector, amplified to the desired value, is telemetered to the ground with multy-

Declassified in Part - Sanitized Copy Approved for Release 2011/12/08 : CIA-RDP80T00246A016600420001-1

Declassified in Part - Sanitized Copy Approved for Release 2011/12/08 : CIA-RDP80T00246A016600420001-1

channel and high-speed sampling rate system.

Ionic current, as a time function, is recorded as a number of periodic "peaks", each of them corresponding to the ions of a certain mass #/. The distamce between the peak and the beginning of the mass-spectrum is the measure of its mass number, and the peak amplitude is nearly proportional to the concentration of the ions with this mass ##/.

#/ Supposing, that every ion carries a single elementary charge.

##/ with a precision to possible effects of mass discrimination in draving field region and in the analyzer itself.

Declassified in Part - Sanitized Copy Approved for Release 2011/12/08 : CIA-RDP80T00246A016600420001-1

Declassified in Part - Sanitized Copy Approved for Release 2011/12/08 : CIA-RDP80T00246A016600420001-1

Results

The sounding rocket firing, which took place in the morning on June 15, 1960 in the middle latitudes of the European part of the USSR when the Sun elevation was 15°, alongside the usual for these altitudes positive ions of nitrogen oxide No^{+} and molecular oxigen O_2^{+}, detected magnesium ions Mg^{+}. During this experiment for the first time there was used a radio-frequency ionic mass spectrometer of higher sensitivity (Fig.2).

In the altitude range 92 to 206 km some more than 100 spectra were obtained. Five of them have peaks with mass number 24^{+} and 26^{+}. Three of these spectra are obtained at the ascent and two - at the descent. These spectra and also some previous and following ones are shown in Fig.3. One can see good correspondence of the heights where the peaks with M = 24 and 26 were recorded at the ascent and descent. So, the spectra with maximum amplitude of these peaks are obtained at the altitudes 103,5 and 105 km, respectively. As the period of mass scanning was equal to 3 sec, what is equivalent to $\sim$ 4 km height variation, such a coincidence of the heights is more than satisfactory.

Mass number of magnesium is 24. Alongside the isotope Mg^{24} there also exist isotopes Mg^{25} and Mg^{26}, their relative abundance being 78.6%, 10.1% and 11.3%, respectively /10/. If the recorded ions with M = 24 and 26 are the magnesium ions, the peaks amplitudes ratio must be equal to 7.

Declassified in Part - Sanitized Copy Approved for Release 2011/12/08 : CIA-RDP80T00246A016600420001-1

Declassified in Part - Sanitized Copy Approved for Release 2011/12/08 : CIA-RDP80T00246A016600420001-1

The results of the peaks amplitudes measurements are given in the following Table:

Time T sec	Height H km	Relative intensities i_{24}/i_{26}	$\frac{i_{Mg^+}}{i_{No^+} + i_{O_2^+} + i_{Mg^+}}$	Concentration $[Mg^+]$, cm^{-3}
I20	99,5	-	< 0.0I	< 400
I23	I03.5	I0 ± 2.4	0.I7 ± 0.0I	I3600
I26	I08.0	9 ± 6	0.02 ± 0.0I	I600
I29	II2.0	-	< 0.00I	< I60
I35	I20.0	-	0.005 ± 0.00I	400
4I8	I09.0	-	0.03 ± 0.0I6	2400
42I	I05.0	9 ± 5	0.I7 ± 0.02	I3600
424	I00.5	-	< 0.02	< I600

Average 9.3 ± 5

Taking into account possible systematic errors, we consider, that the received value 9.3 ± 5 proves the suggested indentification of ions with M = 24 and 26 with magnesium ions. The isotope Mg^{25} is not detected due to low resolution. Some asymmetry of the peak Mg^{24} base points to its presence (see the spectrum for M = I23 sec.)

Having at hand independent measurements of electron concentration in the atmosphere one can compute absolute concentrations of positive ions, recorded by mass-spectrometer. Then we assume the following: I/ the sum of positive ions concentration is equal to electron concentration, i.e. there are no negative

Declassified in Part - Sanitized Copy Approved for Release 2011/12/08 : CIA-RDP80T00246A016600420001-1

Declassified in Part - Sanitized Copy Approved for Release 2011/12/08 : CIA-RDP80T00246A016600420001-1

ions: $\sum [M^+] \cdot n_e$; 2/ The sum of ion peaks amplitudes in the mass-sphectrogram is proportional to the total positive ions concentration: $\sum i_{M^+} = K \sum [M^+]$; 3/ the ratio of ion peaks amplitudes ratio of corresponding ions in the atmosphere:

$$i_{M_1^+} / i_{M_2^+} = [M_1^+] / [M_2^+]$$

So, the ion M_I absolute concentration can be found from the relation: $[M_1^+] = i_{M_1^+} \cdot n_e / \sum i_{M^+}$.

The ratio maximum intensity of the magnesium ion peaks to the total intensity of all the recorded ionosphere ~~compone~~ components is equal to = 0.I7. During this recket firing electron concentration was determined by other investigators by means of rocketborn U.H.F. dispersion interferometer analogous to what was described in the paper /II/. At the I00 - II0 km altitude n_e = 8 x $I0^4$ cm^{-3} , hence, maximum concentration of magnesium ions at the I03.5 - I05 km altitude $/Mg^+/$ = = I.36 x $I0^4$cm.

Fig.4 shows the recorded magnesium ions concentration variation with height and possible profile of the layer. Assuming the half width of the layer equal to 5 km, the total number of ions in the unit column will be equal to 7 x $I0^9$ cm^{-2}. Naturally owing to few experimtntal points /spectra/ the given layer profile can be considered as only conditionally presenting the real patern of Mg^+ ions distribution.

Note the certain record of Mg^+ ions in the spectrum, obtained during the flight at the I20 km altitude /Fig.5/. In the previous and following spectra M = 24 peak is lacking. Thus, we see, that there exist two maxima of magnesium ions concentration at the ~ I04 and ~I20 km altitude.

Declassified in Part - Sanitized Copy Approved for Release 2011/12/08 : CIA-RDP80T00246A016600420001-1

Declassified in Part - Sanitized Copy Approved for Release 2011/12/08 : CIA-RDP80T00246A016600420001-1

In the spectrum of T = 135 sec (120 km altitude) there is a peak with M = 28, which is lacking in all previous and many following spectra. Its possible identification will be discussed later.

Studying the spectrum of T = 123 sec, obtained at the ascent at the 103.5 km altitude, (Fig.3) attentively, one can see an appreciable peak of ion current with M = 40^+.

As the previous and following spectra lack M = 40 peak, its detection can be,naturally, connected with simultaneous appearance of Mg^+ ions and refferred to Ca^+ ions presence in this layer. Relative abundance of Ca^{40} isotope makes up 97%.

A^{40} is another stable isotope with M = 40 and great relative abundance, however, for some reasons this identification is unacceptible. And otherwise, in the light of the obtained data of ionised CaII /12, 13/ lines presence in the twilight spectra the identification of $M=40^+$ peak with Ca^+ ions is doubtless. Ca^+ ions peak cannot be observed in other spectra /Fig.3/, as there its amplitude must be less than the minimum-detectable one.

At last, there is one more important peculiarity in the spectra for the rocket firing on June 15, 1960. As a result of transient processes of mass-scanning at the end of each spectrum there is normally recorded a small "ridge" of ion current, not associated with any ions. Mass range of the used device MX-6403 in the ion analysis regime comes to an end in M=56 region and this mass cannot be normally reproduced in the spectrum.

Declassified in Part - Sanitized Copy Approved for Release 2011/12/08 : CIA-RDP80T00246A016600420001-1

Declassified in Part - Sanitized Copy Approved for Release 2011/12/08 : CIA-RDP80T00246A016600420001-1

Nevertheless, at last in two spectra at the ascent at the altitudes, corresponding to M^+ ions appearance (100-105 km) the ion currents at the end of the scanning are abnormally high. The same is observed in the spectra of the descent at the same altitude. The only possible explanation of the mentioned peculiarities is the assumption, that the given altitude range alongside the definitely recorded Mg^+, O^+, O_2^+ and Ca^+ ions there are also many ions with mass number 56^+. The only stable isotope with M=56 with great relative abundance is the isotope Fe^{56} (91,7%) what defines the possible identification. Fe^+ ions concentration in the layer maximum must be estimated in the order of magnitude close to M^+ ions concentration, i.e. $[Fe^+] \sim 1.5 \times 10^4 cm^{-3}$ at the 101 km altitude.

During the latest experiment in the altitude range 100 to 120 km the detection of ions of metals led to thorough study of previously obtained in analogous rocket firings telemetric records, especially in the region of 100-110 km.

It is necessary to take into consideration the fact, that the used method was not specially intended and was not provided for relatively "fine-structural" measurements of ion composition variation with height. Thus, lack of any definite orientation of container after its separation from the rocket, for instance, is a limiting factor. At the 100 km altitude /when the top is about 200 km/ container moves at the rate of 1,5 km/sec, though the mean thermal velocity of the ion with M=30, when the temperature is 300^oK, will be about 0,4 km/sec. Under these conditions the mass-spectrometer sencitivity greatly depends on the aspect of the entrance of the tube relative to the velocity vector.

Declassified in Part - Sanitized Copy Approved for Release 2011/12/08 : CIA-RDP80T00246A016600420001-1

Declassified in Part - Sanitized Copy Approved for Release 2011/12/08 : CIA-RDP80T00246A016600420001-1

Therefore, at the 100-120 km altitude where there are thin layers of non-typical for nitrogen-oxigen atmosphere ions of metals, measurements were not always possible, as the container orientation was not necessary optimal. Comparatively large period of mass-scanning prevented the detection of thin ion layers. The mass-scanning period of RMS-I device /7/, which was used in 1957-1958, was 1,7 sec, which corresponds to 2,5 km change in height. Mass-scanning of spectrometers, used in the following experiments /1959-1960/ was 3 sec, and H=4 km, respectively. Sometimes, there were limiting factors, such as insufficient sencitivity of the device or high noise level.

Nevertheless, while looking through the mass-spectra records, obtained by sounding rocket firing on August 2, 1958, the sun elevation being 36^{o}, we also found in two of them, corresponding to the altitudes about 105 km at the ascent and descent, ion peaks with $M=56^{+}$, identified with ions of ferrum Fe^{+}. Possible error of mass number determination in this experiment by no means prevails ± 1 atomic mass unit, as the device ranged to M=62.

As is clear from the comparison of the peaks amplitudes of Fe^{+} ions and "normal" for this altitude ions of nitrogen oxide NO^{+} and molecular oxigen O_2^{+} /Fig.6/ ferrum ions concentration is an appreciable part of the total ionic /electron/ concentration. Unfortunately, no measurements of electron concentration were carried out during the rocket firing on August 2, 1958, therefore possible estimates are less reliable. If to use the results of Ne measurements, obtained during the sounding rocket firing on August 27,1958

Declassified in Part - Sanitized Copy Approved for Release 2011/12/08 : CIA-RDP80T00246A016600420001-1

Declassified in Part - Sanitized Copy Approved for Release 2011/12/08 : CIA-RDP80T00246A016600420001-1

/14/, the Sun elevation being 18^0, in the conditions, close to those of the measurements on August 2, 1958, the recorded ion concentration will be: $[Fe^+] \simeq 1.2 \ 10^4 cm^{-3}$.

It is clear from the spectra in Fig. 6, that ions with M=28 are recorded in the same limited altitude range, as ions of Fe^+. The most natural identification of these and molecular nitrogen N_2^+ ions is not the only possible one#/. The element with M=28 is silicon and this identification seems to be in harmony with the results, given above. The estimate of maximum concentration of ions with $M=28^+$ according to the spectra in Fig.6 gives the value $7.5 \times 10^3 cm^{-3}$.

If we identify M=28 with N_2^+ ions, we have to admit, that their appearance in E-region of the ionosphere at the altitude of 105 km is unexpected and needs special explanation, in spite of the fact, that nitrogen is the main compound of the atmosphere at these altitudes. The question of the reasons of molecular nitrogen ionisation in the earth atmosphere is not yet solved.

In the light of ideas of the work /15/ and taking into account the new data of HeII line absorbtion λ = 304 A /16/, according to which this radiation, capable of ionising nitrogen molecule, is absorbed in the altitude range 210-150km, A.D. Danilov's point of view, explaning molecular nitrogen ionisation by

---

#/The identification of ions with $M=28^+$ with Fe^{++} is formally possible, though hardly probable, as mass-spectrometer devides ions according to the ratio of their mass to the charge, and single charged ions with M=28 cannot be separated from twice ionised particles with M=56. High resolution is necessary for the $^{56}Fe^{++} - {}^{28}N_2^+$ doublet separation.

Declassified in Part - Sanitized Copy Approved for Release 2011/12/08 : CIA-RDP80T00246A016600420001-1

Declassified in Part - Sanitized Copy Approved for Release 2011/12/08 : CIA-RDP80T00246A016600420001-1

charge transfer reaction with atomic nitrogen ions: $N_2 + N^+ \rightarrow N_2^+ + N$ /5/. This, undoubtedly, must be true for the altitude range 250 km and more. However, it is clear, that N_2^+ ions appearance in E-region at the I00-I20 km altitude can be neither due to direct photoionisation, N_2 /there are no corresponding radiation quanta/, nor due to charge transfer reaction /there are no N^+ ions /I7/ /.

Thus, the appearance of ions with $M = 28^+$ in E-region must: testify to some other, N_2 ionisation processes, not associated with solar radiation, or these ions must be identified with silicon ions Si^+.

Such indentification, as was already said, is in harmony with the detection of Mg^+, Ca^+ and Fe^+ ions in this region. As is generally Known, magnesium, silicon and ferrum /alonside oxigen/ are the elements, which prevail in stone meteors.

The recorded ratio of magnesium and calcium ions concentrations $[Mg^+]/[Ca^+] \approx 25 \pm 8$, is close to the ratio of the number of atoms of the mentioned elements in meteors: $[Mg]/[Ca] = 15/18$. It is understandable from the point of view of meteor hipothesis of the detected ions origin, because Mg and Ca atoms ionisation, (whether it is photoionisation or ionisation by their interaction with atmospheric molecules), as well as recombinztion of Mg^+ and Ca^+ ions, must be going on in the same way, As physical and chemical characteristics of these metals are alike, the constants of ionisation and recombination

Declassified in Part - Sanitized Copy Approved for Release 2011/12/08 : CIA-RDP80T00246A016600420001-1

Declassified in Part - Sanitized Copy Approved for Release 2011/12/08 : CIA-RDP80T00246A016600420001-1

processes must almost coinside,

Estimates of the total number of Ca ions in the unit column, made by the obtained spectra / $[Ca^+] \sim 540\ cm^{-3}$ $N_{Ca^+} \geq 3 \cdot 10^8\ cm^{-2}$ / by twilight intencity of Ca II lines, show good correspondence: $N_{Ca^+} \sim 5 \cdot 10^8\ cm^{-2}$ /I2/.

The results of the work /I2/ are comparable with the data, as far as they were obtained in the same month /June/, during the period of daytime meteor showers activity, Perseids and Arietids /I9/.

The altitudes of "non-typical" for the Earth atmosphere ions of metals appearance are specific for meteor phenomema: in the region I00 to I20 km the smallest of all vaporising in the atmosphere meteor particles loose their cosmic speeds and vaporize totally or partially/ and, hence, at most contribute both from the point of view of energy and quantity of the substance, entering the atmosphere/.

As it is known, that in meteor spectra the lines of ionised metal - ferrum, magnesium, calcium and silicon /20/ - are directly observed, an important role of the mechanism of fast-moving meteor substance atoms ionisation during in elastic collisions with atmospheric molecules is doubtless. Naturally, besides these, processes of Ca, Mg, Fe and Si neutral atoms photoionisation by ultraviolet solar radiation go on in the day time /2I/.

Given results prove the hipothesis by Nicolet /2I/

Declassified in Part - Sanitized Copy Approved for Release 2011/12/08 : CIA-RDP80T00246A016600420001-1

Declassified in Part - Sanitized Copy Approved for Release 2011/12/08 : CIA-RDP80T00246A016600420001-1

about the leading role of meteros in night ionisation in E-region. The altitudes, where the layers were detected, fully coinside with the altitudes of the hight E-layer, determined by radio-observation (I00 - I05 km, see /2I/), and ionic concentrations of metals are equal in the order of magnitude to the night electron concentration values in E-region ($\sim I0^4 cm^{-3}$.

It seems probable, that with some improvement of the method (with the same or a little higher sensitivity and resilution) ion mass spectrum analysis in E-rebion may be used for definition of chemical composition of such sizes meteors which do not reach the ground, and hence, cannot be analysed by other methods. Particularly, we hope to get information about the composition difference of particles of different meteor showers and also sporadic and showers meteors.

References: see the Russian text.

Declassified in Part - Sanitized Copy Approved for Release 2011/12/08 : CIA-RDP80T00246A016600420001-1

Declassified in Part - Sanitized Copy Approved for Release 2011/12/08 : CIA-RDP80T00246A016600420001-1

Fig.I The scheme of installation of radio-frequency mass-spectrometer in the container.

Fig.2. Radio-frequency mass-spectrometer, used during the rocket firing on June I5, I960.

Fig.3. Positive ions mass spectra, obtained by the morning rocket firing on June I5, I960. All ion components are marked by corresponding chemical symbols. The peaks in the spectra at the descent, not marked by symbols, correspond to contamination ions.

Fig.4. Magnesium ions concentration variation with height in the atmosphere,

o o o - variation at the ascent,

● ● ● -variation at the descent.

Possible profil of Mg^+ ions layer is marked with dotted line.

Fig.5 The same as Fig.3. The spectra show the existence of the additional thin layer of ions with M = 24 $/Mg^+/$ and M = 28 $/N_2^+$ or $Si^+/$ at the I20 km altitude.

Fig.6. Positive ions mass spectra, obtained by the day-time rocket firing on August 2, I958. The spectra show the existence of the layers of ions with M = 56 $/Fe^+/$ and M = 28 $/Si^+$ or N_2^+ /.

Declassified in Part - Sanitized Copy Approved for Release 2011/12/08 : CIA-RDP80T00246A016600420001-1

Declassified in Part - Sanitized Copy Approved for Release 2011/12/08 : CIA-RDP80T00246A016600420001-1

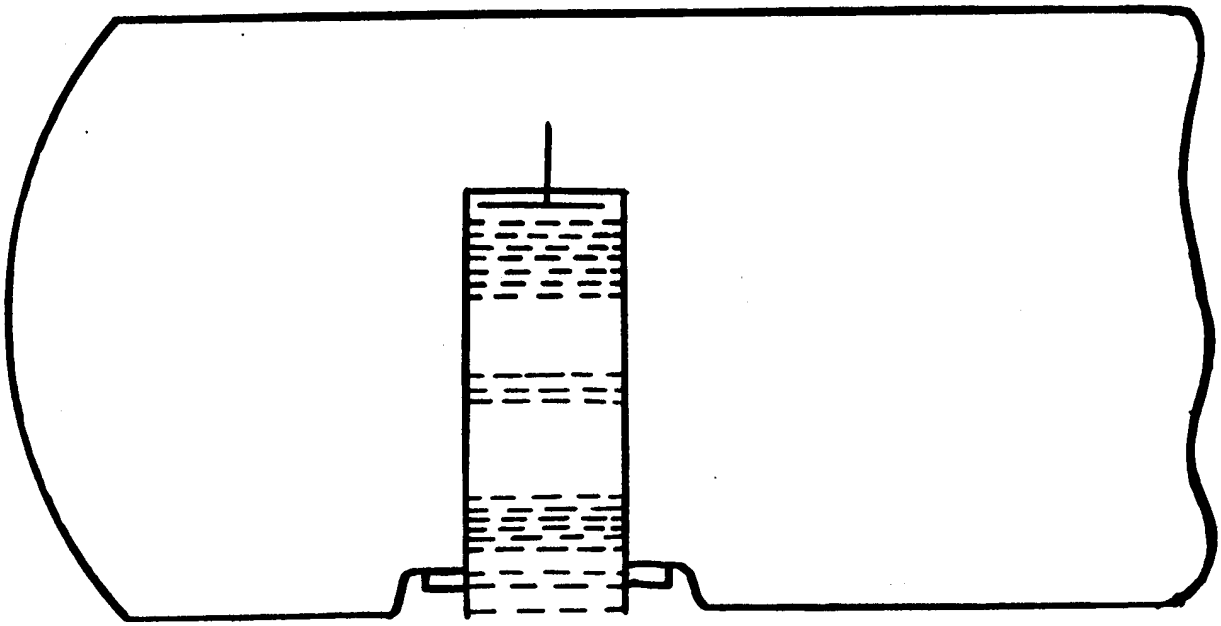

Declassified in Part - Sanitized Copy Approved for Release 2011/12/08 : CIA-RDP80T00246A016600420001-1

Declassified in Part - Sanitized Copy Approved for Release 2011/12/08 : CIA-RDP80T00246A016600420001-1

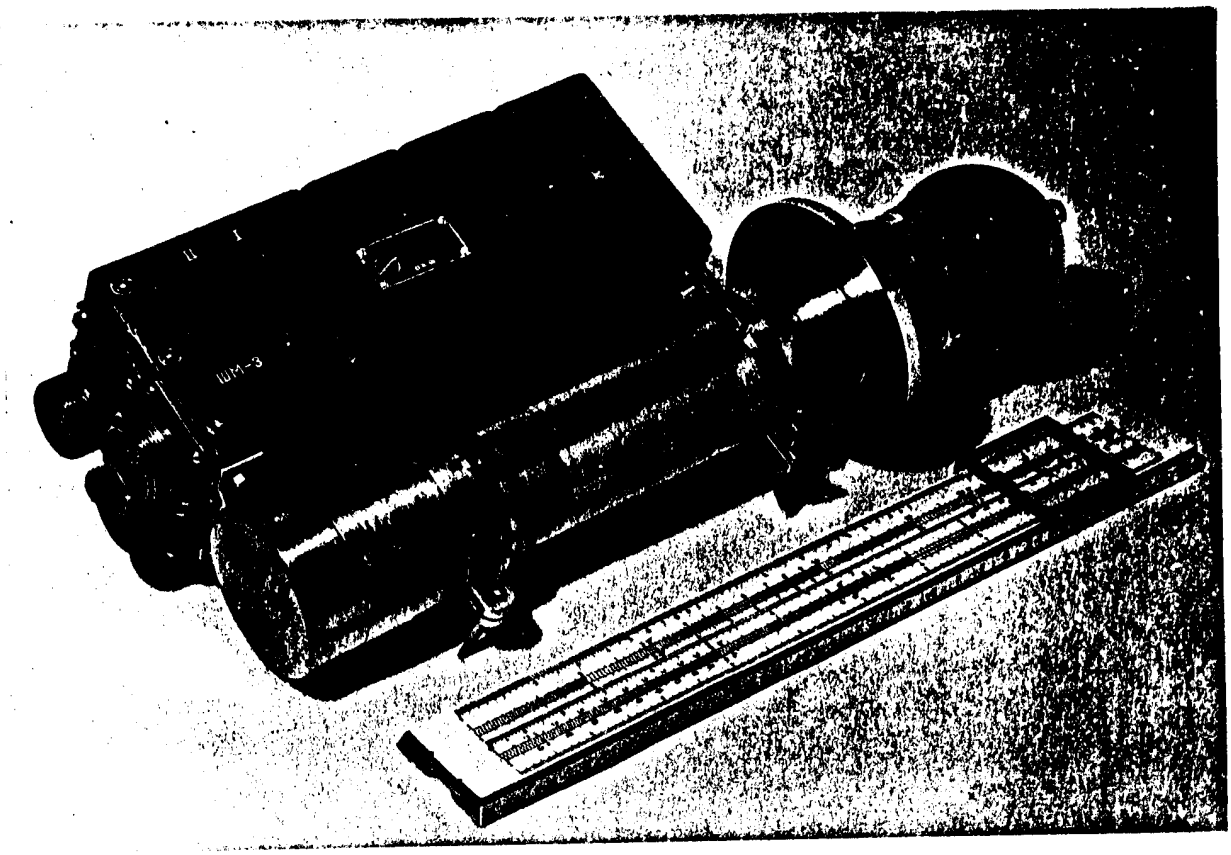

Declassified in Part - Sanitized Copy Approved for Release 2011/12/08 : CIA-RDP80T00246A016600420001-1

Declassified in Part - Sanitized Copy Approved for Release 2011/12/08 : CIA-RDP80T00246A016600420001-1

Восходящая ветвь

Нисходящая ветвь

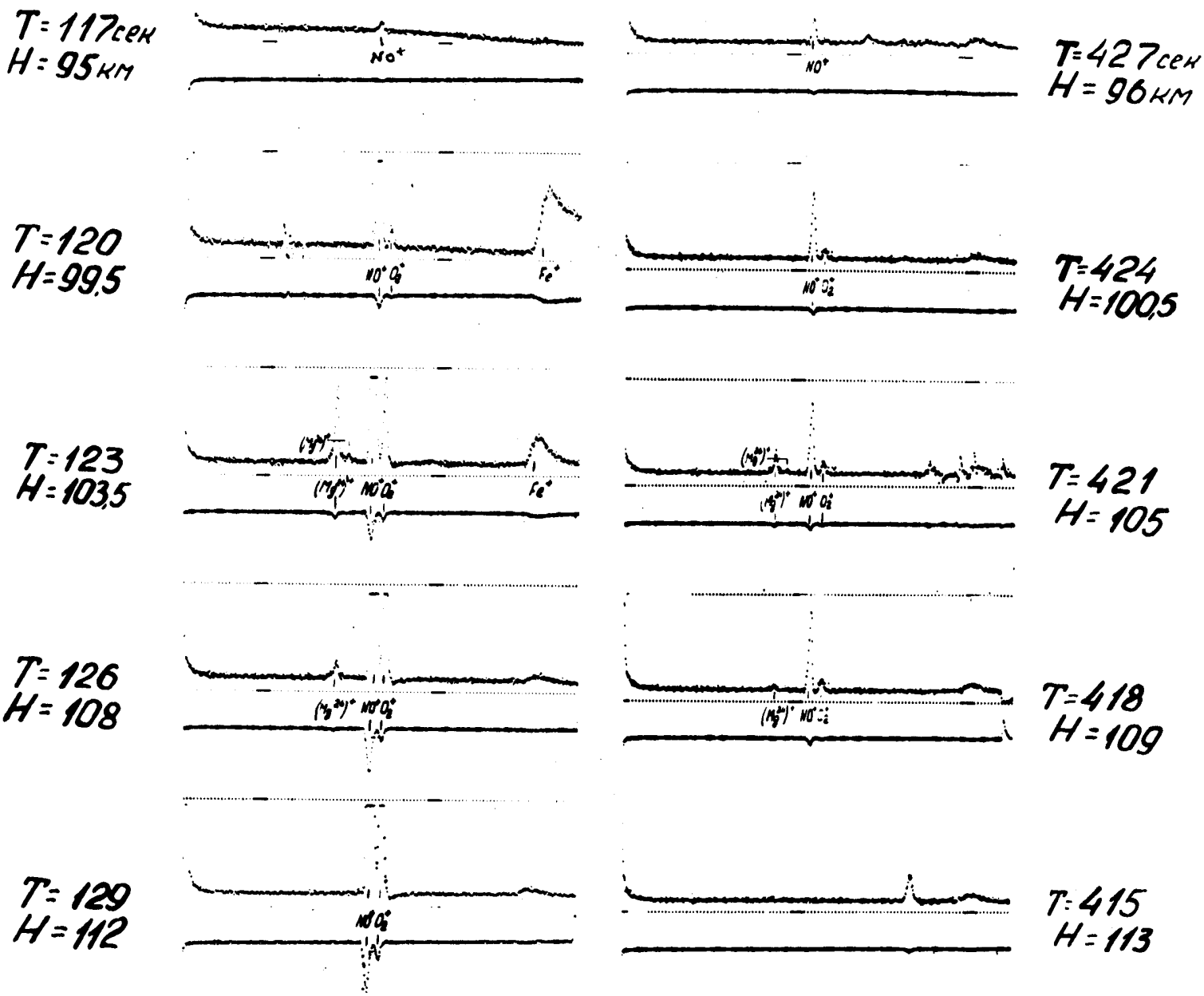

Declassified in Part - Sanitized Copy Approved for Release 2011/12/08 : CIA-RDP80T00246A016600420001-1

Declassified in Part - Sanitized Copy Approved for Release 2011/12/08 : CIA-RDP80T00246A016600420001-1

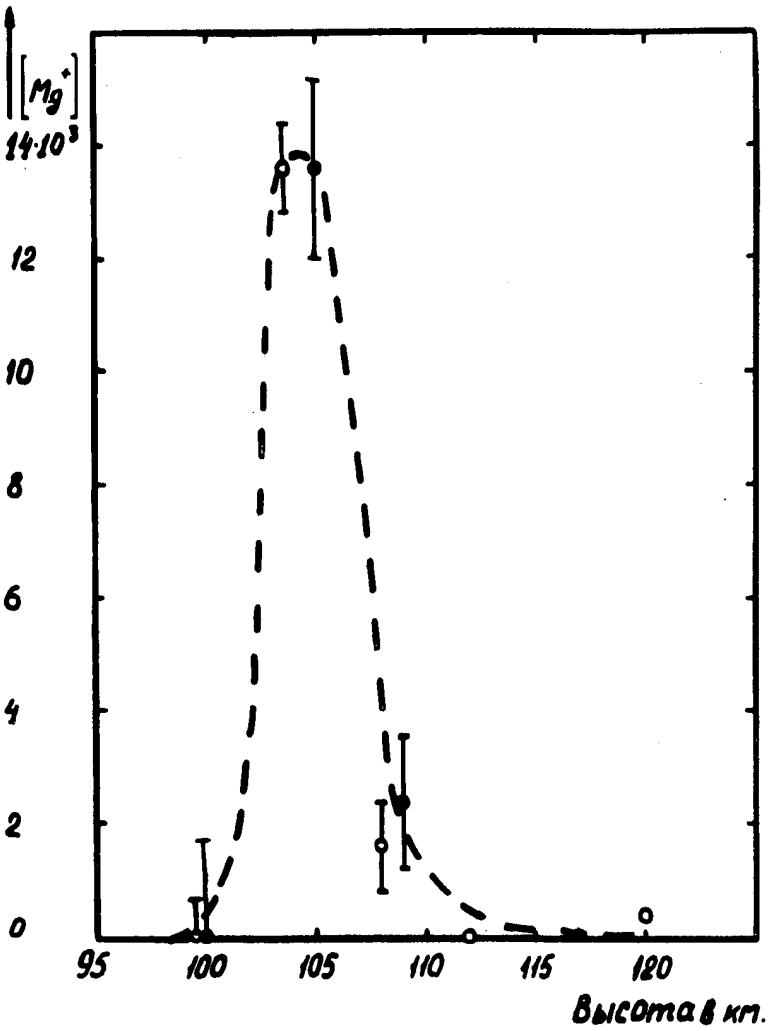

Declassified in Part - Sanitized Copy Approved for Release 2011/12/08 : CIA-RDP80T00246A016600420001-1

Declassified in Part - Sanitized Copy Approved for Release 2011/12/08 : CIA-RDP80T00246A016600420001-1

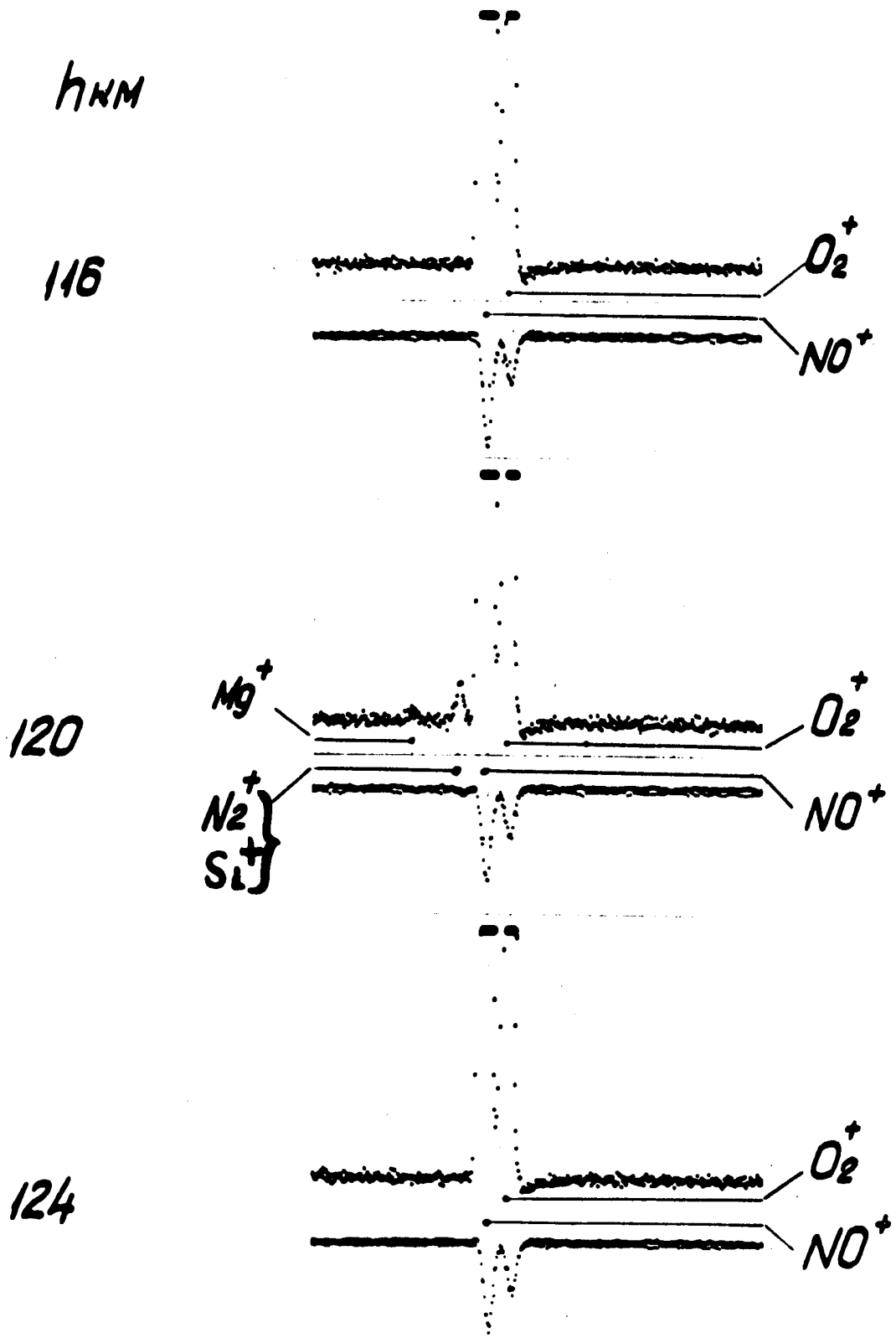

Declassified in Part - Sanitized Copy Approved for Release 2011/12/08 : CIA-RDP80T00246A016600420001-1

Declassified in Part - Sanitized Copy Approved for Release 2011/12/08 : CIA-RDP80T00246A016600420001-1

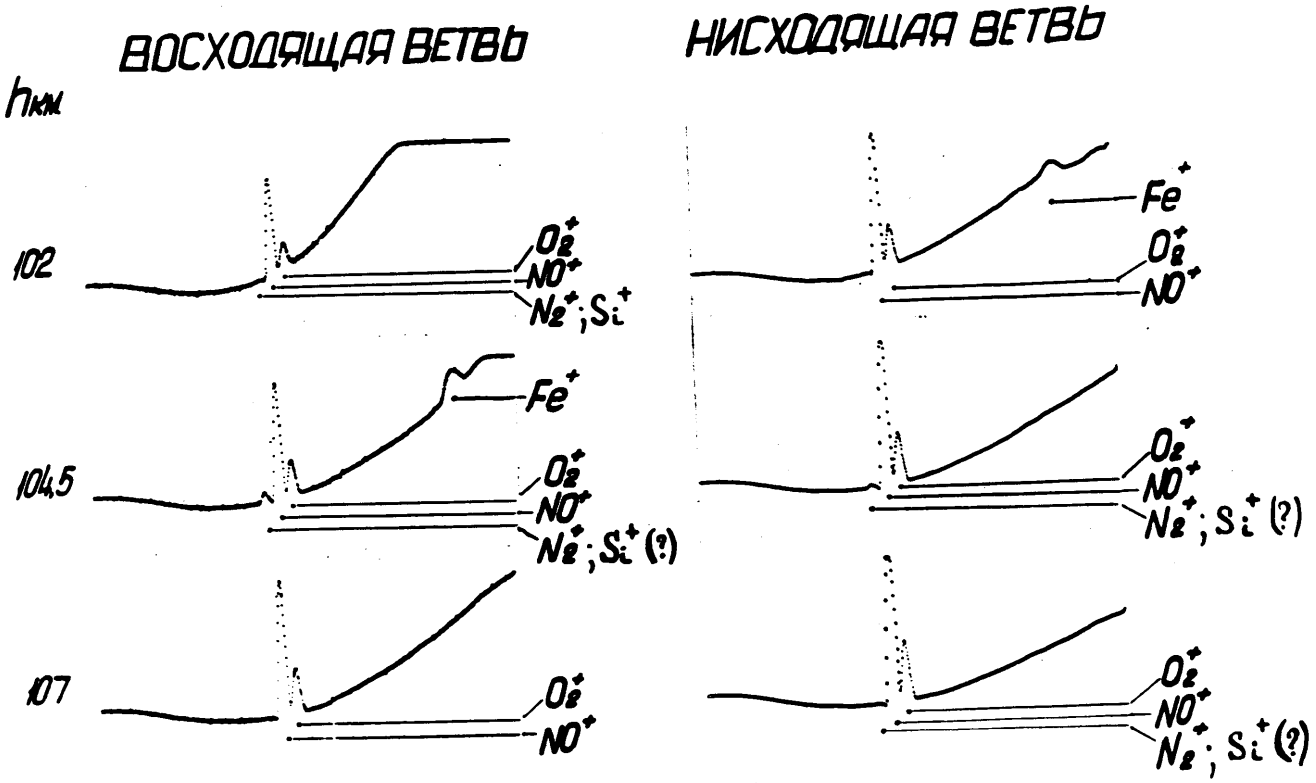

Declassified in Part - Sanitized Copy Approved for Release 2011/12/08 : CIA-RDP80T00246A016600420001-1

Declassified in Part - Sanitized Copy Approved for Release 2011/12/08 : CIA-RDP80T00246A016600420001-1

#4 1.10

by A.E.MIKIROV (English) (12pp)

5. AEROSOLE SCATTERING COEFFICIENT MEASUREMENT AT THE 80-I00 km.

The measurements of the sky brightness distribution at altitudes is of great interest both from geophysical and practical points of view.

It is common knowledge that the sky brighness in the upper atmosphere is the combination of both the atmosphere luminosity and scattered light. In the day-time atmosphere glow itself makes negligible contribution to the total sky brightness, produced mainly by scattering effect by gas molecules and atmosphere aerosoles.

Such investigations can be carried out both by indirect measurements /twilight method/ and direct ones /vertical atmosphere sounding by means of balloons and rockets/.

The day sky brightness investigation by means of rockets began in I946. In these experiments there were sometimes used photometers, sometimes - photocameras. The obtained results give alternative data of day sky brightness.

Thus, for instance, Milly's experiments /I/ show, that the sky brightness decreases with height and at the 35 km altitude is of the order of 2-3% of the sky brightness near the Earth surface.

At the 70 km altitude the sky brightness decreases 2 times more and further remains constant up to the I35 km altitude.

On the basis of these data we came to the conclusion, that

Declassified in Part - Sanitized Copy Approved for Release 2011/12/08 : CIA-RDP80T00246A016600420001-1

Declassified in Part - Sanitized Copy Approved for Release 2011/12/08 : CIA-RDP80T00246A016600420001-1

at the 135 km altitude these exists a luminous layer, the nature of which is difficult to explain.

Bates and Dalgarno /2/ showed, that such glow cannot be produced by the Earth atmosphere fluorecsence under the influence of the solar extreme-ultraviolet radiation.

Other authors showed, that it cannot be explained by zodiacal glow. Morosov V.M. and Shclovsky I.S. /3/ reject the assumption, that it is the existence of the sufficient number of aerosoles in the upper atmosphere, that causes this glow.

Berg's measurements /4/ have somehow slightly changed the notion of the day sky brightness. According to their data the day sky brightness at the 80 km altitude is 8.10^{-5} stilb, i.e. about 800 times more than the night sky brightness. Berg used cameras for his measurements, however the measured brightness was insufficial to make appreciable blackening on photoemulsion. Based on this he made a conclusion, that at the 80-280 km altitude the day sky brightness is 2.10^{-5} times less than that near the Earth surface. He found no luminous layers.

The latest experiments were performed by Birukova /5/ who, like Berg, used cameras for the sky brightness measurements. According to her data the sky brightness at the 56 km altitude is 5,2 apostilb. If according to Fisenkova-Pjaskovsraja /6/, the sky brightness near the Earth surface is 5000 apostilb, one can conclude, that at the altitude from 0 to 56 km the sky brightness fall 10^3 times. But at higher altitudes no measurements were taken by her. Thus, sufficiently precise brightness value, and spectral energy distribution in the upper atmosphere remained unknown.

Declassified in Part - Sanitized Copy Approved for Release 2011/12/08 : CIA-RDP80T00246A016600420001-1

Declassified in Part - Sanitized Copy Approved for Release 2011/12/08 : CIA-RDP80T00246A016600420001-1

We measured the day sky brightness at different altitudes in 4 directions by means of photoelectric photometer, designed and produced in accordance with the technical task of the Institute.

The apparatus is a high sensitive photoelectric photometer with the viewing angle of the order of 10°, the measurements with it being taken by immediate comparison of the external radiation signals with the standard signal, received from luminous compound phosphor.

The apparatus block-scheme is shown in Fig.I. As can be seen from Fig.I the apparatus optical scheme consists of quartz lens, light filters, neutral absorbing filters, a concave spherical mirror and a photomultiplier.

The apparatus is equipped with a device which allows to agust automatically one after another light filters, a free window, constant luminous compound phosphor and neutral absorbing filters on the light beam way.

The device, is shown in Fig.I as 2 disks.

The neutral absorbing filters, included in the scheme, provide for all filters, free window and luminous compound phosphor to have sufficiently wide limits of the brightness value variation, i.e. allows to make quite reliable measurements when the measured value varies more than 10^3 times.

The day sky scattered light, having passed the lens, the light filter or the free window and the neutral absorbing filter gets on - to the spherical mirror, which sends it to the photocathode. FEU-25 is used as the light receiver, with sufficient sensitivity it is the most stable, from the variation point of view.

Declassified in Part - Sanitized Copy Approved for Release 2011/12/08 : CIA-RDP80T00246A016600420001-1

Declassified in Part - Sanitized Copy Approved for Release 2011/12/08 : CIA-RDP80T00246A016600420001-1

For photomultiplier current amplification two cascade amplifier of alternating current is used in the apparatus. The light beam modulation is performed by rotating tooth disk, fastened on electric engine axis. The anchor of electromagnetic generator, giving reference, voltage for synchronous detector, is installed on the same electric engine axis.

The apparatus provides for a contact, which gives an impulse, thus fixing the beginning of each cycle of measurements.

All above mentioned allowed to obtain the apparatus sensitivity of the order of $0,9 \cdot 10^{-8}$ stilbs for integral light and $1,5 \cdot 10^{-10}$ $\frac{\text{w}}{\text{cm}^2 \cdot \text{st} \cdot \mu}$ for separate wave lengths. The neutral absorption filters included in the scheme widened the range of the measured breightness from $0,5 \cdot 10^{-8}$ to $0,5 \cdot 10^{-5}$ stilbs.

The brightness of the constant luminous conpound phosphor of different instruments was different and varied from $0,8 \cdot 10^{-8}$ to $3,7 \cdot 10^{-8}$ stilbs.

The apparatus, described above was used for sky brightness measurements up to 100 km.

A number of experiments was carried out for the definition of the upper atmosphere brightness. The best experiments from the point of view of the sensor optical axcises disposition in space were experiment N4, performed in the northern latitudes, and experiment N6, performed in the middle latitudes of the USSR.

The sun in the first case composed with the horizon an angle $\beta_\odot = 1^\circ 50'$, and in the second case $\beta_\odot = 0^\circ 40'$. The results

Declassified in Part - Sanitized Copy Approved for Release 2011/12/08 : CIA-RDP80T00246A016600420001-1

Declassified in Part - Sanitized Copy Approved for Release 2011/12/08 : CIA-RDP80T00246A016600420001-1

of the processing are given in Fig.2, where brightness values in stilbs are plotted on the abciss and height in km - on the ordinate. The curves clearly show, that in the middle latitudes the sky brightness is more, than in the northern latitudes, and this can be accounted for only by the great number of scattering particles.

For comparison Fig.3 gives the measured brightness values and all known data, obtained by other authors. Besides, it gives the sky brightness of absolutely clean atmosphere.

The brightness values, received experimentally, are slightly higher than the Rayleigh ones. This may point to the existence of aerosoles in the atmosphere.

As is known, according to experimental data the atmosphere optical density can be found from the equation.

$$S_\lambda = \frac{S_{o\lambda}}{4\pi} \sec\theta \int_0^{\infty} e^{-t \sec\xi} \cdot e^{-(H-\tau)\sec\theta} \gamma(t\theta)\, dt \qquad (5)$$

where $S_{o\lambda}$ - the source intensity before entering the atmosphere;

S_λ - the intensity of the observed scattered radiation;

$\gamma(t\theta)$ - the indicatrix of scattering. Considering $\gamma(t\theta) = \frac{3}{4}(1-\cos^2\varphi)$, what is quite acceptable for the scattering angles $180^\circ \div 120^\circ$, and assuming $\tau \ll 1$, equation (5) can be written as follows:

$$S_\lambda = \frac{S_{o\lambda} \cdot 3}{16} m(1+\cos^2\varphi)\tau_\lambda = \frac{3}{16} S_{o\lambda} m(1+\cos^2\varphi)(\tau_{\lambda\,rayl} + \tau_{\lambda\,aer})$$

where $\tau_{\lambda\,rayl}$ - optical depth, corresponding to the Rayleigh scattering,

Declassified in Part - Sanitized Copy Approved for Release 2011/12/08 : CIA-RDP80T00246A016600420001-1

Declassified in Part - Sanitized Copy Approved for Release 2011/12/08 : CIA-RDP80T00246A016600420001-1

τ_{ain} - optical depth, corresponding to scattering on the particles according to Mie's law.

Thus, in order to determine the optical depth as the optical depth as the Rayleigh one τ_{rayl} , and as aerosole component τ_{ain} , it will be quite enough to measure the scattered radiation intensity in 2 waves lengths or in 2 different angles of the indicatrix of scattering.

For determination of the number of aerosoles in an atmosphere layer it is sufficient to have the measurements data of the scattered light brigtness at the upper and lower boundary of the layer and then the aerosole optical depth of the latter will be equal to difference:

$$\tau_{ain\ layer} = \tau_{ain}(h+\Delta h) - \tau_{ain}(h)$$

whence assuming τ_{ain} of the layer $= K(\rho)\pi r^2 N \Delta h$

$$\beta_{ain} = K(\rho)\pi r^2 N$$

one can define the value of aerosole scattering coefficient where $K_{(\rho)}$ - Houghton-chalker coefficient,

N - the number of scattering particles in I cm^3.

r - the mean radium of a scattering particle.

Fig.4 gives β_{ain} values for the nothern and middle latitudes of the USSR. Besides, it gives scattering coefficient values for absolutely clean atmosphere (β_{rayl}) for comparison. The results , presented in Fig.4 , show, that from 80- to 100 km there exists an aerosole layer with the maximum situated at the 85 km altitude in the middle latitudes and at 92 km in the

Declassified in Part - Sanitized Copy Approved for Release 2011/12/08 : CIA-RDP80T00246A016600420001-1

Declassified in Part - Sanitized Copy Approved for Release 2011/12/08 : CIA-RDP80T00246A016600420001-1

nothern latitudes, the number of aerosoles being greater in the middle latitudes, than in the nothern ones.

By means of Fig.4 data one can measure the aerosole layer concentration and density. Let us assume $(K_\beta) = 4$, in other words, we shall consider, that scattering takes place on the particles with the maximum scattering coefficient, what corresp corresponds to $r = 0,4\ \mu$. It means, that we give the estimate of the minimum aerosole substance quantity. If we assume specific density of aerosole substance to be equal to 3 g/cm^3, in the layer maximum (for the middle latitudes) $N = I.IO^{-3}$ I/cm^3, $\rho = 8.IO^{-I6}$ g/cm^3 and for the nothern latitudes N $0,6^{0}IO^{-3}$ I/cm^3, $\rho = 4,8.IO^{-I6}$ g/cm^3.

Declassified in Part - Sanitized Copy Approved for Release 2011/12/08 : CIA-RDP80T00246A016600420001-1

Declassified in Part - Sanitized Copy Approved for Release 2011/12/08 : CIA-RDP80T00246A016600420001-1

R E F E R E N C E S

I. Miley H.A., Callengton E.H., Bedinger J.L. - Trans.Amer.Geophys.Union , I953, v.34, N 5.

2. Bates D.R., Dalgarno A. - J. Amer.Ter.Phys., I954, v.5 (5/b) p. 329-334,

3. Morosov V.M., Chklovskii I.E. - Isv. AN SSSR, ser. geophys. N 4, I956, p. 464-468

4. Berg O. - J. of Geophys. Research, I955, v.60, N 3.

5. Birjukova L.A. - Trudy TSAO, I959.

6. Fisenkova-Pjaskovskaja E.V., Isv.AN SSSR, I957.

Declassified in Part - Sanitized Copy Approved for Release 2011/12/08 : CIA-RDP80T00246A016600420001-1

Declassified in Part - Sanitized Copy Approved for Release 2011/12/08 : CIA-RDP80T00246A016600420001-1

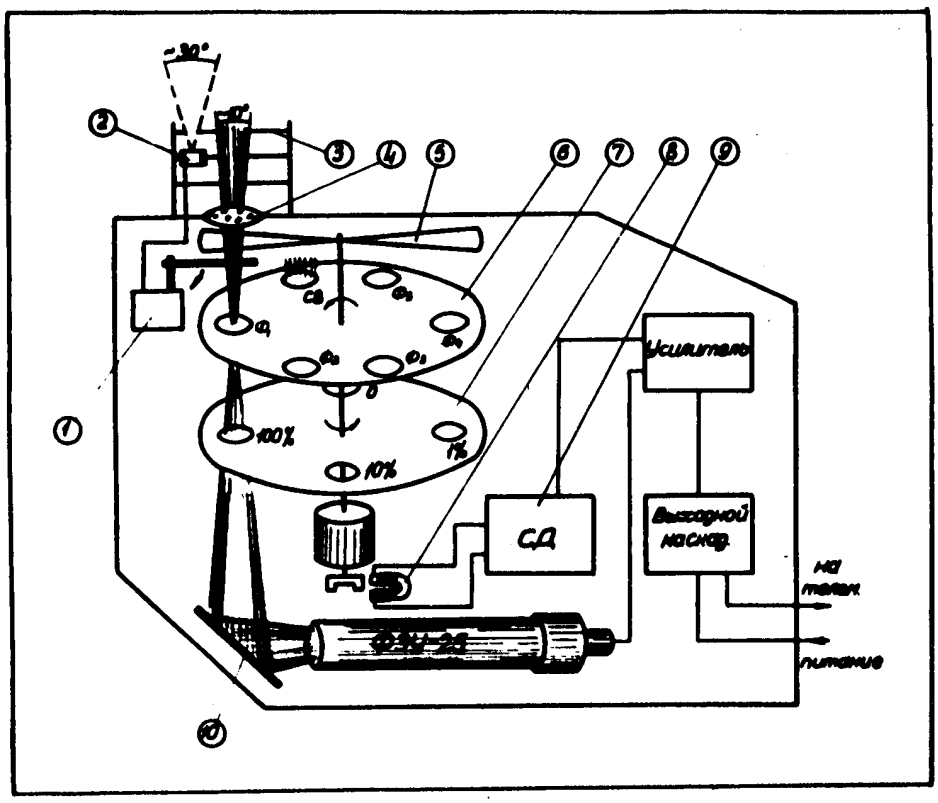

Declassified in Part - Sanitized Copy Approved for Release 2011/12/08 : CIA-RDP80T00246A016600420001-1

Declassified in Part - Sanitized Copy Approved for Release 2011/12/08 : CIA-RDP80T00246A016600420001-1

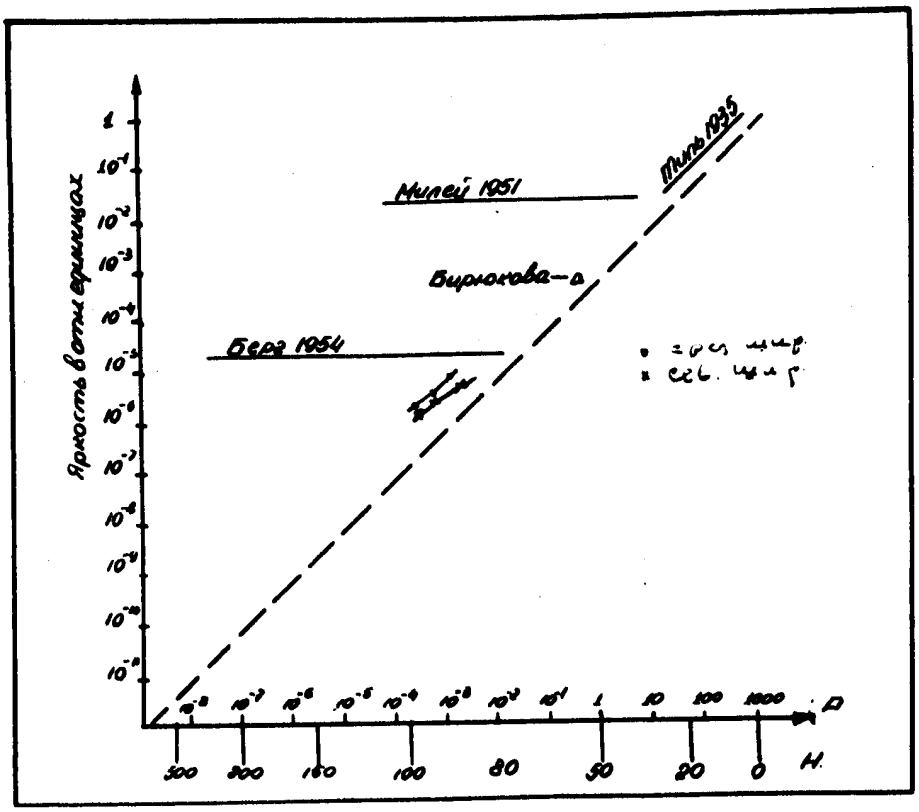

Declassified in Part - Sanitized Copy Approved for Release 2011/12/08 : CIA-RDP80T00246A016600420001-1

Declassified in Part - Sanitized Copy Approved for Release 2011/12/08 : CIA-RDP80T00246A016600420001-1

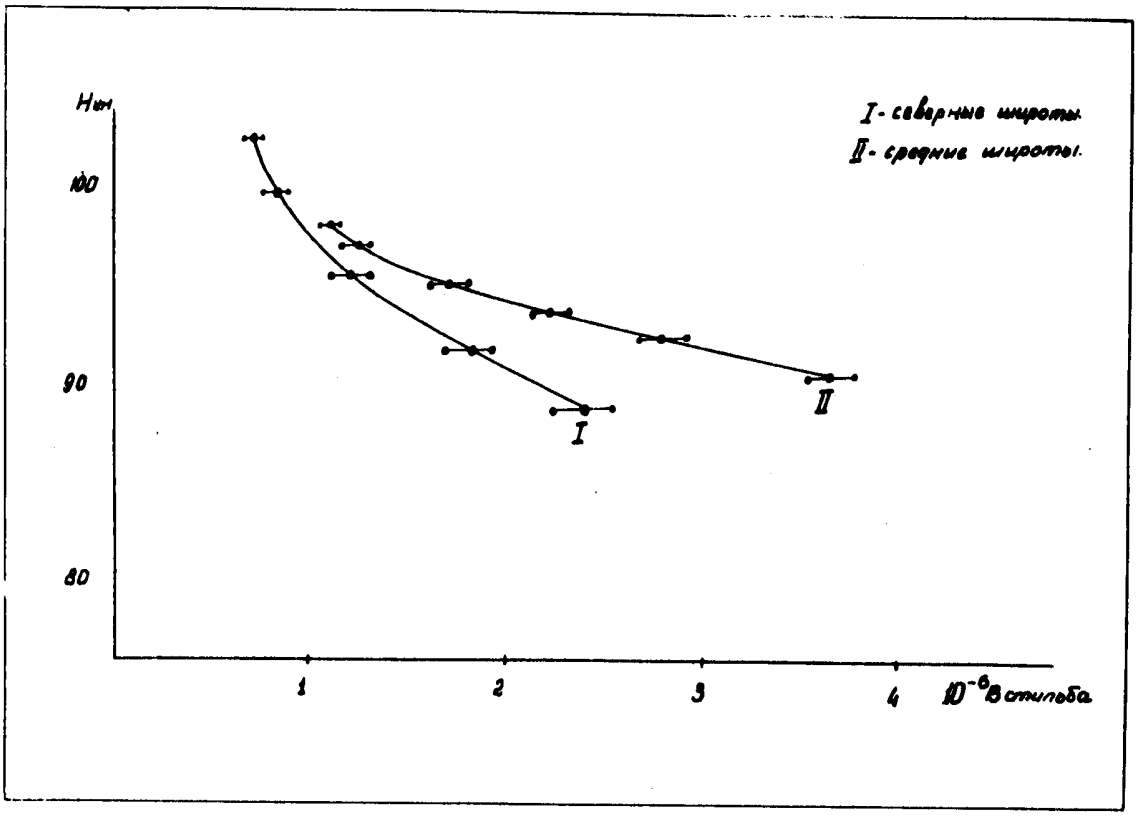

Declassified in Part - Sanitized Copy Approved for Release 2011/12/08 : CIA-RDP80T00246A016600420001-1

Declassified in Part - Sanitized Copy Approved for Release 2011/12/08 : CIA-RDP80T00246A016600420001-1

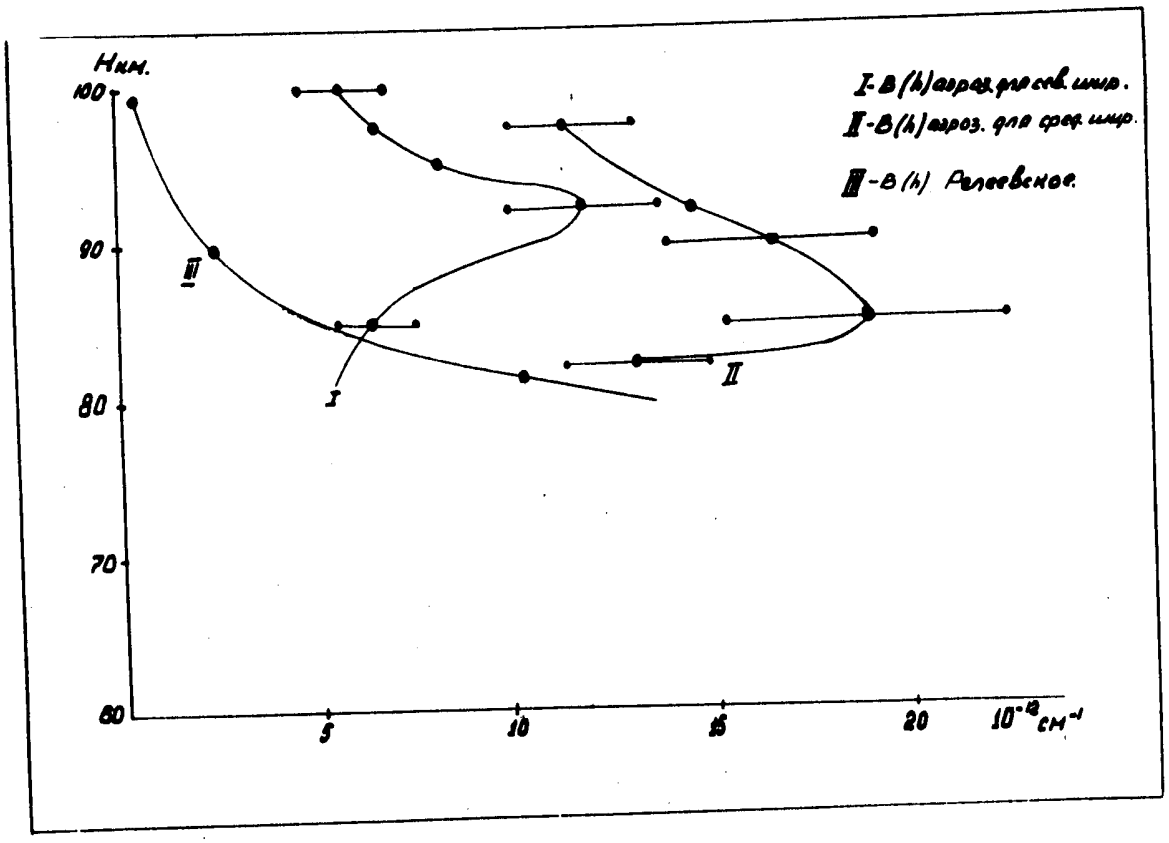

Declassified in Part - Sanitized Copy Approved for Release 2011/12/08 : CIA-RDP80T00246A016600420001-1

Declassified in Part - Sanitized Copy Approved for Release 2011/12/08 : CIA-RDP80T00246A016600420001-1

1.12

A.A.POKHUNKOV. (English) (17pp)

6. GRAVITATIONAL SEPARATION, COMPOSITION AND STRUCTURAL PARAMETERS OF THE ATMOSPHERE AT THE ALTITUDES ABOVE 100 KM.

Abstract.

The results of measurements of the Earth atmosphere neutral composition, made with radio-frequency mass-spectrometer during 2 soundings of geophysical rockets in the middle latitudes of the USSR: in September, 1960 (night) and in November, 1961 (day) are given. Gravitational separation of Ar and N_2 gases is found. According to the first sounding data the height of the beginning of separation is about 110 km. The atmosphere temperature distribution was measured up to the 210 km altitude for the night experiment and 300 km - for the day-time experiment. During the night experiment the distribution of relative and absolute concentrations of N_2 O_1 and O_2 was found up to the 210 km altitude. At the 100 to 210 km altitudes there was also estimated mean molecular weight, pressure and density of the atmosphere.

The limiting concentrations values of the following minor admixtures in the atmosphere: N_1, NO, H_2O, OH, H, and He are given.

During the night experiment at the 100 and 130 km altitudes magnesium oxide MgO of meteoric origin was detected.

At 00.56 local time, on September 23, 1960 in the middle latitudes of the European part of the USSR a geophysical rocket was launched to the 210 km altitude. During this sounding the container, separated from the rocket, was equipped with a 5-cascade

Declassified in Part - Sanitized Copy Approved for Release 2011/12/08 : CIA-RDP80T00246A016600420001-1

Declassified in Part - Sanitized Copy Approved for Release 2011/12/08 : CIA-RDP80T00246A016600420001-1

high sensitive radio-frequency mass-spectrometer (minimum registered current $4 \cdot 10^{-14}$A corresponds to partial pressure $5 \cdot 10^{-10}$mm mercury column) with mass ranges from 1 to 4 and from 12 to 60 atomic mass units. Detailed technical characteristics of the apparatus and the scheme of its installation on the container are given in work (1).

Neutral composition measurements by mass-spectrometer were carried out after the container separation at the distances up to a few hundreds of meters from the rocket.

The particularity of this experiment mass-spectra is the characteristic inherent only in atmospheric components periodic modulation of ion currents, produced by arbitrary container rotation in its flight and by pressure head effect. While the experiment data processing this sircumstance allowed to take into consideration desorption of the container surface. The spectra recorded the ion peaks, corresponding to the gases with the following mass numbers: 1,2,12,14,16,17,18,28,29,30,32,34,36,40,42 and 44, which were identified with H_1,H_2,C,N_1,O_1, OH,H_2O,N_2,N_1^{14},N_1^{15},NO,O_2,O_1^{16},O_1^{18}, Ar^{36},Ar^{40},$Mg^{26}O$,CO_2 and N_2O, respectively. Besides at the 100 to 125 km altitudes during the ascent and the descent there were recorded the gases with mass numbers 9 and 10, which finally are not yet identified.

On November 15,1961 at 16.00 p.m. local time a geophysical rocket was launched up to the 430 km altitude. Neutral composition measurements in this launching were carried out with a mass-spectrometer, installed in the head of the rocket under the separated nose cone. The used 5-cascade radio-frequency mass-spectrometer does not differ from the described in (1) and used in the night experiment of 1960 - one in sensitivity, resolving

Declassified in Part - Sanitized Copy Approved for Release 2011/12/08 : CIA-RDP80T00246A016600420001-1

Declassified in Part - Sanitized Copy Approved for Release 2011/12/08 : CIA-RDP80T00246A016600420001-1

power and mass range.

The apparatus was put to operation and began to record atmospheric gases mass spectra at the 130 km altitude.

Some results of mass-spectrogrammes treatment on the ascent of the free rocket flight tragectory, where all the angles of attack of the apparatus remained equal to 0°, are given below.

Gravitational separation.

The study of Ar and N_2 ion currents ratio variation with height in both experiments, presented in Fig.1, shows, that both in the night and day atmosphere there is gravitational separation of these gases. The comparison of these ion currents laboratory ratio, corresponding to Ar content in the ground layer, with the values, obtained during the sounding, taking into consideration the mass selection coefficient (2), shows, that gravitational separation in the night atmosphere begins at ~~th~~ the 105-110 km altitude.

As for the day atmosphere the direct definition of this level turned to be difficult due to the measurements being carried out at the altitudes above 130 km, where, as can be seen from Fig.1, there is an appreciable separation of Ar and N_2. The obtained results are in agreement with the data of 2 experiments, performed in the mornings in summer of 1959 (3,4) in the USSR, and also with the data of American authors, who studied the upper atmosphere layers at 59°N (5). As to the conclusion of the absence of gravitational separation in the atmosphere above White Sands (6) at 32°N, one has to agree with B.A.Mirtov /7/, doubting the results, obtained by American authors, due to unsatisfactory method of the experiment.

Declassified in Part - Sanitized Copy Approved for Release 2011/12/08 : CIA-RDP80T00246A016600420001-1

Declassified in Part - Sanitized Copy Approved for Release 2011/12/08 : CIA-RDP80T00246A016600420001-1

Atmosphere temperature.

According to Dalton's law the barometric formulae is used for gases concentrations distribution in the atmosphere above the gravitational separation level, this formulae allows to compute the atmosphere temperature and its variation with height according to the scale height H=RT/Mg of any component.

The absence of the container orientation in the night experiment of 1960 determined the computation method. The temperature was estimated according to the steepness of the slope of Ar and N_2 ion currents ratio variation curve (Fig.1), as this ratio variation with the accuracy to the proportionality coefficient is equal to Ar and N_2 relative concentration variation. The scale height $H=RT/(M_A-M_N)g$ was found according to the slope steepness for the barometric formulae defining Ar and N_2 relative concentration variation with height. The temperature was estimated in this way up to the 185 km altitude. From 185 to 210 km the temperature was estimated by linear extrapolation. The errors of the temperature definition make up about 10% of the measured value. The estimated values of the night atmosphere temperature are listed in Table 1.

As during the day experiment of 1961 the instrument orientation was constant (angle of attack=0^o), the temperature was computed from the curve inclination of N_2 ion current variation (Fig.2) which characterises the atmosphere nitrogen concentration variation with height. The calculation of the velocity head gives the following formulae for the scale height, from which the temperature was estimated:

$$H = H_o \frac{(2h_m - h)}{(2h_m - h) - H_o}$$

where H_o - the scale height for N_2 concentration variation

Declassified in Part - Sanitized Copy Approved for Release 2011/12/08 : CIA-RDP80T00246A016600420001-1

Declassified in Part - Sanitized Copy Approved for Release 2011/12/08 : CIA-RDP80T00246A016600420001-1

inside mass-spectrometer analyser, estimated directly from the steepness of the slope of N_2 ion current variation curve (Fig.2), h_m=430 km - the maximum height of the rocket ascent, h- the height, where H_o was measured.

Temperature values are in agreement when Ar ion current variation with height is used. The atmosphere temperature computation was limited in this experiment to the 300 km altitude due to the effect of desorption from the rocket becoming appreciable at higher altitudes. The obtained day atmosphere temperature values are also listed in Table 1.

The main composition, pressure and density of the atmosphere.

According to the data of 2 experiments, carried out at the altitudes above 100 km the main components, determining the atmosphere density are N_2, O_1 and O_2. In the altitude range 100 to 150 km there were recorded the isotopes $N_2(N^{14}, N^{15})$ with mass number 29 a.m.u., and at the 100 - 126 km altitudes - the isotopes $O_2(O^{16}, O^{18})$ with mass number 34 a.m.u.

Relative concentrations of these isotopes at the observed altitudes are practically constant and equal to $(7,6 \pm 0,6) \times 10^{-3}$ for N_2 and $(4,1 \pm 0,6) \times 10^{-3}$ for O_2, respectively, what is in good agreement with relative spread $7,6 \cdot 10^{-3}$ for $N^{14}.N^{15}$ isotope and $4 \cdot 10^{-3}$ for $O^{16}.O^{18}$ isotope (8). The study of the atmosphere composition by means of mass-spectrometer at the altitudes, where there exist chemically active atomic components, which can partially recombinate or combine with the analyser inner walls material, presents appreciable difficulties.

In work (1) on the basis of comparison of the experiments,

Declassified in Part - Sanitized Copy Approved for Release 2011/12/08 : CIA-RDP80T00246A016600420001-1

Declassified in Part - Sanitized Copy Approved for Release 2011/12/08 : CIA-RDP80T00246A016600420001-1

performed with mass-spectrometer analysers of different designs, there was received the correction factor, which takes into account possible reactions inside the analyser, which change the analysing gases composition. By means of the night experiment data with due regard for this factor there were obtained concentrations of the main atmpsphere gases: O_1, O_2 and N_2 and the mean molecular weight of the air in the altitude range 100-210 km was estimated (see Table 1).

Using the laboratory data of N_2 ion current variation with partial pressure inside the analyser there was estimated N_2 pressure at the 210 km altitude (excluding the background of gas separation from the container) in the hight experiment. Due to absence of the data of the container orientation during the flight, N_2 pressure distribution in the altitude range 100-210 km was estimated according to the barometric formulae with the use of atmospheric temperature values, estimated in the same experiment. The obtained N_2 pressure distribution is shown in Fig.3, curve 2. Further computations with the use of O_I, O_2 and N_2 relative concentrations data allowed to find the distribution of the main atmosphere gases absolute concentrations, night atmosphere pressure and density at the 100-210 km altitudes. The results of these computations are listed in Table I.

As in the day experiment of 1961 the mass-spectrometer analyser had no shielding grid with positive potential, contrary to the mass-spectrometer in the night experiment of 1960, alongside with neutral particles it recorded atmospheric ions, passing freely the ion source region. This resulted in the fact that neutral atomic oxigen could be found inspectrogrammes only of the 130 to 160 km altitudes, and at 160 to 430 km

Declassified in Part - Sanitized Copy Approved for Release 2011/12/08 : CIA-RDP80T00246A016600420001-1

Declassified in Part - Sanitized Copy Approved for Release 2011/12/08 : CIA-RDP80T00246A016600420001-1

the main part of the ion current was produced by atomic oxygen atmosphere ions. In the altitude range I30-I60 km O_I and N_2 ion currents ratios are equal in both experiments. This testifies to the fact, that in view of different analysers designs atomic oxigen relative concentration at the I30-I60 km altitude is slightly higher in the day experiment, than in the night one. The aim of the further treatment of the day experiment materials is quantitative verification of O_I, O_2 and N_2 relative concentrations values.

As to atomic nitrogen N_I, its concentration in the night atmosphere at the I00-2I0 km altitude does not prevail I-2% of N_2 concentration.

According to the extrapolation computations, made on the basis of the obtained data by means of the barometric formulae N_2 plays the predominant role in atmosphere density up to about 280 km where the equality of densities $\rho(N_2) = \rho(O_1)$ is observed.

Minor admixtures in the atmosphere

Helium. In the limits of the apparatus sensitivity after the opening of the analysers neutral He was recorded in no spectra, what allows to affirm, that at the altitudes above I00km He concentration does not prevail 6×10^7 particles/cm^3.

H_2O, OH, H_I and H_2 According to the night experiment data H_2O ion current variation pattern decreases with height and is symmetrical relative to the top.

Declassified in Part - Sanitized Copy Approved for Release 2011/12/08 : CIA-RDP80T00246A016600420001-1

Declassified in Part - Sanitized Copy Approved for Release 2011/12/08 : CIA-RDP80T00246A016600420001-1

As can be seen from Fig.4 H_2O ion current modulation, produced by the change of inlet position relative to the contrary inflow is slightly pronounded in comparision with N_2(Fig.3). This points to the fact, the apparatus records mainly H_2O, carried to the upper atmosphere layers on the container surface. The maximum value of H_2O partial pressure in the upper atmosphere, estimated according to the ion current modulation depth does not prevail $3 \cdot 10^{-7}$ mm mercury column at the II5 km altitude, or 0,6% of the total atmosphere pressure. This value must be cosidered as the upper boundary of H_2O content in the atmosphere, as ion current modulation can be produced mainly due to the increase of the number of H_2O reflected molecules, entering the analyser when the latter changes its orientation relative to the contrary flow.

Hydroxile OH recorded by the mass-spectrometer with the accuracy to the measurements errors is produced by H_2O dissociation in the ion source of the apparatus, what is confirmed by the agreement of laboratory and flight ion current ratios values $J(OH)/J(H_2O)$.

Thus, assuming the measurements error value to be the upper limit of OH content in the atmosphere, we find, that the content of hydroxile OH at the altitudes above I00 km does not prevail $6 \cdot 10^{-3}$% of the total atmosphere pressure.

H_I ion current pattern has analogous with H_2O and OH character of variation with height, what points to the dissociative connection of H_I and H_2O (Fig.4).

However, beginning from I45 km H_I ion current decreases

Declassified in Part - Sanitized Copy Approved for Release 2011/12/08 : CIA-RDP80T00246A016600420001-1

Declassified in Part - Sanitized Copy Approved for Release 2011/12/08 : CIA-RDP80T00246A016600420001-1

slower, than it is necessary for maintaining laboratory relation of ion currents $J(H_2O) : J(OH) : J(H_1)$ H_I concentration at the altitudes above 150 km, corresponding to excess ion current, is about 10^8 particles/cm^3. This excess of H_I does not contradict to the explanation of its existence by atmosphere hydrogen, but final conclusions demand some additional experiments to be performed. Apparently atomic hydrogen H_I recombination inside the analyser fully accounts for the formation of molecular hydrogen H_2, found at the altitudes up to 130km, what is backed by H_I and H_2 ion courrents correlation. As a result of this, in the absence of H_2 in the spectra at the altitudes above 130 km, the upper limit of H_2 concentration in the atmosphere above 100 km will give the value of $3 \cdot 10^7$ particles/cm^3.

NO. At the 130-180 km altitudes during the night sounding there was recorded negligible quantity of neutral nitrogen oxide NO. Its concentration did not prevail 0,1% of N_2 concentration.

As the appreciable part of NO^+ ions could be formed inside the analyser as a result of charge-transfer reactions of the following type: $O^+ + N_2 = NO^+ + N$, the given value can be considered to be only the upper limit of NO concentration in the atmosphere at the 130-180 km altitude.

Atmospheric admixture of extra-terrestrial origin.

During the night experiment ascent and descent of the rocket at the 103-126 km altitudes there was detected gas with mass number 42 , indentified with the oxide of Mg isotope, i.e. $Mg^{26}O$. The oxides of 2 other isotopes with mass numbers 40 and 41 cannot be singled out on the spectrogrammes due to the following reasons:

Declassified in Part - Sanitized Copy Approved for Release 2011/12/08 : CIA-RDP80T00246A016600420001-1

Declassified in Part - Sanitized Copy Approved for Release 2011/12/08 : CIA-RDP80T00246A016600420001-1

The ion peak of the main oxide $Mg^{24}O$ was recorded simultaneonsly with Ar ion current, which was an order of madnitude more than $Mg^{24}O$ amplitude. And $Mg^{25}O$ ion peak coinsided with negative impulse from Ar ion peak /due to the amplifier super correction/.

$Mg^{26}O$ and N_2 relative concentrations variation is shown in Fig.5. Absolute concentration of all Mg oxides, obtained with the consideration of their relative distribution is equal to about $I \cdot IO^9$ particles/cm^3 at the I03-I26 km altitudes. Stone meteors, where MgO content can be up to 40,2% of the total weight, are apparently, the atmosphere source of MgO /9/. At the same time stone meteors comprise the main part /86%/ of all meteors, reaching the Earth /IO/ from the point of view of their weight.

MgO can be formed in the atmosphere in two ways. One part of the molecules originates as a result of direct meteor evaporation and the other - when vaporised Mg atoms oxidize in the atmosphere.

Therefore the absence of metallic Mg in the spectrogrammes is explained both by very small (0,03%) quantity of Mg in metallic phase in meteor substance content (II) and by the existence of considerable quantities of atomic oxigen , with which free Mg can combine at the I03-I26 km altitudes.

$Mg^{26}O$ relative concentration decrease above II7-II8 km is in agreement with gravitational separation of gases at the altitudes above I05-II0 km. The decrease of relative concentration below II7 km can be accounted for by the existence of an extensive layer transitive from the atmosphere with

Declassified in Part - Sanitized Copy Approved for Release 2011/12/08 : CIA-RDP80T00246A016600420001-1

Declassified in Part - Sanitized Copy Approved for Release 2011/12/08 : CIA-RDP80T00246A016600420001-1

the diffusion pattern of mixing of the gases.

In this transition layer the gravitational separation which is just beginning is partially disturbed by separate flows from the turbulent atmosphere, laying below. As to MgO, this circumstance leads to the fact, that MgO concentration in this transition layer from 105-110 km to 117-118 km will decrease on the account of partial mixing with the atmosphere layer, situated below the layer of total meteor evaporation and therefore not containing MgO.

The author is greatful to B.A.Mirtov for the usefull discussion, A.A.Perno, R.F.Starostina and G.I.Podsoblyayeva for their help in the experiment procession and treatment of the material.

Declassified in Part - Sanitized Copy Approved for Release 2011/12/08 : CIA-RDP80T00246A016600420001-1

Declassified in Part - Sanitized Copy Approved for Release 2011/12/08 : CIA-RDP80T00246A016600420001-1

Fig.I - Ar and N_2 ion currents ratio variation with height. I and 2 - ascent and descent of the flight (night,I960), 3 - ascent (day,I96I).

Fig.2 - Variation of N_2, O_I, O_2 and Ar neutral gases ion currents on the ascent during the day experiment of I96I.

Fig.3 - I - N_2 ion current variation with height of the ascent with different orientations of the mass-spectrometer (night,I960) 2 - N_2 pressure variation in the atmosphere counted according to the barometric formulae.

Fig.4 - H_2O, OH, H_I and H_2 ion currents variation with height (time) on the ascent of the flight.

Fig.5 - $Mg^{26}O$ relative concentration variation with height on the ascent and descent of the flight.

Declassified in Part - Sanitized Copy Approved for Release 2011/12/08 : CIA-RDP80T00246A016600420001-1

Declassified in Part - Sanitized Copy Approved for Release 2011/12/08 : CIA-RDP80T00246A016600420001-1

R E F E R E N C I E S

1. A.A.POKHUNKOV - Iskusstvennye sputniki zemli, ed.12, 1962, (in print)
2. A.I.REPNEV - Trudy TS A O, ed. 29, 66-73, 1960.
3. A.A.POKHUNKOV - Izvestija AN SSSR, ser. geofiz., No.11, 1649-1657, 1960.
4. A.A.POKHUNKOV - Iskusstvennye sputniki zemli, ed. 7, 89-100, 1961.
5. E.B.MEADOWS and J.W.TOWNSEND - Proc. of the first Internat. Space Science Symposium, Nice, 175-198, 1960.
6. E.B.MEADOWS and J.W.TOWNSEND - J.of Geophys. Res., v. 61, 576, 1956.
7. B.A.MIRTOV -Gazovyi sostav atmosphery zemli. Izd.ANSSSR 1961.
8. G.SIBORG,I.PERLMAN, G.KHOLLENDER - Tablitsa izotopov, I.L. Moskva, 1956.
9. L.G.KVASHA- Meteoritika, ed.14, 75-85, 1956.
10. B.U.LEVIN, S.V.KOZLOVSKAJA, A.G.STARKOVA - Meteoritika, ed. 14, 38-53, 1956.
11. .NODDACK - J. u. W. Naturwissenschaft, Heft 35, 757-764, 1930.

Declassified in Part - Sanitized Copy Approved for Release 2011/12/08 : CIA-RDP80T00246A016600420001-1

Declassified in Part - Sanitized Copy Approved for Release 2011/12/08 : CIA-RDP80T00246A016600420001-1

Таблица I.

15Nov. 1961 16h00m. l.t.		23 September 1960, 0h56m loc. time.						
h Km	T °K	T °K	$n(N_2)$ cm^{-3}	$n(O_2)$ cm^{-3}	$n(O_1)$ cm^{-3}	M a.m.u.	p mm. Hg.	ρ $gm.cm^{-3}$
100		215	$7,4.10^{12}$	$1,8.10^{12}$	$6,8.10^{11}$	27,9	$2,5.10^{-4}$	$4,9.10^{-10}$
110		265	$1,7.10^{12}$	$4,0.10^{11}$	$2,1.10^{11}$	27,6	$6,4.10^{-5}$	$1,1.10^{-10}$
120		325	$4,8.10^{11}$	$1,1.10^{11}$	$7,9.10^{10}$	27,2	$2,3.10^{-5}$	$3,1.10^{-11}$
130	600	395	$1,7.10^{11}$	$3,8.10^{10}$	$3,5.10^{10}$	26,9	$1,0.10^{-5}$	$1,1.10^{-11}$
140	770	490	$7,6.10^{10}$	$1,6.10^{10}$	$1,9.10^{10}$	26,5	$6,7.10^{-6}$	$5,0.10^{-12}$
150	900	600	$3,6.10^{10}$	$7,3.10^{9}$	$1,1.10^{10}$	26,1	$4,3.10^{-6}$	$2,3.10^{-12}$
160	1000	715	$1,9.10^{10}$	$3,6.10^{9}$	$6,5.10^{9}$	25,8	$2,7.10^{-6}$	$1,2.10^{-12}$
170	1140	785	$1,1.10^{10}$	$2,1.10^{9}$	$4,4.10^{9}$	25,5	$1,8.10^{-6}$	$7,5.10^{-13}$
180	1170	825	$7,3.10^{9}$	$1,3.10^{9}$	$3,2.10^{9}$	25,1	$1,2.10^{-6}$	$4,9.10^{-13}$
190	1190	860	$5,0.10^{9}$	$8,0.10^{8}$	$2,5.10^{9}$	24,9	$7,3.10^{-7}$	$3,4.10^{-13}$
200	1250	895	$3,3.10^{9}$	$5,0.10^{8}$	$1,9.10^{9}$	24,4	$5,3.10^{-7}$	$2,4.10^{-13}$
210	1290	925	$2,3.10^{9}$	$3,2.10^{8}$	$1,5.10^{9}$	24,1	$3,8.10^{-7}$	$1,6.10^{-13}$
250	1360							
300	1560							

Declassified in Part - Sanitized Copy Approved for Release 2011/12/08 : CIA-RDP80T00246A016600420001-1

Declassified in Part - Sanitized Copy Approved for Release 2011/12/08 : CIA-RDP80T00246A016600420001-1

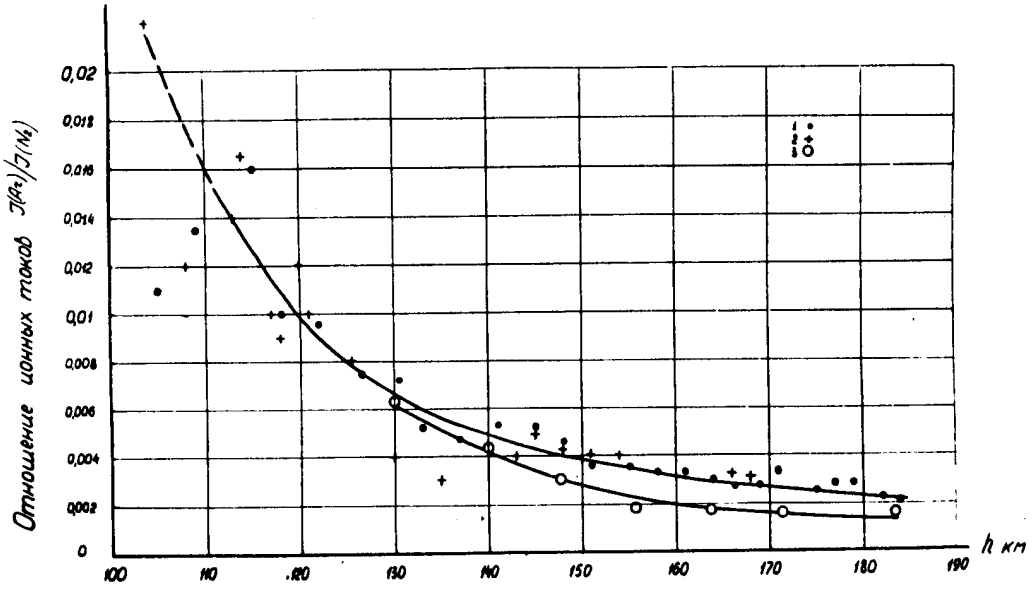

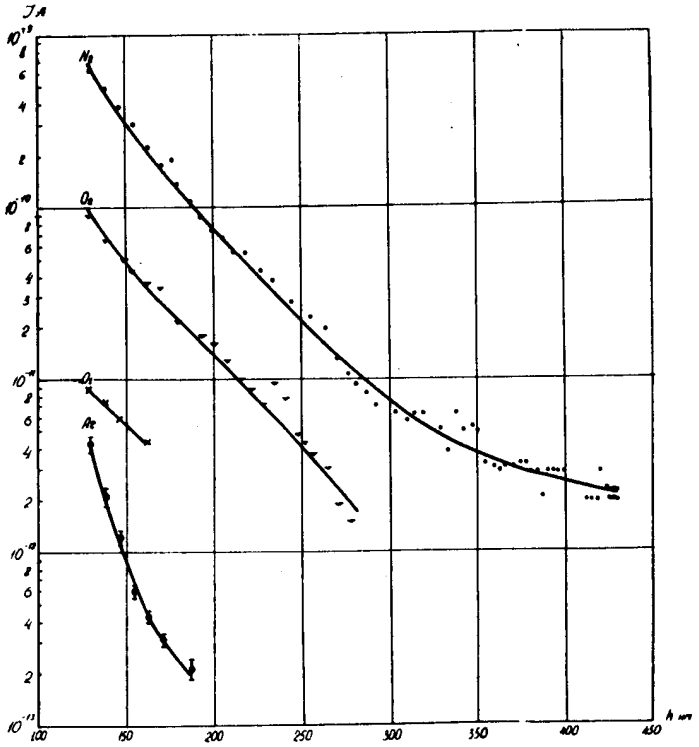

Declassified in Part - Sanitized Copy Approved for Release 2011/12/08 : CIA-RDP80T00246A016600420001-1

Declassified in Part - Sanitized Copy Approved for Release 2011/12/08 : CIA-RDP80T00246A016600420001-1

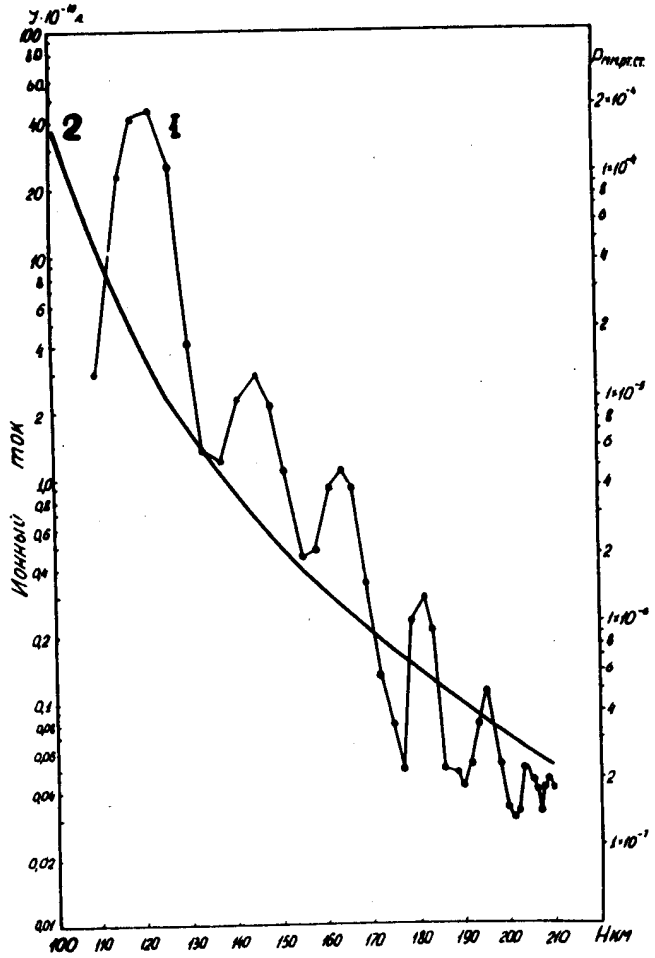

Declassified in Part - Sanitized Copy Approved for Release 2011/12/08 : CIA-RDP80T00246A016600420001-1

Declassified in Part - Sanitized Copy Approved for Release 2011/12/08 : CIA-RDP80T00246A016600420001-1

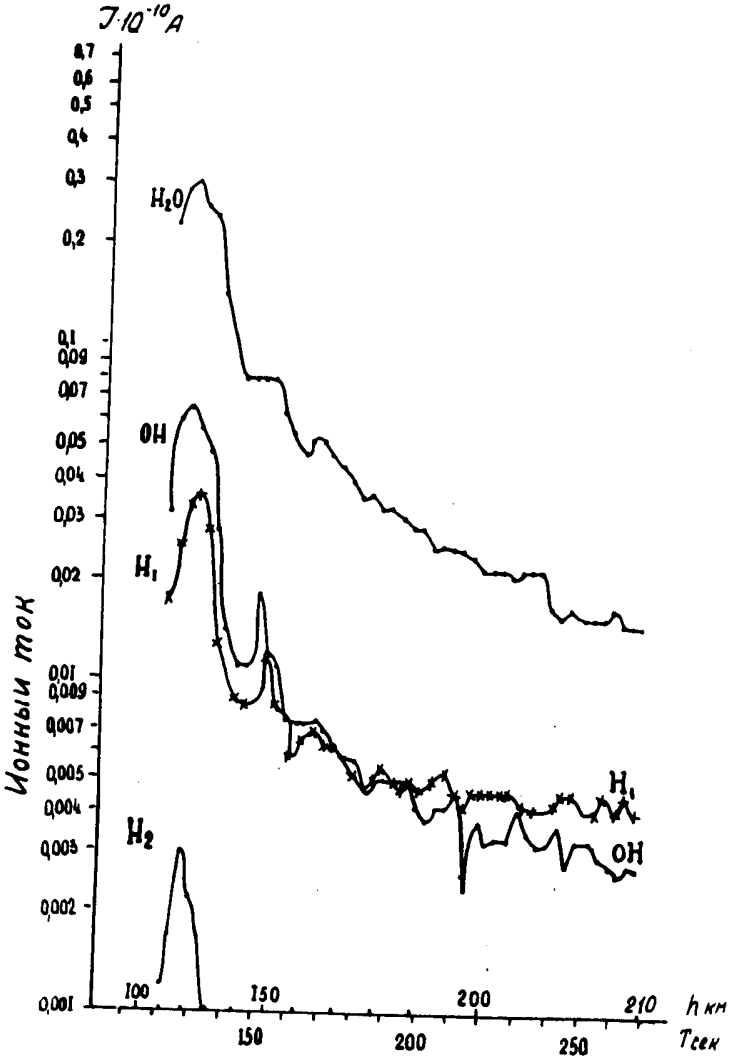

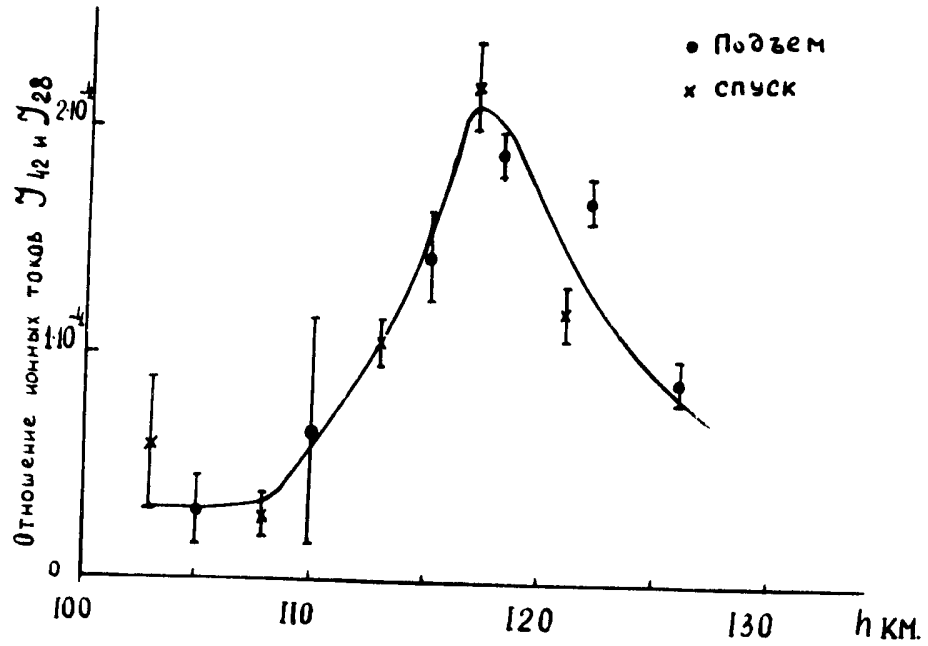

Declassified in Part - Sanitized Copy Approved for Release 2011/12/08 : CIA-RDP80T00246A016600420001-1

Declassified in Part - Sanitized Copy Approved for Release 2011/12/08 : CIA-RDP80T00246A016600420001-1

7. "ON EFFECTS PRODUCED BY A BODY MOVING FAST IN PLASMA"

by Y.L.Alpert, A.V.Gurevich and L.P.Pitayevsky (English) (9 pp)

Summary I.

1. Particle Concentration Disturbance and the Electric Field in the Vicinity of the Body.

The work presented deals with a theoretical investigation of electromagnetic disturbances caused by a body, for instance, by an artificial Earth satellite, moving in a plasma (the ionosphere). The indicated problem is of considerable interest for two causes.

Firstly, during measurements of the gas density, ion and electron concentration, of the electric field, the temperature and other parameters of the undisturbed medium by means of artificial satellites or space probes around the body surface, it is necessary to have an idea on disturbances of these values caused by the body itself, which, as we shall see, can be very large and extend at a large (in comparison with the body dimensions) region.

Secondly, of great interest is the investigation of the electromagnetic wave scattering on the perturbed region -- on the "trail" of the body which is carried together with the body along its orbit.

It should be also borne in mind that problems connected

Declassified in Part - Sanitized Copy Approved for Release 2011/12/08 : CIA-RDP80T00246A016600420001-1

Declassified in Part - Sanitized Copy Approved for Release 2011/12/08 : CIA-RDP80T00246A016600420001-1

with the body motion in a rarefied plasma are very peculiar and by themselves are of theoretical interest.

The satellite motion in a rarefied medium has been investigated by several authors. However, the majority of the authors were interested only in the calculation of the friction force acting on the body (1). In some works the structure of the disturbed zone was studied (Kraus and Watson (2), Rand (3)), and only for the case of a weakly charged body with dimensions small as compared with the Debye radius. That is why their results have no direct relation with the motion of actual satellites in the ionosphere. Besides, using the perturbation theory these authors dropped the term of the second approximation essential in this case. Therefore their results are incorrect at large distances from the body.

In our works we studied directly electromagnetic effects produced under actual conditions by a satellite moving in plasma (4-7). Some of the results obtained are given below. In this complex of problems of great interest is calculation of a particle flux in the vicinity of the body. Besides, the case is important when the body velocity becomes commensurate with the thermal velocity of particles or lower than it, and the body dimensions become commensurate with the Debye radius, when the effect of the electric field is especially significant. This takes place at the transition into interplanetary space. However, the results of the analysis of this problem have not been considered here.

Declassified in Part - Sanitized Copy Approved for Release 2011/12/08 : CIA-RDP80T00246A016600420001-1

Declassified in Part - Sanitized Copy Approved for Release 2011/12/08 : CIA-RDP80T00246A016600420001-1

The body motion in the upper atmosphere usually takes place in conditions when the particle free paths are large as compared to the body dimensions, and the body interacts with neutral molecules and atoms, ions and electrons. Since it moves with a hypersonic velocity $V_0 \gg \sqrt{\frac{8\kappa T}{\pi M}}$ where $\sqrt{\frac{8\kappa T}{\pi M}} = \bar{v}_T$ is the mean thermal velocity of ions and neutral particles, their concentrations around the body are considerably perturbed.

In front of the body naturally an excess of particles appears due to reflection of the incident flux from the body surface. The "condensation region" is formed here.

On the rear of the body, to the contrary, the rarefaction region is formed since the body "sweeps out" the particles and the latter have not enough time to fill this region completely, since Vt << Vo. Partial filling of the rarefaction region takes place differently for neutral particles, ions and electrons. Neutral particles fill the swept out zone due to particles falling from the outside with transversal velocities on the order of the thermal velocity. Due to the outer magnetic field effect which takes place in the ionosphere and also due to the influence of the electric field which is formed, ions and electrons fill the rarefied region in a more complicated way. The electric field effect for ions is not decisive in this case, since the energy of incident particles is on the order of $Mv_0^2 \gg \kappa T$ that is considerably exceeds their thermal energy $e\varphi \sim \kappa T$ On the contrary, the electron distribution is fully

Declassified in Part - Sanitized Copy Approved for Release 2011/12/08 : CIA-RDP80T00246A016600420001-1

Declassified in Part - Sanitized Copy Approved for Release 2011/12/08 : CIA-RDP80T00246A016600420001-1

determined by the electric field and for them the Boltzmann distribution is always true. The main influence on ion filling is exerted by the outer magnetic field which retains particles hindering the filling of the rarefied region by ions. The character of the filling and the rarefaction region dimensions essentially depend on the angle between the body motion velocity Vo and the magnetic field vector $\vec{H}_0$.

The solution of the above mentioned problems requires kinetic consideration, since it is meant that the particle freepath Λ is much larger than the linear dimensions of the body Ro. In the coordinate system connected with the moving body the particle distribution is stationary and is described by kinetic equations

$$\vec{v}\frac{\partial f_M}{\partial \vec{r}} - \frac{1}{M}\frac{\partial U}{\partial \vec{r}}\frac{\partial f_M}{\partial \vec{u}} = 0 \qquad (1)$$

$$\vec{v}\frac{\partial f_e}{\partial \vec{r}} - \left\{\left(\frac{e}{m}\frac{\partial \varphi}{\partial \vec{r}} + \frac{1}{m}\frac{\partial U}{\partial \vec{r}}\right) - \frac{e}{mc}\left[\vec{H},\vec{v}+\vec{v}_0\right]\right\}\frac{\partial f_e}{\partial \vec{u}} = 0 \qquad (2)$$

$$\vec{v}\frac{\partial f_i}{\partial \vec{r}} - \left\{-\frac{e}{M}\frac{\partial \varphi}{\partial \vec{r}} + \frac{1}{M}\frac{\partial U}{\partial \vec{r}} + \frac{e}{Mc}\left[\vec{H},\vec{v}+\vec{v}_0\right]\right\}\frac{\partial f_i}{\partial \vec{u}} = 0 \qquad (3)$$

In equations (1)-(3) $f_M(\vec{r},\vec{u})$, $f_e(\vec{r},\vec{u})$ and $f_i(\vec{r},\vec{u})$ are distribution functions of neutral particles, electrons and ions, e is the electron and ion charge, m and M are electron and ion masses, $\varphi=\varphi(\vec{r})$ is the electric field potential, H is the outer magnetic field $U=U(r-V_0t)$ is the potential energy of the interaction of particles with the body surface $\vec{u}=\vec{v}+\vec{v}_0$. At infinity naturally f_M, f_i and fe are Maxwellean functions. The electric field, which is formed due to the difference in electron and ion concentrations in the disturbed zone, is defined by the Poisson equation, $\Delta\varphi = 4\pi e\left(\int f_e(\vec{r},\vec{u})d^3u - \int f_i(\vec{r},\vec{u})d^3u\right)$ with boundary conditions.

Declassified in Part - Sanitized Copy Approved for Release 2011/12/08 : CIA-RDP80T00246A016600420001-1

Declassified in Part - Sanitized Copy Approved for Release 2011/12/08 : CIA-RDP80T00246A016600420001-1

Neutral Particle Disturbance

The distribution of neutral particles is determined by equation (1). Its solution is obtained for mirror and diffuse reflections of particles from the surface. For the density behind the sphere of radius Ro distribution $\frac{n_M(\rho,z)}{n_{M_0}}$ is obtained presented in Fig.1 for $\sqrt{\frac{MV_0^2}{2KT}}=8$. As seen from the figure, the extended rarefaction region is formed here, in which $z \sim 10R_0$ before the distance $n_M \leq 0{,}5 n_{M_0}$ is reached. The dependence of the particle density in the condensation region in front of the body for different ρ and z at mirror reflection is shown in Fig.2. It is seen from the figure that close to the body surface the neutral particle concentration is increased two-fold at a distance 0.2 Ro from the body surface $\frac{n}{n_{M_0}} = 1.5$ and at a distance of a radius $\frac{n}{n_{M_0}} = 1.1$. With the increase of the distance from the body surface the concentration disturbances in the condensation region decrease more rapidly than in the rarefaction region.

The particle concentration distribution in the condensation region at diffuse scattering is shown in Fig.3. In this case the reflected particle concentration near the body surface is much higher than in the case of a secular reflection. Let us note that since the velocity of the incident particle flux is much larger than the thermal velocity, the collisions of particles filling the rarefied region with the body surface are of little probability and at large distances they weakly affect the particle concentration.

Declassified in Part - Sanitized Copy Approved for Release 2011/12/08 : CIA-RDP80T00246A016600420001-1

Declassified in Part - Sanitized Copy Approved for Release 2011/12/08 : CIA-RDP80T00246A016600420001-1

This means that the concrete shape of the body in the rarefied zone at distances $z >> Ro$ is insignificant, of importance is only the shape of maximum body cross-section in the plane orthogonal to the incident stream. Corresponding calculations for the body with a cross-section S lead to a very simple and graphical formula

$$n_M(\rho,z)=n_{M_0}\left(1-\frac{SMv_0^2}{2\pi\kappa T}\frac{1}{z^2}\exp\left(-\frac{Mv_0^2}{2\kappa T}\frac{\rho^2}{z^2}\right)\right) \qquad (5)$$

Ion and Electron Disturbances

The set of equations (2-4) describes the ion and electron distribution functions and the electric field. In the general case it is very complex. However, taking into account that the Maxwell-Boltzmann distribution is true for electrons it can be solved

$$N_e(\vec{r},\vec{u})=N_0\left(\frac{M}{2\pi\kappa T}\right)^{3/2}\exp\left(-\frac{Mu^2+e\varphi(r)}{2\kappa T}\right),$$

For ions as the first approximation the electric field effect can be ignored.

With the magnetic field taken into account when $\vec{v}_0 \parallel \vec{H}$ for a circular cross-section of the body of radius Ro in the plane perpendicular to the direction of the motion we obtain for the ion concentration in the rarefied zone

$$N_i(\rho,z)=N_{i0}-2N_{i0}\exp\left\{-\frac{\rho^2}{(2\rho_H\sin\frac{\Omega_H z}{2v_z})^2}\right\}\int_{R_0/2\rho_H|\sin\frac{\Omega_H z}{2v_z}|}^{\infty} ue^{-u^2}I_0\left(\frac{\rho u}{\rho_H|\sin\frac{\Omega_H z}{2v_z}|}\right)du. \qquad (6)$$

Here $\Omega_H=\frac{eH}{MC}$ is the gyromagnetic frequency $\rho_H=\frac{c}{eH}\sqrt{\kappa TM}$ is the average Larmor ion radius, Io is the Bessel function from an imaginary argument. From formula (6) is evident that in the close zone the magnetic field effect is of little importance as it should be. At $z > \frac{v_0}{\Omega_H}$ the

Declassified in Part - Sanitized Copy Approved for Release 2011/12/08 : CIA-RDP80T00246A016600420001-1

Declassified in Part - Sanitized Copy Approved for Release 2011/12/08 : CIA-RDP80T00246A016600420001-1

magnetic field effect is, to the contrary, very great $N_i(\rho,z)$ is a periodic function z with a period $\tau_z = \frac{2\pi v_0}{\Omega_H}$. In Fig.4 corresponding curves of equal values $N_i(\rho,z)/N_{io}$ are shown for Ro-ρn and $\sqrt{\frac{MV_0^2}{2KT}} = 8$. In this case the variation period $\frac{\Delta N_i}{N_{io}}$ expressed in radii of the sphere Ro, is equal to 50.24. When the body moves orthogonally to $\vec{H}_0$ ($\vec{H}_0 \perp \vec{v}_0$) the structure of the disturbed zone is more complicated. The dependence of surfaces $\frac{N_i}{N_{io}} = 0.8$ for $\rho_H = 0.3$ Rx and $\frac{N_i}{N_{io}} = 0.93$ for $\rho_H = R_x$ on x, y, z for the body of a square cross-section, when $\sqrt{\frac{MV_0^2}{2KT}} = 8$ is shown in Fig. 5, 6. In contrast to the case of the longitudinal body motion ($\vec{v}_0 \parallel \vec{H}$) the disturbance does not remain constant and decreases with distance as $\frac{1}{z}$. Let us remind here that in the case when $H = 0$ $\frac{\Delta N_i}{N}$ decreases with distance proportionally to $\frac{1}{z^2}$, while at $\vec{H} \parallel \vec{v}_0$ the ratio $\frac{\Delta N_i}{N_{io}}$ does not decrease at all with the increase of distance when the collision frequency $\nu = 0$.

The Electric Field Around the Body.

Using the Boltzmann distribution for the electron density we have the equation for the potential $\varphi(z)$ around the body

$$\Delta\varphi(\vec{r}) = -4\pi e N_0 \left(\frac{N_i(\vec{r})}{N_0} - \exp\left[-\frac{e\varphi(\vec{r})}{KT} \right] \right), \qquad (7)$$

where $N_i(\vec{r}) = \int f_i \, d^3u$ is the ion density, No is the undisturbed electron density. Since we consider the case when Ro >> D (D is the Debye radius), the solution of (7) gives the following expressions for $\varphi(z)$ with an accuracy to the terms on the order of $\frac{1}{\ln A}$ in the vicinity of the body

Declassified in Part - Sanitized Copy Approved for Release 2011/12/08 : CIA-RDP80T00246A016600420001-1

Declassified in Part - Sanitized Copy Approved for Release 2011/12/08 : CIA-RDP80T00246A016600420001-1

and with an accuracy on the order of $\frac{1}{A}$ at a large distance from the body ($A = \frac{Ro}{D}$)

$$\varphi(\vec{r}) = \begin{cases} \frac{\kappa T}{e} \ln \frac{N_0}{N_i(\vec{r})} & \text{at } \frac{N_i(\vec{r})}{N_0}\left(\frac{R_0}{D}\right)^2 \geq 1, \\ \frac{\kappa T}{e} \ln A & \frac{N_i(\vec{r})}{N_0}\left(\frac{R_0}{D}\right)^2 \leq 1. \end{cases} \quad (8)$$

The distribution of the potential in the vicinity of a spherical body determined by formula (8) is shown in Fig.7. Since in the ionosphere $\ln A \sim 10$, the potential φ in the maximum rarefaction region is by an order of magnitude greater than $\frac{\kappa T}{e}$ i.e. $\varphi \sim 1$ volt. In front of the body φ, to the contrary, is only of the order of $\frac{\kappa T}{e}$ i.e. $\varphi \sim 0{,}05 \div 0{,}1$ volt.

Results of the calculation of $\varphi(z)$ for the body with a metallic surface are presented in Fig.8. From the figure is evident that the φ potential variation close to the surface (in the region of maximum rarefaction) has changed considerably as compared to the case of the reflecting sphere, as it should be. However, the maximal value of φ is, as before, $\frac{\kappa T}{e} \ln A$. It is reached not close to the surface of the sphere, but at a distance on the order of Ro from it.

The electric field which is formed due to the plasma disturbance caused by the moving body is calculated above ignoring the reverse effect of the electric field on the perturbation, i.e. on the ion motion. Actually this is of course true only to a first approximation. It stands to reason that the electric field affects the ion motion. However, as already indicated above, due to a large ion velocity with respect to the body, this influence is not predominant or the problem considered here, since $MV_0^2 \gg e\varphi(z)$.

We have shown that with a strict account of the electric field in the general case, when $H = 0$, the ion density

Declassified in Part - Sanitized Copy Approved for Release 2011/12/08 : CIA-RDP80T00246A016600420001-1

Declassified in Part - Sanitized Copy Approved for Release 2011/12/08 : CIA-RDP80T00246A016600420001-1

disturbance decreases at a large distance from the body proportionally to $\frac{1}{z^2}$, which coincides with the results obtained above without the electric field taken into account. This shows, in particular, that the results of Kraus and Watson (2) who obtained the decrease $\sim \frac{1}{z^3}$ are erroneous.

Declassified in Part - Sanitized Copy Approved for Release 2011/12/08 : CIA-RDP80T00246A016600420001-1

Declassified in Part - Sanitized Copy Approved for Release 2011/12/08 : CIA-RDP80T00246A016600420001-1

8. "ON EFFECTS PRODUCED BY A BODY MOVING FAST IN PLASMA"

Y.L.Alpert, A.V.Gurevich and L.P.Pitayevsky

Summary II

II. Radio Wave Scattering on the Body "Trail"

The electron inhomogeneity which is produced around the body leads to the scattering of incident radio waves. The structure of the scattered electromagnetic wave field changes in a complex manner depending on the angle between the incident wave and the direction towards the observer, on the angle between the magnetic field and the body motion direction, on the wavelength and plasma parameters.

At the scattering the body rarefaction region plays the greatest role. Due to the influence of the outer magnetic field, as we have seen, for instance, in the case of the motion along the field, the rarefaction region is of a cylindrical form with a periodically changing surface $N(z) = \text{const}$. Along the magnetic field the length of this formation is on the order of the ion free path. Its transversal dimension is on the order of the linear dimensions of the body Ro or the ion Larmor radius $\rho_H = \frac{v_0}{eH/Mc}$.

Since cases of artificial satellite or rocket motions in the ionosphere or interplanetary medium which are of actual interest to us correspond to the case

$$\Lambda \gg R_0 , \qquad (1)$$

Declassified in Part - Sanitized Copy Approved for Release 2011/12/08 : CIA-RDP80T00246A016600420001-1

Declassified in Part - Sanitized Copy Approved for Release 2011/12/08 : CIA-RDP80T00246A016600420001-1

the theoretical calculation requires the solution of the kinetic problem. Keeping in mind that frequencies usually used satisfy the condition

$$\omega \gg \omega_H \tag{2}$$

(where $\omega_H = \frac{eH}{mc}$ is the electron Larmor frequency) we can assume

$$\varepsilon = 1 - \frac{4\pi N e^2}{m\omega^2} = 1 - \frac{\omega_0^2}{\omega^2}, \qquad \delta\varepsilon = -\frac{\omega_0^2}{\omega^2}\delta N(z) \tag{3}$$

and use the perturbation method for the calculation of the scattering at distances larger than the wavelength. The electric field of the scattered wave E' and the effective scattering cross-section in the element of the body angle dO are as follows:

$$E' = \frac{e^2}{m\omega^2\varepsilon}\,\frac{e^{iKR}}{R}\left[\bar{K}'\left[\bar{K}'\bar{E}_0\right]\right] N\bar{q} \tag{4}$$

$$\sigma = \frac{1}{16\pi^2\varepsilon^2}\left(\frac{\omega_0}{\omega}\right)^4 \frac{(Nq)^2}{N_0^2} K^4 \sin^2\psi_1\, dO \tag{5}$$

In formulae (4) and (5) $\bar{E}_0$ and $\bar{K}$ are the electric field amplitude and the wave vector of the incident wave, respectively, $\bar{K}'$ is the wave vector of the scattered wave, ψ_1 is the angle between $\bar{k}'$ and $\bar{E}_0$, No is the undisturbed electron density

$$N_q(q) = \int \delta N(\bar{z}) \exp(-i\bar{q}\bar{z})\, d^3z, \tag{6}$$

the Fourier-component of the electron disturbance $\delta N(z)$,

$$\bar{q} = \bar{K}' - \bar{K}, \qquad |q| = 2K\sin\frac{\psi}{2} \tag{7}$$

ψ is the scattering angle (between $\bar{K}$ and $\bar{K}'$) and d^3z is the volume element.

The N_q function can be determined in a more straightforward way directly from the kinetic equation. This makes it possible to solve the problem stricter and to take into account the influence of the electric field and the collision frequency

Declassified in Part - Sanitized Copy Approved for Release 2011/12/08 : CIA-RDP80T00246A016600420001-1

Declassified in Part - Sanitized Copy Approved for Release 2011/12/08 : CIA-RDP80T00246A016600420001-1

between particles which considerably affect the scattering at distances from the body larger than its dimensions. This region makes the greatest contribution to scattering.

Let us determine the ion distribution function with respect to velocities $\bar{u}$ and coordinates $\bar{r}$ in the form:

$$\left.\begin{aligned} f(\bar{u},\bar{r}) &= f_0(u) + f'(\bar{u},r) \\ f_0(\bar{u}) &= N_{i_0}\left(\frac{M}{2\pi\kappa T}\right)^{3/2} \exp\left(-\frac{Mu^2}{2\kappa T}\right) \end{aligned}\right\} \qquad (8)$$

Due to the fact that the body velocity is much lower than the electron velocity ($v_0 << \sqrt{\frac{kT}{m}}$), the electron density is expressed by the Boltzmann formula:

$$N(r) = N_0 \exp\left[\frac{e\varphi(r)}{\kappa T}\right]. \qquad (9)$$

As a result of this, N_q calculation reduces to the solution of the kinetic equation for ions and the Poisson equation which are written in the coordinate system, where the body is at rest in the form:

$$\left.\begin{aligned} &i\bar{q}(\bar{u}-\bar{v}_0)f_{\bar{q}} + \frac{e}{Mc}[\bar{u}H_0]\frac{\partial f_q}{\partial u} + \nu f_q - \frac{f_0}{N_0}\int f_q d^3u + \frac{e}{\kappa T} f_0 \cdot i\bar{q}\bar{u}\varphi_{\bar{q}} = \mathcal{J}(u)\Phi(qR_0,\cos\theta), \\ &q^2\varphi_{\bar{q}} = 4\pi e\left\{\int f_q d^3u - N_{\bar{q}}\right\}, \\ &N_{\bar{q}} = \frac{N_0 e}{\kappa T}\varphi_{\bar{q}}, \end{aligned}\right. \qquad (10)$$

where $f_q(\bar{q},\bar{u}) = \int f' e^{-i\bar{q}\bar{r}} d^3r$, $\varphi_q(\bar{q}) = \varphi e^{-i\bar{q}\bar{r}} d^3r$.

The right side of equation (10) has the meaning of "the integral of collisions" of ions with the body and is written in assumption that all incident ions are neutralized by the body (a metallic one). In this case we have:

$$\mathcal{J}(u) = \pi R_0^2 f_0 v_0, \qquad (11)$$

$$\Phi(qR_0,\cos\theta) = 2\int_0^{\pi/2} \sin\vartheta\cos\vartheta\, e^{iqR_0\cos\vartheta\cos\theta}\, \mathcal{J}_0(qR_0\sin\vartheta\sin\theta)\, d\vartheta, \qquad (12)$$

where $\cos\theta = \frac{\bar{q}\bar{V}_0}{qV_0}$ and $\mathcal{J}_0$ is the Bessel function. The effective collision frequency is introduced in such a form

Declassified in Part - Sanitized Copy Approved for Release 2011/12/08 : CIA-RDP80T00246A016600420001-1

Declassified in Part - Sanitized Copy Approved for Release 2011/12/08 : CIA-RDP80T00246A016600420001-1

that the law of particle preservation should not be violated. Then the collision integral Y has the form:

$$Y=-\nu\left(f-\frac{f_0}{N_0}\int f d^3u\right)=-\nu\left(f'-\frac{f_0}{N_0}\int f' d^3u\right) \qquad (13)$$

As a result of the integration of (10) we have ultimately:

$$N_q=\frac{-\pi R_0^2 N_0 V_0}{\Omega}\,\frac{\int_0^\infty \exp\left\{\frac{iq v_0-\nu}{\Omega}x-\frac{\kappa T}{2M\Omega^2}\left(q_z^2x^2+4q_\perp^2\sin^2\frac{x}{2}\right)dx\right\}}{\left[2+\frac{iq v_0-2\nu}{\Omega}\int_0^\infty \exp\left\{\frac{iq v_0-\nu}{\Omega}x-\frac{\kappa T}{2M\Omega^2}\left(q_z^2x^2+4q_\perp^2\sin^2\frac{x}{2}\right)dx\right\}\right]}\,\Phi(qR_0\cos\theta) \qquad (14)$$

where $\Omega=\frac{eH}{Mc}$, q_z and $q_\perp$ are longitudinal and transversal components of $\bar{q}$ relative to the magnetic field $\bar{H}$.

It should be noted that though formula (14) is derived as a general one, the effect of the electric field on the right side of (10) is not taken into account with sufficient consistency and the collision integral is also introduced not rigidly. How essential it is can be found by a stricter analysis which is very difficult to conduct.

Substituting (14) into (5) after some calculations we obtain the differential effective scattering cross-section in the coordinate system connected with the body in the form

$$\sigma(\vartheta_1,\vartheta_2,\varphi)=\left\{\frac{1}{16}\left(\frac{\omega_0}{c}\right)^4\frac{R_0^4v_0^4}{\Omega_H^2}\sin^2\psi_1\right\}F_3'(\alpha,\beta,\gamma,\delta)\cdot\left|\Phi(qR_0,\cos\theta)\right|^2, \qquad (15)$$

where ϑ_1 and ϑ_2 designations are evident from Fig.1, $\bar{q}=\bar{K}'-\bar{K}$ is a bisector of the angle between

$$F_3'(\alpha,\beta,\gamma,\delta)=\frac{F_1'^2+F_2'^2}{(2-2\beta F_1'-\alpha F_2')^2+(\alpha F_1'-2\beta F_2')^2} \qquad (16)$$

$$\left.\begin{aligned}F_1'&=e^{-\delta}\int_0^\infty\cos\alpha x\exp(-\beta x-\gamma x^2+\delta\cos x)dx,\\ F_2'&=e^{-\delta}\int_0^\infty\sin\alpha x\exp(-\beta x-\gamma x^2+\delta\cos x)dx,\end{aligned}\right\} \qquad (17)$$

$$\left.\begin{aligned}&\alpha=\frac{\bar{q}\bar{V}_0}{\Omega_H}=\frac{qV_0}{\Omega_H}(\cos\vartheta_1\sin\vartheta_2+\sin\vartheta_1\cos\vartheta_2\cos\varphi),\quad \beta=\frac{\nu}{\Omega_H},\quad \gamma=\frac{a}{2}\sin^2\vartheta_2,\\ &\delta=\frac{a}{2}\cos^2\vartheta_2,\quad a=\frac{\kappa T}{M\Omega_H^2}q^2,\quad q^2=4\frac{\omega^2}{c^2}\left(1-\frac{\omega_0^2}{\omega^2}\right)\sin^2\frac{\psi}{2}\end{aligned}\right\} \qquad (18)$$

Declassified in Part - Sanitized Copy Approved for Release 2011/12/08 : CIA-RDP80T00246A016600420001-1

Declassified in Part - Sanitized Copy Approved for Release 2011/12/08 : CIA-RDP80T00246A016600420001-1

The main features of the effective scattering cross-section (15) are determined by the scattering function $F_3'(\alpha, \beta, \gamma, \delta)$, which was tabulated by us on an electronic computer for three heights of the ionosphere $z = 300, 400, 700$ km.

Analysis of $F_3(\vartheta_1, \vartheta_2, \varphi)$ shows that depending on angles ϑ_1, ϑ_2 and φ between $\vec{v}_0$ and $\bar{H}$, the normal $\vec{R}$ to $\vec{Ho}$ and $\bar{q}$ and planes $(\vec{v}_0 \vec{H})$ and $(\vec{q} \vec{H})$, $F_3'(\vartheta_1, \vartheta_2, \varphi)$ is a multilobe sharply directed function with the main maximum (0) $\alpha = 0$ at $\vartheta_1 = \vartheta_2 = 0$. Lateral maxima and minima $F_3'(\pm 1 m, \pm 2m \ldots)$ and $(\pm 1$ m, ± 2 m) correspond to the values

$$\alpha_{max} = \pm 1.22, \pm 2.18, \pm 3.15, \pm 4.23$$

$$\alpha_{min} = \pm 0.73, \pm 1.70, \pm 2.91, \pm 3.86$$

As is evident from Fig.2,3 built for the case when $\bar{v}_0 // \bar{H}_0$ $\vartheta_1 = 0$ for $\lambda = 30$ m, $z = 300$ m, $F_3'(\vartheta_2)$ is simmetrical with respect to the value $\alpha_0 = 0$ ($\vartheta_1 = \vartheta_2 = 0$). In this case F_3' does not depend on φ Therefore, the plane $F_3'(\vartheta_2, \varphi)$ is formed as a result of $F_3'(\vartheta_2)$ rotation about the axis $\bar{H}_0$ (Fig.4). When $\vartheta_1 \neq 0$ ($\vec{v}_0$ is not parallel to $\vec{H}$), $F_3'(\vartheta_1, \vartheta_2, \varphi)$ is asymmetrical with respect to ϑ_2 (Fig.5) and depends on φ. The $F_3'(\vartheta_1, \vartheta_2, \varphi)$ surface has already no axial symmetry (Fig.6).

When $\vec{v}_0 // \vec{H}_0$ as can be easily noted, the main maximum of the effective cross-section lies in the direction of the mirror reflection from $\bar{H}_0$, and, when $\vartheta_1 \neq 0$, it is turned with respect to this direction by the angle ϑ_2 determined from the equation $\alpha = 0$. The main maximum (0)

Declassified in Part - Sanitized Copy Approved for Release 2011/12/08 : CIA-RDP80T00246A016600420001-1

Declassified in Part - Sanitized Copy Approved for Release 2011/12/08 : CIA-RDP80T00246A016600420001-1

is the sharpest and considerably exceeds lateral maxima which is evident from Table I. Effective σ values which correspond to the main maximum and their ratio to the overall effective cross-section of an ideally conducting sphere are given in the same Table for different wavelengths and radii of the sphere Ro and also for the day and night ionospheres. At daytime and, in a number of cases, at night, the effective cross-section $\sigma(0,0)$ of the " trail" main maximum considerably exceeds the effective cross-section of the sphere itself reaching many tens and hundreds of square metres. The scattering increases with height in the range of 300-700 km. With the decrease of the wavelength, σ decreases fast and at $\lambda \lesssim 15$ m it is already small. Thus, at the point of observation, as the body approaches, at first the scattered field monotonously increases, then outbursts are observed due to the lateral and main maxima, after which the scattered wave intensity again decreases monotonously. Practically the scattered field is sufficiently large only during several time intervals $\delta t = \frac{\delta z}{v_o}$ For these time intervals sufficiently intense and narrow maxima pass distances $\delta z \sim z\,\delta\theta$ near the Earth where z is the body height, and $\delta\theta$ is the maximum angular width. It is natural that the effect of scattering from the "trail" is revealed only under the condition when it is larger than the scattering effect of the body itself or is equal to it. This takes place when the body moves close to the magnetic field direction . Analysis of the effective scattering

Declassified in Part - Sanitized Copy Approved for Release 2011/12/08 : CIA-RDP80T00246A016600420001-1

Declassified in Part - Sanitized Copy Approved for Release 2011/12/08 : CIA-RDP80T00246A016600420001-1

cross-section has shown that for the region of ionospheric heights considered here the width δz of the square "illuminated" near the Earth's surface by different lobes is $\delta z \sim$(1-9) km, the burst times $\delta t \sim$(0.2-1) sec., and time intervals between individual bursts $\Delta t \sim$ are (3-5) sec. It is natural that if the region where the body flies is irradiated from several points (see Fig.7) at different angles, the time of the action of the trail scattering effect is considerably increased.

Declassified in Part - Sanitized Copy Approved for Release 2011/12/08 : CIA-RDP80T00246A016600420001-1

Declassified in Part - Sanitized Copy Approved for Release 2011/12/08 : CIA-RDP80T00246A016600420001-1

Table 1.

Values of $F_3'(\vartheta_1=0,\ \varphi=0)_{max}$, σ_{max} and $\frac{\sigma}{\sigma_0}$.

λ_M			30			20			15	
z		300:	400:	700	300	400	700	300	400	700
$F'_{3,max}$	/0/	53,46	134,4	1535	11,07	31,05	479,3	4,82	14,10	241,3
- " -	/1/	9,39	13,18	3,18	-	-	-	-	-	-
- " -	/II/	0,89	1,15	0,62	- -	-	-	-	-	-
- " -	/III/	none	0,21	0,25	-	-	-	-	-	-
				Ro = 1 m						
	σ m^2	15	26	30	3	5,6	0,8	1	2	4
day	$\frac{\sigma}{\sigma_0}$	350	590	630	14	25	36	1,6	3	5
	σ m^2	0,05	2,6	4,6	10^{-2}	0,6	1,3	3.10^{-3}	0,2	0,6
night	$\frac{\sigma}{\sigma_0}$	1.1	60	9,6	5.10^{-2}	2,5	57	10^{-2}	0,3	0,8
				Ro = 3m						
	σ_{M^2}	810	1420	1620	98	184	280	18	35	60
day	$\frac{\sigma}{\sigma_0}$	28	50	58	1	2	2,8	0,3	0,5	0,8
	σ_{M^2}	2,7	142	240	0,3	18	50	6.10^{-2}	35	9
night	$\frac{\sigma}{\sigma_0}$	0,1	5	8,5	4.10^{-3}	0,2	0,6	7.10^{-4}	0,05	0,8

Declassified in Part - Sanitized Copy Approved for Release 2011/12/08 : CIA-RDP80T00246A016600420001-1

Declassified in Part - Sanitized Copy Approved for Release 2011/12/08 : CIA-RDP80T00246A016600420001-1

1.27

9. "CHEMISTRY OF THE UPPER ATMOSPHERE"

by V.I.Krassovsky,
Institute of Physics of the Atmosphere,
USSR Academy of Sciences, Moscow

The atoms of nitrogen and oxygen, and, to a lesser extent, those of hydrogen, carbon and chemically inert helium, are the basic atoms of the upper atmosphere. Despite, however, the scanty assortment of atmospheric atoms and of their ions, the compounds and chemical reactions in which they participate are rather numerous. An extensive, thouth far from complete, list of possible reactions is given, for example in the well-known works by Bates, Nicolet et al. /1,2,3,4 and 5/. More definite information has become available in recent years regarding the electromagnetic and corpuscular radiation of the Sun, which dissociates the molecules of the atmosphere and excites and ionizes its atoms and molecules. Following such primary processes, there begin complicated chemical conversions, and there appears, figuratively speaking an atom-molecular or ion-atom-molecular "kaleidoscope." But modern data on the rates of the possible reactions are quite uncertain and even contradictory. By way of illustration, Table 1 presents data on the rate coefficients of some major reactions in the atmosphere at altitudes from 70 to 100 km. The vagueness of their values is too great. Much energy and great efforts may be applied to compile and solve systems of

Declassified in Part - Sanitized Copy Approved for Release 2011/12/08 : CIA-RDP80T00246A016600420001-1

Declassified in Part - Sanitized Copy Approved for Release 2011/12/08 : CIA-RDP80T00246A016600420001-1

compound equations, but because of the above fact the final result will not prove of any practical value. Many researchers assessed the coefficient of the rate and of the energy of activation of reactions in the atmosphere and in rarefied gases under laboratory conditions, proceeding from a limited number of processes under consideration. Such an approach would be fully justified if the processes under consideration were actually the only ones possible. With the existing uncertainty with regard to the values of the reaction rate coefficients it is impossible to specify reliably the most likely processes of the upper atmosphere. In briefly reviewing the present-day state of the chemistry of the upper atmosphere, it is most advisable to stress the most controversial points.

The principal data on dissociation of molecular oxygen are collected in Table 2. The average daily flux of solar radiation quanta dissociating molecular oxygen has a value of the order of 10^{12} and 8×10^{11} quanta cm^{-2} sec^{-1} in the Runge-Schuman bands and continuum respectively. In polar regions, dissociation of oxygen and nitrogen molecules may be considerably greater owing to the invasion of corpuscles, especially during aurorae. Table 3 shows the process of recombining atomic oxygen the way it had been conceived before hydroxyl radiation of the upper atmosphere was discovered. After this event, however, Bates and Nicolet /1/ and Herzberg on his own /14/ suggested a new mechanism according to which oxygen molecules emerge from ozone molecules and

Declassified in Part - Sanitized Copy Approved for Release 2011/12/08 : CIA-RDP80T00246A016600420001-1

Declassified in Part - Sanitized Copy Approved for Release 2011/12/08 : CIA-RDP80T00246A016600420001-1

oxygen atoms through the mediation of atomic hydrogen which is the catalytic agent. The scheme of such a process is shown in Table 4. An oxygen molecule pair is formed in such reactions from the ozone molecule and the oxygen atom. For energy considerations they account well for the maximum excitation of hydroxyl only to the 9 vibrational level of the basic state. Somewhyt later Krassovsky /15/ suspected thyt more excited conditions of hydroxyl, exceeding this level, may be rapidly destroyed below 80 to 100 km during collisions with oxygen molecules as a result of which ozone and atomic hydrogen will reappear. McKinley, Garvin and Bodart /16/ confirmed by means of laboratory experiments the maximum oxcitation of hydroxyl to the 9 level in an ozone-hydgogen mixture. It was still to be clarified, however, to what extent this is due to the ozone-hydrogen reaction itself, and not to the destruction of strongly-excited hydrixyl by oxygen molecules.

Most remarkable proved to be the enormous power of hydroxyl radiation of the upper atmosphere. On the basis of a vast observation material dealing with middle geographical latitudes, Shefov /17/ determined the mean intensity of hydroxyl bands in the visible and near infrared region of the spectrum. Regretfully enough, the laboratory appraisals of the relative intensities of the bands from the same levels, made by Garvin, Broida and Kostkowsky /18/, led to results differing from those obtained by Shefov. And yet, if one is to proceed from Shefov's data and determine by means of interpolation,

Declassified in Part - Sanitized Copy Approved for Release 2011/12/08 : CIA-RDP80T00246A016600420001-1

Declassified in Part - Sanitized Copy Approved for Release 2011/12/08 : CIA-RDP80T00246A016600420001-1

taking into consideration the linear terms only in an expression of the dipole moment, the intensity of more infrared bands of hydroxyl in the region insufficient for observation, as was done, for instance, by Shklovsky /19/ and, as a variant, by Heaps and Herzberg /20/, it is possible to assess approcimately the average yield of the newly-formed hydroxyl molecules apart from optical transitions from higher states. It may be appraised as 10^{11} cm^{-2} sec^{-1} for every vibrational level of the basic state, beginning with the 9 level and lower. Thus it may be expected that the total number of newly-formed hydroxyl molecules on all the vibrational levels will reach $10^{12}.cm^{-2}$ sec^{-1}. The number of such processes in the upper atmosphere is greater than the number of destructions there of oxygen molecules by Sun radiation in the Runge-Schuman continuum; it is commensurable with the number of destructions of oxygen molecules by its radiation in the Runge-Schuman bands. Although such an appraisal is somewhat vague, there is still the impression that such a yield of new hydroxyl molecules and, consequently, of oxygen molecules, even if it does not exceed the number of dissociated oxygen molecules, undoubtedly constitutes its important part. Reference has been made here to the mean values of the hydroxyl formation rate. Actually, however, considerable fluctuations of intensity of this process take place. Greater intensity of hydroxyl emission has been recorded at higher geographical latitudes /21/.

Declassified in Part - Sanitized Copy Approved for Release 2011/12/08 : CIA-RDP80T00246A016600420001-1

Declassified in Part - Sanitized Copy Approved for Release 2011/12/08 : CIA-RDP80T00246A016600420001-1

After the appearance of the ozone-hydrogen hypothesis, Krassovsky /22 and 23/ assumed that there exist other possibilities for the appearance of hydroxyl radiation. According to his suggestion, reactions referred to in Table 5 are possible in the region where the radiation appears. It is noteworthy that, according to this process, atomic oxygen, in the main, passes into a molecular state not during the union of two oxygen atoms in triple collisions, but as a result, first of the formation from molecular and atomic oxygen in triple collisions of ozone, and then of the reaction of ozone with oxygen atoms. Krassovsky stressed that metastable vibration-excited oxygen and ozone molecules, incapable of being deactivated by radiation, can be preserved for a long time and can stimulate diverse reactions with a coefficient of atomic exchange processes rate of the order of 10^{-10} cm^3 sec^{-1}. Subsequently Norrish et al. /24/ reported on the prolonged existence of such molecules observed by them under laboratory conditions. The maximum excitation of hydroxyl to the 9 level Krassovsky explained by the fact that the vibrational excitation of molecules is limited by the state sufficient only to provide for the appearance of hydroxyl with an excitation not exceeding the 9 vibrational level of the basic state. More highly excited oxygen molecules are destroyed during their collisions with non-excited oxygen molecules, as a result of which there spring oxygen atoms and ozone molecules A similar process has already been referred to in Table 2 (process 2).

Declassified in Part - Sanitized Copy Approved for Release 2011/12/08 : CIA-RDP80T00246A016600420001-1

Declassified in Part - Sanitized Copy Approved for Release 2011/12/08 : CIA-RDP80T00246A016600420001-1

It has been ascertained by means of rocket investigations that a hydroxyl emission emerges in a region whose altitude and thickness change substantially. For example, Parker /25/ made it known that a maximum intensity of this emission was observed in one instance at an altitude of 80 km, and in another case at an altitude of 90 km. Tarasova /26/ even reported about two maxima of hydroxyl emission intensity near the same altitudes. Thus, hydroxyl emission appears considerably higher than originally supposed by Bates and Nicolet /1/ and much lower than originally assumed by Krassovsky /22 and 23/. At the time Krassovsky /15 and 27/ noted that initial acts of molecular oxygen dissociation, due to the dissociating radiation absorbed there, are not sufficient for hydroxyl emission to appear in a non-mixing atmosphere at an altitude of 80 to 90 km. An ozone-hydrogen reaction can in principle take place, however, at such an altitude if there exists a vertical mixing of the atmosphere, which provides for an influs of all the necessary initial products into the reaction zone. To account for the high content of molecular oxygen above 100 km, Nicolet /28 and 29/ took the vertical mixing of the atmosphere into consideration. Inasmuch as the temperature of the atmosphere considerably increases with a decrease in altitude below the temperature minimum at an altitude of some 80 to 90 km, very favourable conditions exist there for vertical mixing. Simultaneously, owing to atmospheric viscosity, a higher region of the atmosphere above

Declassified in Part - Sanitized Copy Approved for Release 2011/12/08 : CIA-RDP80T00246A016600420001-1

Declassified in Part - Sanitized Copy Approved for Release 2011/12/08 : CIA-RDP80T00246A016600420001-1

the temperature minimum will also be involved in this process. Actually circulation in the atmosphere is most likely of a zonal nature. In some places there are upstream flows, in other downstream and in still other places horizontal flows. In the region of the temperature minimum there probably exist regions where there is a slippage of the lower and upper layers. In this case there will always exist an influx of reacting products from below and from above into the intermediate layer. Hence, the lack of coincidence of the hydroxyl emission maximum intensity zone with that of the most intensive ozone formation at altitudes below 50 km cannot be taken as an objection against the ozone-hydrogen hypothesis. On the other hand, the process of mixing will inevitably result in recombination processes taking place more effectively by means of triple collisions at lower altitudes, and not above 100 km where there is a maximum concentration of atomis oxygen but where the lifetime of oxygen atoms in a free state before their reunification with one another or with oxygen molecules considerably exceeds several days.

Bates and Moisiewitsch /30/ advanced a number of objections to Krassovsky's hypothesis. They first pointed out that the primary acts of molecular oxygen dissociation of about 2×10^{11} cm^{-2} sec^{-1} in the region above 100 km do not suffice to ensure the recorded rate of emergence of new hydroxyl molecules, which possibly attains 10^{12} hydroxyl

Declassified in Part - Sanitized Copy Approved for Release 2011/12/08 : CIA-RDP80T00246A016600420001-1

Declassified in Part - Sanitized Copy Approved for Release 2011/12/08 : CIA-RDP80T00246A016600420001-1

molecules cm^{-2} sec^{-1}. The vertical mixing of the atmosphere provides, however, in the case of Krassovsky's mechanism, as in the case of the ozone-hydrogen one, ample reserves to maintain hydroxyl radiation at the recorded level. The upward movement of considerable quantities of ozone, which dissociates there into oxygen molecules and atoms in about an hour's time, may be sufficient for setting up a necessary reserve of atomic oxygen above the region of hydroxyl radiation emergence. The downward movement of substantial quantities of atomic oxygen causes there more intensive processes of formation of both ozone and vibration-excited oxygen molecules than above. It is to be regretted that no comprehensive analysis of the influence of atmosphere mixing on the processes of oxygen dissociation and recombination has yet been published at present. Secondly, Bates and Moisiewitsch /30/ noted that vibration-excited oxygen molecules will be rapidly deactivated in atomic exchange reactions with oxygen atoms, wasting the stored up energy before interacting with hydrogen atoms. There is no doubt that this is valid if the concentration of atomic oxygen greatly exceeds that of atomic hydrogen. But a concemtration of atomic oxygen below 100 km in the region of springing hydroxyl emission has never been ascertained experimentally. It was computed theoretically only on the basis of questionable constants some of which are given by way of illustration in Table 1. In addition, the chemically active excited

Declassified in Part - Sanitized Copy Approved for Release 2011/12/08 : CIA-RDP80T00246A016600420001-1

Declassified in Part - Sanitized Copy Approved for Release 2011/12/08 : CIA-RDP80T00246A016600420001-1

states of ozone were not taken at all into consideration in this case. It is quite possible that at night the concentration of atomic oxygen in the region of emergence of hydroxyl emission does not exceed greatly that of atomic hydrogen or of its compounds. This problem can be solved only by means of direct experiments.

The question regarding the nature of hydroxyl radiation of the upper atmosphere lacks clarity not only because of the uncertainty with regard to the values of the constants of possible reactions. In a personal conversation Shklovsky drew my attention to the fact that present-day information about atomic hydrogen of the upper atmosphere do not corroborate certain hypotheses regarding the formation of excited hydroxyl as a result of low concentrations of atomic hydrogen. Friedman and his colleagues /31/ have shown that the concentration of atomic hydrogen at altitudes over 90 to 100 km hardly exceeds $5 \times 10^{6} cm^{-3}$ or $5 \times 10^{12} cm^{-2}$. Below, at the altitude of homogeneous atmosphere, the concentration of atomic hydrogen is unlikely to be greater than by the number of times equal to the base of natural logarithms. On the other hand, the published extremely high values of the rate of the reaction of atomic hydrogen transformation into perhydroxyl /11/ raises doubts regarding the possible high concentrations of atomic hydrogen in the region of hydroxyl emission emergence. Table 6 gives the value of the mean time of atomic oxagen and hydrogen existence before their transformation into ozone and perhydroxyl during triple

Declassified in Part - Sanitized Copy Approved for Release 2011/12/08 : CIA-RDP80T00246A016600420001-1

Declassified in Part - Sanitized Copy Approved for Release 2011/12/08 : CIA-RDP80T00246A016600420001-1

collisions with oxygen molecules or a third body. Used as example are the largest of the published coefficients of the rates of these reactions (see Table 1). It can be seen that as altitude decreases, the processes of ozone and perhydroxal increase abruptly. At night, when there is no dissociating radiation of the Sun, it is impossible to imagine ways for a reverse process. On the one hand, this would be in support of the ozone-hydrogen hypothesis if there were no appreciable concentrations of atomic oxygen in the reaction zone, in which case newly-formed excited ozone could deactivate before a collisions with oxygen atoms, i.e. before the emergence of a pair of vibration-excited oxygen molecules. But, on the other hand, effective transformation of atomic hydrogen into perhydroxyl does not substantiate this hypothesis. If one is to use the value suggested by Bates and Nicolet /1/ ($\sim 10^{-12} cm^3 sec^{-1}$) for the ozone-hydrogen reaction coefficient rate, and that suggested by Krassovsky /6/ ($\sim 10^{-10} cm^3 sec^{-1}$) for the oxygen-hydrogen reaction, and assuming the concentration of atomic hydrogen as $5 \times 10^6 cm^{-3}$, a concentration of ozone amounting to about $2 \times 10^{11} cm^{-3}$ or 2×10^9 vibration-excited oxygen molevules cm^{-3} would be required respectively to ensure a yield of 10^6 newly-formed hydroxyl molecules $cm^{-3} sec^{-1}$. These values exceed what might be expected. Possibly more acceptable would be the existence of other constants of reaction rates or of greater concentrations of

Declassified in Part - Sanitized Copy Approved for Release 2011/12/08 : CIA-RDP80T00246A016600420001-1

Declassified in Part - Sanitized Copy Approved for Release 2011/12/08 : CIA-RDP80T00246A016600420001-1

atomic hydrogen. This would allow to preserve the former conceptions. New precise experimental data would, however, be required for such an orientation, and these are not yet available. Until then one cannot uphold the viewpoint according to which the values of reaction constants should be rejected unless they support the hypothesis in question.

If subsequently it is really confirmed that the concentration of atomic hydrogen below 100 km is insufficient to provide, in accordance with the well-known hypotheses, for the emergence of a hydroxyl emission of the observed intensity, new ways will have to be found to account for the emergence of a large number of excited hydroxyl molecules. Krassovsky /32 and 33/ has already attempted to make a preliminary excursion into the realm of new presumptions. Table 7 presents a list of some possible reactions with the participation of molecules containing hydrogen. Of particular interest is the chain of reactions given in Table 8. Table 9 depicts the basic regularities of such a chain. For instance, at an altitude of some 80 km, where it may be expected that the concentration of all the molecules and atoms will amount to about $10^{15} cm^{-3}$, of oxygen molecules to about $2 \times 10^{14} cm^{-3}$ and of oxygen atoms to about $10^{9} cm^{-3}$, with $a_3 = 10^{-30} cm^6 sec^{-1}$ and $a_1 = 10^{-13} cm^3 sec^{-1}$, the ratio of the concentration of perhydroxyl and that of atomic hydrogen will be of the order of 2×10^{3}. To ensure v_9 - a yield of newly-formed hydroxyl molecules of about

Declassified in Part - Sanitized Copy Approved for Release 2011/12/08 : CIA-RDP80T00246A016600420001-1

Declassified in Part - Sanitized Copy Approved for Release 2011/12/08 : CIA-RDP80T00246A016600420001-1

10^6 cm^{-3} sec^{-1}, the absolute concentration of perhydroxyl will have to be of a value close to $10^{10} cm^{-3}$. There is nothing improbable about such a value since the total concentration of the particles is as high as $10^{15} cm^{-3}$. In this case the concentration of atomic hydrogen will approximately equal $5 \times 10^6 cm^{-3}$. If atomic hydrogen is to diffuse rapidly upwards in the still higher part of the atmosphere and then dissipate, there may be no greater concentration of atomic hydrogen there under such conditions. The process with the participation of perhydroxyl may provide for excitation of hydroxyl, but not to the high vibration levels of the basic state. Radiation from lower levels is particularly intensive in the radiation of the night sky. This process would not, however, be sufficient to excite higher levels. Other ways, too, of excitation to such levels are required. One of the possibilities lies in the fact that perhydroxyl itself appears in an excited state and preserves it until the reaction with atomic oxygen, thereby providing energy for the formation of more excited hydroxyl.

Vibration-excited oxygen molecules may also provide for an actually recorded less intensive excitation of higher levels. Table 10 gives a list of possible reactions. The Table also depicts the principal regularities for processes 2. For excited hydroxyl to appear in a low concentration of hydrogen, the concentration of non-excited deactivated hydroxyl should be great and that of vibration-excited molecules of oxygen and of its atoms should approximate one

Declassified in Part - Sanitized Copy Approved for Release 2011/12/08 : CIA-RDP80T00246A016600420001-1

Declassified in Part - Sanitized Copy Approved for Release 2011/12/08 : CIA-RDP80T00246A016600420001-1

another. This follows from the fact that a_5 is greater than a_6 by approximately two orders since a_5 corresponds to the reaction with the participation of a vibration - excited molecule. With such concentrations being equal, the hydroxyl concentration will exceed that of atomic hydrogen by two orders or so. For 10^6 new excited hydroxyl molecules $cm^{-3}sec^{-1}$ to emerge, with a concentration of non-excited hydroxyl of the order of $10^8 cm^{-3}$ and a_4 of the order of $10^{-10} cm^{-3}$ sec^{-1}, a concentration of vibration-excited oxygen molecules is required, which attains $10^8 cm^{-3}$. As the concentration of atomic oxygen at night below 90 to 100 km cannot be too high because of its rapidly joining oxygen molecules (see Table 6), vibration-excited oxygen molecules can be preserved for a long time.

The reaction of ozone with non-excited perhydroxyl cannot provide for hydroxyl excitation above the 3 vibration level of the basic state. Therefore the predominating share of hydroxyl emission in the night sky cannot be due to this reaction. If, however, perhydroxyl is first formed in an excited state and preserves it before it enters into a reaction with ozone, the emergence of hydroxyl with excitation to higher levels is possible. It should also be mentioned that as the rate of reactions with excited products is great, the required concentration of excited perhydroxyl may prove to be insignificant. If, however, such conditions do not exist, ozone will be capable of effectively ensuring the recorded hydroxyl radiation of the night sky, provided there is a high concentrat-

Declassified in Part - Sanitized Copy Approved for Release 2011/12/08 : CIA-RDP80T00246A016600420001-1

Declassified in Part - Sanitized Copy Approved for Release 2011/12/08 : CIA-RDP80T00246A016600420001-1

ion of atomic hydrogen.

Very complex changes are observed in hydroxyl radiation of the night sky /21/. Particularly noteworthy is the variable relative population of the various initial levels of hydroxyl and the dissimilar rotational temperature at its bands from the various initial levels. On the face of it, all this is in harmony with the existence of several mechanisms of formation of excited hydroxyl, functioning at various altitudes. The considerable changes in the rotational temperature, up to tens of Kelvin degrees, even during a single night testify to the fluctuation of the altitude of hydroxyl emergence, since, proceeding from energy considerations, they yield to no explanation of substantial changes in temperature at any fixed level of the atmosphere. All this provides a reason in support of the vertical mixing of the upper atmosphere as it can hardly remain unchanged for a long time.

In all the schemes of the above-analyzed processes, attention was given only to the reaction of ozone or of oxygen molecules with atoms or with unstable compounds of hydrogen. The reactions between hydroxyl and hydroxyl, and between perhydroxyl and perhydroxyl, as well as between hydroxyl and perhydroxyl result in the emergence of stable compounds: water or molecular hydrogen. Table 11 enumerates such reactions. As the coefficients of their rate at altitudes of 70 to 100 km may be of the order of 10^{-13} $cm^3 sec^{-1}$, they will remove effectively hydrogen, hydroxyl and perhydroxyl atoms from the reaction zone. If one

Declassified in Part - Sanitized Copy Approved for Release 2011/12/08 : CIA-RDP80T00246A016600420001-1

Declassified in Part - Sanitized Copy Approved for Release 2011/12/08 : CIA-RDP80T00246A016600420001-1

even analyzes the processes initially described by Bates and Nicolet /1/ or later by Krassovsky /22 and 23 /, the concentration of deactivated hydroxyl would reach $10^8 cm^{-3}$ at the observed rate of emergence of newly-formed hydroxyl molecules of the order of $10^{12} cm^{-2} sec^{-1}$ or of $10^6 cm^{-3} sec^{-1}$ as well as with a coefficient of the rate of reaction of non-excited hydroxyl with atomic oxygen of the order of $10^{-12} cm^3$ sec^{-1} and a concentration of atomic oxygen even of the order of $10^{10} cm^{-3}$. That is why the appearance of water vapours during collisions between hydroxyl molecules was accompanied by a removal from the reaction zone of about $2x10^3$ hydroxyl molecules cm^{-3} sec^{-1} or of about $2x10^9$ hydroxyl molecules $cm^{-2} sec^{-1}$. To restore the initial products a considerable greater number of hard quanta would be required than $2x10^9$ quanta $cm^{-2} sec^{-1}$ since molecular hydrogen and water constitute but an insignificant part of the atmosphere and are not, therefore their only absorbers. Apart from photodissociation there may exist other processes, which destroys hydrogen molecules and water vapours into hydrogen atoms or into simpler compounds. Table 12 presents a number of such reactions. Vibrationally excited oxygen molecules may be the effective reducer of the initial products. Even a slight concentration of such molecules,which would be insufficient to provide completely for a hydroxyl emission, is ample enough to maintain the required concentrations of either hydrogen, or hydroxyl or perhydroxyl in the

Declassified in Part - Sanitized Copy Approved for Release 2011/12/08 : CIA-RDP80T00246A016600420001-1

Declassified in Part - Sanitized Copy Approved for Release 2011/12/08 : CIA-RDP80T00246A016600420001-1

zone where this emission emerges. Bates and Nicolet /35/ assumed that the formation of atomic hydrogen may be partly effected owing to the destruction of methane. It should, however, be noted that although they pointed to the way of effective destruction of methane in the upper atmosphere, it is so far impossible to imagine any processes there, leading to its reverse synthesis. For this reason preference has been given in this work to the destruction and synthesis of hydrogen molecules and of water.

The absence of exact values of the above-mentioned reaction rate constants, as well as the lack of reliable information regarding the content of atomic oxygen, ozone, vibrationally excited oxygen molecules, atomic hydrogen, hydroxyl and perhydroxyl in the region of hydroxyl emission emergence does not permit to analyze in detail either the basic process of recombining atomic oxygen or its ramifications. Krassovsky /6,15 and 34/ has assumed that vibrationally excited oxygen molecules provide for reactions in which emissions of the night sky emerge. Along with vibrationally excited oxygen molecules, oxygen molecules with electronic excitation may also partly appear, as a result of which certain emissions of the night sky will appear, belonging to molecular oxygen.

Apparently it has now been widely recognized that at altitudes ranging from 100 to 400 km, molecular nitrogen

Declassified in Part - Sanitized Copy Approved for Release 2011/12/08 : CIA-RDP80T00246A016600420001-1

Declassified in Part - Sanitized Copy Approved for Release 2011/12/08 : CIA-RDP80T00246A016600420001-1

dissociates, in the main, as a result of ionization processes enumerated in Table 13. A dissociative recombination of the molecular ion is their final stage. The coefficient of recombination is most likely assessed by values of the order of $10^{-7} \div 10^{-9} cm^3 sec^{-1}$, depending on the nature of the molecular ion /5/. It is even possible that ionization of atomic oxygen is attended with dissociation of molecular nitrogen as reaction 3b is more effective than direct recombination of an atomic oxygen ion with an electrone (see expression A in Table 13). As the concentration of molecular nitrogen in the above region always exceeds that of electrons, and a_{10} is approximately equal to $10^{-12} cm^3 sec^{-1}$, this condition is valid with a_8 of the order of $10^{-12} cm^3 sec^{-1}$. Besides, some electrons formed during primary photoionization may possess energy sufficient for ionization of one more atom or molecule. Atomic nitrogen does not appear to be the predominant component at altitudes from 100 to 400 km, and reaction 2 is less important than 1, 3a, 4a and 4b. All this leads to the assumption that every act of ionization in the upper atmosphere, whether of a nitrogen molecule or of an oxygen atom, is accompanied approximately by dissociation of one nitrogen molecule.

It has been established at present that short-wave radiation of the Sun with a length wave less or equal to 300Å, absorbed aboce the 150-kilometre level, is the most powerful source of ionization in the upper atmosphere /3b/.

Declassified in Part - Sanitized Copy Approved for Release 2011/12/08 : CIA-RDP80T00246A016600420001-1

Declassified in Part - Sanitized Copy Approved for Release 2011/12/08 : CIA-RDP80T00246A016600420001-1

The total flux of quanta of this radiation may attain 3×10^{10} quanta $cm^{-2} sec^{-1}$. Above 150 km, processes 1 and 2, given in Table 14, are incapable of ensuring an equally effective recombination of atomic nitrogen, which could compensate the above rate of molecular nitrogen dissociation. Process 3 (see Table 14) whose principal regularities are given at the bottom of the Table would most likely be more effective. It is worth noting that a_{12} may be greater than a_{11} since vibrationally excited molecules of nitrogen oxide, formed in the reaction 3a between non-excited products, may interact in reaction 3b. Harteck and Kopsch /37/ give for a_{12} a value as high as $10^{-12} cm^3 sec^{-1}$, and this has been confirmed by rocket experiments with nitrogen oxide in the upper atmosphere, carried out by Pressman, Aschenbrandt, Jursa and Zelikoff /38/. Hence, the concentration of nitrogen oxide molecules will be lower than that of molecular oxygen. With v_{14} approximately equal to 10^4 of the newly-formed nitrogen molecules $cm^{-3} sec^{-1}$, the concentration of molecular oxygen approximately equal to $10^9 cm^{-3}$ and $a_{11} = 10^{-13} \div 10^{-14} cm^3 sec^{-1}$, the required value of atomic nitrogen concentration will be of the order of $10^8 \div 10^9$ cm^{-3}. It does not seem to be improbable.

As early as 1951, Krassovsky /39/ made it public that reaction 1 referred to in Table 15 can provide for the recorded continuum of night sky radiation. The principal regularities of the process are given at the bottom of the

Declassified in Part - Sanitized Copy Approved for Release 2011/12/08 : CIA-RDP80T00246A016600420001-1

Declassified in Part - Sanitized Copy Approved for Release 2011/12/08 : CIA-RDP80T00246A016600420001-1

Table. For a_c Kaufman gives a value attaining $10^{-17} cm^3 sec^{-1}$ /9/. As has been ascertained at present, the major part of the continuum arises below the 150-kilometre level /25/. An agreement with this requires that v_c should not exceed 10^2 quanta $cm^{-3} sec^{-1}$. This means that, for example, with a concentration of oxygen atoms of the order of 10^{10} cm^{-3}, the concentration of nitrogen oxide should be less than $10^9 cm^{-3}$ and, consequently, less than the maximum concentration of molecular oxygen above 150 km. Such a conclusion has already been made above, but for other considerations.

Besides the above-described process of atomic nitrogen recombination, two other, less effective, processes are possible. They are shown in Table 16. Process 1, where oxygen molecule ions are the catalyst, is possible above the 150-kilometre level. Process 2 may occur in the region where vibrationally - excited oxygen molecules exist, below the 100-kilometre level, where atomic nitrogen may be brought in as a result of vertical mixing of the atmosphere. Krassovsky has assumed that the reaction of vibrationally excited oxygen molecules with atomic nitrogen as well as with carbon oxide may be accompanied by excitation of atomic oxygen to a state ^1S which is initial for the radiation of a certain green emission of the night sky / 15 and 34/. Since the energy of dissociation of molecular nitrogen and of nitrogen dioxide into a monoxide is greater than that of molecular oxygen dissociation, additional energy

Declassified in Part - Sanitized Copy Approved for Release 2011/12/08 : CIA-RDP80T00246A016600420001-1

Declassified in Part - Sanitized Copy Approved for Release 2011/12/08 : CIA-RDP80T00246A016600420001-1

is released in such reactions, which is necessary for exciting state ^1S in oxygen atoms. Ozone is likewise capable of oxidizing the atomic nitrogen penetrating downward. Since in all the above cases a vibrationally excited nitrogen oxide molecule emerges, basically in the state $^2\Pi$, a discovery of rotational-vibrational bands of this molecule in the infrared region of the spectrum is not precluded.

The question of localization of the atomic nitrogen recombination region is extremely important in clarifying the nature of expansion of the upper atmosphere in daytime. As is well known, this was noticed when observing the braking of artificial satellites /40,41,42 and 29/. For this process to be explained by heating of the atmosphere with a hard electromagnetic radiation of the Sun with a length wave less or equal to 300Å, the region of the basic recombination of atomic nitrogen, in which the transformation of dissociation energy into heat takes place, should not be very remote from the region on the atmosphere where the above radiation is absorbed. In addition, the acts of recombination should not substantially lag behind those of dissociating radiation absorption. To avoid contradictions with the actually occuring retardation, the latter should not be assumed to exceed approximately 5×10^3 sec. Hence, the average lifetime of atmospheric nitrogen should not, either, exceed this value, provided the heating and expansion of the atmosphere in the region near the

Declassified in Part - Sanitized Copy Approved for Release 2011/12/08 : CIA-RDP80T00246A016600420001-1

Declassified in Part - Sanitized Copy Approved for Release 2011/12/08 : CIA-RDP80T00246A016600420001-1

200-kilometre level are due to the absorption of the Sun's ultra-violet radiation with a length wave less or equal to 300A. The average lifetime of atomic nitrogen, limited by its reaction with oxygen molecules (see process 3 in Table 14), will equal the reciprocal of the product of the molecular oxygen concentration and a_{11}, the coefficient of the reaction 3a rate. If a_{11} is of the order of $10^{-13}cm^3sec^{-1}$, the concentration of molecular oxygen should be of the order of $2x10^9cm^{-3}$. Such a concentration is quite probable at a level somewhat below 200 km.

It is generally believed that atomic exchange reactions with the participation of atom or molecule ions are highly effective /43/. The coefficient of their rate is sometimes even appraised by a value exceeding $10^{-10}cm^3sec^{-1}$ /44/. If one also bears in mind that the reacting products may possess excitation energy, for instance, in the shape of vibrational excitation of molecules, it appears ten that the possible variants of transformations are very numerous. Table 17 gives a list of some ion-exchange reactions, specifying their energy release. With the exact valies of the coefficients of the rates of such reactions lacking, it is not possible, however, to indicate the most probable ways of transformations.

It is possible at present to determine more or less accurately the yield of primary ions. But already when evaluating their equilibrium concentration, uncertainties appear, resulting from the lack of exact values of ion

Declassified in Part - Sanitized Copy Approved for Release 2011/12/08 : CIA-RDP80T00246A016600420001-1

Declassified in Part - Sanitized Copy Approved for Release 2011/12/08 : CIA-RDP80T00246A016600420001-1

recombination coefficients, especially during the dissociative recombination of molecular ions. But th e most important uncertainties lie in the insufficient knowledge of the ion-exchange reaction coefficients.

Even before rocket investigations of the ion composition, Krassovsky /45/, proceeding from the above considerations, assumed that the ion of nitrogen oxide, formed in reaction 3b (see Table 13), must predominate in the upper atmosphere. Later, when it has been established by means of direct sounding that the ion of nitrogen oxide actually prevails at altitudes from 100 to 250 km, Bates and Nicolet /47/ raised objections to Krassovsky's suggestion. They noted that if reaction 3b /see Table 13/ has a rate coefficient of about 10^{-9} $cm^3 sec^{-1}$ (Krassovsky himself assumed the value of 10^{-10} $cm^3 sec^{-1}$ as a rough estimate), all the ions of atomic oxygen will disappear very rapidly at night, being transformed into nitrogen oxide ions. As this has not, however, been observed, Bates and Nicolet believe that the coefficient of reaction 3b-a_8 rate has a value not exceeding 10^{-13} $cm^3 sec^{-1}$. This reaction cannot therefore play any major part in dissociation of molecular nitrogen. They consider more likely the formation of nitrogen molecules as a result of the process of dissociative recombination of the molecular nitrogen ion.

Although on the face of it Bates' and Nicolet's arguments appear convincing, still their unconditional acceptance calls for a full guaranty that reaction 1 (see Table 18)

Declassified in Part - Sanitized Copy Approved for Release 2011/12/08 : CIA-RDP80T00246A016600420001-1

Declassified in Part - Sanitized Copy Approved for Release 2011/12/08 : CIA-RDP80T00246A016600420001-1

has no inverse course. The point is that nitrogen oxide ions are bound to be formed in a vibrationally excited state. If with all that they are capable of preserving their vibrational state for a long time and are in a medium with a high concentration of atomic nitrogen, a reverse reaction appears inevitable. In this case atomic oxygen ions will regenerate owing to the vibrationally excited molecules of nitrogen oxide. Hence process 3b (see Table 13) may prove to be effective and follow its course at a very great coefficient of direct reaction rate a_8, exceeding $10^{10} cm^3 sec^{-1}$, without resulting in a rapid and complete disappearance of oxygen ions. No data seem to be available as yet, which would permit to reject fully such arguments without any hesitation.

Ionization through radiation, with a length wave less or equal to 300Å, related to the number of atoms of the given element, is the same, regardless of the fact whether they are in a molecular or in a free state. The effective section of ionization in oxygen is somewhat larger than in nitrogen /46/. Above 150 km, the number of oxygen atoms is not smaller than that of nitrogen atoms. For this reason oxygen ionization in the upper atmosphere, where its relative content is high, cannot be a minor process. If, notwithstanding Bates' and Nicolet's remarks, the reaction of molecular nitrogen destruction by oxygen ions may be considerable, the process should be sufficiently rapid to destroy molecular

Declassified in Part - Sanitized Copy Approved for Release 2011/12/08 : CIA-RDP80T00246A016600420001-1

Declassified in Part - Sanitized Copy Approved for Release 2011/12/08 : CIA-RDP80T00246A016600420001-1

nitrogen without any appreciable retardation and to make for heating the upper atmosphere during a recombination of its atoms which then sets in rapidly. The maximum admissible retardation has already been roughly estimated as 5×10^3 sec. A complete destruction of molecular nitogen in such a presumed process will culminate in a dissociative recombination of the nitrogen oxide ion. The time constant of this process will equal the reciprocal of the electron concentration product and the coefficient of nitrogen oxide ion dissociation recombination rate, and this reciprocal will not apparently exceed the admissible value of 5×10^3 sec.

In recent years the Institute of Physics of the Atmosphere under the USSR Academy of Sciences /33/ has succeeded in discovering a regular twilight emission of helium with a length wave equal to 10,830Å, corresponding to the transition of helium $2^3P \rightarrow 2^3S$. During aurorae lit up by the Sun, the intensity of this emission is on a considerable increase. Even in ordinary twilight not accompanied by aurorae, its intensity is as high as 10^3 Rayleighs. N.N.Shefov /48 and 49/ ecplained this emission as fluorescence of a metastable state of orthohelium 2^3S in solar radiation. It may appear during a bombardment of ordinary parahelium by electrons with an energy of about 25 ev. These electrons may be the product of ionization of atmospheric atoms and molecules by the Sun's radiation with a length wave less or equal to 300Å or by electrons with an

Declassified in Part - Sanitized Copy Approved for Release 2011/12/08 : CIA-RDP80T00246A016600420001-1

Declassified in Part - Sanitized Copy Approved for Release 2011/12/08 : CIA-RDP80T00246A016600420001-1

energy of several thousand ev, which cause aurorae. Apart from this, ordinary parahelium, when absorbing Sun radiation with a length wave equal to 584 Å may be transferred to the resonance level 2^1P and then, as a result of a cascade transition, may pass on to the metastable level of parahelium 2^1S. Furthermore, such metastable atoms of parahelium, when colliding with thermal electrons of the upper atmosphere, readily change into a metastable state of orthodelium 2^3S. Before deactivation such metastable atoms may exist up to 10^3 sec. Shefov has shown that to produce an ordinary twilight burst helium emission with a length wave equal to 10,830 Å at an altitude of about 1000 km, a concentration of atoms of orthohelium in the state 2^3S of the order of 10 cm^{-3}, formed when parahelium concentrating about 10^6 cm^{-3}, is required. This corresponds to the density of the upper atmosphere at this level, obtained by evaluating the braking of American altitude artificial Earth satellites /50/. Thus it becomes evident that already at such an altitude helium is a substantial component of the Earth's atmosphere. The details can be found in Shefov's original works. This has been mentioned here to draw attention to a search of other metastable states of atoms and molecules in the upper atmosphere, which, being optically inactive, may bring about diverse chemical conversions whose genuine nature may not even be surmised.

All the numerical examples cited above do not mean that they are precisely the most probable ones. They are but intended to illustrate what may happen to the ideas regarding

Declassified in Part - Sanitized Copy Approved for Release 2011/12/08 : CIA-RDP80T00246A016600420001-1

Declassified in Part - Sanitized Copy Approved for Release 2011/12/08 : CIA-RDP80T00246A016600420001-1

chemical conversions in the upper atmosphere if some or other still uncertain constant will prove valid. All this will stimulate a wide and profound discussion. It is quite evident that specified or rater reliable, non-contradictory values of constants possible in the upper atmosphere are required. What is also needed is to ascertain the absolute and relative probabilities of all the transitions of such an important molecule as hydroxyl, and this should be done not only theoretically, but in a reliably experimental way in laboratories. This will allow to compile an exact energy balance of the upper atmosphere, related to the oxygen dissociation energy. It will prove possible owing to the likelihood of fixing the true value of newly-formed hydroxyl molecule yield by the intensity of the hydroxyl emission in the visible and near infrared region of the spectrum, accessible to observations. A thorough study of the processes of formation and deactivation of metastable states of atoms and molecules is highly necessary. Of considerable importance are comprehensive investigations of all the emissions of the upper atmosphere so as to gain a more profound knowledge of its complex chemical processes. Of enormous significance would be complex studies directly in the upper atmosphere at its various levels, in different latitudes, at various hours of day and night, and at different seasons and time periods of solar activity cycles. It is necessary to determine simultaneously the concentration of oxygen and nitrogen molecules and atoms, of hydroxyl, perhydroxyl and water molecules, of atomic and molecular hydrogen, of nitrogen oxide and dioxide, of carbon dioxide

Declassified in Part - Sanitized Copy Approved for Release 2011/12/08 : CIA-RDP80T00246A016600420001-1

Declassified in Part - Sanitized Copy Approved for Release 2011/12/08 : CIA-RDP80T00246A016600420001-1

and monoxide molecules, of vibrationally excited molecules and of all kinds of ions. This is a very difficult task. Perhaps it is even impossible now to point to the actual way of recolving it. But all this is indispensable to eliminate the great number of uncertainties and to gain a clear idea of chemical conversions in the upper atmosphere.

Declassified in Part - Sanitized Copy Approved for Release 2011/12/08 : CIA-RDP80T00246A016600420001-1

Declassified in Part - Sanitized Copy Approved for Release 2011/12/08 : CIA-RDP80T00246A016600420001-1

Table I

References	The rate coefficient of the reaction $cm^6\ sec^{-1}$		
	$O+O+M \rightarrow O_2+M$ [I] (M is O_2)	$O+O_2+M \rightarrow O_3+M$ [I] (M is O_2)	$H+O_2+M \rightarrow HO_2+M$ [I] (M is O_2)
Bates, Nicolet /I/	$\sim 10^{-32}$	$\sim 10^{-34}$	$\sim 10^{-35}$
Krassovsky /6,7/	$\sim 10^{-32}$	$\sim 1.5 \times 10^{-32}$	
Kondrat'ev /8/		10^{-32}	$0.11 \div 1.5 \times 10^{-32}$
Kaufman /9/ [2]	$\leq 10^{-33}$	10^{-33}	10^{-30}
Hoare, Walsh /II/			10^{-30}
Farkas, Sachsse /12/			$\sim 2 \times 10^{-34}$
Benson, Axworthy /13/		2×10^{-34}	

I) Here and below M denotes any atmospheric atom and molecule.

2) According to /10/ the rate coefficient of the reaction $O + O + M \rightarrow O_2 + M$ is also small.

Declassified in Part - Sanitized Copy Approved for Release 2011/12/08 : CIA-RDP80T00246A016600420001-1

Declassified in Part - Sanitized Copy Approved for Release 2011/12/08 : CIA-RDP80T00246A016600420001-1

Table 2

Mainly below 50 km

I. $O_2 + h\nu$ (The Runge-Schumann bands 1925-1760 Å) $\rightarrow O_2^*$ 1)

2. $O_2 + O_2^* \rightarrow O_3 + O$

3. $O_3 + h\nu$ (The Hartley bands 3000-2000 Å) $\rightarrow O_2 + O$

Mainly higher 100 km

$O_2 + h\nu$ (The Runge-Schumann continuum 1760-1250 Å) $\rightarrow$

$\rightarrow O(^1P) + O(^1D)$

I) Here and below an asterisk $(^*)$ denote the excitation of atom or molecule.

Table 3

$O_2 + O + M \rightarrow O_3 + M$

$O_3 + O \rightarrow O_2 + O_2$

$O_3 + O_3 \rightarrow O_2 + O_2 + O_2$

$O + O + M \rightarrow O_2 + M$

Declassified in Part - Sanitized Copy Approved for Release 2011/12/08 : CIA-RDP80T00246A016600420001-1

Declassified in Part - Sanitized Copy Approved for Release 2011/12/08 : CIA-RDP80T00246A016600420001-1

Table 4

$$O_3 + H \rightarrow OH^* + O_2$$

$$OH^* \rightarrow OH + h\nu$$

$$OH + O \rightarrow O_2 + H$$

Table 5

The main reactions

$$O + O_2 + M \rightarrow O_3^* + M$$

$$O + O_3^* \rightarrow O_2^* + O_2^*$$

The reactions of the deactivation O_2^*

$$O_2^* + H \rightarrow OH^* + O$$

$$OH^* \rightarrow OH + h\nu$$

$$OH + O \rightarrow O_2 + H$$

Declassified in Part - Sanitized Copy Approved for Release 2011/12/08 : CIA-RDP80T00246A016600420001-1

Declassified in Part - Sanitized Copy Approved for Release 2011/12/08 : CIA-RDP80T00246A016600420001-1

Table 6

Altitude km	/M/[1] cm^{-3} according to CIRA1961	The mean life time (sec)	
		O in $O+O_2+M \rightarrow O_3+M$	H in $H+O_2+M \rightarrow HO_2+M$
70	$2x10^{15}$	$I.2x10^2$	I.2
80	4.0×10^{14}	$3.Ix10^3$	3.IxI0
90	$6,5 \times 10^{13}$	$I.2x10^5$	$I.2x10^3$
100	10^{12}	$5x10^6$	$5x10^4$

I) Here and below the chemical symbol for an atom ar a molecule the square brackets their concentration.

Table 7

O_2^* (+93.8 kcal/mole) + H_2 → OH^* + OH^* + 75.4 kcal/mole[I)]

O_2^* (+93.8 kcal/mole) + OH → OH^* + O_2^* + 93.8 kcal/mole[I)]

O_2^* (+93.8 kcal/mole) + HO_2 → OH^* + O_3 + 39.8 kcal/mole[I)]

O_3 + HO_2 → OH^* + O_2^* + O_2^* + 30.6 kcal/mole

O + HO_2 → OH^* + O_2^* + 54.0 kcal/mole

1) O_2^* (> + 93.8 kcal/mole) + O_2 → O + O_3

Declassified in Part - Sanitized Copy Approved for Release 2011/12/08 : CIA-RDP80T00246A016600420001-1

Declassified in Part - Sanitized Copy Approved for Release 2011/12/08 : CIA-RDP80T00246A016600420001-1

Table 8

$O + HO_2 \rightarrow OH^* + O_2$		(a_I)	I)
$OH^* \rightarrow OH + h\nu$			
$O + OH \rightarrow O_2 + H$		(a_2)	I)
$H + O_2 + M \rightarrow HO_2 + M$		(a_3)	I)

I) a_I, a_2 and a_3 are the rate coefficients of these reactions.

Table 9

$$[O]\,[HO_2]\,a_I = [O][OH]\,a_2 = [H][O_2][M]\,a_3 = v_9 \quad \text{I)}$$

$$[H] = \frac{v_9}{[O_2][M]a_3} \qquad [OH] = \frac{v_9}{[O]\,a_2} \qquad [HO_2] = \frac{v_9}{[O]\,a_I}$$

$$\frac{[HO_2]}{[H]} = \frac{[O_2][M]\,a_3}{[O]\,a_I}$$

I) v_9 is the amount of new OH^* cm^{-3} sec^{-I}

Declassified in Part - Sanitized Copy Approved for Release 2011/12/08 : CIA-RDP80T00246A016600420001-1

Declassified in Part - Sanitized Copy Approved for Release 2011/12/08 : CIA-RDP80T00246A016600420001-1

Table 10

I. $O_2^* + H_2 \rightarrow OH^* + OH^*$

2a. $O_2^* + OH \rightarrow OH^* + O_2^*$ (a_4) I) 2)

2b. $O_2^* + H \rightarrow OH^* + O$ (a_5) 2)

2c. $OH^* \rightarrow OH + h\nu$

2d. $OH + O \rightarrow O_2 + H$ (a_6) 2)

$$[O_2^*][OH]\, a_4 + [O_2^*][H]\, a_5 = v_{10} \quad 3)$$

$$[O_2^*][H]\, a_5 = [O][OH]\, a_6$$

$$\frac{[OH]}{[H]} = \frac{[O_2^*]\, a_5}{[O]\, a_6}$$

when

$$[OH]\, a_4 \gg [H]\, a_5$$

$$[OH] \sim \frac{v_{10}}{[O_2]\, a_4}$$

I) "2a" is the atom exchange reaction.

2) a_4, a_5 and a_6 are the rate koefficients of these reactions.

3) v_{10} is the amount of new $OH^*\, cm^{-3}\, sec^{-I}$.

Declassified in Part - Sanitized Copy Approved for Release 2011/12/08 : CIA-RDP80T00246A016600420001-1

Declassified in Part - Sanitized Copy Approved for Release 2011/12/08 : CIA-RDP80T00246A016600420001-1

Table II

$OH + H \rightarrow O + H_2$	+ 2.2 kcal/mole
$HO_2 + HO_2 \rightarrow O_2 + O_2 + H_2$	+ 9.2 kcal/mole
$OH + OH \rightarrow O + H_2O$	+ 16.8 kcal/mole
$OH + H\ O_2 \rightarrow O_2 + H_2O$	+ 70.8 kcal/mole
$OH + O_3 \rightarrow HO_2 + O_2$	+ 39.8 kcal/mole
$H + O_3 \rightarrow HO_2 + O$	+ 23.6 kcal/mole

Table 12

($H_2 + O_2 \rightarrow OH + OH$	- 18.4 kcal/mole)
$H_2 + O_2 \rightarrow OH + OH$	
($H_2O + O_2 \rightarrow HO_2 + OH$	- 70.8 kcal/mole)
$H_2O + O_2 \rightarrow HO_2 + O$	

Declassified in Part - Sanitized Copy Approved for Release 2011/12/08 : CIA-RDP80T00246A016600420001-1

Declassified in Part - Sanitized Copy Approved for Release 2011/12/08 : CIA-RDP80T00246A016600420001-1

Table 13

Ia. $N_2 + h\nu \rightarrow N_2^+ + e$ (>16 ev) Ib. $N_2^+ + e \rightarrow N + N$ (a_7) I)

2. $N_2 + h\nu \rightarrow N + N^+$

3a. $O + h\nu \rightarrow O^+ + e$ (> 16 ev)

3b. $O^+ + N_2 \rightarrow NO^+ + N$ (a_8) 1) 3c. $NO^+ + e \rightarrow N + O$ (a_9) I)

4a. $O + e$ (> 13 ev) $\rightarrow O^+ + e + e$ 4b. $N_2 + e$ (> 16 ev) $\rightarrow N_2^+ + e + e$

A. $[N_2]\ a_8 \gg [e]\ a_{10}$ 2)

I) a_7, a_8 and a_9 are the rate coefficients of these reactions.

2) a_{10} is the coefficient of the recombinations of O^+ and electron into O.

Table 14

I. $N + N + M \rightarrow N_2 + M$

2a. $N + O + M \rightarrow NO + M$ 2b. $NO + N \rightarrow N_2 + O$

3a. $N + O_2 \rightarrow NO^* + O$ (a_{II}) 1) 3b. $NO^* + N \rightarrow N_2^* + O$ (a_{12}) I)

$$[O_2]\,[N]\,a_{II} = [NO^*][N]\,a_{12} \sim v_{14} \quad 2)$$

$$[NO^*] = \frac{a_{II}}{a_{12}}\,[O_2]$$

$$[N] \sim \frac{v_{14}}{[O_2]\,a_{II}}$$

I) a_{11} and a_{12} are the rate coefficients of these reactions.

2) v_{14} is the amount of recombinations of N and N into N_2 cm^{-3} sec^{-1}

Declassified in Part - Sanitized Copy Approved for Release 2011/12/08 : CIA-RDP80T00246A016600420001-1

Declassified in Part - Sanitized Copy Approved for Release 2011/12/08 : CIA-RDP80T00246A016600420001-1

Table 15

I. $No + O \rightarrow NO_2 + h\nu\ (a_c)^{I)}$ $\qquad 2.NO_2 + O \rightarrow NO + O_2$

$$[NO][O]\ a_c = v_c^{\ 2)}$$

I) a_c is the rate coefficient of this reaction.

2) v_c is the amount of quanta of the continuum $cm^{-3}\ sec^{-I}$.

Table 16

Ia. $O_2^+ + N \rightarrow NO^{+*} + O$ $\qquad (+ 4.II\ ev)$

Ib. $NO^{+*} + N \rightarrow N_2 + O^+$ $\qquad (- 0.83\ ev)$

Ic. $O^+ + O_2 \rightarrow O_2^+ + O$ $\qquad (+ 1.40\ ev)$

2a. $O_2^* + N \rightarrow NO^* + O$

2b. $NO^* + M \rightarrow NO + M^*$

2c. $NO^* + N \rightarrow N_2^* + O^*$

2d. $NO + N \rightarrow N_2^* + O$

Declassified in Part - Sanitized Copy Approved for Release 2011/12/08 : CIA-RDP80T00246A016600420001-1

Declassified in Part - Sanitized Copy Approved for Release 2011/12/08 : CIA-RDP80T00246A016600420001-1

Table 17

Reactions	Energy ev
$O_2^+ + N_2 \longrightarrow NO^+ + NO$	+ 0.84
$N_2^+ + O_2 \longrightarrow NO^+ + NO$	+ 4.29
$O_2^+ + O \longrightarrow O_2 + O^+$	- I.40
$O_2^+ + N \longrightarrow NO^+ + O$	+ 4.II
$O_2^+ + N \longrightarrow O^+ + NO$	+ 0.01
$N_2^+ + N \longrightarrow N_2 + N^+$	+ I.II
$N_2^+ + O \longrightarrow NO^+ + N$	+ 2.88
$N_2^+ + O \longrightarrow N^+ + NO$	- 2.16
$NO^+ + O \longrightarrow O_2^+ + N$	- 4.II
$NO^+ + O \longrightarrow N^+ + O_2$	- 6.45
$NO^+ + O \longrightarrow NO + O^+$	- 4.10
$NO^+ + N \longrightarrow N_2^+ + O$	- 2.88
$NO^+ + N \longrightarrow O^+ + N_2$	- 0.83
$NO^+ + N \longrightarrow NO + N^+$	- 5.04
$O^+ + O_2 \longrightarrow O + O_2^+$	+ I.40
$O^+ + N_2 \longrightarrow NO^+ + N$	+ 0.83
$O^+ + N_2 \longrightarrow N^+ + NO$	- 4.21
$N^+ + N_2 \longrightarrow N_2^+ + N$	- I.II
$N^+ + O_2 \longrightarrow NO^+ + O$	+ 6.45
$N^+ + O_2 \longrightarrow O^+ + NO$	+ 0.67

Declassified in Part - Sanitized Copy Approved for Release 2011/12/08 : CIA-RDP80T00246A016600420001-1

Declassified in Part - Sanitized Copy Approved for Release 2011/12/08 : CIA-RDP80T00246A016600420001-1

Table 18

$$O^+ + N_2 \rightleftharpoons NO^+ + N$$

Declassified in Part - Sanitized Copy Approved for Release 2011/12/08 : CIA-RDP80T00246A016600420001-1

Declassified in Part - Sanitized Copy Approved for Release 2011/12/08 : CIA-RDP80T00246A016600420001-1

REFERENCES

1. D.R.Bates and M.Nicolet. Journ.Geophys. Res. 55, N 3, 301, 1950
2. D.R.Bates. The earth as a planet. Ed.G.P.Kuiper, p. 576, 1954.
3. P.Harteck, The threshold of space. Ed.M.Zelikoff, p.32, 1957.
4. M.Nicolet. The threshold of space.Ed.M.Zelikoff, p.40,1957.
5. A.Dalgarno. Ann.Géophys. 17, N I, 16, 1961.
6. V.I.Krassovsky. Usp.Fizich.Nauk, USSR, 63, N 4, 673,1957.
7. V.I.Krassovsky. Journ.Atm.Terr.Phys. 10, 49, 1957.
8. V.N.Kondrat'ev.Kinetics of chemical gaseous reactions. Publ.House Academy of Sciences,Moscow,p.283,1958.
9. F.Kaufman.Proc.Roy.Soc. 247A, N 1248,123,1958.
10. W.D.McGrath and R.G.W.Norrish. Proc.Roy.Soc.,242A, N 1230,265,1957.
11. D.E.Hoare and A.D.Walsh, Trans.Faraday Soc.53, 1102,1957.
12. L.Farkas and H.Sachsse. Z.phys.Chem. B27, III, 1934.
13. S.W.Benson and A.E. Axworthy. J.Chem.Phys. 26, 1718,1957.
14. G.Herzberg. J.Roy.Ast.Canada 45, 100,1951.
15. V.I.Krassovsky.Usp.Fizich.Nauk,U.S.S.R., 47, N 4,493,1952; 54, N 3, 469,1954.
16. J.D.McKinley,D.Garvin,M.J.Boudart. The airglow and the aurorae.Ed.E.B.Armstrong and A.Dalgarno. Pergamon Press,London. p. 264, 1955.

Declassified in Part - Sanitized Copy Approved for Release 2011/12/08 : CIA-RDP80T00246A016600420001-1

Declassified in Part - Sanitized Copy Approved for Release 2011/12/08 : CIA-RDP80T00246A016600420001-1

17. N.N.Shefov.Spectral, Electrophotometrical,and Radar Researches of aurorae and Airglow. Publ.House Academy of Sciences,Moscow,N 6, p.21, 1961.

18. D.Garvin, H.P.Broida and H.J.Kostkowsky. J.Chem.Phys. 32, N 3, 880, 1960.

19. I.S.Shklovsky.Izv.Krym.Astrofiz.Obs. 7, 34,1951.

20. H.S.Heaps and G.Herzberg. Z.Phys. 133, 48, 1952.

21. V.I.Krassovsky, N.N.Shefov and V.I. Garin. Journ.Atm. Terr.Phys. 21, 46,1961.

22. V.I.Krassovsky and V.T.Lukashenya.Doklady Acad. Nauk USSR 81, 811, 1951.

23. V.I.Krassovsky. The airglow and the aurorae.Ed. E.B.Armstrong and A.Dalgarno. Pergamon Press,London, p.193, 1955.

24. R.G.W.Norrish,etc. Proc.Roy.Soc. A.233, 455,1956.

25. D.M.Parker. Ann.Géophys. 17, N 1, 67,1961.

26. T.M.Tarasova . Astr.Zirc. U.S.S.R., N 222, 31,1961.

27. V.I.Krassovsky. The airglow and the aurorae. Ed.E.B.Armstrong and A.Dalgarno. Pergamon Press,London. P.197,1955.

28. M.Nikolet. The earth as a planet.Ed.G.P.Kuiper. Pp. 644,1954

29. M.Nikolet,Physics of the upper atmosphere. Ed.J.A.Ratcliffe. P.17.1960.

30. D.R.Bates and B.L.Moiseiwith.Journ.Atm.Terr.Phys. 8, 305,1956.

31. H.Friedman. Proc. 11 Intern.Astronaut.Congress,Stockholm. P.83,1960.

Declassified in Part - Sanitized Copy Approved for Release 2011/12/08 : CIA-RDP80T00246A016600420001-1

Declassified in Part - Sanitized Copy Approved for Release 2011/12/08 : CIA-RDP80T00246A016600420001-1

32. V.I.Krassovsky, Usp.Fizich.Nauk U.S.S.R. 75, N 3,501,1961.

33. V.I.Krassovsky.Plynet.Space Sci. 8, 197,1961.

34. V.I.Krassovsky.Ann.Géophys.14,N 4, 395,1958.

35. D.R.Bates and M.Nicolet.Pub.Astr.Soc.Pacific 62,106,1950.

36. H.E.Hinteregger.Journ.Geophys.Res. 66, N 8, 2367,1961.

37. P.Harteck, V.Kopsch. Z.Phys.Chem. 12,327,1931.

38. J.Pressman, L.M.Aschenbrand, F.F.Marmo, A.S.Jursa and M.Zelikoff.The threshold of space.Ed.M.Zelikoff. P.235.1957.

39. V.I.Krassovsky.Doklady Akad.Nauk U.S.S.R. 78 , 669,1951.

40. M.L.Lidov, Isk.Sput.Zemli. Publ.Hause Academy of Sciences U.S.S.R.,Moscow. N 1, 9, 1958.

41. P.E.El'yasberg and V.D.Jastrebov.Isk.Sput. Zemli. Publ. House Academy of Sciences U.S.S.R.,Moscow. N 4, 18, 1960.

42. G.A.Kollegov.Isk.Sput.Zemli.Publ.House Academy of Sciences U.S.S.R.,Moscow.N 4,31, 1960.

43. H.Eyring, J.O.Hirschfelder and H.S.Taylor.J.Chem.Phys. 4, 479, 1936.

44. R.F.Potter, J.Chem.Phys.23, 2462,1955.

45. V.I.Krassovsky.Izv.Ac.Sci.U.S.S.R.,ser.geophys.,N 4,504,1957.

46. A.Dalgarno and Parkinson,Journ.Atm.Terr.Phys. 18, N 4,1960.

47. D.R. Bates and Nicolet.Journ.Atm.Terr.Phys. 18, 65,1960.

48. N.N.Shefov.Planet.Space Sci.5, 70,1961.

49. N.N.Shefov. Ann.Géophys.17,N 4,1961.

50. H.K.Paetzold and H.Zschörner.Proc.2 Cospar Symposium, Florence,1961.

Declassified in Part - Sanitized Copy Approved for Release 2011/12/08 : CIA-RDP80T00246A016600420001-1

Declassified in Part - Sanitized Copy Approved for Release 2011/12/08 : CIA-RDP80T00246A016600420001-1

by A.D.DANILOV

10. "SOME QUESTIONS, CONNECTED WITH RECOMBINATION AND IONIZATION PROCESSES IN THE EARTH ATMOSPHERE"

I. The knowledge of the value of the effective recombination coefficient in ionosphere α' is of great importance for understanding a number of questions of upper atmosphere physics. The analysis of various photochemical reactions, controling upper atmosphere ionic composition, made in works [1,2,3] allows to investigate diurnal variation of α' value at different altitudes.

At present it is common knowledge that molecular ions dissociative recombination reactions are the basic recombination processes in the upper atmosphere. Work [4] shows, that at least up to the 500-600 km altitudes recombination in the atmosphere is defined by the reactions:

$$NO^+ + e \rightarrow N + O$$
$$O_2^+ + e \rightarrow O + O$$
$$N_2^+ + e \rightarrow N + N$$

and effective recombination coefficient is written in the following form:

$$\alpha' = \alpha \frac{[X_N^+]}{n_e} \qquad /I/$$

where α - rate coefficient of dissociative recombination reactions, $[X_N^+]$ - summary concentration of molecular ions at the given altitude.

As up till now the exact α coefficient value remains questionable, one can consider diurnal variations of α' value

Declassified in Part - Sanitized Copy Approved for Release 2011/12/08 : CIA-RDP80T00246A016600420001-1

Declassified in Part - Sanitized Copy Approved for Release 2011/12/08 : CIA-RDP80T00246A016600420001-1

without assuming a fixed value for this coefficient. As is seen from /I/ α' value is proportional to molecular ions part in the total ion density $[X_M^+]/n_e$ / $n_e = n_i$ /, therefore, the question of α' value dirunal variation comes to the investigation of diurnal variations of molecular ions quantity in the atmosphere.

At present there are no reliable experimental data of atmosphere ion composition variation from day to night. V.G.Istomin's measurements [5,6] taken during morning and evening hours of different days, allow to make only qualitative conclusions. The same can be said about the measurements by Johnson et all [7], taken in more nothern latitudes, than V.G.Istomin's measurements, what makes difficult their mutual comparison.

Works [I-3] deal with photochemical ways of molecular ions formation and there were obtained the following expressions for concentrations ratio

$$\frac{[NO^+]}{[O^+]} \sim \frac{[N_2]}{n_e}; \quad \frac{[O_2^+]}{[O^+]} \sim \frac{[O]}{n_e}; \quad \frac{[N_2^+]}{[O^+]} \sim \frac{[N_2]}{n_e},$$

which turned to be in good correlation with the mentioned experimental data. As can be seen from these expressions, the ratio of molecular ions concentration to the concentration of atomic ions is directly proportional to neutral density and inversely proportional to electron concentration.

In view of the said we transform the ratio $\frac{[X_M^+]}{n_e}$ in formulae /I/ as follows:

$$\frac{n_e}{[X_M^+]} = \frac{[X_A^+]+[X_M^+]}{[X_M^+]} = 1 + \frac{[X_A^+]}{[X_M^+]} = 1 + \frac{[O^+]+[N^+]}{[NO^+]+[O_2^+]+[N_2^+]} \qquad /2/$$

Declassified in Part - Sanitized Copy Approved for Release 2011/12/08 : CIA-RDP80T00246A016600420001-1

Declassified in Part - Sanitized Copy Approved for Release 2011/12/08 : CIA-RDP80T00246A016600420001-1

As, according to experimental data [8] $[N^+]$ at all the altitudes does not prevail I/IO of $[O^+]$, the second term in the fraction numerator can be neglected. As to this fraction denominator, the part of O_2^+ and N_2^+ ions relative to NO^+ ions varies from I/5 -I/IO at low altitudes to I/2 - I at the altitudes of the order of 500 km therefore, assuming an error, fully aware that it is within the factor of two, one can substitute the value I,5 $[NO^+]$ for the fraction denominator. Then formulae /2/ will have the form:

$$\frac{n_e}{[X_N^+]} = 1 + 0.65\,\frac{[O^+]}{[NO^+]}$$

According to [I] $\frac{[NO^+]}{[O^+]} = \frac{\gamma}{\alpha}\cdot\frac{[N_2]}{n_e}$, where γ/α - the ratio of the rate coefficients of charge transfer and dissociative recombination reactions, which was found in the given work to be equal to 10^{-4}. Thus, the resulting formulae for effective recombination coefficient will have the form:

$$\alpha' = \frac{\alpha}{1 + 0.65\cdot 10^{+4}\cdot\frac{n_e}{[N_2]}} \qquad /3/$$

This formulae allows to consider α' value variation from day to night on the basis of diurnal variations of neutral and electron densities at various heights. Diurnal variations of atmosphere density is taken from the work by King-Hile [9], and day to night electron concentrations ratio is taken according to Ja.L.Alpert [10]. Up to the altitudes of the order of 200 km the value $10^4\frac{n_e}{[N_2]}$ in formulae /3/ is small in relation to 1 /what corresponds to small part of

Declassified in Part - Sanitized Copy Approved for Release 2011/12/08 : CIA-RDP80T00246A016600420001-1

Declassified in Part - Sanitized Copy Approved for Release 2011/12/08 : CIA-RDP80T00246A016600420001-1

atomic ions relative to molecular ones/ and α' practically does not vary from day to night. From 200 km to 400 km the ratio $\frac{(\alpha')_{day}}{(\alpha')_{night}}$ is inversely proportional to the relative electron concentrations ratio. Above 400 km diurnal variations both electron and neutral densities must be taken into consideration. Assumed values $\frac{(n_e)_{day}}{(n_e)_{night}}$ and $\frac{(\rho)_{day}}{(\rho)_{night}}$ and the obtained ratios $\frac{(\alpha')_{night}}{(\alpha')_{day}}$ for the I00-600 km altitudes are listed in the following table:

TABLE

H km	I00-I50	I60	I80	200	250	300	350	400	500	600
$\frac{(n_e)_{day}}{(n_e)_{night}}$	I0	20	20	20	20	I8	8	3	2.7	2.7
$\frac{(\rho)_{day}}{(\rho)_{Night}}$	I	I	I	I	I	I	I	I.5	3.8	8.0
$\frac{(\alpha')_{night}}{(\alpha')_{day}}$	I	I.I	I.3	I.6	4.6	I0	6.8	2	0.8	0.34

As can be seen from the table, effective recombination coefficient up to the altitudes of the order of 400 km is higher than in the day time, the greatest α' variations occuring at about the 300 km altitude, reaching an order of the value. Above 500 km effective recombination coefficient has inverse diurnal variation, i.e. decreases at night.

On the basis of the above said it will be not difficult to estimate diurnal variation of the total number of recombinations in an atmosphere column $\int \alpha' n_e^2 dz$. According to the table data the ratio $(\int \alpha' n_e^2 dz)_{day} / (\int \alpha' n_e^2 dz)_{night}$ has the value $3.3\ I0^{I}$.

Declassified in Part - Sanitized Copy Approved for Release 2011/12/08 : CIA-RDP80T00246A016600420001-1

Declassified in Part - Sanitized Copy Approved for Release 2011/12/08 : CIA-RDP80T00246A016600420001-1

2. Experimental data of ion and electron concentration in the ionosphere allow to consider the question of ionising agent absorption in the upper atmosphere.

As is show in [4] the total rate of recombination in a volume unit per second at the given altitude is equal to:

$$\nu_{rec} = \alpha [X_M^+] n_e \qquad /4/,$$

where all the designations are the same as at the beginning of the paper. In equillibrium conditions the recombination rate must be balanced by the ionisation rate:

$$\nu_{rec} = \nu_{ion} = [M] \sigma_i n = [M] j \qquad /5/$$

where $[M]$ - neutral particles concentration in a volume unit, σ_i - ionisation cross-section, n - ionising agent flux at the given altitude, j - ionisation coefficient. The last equality is true only for monochormatic radiation or for the radiation , the cross section of which does not vary with wave length.

Radiation flux value must vary with height and depend upon optical depth of the above atmosphere layers:

$$n = n_\infty \cdot e^{-\tau} = n_\infty e^{-\sigma N_M}$$

where n_∞ - ionising agent flux outside the atmosphere, τ - optical depth, N_M - the number of particles in an atmosphere column above the given level. Denoting $\sigma_i n_\infty$ by j_∞

Declassified in Part - Sanitized Copy Approved for Release 2011/12/08 : CIA-RDP80T00246A016600420001-1

Declassified in Part - Sanitized Copy Approved for Release 2011/12/08 : CIA-RDP80T00246A016600420001-1

/ionization coeffecient outside the atmosphere/ we write the last equality:

$$j = j_\infty \cdot e^{-\sigma N_M} \qquad /6/.$$

As is clear from this equality, j value variation with height under the given atmosphere density is determined by absorption cross-section σ. On the other hand, from equalities /5/ and /4/ one can obtain the following expression for j value at the given altitude:

$$j = \frac{\alpha [X_M^+] n_e}{[M]} \qquad /7/.$$

Fig.I shows the values for the altitude range I00-400 km /point/calculated from formulae /7/. While calculating there were used experimental data of electron [II] and ion [8,6] densities. The value [M] is calculated on the basis of the density experimental data [I2,I3] in supposition, that the par part of molecular nitrogen up to the 400 km altitude remains constant [I4], but O_2 and O concentrations are distributed in accordance with [2].

Fig.I shows as well an absorption exponential curve /6/ in the altitude range I60-400 km, when σ value is equal to $5 \cdot I0^{-I7}$ cm^2. As is seen from this figure the ionization coefficient variation with height at the altitudes above I60 km is well represented by the absorption curve, corresponding to a high absorption cross section $5 \cdot I0^{-I7}$ cm^2. At the same time, one can see from Fig.2, where j - value variation with

Declassified in Part - Sanitized Copy Approved for Release 2011/12/08 : CIA-RDP80T00246A016600420001-1

Declassified in Part - Sanitized Copy Approved for Release 2011/12/08 : CIA-RDP80T00246A016600420001-1

height below I60 km is shown in another scale along the altitude axis, that at low altitudes j - value variation cannot be represented by exponential curve, corresponding to any single absorption cross section for the whole altitude range I00-I60 km.

As can be seen from the curves of Fig.2 the cross section, corresponding to ionizing radiation absorption at these altitudes varies from 10^{-17} cm^2 at the I50-I60 km altitude to 5 10^{-19} cm^2 at the I00-II0 km altitude.

The obtained ionization coefficient variation in the atmosphere seems to be indicative of the following: at the I60-400 km altitudes the ionization in the atmosphere is produced by the agent, having high cross section of absorption by atmosphere components.

Besides, this agent is monochromatic in the sence that its absorption cross section does not vary while this agent is being absorbed a hundred times. The mentioned characteristics lead to a supposition, that at the altitudes above I60 km solar ultraviolet radiation cannot be the ionizing agent. Indeed, firstly, the maximum cross section of absorption by atmosphere components of solar ultraviolet radiation is I.0 10^{-17} cm^2 [I5], the mean value of σ being equal to 3-5.10^{-18} cm^2 [I6]. Secondly, the solar ultraviolet radiation is not monochromatic, i.e. it consists of radiation "parts", having different absorption cross section from the given maximum value to the values of a few units per 10^{-19} cm^2, therefore this radiation absorption at different altitudes must correspond to different σ - values.

Declassified in Part - Sanitized Copy Approved for Release 2011/12/08 : CIA-RDP80T00246A016600420001-1

Declassified in Part - Sanitized Copy Approved for Release 2011/12/08 : CIA-RDP80T00246A016600420001-1

The mentioned particularities of ionizing agent at the altitudes above I60 km lead to a supposition, that these are soft electrons fluxes which can be this agent . Indeed, ionization cross section of oxigen and nitrogen molecules for these electrons is very high and reaches a few units per 10^{-16} cm^2 /Massey and Burhop [17]/, and, besides, this cross section value varies with the energy variation from 30 to 700 ev less than 3 times. Soft electrons fluxes as a possible source of night ionization of F-region of the ionosphere, were regarded in work [18], were the electron flux weakening in the atmosphere was estimated. However, the ionization character at the heights of F-region at night and during solar eclipses allows to assume that in the day-time at the 200-400 km altitudes the ionization is also caused by other agent than solar radiation.

At the same time, the given in Fig.2 ionizing agent absorption cross sections at the altitudes below 160 km are in good correspondence with the point of view that solar ultraviolet radiation is the main ionization source at these altitudes. The absorption cross section, obtained for the 100-160 km altitudes, corresponds to the cross sections which exist in the region of 800 - 100 Å, and the fact of quick cross section variation with height is in good agreement with solar ultraviolet radiation being nonmonochromatic, as it was said above. The diurnal ionization variations and ionization variations during solar eclipses at these heights also indicate that this ionization is caused by solar radiation.

j-values, shown in Fig.1 and 2 are counted in supposition that the rate coefficient of dissociative recombination reactions- α - is equal to 10^{-6} $cm^3 sec^{-1}$. At present some authors assume lower values for it. However, everyone can see, that the obtained

Declassified in Part - Sanitized Copy Approved for Release 2011/12/08 : CIA-RDP80T00246A016600420001-1

Declassified in Part - Sanitized Copy Approved for Release 2011/12/08 : CIA-RDP80T00246A016600420001-1

in this work results do not depend on the absolute value of j-value variation, defining the absorption cross section, will not change, if α -value at all the altitudes is decreased several times. Now let us consider the possible α -value variation with height due to temperature variation. According to Nicolet [19], the maximum different temperatures at the 160 and 400 km altitudes are 950 and 1600°K, respectively. If α coefficient has the temperature dependence received in [20]:

$$\alpha \sim T^{-1/2}$$

these temperatures give the possible 1,3 times decrease of α from 160 to 400 km; when j-value varies a hundred times at the same altitudes. Thus, the possible α variation with height cannot appreciably change the ionization coefficient variation and affect the main conclusion about the high cross section of ionising agent absorption above 160 km.

The knowledge of α -coefficient is, however, necessary for estimation of n_∞ value, i.e. necessary flux of ionizing agent:

$$n_\infty = n_{400} = \frac{\alpha [X_N^+] n_e}{[M] \sigma_i}$$

When α is equal to 10^{-6} - 10^{-7} $cm^3 sec^{-1}$ (this interval of the values now seems to be most correct) in order to explain the observed ionization the flux must be 10^{10} - 10^{11} electrons/cm^2 sec, the mean electrons energy being of the order of 300 ev. The question of such soft electron fluxes existence in the upper atmosphere is discussed in G.S.Ivanov-Kholodny's work and has received the definite answer.

Declassified in Part - Sanitized Copy Approved for Release 2011/12/08 : CIA-RDP80T00246A016600420001-1

Declassified in Part - Sanitized Copy Approved for Release 2011/12/08 : CIA-RDP80T00246A016600420001-1

Fig.I - The ionization coefficient value j variation in the altitude range I00- 400 km.

o o - values, computed according to formulae /7/.

—— - absorption exponent variation /6/ when σ = $= 5 \cdot 10^{-17}$ cm^2.

Fig.2 - Ionization coefficient j value variation in the altitude range I00-I60 km.

o o - value, computed according to formulae /7/.

—— - absorption exponent variation under different absorption cross-section values σ .

Declassified in Part - Sanitized Copy Approved for Release 2011/12/08 : CIA-RDP80T00246A016600420001-1

Declassified in Part - Sanitized Copy Approved for Release 2011/12/08 : CIA-RDP80T00246A016600420001-1

REFERENCES

I.A.D.Danilov "Iskusstvennye sputniki Zemli" N5,60,I960

2.A.D.Danilov "Iskusstvennye sputniki Zemli" N7,56,I96I

3.A.D.Danilov "Iskusstvennye sputniki Zemli" N8,72,I96I

4.A.D.Danilov "DAN SSSR I37/5/,I098,I96I

5.V.G.Istomin "Iskusstvennye sputniki Zemli" NII,94,I96I

6.V.G.Istomin "Iskusstvennye sputniki Zemli" N7,64,I96I

7.C.Y.Johnson,E.B.Meadow,J.C.Holms I94 Rocket Repoert Series NI, I958

8.V.G.Istomin "Iskusstvennye sputniki Zemli" N4,I7I,I960

9.Ja.L.Alpert "Racprostranenie radiovoln i ionosfera" M. I96I, p.I30

I0.D.G.King-Hell Ann.Geoph. I7(2),I62,I96I

II.K.I.Gringauz "Ikusstvennye sputniki Zemli" NI,62,I958

I2.V.V.Mikhnevitch,B.S.Danilin,A.I.Rennev,V.A.Sokolov "Iskusstvennye sputniki Zemli" N3,84,I959

I3.V.V.Mikhnevitch "Iskusstvennye sputniki Zemli" N2,26,I958

I4.A.D.Danilov "Iskusstvennye sputniki Zemli" NI0,98,I96I

I5.A.Dalgarno,D.Parkinson J.A.T.Ph. I8(4),335,I960

I6.K.Watanabe Adv.Geophys. 5,I53,I958

I7.H.S.W.Massey,E.H.S.Burhop "Electronic and ionic impact phenomena" Oxford, I952

I8.L.A.Antonova,G.S.Ivanov-Kholodhy "Geomagnetizm i aeronomija" I/2/,I96I

I9.M.Nicolet "Aeronomy" Preprint I962

20. A.C.Fair,O.T.Fundingsland, K.S.W.Champion, A.U.Aden J. of Appl.Phys. 29,928,I958

Declassified in Part - Sanitized Copy Approved for Release 2011/12/08 : CIA-RDP80T00246A016600420001-1

Declassified in Part - Sanitized Copy Approved for Release 2011/12/08 : CIA-RDP80T00246A016600420001-1

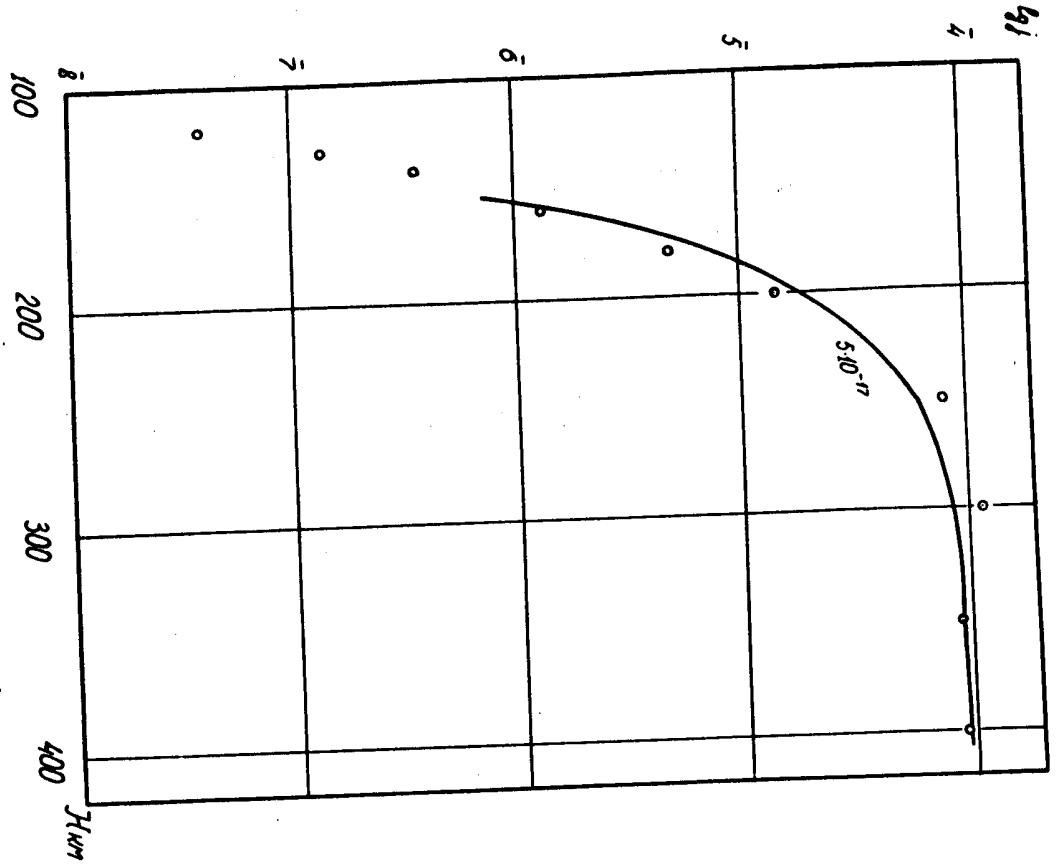

Fig 1

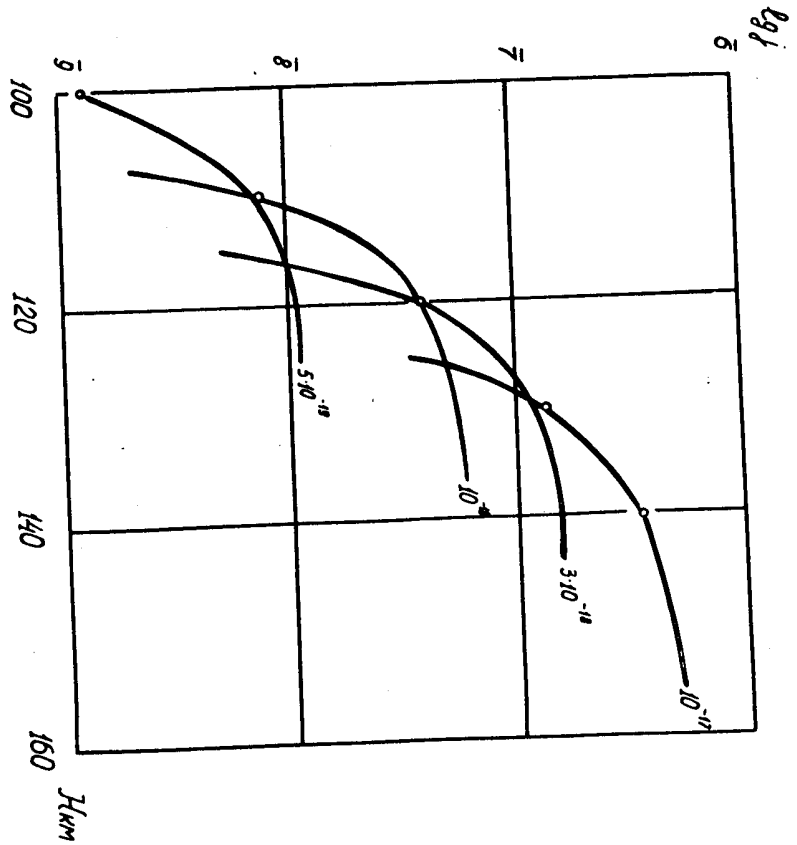

Fig 2

Declassified in Part - Sanitized Copy Approved for Release 2011/12/08 : CIA-RDP80T00246A016600420001-1

Declassified in Part - Sanitized Copy Approved for Release 2011/12/08 : CIA-RDP80T00246A016600420001-1

by G.S.IVANOV-KHOLODNY

11. "ON THE RATE OF IONIZATION AND RECOMBINATION PROCESSES IN THE IONOSPHERE."

(Interpretation of rocket and satellite data)

ABSTRACT

Here it is given an analysis of a number of rocket experiments delt with intensity measurements of the solar extreme ultraviolet ion composition and corpuscular radiation measurements in the ionosphere. This analysis shows that ionization and recombination rates exceed many times the rates used up till now. These conclusions are confirmed by some ground ionosphere experiments. Now it is necessary to reconsider the data obtained earlier which concern effective recombination coefficient estimation in the ionosphere, due to this we have now a new conception of the main elementary processes in the ionosphere.

Declassified in Part - Sanitized Copy Approved for Release 2011/12/08 : CIA-RDP80T00246A016600420001-1

Declassified in Part - Sanitized Copy Approved for Release 2011/12/08 : CIA-RDP80T00246A016600420001-1

In course of development of investigation methods by means of rockets and satellites they contribute considerably to the earth ionosphere study. Particularly there well-known recent achievements in exploring of the ionosphere structure, due to which important properties of the ionosphere structure are brought to light, which were escaping in former investigations carried out with the help of radio-sounding stations: absence of clearly pronounced E and F_1 layer, electron density gradient is very steep in the low part of E layer and slope above n_e maximum, n_e maximum height is fairly constant in F region of the ionosphere ($\sim$300 km) a measurement of n_e absolute value and n_e diurnal variation characteristics at different heights etc. (for instance cf. Nuwell's last review /1/). These data changed old view on the ionosphere, though they regard morphological properties of the ionosphere and do not touch upon its deep physical processes. Meanwhile there were obtained a number of facts of fundamental importance in understanding of elementary processes in the ionosphere. Mainly the following is implied here: 1) solar extreme ultraviolet energy estimation, 2) data concerning the ionosphere ion composition, 3) detection of electron fluxes in the ionosphere. Let us consider these facts and direct consequencies from them.

I. The analysis of solar exteme ultraviolet spectra obtained with the help of spectrographs and spectrometers, mounted on rockets, indicates that the energy of solar radiation, which ionizes the earth ionosphere is about 15 erg/cm^{2}sec (Ivanov-Kholodny and Nikolsky /2/). It should be noted that this value

Declassified in Part - Sanitized Copy Approved for Release 2011/12/08 : CIA-RDP80T00246A016600420001-1

Declassified in Part - Sanitized Copy Approved for Release 2011/12/08 : CIA-RDP80T00246A016600420001-1

exceeds several times that one obtained by Hinteregger on the bases of direct photoelectrical measurements - I.4 - 8 erg/cm^2. .sec. As it is shown in /2/ he did not took into account the absorption of the radiation, caused by N_2 or H_2O, spectral bands of which situated just on the maximum of spectral energy distribution. According to the spectrum constructed in /2/ we may obtain that during the solar maximum activity the radiation flux is equal to $\sim 3.10^{11}$ photon/cm^{2}sec, that considerably exceeds the values which have been used before. Previous to the time of rocket investigations the estimations of this value during solar minimum activity gave the value equal to 5.10^9 photon/cm^{2}sec /3,4/ and it considered to be overestimated. Brightness of the solar active regions according to the theory /5/ and as it was prooved nowadays by rocket experiments in photographing of the Sun in X-rays is $\sim 10^2$ times higher, than that of the undisturbed regions. As during the solar maximum phase active regions occupy $\sim$10 per.cent. of the solar area, so extreme ultraviolet radiation intensity during the solar cycle should vary approximately in 10 times. Thus on the bases of experimental data while studying the ionosphere one should regard the fact of high intensity of the solar ionizing radiation.

Meanwhile, on the bases of ionosphere data concerning n_e and α' as it was more than once computed, a total number of recombination and consequently ionization acts in the ionosphere

Declassified in Part - Sanitized Copy Approved for Release 2011/12/08 : CIA-RDP80T00246A016600420001-1

Declassified in Part - Sanitized Copy Approved for Release 2011/12/08 : CIA-RDP80T00246A016600420001-1

per square centimeter column is only 2 - 5 $.10^9 cm^{-1} sec^{-1}$, that corresponds to the ionization energy of 0.1 - 0.5 $erg/cm^2 sec$, as 30 -50 ev energy is necessary for per ion formation in the atmosphere. This indicates a sharp contradiction between present conception concerning the ionosphere and new rocket data about solar radiation.

On the bases of data concerning the solar extreme ultraviolet spectrum /2/ and upper atmosphere density /6/ the solar radiation penetration through the atmosphere was computed and also it was computed the rate of the ionization q for each height. Using rocket data concerning n_e there was computed the effective recombination coefficient $\alpha_1' = q/n_e^2$ /7/, the results are presented in Table I. Due to some uncertainty in choosing the zenith angle of the sun $Z_\odot$ the values of α_1' are uncertain by the factor I.5-2

TABLE I

h, km	$\alpha_1' = q/n_e^2$	$\alpha_2' = \alpha^* \frac{M^+}{n_e}$
I00	-	4.10^{-7}
I20	$I.5.10^{-7}$	$3.5.10^{-7}$
I40	$I.10^{-7}$	$2.5.10^{-7}$
I60	$I.10^{-7}$	$I.5.10^{-7}$
I80	$I.10^{-7}$	$I.4.10^{-7}$
200	5.10^{-8}	$I.3.10^{-7}$
250	3.10^{-9}	2.10^{-8}
300	$I.10^{-9}$	$I.10^{-8}$
400	5.10^{-10}	$I.10^{-9}$

Declassified in Part - Sanitized Copy Approved for Release 2011/12/08 : CIA-RDP80T00246A016600420001-1

Declassified in Part - Sanitized Copy Approved for Release 2011/12/08 : CIA-RDP80T00246A016600420001-1

2. Let us consider rocket measurements of the atmospheric ion composition, excellently carried out with the help of radio-frequency mass spectrometers by V.G.Istomin and Johnson et al.. Without saying anything about another important aspects of these achievements, we only point out the fact of particular importance, e.g. obtaining a relatively high quantity of molecular ions in the upper atmosphere. It follows directly from this, that recombination in the ionosphere up to 600-700 km height are determined by molecular ion dissociative recombination and the effective recombination coefficient $\alpha_i' = \alpha^* M^+/n_-$ /where α^* is a rate coefficient of dissociative recombination reaction/. It is prooved that α_i' is I - 2 order of magnitude higher than that obtained according to ionospheric data /8,9/. In connection with it let us make two notes: concerning the rate of dissociative recombination α^* and ionospheric measurements of α .

a) Bates and Massey /IO/ were the first to indicate the importance of dissociative recombination reaction for the ionosphere. Bates's first theoretical estimations /II/ gave for $\alpha^* \geq 10^{-7} cm^3 sec^{-1}$ at $T \approx 250^\circ K$, that confirmed laboratory measurements, but contradicted to ionosphere data of that time. On the bases of numerous laboratory measurements, which have been carried out up till now, for $(N_2^+ + e)$ reaction at a low pressure and $T = 300 - 2000^\circ K$ $\alpha^* = 3 - I.10^{-7} cm^3 sec^{-I}$ ($\alpha^* \sim T^{-1/2}$). For $(O_2^+ + e)$ reaction less certain estimations gave $\alpha^* = 5.10^{-8} cm^3 sec^{-I}$. The main molecular ion at $h \leq 500$ km heights is NO^+ therefore in order to compute α' it is necessary to know α^* for $NO^+ + e$ reaction. However the laboratory rate

Declassified in Part - Sanitized Copy Approved for Release 2011/12/08 : CIA-RDP80T00246A016600420001-1

Declassified in Part - Sanitized Copy Approved for Release 2011/12/08 : CIA-RDP80T00246A016600420001-1

measurements of this reaction are less certain, they give for for it , as well as for dissociative recombination reaction of ions of rare gases, α^* value which is approximately equal to that of ($N_2^+ + e$) reaction. A similar value is likely to be obtained from direct experimental data according to measurements of rate decrease of n_e in a cloud while nitric oxide is ejected from a rocket. So at computing $\alpha_2' = \alpha^* M^+ n_-$ one should take $\alpha^* = 3 \cdot 10^{-7} \sqrt{\frac{300}{T}}$ (in Danilov's work /9/ it was taken $\alpha^* = 10^{-6}$). The results of the computation are presented in Table I. These data concerning α_2' are consistent within a factor of 2-3 with the data concerning α_1', except the values of α_1' in n_e maximum region of the ionospher at 250-300 km height. At these heights as well as at higher ones the effect of corpuscular radiation (see item 3) which is not probably taken onto account tends to underestemation of α_1'. In this case as it may be estimated that during the solar maximum activity in the ionosphere per square centimeter column about $4 \cdot 10^{11}$ $cm^{-2} sec^{-1}$ acts of neutralization (compare /8/) are to take place, and this corresponds to $\sim$ 20 $erg/cm^2 sec$ of the ionization energy. Thus the interpretation of new data about ionospheric ion composition is in a good agreement with analyses of solar extreme ultraviolet spectra /8/. This indicates that there exists a crisis in a morden presentation of the ionosphere, and this is enough to assert that there are more intensive recombination and ionization processes than it has been used up till now. Thus we conclude that some former results about the determination of recombination coefficient

Declassified in Part - Sanitized Copy Approved for Release 2011/12/08 : CIA-RDP80T00246A016600420001-1

Declassified in Part - Sanitized Copy Approved for Release 2011/12/08 : CIA-RDP80T00246A016600420001-1

in the ionosphere are to be doubtful.

b) There are several methods to obtain α' in E and F ionosphere regions, these methods are based on measurements of n_e variations during solar eclipses at sunset and sunrise diurnal n_e variations and the like. In general these methods give various and often contradictive results and sometimes they give the same high results as those presented in Table I, and it happens that they give even negative values of α'. The latter may be connected in some cases with incorrect reasoning. The most reliable method of the determination of α' in E and F_I regions is considered to be measurements during solar eclipses. The delay of Δt moment of n_e minimum coming in comparison with the moment of the eclipse minimum phase of E and F_I regions is usually $\lesssim$ 5 min., and according to Rydbeck and Wilhelmson /I2/ foe the regions it gives $\alpha' > 10^{-8}$. To carry out these measure - ments as well as to carry out them during other ionospheric disturbances , it would be necessary to have higher rates of pro processes and more accurate measurements. Therefore for α' determination it is used n_e relative variation during the eclipse By this method for α' 0.5-2.10^{-8} values are obtained. However here it is not taken into account the fact that at the moment of maximal phase about 10-20 percent of solar extreme ultra- violet radiation coming outside the solar disc, as it was recent ly prooved with the help of rocket experiments. Considering this fact a number of authors obtained

Declassified in Part - Sanitized Copy Approved for Release 2011/12/08 : CIA-RDP80T00246A016600420001-1

Declassified in Part - Sanitized Copy Approved for Release 2011/12/08 : CIA-RDP80T00246A016600420001-1

$\alpha' = 0.4 - 1.10^{-7}$ /12 - 16/, though it may happen that higher values can be obtained, especially if we take into account that bright regions of extreme ultraviolet are distributed over the disk nonuniformly. These α' data are in a good agreement with those ones presented in Table I and are supported by other ionosphere measurements. For example, a certain sharp variation of n_e at sunrise and sunset also leads to an unusually high value of α' and measurements of the aurora brightness variation gave also high values of $\alpha' = 10^{-7}-10^{-6}$. In connection with it is also necessary critically to revise the conclusions concerning α', obtaining in diurnal variation of n_e and some other methods. It also necessary critically to reconsider interpretations of another phenomena connected with recombination and ionization rate in the ionosphere.

On the bases of the conclusions of high rates of re - combination ionosphere processes, the main chemical reactions describing elementary ionosphere processes must be revised. Bates and Massy /10/ considering various possible chemical reactions in the upper atmosphere indicated in particular dissociative recombination and ion-atom interchange reactions. Other authors paid great attention to these reactions, however only now it was established that they are of significant importance. Using the data concerning the variations of relative ion composition with the height, Danilov /9/ confirmed that ion

Declassified in Part - Sanitized Copy Approved for Release 2011/12/08 : CIA-RDP80T00246A016600420001-1

Declassified in Part - Sanitized Copy Approved for Release 2011/12/08 : CIA-RDP80T00246A016600420001-1

transformations and disappearances occur mainly in such a way that atomic ion transforms into molecular ones caused by ion- - atom interchange reactions, and neutralization in the ionosphere occurs as a result of dissociative recombination of molecular ions. In this case, as it was shown by Ratcliffe /I9/ electron disappearance rate in the upper part of the ionosphere should be proportinal to n_e but not to n_e^2, as it is in the lower ionosphere. The linear law of electron disappearance at 250-400 km heights is obtained now in a number of experiments and this also confirms that the choice of the abovementioned reactions in the ionosphere was quite true. Rate values of ion formation and ion disapperance at 200 - 400 km hieght obtained eclipse data in /20/ are close to those ones presented in Table I; Van Zandt et.al. /20/ also indicates contradiction between these data and the existent data concerning α'.

3) According to new data concerning the recombination coefficient the ionosphere should be neutralized for a comparatively short period of time after sunset, if there was no additinal night ionization source. Antonova and Ivanov - - Kholodny /2I/ suggested a corpuscular hypothesis to explain night ionosphere ionization. According to this hypothesis a soft ($I0^2$ - $I0^4$ ev) electron flux according to α' new data with power of $\sim$ I erg/cm^{2}sec fall onto the ionosphere. This electron flux may produce some ionization even in the day time /2I/ at 300 km height it may produce ionization exceeding

Declassified in Part - Sanitized Copy Approved for Release 2011/12/08 : CIA-RDP80T00246A016600420001-1

Declassified in Part - Sanitized Copy Approved for Release 2011/12/08 : CIA-RDP80T00246A016600420001-1

the one caused by solar extreme ultraviolet. This assumption may explain the noted difference between data concerning in Table I at 250 ÷ 300 km height obtained in various ways and also a peculiar variation of α' with height, indicated by Danilov /9; 22/, who draws the attention to high effective cross section of the ionizing agent at ~300 km height. It is important to emphasize that the source power necessary for producing electron fluxes in the ionosphere must exceed many times the source power of the earth radiation belts. The hypothesis concerning the soft electron presence in the ionosphere is a significant contribution to the development of new ionospheric point of view, and it is closely connected with high rate conception of ionization and recombination processes in the ionosphere. An experimental foundation for the corpuscular hypothesis is presented in detail in /2I/. Here it should be added that recently Kazatschevskaya et.al. have confirmed by new methods in experiments with thermoluminescent phospor at Antonova's experimental results, the latter obtained that 70-I00 km height the flux of 20-30 kev electrons carried the energy of about $I.IO^{-2}$ erg/cm^{2}sec. steradian. Let us note that we can directly obtain the value of the rate coefficient of the ionization processes consequently near I00 km height $q \approx IO^2$ cm^{-3} sec^{-I}, caused by the abovementioned electrons, and the rate recombination coefficient balancing this night ionization $\alpha' \approx 3.IO^{-6}$.

Declassified in Part - Sanitized Copy Approved for Release 2011/12/08 : CIA-RDP80T00246A016600420001-1

Declassified in Part - Sanitized Copy Approved for Release 2011/12/08 : CIA-RDP80T00246A016600420001-1

So we believe that the whole comlex of new rocket experimental data estimating intensities and solar extreme ultra violet spectrum its distribution over the solar disc and beyond the limb, estimeting ion composition and corpuscular radiation in the ionosphere show that the oppinion concerning rates of recombination and ionization processes which has been formed by the present time, is not true. It was indicated above in what way these ideas concerning elementary processes in the ionosphere should be reconsidered. Here it was found out, that the conclusions delt with high intensities of ionization and recombination processes are also confirmed in a number of ground ionosphere experiments. In connection with it, now it is probably necessary critically to recosider earlier obtained results of effective recombination coefficient measurements. There arises a question of developing new ideas concerning physical--chemical ionosphere processes as well as concerning new interpretion of such phenomena as a general ionosphere behavior and also ionosphere parameter variations dependently on the time of day, season geographical co-ordinates, and also on upeper atmosphere heating, diffusion and drift.

Institute of Applied Geophysics of the Academy of Sciences of the USSR.

Declassified in Part - Sanitized Copy Approved for Release 2011/12/08 : CIA-RDP80T00246A016600420001-1

Declassified in Part - Sanitized Copy Approved for Release 2011/12/08 : CIA-RDP80T00246A016600420001-1

REFERENCES

I. H.E.Newell,Jr., in "Physics of the upper atmosphere", ed by I.A.Ratcliffe, New York - London, I960,p.273.

2. G.S.Ivanov-Kholodny, G.M.Nikolsky, Astronomitch. j., 38,828, I96I., "Prediction and Identification of Emission Lines in Solar Extreme Ultraviolet λ = II00Å" (report presented at this symposium)

3. C.W.Allen, Terr. Magn.Atm. Electr., 53,433,I948.

4. I.S.Chklovsky, Izv.Krymsk.astrofizitch.observatorii,4,80, I949.

5. G.S.Ivanov-Kholodny, G.M.Nikolsky, Astronomitch,j.,38,45,I96I.

6. H.Kallman-Bijl,R.F.Boyd, H.La Gow, S.M.Poloskov, W.Prister, "Cospar International Reference Atmosphere", I96I

7. G.S.Ivanov-Kholodny, Geomagnetizm i Aeronomija (in press)

8. G.S.Ivanov-Kholodny, Dokl. AN SSSR, I37,/—,/—, 327.I96I

9. A.D.Danilov, Dokl. AN SSSR, I37,I098, I96I.

I0. D.R.Bates, H.S.N.Massey,Proc,Phys. Soc., I92,I947

II. D.R.Bates, Phys.Rev., 78,492,I950.

I2. O.E.H.Rydbeck, Wilhelmson,H., Trans. Chalmers Univ. Technol. Gothenberg, Sweden, N I49,3,I954.

I3. J.Hunaert, M.Nicolet, J.Geophys.Res., 60,537,I955.

I4.C.M.Minnis, Nature, I78,33,I956.

I5. C.M.Minnis, J.Atm.Terr.Phys., 9,20I, I956.

I6. J.A.Ratcliffe, "Solar eclipses and the ionosphere", I956,p.306.

I7.M.W.McElhinny, J.Atm.Terr.Phys.,I4,273,I959.

I8. T.A.Chubb, H.Friedman, R.W.Kreplin, R.Blake, A.E.Unsicker, Mém. Soc.roy.Sci.,Liège,4,228,I96I.

I9. J.A. Ratcliffe,JAtm. Terr.Phys., 8,260,I956.

20. T.E.Van Zand, R.B.Norton, C.H.Stonehocker, J.Geophys.Res., 65, 2003, I96I.

2I. L.A.Antonova, G.S.Ivanov-Khohlodny, "Geomagnetizm i aeronomiya",I, I64, I96I "Space ResearchII" Amsterdam, I96I.

22. A.D.Danilov " Some questions connected with recombination and ionization processes in the earth atmosphere" (report presented at the symposium)

23. T.V.Kazatchevskaya (private connections)

24. L.A. Antonova, G.S.Ivanov-Kholodny, Izv. AN SSSR (ser.geof.) N 5,756, I960.

25. L.A.Antonova,Izvastiya AN SSSR (ser.geof.) N9, I437, I96I.

26. Ya.L. Alpert, JETF, I8, 995, I948.

Declassified in Part - Sanitized Copy Approved for Release 2011/12/08 : CIA-RDP80T00246A016600420001-1

Declassified in Part - Sanitized Copy Approved for Release 2011/12/08 : CIA-RDP80T00246A016600420001-1

6/ T.M.TARASOVA

12. "NIGHT SKY MAIN EMISSION LINES INTENSITY DISTRIBUTION WITH HEIGHT"

The results of the preliminary treatment of the experimental data obtained on the 23-d of September, 1960 are presented in this paper.

The aim of the experiment was the investigation of the night sky emission line energy line distribution with height at possible close conditions of the experiment for all the lines (apparatus orientation, closeness of the studied regions of the sky and measurement moments). In the apparatus it is provided simultaneous (with maximal intervals 1.6 sec) measurements of the green line glow (λ =5577 Å) and of the red line (λ =6300 Å atomic oxigen, sodium (λ =5893 Å), hydroxile (9.I00-IQ700 Å), molecular oxigen (λ =3650 Å) and of the continuous spectrum of the night sky (λ =5300 Å).

Declassified in Part - Sanitized Copy Approved for Release 2011/12/08 : CIA-RDP80T00246A016600420001-1

Declassified in Part - Sanitized Copy Approved for Release 2011/12/08 : CIA-RDP80T00246A016600420001-1

I. APPARATUS. A photoelectrical photometer was used, it was raised on a rocket to high atmosphere layers. This photometer as an automatical device, having two optical channels with receivers, providing the apparatus sensitivity in the region of 2600 - 11000 Å. An illumination of the cathodes is made by means of two telescope systems operating parallely. Frequency of filter changing is 0.4 sec. Photometer viewing angle is 6°. The photometer axis is set up parallel to the rocket axis. In order to control apparatus operation stability there is mounted a luminaphor of a constant activity. The record was carried out by means of an oscillator with I2 galvanometers that made it possible to record one and the same energy value in five ranges. The time of the beginning of instrument operation is ($00^{h}56^{m}$) of local time.

2. PROCESSING METHODS AND CALIBRATION. Calibration was carri ed out by means of a band lamp, colour temperature of which and its integral energetic power of light are known. Illumination of the objective of the system was made with the help of a frosted glass, spectral transparency of which and its evenness of illumination were estimated experimentally. Optical characteristics of interferent filters were estimated by means of a monochromator under the same illumination conditions, under which the instrument operates, when measurements are being carried out. Photometer calibration was carried out by means of experimental determination of the frosted glass brightness with the help of a thermal element graduated in absolute energy units, according to a standart lamp. The frosted glass brightness obtained experimentally coinsided with the calculated value obtained according to Plank's equation.

Declassified in Part - Sanitized Copy Approved for Release 2011/12/08 : CIA-RDP80T00246A016600420001-1

Declassified in Part - Sanitized Copy Approved for Release 2011/12/08 : CIA-RDP80T00246A016600420001-1

Data processing was fulfilled in the following way. The apparatus reading when measuring hight sky glow:

$$I_H = C_\lambda (\kappa_\lambda B_\lambda + \ldots b'_\lambda W) \omega S$$

where $b'_\lambda = b'_\lambda + b_\lambda^{OH}$

B_λ - radiation brightness in the line

b_λ - continuous radiation brightness at I Å

$b^{OH}_{\lambda\Delta\lambda}$ - radiation brightness in the corresponding hydroxile band, passing through the filter

ω - solid sight angle in steradians

S - objective area of the system in cm^2

W - the equivalent filter width in Å for 100 per.cent. of penetration which is equal to estimation $W = \int_{-\infty}^{\infty} \kappa(\lambda) d\lambda$ in the investigated wave length

K_λ - filter penetration coefficient,

C_λ - proportionality coefficient, penetration is also taken into account.

When considering the continuous spectrum background we used:

Roach's /I/ assumption, according to which continuous background distribution is taken as identical with the energy distribution in G_2 star spectrum class.

Another method of the background calculation with the use of Shefov's experimental data /2/ leads to certain variation of the absolute values of the intensities, but does not introduce considerable changes into the relative glow intensities distribution with height.

For the emission of OH and O_2 the continuous background was not considered at all. The accuracy of the intensity estimation in absolute unit is 30 R. The accuracy of the relative line intensity

Declassified in Part - Sanitized Copy Approved for Release 2011/12/08 : CIA-RDP80T00246A016600420001-1

Declassified in Part - Sanitized Copy Approved for Release 2011/12/08 : CIA-RDP80T00246A016600420001-1

estimations is I5-20 per cent.

The paper presents the data, obtained at the ascending branch of the rocket trajectory from the height of H=65 km (when the instrument starts operating) up to the height of 200km

The orientation accuracy estimations for the height range of 65-I00 km is $\pm_2$o, for I00-I30 km - $\pm$I0^o and for I30-I90 km - $\pm$20^o. The apparatus movement at the ascending trajectory branch may be described in the following way: in the region of 65-75 km the axis is directed to the zenith, beginning with 75 km height the apparatus starts turning and this is followed by increasing of the measuring intensity value caused by the ray path increase. At the height of I30 km the apparatus axis is directed just vertically down, at I70-200 km height the apparatus keeps on rotating and its axis is again directed towards the zenith.

3. EXPERIMENTAL DATA are listed in Table I and illustrated in graphs No.I-6. In the first line of the Table there is presented the agent that causes a glow; in the second line the investigated spectrum region; in the third one-filter spectral characteristics which were obtained in view of spectral multiplier sensitivity; in the fourth line - energy values, which were obtained on the ground on the eve of the rocket experiment. For OH and O_2 emission there are relative intensities I, as for the rest of the components there are absolute intensity values in Rayleigh: J_Σ - summary intensity measured by the apparatus in the given spectrum region $E_{\lambda+OH}$ is the energy of the line plus the energy of the corresponding hydroxile band (the latter is taken from literature data)

Declassified in Part - Sanitized Copy Approved for Release 2011/12/08 : CIA-RDP80T00246A016600420001-1

Declassified in Part - Sanitized Copy Approved for Release 2011/12/08 : CIA-RDP80T00246A016600420001-1

/3/ and E_λ - the energy in the emission line; in the fifth line - the same values, recorded by the photometer at the time of passing H=65 km[x] directed towards the zenith (↑). In the sixth line - the data, obtained by the apparatus at I30 km height the axis is directed vertically down (↓). The data obtained at I30 km, when the apparatus axis is directed towards the Earth, may be distorted by an additional light source from the Earth. However, practical equality of OH emission energy ratio in the nearest infrared spectrum region to the green line emission observed at the heights of 65 (↑) and I30 (↓) indicates that both cases we deel with the atmosphere own emission. When an additional light source appears should sharply decrease this ratio due to considerable difference of a spectral energy distribution in the night sky and in an electrical lamp. In the seventh line there are emission values, recorded by instruments at I80 km height, when the axis is directed towards the zenith; in the last line - the energy difference, obtained in lines 5 and 6, that determines the glow intensity coming from the heights exeeding I30 km.

In Fig.I-6 the apparatus climb height is plotted on the abscisse: in all the Figures curve 3 gives the intensity recorded by the photometer in the position it appeared to be at the moment of measuring(the curve is drawn according to four scales

[x] - in the text (↑) means that the apparatus axis is directed towards the zenith, and (↓) means that it is directed vertically down.

Declassified in Part - Sanitized Copy Approved for Release 2011/12/08 : CIA-RDP80T00246A016600420001-1

Declassified in Part - Sanitized Copy Approved for Release 2011/12/08 : CIA-RDP80T00246A016600420001-1

which are provided by the oscillator with galvanometer); curve I gives the intensity reduced to the zenith, which is obtained from curve 3 after the introduction of a correction for the ~~zenit~~ zenith distance according to the following equation:

I) for the case when the layer is above the apparatus

$$J_\theta = J_z \sec \alpha \qquad \text{where } \sin\alpha = \frac{R}{R+H}\sin\theta$$

2) for the case when the apparatus is moving in the layer

$$J_\theta = -\cos\theta\,(R+H_0) + \sqrt{\cos^2\theta\,[R+H_0]^2 + 2J_z(R+H_0) + J_z^2}$$

where J_z - the intensity when one obverves it in the zenith direction;

θ - the angle of the apparatus and the vertical;

R - the earth radius

H_0 - the apparatus altitude.

H - the layer altitude.

When calculating corrections for the maximum upper boundary of the layer for λ = 9100 - 10700 Å , λ= 8650 Å , λ= 5577 Å the altitude of 120-130 km was taken; according to our data there is no glow alone these altitudes.

In all the Figures on curve 3 arrows show the altitude range for which the correction for the zenith angle is less than 20 per.cent, the arrow direction is the directrion of the apparatus axis.

Curve 2 is obtained by differentiation of curve I and it gives emission in atmosphere volume units.

4. DISCUSSION OF THE RESULTS

I) Hydroxile emission (9100 - 10700 Å)

As it is seen from the Table and Fig.I the energy value, recorded at the altitude of 65 km (↑), when recording a glow

Declassified in Part - Sanitized Copy Approved for Release 2011/12/08 : CIA-RDP80T00246A016600420001-1

Declassified in Part - Sanitized Copy Approved for Release 2011/12/08 : CIA-RDP80T00246A016600420001-1

is the whole depth of the atmosphere above 65 km, coinsides with the accuracy of test errors, with the energy value, obtained at the I30 km altitude, when measuring glow in the 0-I30 km layer.

The glow energy distribution with height is given in Plot No.I, curve I, which was obtained when the apparatus was crossing it. As it is seen from this Plot the glow is concentrated in the layer the low boundary of which is at H = 73 ± 2 km, and the upper one is at H = II0 ± I0 km. The layer gravitation center is situated at H = 78 ∓ 2 km. At H= I80 km the photometer records only continuous radiation energy and this is less than I0 per.cent of the energy at H = 65 km. At the altitudes below 65 km there probably exists glow in the region of 9I00-I0700 Å , as $J_{65}(\downarrow)$ $J_{I30}(\downarrow)$ expected energy values are, however, within the limits of the test accuracy.

2) $O_2(0\text{-}I)$ molecular oxygen emission.

The data for $O_2(0\text{-}I)$ presented in the Table and Fig.2 show that in the region of λ = 8650 Å a glow is concentrated in the layer, situated between the altitudes of 65 and I30 km, as energy value, recorded at 65 km ($\downarrow$) is practically equal to that one recorded at the I30 km altitude ($\downarrow$) and $J = f(H)$ = const at H = 65 - 74 km. At altitudes exceeding I80 km the glow is lacking, only the continuous radiation energy is measured and it is as it is seen from Fig.2 less than I0 per.cent of the energy at H=65 km. From curve I, Plot 2, where the vertical emission distribution is given, it is clear that the low layer boundary is at H=74±2 km, and the upper one is at H = II0 ± I0 km. The layer gravitation center is situated

Declassified in Part - Sanitized Copy Approved for Release 2011/12/08 : CIA-RDP80T00246A016600420001-1

Declassified in Part - Sanitized Copy Approved for Release 2011/12/08 : CIA-RDP80T00246A016600420001-1

at H = 8I ± 2 km.

According to preliminary estimates the molecular oxygen energy radiation value is 50 per.cent of the summary energy, coming through the filter; 50 per.cent of the glow is induced by the hydroxile glow and the hight sky continuous spectrum background. As the energy value of J_H = I30 (I) is somewhat higher than $J_{H=65}$ (I) it is likely that below 65 km there exists glow in the region of λ = 8650 Å , however expected energy values are in the range of experimental accuracy.

3. Night Sky Glow Continuous Spectrum

As it is seen from Plot 3 for the region of λ = 5300 Å in the height range of 64-75 km the part of the curve $J = f(H)$ =const, which is characteristic for the case when the layer is above the apparatus (see Fig.I and 2) is lacking. The intensity begins decreasing, when the apparatus starts operating and goes on up to the altitudes exceeding I30 km. This can be seen from the Table data analysis: at H=65 km the energy value computed in Å is equal to I R/Å ; at the I30 km altitude this value is equal to 0.4 R/Å. Comparing these figures we can conclude that the energy of the radiation, coming from the altitudes exceeding I30 km, should be no less than 0.6 R/Å. Actually the energy value recorded at I80 km altitude gives only 0.4 R/Å. This testifies to the fact that above I30 km in the region of λ = 5300 Å, there exists glow, which is of an atmospheric origion. Thus the star background is not more than 30 per.cent of all the intensity. The analysis of the obtained data show that for the emission in the region of λ =5300 Å one does not observe more or less pronounced layers: the glow is continuously decreasing from 65 km height up to I30-I80km heights. The low

Declassified in Part - Sanitized Copy Approved for Release 2011/12/08 : CIA-RDP80T00246A016600420001-1

Declassified in Part - Sanitized Copy Approved for Release 2011/12/08 : CIA-RDP80T00246A016600420001-1

layer boundary is not recorded by the apparatus as according to Plot 3, it was to be located below 65 km.

Comparing the data obtained for the spectrum region of $\lambda\lambda$ = 9I00-I0700 Å and λ = 8650 Å , one can see that below 65 km the glow is likely to exist in the both regions. This may be explained by the presence at low altitudes of the glow responsible for the continuous spectrum in the night sky. This assumption is cosistent with the absence of the low glow boundary in the region of λ = 5300 Å .

4. Atomic Oxygen Radiation O('S) λ = 5577 Å.

Analysing the Table one can see that the energy value for the atomic oxigen green line, obtained from the altitude of 65 km (↑), when the apparatus is directed to the zenith, is equal to the energy value, recorded by the apparatus when its axis was directed vertically down at H = I30 km (↓). This testifies to the fact that the glowing layer is situated between the altitudes of 65 and I30 km. The absence of the glow at altitudes exceeding I80nkm is also proved by the summary energy measurements recorded in the given filter at the altitude of I80 km, where the value equal to the night sky continuous radiation energy is recorded (see the last Table line). Analysing the data, obtained when the apparatus was coming through the layer , we can precise the energy distribution at the altitudes of 70-I00 km: so, from Plot No.4 it is seen that the λ = 5577 Å glow is originated in the layer, which has a pronounced lower boundary

Declassified in Part - Sanitized Copy Approved for Release 2011/12/08 : CIA-RDP80T00246A016600420001-1

Declassified in Part - Sanitized Copy Approved for Release 2011/12/08 : CIA-RDP80T00246A016600420001-1

at 82±2 km and the upper one at H=II0±I0 km, and the layer gravitation center is situated at H=90±2 km.

5. Sodium Emission (λ=5893 Å)

Using the same method of treating, as for the line of λ =5577Å we shall obtain the same result; at the altitude of 65 km the energy of $E_{\lambda+OH}$ equal to 3I0 R was recorded by the apparatus directed to the zenith. At the altitude of I30 km this value was only 200 R. This means that the main part of the glow remained above I30. This conclusion is backed by the measurements, obtained at I80 km altitude, where the apparatus directed to the zenith recorded the energy equal to 90 R. This value is by 20 R less than the difference $J_{H=65}^{(\uparrow)} - J_{H=130}^{(\downarrow)}$ characterizing the energy, which the apparatus directed to the zenith is to record at I30 km.

As it is seen from Fig.4 , at altitudes less than I30 km, the apparatus recorded a layer, located at the altitudes 70-I00 km. According to the sharp glow intensity decrease caused by the apparatus penetration into the layer, as it was similarly observed for λ =5577 Å, λ=8656 Å and OH glow, the layer gravitation center is situated at the altitude of 80-85 km. The lower layer boundary is at 70 km and the upper one is uncertain.

The analysis of all the obtained data shows that Na glow is not concentrated in one narrow layer, but it has a peculiar glow distribution with altitude: besides the glow layer located in the 70-80 km region there is glow at the altitudes exceeding I80 km. As for the nature of the glow

Declassified in Part - Sanitized Copy Approved for Release 2011/12/08 : CIA-RDP80T00246A016600420001-1

Declassified in Part - Sanitized Copy Approved for Release 2011/12/08 : CIA-RDP80T00246A016600420001-1

distribution in the range of I30-I8^{0} km, it is difficult to come to any conclusion as the energy radiation value, which can be concentrated in the air region of I30-I80 km is very small(20-30 R).

6. Atomic Oxigen Radiation O('D) λ=6300 Å

Fig.6 gives radiation distribution with height in the region of λ=6300 Å, curve 3 - for the energy value without background of $\mathcal{J}_{\lambda+OH}$.

As it is seen from the Figure and the Plot, the apparatus, directed to the zenith at 65 km altitude (1) recorded the value of $\mathcal{J}_{\lambda+OH}$ =300 R. The apparatus directed vertically down measured the value $\mathcal{J}_{\lambda+OH}$=I30 R. at the altitude I30 km (1). These values are not equal as it was observed for the emission of λ=5893 Å. The difference $\mathcal{J}^{(1)}_{H=65} - \mathcal{J}^{(1)}_{H=130}$ giving the radiation energy value coming from the altitudes exeeding I30 km, is I70 R.

Energy measurements by the apparatus directed to the zenith at the altitude of I80 km showed that there exists glow at altitudes exceeding I80 km, however the energy value fixed in this case is much less than the abovementioned difference, and it is of 80-I00 R. Hence, in the atmosphere depth in the range of I30-I80 km there is glow in the investigated spectrum region. As at these altitudes according to point I0 there is no hydroxile glow, one may conclude, that the agent, causing glow in the region λ =6300 Å at the altitudes of I30-I80 km is atomic oxigen O ('D).

Declassified in Part - Sanitized Copy Approved for Release 2011/12/08 : CIA-RDP80T00246A016600420001-1

Declassified in Part - Sanitized Copy Approved for Release 2011/12/08 : CIA-RDP80T00246A016600420001-1

Thus 50 per cent of the radiation in the line λ=6300 Å° induced by the atmosphere glow above I30 km is concentrated at the altitudes exceeding I80 km,=and 50 per cent of it - altitudes in the range of I30-I8o.

Whether there is any glow of λ =6300 Å below I30 km it is difficult to decide for certain because of the fact that the main part of the radiation in this region belongs to hydroxile radiation the distribution with height of which is not known. If we assume that in the region of λ -6300 Å it is approxemately the same as that of 9I00-I0700 Å, then it follows from the data analysis, that below I30 km there is glow in the line λ =6300 Å. This conclusion needs to be tested experimentally.

Declassified in Part - Sanitized Copy Approved for Release 2011/12/08 : CIA-RDP80T00246A016600420001-1

Declassified in Part - Sanitized Copy Approved for Release 2011/12/08 : CIA-RDP80T00246A016600420001-1

TABLE I

I	Agent	Hydroxile	Molecular Oxigen O_2(O-I)	Continuous glow spectrum	Atomic oxigen O('S)	Sodium	Atomic oxigen O('D)
II	λ	9100-10700 Å	8650 Å	5300 Å	5577 Å	5893 Å	6300 Å
III	W		56	49	38.5	52	79
	K_λ		0,20	0,26	0,17	0,26	0,33

Absolute glow intencity in Rayleigh

	Relative →		Intencity	full	by I Å	E_λ^{5577}	$E_{\lambda,OH}$	$E_{\lambda,OH}$
IV	0	14	21	220	1.2R/Å	240	270	250
V	65 (↓)	16	22,5	185	1R/Å	200	300	300
VI	180 (↓)	18	25	72	0.4R/Å	210,5	200	180
VII	180 (↓)	1	2	75	0.4R/Å	0	90	80-100
VIII		Energy difference $E_{65(\downarrow)}-E_{180}$		113	0.6R/Å	10	110	170

Layer location altitudes

layer gravitation center	78 ± 2	84 ± 2	64 - 180	32 ± 2	80-85	~180
lower boundary	73 ± 2	74 ± 2	6 < 64	80 82	70-85	~180
upper boundary	100 ± 2	100 ± 2	>180	100	>200	>200

Declassified in Part - Sanitized Copy Approved for Release 2011/12/08 : CIA-RDP80T00246A016600420001-1

Declassified in Part - Sanitized Copy Approved for Release 2011/12/08 : CIA-RDP80T00246A016600420001-1

Fig.I - OH glow intensity distribution with height
1.- relative intensity, reduced to the zenith;
2- emission in volume units;
3 - photometer indications which are not reduced to the zenith.

Fig.2 - glow intensity distribution with height in the region of 8650 Å
I.- relative intensity reduced to the zenith;
2- emission in volume units;
3 - photometer indications, which are not reduced to the zenith;

Fig.3 - glow intensity distribution with height in the region of 5300 Å
1.- glow intensity reduced to the zenith (along the upper scale - relative, along the low one - absolute)
2 - photometer indications, reduced to the zenith (here we have the same scale notation as that for curve I)

Fig.4 - radiation intensity distribution of 5587 Å with height.
1 - absolute glow intensity in the zenith, without background
2 - emission in volume units

Fig.5 - glow intensity distribution with height in the region of 5893 Å
3 and 3' - absolute glow intensity, which is not reduced to the zenith: 3' - summary energy; 3 - energy, without background.

Fig.6 - glow intensity distribution with height in the region of 6300 Å.
- absolute glow intensity, without background (which is not reduced to the zenith)

Declassified in Part - Sanitized Copy Approved for Release 2011/12/08 : CIA-RDP80T00246A016600420001-1

Declassified in Part - Sanitized Copy Approved for Release 2011/12/08 : CIA-RDP80T00246A016600420001-1

REFERENCES

I.F.E.Roach Manual for phitimetric observations of the airglow during the International Geophysical Year. National bureau of standarts 5006, I-33, I956.

2.N.I.Chefov Spektralnye elektrofotometritcheskie i radiolokatsionnye issledovanija poljarnykh sijanii i svetchenija notchnogo neba. N 2-3 Moskva I960,p.57

3.N.I.Chefov Spectralnye electrofotometricheskie i radiolokatsionnye issledovanija poljarnukh sijanii i svetchenija notchnogo neba. N 6 Moskva I96I p.2I

Declassified in Part - Sanitized Copy Approved for Release 2011/12/08 : CIA-RDP80T00246A016600420001-1

Declassified in Part - Sanitized Copy Approved for Release 2011/12/08 : CIA-RDP80T00246A016600420001-1

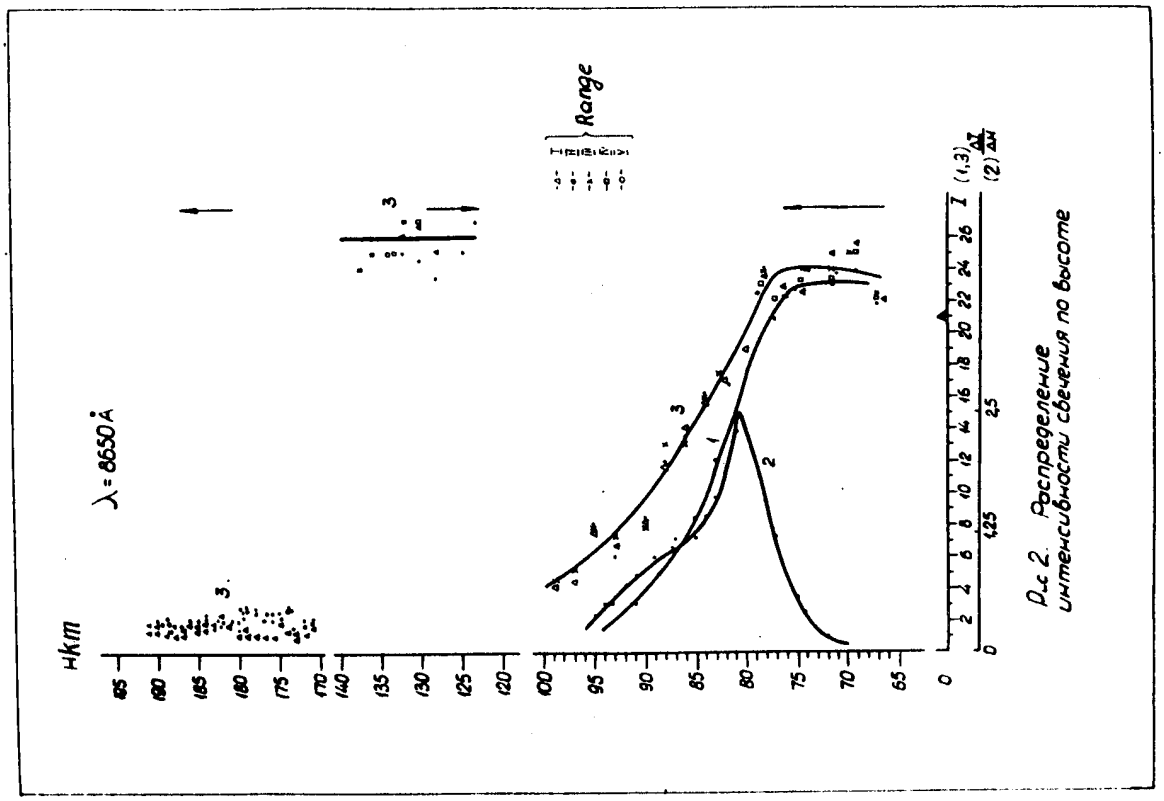

Рис 2. Распределение интенсивности свечения по высоте

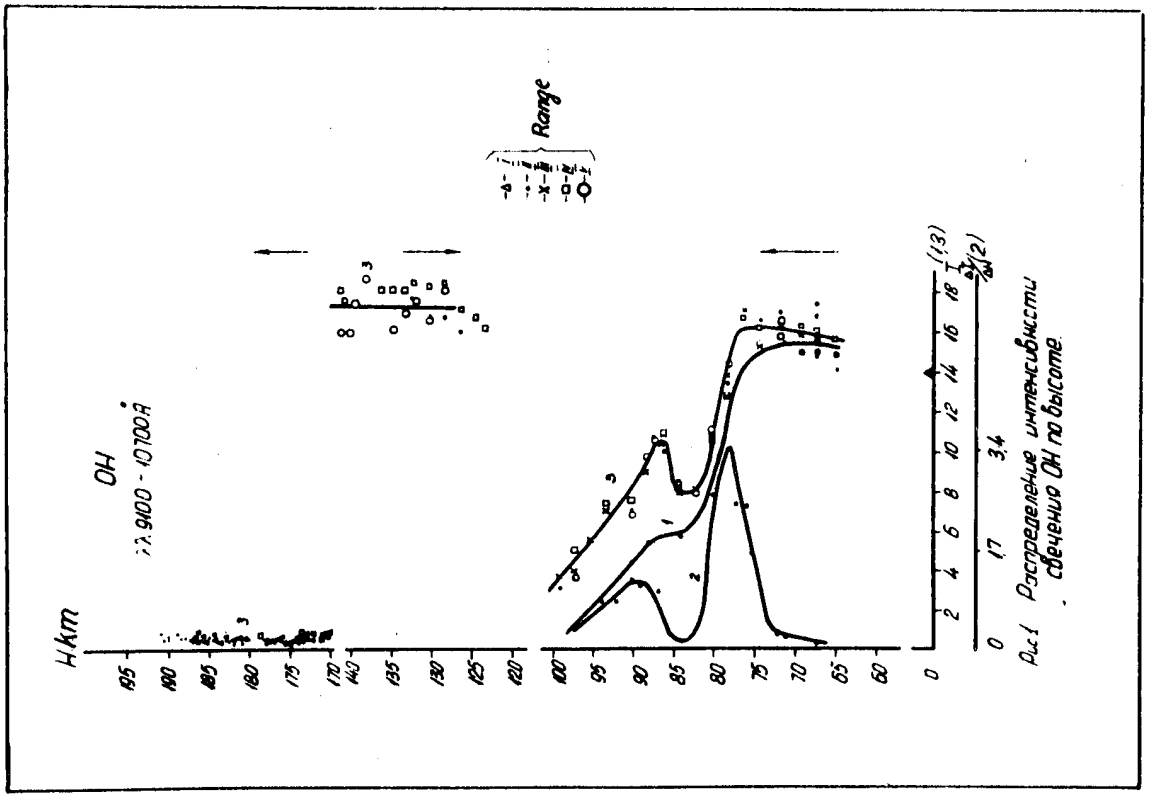

Рис 1 Распределение интенсивности свечения ОН по высоте

Declassified in Part - Sanitized Copy Approved for Release 2011/12/08 : CIA-RDP80T00246A016600420001-1

Declassified in Part - Sanitized Copy Approved for Release 2011/12/08 : CIA-RDP80T00246A016600420001-1

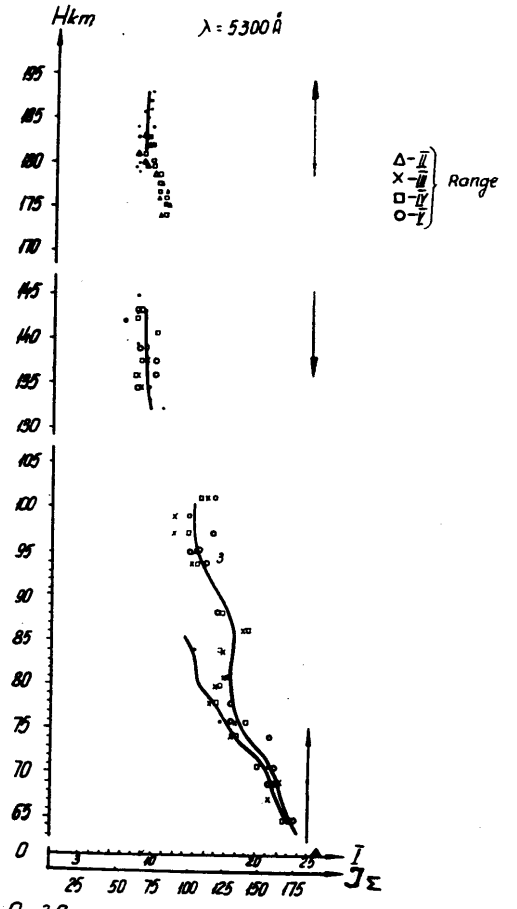

Рис.3 Верхняя шкала - относительная интенсивность свечения
Нижняя шкала - абсолютная интенсивность в рейл.

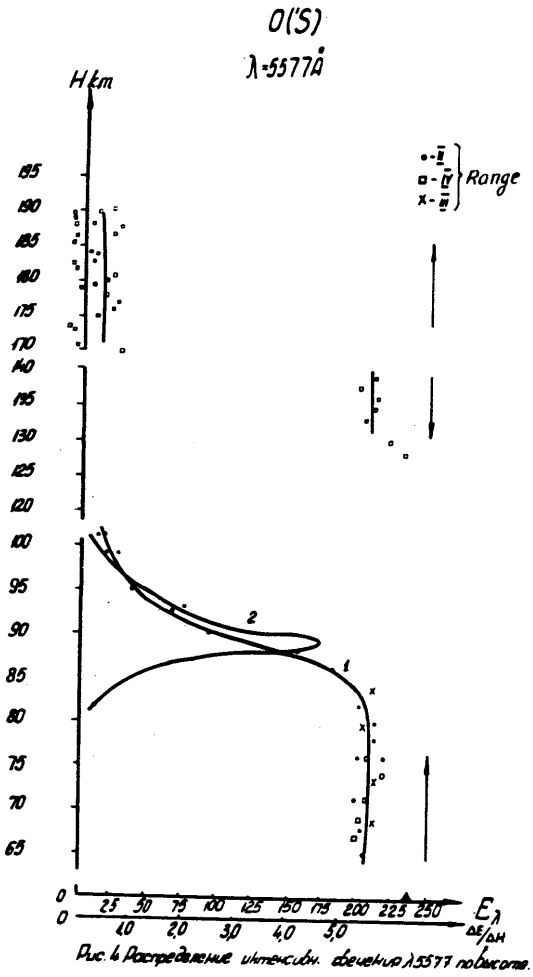

Рис. 4 Распределение интенсивн. свечения λ5577 по высоте.

Declassified in Part - Sanitized Copy Approved for Release 2011/12/08 : CIA-RDP80T00246A016600420001-1

Declassified in Part - Sanitized Copy Approved for Release 2011/12/08 : CIA-RDP80T00246A016600420001-1

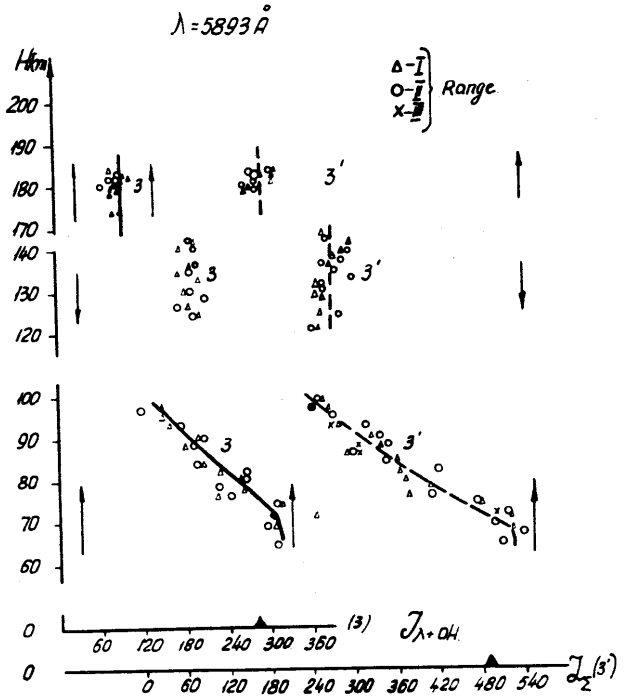

рис. 5 Распределение свечения в области λ 5893 по высоте.

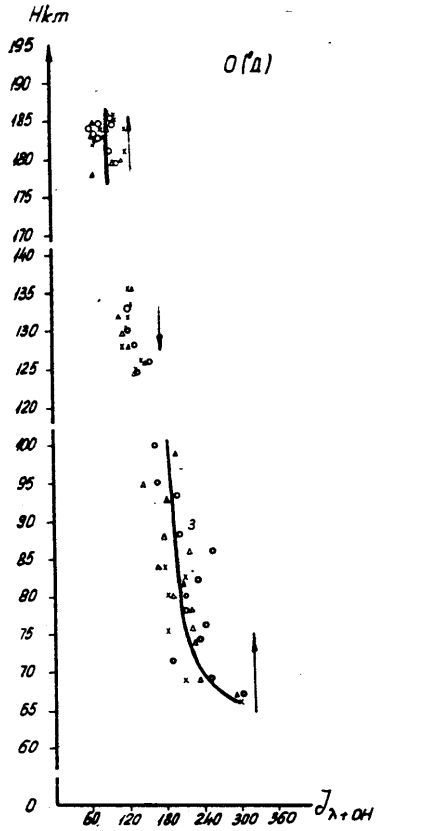

Рис. 6 Распределение энергии свечения λ = 6300 Å по высоте.
Δ-I
O-II
X-III
Range

Declassified in Part - Sanitized Copy Approved for Release 2011/12/08 : CIA-RDP80T00246A016600420001-1

Declassified in Part - Sanitized Copy Approved for Release 2011/12/08 : CIA-RDP80T00246A016600420001-1

13. "ON SOME RESULTS OF THE EARTH'S MAGNETIC FIELD INVESTIGATIONS IN OUTER SPACE"

by S. Sh.Dolginov and N.V.Pushkov

The aim of this paper is to compare some results of magnetic measurements carried out on high-altitude space rockets and artificial Earth satellites at distances 2-10 R_E.

The magnetic measurements carried out up to the present time in outer space at these distances, in spite of their reconnaisance character, have given the experimental material touching upon the fundamental problems of geomagnetism.

The investigations were carried out under different geophysical conditions and with different instrumentation. As the experiments are complex and few, a question arises on the degree of the agreement of the experimental data obtained from different experiments, especially because the quantitative comparison of the results of magnetic and radiation measurements carried out simultaneously encounters now a number of difficulties.

The discussion of the results of magnetic measurements carried out in outer radiation belts at distances 2-10R_E will be difficult without the data on the degree of the agreement of the measured and calculated field values at low altitudes in the nearest vicinity of the Earth obtained in different regions of the globe by means of Sputnik III (1958) and Avanguard III (1959).

Declassified in Part - Sanitized Copy Approved for Release 2011/12/08 : CIA-RDP80T00246A016600420001-1

Declassified in Part - Sanitized Copy Approved for Release 2011/12/08 : CIA-RDP80T00246A016600420001-1

Measurements within the Range 1.04-1.5R_E

Comparison of the field values measured over the U.S.S.R territory within the altitude range of 230-800 km with the values of the field intensity calculated on the basis of 62 coefficients of Gauss series (n = 9, m = 6) (1) has made it possible to establish their correlation within the limits of 0.1 - 1 per cent over the most part of the U.S.S.R. territory including the Siberian world magnetic anomaly (2). The differences between the measured and calculated field values are of a systematic character.

The estimate of the accuracy of the analytic presentation of the field over the U.S.S.R. territory including the region of the Siberian anomaly, the estimate of the accuracy of the exclusion of the magnetic deviation effect on these portions of the trajectory allow to make a supposition that the observed differences can be explained by the chart errors, by the analytic presentation errors and by the errors of the exclusion of the deviation.

Magnetic measurements over different regions of the globe within the latitude range of $\pm 30^{\circ}$ and within the altitude range of 510-3,750 km over the Earth's surface were carried out by means of a proton precession magnetometer installed on the American satellite "Avanguard III". The deviations of the measured values from the calculated ones in a height range of 500-700 km detected in the American experiment, reach 300-500 gammas (3).

Declassified in Part - Sanitized Copy Approved for Release 2011/12/08 : CIA-RDP80T00246A016600420001-1

Declassified in Part - Sanitized Copy Approved for Release 2011/12/08 : CIA-RDP80T00246A016600420001-1

Over the predominant number of regions over which information was obtained in the American experiment the calculated values of the field turned out to be larger than measured ones, though there are regions with opposite values.

Until the coefficients of the analytic presentation of the field used for the comparison in the American experiment are not published, it is impossible to give a complete comparison of the results of the two experiments, but we can state that within the altitude range equal for the both experiments (500-800 km) in different latitudinal belts (35-65° and ± 30°) the measured and calculated field values differ within 0.5%-1%.

The measurements made with the satellite "Avanguard III" within the altitude range of 800-3,750 km have shown that the difference between the measured and calculated field values decreases in an absolute magnitude, but slower than the field decreases (4).

Therefore, the percentage deviation of the measured values from the calculated ones increases with the growth of height from 0.6% to 1.3%. It is quite possible that such a variation in the percent values of the deviations is determined not only by the errors of the analysis, but also by the influence of some external constant sources.

II. Measurements of the Magnetic Field Within the Altitude Range of 2-10 R_E. To obtain the experimental data on the magnetic field intensity at distances of 2-10 Earth radii was considered one of the most important tasks of the program of investigations in outer space, since the magnetic

Declassified in Part - Sanitized Copy Approved for Release 2011/12/08 : CIA-RDP80T00246A016600420001-1

Declassified in Part - Sanitized Copy Approved for Release 2011/12/08 : CIA-RDP80T00246A016600420001-1

storm and aurora theory allowed the possibility of producing electric current systems at thesee distances at least during magnetic disturbances.

The discovery of the radiation belts at such heights which exist constantly about the Earth has considerably changed our conceptions on properties of space at distances of 2-10 R_E.

Magnetic investigations in the outer radiation belt were made in the Soviet Union in 1959 on Luniks I and II and in the U.S.A. in 1958, 1959, 1960 and 1961 on 'Pioneer I', Pioneer II, "Explorer VI" and "Explorer X".

It seems reasonable to compare the results of the experiments performed under relatively equal geophysical conditions.

a) Magnetic Investigations on Magnetically Quiet Days.

It might be considered with a certain degree of conditionality that the experiments on Lunik II and on the "Explorer X" were carried out on magnetically quiet days, at least on the portion of the trajectories at 2 - 10 R_E.

Lunik II was launched on 12th September, 1959. The measurements were made by a three-component magnetometer of magnetically saturated type. Metrological properties of the instrumentation in use and the results of measurements were described in papers (5), (6). The instruments of this type are relative. However, due to the container rotation and the sensitivity of each of the channels to the field sign there was the possibility of determining the correction relative to the field absolute zero for each of the channels

Declassified in Part - Sanitized Copy Approved for Release 2011/12/08 : CIA-RDP80T00246A016600420001-1

Declassified in Part - Sanitized Copy Approved for Release 2011/12/08 : CIA-RDP80T00246A016600420001-1

and to control the zerostability in flight.

Fig.1 gives the results of the field measurements on the ground portion of the trajectory at distances of 18,000-50,000 kilometres from the Earth's centre.

Curve 1 represents the measured field values. The dashed curve 2, represents the calculated field values. The difference between curves I and 2 is presented by curve 3.

Smoothed curve 4 shows the most probable difference between curves 1 and 2, which is free from the possible errors linked with some nonsimultaneity of the interrogation of each of the channels at measurements on the rotating container, subjected to precession.

Curves 1 and 2 are quite near with each other at distances more than 28,000 km from the Earth's centre. At lower distances from the Earth the difference between the curves increases. At a distance of 18 thousand kilometres the difference is (according to curve 4) 130 gammas. At closer distances the instrument was off-scaled.

The difference between curves 1 and 2 at a distance of 18,000 km is according to curve 4 approximately 8 per cent and according to curve 3 approximately 11 per cent from the value of the dipole field at this distance.

This considerably exceeds the above considered differences between the calculated and measured values at low altitudes.

The first eight coefficients of the Gauss series used in calculating curve 2 and theoretical curves along the

Declassified in Part - Sanitized Copy Approved for Release 2011/12/08 : CIA-RDP80T00246A016600420001-1

Declassified in Part - Sanitized Copy Approved for Release 2011/12/08 : CIA-RDP80T00246A016600420001-1

trajectories of Sputnik III differ little. At a distance of 18,000 km the difference determined by the difference of g_1^0 coefficients amounts only to a few gammas.

The curve calculated with the help of Finch and Leaton's coefficients would be above curve 2. The difference between the calculated and measured values would be by 30 gammas greater at a distance of 18,000 km.

Thus, it appears that the observed differences between the calculated and measured field values lie beyond the limits of the uncertainty in the knowledge of the coefficients of the dipole and quadruple terms of the Gauss series.

At such exclusively high accuracy in determining radial distances which was achieved during the launch of Lunik II curve 4 seems to lie beyond the limits of the experimental errors.

The results of measurements on Lunik II on comparable positions of the trajectory (18,000-45,000 km) turned to be in a good agreement with the results of measurements made on "Explorer X" by meansof an absolute rubidium magnetometer (7) on March 25, 1961. Curve 4 of the Soviet experiment by the sign of the effect and the order of magnitude is analogous to the curves of the difference between the measured and calculated field values reported by Heppner and his collaborators from the data of the "Explorer X" magnetometer. The differences between the measured and calculated field values (from the coefficients of Finch and Leaton's analysis) in the American experiment amounted to 5% and 8% at a distance of 18,000 km correspondingly to two variants of the

Declassified in Part - Sanitized Copy Approved for Release 2011/12/08 : CIA-RDP80T00246A016600420001-1

Declassified in Part - Sanitized Copy Approved for Release 2011/12/08 : CIA-RDP80T00246A016600420001-1

rocket trajectory.

In the published reports on "Pioneer I", "Pioneer V" and "Explorer VI" experiments (8,9,10) there are no data on the Gauss series coefficients from which the theoretical curves were calculated.

From the data of the "Pioneer I", "Pioneer V", and "Explorer VI" experiments conclusion was drawn that up to 5 Earth radii, the magnetic field strictly follows the dipole distribution law (11) or differs from it very little (12).

All these experiments were carried out by means of rotating coils which measured the field component transversal to the spin axis. The instruments had logarithmic scales with high senitivity in weak fields and cruder sensitivity in strong fields.

Estimating the measurement errors due to possible mistakes in defining the coil rotation axis the experimenters considered as errors the 25-30 per cent deviationsof the theoretical curves from the measured value observed at distances of 25 R_E in "Explorer VI" experiments (These deviations, as a rule, had a positive sign, that is, the measured values were higher than the theoretical ones).

Because of this we have the right to conclude that using only the magnetic measurements data the authors of the experiments on "Explorer VI" could consider the field at distances of 2 -3R_E as coinciding with the calculated one within the limits of the accuracy, estimated by them.

Declassified in Part - Sanitized Copy Approved for Release 2011/12/08 : CIA-RDP80T00246A016600420001-1

Declassified in Part - Sanitized Copy Approved for Release 2011/12/08 : CIA-RDP80T00246A016600420001-1

Using the data on the particle spatial-energy distribution (12) the authors of the Explorer VI experiment have come to the conclusion that there are no considerable deviations in the geomagnetic field at distances less than 30,000 km.

The measurement results obtained in the abovementioned experiments at distances $\geq 5 R_E$ may be interpreted in a quite different way. According to Explorer VI data the deviations of the measured field values from the calculated ones amounted 60%-75% from the dipole field value at these distances. Besides, the difference curves gradients considerably differed from the normal field gradients at these distances. This made the authors of the experiments conclude that the effects observed are connected by a current system at a distance of 10 R_E. With the same success the effect was explained by Chapman and Akasofu (13) by a current system at a distance of 6 R_E.

The similar effects were recorded at these distances during Luniks I and II flights. However, it was estimated that these effects in the experiments on Lunik I might be ascribed to the measurement errors, though the possibility was not excluded that the fluctuations observed were of the geophysical nature.

In the experiment on "Explorer X" at 5-6R_E distances there were no effects observed in the field scalar magnitude, equal in size and similar in gradients to the effects revealed in the experiment on "Explorer VI" in the transversal field component. Considerable deviations were observed in

Declassified in Part - Sanitized Copy Approved for Release 2011/12/08 : CIA-RDP80T00246A016600420001-1

Declassified in Part - Sanitized Copy Approved for Release 2011/12/08 : CIA-RDP80T00246A016600420001-1

the field scalar magnitude T at 7 R_E distances and earlier deviations in the field direction were found. This is an extremely important circumstance. On this basis the authors of the experiment on "Explorer X" have come to the conclusion that the observed effects at these distances may be ascribed to the current system as well as to the possible effect of the solar wind and to superimposed interplanetary fields. Comparing the results of measurements on "Explorer VI" and "Explorer X" at 5-6R_E distances one should take into account some differences in geophysical conditions of the experiments. So the deviations observed on "Explorer VI" on August 9, 10, 24 and 25 could be connected (14) with a group of small disturbances without a sudden commencement by the amplitudes which do not belong to the class of magnetic storms, but which have common typical peculiarities at many observatories.

b) Magnetic Measurements on Magnetically Disturbed Days.

Magnetic measurements at distances of 2.5-6 R_E during magnetic disturbances with a typical sudden commencement and during the disturbance sufficiently intense on the Earth's surface were carried out during the flights of Lunik I and the satellite "Explorer VI".

As it is known (15), the Lunik I magnetometer during flight on January 2, 1959, detected considerable deviations of the measured field values from the calculated ones at distances of 14,500-25,000 km. (Fig. 2).

The curve of the measured field values was marked by a general depression and, besides, by the region where the

Declassified in Part - Sanitized Copy Approved for Release 2011/12/08 : CIA-RDP80T00246A016600420001-1

Declassified in Part - Sanitized Copy Approved for Release 2011/12/08 : CIA-RDP80T00246A016600420001-1

gradients considerably differed from the spatial gradients of the theoretical curve .

The materials collected by the authors (16) on the geophysical situation of the experiment are of extreme importance to the interpretation of the measurement results on Lunik I. The data of sixteen magnetic observatories and two terrestrial current observatories have shown that the day of January 2, 1959, including the hours of Lunik I flight were marked by a weak, but world magnetic disturbance with the amplitude of a sudden commencement. Sc ~10 grammas and the value Dst of the variation of ~ 20 gammas (Fig.3). The disturbance began 5 hours before this zone was passed by the space rocket. The disturbance was caused by an attenuating active region on the sun which 28 days before produced a strong magnetic storm. About 20 auroral stations observed aurorae on January 2, 1959.

One may note then the following:

The ~~summary~~ total energy release recorded during the passage of the outer zone by the instruments of Luniks I and III was the same and was 1.5 times less than the energy release, recorded during Lunik II flight (17) on a quiet day. During Lunik III flight a magnetic disturbance took place which began 3 hours before the launching (H average daily values were 50 gammas lower than H daily values on quiet days):

From the data of "Explorer VI" for the first hours of the storm initial phase the instruments sensitive to the bremsstrahlung electrones (18, 19) show the decrease of the

Declassified in Part - Sanitized Copy Approved for Release 2011/12/08 : CIA-RDP80T00246A016600420001-1

Declassified in Part - Sanitized Copy Approved for Release 2011/12/08 : CIA-RDP80T00246A016600420001-1

radiation intensity in the outer zone. Comparing the levels of the energy release registered in the Lunik I and III flights with that recorded in Lunik II flight one can conclude that the day of Lunik I experiment should be considered a disturbed one, not only from the data of magnetic ground stations, but also judging from the general tendency in the situation in the zone during magnetic disturbances which was established directly by means of radiation detectors.

The difference between the measured and calculated field values revealed in Lunik I flight at distances of 14,000-22,000 km from the Earth's centre, was probably determined by the effect of the reasons always effective (that is also on magnetically quiet days) and by the effect of additional sources originated at 2.5-3.5 R_E distances during magnetic storms.

The explanation of anomalous effects on the distribution of the Earth s magnetic field, at 2.5-3.5 R_E distances revealed during Lunik I and II flights naturally should be sought in magnetic phenomena arising during the motion of charged particles in the Earth's magnetic field. In connection with this qualitative comparisons were made of the geomagnetic curves and the ~~curves of~~ spatial energy radiation distribution curves obtained by S.N.Vernov, A.E.Chudakov, J.Van Allen and their collaborators. Then we wanted to find proofs that the 2.5-3.5 R_E space is magnetically active in the published materials of radiation investigations on "Explorer VI" (18) which showed that at these distances the largest variations are observed in the spectrum of high

Declassified in Part - Sanitized Copy Approved for Release 2011/12/08 : CIA-RDP80T00246A016600420001-1

Declassified in Part - Sanitized Copy Approved for Release 2011/12/08 : CIA-RDP80T00246A016600420001-1

energy particles which the authors connected with the field variation at these distances. A stable splitting of the outer zone (18) is also observed and the region of anomalous effects in the magnetic field coincides with the region of the largest gradients of the radiation energy curves (20).

On the other hand, a number of authors pointed out to the discrepancy (in the quantitative character of the effects in the magnetic field with the intensity of radiation (12, 21).

On the basis of paper (21) the authors (5) expressed the supposition, that the radiation belt protons not yet discovered, are chiefly responsible for the observed magnetic effects at 2.5-3.5 R_E distances. The electrons contour magnetically active regions being very sensitive to the field distribution.

Of paramount importance are the data on the magnetic disturbance effect at a distance of 24,000 km observed during the magnetic storm on August 16-17, 1960, by the satellite "Explorer VI" published rather recently. A disturbance effect of about 380 gammas in the transversal field component was recorded at a distance of 24,000 km.

Since the satellite at 4 R_E distance was close to the geomagnetic equator, one can conclude that the disturbance amounted to 70-80% of the dipole field value at these distances. The publication does not contain information on the spatial distribution of the effect in the nearest vicinity

Declassified in Part - Sanitized Copy Approved for Release 2011/12/08 : CIA-RDP80T00246A016600420001-1

Declassified in Part - Sanitized Copy Approved for Release 2011/12/08 : CIA-RDP80T00246A016600420001-1

of 4 R_E. Proceeding from the fact that) st-variation by the data of terrestrial stations was about 12 0 gammas, that is, 3 times lower than the effect at 4 R_E, one can conclude that the spatial gradients of the effect differed from the dipole field gradient.

Comparing the effect at a distance of 21,000-23,000 km in Lunik I experiment and the corresponding effect on the Earth's surface with the analogous effects in Explorer VI experiment on August 16-17, it is necessary to note a better agreement of these effects in the last case. From this point of view the agreement between the effect on the Earth's surface and that at a distance of 24,000 km on "Explorer VI" may be established with more physical ~~definite~~ models of the current ring than it was achieved by the authors. (16).

In addition to the experiments made directly in this region one should use the data of "Avanguard III" obtained during the magnetic disturbances (3) to solve the magnetic storm sources localization problem.

Comparing the signs of the disturbance effects on the Earth's surface and at the height of the satellite flight the authors of the experiment have concluded that the disturbance sources are situated near the slit between the outer and inner radiation zones.

We have reviewed the not numerous experiments aimed at measuring the Earth's magnetic field by means of magnetometers in the outer radiation zone.

We should stress once more that all the experiments conducted so far had certain limitations which in a different degree influenced the accuracy of measurements and

Declassified in Part - Sanitized Copy Approved for Release 2011/12/08 : CIA-RDP80T00246A016600420001-1

Declassified in Part - Sanitized Copy Approved for Release 2011/12/08 : CIA-RDP80T00246A016600420001-1

the unique character of the result.

In spite of this in a number of experiments (5,7,15,12, 3) deviations were detected from the theoretically calculated field values lying beyond the limits of the known errors. Comparing the results of these measurements one can indicate two magnetically active regions at 2.0-1.0 R_E distance in the space of the magnetosphere:

1) at 2.5-3.5 R_E distances;

2) at > 6 R_E distance.

In the region of 2.5-3.5 R_E a current system is apparently localised which during magnetic disturbances becomes especially intense and is responsible for the main phase of the magnetic storm. These regions should be the subject of especially intensive investigations.

It seems that as a result of the magnetic and radiation investigations performed the following conceptions in geomagnetism based on the analysis of the terrestrial data have become less hypothetical.

1) The existence of the outer part of the Earth's constant magnetic field;

2) The existence of the outer part of secular variations of the constant field;

3) The existence and localization of the ring current of magnetic storms.

Declassified in Part - Sanitized Copy Approved for Release 2011/12/08 : CIA-RDP80T00246A016600420001-1

Declassified in Part - Sanitized Copy Approved for Release 2011/12/08 : CIA-RDP80T00246A016600420001-1

REFERENCES

1. Benkova N.P., Tyurmina L.O., Geomagnetizmi. Aeronomiya, Vol.3. 1961, N 1 and 3.

2. Dolginov S. Sh., Zhuzgov L.N., Pushkov. N.V., Tyurmina, L.O., Fryazinov I.V.

3. Some Results of the Measurements of the Earth's Constant Magnetic Field from Sputnik III over the USSR Territory (The Report presented to the present Symposium).

3. Heppner J.P., Cain J.C., Shapino, I.R., Stolarik J.D., Space Research I, Amsterdam, 1960.

4. Heppner, J.P., Skilman, T.L., Cain J.C., Space Research II, 1961, p.681.

5. Dolginov S.Sh., Yeroshenko E.G., Iskusstvennye Sputniki Zemli, 1960, N.5.

6. Dolginov S.Sh., Teronenko E.G., Zhuzgov L.N., Pushkov N.V., Geomagnetism i Aeronomiya, Vol.1, N.1, 1961.

7. Heppner, J.P., Ness N.F., Skilman T.L., Scearce C.S., Contributions to 1961 Kyoto Conference, Preprint.

8. Sonnett C.P., Smith E.J. Sims A.R., Space Research I, 1960

9. Smith E.J., Coleman, P.J., Judge D.F., Sonett, C.P., J.Geophys. Res., 1960, 65, N6

10. Sonett C.P., Smith E.J., Judge D.L., Coleman P.J, Physical Review Lett. Vol.4, N.4, 1960.

11. Rossi B. Trans. American Geophysical Union, Vol.41, N3, 1960.

Declassified in Part - Sanitized Copy Approved for Release 2011/12/08 : CIA-RDP80T00246A016600420001-1

Declassified in Part - Sanitized Copy Approved for Release 2011/12/08 : CIA-RDP80T00246A016600420001-1

12. Smith E.Rosen, A, Ballistic Missiles and Space Technology 1960, N.3.

13. Akasofu S.I., Cain J.C., Chapman S, J.Geophys.Res., Vol.66, N.12, 1961.

14. Antsilevich G.M., Geomagnetism i Aeronomiya, Vol.I. N 3, 1961.

15. Dolginov S.Sh, Pushkov N.V., Doklady Akademii Nauk SSSR, 129, N1,77, 1959.

16. Antsilevich, M.G., and Shevnin A.D., Doklady Akademii Nauk, 135, N 2, 1960.

17. Vernov S.N., Chudakov A.E., Vakulov L.V., Gorchakov E.V., Logachev Yu. I. Geomagnetism i Aeronomiya, Vol.1, N6. 1960.

18. Fan C., Meyer, P.Simpson J.J., Geophys.Res. Vol.66, N 9, 1961.

19. Arnoldy R.L., Hoffman R.A., Winckler J.R., J.Geophys. Res.Vol 65, N.5. 1960.

20. Van Allen J.A., Frank L.A., Nature, 184, 219, 1959.

21. Gringauz K.I., Kurt, V.I., Moroz V.I., Shklovsky, I.S., Astronomichesky Zhurnal Vol.XXXVII, issue 4, 1960.

22. Singer S.F., Trans.Amer.Geophys.Union 38, 175, 1957.

Declassified in Part - Sanitized Copy Approved for Release 2011/12/08 : CIA-RDP80T00246A016600420001-1

Declassified in Part - Sanitized Copy Approved for Release 2011/12/08 : CIA-RDP80T00246A016600420001-1

by S.Sh.Dolginov, L.N.Zhuzgov, N.V.Pushkov,
L.O.Tyurmina, I.V.Fryazinov

14.

"Some results of the constant geomagnetic field measurements carried out from Sputnik III over the territory of the USSR"

Measurements of the Earth's magnetic field in interplanetary space envisaged by the Soviet IGY program were carried out in May-June 1958 from Sputnik III.

Objectives of this experiment, a preliminary report on the character of the experimental data obtained and a detailed description of the measuring apparatus were presented in paper (1,2,3).

The Sputnik III magnetometer measured the scalar value of the geomagnetic field intensity and the satellite orientation with respect to the geomagnetic field vector.

Knowledge of the orientation angles of the satellite body with respect to the geomagnetic field made it possible to determine parameters of the satellite motion and its absolute orientation. The theory of the question, the technique of solving this problem and the results of determining Sputnik III rotation and orientation parameters are expounded in paper (4).

Comparison of measured values of the intensity of the geomagnetic field with the values of this intensity calculated on the basis of the coefficients of the geomagnetic potential

Declassified in Part - Sanitized Copy Approved for Release 2011/12/08 : CIA-RDP80T00246A016600420001-1

Declassified in Part - Sanitized Copy Approved for Release 2011/12/08 : CIA-RDP80T00246A016600420001-1

expansion in a series in spherical harmonics made it possible to establish their correspondence within 0.I-I% over the most part of the territory of the USSR including the Siberian world magnetic anomaly and up to 2. over eastern boundaries of the territory of the USSR and adjoining seas.

Difference between measured and calculated values of the field are of a systematic character and have a constant sign.

The evaluation of the precision of an analytic presentation of the field over the territory of the USSR and possible errors of presentation over the boundary territories makes it possible to express a supposition that discrepancies observed can be explained in the main by errors of analytic presentation and partly by errors of measurements.

Thus, in the constant magnetic field over the USSR a noticeable part was not revealed which would not correspond to the ground distribution of the field beyond the limits of the accuracy of comparisons and the accuracy of initial charts (±200 gammas).

In the present report the conclusions expounded above are illustrated by a limited number of typical magnetograms obtained on circuits which traversed the whole territory of the USSR. More detailed data will be published soon.

The exposition of immediate materials will be opened by a brief description of metrological properties of the apparatus in use and the technique of excluding the magnetic interference aboard the satellite from Sputnik III magnetograms.

Declassified in Part - Sanitized Copy Approved for Release 2011/12/08 : CIA-RDP80T00246A016600420001-1

Declassified in Part - Sanitized Copy Approved for Release 2011/12/08 : CIA-RDP80T00246A016600420001-1

I. Metrological Features of the Apparatus and the Technique of Excluding the Magnetic Deviation

Magnetic measurements from Sputnik III were the first magnetic survey made from a space vehicle.

The high accuracy of the determination of the satellite coordinates in time and high informative capacities of telemetry have favoured the conducting of the experiment.

The main difficulty in carrying out the experiment aimed at measuring the magnetic field was connected with a considerable magnetic interference. The latter took place on board the satellite due to a large number of various instruments designed for other experiments which contained magnetic parts.

This served one of the reasons for a refusal from the use of a proton magnetometer and for a use of a magnetometer with automatic orientation of a magnetically saturated sensor with respect to the total vector equipped with two elements for measuring the satellite orientation and, hence, the magnetic interference vector with respect to the field vector.

Due to precessional character of the satellite rotation it was possible to exclude the main part of the magnetic interference.

Being a relative instrument, the magnetometer in use was fixed to absolute values of the field by means of a proton magnetometer.

The stability of the zero point of the magnetometer was determined by the stability of the special source of the

Declassified in Part - Sanitized Copy Approved for Release 2011/12/08 : CIA-RDP80T00246A016600420001-1

Declassified in Part - Sanitized Copy Approved for Release 2011/12/08 : CIA-RDP80T00246A016600420001-1

compensation network which was not switched off. Laboratory tests of the similar source of stable current during 25 days have shown changes in current which are equivalent to the magnetometer zero drift o 135 gammas for 21 days with the average velocity of the change 5 gammas/day. For the latter four days the drift velocity increased to 12 gammas/day.

The drift of the magnetometer aboard the satellite could be also checked up by comparing differences between experimental values of the field and theoretical values on the circuits having close coordinates φ , λ, h and even coinciding values φ and λ . Such circuits took place on days with 1-2 day interval and on days with 17-20 day interval. The accuracy of one counting as a result of deciphering of the telemetry is evaluated 20 gammas from the results of laboratory tests. The readings of the instrument were transmitted practically continuously during the contact. The main error in measurements is connected with the error of excluding the magnetic deviation. The exclusion of the magnetic deviation was carried out in such a way.

Sputnik III magnetic interference vector created by solid magnetic materials and constant electric circuits performed a regular precessional motion with a precession angle close to 90° and a slow rotation about the longitudinal axis. The rotation about the longitudinal axis decelerated rather quickly.

Since the precessional motion velocity was sufficiently high, the magnetic interference produced the field variations whose gradients essentially differed from the gradients of the

Declassified in Part - Sanitized Copy Approved for Release 2011/12/08 : CIA-RDP80T00246A016600420001-1

Declassified in Part - Sanitized Copy Approved for Release 2011/12/08 : CIA-RDP80T00246A016600420001-1

Earth's magnetic field at high altitudes. Due to this, smooth field variations connected with the change of height and

Declassified in Part - Sanitized Copy Approved for Release 2011/12/08 : CIA-RDP80T00246A016600420001-1

Declassified in Part - Sanitized Copy Approved for Release 2011/12/08 : CIA-RDP80T00246A016600420001-1

coordinates of the satellite relative to the Earth's surface were modulated by quicker ocillations, the frequency of which coincided with the frequency of the precessional motion, as seen from the curves of Fig.1

If T_ε is the geomagnetic field vector, T_i is the magnetic interference vector, and φ is the angle between them, then the scalar value of the total vector T_t will be determined from the formula

$$T_t = \left|\vec{T}_i + \vec{T}_\varepsilon\right| = \sqrt{T_\varepsilon^2 + T_i^2 - 2T_i T_\varepsilon \cos\varphi} \qquad (I)$$

Due to the small magnitude of the T_i value as compared with T_ε, the above expression can be expanded in a series in powers of T_i

$$T_\varepsilon = T_t - T_i \cos\varphi + \frac{1}{2}\frac{T_i^2}{T_\varepsilon}\sin^2\varphi + \ldots$$

Restricting ourselves with the first term, we shall obtain:

$$T_\varepsilon = T_t - T_i \cos\varphi \qquad (2)$$

Thus, it is assumed that due to the small magnitude of the vector T_i, the magnetic interference changed only the magnitude of the geomagnetic field intensity and did not change considerably its direction, and the satellite magnetometer measured the Earth's magnetic field intensity and the projection of the magnetic interference vector on the direction of the Earth's magnetic field changing in magnitude and sign.

If X, Y, Z represent a recangular system of coordinates connected with the body of the satellite, j is an angle between

Declassified in Part - Sanitized Copy Approved for Release 2011/12/08 : CIA-RDP80T00246A016600420001-1

Declassified in Part - Sanitized Copy Approved for Release 2011/12/08 : CIA-RDP80T00246A016600420001-1

vector T_i and the Z-axis, φ is an angle between the projection of T_i on the plane XOZ and the Y-axis, λ and Δ are analogous angles of the measuring element of the magnetometer with a system of coordinates XYZ (Fig.2, a, b, c) (4), then we have

$$\cos \Psi = \cos j \cos \lambda + \sin j \sin \lambda \cos (\Delta + \varphi) \tag{3}$$

Angles λ and Δ were determined from the readings of the magnetometer orientation sensors.

Having assumed, as the first approximation, that the interference is of a dipole character, we obtain from (2) and (3)

$$T_i \cdot \cos \Psi = T_i \cos j \cdot \cos \lambda + T_i \sin j \cdot \sin \lambda \cdot \cos (\Delta + \varphi) =$$
$$= Z_i \cos \lambda + H_i \sin \lambda \cdot \cos (\Delta + \varphi). \tag{4}$$

where Zi and Hi are the interference vertical and horizontal components. They were preliminarily estimated at the satellite model.

In fact, in accordance with the actual disposition of the main sources creating interferences, the magnetic interference was not of a dipole character. Magnetograms were subjected to harmonic analysis with the use of segments equal to precession periods. As a result of harmonic analysis, it was established that the deviation is represented in the main by three harmonics.

In accordance with this, the value of the magnetic deviation as a function of time for magnetograms should be searched for not from formula (4), but in the form of a number of spherical

Declassified in Part - Sanitized Copy Approved for Release 2011/12/08 : CIA-RDP80T00246A016600420001-1

Declassified in Part - Sanitized Copy Approved for Release 2011/12/08 : CIA-RDP80T00246A016600420001-1

functions.

$$T_i = Z_1 \cos\lambda + H_1 \sin\lambda \cdot \cos(\Delta + G_1) + Z_2\left(\cos 2\lambda - \frac{1}{3}\right) +$$
$$+ H_2 \sin 2\lambda \cdot \sin(\Delta + G_2) + H_2'(1 - \cos 2\lambda)\cdot \sin(2\Delta + G_3) + Z_3\left(\cos 3\lambda - \frac{3}{5}\cos\lambda\right) \quad (5)$$

where Z_n H_n and G_n are constant coefficients, Δ and λ are angles of the turn of the satellite body with respect to the magnetic field vector. It is obvious that expression (4) is the first harmonic of expression (5), its dipole part.

The determination of the coefficients of formula (5) reduced to the selection of such a combination of the vector components of the first and second harmonics which ensured the optimum agreement between the magnetic deviation curve calculated from formula (5) and the experimental magnetogram. This method has a certain sensitivity which limits a unique selection of the deviation coefficients. One of the sources of dispersion in the values of deviation coefficients determined on different circuits lies in the errors of the determination of the "zero" counting from orientation generators. Determined by two independent methods "zeros" of the orientation generators sometimes differ within $\pm 5^0$. As calculations have shown, non-singularity of the choice of the deviation coefficients (in the assumption that they should be constant on all circuits) leads to errors $\pm$ 100 gammas in average smoothed experimental curves (curves 3 in Fig.4). The error is a little bit higher where modulation on magnetograms is not deep. The main part of the magnetic interference corresponded to three initial terms of expression (5).

Fig.1 presents a magnetogram obtained on one of the circuits of the satellite flight (curve 1). Curve 2 is

Declassified in Part - Sanitized Copy Approved for Release 2011/12/08 : CIA-RDP80T00246A016600420001-1

Declassified in Part - Sanitized Copy Approved for Release 2011/12/08 : CIA-RDP80T00246A016600420001-1

obtained from curve I after excluding the first harmonic of deviation. Curve 3 is obtained from curve 2 by means of a graphical exclusion of the second harmonic and higher harmonics. Subsequently it was decided to select deviation coefficients of the first harmonic and of higher harmonics on a computer. The machine determines smoothed curves3which subsequently are used for comparison with calculated curves (curves 1 and 2 in Fig.4).

After the exclusion of the magnetic deviation effect from the curves of the magnetograms, we have no right to speak about possible peculiarities of the geomagnetic field whose spatial dimensions were close to linear dimensions of the deviation waves. Thus, we can solve the problem of the degree of the correspondence of modern magnetic charts to the actual distribution of the geomagnetic field intensity only generally, in its basic features.

II. Comparison of Measured and Calculated Values of the Geomagnetic Field at High Altitudes

To elucidate the problem of the degree of the correspondence of modern magnetic charts to the actual distribution of the geomagnetic field, a calculation was made of the field total intensity scalar magnitude for points located at the portions of Sputnik III trajectory over the territory of the USSR.

By the time when the present work was being carried out there were no ready magnetic charts for epoch 1958. Therefore the following technique was used:

Declassified in Part - Sanitized Copy Approved for Release 2011/12/08 : CIA-RDP80T00246A016600420001-1

Declassified in Part - Sanitized Copy Approved for Release 2011/12/08 : CIA-RDP80T00246A016600420001-1

I. From the data of spherical harmonic analysis of the geomagnetic field for previous epochs N.P.Benkova and L.O.Tyurmina (5) have made extrapolations for epoch 1958 of all the potential coefficients g_n^m and h_n^m of the geomagnetic field up to n=6, m=6. Extrapolation was made in

Declassified in Part - Sanitized Copy Approved for Release 2011/12/08 : CIA-RDP80T00246A016600420001-1

Declassified in Part - Sanitized Copy Approved for Release 2011/12/08 : CIA-RDP80T00246A016600420001-1

accordance with empirically established peculiarities of the secular variations of each of the coefficients.

Using the general formula of the field potential with these extrapolated values of the coefficients, calculations of the scalar value of the field intensity T for points along Sputnik III trajectories were carried out as well as calculations of the Z-component of the field for the uniform network of the ground points on the territory of the USSR. The values of T on basis of the calculations are shown by curves (2) in Fig.4 and in subsequent figures.

2. Values of the Z-component of the field calculated from the above extrapolated coefficients were compared with Z--components of the chart of the USSR previously reduced to epoch 1958 for secular variations. Compilers of the chart are V.P.Orlov and N.V.Adam. The comparison has revealed the existence of discrepancies up to 1,500 gammas between these two charts of ground values of the vertical Z-component.

Such considerable discrepancies could be the consequence of different accuracy of initial data which were the basis of charts compared, of different accuracy of two methods used for taking into account the field secular variations and possibly of the peculiarity of the secular variations of the magnetic field over Eurasia.

In any case it was obvious that extrapolated coefficients unsatisfactorily present the magnetic chart of the USSR on the Earth's surface.

Declassified in Part - Sanitized Copy Approved for Release 2011/12/08 : CIA-RDP80T00246A016600420001-1

Declassified in Part - Sanitized Copy Approved for Release 2011/12/08 : CIA-RDP80T00246A016600420001-1

In this connection a lim ted problem was set: to correct the coefficients g_n^m and h_n^m in such a waythat a good analytic presentation of the Z chart of the USSR be achieved. The technique of the correlation of the coefficients is expounded in paper (5). The satisfactory presentation of the chart of the vertical component of the USSR geomagnetic field was achieved with the use of corrected coefficients of the potential $g_n'^m$ to n=9 and m=6. Differences between the field values on the Z-chart of the USSR and those values calculated from the corrected coefficients $g_n'^m$, as a rule, are of the order of 200 gammas and lower, and only in several points they reach greater values. The accuracy of the field presentation beyond the borders of the USSR was not verified. The values of the scalar values of the total vector T along the segments of Sputnik III trajectories calculated from these coefficients are presented in Fig.4 and subsequent figures by curves I.

For convenience of the reviewing the material the trajectories of circuits used for illustrations are indicated against the background of the chart of isodynames of the modulus of the intensity T of the normal geomagnetic field of the USSR. (Fig.3). Numbers of circuits corespond to numbers on magnetograms. Direct circuits coming in the direction from south-west to north-east traversed the territory of the USSR at altitudes of 240-800 km. Inverse circuits coming from north-west to south-east traversed the territory of the USSR at altitudes of 300-800 km.

The main peculiarity of the magnetic field at the territory

Declassified in Part - Sanitized Copy Approved for Release 2011/12/08 : CIA-RDP80T00246A016600420001-1

Declassified in Part - Sanitized Copy Approved for Release 2011/12/08 : CIA-RDP80T00246A016600420001-1

of the USSR is the East-Siberian maximum of the geomagnetic field intensity. The centre of this maximum has not yet been sufficiently investigated by round magnetic surveys. According to the data at our disposal it was situated in epoch I950 between the Yenisei and Lena Rivers at a latitude of 60° and at a longitude I08°E. The value of the field in this region exceeded 6I,500 gammas. Thus, the Asian maximum exceeds the value of the magnetic field intensity on the North Magnetic Pole.

Agreeing very close over the European part of the Soviet Union the calculated curves I and 2 start to disagree with the transition to East and reach discrepancies up to I,000 gammas within the range of longitudes 75-I06°E. They reach the maximum value up to I,700 gammas at longitudes 95-97°E. Curves I and 2 agree again at longitudes I40-I46° for circuits traversing the Soviet Union from South-West to North-East.

Experimental curves 3 pass very close from curves I over the territory of the Soviet Union. Passing above curves I in the extreme South-West of the USSR (maximaly by 250 gammas) experimental curves 3 gradually approach the former and the difference reaches zero at longitudes about 55°E. Over the Asian part of the USSR experimental curves 3 pass invariably lower than curves I within the limits 50 to 300-400 gammas. On many circuits this difference decreases up to 200-I00 gammas over the region of the intensity maximum (λ=90-II0°E). East of the intensity maximum over the land boundary of the USSR and East from it, experimental curves 3 pass lower than

Declassified in Part - Sanitized Copy Approved for Release 2011/12/08 : CIA-RDP80T00246A016600420001-1

Declassified in Part - Sanitized Copy Approved for Release 2011/12/08 : CIA-RDP80T00246A016600420001-1

both calculated curves which, as was already mentioned, practically coincide at these longitudes. Almost in all cases over this territory (due to definiteness of the direction of the kinematic moment vector around which precession takes place) the modulation amplitude under the action of the interference vector turned to be not deep which, as mentioned before is connected with large errors in the exclusion of the deviation. Besides, the accuracy of the analytic presentation of the field over eastern boundaries of the territory is also lower due to some limitations which took place in determining coefficients $g_n^{'m}$ and h_n^m.

Thus, the basic peculiarities of the geomagnetic field at the most part of the territory of the U.S.S.R., including the world anomaly, correspond well both at the Earth's surface, and at altitudes of Sputnik III flight to the found analytic presentation of the field with coefficients corrected on the chart of the vertical component of the U.S.S.R. and, hence, in the constant magnetic field of the Earth over the U.S.S.R. there is no noticeable part which would not correspond to the terrestrial distribution of the field within the reached accuracy of comparisons (± 200 gammas). The found analytic presentation of the field at the territory of the U.S.S.R., as measurements from Sputnik III have shown, represent the field less satisfactorily on the eastern boundary of the U.S.S.R. territory and adjoining seas. To verify the applicability of coefficients $g_n^{'m}$ and h_n^m beyond the territory of the U.S.S.R. a programme of calcula-

Declassified in Part - Sanitized Copy Approved for Release 2011/12/08 : CIA-RDP80T00246A016600420001-1

Declassified in Part - Sanitized Copy Approved for Release 2011/12/08 : CIA-RDP80T00246A016600420001-1

tions on the Earth's surface is planned.

The East-Siberian world magnetic anomaly has repeatedly attracted the magnetologist's attention, when they investigate the problems of geomagnetism, particularly, the features of the

Declassified in Part - Sanitized Copy Approved for Release 2011/12/08 : CIA-RDP80T00246A016600420001-1

Declassified in Part - Sanitized Copy Approved for Release 2011/12/08 : CIA-RDP80T00246A016600420001-1

secular variations of the residual field obtained from the normal geomagnetic field by subtracting of its dipole part. One of the estimations of the secular variation rate can be made from the consideration of the change in the position of the centre of the anomaly in time. (Speaking of the centre of the anomaly we mean a symmetric point of the oval of the maximal isodyname). Some of the Sputnik III circuits traversed close this region (Fig.3), and, therefore, it is possible to estimate the position of the intensity maximum of the total vector. From a combination of circuits denoted in Fig.3 (No. 2, 3, 8 and some others) the position of the maximum for I958 and the above mentioned altitude of 250 km can be indicated:

$\lambda = 110\text{-}111^\circ E, \quad \varphi = 62^\circ N$

These coordinates lie within the limits of the maximal isodyname of the normal field chart for epoch I950 (Fig.3).

Declassified in Part - Sanitized Copy Approved for Release 2011/12/08 : CIA-RDP80T00246A016600420001-1

Declassified in Part - Sanitized Copy Approved for Release 2011/12/08 : CIA-RDP80T00246A016600420001-1

References

I. N.V.Pushkov, S.Sh.Dolginov, Uspekhi Fiz. Nauk, 63, 64, I957.

2. S.Sh.Dolginov, L.N.Zhuzgov, N.V.Pushkov, Artificial Earth Satellites, 2, 50, I958.

3. S.Sh.Dolginov, L.N.Zhuzgov, V.A.Selyutin, Artificial Earth Satellites, 4, I35, I960.

4. V.V.Beletsky, Yu.V.Zonov, Artificial Earth Satellites, 7, 32, I96I.

5. N.P.Benkova, L.O.Tyurmina, Geomagnetism and Aeronomy, USSR, I, 87 and p.452, I96I.

Declassified in Part - Sanitized Copy Approved for Release 2011/12/08 : CIA-RDP80T00246A016600420001-1

Declassified in Part - Sanitized Copy Approved for Release 2011/12/08 : CIA-RDP80T00246A016600420001-1

Figures

Fig. 1. The character of experimental curves of Sputnik III magnetometer.

1. Record of the intensity of the scalar magnitude of the total field vector.
2. An experimental curve after exclusion of the first harmonic of magnetic deviation.
3. An experimental curve after exclusion of high harmonics.

4, 5. Changes of angles λ and Δ (see Fig. 2 c) with time.

Fig. 2. Graphical presentations for determination of the dipole part of magnetic deviation as a function of orientation angles.

Ti - magnetic interference vector

T_ξ - geomagnetic field vector.

$\mathcal{J}$ and σ - angles formed by the magnetic interference vector with the coordinate system in the satellite.

λ and Δ - angles formed by the magnetometer measuring pickup (the geomagnetic field vector) with the same coordinate vector.

φ - a spherical angle between the magnetic interference vector and the geomagnetic field vector.

Fig. 3. The chart of the modulus of the intensity of the normal geomagnetic field of the USSR for epoch 1950 with projections of the segments of Sputnik III trajectories. Numbers of the segments of trajectories correspond to numbers on magnetograms of Fig. 4,5,6,7

Fig. 4,5,6,7. Experimental and calculated magnitudes of the scalar value of the geomagnetic field total vector along the segments of trajectories.

Curve 1 solid - calculated values of the field according to coefficients determined from the chart of the vertical component of the USSR.

Curve 2 (long dashed) calculated values of the field according to extrapolated coefficients of the potential analyses made earlier.

Curve 3 (short dashed) - an experimental curve after

Declassified in Part - Sanitized Copy Approved for Release 2011/12/08 : CIA-RDP80T00246A016600420001-1

Declassified in Part - Sanitized Copy Approved for Release 2011/12/08 : CIA-RDP80T00246A016600420001-1

exclusion of the influence of magnetic deviation.
Curve 4 - the altitude of the flight
Curve 5 (modulated solid) - Sputnik III magnetometer record.

Declassified in Part - Sanitized Copy Approved for Release 2011/12/08 : CIA-RDP80T00246A016600420001-1

Declassified in Part - Sanitized Copy Approved for Release 2011/12/08 : CIA-RDP80T00246A016600420001-1

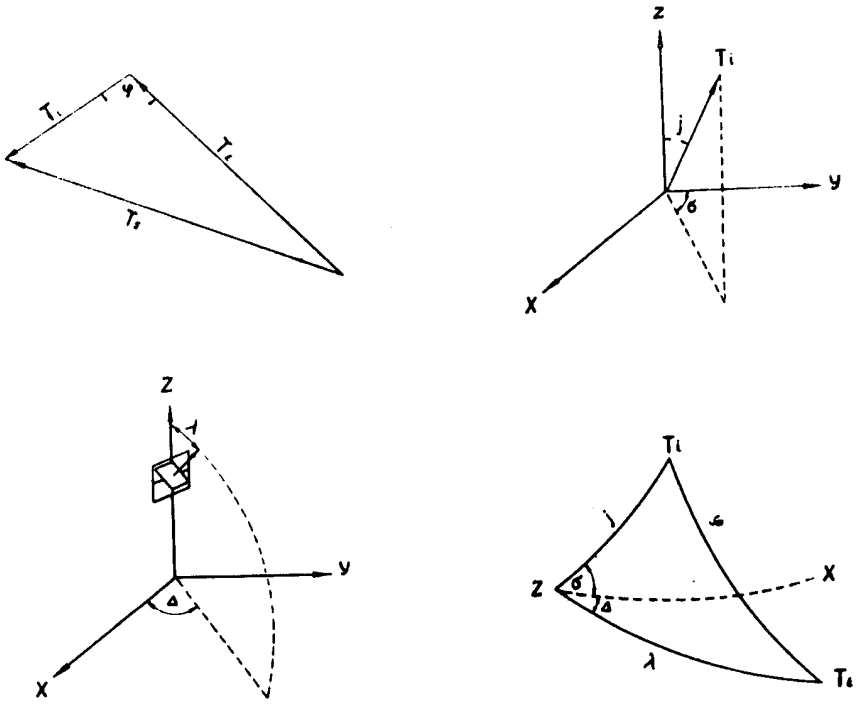

$$T_s^2 = T_e^2 + T_i^2 - 2 T_e T_i \cos\varphi$$

$$T_e = T_s - T_i \cos\varphi$$

$$T_i \cos\varphi = T_i \cos J \cos\lambda + T_i \sin J \sin\lambda \cos(\Delta+\sigma) =$$

$$= Z_i \cos\lambda + H_i \sin\lambda \cos(\Delta+\sigma)$$

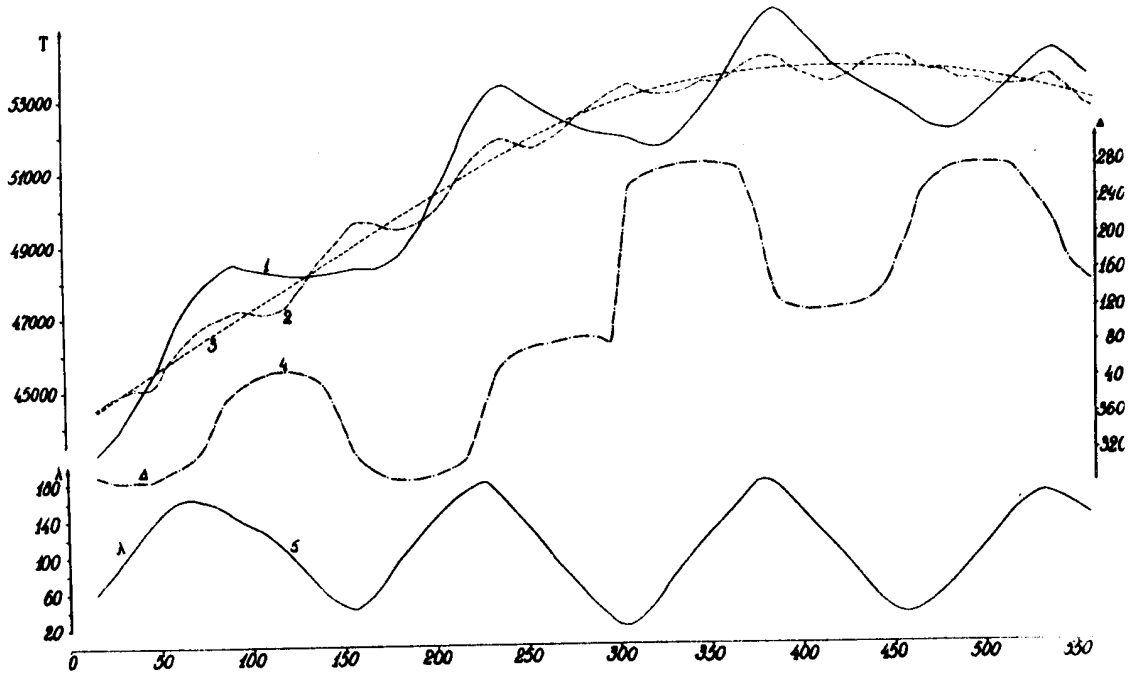

Declassified in Part - Sanitized Copy Approved for Release 2011/12/08 : CIA-RDP80T00246A016600420001-1

Declassified in Part - Sanitized Copy Approved for Release 2011/12/08 : CIA-RDP80T00246A016600420001-1

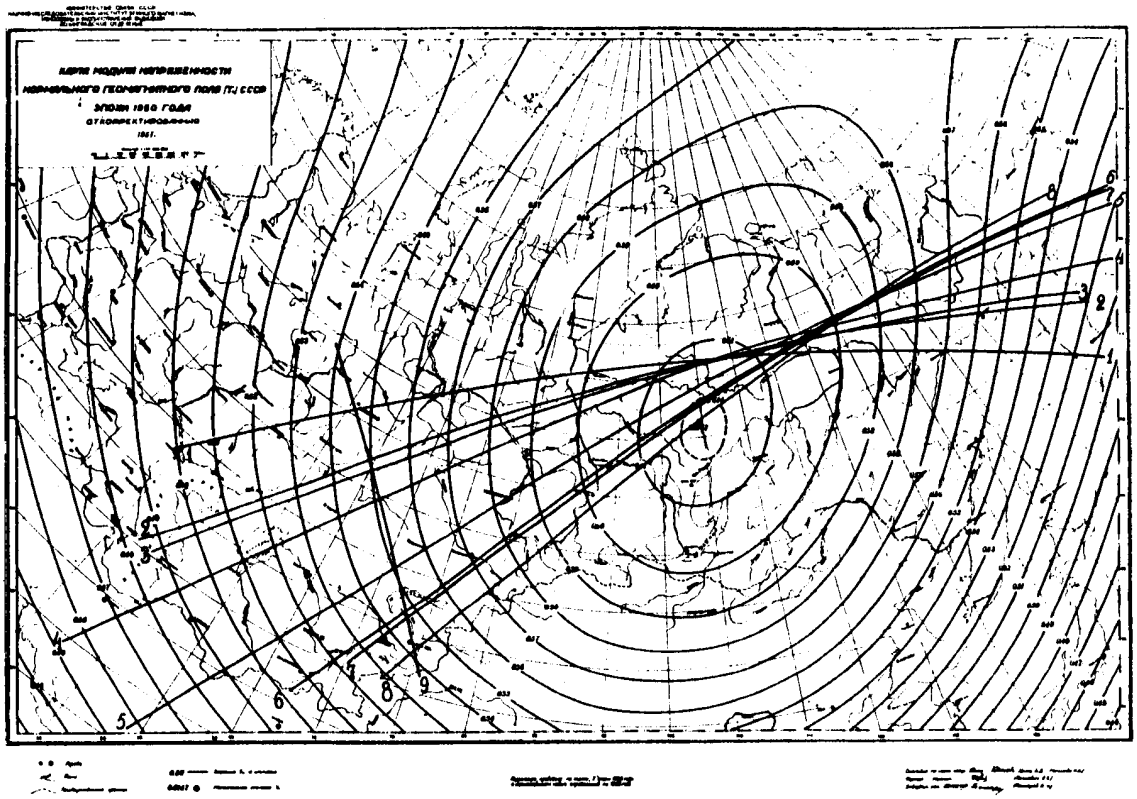

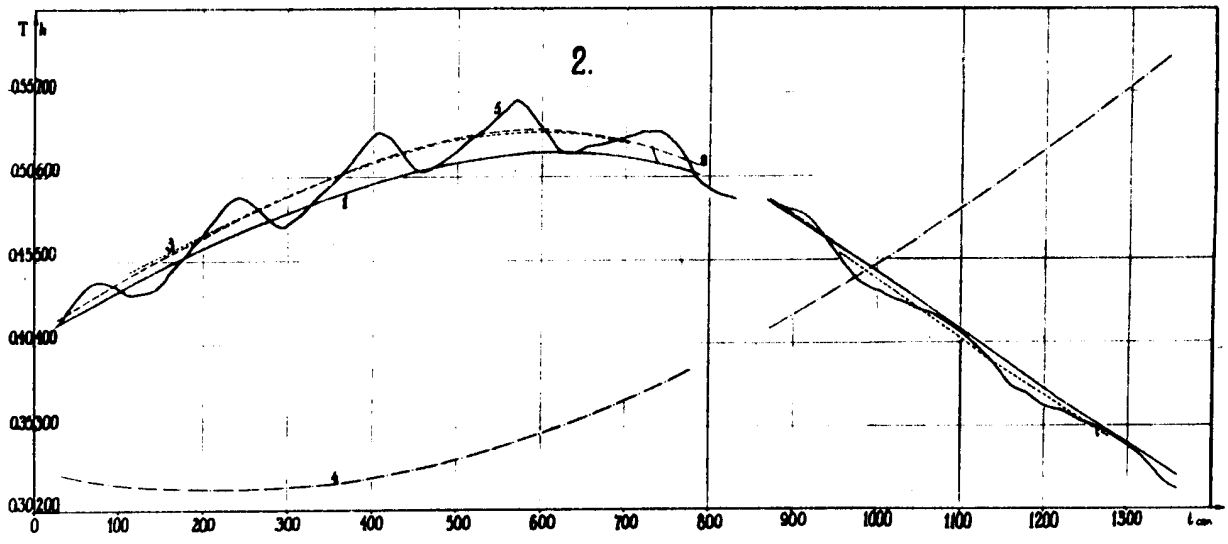

Declassified in Part - Sanitized Copy Approved for Release 2011/12/08 : CIA-RDP80T00246A016600420001-1

Declassified in Part - Sanitized Copy Approved for Release 2011/12/08 : CIA-RDP80T00246A016600420001-1

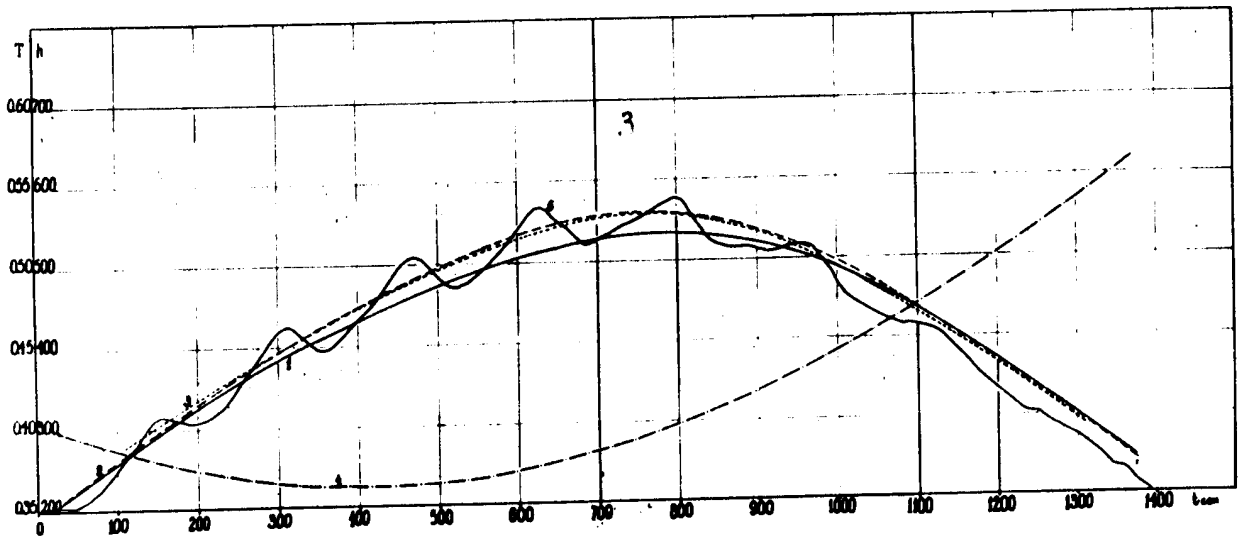

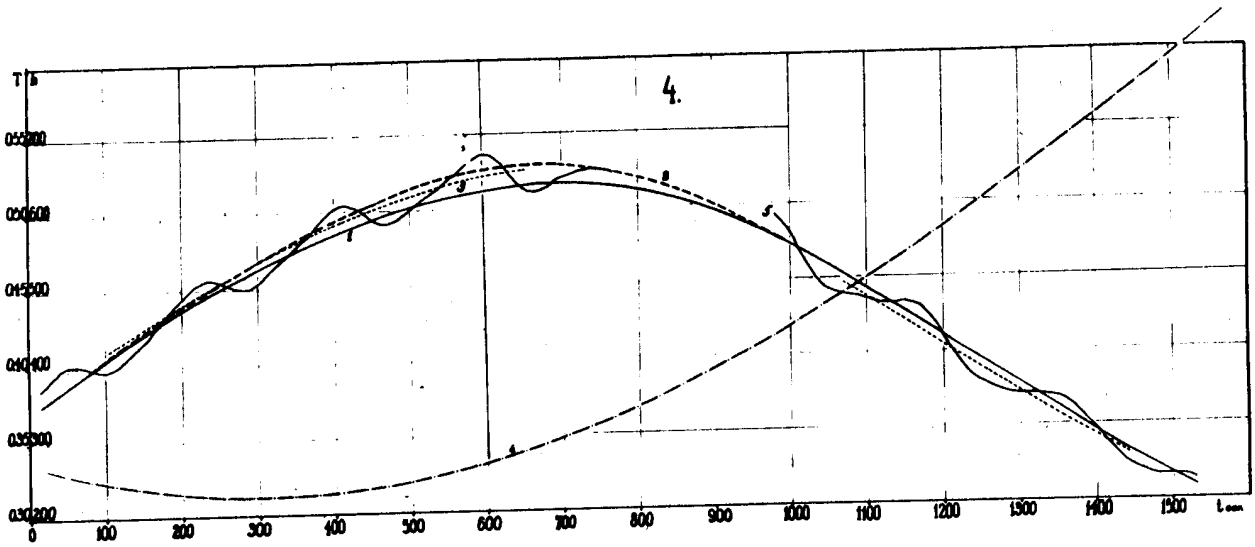

Declassified in Part - Sanitized Copy Approved for Release 2011/12/08 : CIA-RDP80T00246A016600420001-1

Declassified in Part - Sanitized Copy Approved for Release 2011/12/08 : CIA-RDP80T00246A016600420001-1

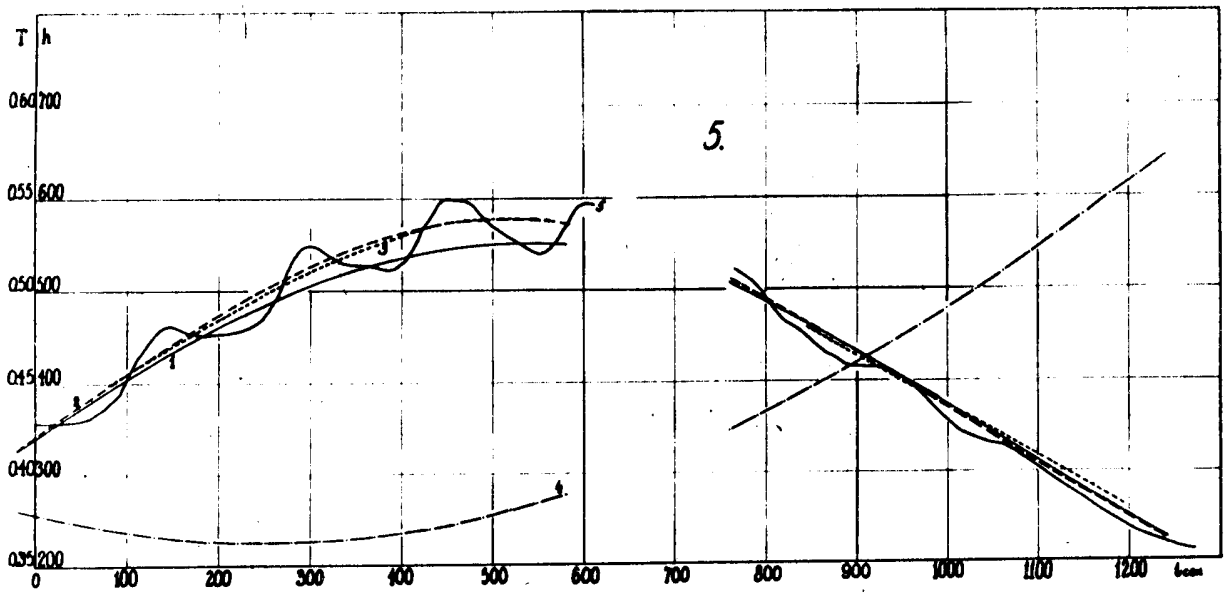

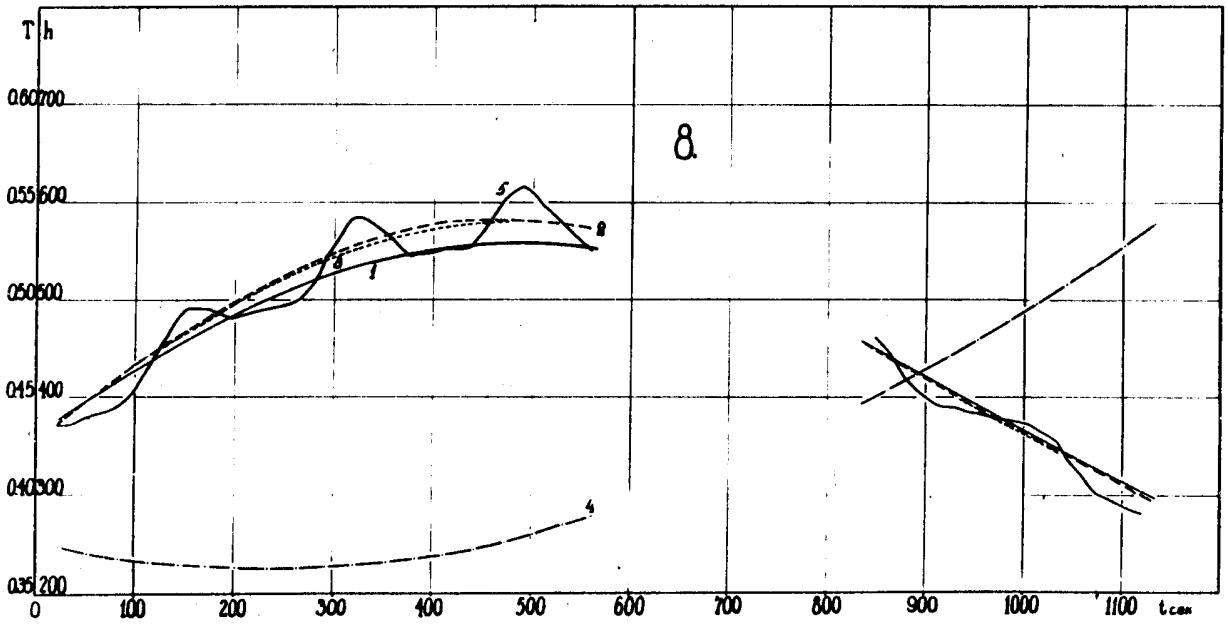

Declassified in Part - Sanitized Copy Approved for Release 2011/12/08 : CIA-RDP80T00246A016600420001-1

Declassified in Part - Sanitized Copy Approved for Release 2011/12/08 : CIA-RDP80T00246A016600420001-1

16. "INVESTIGATIONS OF RADIATION DURING FLIGHTS OF SATELLITES, SPACE VEHICLES AND ROCKETS"

by S.N. Vernov, E.V. Gorchakov, Yu. I. Logachev, V.E.Nesterov, N.F. Pisarenko, I.A. Savenko, A.E. Chudakov, P.I. Shavrin.

In the present brief report we give experimental results obtained from the second and the third space vehicles and on the space rocket launched towards Venus, as well as some data previously obtained on the third Soviet earth satellite (launched May 15, 1958; apogee - 1,800 km, perigee - 250 km).

The flight of the second and the third space vehicles took place on August 19-20 and December 1-2, 1960 respectively. The second space vehicle's orbit was close to the circular (perigee-306 km, apogee - 339 km), the period of circulation being 90.7 min. The altitude of the perigee of the third space vehicle was 187.3 km that of the apogee was 265 km, and the circulation period was 88.6 min.

The interplanetary automatic station was launched towards Venus on February 12, 1961.

1. The OUTER RADIATION BELT

§ 1. The Geographical Location of the Belt at Small Altitudes

From the data of the third earth satellite for altitudes of 300-600 km in the Northern hemisphere, and about 1,500 km in the Southern hemisphere, the mean geomagnetic latitude of the high latitude boundary of the outer radiation belt proved to be equal to $69^{\circ} \pm 2^{\circ}$ in the Northern hemisphere in the interval of geographical longitudes 30° W.L.-120° W.L. and $65^{\circ} \pm 2^{\circ}$ in the Southern henisphere in the interval of Longitudes 30° E.L.-180° E.L.

Declassified in Part - Sanitized Copy Approved for Release 2011/12/08 : CIA-RDP80T00246A016600420001-1

Declassified in Part - Sanitized Copy Approved for Release 2011/12/08 : CIA-RDP80T00246A016600420001-1

The investigation carried out on the second and the third space vehicles made possible for the first time a detailed study of the outer radiation belt near the Earth at all longitudes, since the 24-hour memorising device provided simultaneous and continuous information on the radiation intensity along the flight trajectory of all the vehicles around the whole Earth in an interval of geographical latitudes $\pm 65^{\circ}$. The apparatus consisted of a CTC-5 gas-discharge counter and two scintillation counters, one of which was inside the satellite protected by leyer of matter of 5 ÷ 150 g/cm^2. This scintillation counter consisted of ФЭУ -16 photomultiplier and a NaI (Tl) crystal 30 mm in diameter and 14 mm in height, and with a 25 kev energy threshold of a counting channel. Also registered was the total energy release in the crystal from the anode current of the pholomultiplier. The memorising device questioned the counters every three minutes.

Fig.1 gives the detector readings for one of the sections of the third space vehicle's flight trajectory. It will be seen from the figure that in a number of places an increase in the counting rate of the scintillation counter was observed, accompanied by a comparatively slight increase of energy release and the counting rate of the gas-discharge counter, A detailed analysis has shown that such a sharp increase in the counting rate of the scintillation counter was caused by registration of bremsstrahlung due to interaction between electrons of the Earth's radiation belts and the vehicle's skin.

Fig.2 shows the location of the maximum of the outer radiation belt at various longitudes.

It will be seen from Fig.2 that experimentally determined

Declassified in Part - Sanitized Copy Approved for Release 2011/12/08 : CIA-RDP80T00246A016600420001-1

Declassified in Part - Sanitized Copy Approved for Release 2011/12/08 : CIA-RDP80T00246A016600420001-1

intensity maxima in one hemisphere lie on the same curve as the magnetically conjugated points for the intensity maxima of the other hemisphere (the magnetically conjugated are the end points of the line of force of the geomagnetic field on the Earth's surface in the different hemispheres). This has given grounds to indicate the location of the radiation belt maximum not only at longitudes in which space vehicles crossed the belt but also in the interval of longitudes of 80°West and 60° East. Calculation of conjugated points was made according to magnetic measurements on the Earth's surface (I). Solid lines indicates the mirror-point trajectory calculated with the use of adiabatic integral invariants (Cladis and Dessler)

Fig.3 shows the geographical distribution of radiation determined from the bremsstrahlung at an altitude of 300 km. The numbers on the lines of equal intensity correspond to the counting rate of the scintillation counter in pulses/cm^2 sec. The mean bremsstrahlung energy was equal to approximately 2.10^5ev, while the counting rate of the scintillation counter - 400 pulses/cm^2 sec.- corresponds to an electron flux 2.10^5 $\frac{\text{particles}}{cm^2 \text{ sec.}}$ with a mean energy of the order of 3.10^5ev. Comparison of the geographical distribution of the radiation intensity registered by the scintillation counters on the second and the third satellites shows that the location of the outer radiation belt changed only in the South Atlantic (Fig. 3 and 4), possibly because of the magnetic storm of Nov.30 - Dec.1, 1960 (2).

§2. Intensity Measurement of Charged Particles After the Chromospheric Flare of July 7, 1958.

The chromospheric flare (3+) took place on July 7, 1958 and lasted from 0058 till 0414 universal time /3/. At

Declassified in Part - Sanitized Copy Approved for Release 2011/12/08 : CIA-RDP80T00246A016600420001-1

Declassified in Part - Sanitized Copy Approved for Release 2011/12/08 : CIA-RDP80T00246A016600420001-1

2030 u.t. The third Soviet satellite registered, while passing through the outer radiation belt, an 8.3-fold increase of ionization (Fig.5), i.e. 16 hours after the end of the chromospheric flare but several hours before the beginning of the magnetic storm. Then the ionization increased by several orders of magnitude.

At the same time the arrival of solar protons was observed by the balloons /7/. However the intensity of solar protons was not sufficient to explain the ionization increase measured by the satellite. Thus it is reasonable to suppose that the ionization increase is caused by the increase of intensity in the outer radiation belt.

§3. New Data on the Study of the Outer Radiation Belt During Flights of Space Rockets

Comparison of the results obtained during the flights of the first and the second space rockets, and also of the Venus probe shows that in the absence of the magnetic storms the outer radiation belt remained stable for over two years (Fig.6). The indication was also recieved that the spectrum of radiation remained constant over distances from 32,000 to 40,000 km.

§4. On the Question of Altitude Denendence of Particle Intensity in the Outer Radiation Belt

The first space rocket's flight trajectory crossed the line of force of the dipole field located 25,000 km from the centre of the Earth in the Equatorial plane three times, at distances of 8,700 , 11,000 and 19,250 km. The angular distribution of particles in the Equatorial plane was calculated from intensities measured at these points. This distribution was given in the form of $\sim \sin^n\theta$, where θ is the angle between the vector of particle

Declassified in Part - Sanitized Copy Approved for Release 2011/12/08 : CIA-RDP80T00246A016600420001-1

Declassified in Part - Sanitized Copy Approved for Release 2011/12/08 : CIA-RDP80T00246A016600420001-1

velocities and the line of force (a pitch-angle). The magnitude of n proved to be of the order of 1. Further it was assumed that n = 1 for all particles with mirror points lying above 1,000 km and that n = 16 for particle whose mirror points are located at altitudes between 150 and 1,000 km (which is in agreement with experiment carried out on the "Javeline" rocket), while there are no particles with mirror points below 150 km. Fig.7 shows the altitude dependence of the intensity I calculated under such assumptions, along a line of force located 25,000 km from the Earth's centre in the Equatorial plane. If we know the altitude dependence and the atmospheric density at various altitudes /4/, we can establish the dependence of the magnitude W on the altitude. This magnitude is proportional to the energy scattered in the atmosphere by the particles of the belt per unit length of the field tube, per unit time. As it is seen from Fig.7 at altitudes lower than 2000 km magnitude W does not remain constant but decreases sharply with the increase of altitude. It means that the intensity of particles in the radiation belt at these altitudes changes more slowly than the density of the atmosphere. If the distribution of the particles along a force line was determined by the downward motion of mirror points due to the Coulomb scattering, the intensity of particles would be reciprocal of the atmospheric density.

Thus we may suppose that the altitude dependence of intensity at altitudes of the order of 1,000 km is determined by the downward drift of mirror points caused by oscillations of magnetic mirrors, and at low altitudes by a drift caused by Coulomb scattering.

Fig.8 shows how the intensity of bremsstrahlung depends on the intensity of the magnetic field in the magnetically conjugated

Declassified in Part - Sanitized Copy Approved for Release 2011/12/08 : CIA-RDP80T00246A016600420001-1

Declassified in Part - Sanitized Copy Approved for Release 2011/12/08 : CIA-RDP80T00246A016600420001-1

regions. The numbers denote numeration of areas whose geographic coordinates are given in Table 1. Points corresponding to magnetically conjugated regions are joined by straight lines (solid for the second satellite and dotted for the third). The intensity for each region has been obtained by means of averaging the background caused by cosmic rays being subtracted.

On the bases of Table 1 and Fig.8 it can be shown that there (Points 8,10,17) are three regions in which noticeable intensity, distinct from the background, is observed, although mirror points in conjugated regions should be located in the denser layers of the atmosphere (or even underground), if the magnetic field in these regions is not very sharply different from the dipole. Detailed study of this phenomenon may shed light on the mechanism of electronic acceleration in the outer radiation belt. This means that the radiation recorded at points 8,10,17 is not a geomagnetically trapped radiation, but may represent electrons directly accelerated in the Earth's magnetic field, apparently due to the blast waves.

II. THE INNER RADIATION BELT

§1. The Stability of the Belt

From the data of the third Earth satellite the proton intensity in the inner radiation belt during the first three weeks (May 15 - June 3, 1958) remained stable, within several per cent.

The magnetic field of the Earth during this period was quiet enough, the largest chromospheric flares having importance 2+.

§2. Detection of the Inner Radiation Belt in the Region of the Brazil Magnetic Anomaly at Altitudes of 200-300 km

From Fig.3 it follows that at low geographical latitudes near

Declassified in Part - Sanitized Copy Approved for Release 2011/12/08 : CIA-RDP80T00246A016600420001-1

Declassified in Part - Sanitized Copy Approved for Release 2011/12/08 : CIA-RDP80T00246A016600420001-1

the coast of Brazil the counting rate of the scintillation counter, according to the data of the second space vehicle, was anomalously high. It was found that in this region there is a large area with an anomalously small module of the magnetic field intensity reaching 0.25 oersted. Comparison of the counting rate of the Geiger counter with that of the scintillation counter has shown that in the eight points presented on Fig.9 by black circles there are charged particles within the radiation registered, for the ratio of the mentioned counting rates in these points is high and lies in the interval of 7-28%. These particles may be either electrons with an energy of > 5 mev (which is hardly presumable) or protons of the inner radiation belt. From Fig.9 it can easily be seen that the points in which charged particles were observed are mainly located in the central part of the magnetic anomaly. Also located in this region are two points (Nos. 4 and 5), in which the third space vehicle registered charged particles, i.e. 100 km lower, but the intensity of such particles was less almost by one order, and the area of the region was substantially less.

It will be seen from Fig.3 that there exists a transitional region between the inner and the outer radiation belts, in which the intensity of the bremsstrahlung is half that observed at the maximum of the inner belt, and a quarter that of the maximum of the outer belt at this altitude.

III. COSMIC RAYS

Study of cosmic ray distribution near the Earth makes it possible to study the character and structure of the geomagnetic field and to verify the correctness of theoretical approximations

Declassified in Part - Sanitized Copy Approved for Release 2011/12/08 : CIA-RDP80T00246A016600420001-1

Declassified in Part - Sanitized Copy Approved for Release 2011/12/08 : CIA-RDP80T00246A016600420001-1

of this field. Such investigation are carried out in two directions.

§1. Determination of the Equator of Cosmic Rays

Practically at the same time, the second and the third space ships made measurements of the respective 22 and 18 latitudinal curves understorted by the radiation belts, for each of which an empirical formula was found, by the method of least squares, describing the latitudinal dependence, a parabola of the second degree being the approximating function. From the empirical formulas 40 significances were obtained of minima of cosmic ray intensity. The solid line in Fig.10 shows the location of the cosmic ray equator obtained as a result of averaging of the data obtained on the second space vehicle (one detector) and on the third space vehicle (two detectors). Averaging was conducted for points lying at 5° longitudinal intervals. The results of this averaging are shown in Fig.10 by experimental points. The mean ~~quadratic~~ separate error in three-dimensional determination of the location of each point of the equator is equal, on the average, to 1°. The Equator measured is located in fairly good agreement with the Equator calculated by Kellogg in an 2^6-pole approximation /5/.

The experiment conducted shows the advantages of employing satellites to determine the cosmic ray equator as compared with investigations on the Earth's surface.

§2. Study of Planetary Distribution of Cosmic Rays

Fig.11 shows the results of determination of the planetary distribution of cosmic ray intensity obtained from data on the counting rate of the gas-discharge counter, installed on the second space vehicle (solid lines). For this use was made of em-

Declassified in Part - Sanitized Copy Approved for Release 2011/12/08 : CIA-RDP80T00246A016600420001-1

Declassified in Part - Sanitized Copy Approved for Release 2011/12/08 : CIA-RDP80T00246A016600420001-1

pirical formulas obtained by the method of least squares approximating the latitudinal dependence by second-degree parabolas, and the geographical coordinates were determined from the parabolas' points of intersection with straight lines corresponding to given counting rates.

The dotted line in Fig.11 shows the lines of equal magnetic rigidity calculated by Webber /6/. Comparison of the two families of lines shows that the general pattern of the lines of equal cosmic-ray intensity coincides with the topography of magnetic rigidity. However, considerable discrepancies are discovered when a detailed comparison is made.

Declassified in Part - Sanitized Copy Approved for Release 2011/12/08 : CIA-RDP80T00246A016600420001-1

Declassified in Part - Sanitized Copy Approved for Release 2011/12/08 : CIA-RDP80T00246A016600420001-1

Table I

Region	Geographical Longitude	Geographical Latitude	The second space Vehicle		The third space Vehicle	
			The Mean Value of the Intensity of Magnetic Field (oersteds)	The Mean Intensity of Particles pulses $cm^{-2}\ sec^{-1}$	The Mean Value of the Intensity of Magnetic Field(oersteds)	The Mean Intensity of Particles pulses $cm^{-2}\ sec^{-1}$
I	I05-I40°E	40-55°S	0,55	I2	0,574	I4
2	I05-I40°E	52-65°N	0,525	28	0,567	8
3	80-II0°E	35-60°S	0,485	28	0,496	20,6
4	85-I05°E	55-65°N	0,515	75	0,535	4,5
5	60-80°E	40-65°S	0,412	22,5	0,419	23
6	20-65°E	55-65°N	0,455	I4,9	0,484	I
7	20-55°E	40-65°S	0,350	I07	0,376	58,6
8	20W20°E	60-65°N	0,400	6,8	0,457	I,5
9	20E80°W	52-65°S	0,344	204		
I0	85-75°W	45-57°N	0,476	I4		
II	85-I20°W	20-65°S	0,440	6I	0,432	6I
I2	75-95°W	40-55°N	0,492	86	0,529	36
I3	I20-I50°W	50-65°S	0,486	48	0,520	5I
I4	90-II5°W	45-60°N	0,5I0	22	0,545	47
I5	I55WI65°E	50-65°S	0,5I6	I6	0,555	35+28
I6	II5-I50°W	45-65°N	0,504	34	0,5I2	I7,6
I7	I45-I63°E	55-65°S	0,565	6	0,567	I3,5
I8	I50WI60°E	50-65°N	0,476	65	0,493	I8,5

Declassified in Part - Sanitized Copy Approved for Release 2011/12/08 : CIA-RDP80T00246A016600420001-1

Declassified in Part - Sanitized Copy Approved for Release 2011/12/08 : CIA-RDP80T00246A016600420001-1

REFERENCES

1. E.H.Vestine, W.L. Planet Space Sci 1285 /1959/.
2. Magnetic and Solar Data, J. Geophys Res.66, 1279, No.4 /1961/.
3. Solar Data No.7 /July/ 1958.
4. 1/M.Nicolet Planet Space Science 5, No.1, 1961.
   2/ F.S.Johnson Geophys Res.65, No.2,577 /1960/.
   3/ A.I.Dessler, E.H.Parker, J. Geophys Res.64, No.12, 2239 /1960/.
5. P.I.Kellogg. J. Geophys. Res 65, 2701 (1960)
6. W.R.Webber, Nuovo Cimento, Suppl.II, 5 /1957/.
7. Charahchan A.N., Tulinov V.F., Charahchan T.N. ЖЭТФ 39, 249 (1960)

Declassified in Part - Sanitized Copy Approved for Release 2011/12/08 : CIA-RDP80T00246A016600420001-1

Declassified in Part - Sanitized Copy Approved for Release 2011/12/08 : CIA-RDP80T00246A016600420001-1

CAPTIONS TO FIGURES

Fig.1. Detector readings for a part of the flight trajectory of the third space vehicle, Dec. 1-2, 1960. The upper curve is the counting rate of the scintillation counter with a threshold of 25 kev. The middle curve denotes the energy release rate in the NaI (Tl) crystal. The lower curve denotes the counting rate of the gas-discharge counter.

Fig.2. Distribution of maxima of radiation intensity in the radiation belts, according to data provided by the second and the third space vehicles. Circles denote data for the second vehicle, and squares data for the third vehicle. Crosses denote the conjugated points

Fig.3. Radiation distribution in the zones, determined according to bremsstrahlung from the measurements made by the second space vehicle. The numbers on the line of equal intensity correspond to the counting rate of the scintillation counter in pulses/cm^2 sec.

Fig.4. Distribution of the intensity in the zones determined by the bremsstrahlung, according to measurements obtained by the third space vehicle. The numbers on the line of equal intensity correspond to the counting rate of the scintillation counter in pulses/cm^2 sec.

Fig.5. Increase of ionization in the crystal according to measurements taken on July 7-9, 1958. On the Y-axis is put the logarithm of the difference of the observed and the mean ionization value; observation time is given on the abscissa-axis. Shaded sections denote duration of the chromospheric flare, and arrows the beginning and the end of the magnetic storm. The empty circle denotes the ionization calculated

Declassified in Part - Sanitized Copy Approved for Release 2011/12/08 : CIA-RDP80T00246A016600420001-1

Declassified in Part - Sanitized Copy Approved for Release 2011/12/08 : CIA-RDP80T00246A016600420001-1

from data recieved by Charakchian and others /7/.

Fig.6. Energy release as dependent on distance for the first and the second space rocl ts and for the flight of February 12, 1961.

Fig.7. Dependence of I on altitude along a line of force 26,000 km distant from the Earth center in the Equatorial plane. W is a magnitude proportional to energy losses. h - distance from the Earth surface.

Fig.8. Dependence of the mean intensity of the bremsstrahlung of electrons in the outer radiation belt on a certain averaged intensity of the magnetic field on the Earth's surface, for a number of regions, according to data obtained on the second (empty circles) and the third (shaded circles) space vehicles. The points corresponding to magnetically conjugated regions are connected by solid (the second space vehicle) and dotted (the third space vehicle) lines. Geographical location of the regions corresponding to the given points are presented in Table 1.

Fig.9. The region of enhanced radiation in the South Atlantic, according to measurements on the third space vehicle. Black circles indicate those points in which protons were observed by the second space vehicle. Solid lines are for equal intensity, according to the data of the scintillation counter; dotted lines denote the parts of the third space vehicle's trajectory; dot-and-dash lines are for equal intensity of the magnetic field B; the values of B are given in oersteds

Declassified in Part - Sanitized Copy Approved for Release 2011/12/08 : CIA-RDP80T00246A016600420001-1

Declassified in Part - Sanitized Copy Approved for Release 2011/12/08 : CIA-RDP80T00246A016600420001-1

Fig.10. Location of the Equator of cosmic rays according to measurements on the second and the third space vehicles. The dotted curve indicates the equator of cosmic rays calculated by Kellogg in the 2^6-pole approximation.

Fig.11. Planetary distribution of cosmic ray intensity according to the data of the second space vehicle. The numbers in the right correspond to the counting rate of the gas-discharge counter in pulses/cm^2sec. Dotted lines denote equal magnetic rigidity according to Webber. Numbers on these lines correspond to the cut-off rigidity in Bev.

Declassified in Part - Sanitized Copy Approved for Release 2011/12/08 : CIA-RDP80T00246A016600420001-1

Declassified in Part - Sanitized Copy Approved for Release 2011/12/08 : CIA-RDP80T00246A016600420001-1

Fig. 1.

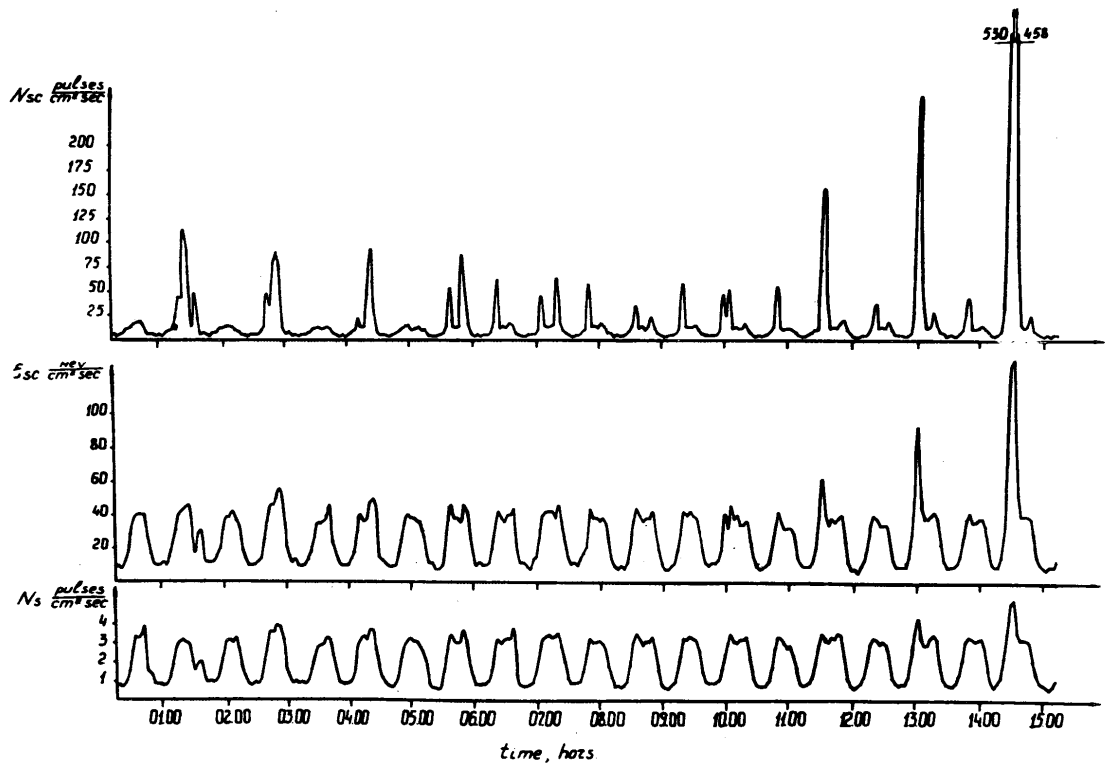

Declassified in Part - Sanitized Copy Approved for Release 2011/12/08 : CIA-RDP80T00246A016600420001-1

Declassified in Part - Sanitized Copy Approved for Release 2011/12/08 : CIA-RDP80T00246A016600420001-1

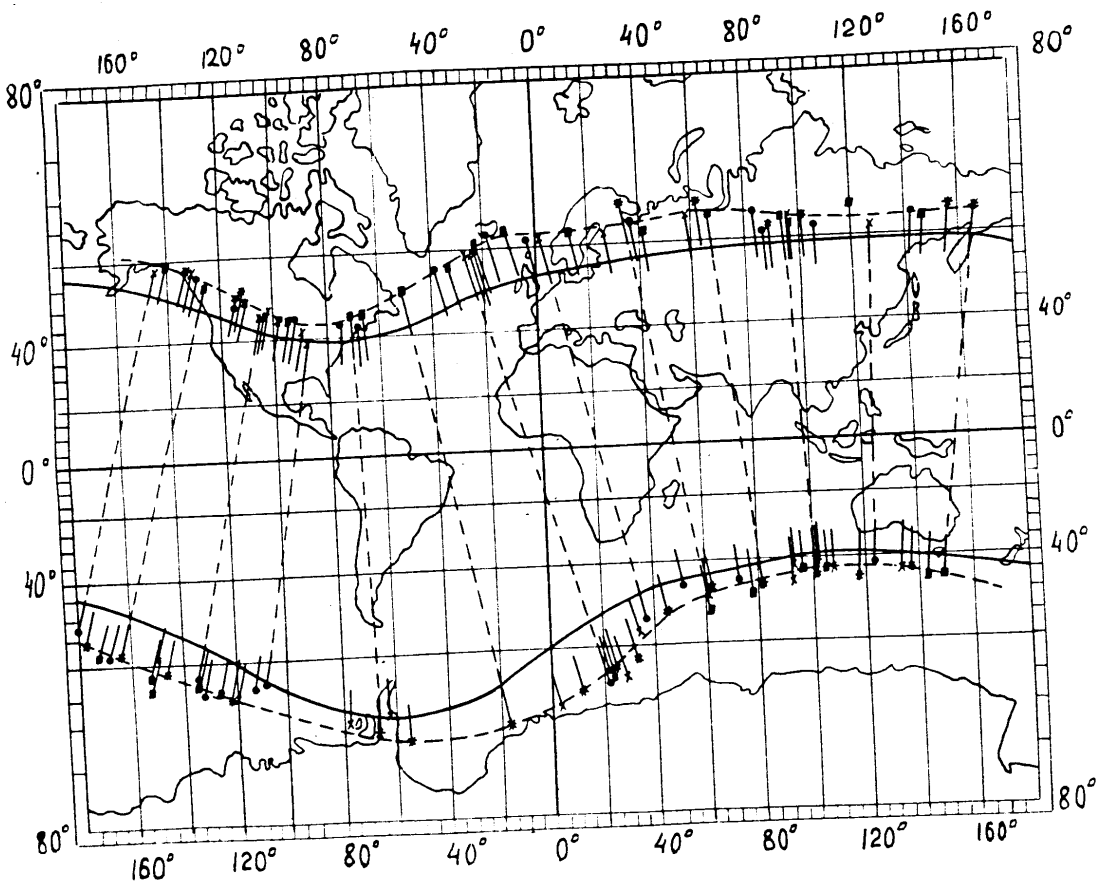

Fig 2

Declassified in Part - Sanitized Copy Approved for Release 2011/12/08 : CIA-RDP80T00246A016600420001-1

Declassified in Part - Sanitized Copy Approved for Release 2011/12/08 : CIA-RDP80T00246A016600420001-1

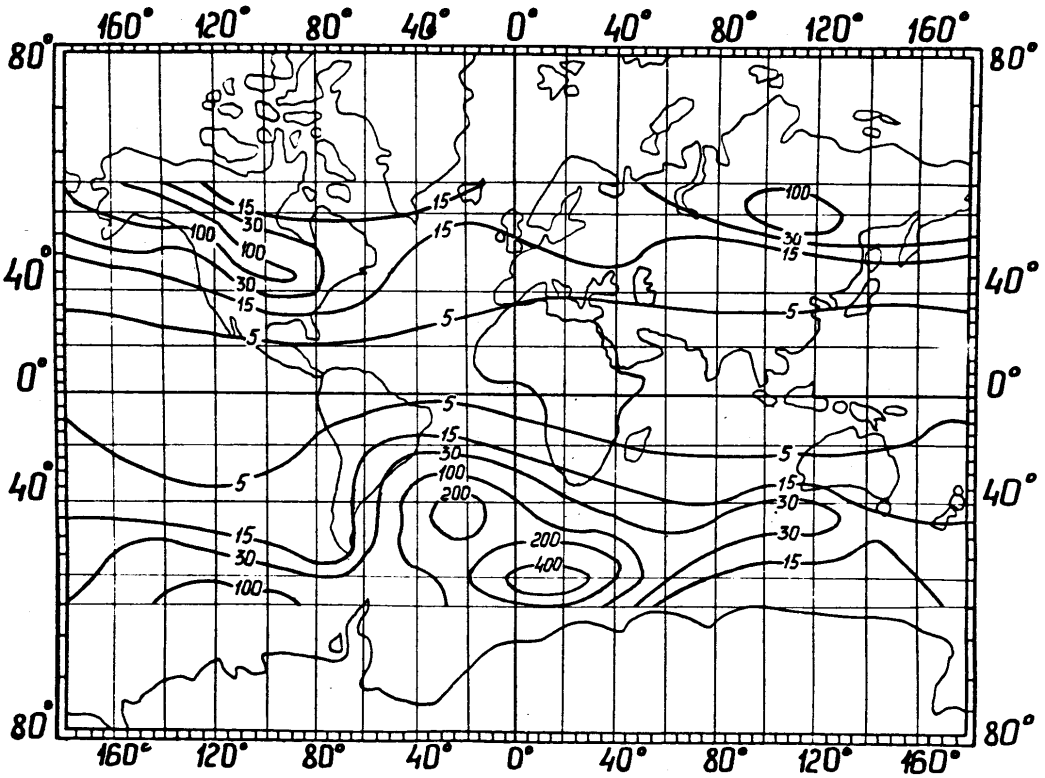

Fig 3

Declassified in Part - Sanitized Copy Approved for Release 2011/12/08 : CIA-RDP80T00246A016600420001-1

Declassified in Part - Sanitized Copy Approved for Release 2011/12/08 : CIA-RDP80T00246A016600420001-1

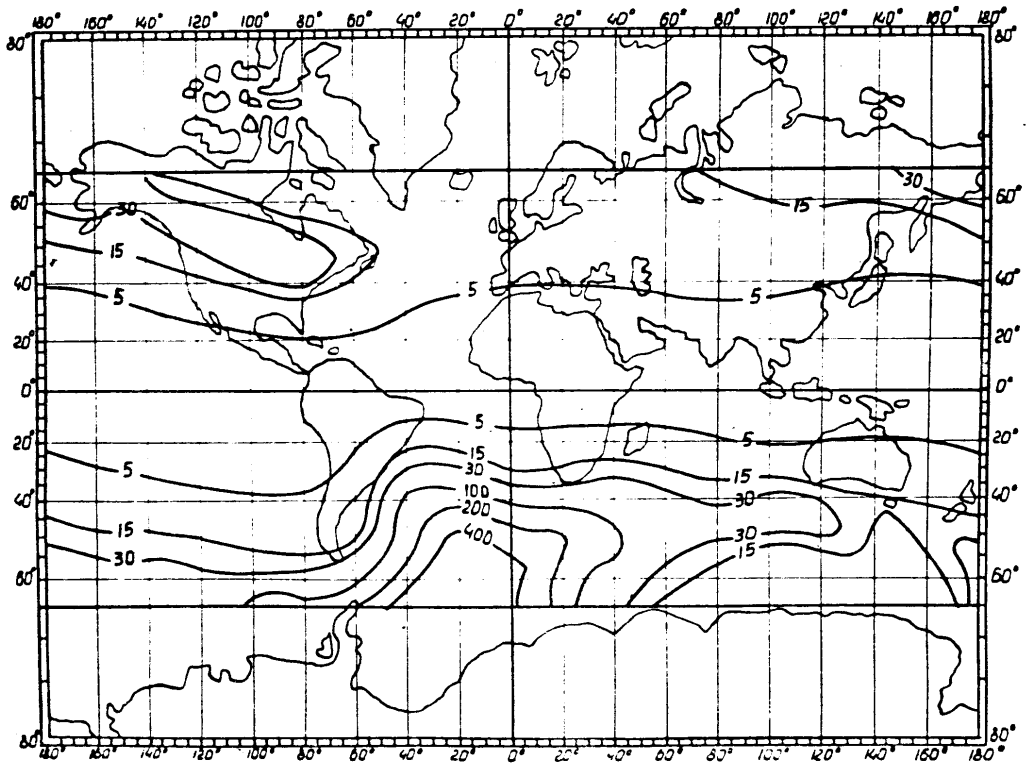

Fig 4

Declassified in Part - Sanitized Copy Approved for Release 2011/12/08 : CIA-RDP80T00246A016600420001-1

Declassified in Part - Sanitized Copy Approved for Release 2011/12/08 : CIA-RDP80T00246A016600420001-1

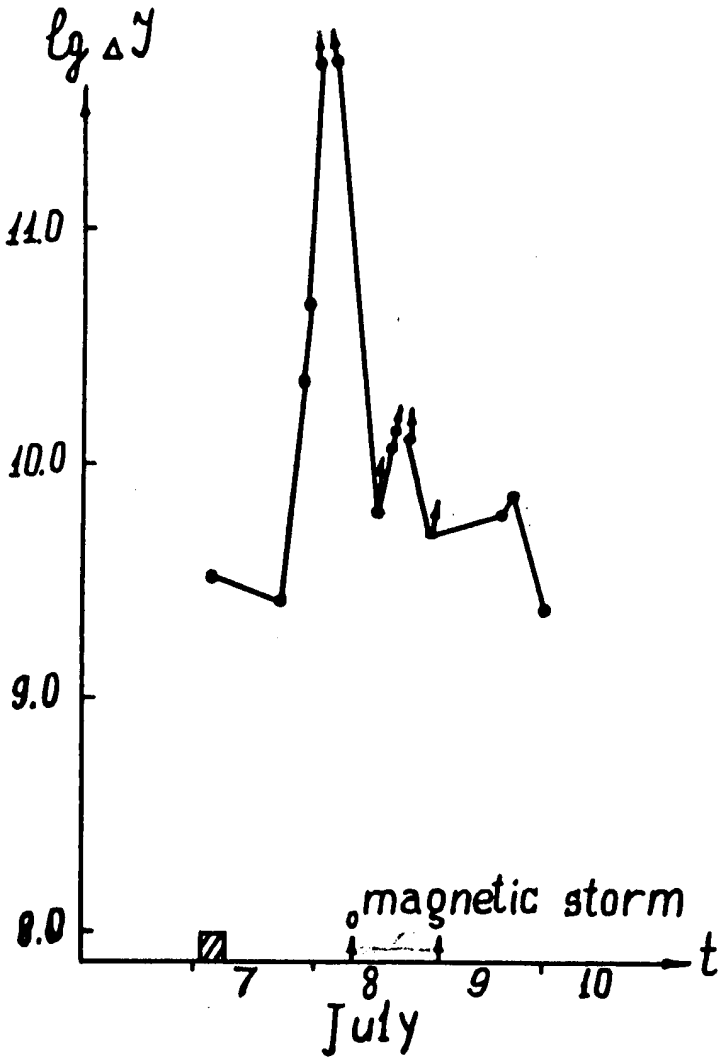

Fig. 5.

Fig 5

Declassified in Part - Sanitized Copy Approved for Release 2011/12/08 : CIA-RDP80T00246A016600420001-1

Declassified in Part - Sanitized Copy Approved for Release 2011/12/08 : CIA-RDP80T00246A016600420001-1

Fig. 6

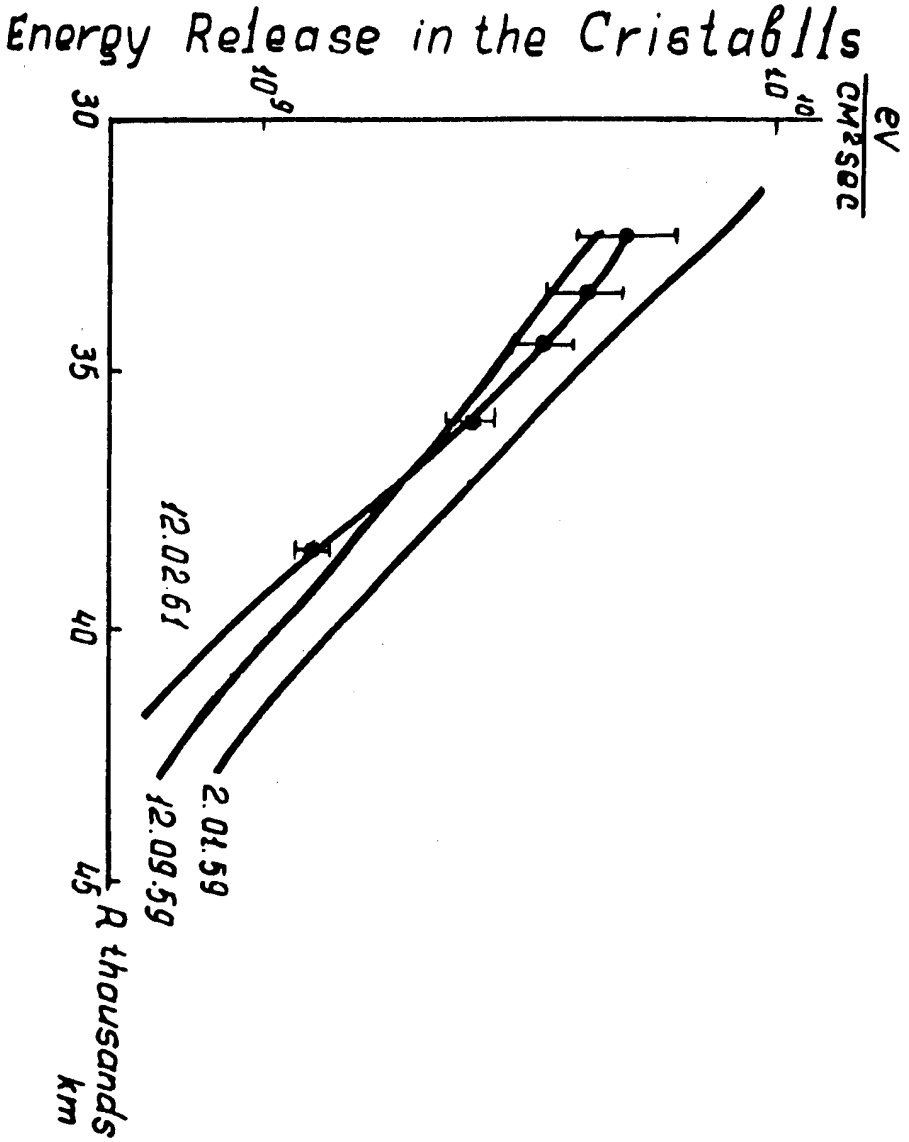

Declassified in Part - Sanitized Copy Approved for Release 2011/12/08 : CIA-RDP80T00246A016600420001-1

Declassified in Part - Sanitized Copy Approved for Release 2011/12/08 : CIA-RDP80T00246A016600420001-1

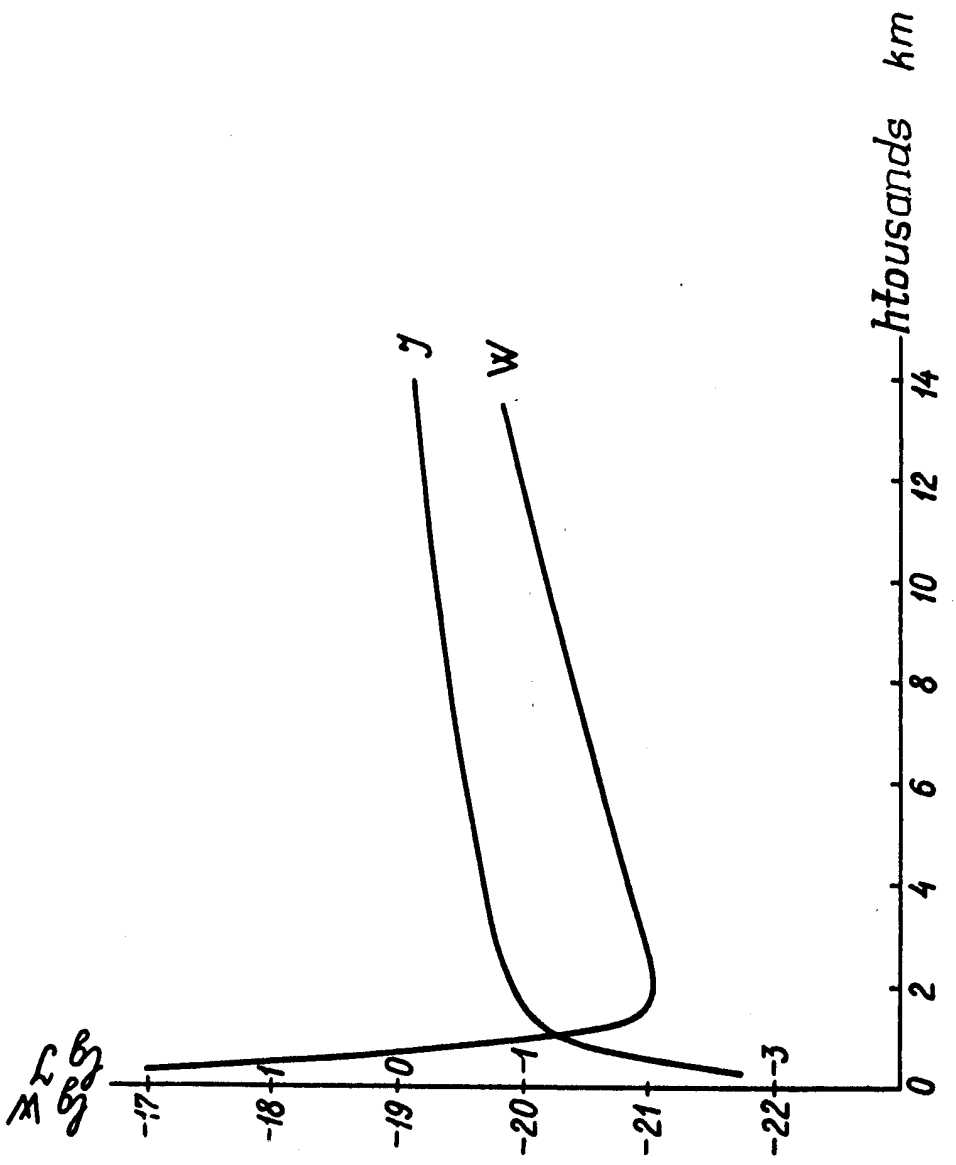

Fig 7

Declassified in Part - Sanitized Copy Approved for Release 2011/12/08 : CIA-RDP80T00246A016600420001-1

Declassified in Part - Sanitized Copy Approved for Release 2011/12/08 : CIA-RDP80T00246A016600420001-1

Fig 8

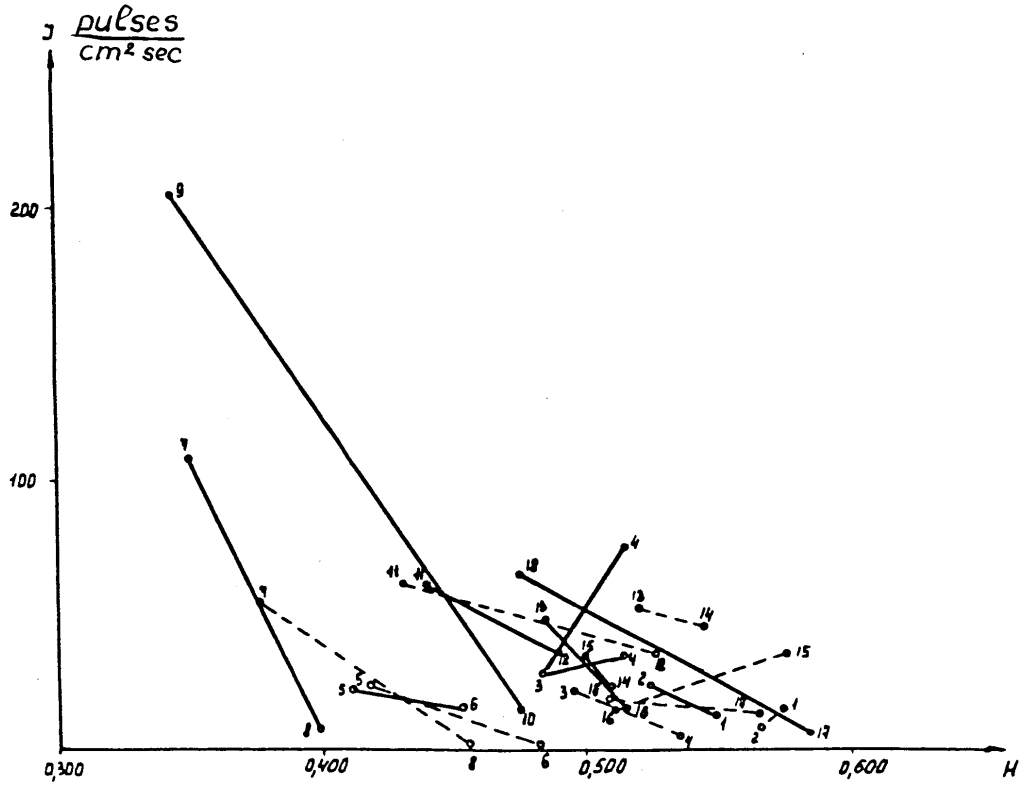

Declassified in Part - Sanitized Copy Approved for Release 2011/12/08 : CIA-RDP80T00246A016600420001-1

Declassified in Part - Sanitized Copy Approved for Release 2011/12/08 : CIA-RDP80T00246A016600420001-1

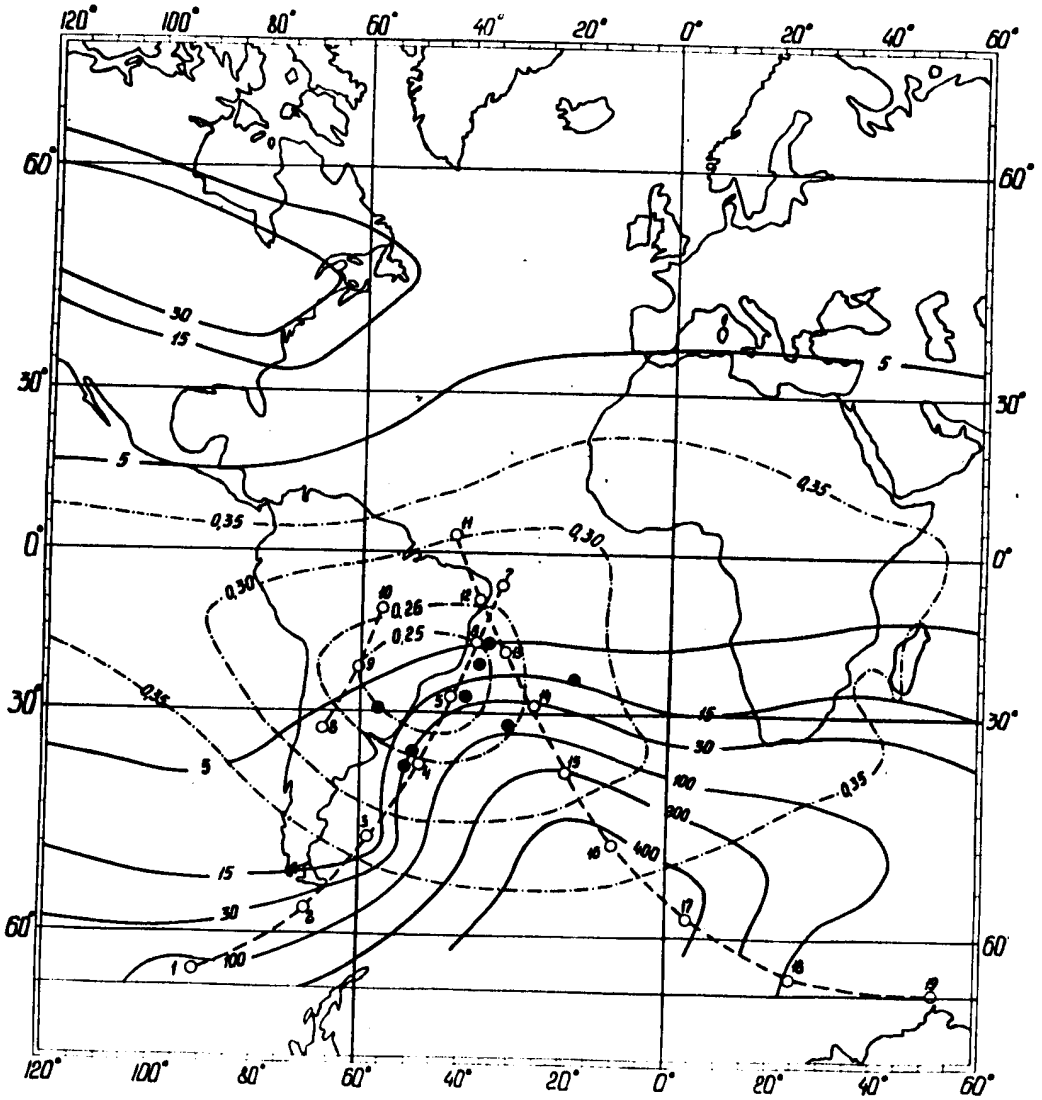

Fig 9

Declassified in Part - Sanitized Copy Approved for Release 2011/12/08 : CIA-RDP80T00246A016600420001-1

Declassified in Part - Sanitized Copy Approved for Release 2011/12/08 : CIA-RDP80T00246A016600420001-1

Fig 10

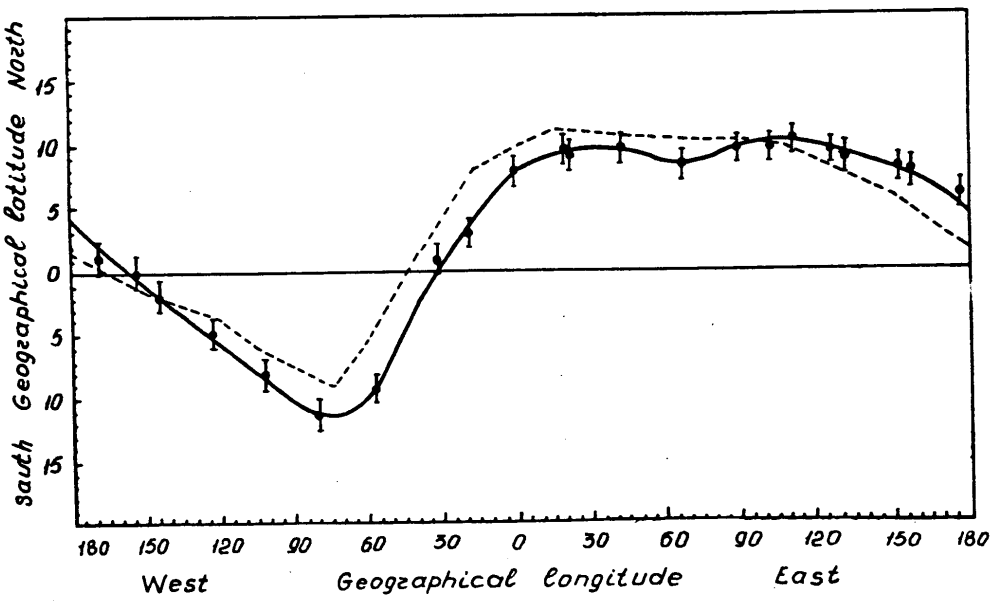

Declassified in Part - Sanitized Copy Approved for Release 2011/12/08 : CIA-RDP80T00246A016600420001-1

Declassified in Part - Sanitized Copy Approved for Release 2011/12/08 : CIA-RDP80T00246A016600420001-1

Fig 11

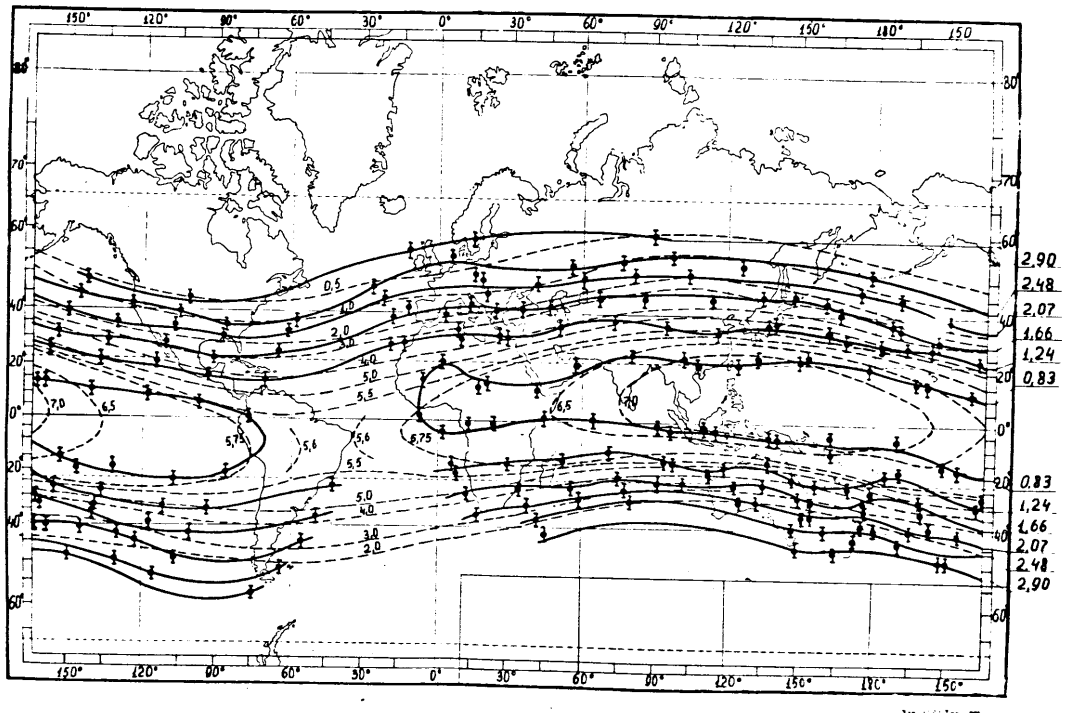

Declassified in Part - Sanitized Copy Approved for Release 2011/12/08 : CIA-RDP80T00246A016600420001-1

Declassified in Part - Sanitized Copy Approved for Release 2011/12/08 : CIA-RDP80T00246A016600420001-1

17.

by V.I.Afanasyeva, J.D.Kalinin

"Solar Corpuscular Streams by the IGY Data"

Undoubtedly, direct measurements with the help of cosmic rockets are most valuable for investigation of phenomena in interplanetary space. However, the analysis of ground geomagnetic data together with geliophysical ones may give some information about the same phenomena. In particular, it is possible to determine more or less difinitely the location of solar corpuscular streams in space at any moment of time. This is possible when streams are as far from the Earth as 0.5 astronomic unit. As long as 1960 one of the authors worked out a conception on geomagnetic storm families. A storm family was called a group of geomagnetic disturbances causally connected with one and the same corpuscular stream. Generally, a family consists of one geomagnetic storm, in a general sense of this notion, and a group of weaker disturbances on the previous and the days following storm days. Sometimes a storm begins a family or completes it. A favourable location of one of the Soviet magnetic observatories in Srednikan (Jakutia) helped to expose families. The presence of two world geomagnetic anomalies - in Siberia and in Canada - created in Srednikan the conditions of an extremely vivid alternation of disturbed and relatively calm periods within storm families. The families.defined by the data of Srednikan were confirmed by the materials of mutualy for away observatories: Guama, Mirnii, Big-Delta, Littel-America. Most often activity within a certain family gradually increases to the middle of the family and then decreases to its and. The duration of families are different from 2-3 days to 5-7 days and more. By the conceptions of the authors a family is created by a corpuscular stream

Declassified in Part - Sanitized Copy Approved for Release 2011/12/08 : CIA-RDP80T00246A016600420001-1

Declassified in Part - Sanitized Copy Approved for Release 2011/12/08 : CIA-RDP80T00246A016600420001-1

that has a relatively narrow most dense core and a very enormous diffusive periphery. The core may be identified with the stream in a general sense of this conception in storm theories. Diffusive periphery is created by the dispersion of the core material. Streams or their cores may be considered as the geophisics. used to think distorted in accordance with their radial speed. A new moment, introduced by the autors into this consideration, is the account of the values $\Delta\varphi$ - the differences of heliographic latitudes widths of streams and the Earth. In other words, stream cores are those, having heliographic latitudes equal to the latitudes of active regions on the Sun, which may be considered as stream origin. Therefore, in most cases stream cores appear to be situated outside the ecliptic plane and the Earth passes through the diffusive periphery of the stream and does not touch the stream core.

On the basis of these conceptions,(a more detailed description of which is published) the authors gave the analysis of the situation in July 1959 at the Assembly of the Geodezy and Geophysics Union in Helsinky [2] . On the same basis one of the authors succeeded in explaining variations from day to day S q--variations by corpuscular effects [3].

At present there is a catalogue of storm families for the whole period of the IGY. For this period there found out 162 families covering 468 days from the IGY 549 days. As to storm intensity that is maximum activity in a family, 162 families are distinguished as follows: 11 families have very large storms 9- large storms and 23-moderate ones. As to the rest 119 families 41 have small storms, and 78 have simple disturbances.

The objectivity in finding out families and their reference

Declassified in Part - Sanitized Copy Approved for Release 2011/12/08 : CIA-RDP80T00246A016600420001-1

Declassified in Part - Sanitized Copy Approved for Release 2011/12/08 : CIA-RDP80T00246A016600420001-1

to certain regions on the Sun was checked up by the analysis of 27-day recurrence in families, which the authors and not use in defining families. It appeared, that 162 families may be ascribed to 119 solar corpuscular streams, as a number of streams created not one, but several storm families (up to 4-5) with neighbouring rotations of the Sun. If the reference of the families to active regions on the Sun were subjective, in a number of family 27 day recurrence it would be found out, that in certain rotations of the Sun a family is ascribed to an active region with only heliographic coordinates, and in other rotations a family from the some 27 day recurrence is ascribed to the activity in the other hemisphere of the Sun. However it did not happen. Such a succession of families appeared to be ascribed to only one active region. Even more, each family has its own value of Δt (time for corpuscular run from the Sun to the Earth orbit) and it appeared to be like one and the same family 27 day succession in all the families.

Therefore the authors suggest their family catalogue, as a catalogue of solar corpuscular streams, causing on the Earth during the IGY geomagnetic activity, and in half cases these streams did not from storms in a general sense, providing only disturbances and therefore could not be found out in a general approach to the question.

The figure showed 27 day diagram of all the families. Each family is given as a triangle. The triangle base is a family duration, the height is proportional to the maximum activity. The upper top of each triangle is placed in a division for days with the maximum activity in a given family.

Declassified in Part - Sanitized Copy Approved for Release 2011/12/08 : CIA-RDP80T00246A016600420001-1

Declassified in Part - Sanitized Copy Approved for Release 2011/12/08 : CIA-RDP80T00246A016600420001-1

One can note that all the families with very large storms appeared to be reffered to active regions, whose geographic latitudes are $\Delta\varphi$ different from the Earth latitude with the averge $\Delta\varphi = 6^\circ$. Families with large storms are $\Delta\varphi = 11967$ families from 162 were connected with regions with $\Delta\varphi \neq 10^\circ$. The families with $\Delta\varphi > 26^\circ$ appeared to be only 6, and only one of them has a large storm, and the other has a moderate one. Some additional information about the way of controling the catalogue can be found in literature [4] . In a table form the catalogue of storm families was placed in the supplement. The catalogue gives the dates of family commencements and ends, the dates of the maximum activity and the characteristics of this maximum activity by the scale-very large, large, moderate, small storms and simply disturbances as well as the dates of passing the central meridian of the Sun by that active region, to which a given family is refered, geliographical latitude of this region and values $\Delta\varphi$ and Δt .

The authors hope, that some investigators will be able to use the catalogue for the analysis of the IGY data.

Declassified in Part - Sanitized Copy Approved for Release 2011/12/08 : CIA-RDP80T00246A016600420001-1

Declassified in Part - Sanitized Copy Approved for Release 2011/12/08 : CIA-RDP80T00246A016600420001-1

Literature

I. Afanasieva V.I. Geomagnetic storm families and solar corpuscular streams. Geomagnetism and aeronomy, I N°1 1961, 59

2. V.I.Afanasieva and J.D.Kalinin. Solar corpuscular streams and geomagnetic field in July 1959 Symposium on the July 1959 Events, Helsinki, July 1960

3. V.I.Afanasieva. Corpuscular nature of a day-to day alteration of calm solar-daily geomagnetic variations. Geomagnetism and Aeronomy N°4,1961, 561

4. V.I.Afanasieva. Geomagnetic storm families during the International geophysical year. Geomagnetism and Aeronomy, 2 N°3, 1962. (being under publication).

Declassified in Part - Sanitized Copy Approved for Release 2011/12/08 : CIA-RDP80T00246A016600420001-1

Declassified in Part - Sanitized Copy Approved for Release 2011/12/08 : CIA-RDP80T00246A016600420001-1

Table 1

N	Dates Commencements and ends of family	Maxim. activity	Characters-tics	C.M.	φ	Δφ	Δt
I	2	3	4	5	6	7	8
I	1957 VI-29-VII	30-VI	VG	29-VI	10°N	7°	1
2	VIII 5-9	5-VII	M	2-VII	17 S	21	3
3	II-15	12-VII	d	9-VII	10-20N	11	3
4	16-18	16-VII	d	14-VII	8-10N	4	2
5	18-20	19-VII	d	16-VII	10 S	15	3
6	21-23	22-VII	m	20-VII	8 N	3	2
7	24-26	24-VII	d	2I-VII	10 N	5	3
8	27-30	29-VII	d	26-VII	6 N	0	3
9	3I-2VIII	I-VIII	d	29-VII	6 N	0	3
10	VIII 3-4	3-VIII	L	I-VIII	8 N	2	2
11	5-7	6-VIII	m	4-VIII	10-23 N	10	2
12	12-14	13-VIII	L	9-VIII	6 N	0	4
13	17-20	18-VIII	d	14-VIII	7 N	0	4
14	20-22	21-VIII	d	18-VIII	7 N	0	3
15	25-28	27-VIII	d	24-VIII	7 N	0	3
16	29-31	30-VIII	m	25-VIII	10 N	3	4
17	IX 2-3 IX	3-IX	VG	30-VIII	5-12 N	1	4
18	4-8	5-IX	G	2-IX	7 N	0	4
19	9-10	9-IX	d	6-IX	22 S	29	3
20	13-14	13-IX	VG	10-IX	8-18 N	6	3
21	15-18	17-IX	d	13-IX	12-15 N	6	4
22	21-26	23-IX	VG	19-IX 21-IX	10 N 8	3 I	4 2
23	IX 29-I-X	29-IX	VG	26-IX	5-8 N	0	3
24	X 3-4	3-X	d	I-X	15 N	8	2
25	9-12	11-IX	L	7-X	15 N	9	4
26	13-15	14-X	m	II-X	15-20 N	11	3
27	X 20-I XI	21-X	L	18-X	25 S	30	3
28	XI 1-4 XI	3-XI	d	I-XI	15-20 S	22	2
29	5-8	6-XI	m	3-XI	15 N	19	1

Declassified in Part - Sanitized Copy Approved for Release 2011/12/08 : CIA-RDP80T00246A016600420001-1

Declassified in Part - Sanitized Copy Approved for Release 2011/12/08 : CIA-RDP80T00246A016600420001-1

1	2	3	4	5	6	7	8
30	XI 8-10 XI	9-XI	L	6-XI	I5° S	I8°	3
31	I0-I6	I2-XI	L	9-XI	7 N	4	3
32	I7-I9	I8-XI	m	I4-XI	7 N	5	4
33	20	20-XI	d	I8-XI	I0 N	8	2
34	22	22-XI	d	2I-XI	I8 N	I6	I
35	23-29	26-XI	G	25-XI	I N	0	I
36	XII I-4 XII	2-XII	d	29-XI	I5 S	I6	3
37	5-7	5-XII	L	3-XII	I5 S	I5	2
38	9-I3	I0-XII	L	8-XII	20 N	20	2
39	I4-I8	I5-XII	L	II-XII	I0 N	II	4
40	I9-20	I9-XII	L	I7-XII	22 S	20	2
41	25-27	26-XII	d	24-XII	25 S	23	2
42	30-2 I-I958	3I-XII	G	28-XII	0	0	3
43	I958 5-7 I	6-I	d	3-I	I8 N	22	3
44	8-I0	9-I	d	4-I	I5 S	II	5
45	I0-I4	I3-I	d	7-I	5-I0 N	I4	6
46	I4-I6	I5-I	d	II-I	I8° S	I5	4
47	I7-I9	I8-I	m	II-I	I0 S	5	7
48	I9-20	20-I	L	I6-I	0-I0 S	0	4
49	22-24	23-I	L	I7-I	I2 N	I7	6
50	25-26	25-I	d	I8-I	20 N	26	7
51	26-27	26-I	d	2I-I	25 N	3I	5
52	28-30	29-I	d	26-I	I5 N	9	3
53	30-2-II	I-II	d	28-I	I0 S	4	4
54	II- 3-6	5-II	L	I-II	5 S	I	4
55	7-8	8-II	L	4-II	I0 N	I6	4
56	9-I0	I0-II	L	6-II	I0 S	3	4
57	II-I3	II-II	VG	8-II	I3 S	6	3
58	I4-I5	I4-II	L	9-II	20 S	I3	5
59	I6-I9	I7-II	L	I3-II	I0 N	I7	4
60	I9-2I	2I-II	L	I7-II	5 N	I2	4
61	22-24	23-II	L	I8-II	8N-0	II	5
62	27-28	28-II	d	25-II	I0 S	3	3
63	III 3-8 III	5-III	L	I-III	23 S	I6	4
64	9-I3	I3-III	m	7-III	I5 S	8	6
65	I4-I6	I5-III	d	I3-III	I5 N	22	2
66	I7-22	I9-III	m	I8-III	I3 N	20	I
67	23-27	25-III	m	22-III	25 N	32	3
68	28-29	28-III	d	24-III	25 S	32	4

Declassified in Part - Sanitized Copy Approved for Release 2011/12/08 : CIA-RDP80T00246A016600420001-1

Declassified in Part - Sanitized Copy Approved for Release 2011/12/08 : CIA-RDP80T00246A016600420001-1

1		2		3	4	5	6		7	8
69	III	30-I	-IУ	30-II	L	27-II	5°	S	2°	3
70	IУ	I-3		2-IУ	I	30-II	20	S	I3	3
7I		3-7		5-IУ	m	4-IУ	I5	S	9	I
72		8-9		9-IУ	d	7-IУ	I5	N	2I	2
73		I0-I2		II-IУ	d	9-IУ	I5	N	2I	2
74		I3-I5		I4-IУ	m	I3-IУ	I0	N	I6	I
75		I5-20		I7-IУ	m	I4-IУ	I0	N	I5	3
76		20-22		22-IУ	d	I9-IУ	20	N	25	3
77		22-24		23-IУ	d	I9-IУ	I8	N	23	4
78		24-27		25-IУ	d	2I-IУ	22	S	I7	4
79		27-30		29-IУ	m	25-IУ	I0	N	I4	4
80	У	I-3	У	I-У	d	29-IУ	I5	S	II	2
8I		4-6		5-У	d	I-У	I7	N	2I	4
82		7-9		8-У	d	3-У	I5	S	I2	5
83		9-II		I0-У	d	7-У	3	N	7	3
84		I2-I6		I4-У	m	9-У	8	N	II	5
85		I6-20		I8-У	L	I4-У	20	S	I8	4
86		20-23		2I-У	d	I6-У	20	S	I8	5
87		24-28		26-У	m	22-У	8	N	9	4
88		29-30		29-У	m	25-У	7	N	8	4
89	У	30-I	УI	3I-У	VG	25-У	7	N	8	6
90	УI	2-3		2-УI	LJ	30-У	I5	S	I5	3
9I		4-6		5-УI	d	I-УI	I5	S	I5	4
92		6-7		6-УI	m	3-УI	I0	N	I0	3
93		8-I3		9-УI	G	5-УI	I0	N	9	4
94		I4-I6		I5-УI	L	I0-УI	25	N	24	5
95		I7-I9		I8-УI	d	I3-УI	I5	N	I4	5
96		I9-20		I9-УI	d	I7-УI	I5	N	I3	2
97		20-23		2I-IУ	G	I8-IУ	I5	N	I3	3
98		24-27		24-УI	d	22-УI	5	N	3	2
99		28-30		29-УI	VG	24-УI	I0	N	7	5
I00	УI	30-2	УII	I-УII	d	29-УI	0		3	I
I0I	УII	3-6		4-УII	L	I-УII	9	N	6	3
I02		7-9		8-УII	VG	4-УII	5	N	I	4
I03		9-I3		I2-УII	d	7-УII	25	N	2I	5
I04		I3-I5		I4-УII	d	I0-УII	30	N	26	4
I05		I6-I9		I8-УII	L	I5-УII	I5	N	I0	3
I06		20-2I		20-УII	L	I8-УII	I0	N	5	2
I07		2I-23		2I-УII	L	I9-УII	4	S	9	2

Declassified in Part - Sanitized Copy Approved for Release 2011/12/08 : CIA-RDP80T00246A016600420001-1

Declassified in Part - Sanitized Copy Approved for Release 2011/12/08 : CIA-RDP80T00246A016600420001-1

1	2	3	4	5	6	7	8
I08	VII 24-26	25-VII	L	2I-VII	20° N	I5°	4
I09	27-28	27-VII	L	25-VII	I5 N	9	2
II0	29-3I	30-VII	d	25-VII	I5 S	2I	5
III	VII-3I-4-VIII	I-VIII	d	3I-VII	I0 N	4	I
II2	VIII- 5-7	6-VIII	d	3-VIII	I0 S	I6	3
II3	6-8	7-VIII	L	4-VIII	I0 S	I6	3
II4	9-I2	I0-VIII	d	8-VIII	25 N	I9	2
II5	I3	I3-VIII	L	9-VIII	I0 S	I7	4
II6	I4-I5	I5-VIII	d	I2-VIII	I5 S	22	3
II7	I6-20	I7-VIII	G	I2-VIII	I5 S	22	5
II8	2I-23	22-VIII	m	I8-VIII	28 N	2I	4
II9	24-25	24-VIII	G	2I-VIII	I5 N	8	3
I20	26-29	27-VIII	m	25-VIII	5 N	2	2
I2I	30-3I	3I-VIII	d	28-VIII	I0 N	3	3
I22	IX I-2 IX	I-IX	d	30-VIII	I0 S	I7	2
I23	3-5	4-IX	VG	3I-VIII	5 S	I2	4
I24	7-I0	8-IX	L	4-IX	20 N	I3	4
I25	I2-I3	I2-IX	d	8-IX	I0 S	I7	4
I26	I4-I7	I6-IX	L	I4-IX	I0 S	I7	2
I27	I8-I9	I8-IX	d	I4-IX	I0 S	I7	4
I28	20-22	2I-IX	d	I7-IX	I0 N	3	4
I29	24-26	25-IX	G	20-IX	20 S	27	5
I30	27-29	27-IX	d	22-IX	I0 N	3	5
I3I	IX 30-I X	30-IX	L	27-IX	5 S	I2	3
I32	X 2-4	3-X	L	30-IX	I0 S	I7	3
I33	5-6	5-X	d	3-X	I0 S	I6	2
I34	6-8	7-X	d	4-X	I5 S	2I	3
I35	I2-I3	I3-X	d	9-X	20 N	I4	4
I36	I4-I6	I5-X	d	II-X	20 N	I4	4
I37	I6-2I	I9-X	d	I4-X	I5 S	2I	5
I38	22-23	23-X	m	20-X	4 S	9	3
I39	24-25	24-X	G	22-X	I0 S	I5	2
I40	26-27	27-X	m	23-X	I0 S	I5	4
I4I	28-3I X	28-X	L	24-X	7 S	I2	4
I42	XI I	I-XI	d	30-X	I5 S	I9	2
I43	2-4 XI	2-XI	L	30-X	I5 S	I9	3
I44	6-8	7-XI	d	3-XI	I5 S	I9	4
I45	9-II	I0-XI	d	3-XI	I0 N	7	7
I46	II-I3	I2-XI	d	5-XI	I5 N	I2	7
I47	I4-I7	I4-XI	d	I0-XI	I5 N	I2	4

Declassified in Part - Sanitized Copy Approved for Release 2011/12/08 : CIA-RDP80T00246A016600420001-1

Declassified in Part - Sanitized Copy Approved for Release 2011/12/08 : CIA-RDP80T00246A016600420001-1

1	2		3	4	5	6		7	8
I48	XI I8-2I		I9-XI	d	I6 XI	I5°	S	I7 °	3
I49	23-27		25-XI	d	23-XI	I0	S	I2	2
I50	28-29	XI	28-XI	d	25-XI	I0	S	II	3
I5I XII	I-2	XII	2-XII	d	30-XI	I3	S	I4	2
I52	4-5		4-XII	VG	30-XI	I5	S	I5	4
I53	6-7		6-XII	d	4-XII	8	N	8	2
I54	8-9		8-XII	d	5-XII	8	S	8	3
I55	I3-I4		I3-XII	m	II-XII	0		I	2
I56	I5-I6		I6-XII	d	I3-XII	0		I	3
I57	I7		I7-XII	m	I5-XII	7	N	8	2
I58	I9-2I		I9-XII	d	I7-XII	25	N	27	2
I59	22-25		23-XII	d	20-XII	5	S	3	3
I60	25-27		26-XII	d	23-XII	20	N	22	3
I6I	28-29		28-XII	d	26-XII	I5	S	I2	2
I62	30-3I	XII	30-XII	d	27-XII	20	S	I7	3

Declassified in Part - Sanitized Copy Approved for Release 2011/12/08 : CIA-RDP80T00246A016600420001-1

Declassified in Part - Sanitized Copy Approved for Release 2011/12/08 : CIA-RDP80T00246A016600420001-1

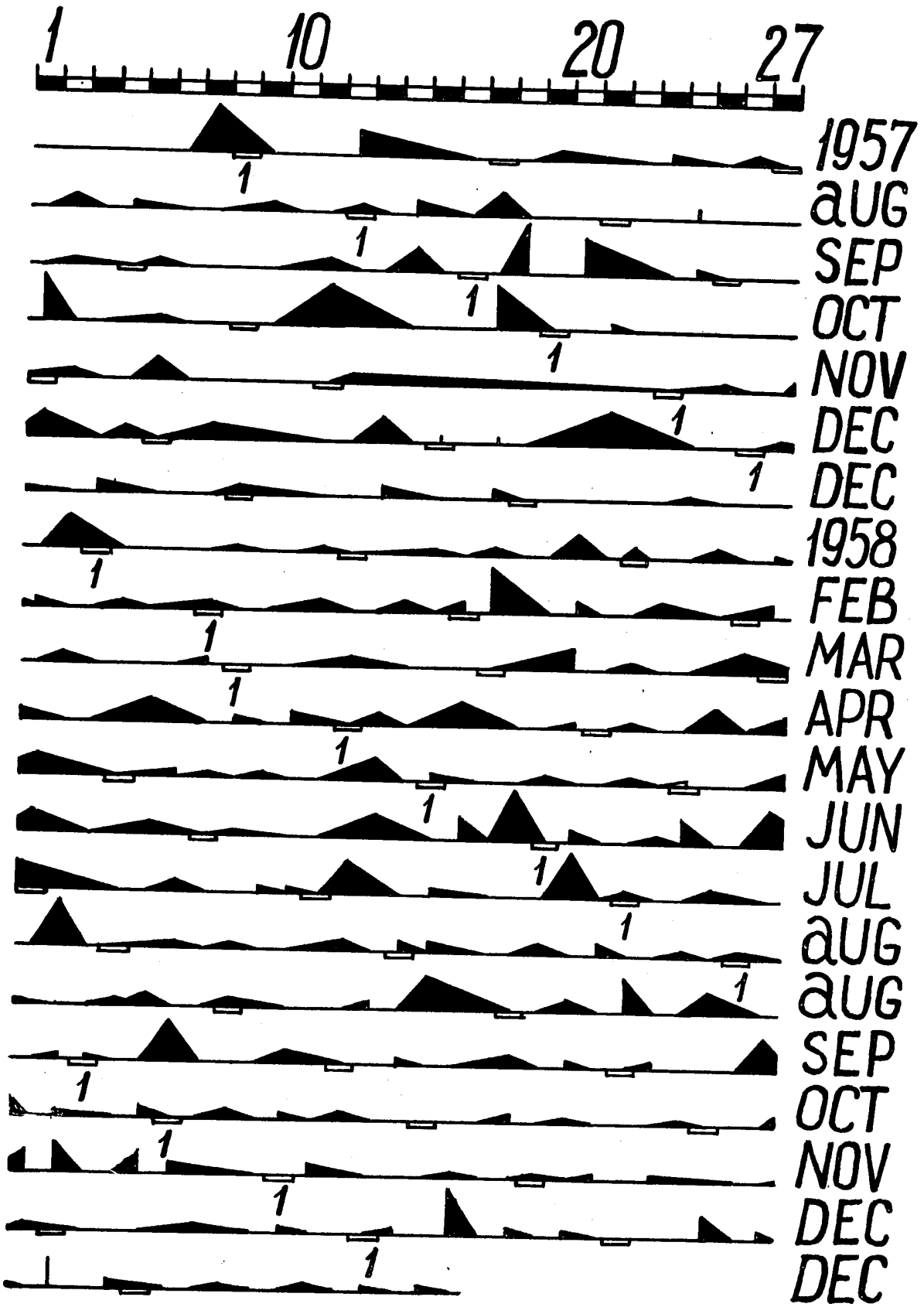

Declassified in Part - Sanitized Copy Approved for Release 2011/12/08 : CIA-RDP80T00246A016600420001-1

Declassified in Part - Sanitized Copy Approved for Release 2011/12/08 : CIA-RDP80T00246A016600420001-1

2.11

18. "DIRECT OBSERVATIONS OF SOLAR PLASMA STREAMS AT A DISTANCE OF ~1,900,000 KM FROM THE EARTH ON FEBRUARY 17, 1961, AND SIMULTANEOUS OBSERVATIONS OF THE GEOMAGNETIC FIELD."

b/ K.I.Gringauz, V.V.Bezrukikh, S.M.Balandina, V.D.Ozerov, R.E.Rybchinsky.

Abstract

Final results are presented of the processing of the data of the experiment aimed at investigating solar plasma streams from the Venus probe launched on February 12, 1961.

Preliminary results were reported by K.I.Gringauz at the Second International Space Science Symposium in Florence in 1961.

The results are compared with the geomagnetic field simultaneous observations.

In K.I.Gringauz' report at the Space Science Symposium in April 1961 in Florence (1) the preliminary information was given on the results of the experiment carried out by means of charged particle traps on the Soviet Venus probe launched on February 12, 1961. In the present report final, somewhat corrected results of measurements are presented. They are compared with the results of the simultaneous registration of the geomagnetic field variations on the Earth.

Let us remind that at the said probe two three-electrode traps were installed among the scientific instruments. They differed only by some design changes from the traps mounted on Lunik II by means of which in 1959 solar plasma streams were recorded for the first time outside the geo-

Declassified in Part - Sanitized Copy Approved for Release 2011/12/08 : CIA-RDP80T00246A016600420001-1

Declassified in Part - Sanitized Copy Approved for Release 2011/12/08 : CIA-RDP80T00246A016600420001-1

magnetic field (2). The changes introduced into the design were directed to the reduction of its weight and further decrease of the collector current component produced by the photoelectron and secondary emission from the inner grid of the trap.

The potentials of the outer grids of the traps on the Venus probe were $\varphi'_{g_2} = 0$ and $\varphi''_{g_2} = +50$ volts. During the measurements the traps retained definite orientation with respect to the direction to the Sun and to the velocity vector due to which collector current variations caused by the body rotation described in (2) and (1) could not take place.

Fig.1 gives the results of the measurements of the trap collector currents during three radiotelemetry transmissions from the Venus probe. Table 1 gives the time t of the beginning of each of these transmissions and the distance R of the probe from the Earth's centre which corresponds to the beginning of the radio contact.

Table 1

No.of Transmission Received	t (Moscow Time)	R (Km)
1	12.II.1961 6h 45m	30,000
2	12.II.1961 14h 25m	170,000
3	17.II.1961 14h 35m	1,900,000

Declassified in Part - Sanitized Copy Approved for Release 2011/12/08 : CIA-RDP80T00246A016600420001-1

Declassified in Part - Sanitized Copy Approved for Release 2011/12/08 : CIA-RDP80T00246A016600420001-1

While considering Fig.1 one should bear in mind that the collector current amplifier with the outer grid potential equal to 0 had a characteristic which consisted of two linear portions. The slope of the upper portion was comparatively low. The maximum measured current was close to 8.10^{-8} amperes. The trap collector current amplifier with $\varphi_{g_2} = +50$ volts had a characteristic close to linear one. The maximum measured current was equal to 2.10^{-9} amperes.

As it should be expected the collector current modulation, which took place in previous similar experiments, was absent in this case, as is evident from the graphs of Fig.1.

Let us note that the recorded currents are somewhat lower than those determined by the positive ion fluxes get into the trap at the expense of the currents produced by the emission of photoelectrons from the inner grid. However, from the materials given in (1) and (2) it can be seen that the photocurrent from the inner grid in the traps on the first space probes did not exceed 5.10^{-10} amperes, while in the traps on the Venus probe it was considerably lower, since the inner grid transparency was increased.

During the first reception of signals the currents of both traps oscillated near zero values. The Venus rocket was at distances of 30,000 ÷ 45,000 km from the Earth's centre, i.e. in the outer part of the second radiation belt. The absence of considerable negative collector currents in the traps during the first radio contact testifies once more to the absence in the second radiation belt of soft electron

Declassified in Part - Sanitized Copy Approved for Release 2011/12/08 : CIA-RDP80T00246A016600420001-1

Declassified in Part - Sanitized Copy Approved for Release 2011/12/08 : CIA-RDP80T00246A016600420001-1

fluxes on the order of 10^{10} cm^{-2} sec^{-1} postulated by the majority of the investigators of this belt in 1959-1961. A more detailed consideration of this problem is given in the report by Gringauz, Balandina, Bordovsky and Shutte at the present symposium (3).

During the second radio-contact low positive currents were registered in both traps. Considerably larger currents were recorded in the traps during the third radio contact.

The current of the trap with the outer grid potential $\varphi_{g_2} = +50$ volts is equal to 2.10^{-9} amperes, i.e. corresponds to the maximum value of the current which could be recorded by the collector current amplifier of this trap. The simultaneous current in the trap with the zero potential on the outer grid is equal to $\sim 3.3.10^{-9}$ amperes. This value apparently determines the N^+ value of the positive corpuscular stream which took place during the third radio contact, namely $\sim 10^9$ sec^{-2} sec^{-1}. With the accuracy up to the measurements errors the stream value was constant during the third radio contact.

During the third reception of signals a magnetic storm with a gradual commencement took place on the Earth, which started on February 17 about 12 hours Moscow time and lasted for several days.

Fig.2 presents collector currents graphs in the traps for each radio contact on the same time scale and the results of the simultaneous registration of the magnetic field parameters according to the data of the Central Magnetic Observatory (Moscow). The latter represent the records of

Declassified in Part - Sanitized Copy Approved for Release 2011/12/08 : CIA-RDP80T00246A016600420001-1

Declassified in Part - Sanitized Copy Approved for Release 2011/12/08 : CIA-RDP80T00246A016600420001-1

the Lacourt magnetograph recorders which registered the geomagnetic field intensity horizontal component H and the angle of the magnetic declination D.

The problem of the correlation between the intensity variations of solar corpuscular stream affecting the Earth's magnetosphere and the geomagnetic field variations during the magnetic storm produced by this stream is not sufficiently clear at present.

Some of the authors believe that for the first hours of the magnetic storm the geomagnetic field fluctuations correspond to the fluctuations of the corpuscular stream and then this correspondence is violated due to the action of the electric current systems which appeared in the ionosphere under the influence of corpuscular streams (4).

This would have been checked up if we had had at our disposal simultaneous long time observations of the corpupuscular stream variations in interplanetary space outside the geomagnetic field and of the magnetic field variations on the Earth. Due to the shorttime (half an hour) duration of the third radio contact the experimental results obtained from the Venus probe have not provided us with such an opportunity.

Nevertheless it is interesting to make an attempt at establishing the correlation between these values assuming that the geomagnetic disturbance value is determined at this time by the corpuscular stream getting into the Earth's magnetic field. It is necessary to take into account that between the moment of the registration of the density of

Declassified in Part - Sanitized Copy Approved for Release 2011/12/08 : CIA-RDP80T00246A016600420001-1

Declassified in Part - Sanitized Copy Approved for Release 2011/12/08 : CIA-RDP80T00246A016600420001-1

some part of the corpuscular stream on the probe and the moment of the contact of the same part of the stream with the Earth's magnetosphere some time has elapsed determined by the mutual location and mutual velocities of the motions of this part of the corpuscular stream, of the Earth and the rocket.

Fig.3 presents the mutual location of the Venus probe and the Earth during the third radio contact. The Venus rocket was at a distance of 1.89 million kilometres from the Earth. The distance from the Sun to it was by 1.54 million kilometres less than the distance from the Sun to the Earth. At the same time it somewhat lagged behind the Earth in its angular motion about the Sun.

It should be borne in mind that the tangential velocity of the corpuscular stream motion at a distance of 1 Astronomical Unit exceeds the Earth's orbital velocity by a factor of 14.

Trying to estimate the delay of the moment of the contact of some region of the stream with the Earth relative to the moment of its contact with the rocket some suppositions about the stream shape should be made. This stream region can come into contact with the Venus probe and then with the Earth by its front (the time τ of the delay of these phenomena will be determined by the radial velocity of corpuscles), or by its lateral surface (in this case τ depends also on the stream tangential velocity equal to $\sim$ 400 km/sec.). Cases are also possible when this region of the stream comes into contact with the Venus

Declassified in Part - Sanitized Copy Approved for Release 2011/12/08 : CIA-RDP80T00246A016600420001-1

Declassified in Part - Sanitized Copy Approved for Release 2011/12/08 : CIA-RDP80T00246A016600420001-1

probe by its front and with the Earth by its lateral surface.

The radial velocity (V rad.) roughly estimated from the delay of the moment of the beginning of the magnetic storm relative to the moment of the passage of the active region on the Sun through its central meridian turned to be equal to ~ 400 km/sec for the storm on February 17, 1961.

Taking into account all these suppositions the time τ turned to be within the limits of 64-110 minutes. The boundaries of the hatched area in Fig.2 are determined by the moments of the beginning and the end of the third reception of the signals with the greatest and lowest delay time taken into account.

In this region and its closest vicinities the H fluctuation reached about 100 gammas.

It should be noted that the value N^+ measured by us is close to the maximum value N+ obtained in the experiment by Bridge, Dilworth and others (5) on the Explorer X satellite, and the velocity of corpuscles detemmined by the indicated indirect method is close to the corresponding mean value directly measured in the experiment (5).

Acknowledgment

The authors are grateful to V.I.Afanasyeva, Yu.D.Kalinin and E.R.Mustel for fruitful discussion.

Declassified in Part - Sanitized Copy Approved for Release 2011/12/08 : CIA-RDP80T00246A016600420001-1

Declassified in Part - Sanitized Copy Approved for Release 2011/12/08 : CIA-RDP80T00246A016600420001-1

References

1. K.I.Gringauz, Space Research II, 1961, North-Holland Publishing Company, Amsterdam, p.539.

2. K.I.Gringauz, V.V.Bezrukikh, V.D.Ozerov and R.E.Rybchinsky, Doklady Akad.Nauk SSSR. Vol.131, 1301,1960; "Iskusstvennye Sputniki Zemli", The Publishing House of the USSR Academy of Sciences, 101, 1961.

3. K.I.Gringauz, S.M.Balandina, G.A.Bordovsky, N.M.Shutte, The Report at the Present Symposium.

4. V.I.Afanasyeva, Proc.of the Institute for Terrestrial Magnetism, the Ionosphere and Radio Wave Propagation of the USSR Academy of Sciences, 12 (22), 63-67, 1957.

5. H.S.Bridge, C.Dilworth, A.J.Lazarus, E.F.Lyon, B.Rossi and F.Scherb, Direct Observations of the Interplanetary Plasma, Report at the Kyoto Conference, September, 1961.

Declassified in Part - Sanitized Copy Approved for Release 2011/12/08 : CIA-RDP80T00246A016600420001-1

Declassified in Part - Sanitized Copy Approved for Release 2011/12/08 : CIA-RDP80T00246A016600420001-1

by Mogilevsky E.I.

19. "Corpuscular solar streams with force-free magnetic fields"

1) In the hypothesis given below one has made an attempt to find out some main properties and the structure of a corpuscular stream from the observational data and the analysis of plasma movements in active regions of the Sun with a bipolar magnetic field. The magnetic field of such a stream, whose energy exceeds the kinetic energy of the stream, is not a frozen magnetic field in a stream plasma, but a force free field of a closed system of the stream plasma. The stability of such a stream and main features of interaction of it with the magnetosphere and ionosphere of the Earth are determined not by a stream plasma, but by the direct influence of a force-free magnetic field of the stream.

2) Recent numerous observations of the Sun prove that all the combination of complex phenomena in the active regions on the Sun is determined by the development of local magnetic fields. The generation and outcome of geoeffective corpuscular streams are also determined by varying local magnetic fields. In the region of the geoeffective stream origin (upper chromosphere end the corona) the magnetic field can appear only as a result of a successive movement of chromospheric plasma clouds, carrying its own magnetic field [1]. The outcome of the magnetic field into the corona as a result of wave processes and diffusion is non-effective [1,2]. As a necessary consequence of chromospheric-coronal plasma compressibility, the conditions of Helmholtz movement are not valid when the plasma is moving. As a result the plasma cloud moving into the corona obtains its own

Declassified in Part - Sanitized Copy Approved for Release 2011/12/08 : CIA-RDP80T00246A016600420001-1

Declassified in Part - Sanitized Copy Approved for Release 2011/12/08 : CIA-RDP80T00246A016600420001-1

forcefree magnetic field [1].

A forcefree character of the magnetic field of a plasma cloud is also seen from the analysis of the conditions of the stability of the current system with the spiral symmetry, arising in a plasma cloud moving in the outer bipolar magnetic field of the active region. The field of such a cloud reminds us of a magnetic field of a stellorator. If the characteristic sizes and density of a plasma cloud with the magnetic field exceed the critical values ($L > 10^{10}$ cm , $n < 10^{8}$ cm^{-3}), then such a cloud moving in the corona does not decay and may go radially outward to the direction of the Earth. By twisting a toroidal magnetic field of the plasma cloud, arising in moving in the outer dipole field, the current field is strengthed up to ~ 50 gausses at the cloud boundary. A relatively large magnetic field and its forcefree character guarantee a cloud stability in the solar corona region and in its movement in an interplanetary space. Magnetic fields of active prominences may serve as an analogy of such magnetic fields in moving plasma clouds. As the observations [3,4] show, the magnetic fields in moving streams of prominences achieve several hundred gausses. It corresponds to the condition of a considerable excess of the magnetic field energy over the kinetic energy of the stream. In generating a plasma stream with a sufficiently strong forcefree magnetic field in its environment an acceleration of a certain part of quick thermal protons and electrons of the Maxwell tail becomes possible. Electrons accelerated up to energy of several dozen Mev will give synchronous radiation (radiobursts of type IV); accelerated protons, trapping into the magnetic field of the stream, come together with the solar

Declassified in Part - Sanitized Copy Approved for Release 2011/12/08 : CIA-RDP80T00246A016600420001-1

Declassified in Part - Sanitized Copy Approved for Release 2011/12/08 : CIA-RDP80T00246A016600420001-1

stream to the Earth magnetosphere and cause polar blackouts. For rather weak magnetic fields of the stream (for instance, unconnected with chromospheric flares) such a process of generation may appear non-effective.

3) It is necessary to underline that a plasma cloud with the force-free field differs principally from the moving plasma with the frozen magnetic field , connected with the Sun, as it. was considered in a number of papers[5]. The authors of this works have not determined the energy, necessary for stretching the magnetic shell with the plasma over the distance of at least dozens of astronomic units. The exact solution of such a task due to its non-linearity, is very difficult, and even an approximate estimation shows that the process of magnetic envelope stretching into an interplanetary plasma requires the energy of many orders greater than the energy of the active region on the Sun[1, 6]. Even these facts are sufficient to refuse the model of a corpuscular stream in a form of a expanding shell. Besides the long-existing corpuscular stream with a stretched magnetic shell should turn into a very twisted spiral due to a solar rotation . The Solar corona structure, investigated in detail during solar eclipses, does not indicate to the presence of any twisting of the coronal streamers. All these difficulties are naturally dropped off for the corpuscular stream model, consisting of a number of plasma clouds unconnected with the Sun. Then current systems from force-free magnetic fields. For such a stream it is possible to calculate a disturibution of a density and a simplified picture of the magnetic field. Such a calculated scheme is presented in fig.I.The interaction of the stream magnetic field with the magnetic field of the active region on the Sun determines

Declassified in Part - Sanitized Copy Approved for Release 2011/12/08 : CIA-RDP80T00246A016600420001-1

Declassified in Part - Sanitized Copy Approved for Release 2011/12/08 : CIA-RDP80T00246A016600420001-1

kinematics and energetics of all plasma cloud succession with the force-free field, composing a geoeffective corpuscular stream [6,7]. Fig. 1 shows, that in a case of plasma clouds with force-free fields the effect of a reverse correlation between the strength of a magnetic field and the value of a concentration of a stream plasma should be noted. In the region of the plasma "core" itself (region A), where we have a system of weakly decaying currents, the magnetic field is almost absent and vice versa in region B, having a greater volume where we have a magnetic field, the plasma density is minimum. In region B , like in a magnetic trap, there might be highenergetic protons of solar cosmic-rays (particularly soft ($\varepsilon \lesssim 10^8$ eV) cosmic rays). Simultaneous measurements of plasma concentration (or plasma flux) and the magnetic field, which have began being made by means of cosmic rockets at substantial distances from the Earth, can allow to solve a question whether the stream is a plasma with a frozen magnetic field (as it is usually approached) or our scheme is true. Such measurements on the Soviet cosmic station, flying to the Venus [8] and on the American Satellite "Explorer X" indicate to the correctness of the model considered. Under the condition $\mathcal{E}_{magn} > \mathcal{E}_{kin}$ the plasma stream with a force-free magnetic field of the structure considered goes through a rarefied interplanetary plasma almost without essential changes. A certain decrease of the current intensity in a plasma "body" of the stream will bring to a decrease of the magnetic field strength, but the character of the field remains force-free.

4). As it is known [9], the plasma stream moving at an

Declassified in Part - Sanitized Copy Approved for Release 2011/12/08 : CIA-RDP80T00246A016600420001-1

Declassified in Part - Sanitized Copy Approved for Release 2011/12/08 : CIA-RDP80T00246A016600420001-1

ultrasonic speed in the interaction with the Earth magnetosphere flows round it, causing the effect of the field "compression". An explanation of penetration of the stream plasma even into outer parts of the magnetosphere comes across a number of principal difficulties. In the considered scheme a force-free magnetic field of an impinging stream causes essential effects in the magnetosphere long before a possible penetration of the stream plasma into the magnetosphere. In the first approximation this influence may be described by the consideration of the impigment at an ultrasonic speed of the side and fore front of the stream magnetic field. The latter may be considered as a movement of a quaziplane magnetic piston in the outer plasma of the Earth exosphere. In this case the interaction of the stream field with the magnetosphere causes longitudinal and transverse waves, travelling to the Earth surface. The scheme of the geomagnetic field disturbances, is like the one considered by Piddington [10] The calculations show that longitudinal weak shock waves carry the greatest flux of magnetic energy. A somewhat less flux of energy will be connected with transverse waves. As in the considered scheme the energy of a force-free magnetic field of the stream 2÷3 orders exceeds its kinetic energy and a very effective transfer of energy from the stream takes place, so only in this case an energy of $\sim 10^{26} \div 10^{27}$ ergs (that is sufficient to cause a geomagnetic disturbance) can be transferred to the Earth magnetosphere. A number of peculiarities during geomagnetic disturbances and disturbances in ionosphere connected with them can be analysed in the light of the scheme considered.

Declassified in Part - Sanitized Copy Approved for Release 2011/12/08 : CIA-RDP80T00246A016600420001-1

Declassified in Part - Sanitized Copy Approved for Release 2011/12/08 : CIA-RDP80T00246A016600420001-1

Литература

I. Могилевский Э.И., Геомагнетизм и аэрономия, I96I , I, № 2, I53

2. Osterbock D.E., Astrophys.J.,I96I,I34,347.

3. Ишша Б.А., Геомагнетизм и аэрономия, I962 , 2 (в печати).

4. Zirin H.,a.A;B.Severny, The observatory,I96I,8I, N 923, I55.

5. Piddington J.H., Phys.Rev.I953,II2, 589.
T.Gold, Nuovo cimento,I959,I3,Suppl.No.I,3I8.
Astrophys.J.,Suppl.Ser.,I960,4, 406.

6. Могилевский Э.И. Геомагнетизм и аэрономия, I962, 2, (в печати).

7. Могилевский Э.И. Тр. ин-та земного магнетизма (ИЗМИР), I95I, вып. 6 (I6а), 3.

8. Долгинов С.Ш., Кузгов Л.Н., Ярошенко Е.Г., Геомагнетизм и аэрономия, I962, 2 (в печати)

9. Мигулев В.И. ДАН СССР, I959, I24, № 5, I00I; I26, № 3, 52I.

I0. Piddington J.H., Mon.Not.R.A.S.,I955,II5,67I;
J.Geoph.Res.,I960,65,NI,93.

Declassified in Part - Sanitized Copy Approved for Release 2011/12/08 : CIA-RDP80T00246A016600420001-1

Declassified in Part - Sanitized Copy Approved for Release 2011/12/08 : CIA-RDP80T00246A016600420001-1

2.16

by S.M.Pologkov, A.E.Mikirov

20.

ELECTROPHOTOMETRY OF THE CHOSEN REGION OF OUTER SOLAR CORONA IN THE VISUAL SPECTRUM REGION DURING THE FULL SOLAR ECLIPSE ON FEBRUARY I5, I96I.

The aim of the experiment was an investigation of brightness distribution in the visual spectrum region close to the Sun space, including the outer corona, then investigation of brightness distribution in the visual spectrum part of the outer corona and the sky region enveloped with measuring.

According to the spectrum, measurements cover the range from 3200 to 6200 Å. Further it was supposed to measure the sky region begining with the Solar edge up to the distance equal to 28 $R_\odot$.

As the container orientation turned out to be different from that of the calculated one another Solar corona part had been measured.

Supposed and really measured Solar corona regions are presented in Fig.I.

Measurement Methods

Measurements were carried out by means of electrophotometer "Donc-2", given in Fig.2.

Electrophotometer "Donc-2" is a camera -obscura with f=44 mm in which a picture of the investigated sky region is projected on a photocathode.

The 0,I9 x 4.2 mm slit, that corresponds to angle dimensions of 0.I5 x 5.5°, gradually moves before the photocathode.

Declassified in Part - Sanitized Copy Approved for Release 2011/12/08 : CIA-RDP80T00246A016600420001-1

Declassified in Part - Sanitized Copy Approved for Release 2011/12/08 : CIA-RDP80T00246A016600420001-1

The scanning slit makes a reverse - progressive movement. A slit movement direction is shown by an arrow in Fig.2. During variations cycle which goes on for 2 sec., the slit manages to scan 14° in progressive and reverse direction. A disc with holes is placed before the alit what permits to modulate the coming radiation with the frequency of 247 c.p.s.. A photomultiplier of "ФЭУ-25" type with an antimony-zesium cathode sensitive to the region of 3000-6200 Å ,e.g. sensitiv to that region, inside of which the maximum intensity of the scattered radiation is locatited, is used as a receiver of the radiation.

A signal taken from the cathode follower comes in to the inlet of the telemetering system.

The instrument calibration was produced on bench photometer. A standart lamp was used as a light source with a known light intensity and colour temperature (2800°K). A light filter of "C" type, turning the source temperature into a colour temperature 6500°K was put before the light source.

The instrument was placed at a definite distance from the light source. A frosted glass with a known trasmission coefficient was placed before the instrument. The frosted glass brightness, measured by the instrument while calibrating, varied within necessary limits with the help of light filters of "HC" type.

The instrument can measure brightnesses from 4.10^{-7} to $1.6 \cdot 10^{4}$ stibls, i.e. in the range of three orders of brightness variations.

Declassified in Part - Sanitized Copy Approved for Release 2011/12/08 : CIA-RDP80T00246A016600420001-1

Declassified in Part - Sanitized Copy Approved for Release 2011/12/08 : CIA-RDP80T00246A016600420001-1

It is known that the total brightness of the solar corona is of the order of $I.5 \cdot IO^{-I}$ stilb, consequently the instrument at the suggested orientation has to be scaled out up to the distance of the order of several solar radii and to measure brightnesses at the distance from IO and more solar radii.

Actually the orientation turned out to be different but as useful as it could be at the actual picture of measuring, and a very interesting corona region from II to 33 $R_\odot$ was measured (see Fig.1).

Measurements Results

Measurements results are given in Fig.3. What conclusions one could come to considering the obtained results? At first let us assume, that the results given in Fig.3, illustrate the brightness distribution in the region from II to 33 $R_\odot$, which are burdened neither by instrumental errors nor by other disturbing effects.

This problem concerning instrumental errors on other possible disturbing effects will be partially considered later. So, let the observed picture of the brightnesses be corresponding to the brightnesses of the observed outer corona region when the photometer slit is moving over it. If it is so, the only possible conclusion from these results may be the one, that the outer corona is presented as an extremely inhomogeneous formation with the size of inhomogeneities of the order of 6' of arc (in grade dimension) that corresponds to 280 thousand km in the linear dimension.

What bases is this conclusion put on? Really, let us assume, that the scattering substance is distributed in such a way, that

Declassified in Part - Sanitized Copy Approved for Release 2011/12/08 : CIA-RDP80T00246A016600420001-1

Declassified in Part - Sanitized Copy Approved for Release 2011/12/08 : CIA-RDP80T00246A016600420001-1

scattering radiation intensity (the corona brightness) falls equally (isotropiccally) according to a certain power low, let it be according to the law of $\rho^{2,5}$ (where ρ - is the distance from ⊙ to the scattering light element of the volume). or according to some other one (power law). It is clear, that even at the uniform distribution in light scattering substance space this brigthness decrease will occur according to the law ρ^{2}, and for gradually decreasing density - according to another low apporximated by higher powers at ρ .

If we assume it then at the described scanning by the slit of the corona region , it is easy to show that we are to obtain the following picture (theoretical one) of brightnesses variations; a measured brightness should vary according to the cosine law (in the corresponding power), i.e. inside of the measured region, if ρ is varying according to a power law. i.e. if α angle is read as it is shown in Fig.I.

However from Fig.3, we see, that the actual picture of brightnesses variation does not completely correspond to the theoretical one . Only at some moments we have measurements regions, where brightnesses variation is like the cosine curve variation.

Further more, from Fig.3 we see, that in some cases instead of expected intensity increase a considerable decrease is recorded in general it has no strictly regular character. However, the maximum and minimum values correspond to these ones which were expected according to Van de Hulst:

The maximum for values of R_o = II

and the maximum value for values of R_o = 30

Declassified in Part - Sanitized Copy Approved for Release 2011/12/08 : CIA-RDP80T00246A016600420001-1

Declassified in Part - Sanitized Copy Approved for Release 2011/12/08 : CIA-RDP80T00246A016600420001-1

For a comparison we give brightness data from Van de Hulst and Blackwell's work /I/, /2/ (see Fig.4).

What does it testify to?

We believe, that considering all the obtained results, evidently one could come to the only conclusion, that substance scattering the light in the outer corona is distributed extremely inhomogeneously, i.e. it has inhomogeneous structure with inhomogeneities sizes less than 6' of arc.

Angular sizes of the inhomogeneities (6' of arc) are obtained from the used brightness measurements methods, i.e. a sycle of measurement is equal to I sec. For this time at the used telemetric methods (I25 information at I sec) a record of I25 brightness estimations is obtained (i.e. I25 points in Fig.5). It is clear that from point to point the slit manages to cover the distance equal to 6'.

The conclusion, that the outer corona has a inhomogeneous structure, generally speaking, corresponds to that one, which has been made in Vitkevitch's work /3/, concerning the so called suppercorona of the Sun, observed by radiotechnical methods, during a solar eclipse of Crabe nebula.

Those measurements concern the same distances from the Sun, as in our case. The inhomogeneities in the suppercorona obviously, describe jet character of the solar corpuscular fluxes, forming electron-isotopic suppercorona.

Thus, according to V.V.Vitkevitch's data, though they were made with high degree of reliability, one can judge only of electron inhomogeneities sizes. While our data, generally

Declassified in Part - Sanitized Copy Approved for Release 2011/12/08 : CIA-RDP80T00246A016600420001-1

Declassified in Part - Sanitized Copy Approved for Release 2011/12/08 : CIA-RDP80T00246A016600420001-1

speaking, concern both scattering on the dust, and scattering by free electrons. At first it seemed, that only dust substance of interplanetary component is responsible for the light scattering at this region, if we are of the same opinion as that of Van de Hulst /I/, /5/.

Howadays, these ideas are additionally considered in Blackwell's works. However, dust component contribution into the outer corona brightness is the main one and it comprises 90 per.cent. of the total brightness. So, scattering on the free electrons comprises less than IO per.cent of the total brightness.

Consequently V.V.Vitkevitch's results may be compared with ours, but it hardly should be sāid that these these works c confirm each other. It would be seccurer to say that obtained by us results about the outer corona structure and inhomogeneities sizes in it do not controdict to V.V.Vitkevitch and Havish's ones /4/.

While considering the reliability of the obtained results we looked through possible effects, which could influence on the results. It may be light from other possible light sources (not of the corona) and instrumental errors.

Only of the own lumenocity and the aerth atmosphere brightness in the region of a complete shadow and possible black out eaused by ring of dawn were considered from possible strange light sources. There is no other hinderances.

Declassified in Part - Sanitized Copy Approved for Release 2011/12/08 : CIA-RDP80T00246A016600420001-1

Declassified in Part - Sanitized Copy Approved for Release 2011/12/08 : CIA-RDP80T00246A016600420001-1

It appeared, that possible hinderances and instrumental effects do not exceed by its value IO per.cent. of the measured brightness value, e.i. IO^{-7} stilb.

Thus, the conclusion concerning the inhomogeneous structure of the outer corona, apparently, is true,

Declassified in Part - Sanitized Copy Approved for Release 2011/12/08 : CIA-RDP80T00246A016600420001-1

Declassified in Part - Sanitized Copy Approved for Release 2011/12/08 : CIA-RDP80T00246A016600420001-1

REFERENCES

I.H.C. van de Hulst — Ap.J. I05, 47I, I947

2.D.E. Blackwell, — M.N. II5, 629, I955

3.M.F. Jaghom, — M.N. I22, I62, I96I

4.V.V. Vitkevitch

5. "Solntse", IL, I957, p.225-24I

6.A.E.Mikirov, DAN, I42, N3, I962

7.V.I.Mjukhjurja Trudy GGO, vyp. 93, I959

Declassified in Part - Sanitized Copy Approved for Release 2011/12/08 : CIA-RDP80T00246A016600420001-1

Declassified in Part - Sanitized Copy Approved for Release 2011/12/08 : CIA-RDP80T00246A016600420001-1

2.21

by G.S. IVANOV-KHOLODNY, G.M. NIKOLSKY.

21. "PREDICTION AND IDENTIFICATION OF EMISSION LINES IN THE SOLAR EXTREME ULTRAVIOLET $\lambda \leq 1100$ Å."

The solar extreme ultraviolet radiation intensity definite ion is of paramount importance to understand ionization, excitation, heating and other physical processes in the Earth ionospere, in interplanetary media, and in the Sun atmosphere. Recently direct rocket measurements of the solar extreme ultraviolet and X-ray radiation power have been a great success and gave some results, however they are faced with certain experimental difficulties when carrying out absolute energy measurements in rather various spectral regions. It is a theory that should contribute in overcoming these difficulties. Spectral investigations gave especially important information.

Beginning with 1958 a number of spectral rocket measurements of solar radiation in $\lambda=1100$ Å region were carried out

Declassified in Part - Sanitized Copy Approved for Release 2011/12/08 : CIA-RDP80T00246A016600420001-1

Declassified in Part - Sanitized Copy Approved for Release 2011/12/08 : CIA-RDP80T00246A016600420001-1

and about 200 emission lines were recorded. Solution of the solar extreme ultraviolet spectrum is one of the most interesting problem resulting from modern rocket investigations and raised before astrophysics and spectroscopy. Though many attempts were undertaken but up till now one had succeeded in identifying less than a half of all the observed lines and more than a half of identifications undertaken by various authors were not consistent. Evidently one could come to final conclusions concerning the correctness of identification only after the analysis of the line intensities and to do this we should have a certain comprehension of physical conditions in the transition layer and in the solar corona.

I. PREDICTION

The authors in paper /1/ established line theoretical intensities of the solar extreme ultraviolet. Radiation intensity of a certain ion in the corona and in the transition region between the corona and the chromosphere can be defined by generalized measure of emission

$$\Delta\varphi = \int_{h(T_1)}^{h(T_2)} n_e^2 T^{-1/2}\, dh,$$

where n_e, T - electron concentration and temperature; $h(T_1)$ and $h(T_2)$ - layer bounderies, where this ion emits. To plot $\Delta\varphi(T_i)$ as a function of the ionization temperature T_i in the whole interval between 10^4 and 10^6 ^oK experimental intensity estimation

Declassified in Part - Sanitized Copy Approved for Release 2011/12/08 : CIA-RDP80T00246A016600420001-1

Declassified in Part - Sanitized Copy Approved for Release 2011/12/08 : CIA-RDP80T00246A016600420001-1

of 27 sufficiently bright reliably identified lines were used as the initial date. These lines were arranged in spectral regions around L_α line. T_i, T_1 and T_2 temperature values for each ion were estimated on the bases of the developed ionization theory. It was adopted that excitation is resulted from an electron collision and it is balanced by spontaneous transitions. In most cases information about oscillator strength is not available, therefore approximate values were taken for them. The use of $\Delta\varphi(T_i)$ function gives an apportunity of calculating I_λ spectral line intensities without any knowledge of a transition region model. It was considered that all the suitable ionization stages of each element and all the atomic transitions for which Laport's rules and selection rules are true. In work /1/ there was presented the total list consisting of 480 most bright emission lines which are to be observed in the solar extreme ultraviolet spectrum 20 - 2000 Å and about 400 lines of them are in the spectral region $\lambda = 1100$ Å.

II. IDENTIFICATION

Theoretically predicted lines and their intensities were compared with experimental spectral data concerning the solar extreme ultraviolet radiation obtained by rockets. Work /2/ by Violett and Rense gives wave lenghts and visual intensities

Declassified in Part - Sanitized Copy Approved for Release 2011/12/08 : CIA-RDP80T00246A016600420001-1

Declassified in Part - Sanitized Copy Approved for Release 2011/12/08 : CIA-RDP80T00246A016600420001-1

"i" of 130 lines in the spectral region 84-1100 Å. Works /3,4/ by Hinteregger present photoelectrical spectrum records in absolute units of energy, where one can find 180 lines in the spectral region 60-1100 Å. Wave lengths for those lines were estimated by us only approximately. Though the most bright lines were observed by all the authors mentioned before together, there exist however non-consistences even among bright lines, and the matter might be cleared out only with the help of a proposed line prediction. It appeared that there are several false lines both in Violett and Rense's /2/ spectra (evidently because of a low quality of spectrograms) and in Hinteregger's /3,4/ the latter is probably connected with fluctuations of the background and the influence of the absorption bands of atmosphere molecular nitrogen and water vapour released by a rocket and apparatus.

From the total number of 225 lines, observed in /2/ and /3,4/ we managed to identify 180 lines with the help of the predicted list of lines /1/. Thus almost all really observed lines were identified while more than a half of unidentified lines were simply false. It should be emphasized that all the most bright lines predicted theoretically were recorded in Violett and Rense's spectra and in Hinteregger's record. However several extreme ultraviolet lines belonging to Ca XII - XV, A XI etc. which have too high ionization potential - 600-800 ev were not recorded. The results of the identification of the observed

Declassified in Part - Sanitized Copy Approved for Release 2011/12/08 : CIA-RDP80T00246A016600420001-1

Declassified in Part - Sanitized Copy Approved for Release 2011/12/08 : CIA-RDP80T00246A016600420001-1

lines are presented in following Table 1.

In Table I "?" - marks the lines, which are likely to be false; "+?" - marks the questionable identifications for which the wave lengths are available but theoretical intensity estimations are more than an order of magnitude less. As far as the data of Table I are concerned the following should be pointed out. In the solar extreme ultraviolet spectra the most abundant elements H, He, C, Ne, Mg, Si, and Fe were observed at all the ionization stages up to the coronal stage, and lines of more rare elements N, Al, S, A, Ca, Ni were observed as well. Probably further experiments will give an opportunity of observing weaker lines the list of wave lengths and expected intensities of which are given by the authors in paper /I/. Among the experimental data of works /2/ and /3,4/ we can find many / $\sim$ I5/ lines observed in the second and third orders as grazing incident spectrograph was used. Examination of Table I data shows that the discrepancy between Violett and Rense's /2/ and Hinteregger's /3,4/ experimental data is more distinguished in the region 500-I000 Å than in the region $\lambda <$ 500 Å. Line identifications are also poorer in the range 500-I000 Å and this we can probably connect with the fact that these experimental data are less reliable (compare the region 850-958 Å where N_2 bands fall). From all I80 identifications 40 ones, which belong to weak lines, are considered to be questionable though they may turn out to be true. Almost half

Declassified in Part - Sanitized Copy Approved for Release 2011/12/08 : CIA-RDP80T00246A016600420001-1

Declassified in Part - Sanitized Copy Approved for Release 2011/12/08 : CIA-RDP80T00246A016600420001-1

of the latter lines (20-30) which ~~have not be~~ unidentified ~~by us~~ and cannot be considered false are probably not identified because of incorrectness of their theoretical line estimations intensity (absence of data about terms and oscillator strenth of some ion, and imperfection of ionization and excitation theories) or the matter can be connected with intercombination transitions which were but little considered in /1/. Thus from 4 intercombination transitions for coronal ions indicated by Pecker and Rohrlich /5/ as it is shown in Table 1 three of them correspond to the observed lines.

III. RADIATION INTENSITY

On the bases of the proposed prediction and line identification one can estimate the flux of the extreme ultraviolet radiation of the Sun and that is of great importance for understanding ionization processes both in the Sun (chromosphere and solar prominences) and in the ionosphere and also in interplanetary space. A comparison of theoretical /1/ and experimental /3-4/ data concerning the reliably identified line intensities seen in Fig. 1, shows that these data in the spectral regions 60-200 Å and 900-1100 Å mainly did not differ more than a factor of 2-3. This testifies particularly to a high accuracy of a prediction of line intensities in /1/. In the X-ray range 60-200

Declassified in Part - Sanitized Copy Approved for Release 2011/12/08 : CIA-RDP80T00246A016600420001-1

Declassified in Part - Sanitized Copy Approved for Release 2011/12/08 : CIA-RDP80T00246A016600420001-1

Å intensity estimations agree at average with results of rocket measurements carried out by means of photon counters /6/ and in the spectral range around [illegible] - they agree with available rocket measurements of line intensities, which were used in computation of theoretical intensities. Thus there is a possibility of correct confrontation of solar radiation intensities in rather various spectral regions theoretically. However, in the spectral region 200-900 Å in Fig. 1 one can see a systematic variation of the ratio of the observed intensties to theoretical ones. As far as it is difficult to expect a systematic variation of theoretical value [illegible] with a wave length, it is probably connected with the fact that spectral apparatus sensitivity variations were not carefully taken into account. According to Fig. 1 the apparatus sensitivity in 250-400 Å is - 1 - 1.5 orders less than that accepted in /4/. It might be induced by absorption in the atmosphere layer overhead the rocket during spectrum record or by water vapour released by design details situated near the light beam. The latter is more possible as the maximum in the water vapour absorption spectrum is also situated in 250-400 Å /7/. The conclusion concerning the influence of effects of absorption of radiation upon experimental data is also justified in Violett and Rense's data , as it is seen in Fig. 2. It is clear from Fig. 2 that visual intensities are also under - estimated in the region 250-400 Å if compared with theoretical intensities.

Declassified in Part - Sanitized Copy Approved for Release 2011/12/08 : CIA-RDP80T00246A016600420001-1

Declassified in Part - Sanitized Copy Approved for Release 2011/12/08 : CIA-RDP80T00246A016600420001-1

Corrected for an absorbtion effect the curve of averaged spectral energy distribution in the solar extreme ultraviolet was plotted in Fig,3. Points of the stepped curves in Fig. 3 are obtained by averaging theoretical intensities of all the lines /I/ according to wave length intervals of $\Delta\lambda = 50$ Å; and circles are obtained by avereging the identified lines presented in Table I. As the both data for $\lambda > 400$ Å coinside mainly all the strong lines are identified in this spectral region.

Spectral energy distribution in extreme ultraviolet of the Sun reveals the maximum in the region 200-400 Å with power density ~ 0.05 erg/sm^{2}sec Å. This radiation originates from the upper layer of the transition region. The main part of the solar extreme ultraviolet radiation energy is concentrated in 200-400 Å, near the Earth this energy is approximately equal to 7.5 erg/sm^{2}sec. Besides the gross maximum in the region 200-400 Å one can notice several maxima more in Fig.3 in the wave length regions 60-I00, 550-650,750-850, and 960--I050 Å. To precise the spectrum structure in the region λ.400 Å averaging line intensities according to the spectrum inter - vals $\Delta\lambda = I0$ Å (shown by points) was carried out. It is interesting to indicating that in Hinteregger's /2,3/ registrogrammes it is observed an accumulation of strong lines in the marked region. The maximum in the most extreme ultra- violet region 60-I00 Å is the most interesting as it corresponds to coronal highly ionized

Declassified in Part - Sanitized Copy Approved for Release 2011/12/08 : CIA-RDP80T00246A016600420001-1

Declassified in Part - Sanitized Copy Approved for Release 2011/12/08 : CIA-RDP80T00246A016600420001-1

ion radiation. We believe, that coronal radiation variations during eleven year cycle of solar activity, will effect particularly the intensity and location of this maximum in the solar extreme ultraviolet spectrum. While radiation variations of the transition layer is mainly connected with the maximum in the range 200-400 Å.

Energy of emission lines in the whole extreme ultraviolet during of the solar maximum activity is 14.7 erg/sm^{2}sec in the spectrum region $\lambda \leq 1100$ Å, if estimated only according to the identified lines. Actually the energy may be slightly higher. Preliminary estimations of the total energy /8/ gave 10-100 erg/sm^{2}sec. It is interesting to note that Allen /9/ also comes to the conclusion that the solar extreme ultraviolet radiation intensity is much higher than it has been used to accept according to ionosphere data (~ 1-0.1 erg/cm^{2}sec.). According to Allen /10/ the total energy of the estimated lines is ~5 erg/sm^{2}sec. The estimation presented here shows that the main part of the solar extreme ultraviolet radiation energy is concentrated in a line spectrum and these energy exceeds the continuous radiation energy of the transition layer and the corona many times./8/.

Declassified in Part - Sanitized Copy Approved for Release 2011/12/08 : CIA-RDP80T00246A016600420001-1

Declassified in Part - Sanitized Copy Approved for Release 2011/12/08 : CIA-RDP80T00246A016600420001-1

SUMMARY

In this paper we discussed allowed atomic transitions for proper ionization stages of all the elments and here it was given the prediction of solar emission lines and their intensities, about 400 lines of which are in the spectrum region $\lambda \leq 1100$ Å. Taking into account the line intensities /1/.180 from ~225 of solar emission lines in the region 60-1100 Å observed by means of rockets /2,3,4/ were identified. It is obtained the spectral energy distribution of the solar extreme ultraviolet, and maxima were found out in the wave length region of 50-100 (the corona), 200-400 (an upper part of the transit ion layer),550-650, 750-850, 950-1050 Å. The total radiation energy was estimated near the Earth ·15 erg/cm^2sec., half of it being concentrated 200-400 Å.

Declassified in Part - Sanitized Copy Approved for Release 2011/12/08 : CIA-RDP80T00246A016600420001-1

Declassified in Part - Sanitized Copy Approved for Release 2011/12/08 : CIA-RDP80T00246A016600420001-1

Fig. 1 - Ratio variations of experimental to theoretical intensities $I[3,4]/I[1,1]$ depending upon λ, - according to data /3/, • - according to data /4/, ——— - average curve.

Fig. 2 - Ratio variations $i[2]/I[1,1]$ depending upon λ plotted according to data /2/. - - - - average curve, — - - - calibration curve according to /9/.

Fig. 3 - Spectral energy distribution of solar line radiation in the region 30-1100 Å. - averiging according to wave length intervals $\Delta\lambda$=50 Å of radiation energy of all the theoretical lines. • - the same according to $\Delta\lambda$=10 Å, ◦ - averaging according to $\Delta\lambda$=50 Å of the reliably identified lines, presented in Table I.

Declassified in Part - Sanitized Copy Approved for Release 2011/12/08 : CIA-RDP80T00246A016600420001-1

Declassified in Part - Sanitized Copy Approved for Release 2011/12/08 : CIA-RDP80T00246A016600420001-1

Литература

1. Г.С.Иванов-Холодный, Г.М.Никольский, Астрономич. ж., 38, 23, 1961.

2. K.Violett, E.A.Hones, Astrophys. J., 132, 954, 1960.

3. H.S.Hinteregger, Astrophys. J., 132, 801, 1960.

4. H.S.Hinteregger, J.Geophys.Res., 66, 2367, 1961.
Symposium COSPAR, Florence, 1961 (preprint).

5. C.Pecker, F.Roberlich, Mem.Soc.roy.sci., Liège, 4, 265, 1961.

6. H.Friedman, in "Space Astrophysics", ed. by W.Miller, NY, 1961, p. 107.

7. K.Watanabe, Adv. Geophys., 2, 153, 1953.

8. Г.С.Иванов-Холодный, Г.М.Никольский, Астрономич. ж., 38, 45, 1961.

9. C.W.Allen, Mem.Soc.roy.sci., Liège, 4, 77, 1961.

Declassified in Part - Sanitized Copy Approved for Release 2011/12/08 : CIA-RDP80T00246A016600420001-1

Declassified in Part - Sanitized Copy Approved for Release 2011/12/08 : CIA-RDP80T00246A016600420001-1

Experimente				Identification [1]			
λ[Å]	i[2]	λ[3,4]	I[3,4]	Ion	λ	I	Remarks
1	2	3	4	5	6	7	8
		62	0.01	Fe XIV	59.6	0.05	
				S VIII	61.6	0.006	
				Ni XIV	(63)	0.005	
		66	0.01	Si VI	(67)	0.003	
		69	0.015	Si VIII	69.7	0.02	
		74	0.015	Fe XIII	(75)	0.05	
83.9	30	83	0.02	Fe XII	(80)	0.06	
		93	0.015	Fe X	(95)	0.05	
103.7	25			Fe IX	103.6	0.03	
109.3	20						
111.5	5	111	0.005	Si VI	111.3	0.01	
113.6	20						
115.8	5			O VI	115.8	0.005	
117.9	10	120	0.005	Si V	117.9	0.01	
		132	0.004	Fe VIII	130.9	0.01	
				O VI	132.3	0.005	
133.5	15	138	0.004	Fe VI	133.6	0.005	
150.0	10	149	0.003	O VI	150.1	0.015	
		166	0.01	A X	(166)	<0.015	+?
169.9	15	169	0.03	A X	(171)	<0.007	II ord.
171.1	5			Fe VI	171.2	0.002	+?
171.9	5						?
172.7	5			O V	172.2	0.002	+?
174.3	30	174	0.045	O VI	172.9	0.02	
		180	0.055				II ord.?
184.7	5	187	0.035	O VI	184.1	0.03	
		192	0.10	S XI	(191)	0.15	
		194	0.05	Fe VIII	195.7	0.02	
		198	0.03	O VIII	198.6	0.05	
		201	0.03	O VIII	202.6	0.03	
209.9	10	204	0.07	Fe XIV	(211)	0.1	
226.3	5	229	0.07	Fe XIII	(230)	0.2	
				Si XII	(230)	0.2	

Declassified in Part - Sanitized Copy Approved for Release 2011/12/08 : CIA-RDP80T00246A016600420001-1

Declassified in Part - Sanitized Copy Approved for Release 2011/12/08 : CIA-RDP80T00246A016600420001-1

1	2	3	4	5	6	7	8
		218	0.055	A	XII (221)	0.02	
				Mi	XV (220)	<0.05	
		222	0.035	Fe	XIV (223)	0.3	
				Si	IX 223.7	0.1	
		226	0.045	Si	IX 225.0	0.07	
				Ca	XV (225)	<0.1	
229.1	10			Si	VIII 230.0	0.003	+?
231.0	20	232	0.02	S	XII 231.5	0.1	
				Fe	XV (232)	0.1	
234.6	5						?
237.1	10						?
238.5	5	238	0.025	Fe	XII (238)	0.2	
				Fe	VII 239.9	0.06	
243.3	10	243	0.025	Mo	II 243.0	0.0005	
				Fe	VII 243.4	0.002	
		249	0.025	Fe	XIII(250)	0.7	
		252	0.003	S	XI (253)	0.06	
257.1	20	257	0.003	S	X (258)	0.03	
				Si	X 258.4	0.06	
260.0	5	259	0.01	S	X (260)	0.05	
261.2	15			Ni	VI 260.5	0.002	+?
				Fe	XVI (262)	<0.05	
		264	0.003	Fe	XIV (264)	0.05	
266.4	10	266	0.003	S	X (265)	0.03	
				Fe	XIV (266)	0.15	
272.3	5	273	0.005	Si	X 272.1	0.05	
276.3	5	276	0.009	Si	VII 275.4	0.06	
				Fe	XIV (276)	0.2	
		278	0.006	Si	X 277.3	0.1	
				Mg	VII 278.4	0.2	
280.0	5			O	IV 279.7	0.01	
				Si	X 280.0	0.006	
281.4	5	282	0.002	Fe	XII (283)	0.04	
		285	0.035	Fe	XIV (285)	0.3	
289.1	10	289	0.002	S	XII (290)	<0.05	
				Ni	XV (290)	<0.02	

Declassified in Part - Sanitized Copy Approved for Release 2011/12/08 : CIA-RDP80T00246A016600420001-1

Declassified in Part - Sanitized Copy Approved for Release 2011/12/08 : CIA-RDP80T00246A016600420001-1

1	2	3	4	5	6	7	8
		297	0.003	[illegible]	(303)	0.2	
		296	0.002	Fe VI	(295)	0.025	
				Si IX	296.2	0.04	
299.2	30	299	0.009	[illegible]	(298)	<0.5	
				S XII	(302)	<0.1	
303.8	20	303	0.13	Si [illegible]	303.6	0.06	
				Be II	303.8	0.13	
		305	0.01	Al IX	305.1	0.02	
		307	0.001	Al VI	(307)	0.003	
310.1	10	311	0.009	Si VII	(317)	0.01	
				S XIII	(311)	<0.02	
				Si XIII	(312)	0.01	
		313	0.005	Si XVI	(313)	<0.02	
				C IV	312.4	0.03	
				Mg VIII	315.0	0.03	
		316	0.002	Si XIV	(316)	0.02	
				Si VIII	316.2	0.1	
		319	0.002	Mg VII	319.0	0.01	
		321	0.005	Si VIII	319.8	0.15	
		326	0.009	Fe XII	(324)	0.02	
328.0	10	335	0.027	Fe XVI	336.2	<0.5	
		339	0.004	Mg VIII	339.0	0.08	
342.6	5	343	0.005	Fe XIV	(342)	0.2	
344.7	20	347	0.01	Si IX	345.0	0.15	
				Fe X	347.0	0.35	
		349	0.003	Si IX	349.8	0.2	
352.9	5	352	0.006	Fe XIII	(350)	0.3	
354.9	30	354	0.005	Fe XII	(350)	0.1	
				Fe XIV	(356)	0.4	
		359	0.012	Fe XII	(360)	0.2	
				Fe XIII	(360)	0.15	
		363	0.005	Fe XVI	361.7	<0.3	
				Fe X	(367)	0.15	
		368	0.02	Mg IX	368.2	0.08	
				Fe XII	(369)	0.3	
372.2	10			Fe XIII	(373)	0.4	
373.6	15	375	0.002	O III	374.1	0.03	

Declassified in Part - Sanitized Copy Approved for Release 2011/12/08 : CIA-RDP80T00246A016600420001-1

Declassified in Part - Sanitized Copy Approved for Release 2011/12/08 : CIA-RDP80T00246A016600420001-1

1	2	3	4	5	6	7	8
379.0	25	378	0.004	Fe XI	(376)	0.02	
				Na VII	331.3	0.008	
		383	0.002	Al VIII	383.7	0.007	
				C IV	384.2	0.006	
				Al IX	385.0	0.01	
		387	0.004	Fe XIII	(386)	0.65	
		391	0.003	Al IX	392.4	0.015	
		404	0.004	Mg VI	403.3	0.13	
		416	0.003	Ne V	416.5	0.03	
419.4	10	413	0.006	C IV	419.5	0.05	
		420	0.002	S XIV	(421)	<0.02	◆ ?
		429	0.002	Ne VII	429.2	0.03	
430.7	10	432	0.002	Mg VIII	430.5	0.05	
435.1	25	437	0.005	Mg VII	431.3	0.03	
				Mg VII	434.9	0.14	
				Mg VIII	436.7	0.1	
		441	0.003	Mg VIII	442.2	0.003	◆?
		445	0.004				
448.0	15	449	0.003	S XIV	(446)	<0.01	
		456	0.003	Si IV	457.8	0.001	◆?
		463	0.003	Na V	463.3	0.004	◆?
463.8	10	467	0.006	Ne VII	(464)	0.03	
		473	0.002				
477.4	15						
483.7	10	484	0.005	Ne V	483.0	0.08	
495.0	5	494	0.005	Na VI	494.3	0.005	◆?
498.3	5	500	0.005	Si XII	499.3	0.06	
503.9	15	503	0.004				IIIord
		507	0.003				
		514	0.004				
		521	0.01	Si XII	521.1	0.03	
				Na I	522.2	0.01	
525.8	15	525		O III	525.8	0.005	
				Fe IV	526.2	0.01	
		529	0.004	A V	527.7	0.002	◆?
535.3	5						
536.5	5	537	0.002	Na I	537.0	0.04	
538.8	5			C III	538.3	0.001	◆?

Declassified in Part - Sanitized Copy Approved for Release 2011/12/08 : CIA-RDP80T00246A016600420001-1

Declassified in Part - Sanitized Copy Approved for Release 2011/12/08 : CIA-RDP80T00246A016600420001-1

1	2	3	4	5	6	7	8
				C II	539.I	0.02	
539.2	5	540	0.003	Ne IV	541.I	0.04	
				Be IV	542.0	0.03	
		543	0.003	Ne IV	543.9	0.I2	
		55I	0.005	Al XI	(550-	0.004	
				Ca VII	551.5	0.002	
553.7	I0	555	0.0II	O IV	554.1	0.I	
		560	0.002	Ne VI	559.6	0.0I5	
		565	0.003	Ne VI	562.8	0.02	
				Si XI	565.I	0.03	
		569	0.0I7	Fe V	569.9	0.I7	
572.9	5	?		Ne V	572.3	0.23	
576.6	I0						
578.5	I0	573	0.004				
580.6	I0						
581.5	I0	58I	0.004	Ca VIII	582.8	0.002	+ ?
				Si IX	583.9	0.02	
584.7	I0	585	0.003	Ne I	584.4	0.7	
589.9	5						?
593.6	5	592	0.003	Si XI	59I.2	0.007	
597.9	5	599	0.003	O III	597.8	0.005	+ ?
599.2	5			O III	599.6	0.0I	+ ?
602.9	5						
607.6	50	606	0.05				II ord.
608.5	5	608	0.006	O IV	608.4	0.I	
609.8	5			O IV	609.8	0.3	
6II.4	5			O III	6I0.8	0.005	+?
6I4.9	20						
6I7.2	25	6I7	0.002				II ord.
		622	0.0I	K IX	62I.4	0.00I	+ ?
625.I	5	625	0.003	Mg X	624.9	0.025	
				O IV	625.I	0.03	
630.3	20	629	0.02	O V	629.7	0.3	
635.5	I0	634	0.002	Ca VII	633.8	0.003	+ ?
		638	0.003	Fe XVI	637.2	< 0.I	
644.9	20			Ca V	646.6	0.00I	+ ?
651.5	I0	653	0.00I	C II	65I.3	$\sim I0^{-6}$	?
		66I	0.003	A XIII	658.7		[5]
		670	0.0I				II ord.
		676	0.003	Ca IX	673.0	0.00I	+ ?

Declassified in Part - Sanitized Copy Approved for Release 2011/12/08 : CIA-RDP80T00246A016600420001-1

Declassified in Part - Sanitized Copy Approved for Release 2011/12/08 : CIA-RDP80T00246A016600420001-1

1	2	3	4	5	6	7	8
		682	0.004	Na IX	(682)	0.005	+ ?
697.3	I5	699	0.004	N III	697	0.00I	+ ?
694.5	25	695	0.005	Mg IX	692.4	0.03	+,II ord.
		700	0.00.	A VIII	700.4	0.004	+ ?
703.3	20	704	0.0I	O III	(703)	0.06	
707.9	20			S VI	706.5	0.002	+ ?
		7I0	0.005	Mg IX	7I0.3	0.0I	+ ?
		720	0.0I				II ord.
		729	0.007	S III	728.7	0.002	
737.I	I5	738	0.0I				II ord.
		745	0.004				III ord.
754.8	I0	752	0.004				
		762	0.005	O V	(760)	0.03	
764.5	I0	767	0.007	N IV	765.I7	0.0I	
		77I	0.0I	Ne VIII	770.5	0.09	
779.4	5	78I	0.007	Ne VIII	780.3	0.06	
		786	0.004	O IV	787.7	0.2	
79I.2	5	790	0.0I4	O IV	790.2	0.1	
		793	0.005	Na VIII	793.3	0.00I	+?
		802	0.002	Cl VII	800.7	0.00I	+?
809.4	5	803	0.002	O IV	809.7	0.002	+?
8I0.9	5	8I2	0.002				
8I5.3	5	8I8	0.005				
822.5	5	82I	0.003	A V	822.2	0.00I	+ ?
823.0	5						?
825.6	5	824	0.004	A V	827.2	0.002	+ ?
829.9	I0	829	0.004				
834.0	5			O II	833.3	0.I	
				O III	833.7	0.I	
835.2	5	835	0.0I5	O II	834.5	0.I5	
				O III	835.2	0.I5	
838.7	5			A V	838.0	0.00I	+ ?
		846	0.003	A IV	843.8	0.002	+ ?
852.6	I0	852	0.0I	A IV	850.6	0.002	+,IIIoni.
855.4	30						
858.2	I0	850	0.003	C II	858.I	0.002	+ ?
859.4	20			C II	858.6	0.004	+ ?

Declassified in Part - Sanitized Copy Approved for Release 2011/12/08 : CIA-RDP80T00246A016600420001-1

Declassified in Part - Sanitized Copy Approved for Release 2011/12/08 : CIA-RDP80T00246A016600420001-1

1	2	3	4	5	6	7	8
		868	0.003				?
		871	0.005				?
		877	0.01				?
		880	0.01				?
		887	0.003				?
		893	0.005	Ne	VII	(892)	0.1	
902.9	5	901	0.003	C	II	903.6	0.01	
905.5	5			S	II	906.9	0.001	+ ?
911.4	100	912	0.040					III ord.
913.0	10							?
914.2	50	914	0.013					
916.0	10	917	0.005	N	II	916.0	0.001	+ ?
		921	0.003	N	IV	922.3	0.002	+ ?
		925	0.005	N	IV	923.3	0.004	+ ?
932.2	10	932	0.003	S	VI	933.4	0.02	
		937	0.007	H	I	937.3	0.003	
940.9	10							?
943.7	10	942	0.004	S	VI	944.5	0.01	
		949	0.003	H	I	949.7	0.015	
960.5	10							?
961.4	10	961	0.003					
964.5	10							?
970.1	10							?
972.9	10	972	0.02	H	I	972.5	0.01	
977.9	30	976	0.03	C	III	977.0	0.6	
		986	0.005					?
990.0	15	992	0.007	N	III	(991)	0.01	
		999	0.013					IIIord.
		1006	0.014					III ord.
1009.8	10	1009	0.004	C	II	1010.7	0.001	+ ?
1013.3	15	1013	0.002	S	III	1012.6	0.006	
1014.1	10	1018	0.004					
1019.7	10							?
1022.0	10							?
1025.7	60	1024	0.04	H	I	1025.7	0.14	
1028.7	10							?
1030.3	15							?
1032.2	30	1029	0.03	C	VI	1031.9	0.06	
1038.2	40	1035	0.02	C	II VI	1036.3 1037.6	0.05	

Declassified in Part - Sanitized Copy Approved for Release 2011/12/08 : CIA-RDP80T00246A016600420001-1

Declassified in Part - Sanitized Copy Approved for Release 2011/12/08 : CIA-RDP80T00246A016600420001-1

1	2	3	4	5	6	7	8
1018.1	10	1018	0.004				
1019.7	10						?
1022.0	10						?
1025.7	60	1024	0.04	R I	1025.7	0.14	
1028.7	10						?
1030.3	15						?
1032.2	30	1029	0.03	0 VI	1031.9	0.06	
1033.2	40	1035	0.02	C II	1036.3	0.05	
				O VI	1037.6		
1040.9	5	1040	0.007	O I	1040.1	0.01	
1048.9	5	1049	0.004	Si V:I	1048.9		[5]
1051.4	10						
1058.7	10	1055	0.007	Al VIII	1058.7		[5]
1065.3	15	1063	0.007	S IV	1062.7	0.005	+?
		1073	0.004	S IV	1073.3	0.01	
		1080	0.013				III ord
1035.1	10	1033	0.013	N II	1035	0.01	
		1091	0.01				
		1100	0.01				

Declassified in Part - Sanitized Copy Approved for Release 2011/12/08 : CIA-RDP80T00246A016600420001-1

Declassified in Part - Sanitized Copy Approved for Release 2011/12/08 : CIA-RDP80T00246A016600420001-1

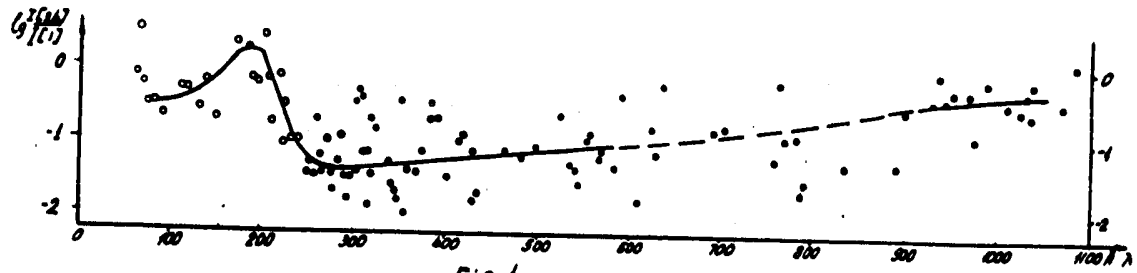

Fig. 1

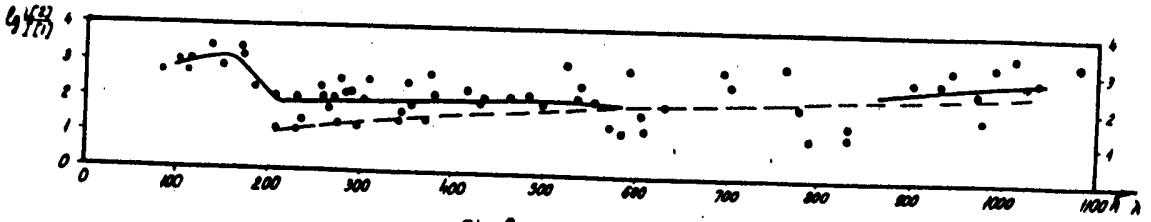

Fig. 2

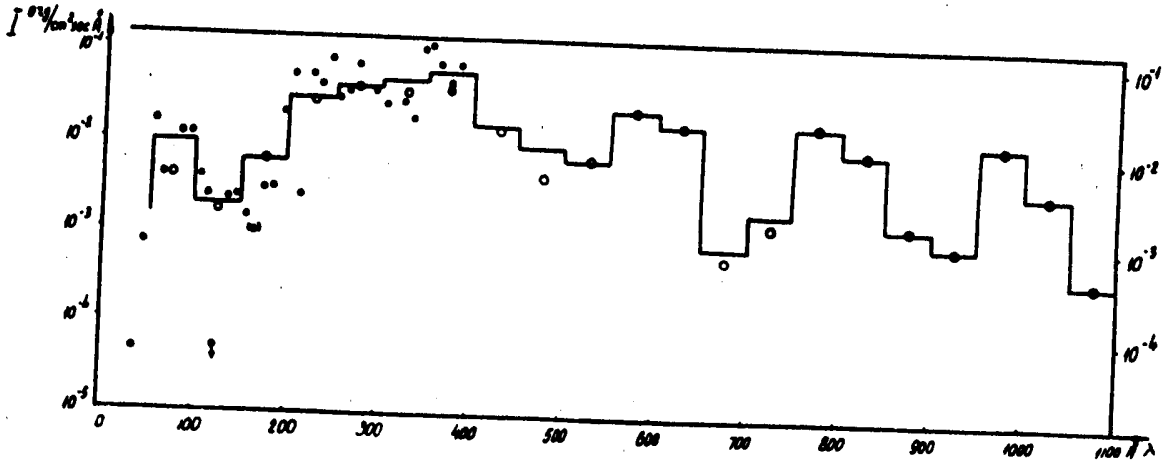

Fig. 3

Declassified in Part - Sanitized Copy Approved for Release 2011/12/08 : CIA-RDP80T00246A016600420001-1

Declassified in Part - Sanitized Copy Approved for Release 2011/12/08 : CIA-RDP80T00246A016600420001-1

2.50

by S.Mandelstam, B.Vasilyev, J.Voronko,
I.Tindo, A.Shurygin
(The Lebedev Physical Institute
Academy of Sciences of the USSR,
Moscow).

22.

"Measurements of Solar X-ray Radiation"

Summary

The flux of solar X-rays radiation below 10Å was measured on July 21,1959 by vertical flights of two geophysical rockets, on August 19-20,1960 during the flight of the spaceship-sputnik II, on December 1-2,1960 during the flight of the spaceship--sputnik III, and on February 15,1960 by vertical flight of a geophysical rocket during the total phase of the solar eclipse.

Introduction

In the present report a summary is given of the results of the measurements of solar X-ray radiation in the region of the spectrum below 10Å performed in the last years at Physical Institute of the USSR Academy of Sciences.

A theoretical investigation of shortwave part of solar radiation including the soft X-rays was made by Shklovsky /1/, Elwert /2/, de Jager /3/, Kazachevskaya and Ivanov-Kholodny /4/.

Declassified in Part - Sanitized Copy Approved for Release 2011/12/08 : CIA-RDP80T00246A016600420001-1

Declassified in Part - Sanitized Copy Approved for Release 2011/12/08 : CIA-RDP80T00246A016600420001-1

The first and extensive experimental investigations of this radiation was carried out by H.Friedman and his colleagues since 1949 /5/.

The results obtained are of considerable interest for understanding physical processes taking place in outer atmospheres of the Sun and of the influence of solar shortwave radiation on the Earth's atmosphere. Theoretical calculations, however, are based on schematic conceptions on the structure of the solar corona and on very approximated values of quantities used in these calculations. The experimental material available naturally is very limited. Therefore, it seems rational to contunue theoretical calculations and accumulate systematical experimental measurements.

We have chosen for the first step measurements of the radiation flux near the shortwave limit of the solar spectrum - below 10Å. This radiation comes from the hottest regions of the solar corona, is subject to rapid variations and penetrates into the Earth's atmosphere most deeply.

In our experiments end-window photon counters with mica and metallic film-windows served as filters was used. Pulses from counters were amplified and shaped by electron circuit, counted by trigger binary stage scaler and transmitted by a telemetry system to Earth. Each measuring channel consisted of one or several photon counters connected in parallel and all transistorized adjusting circuits, input circuit, scaler circuit and output circuit /fig.1/. These channels in all the experiments were mainly the same, differing only in the type

Declassified in Part - Sanitized Copy Approved for Release 2011/12/08 : CIA-RDP80T00246A016600420001-1

Declassified in Part - Sanitized Copy Approved for Release 2011/12/08 : CIA-RDP80T00246A016600420001-1

of the counter, the number of the binary stage and the output to the telemetry system /6/.

The absolute efficiency of the samples of the counters of each type was measured for emission lines /7/ together with A.P.Lukirsky. The sensitivity of the counters used in the flying apparatus was measured from the continuous spectrum of the tungsten anode and is known only with the accuracy of factor 2-3.

2. Measurements by means of geophysical rockets

Measurements were made at two vertical launchings of geophysical rockets to a height of about 105 km., in the morning and in the evening on July 21,1959, at the solar zenith angle about 90° /8/.

Counters were used with mica windows /1.6 mg/cm^2/ with a sputtered layer of aluminium about 2 microns thick. The counters were placed in the rocket instrumentation container. At the ascent of the rocket the container separated from it, self-oriented towards the Sun and was oriented both at the remaining ascending and descending portions of the trajectory up to the entry to the dense layers of the atmosphere.

Because of the indications to the possibility of the existence of fast corpusculs at altitudes of 70 km. and higher altitudes, special measures were taken to ensure protection from these fast corpusculs and to check up that the radiation recorded was really solar X-ray radiation. In the first laun-

Declassified in Part - Sanitized Copy Approved for Release 2011/12/08 : CIA-RDP80T00246A016600420001-1

Declassified in Part - Sanitized Copy Approved for Release 2011/12/08 : CIA-RDP80T00246A016600420001-1

ching the detector block contained two identical counters directed to the Sun. One of the counters had magnetic shielding from electrons effective to the energy of 15-20 kV., while the other control counter, had no protection. Such a combination of counters has made it possible to estimate the number of ounts due to bremsstrahlung produced at the counters windows by low-energy electrons. To estimate the contribution of faster electrons not deviated by magnetic shielding, a control counter was used in the second launching which had /as the working counter/ magnetic protection, but was turned from the direction to the Sun by the angle of 15° and, therefore, recorded only radiation of nonsolar origin. In both experiments interferences from corpusculs were not revealed. The recorded radiation would be ascribed to solar X-ray radiation. Fig.2 shows the counting rate versus time for the working and control counters in the evening launching. The increase of the background at the altitude 30-40 km. is due to the cosmic rays.

From the data on the variation of the counters' counting rate with the height of the container ascent, and from the data on the atmospheric density, the atmosphere absorption coefficients and the counter spectral sensitivity curve one can calculate the energy distribution and the energy flux in the part of the solar spectrum under investigation, extrapolated to the top of the Earth's atmosphere. The results of the calculations are given in fig.3 /the calculations for the 8-10Å region and lower than 3Å are very inexact and, therefore,

Declassified in Part - Sanitized Copy Approved for Release 2011/12/08 : CIA-RDP80T00246A016600420001-1

Declassified in Part - Sanitized Copy Approved for Release 2011/12/08 : CIA-RDP80T00246A016600420001-1

are indicated by dashes/. The energy enclosed in the region below 10Å is $7{,}3 \cdot 10^{-4}$ and $3.2 \cdot 10^{-4}$ erg/cm^2 sec. respectively. Taking account the possible inaccurasy by 2-3 times in the value of the absolute counter-efficiency it is difficult to state if this difference in energies in the morning and the evening flights is real. The solar activity on the day of the launching was considerable; during the day several solar flares were recorded. In the moment of the first launching there are no solar flares; the moment of the second launching coincided with the stage of the attenuation of the class 1 solar flare.

The dashed line in fig.3 shows the Bremsstrahlung intensity calculated according to the expression

$$N_\lambda = \text{Const} \cdot \frac{dt}{\lambda} \exp\left\{-\frac{hc}{\lambda T_e \lambda}\right\} \quad /1/$$

for Te $4.5 \cdot 10^6$ and normalized so that it coincides with the curve 1 at $\lambda = 7$Å. As evident from fig.3, this curve reproduces well the chape of the experimental curves.

3. Measurements by means of spaceships-sputniks

These measurements were carried out during the flights of spaceship-sputniks II and III on August 19-20 and December 1-2, 1960. The aim of the investigations was the measurement of the radiation flux during longer time intervals /9/. In the instrumentation used on spaceship II - six photon counters with beryllium windows /15mg/ cm^2/ - served as the main radiation detectors. The counters were installed outside the ship and their axes were oriented along six mutually perpendicular directions.

Declassified in Part - Sanitized Copy Approved for Release 2011/12/08 : CIA-RDP80T00246A016600420001-1

Declassified in Part - Sanitized Copy Approved for Release 2011/12/08 : CIA-RDP80T00246A016600420001-1

The counter windows had magnetic shielding effective for electrons with energies up to 15-20 kw. The thickness of the aluminium walls of the detector block bodies was 3 mm. All the counters were connected in parallel and coupled to the common counting circuit with the capacity of 20 binary stage. The state of the last twelve binary stages in the scaling circuit were read out every three minuts by the memory device. By the end of the 24-hour flight of the ship all the stored information was on command transmitted by the telemetry system to Earth. The difference of two neighbouring readings gave the number of pulses recorded during the time of 3 minutes by all the six counters. Besides, in the moments of the radio communication of the ship with the Earth the counters counting rate was transmitted directly through the telemetry system. This system remained switched on also for some time after the end of the work of the memory device.

Fig.4 presents the results of the measurements — the record of the counter counting rates derived from the memory device /Moscow time/. In the lower part of the picture time intervals are indicated during which the ship was in the Earth's shadow /the moments of the entry and exit from the shadow are rounded off to 1 minute/. In fig.5 samples of the direct telemetric records are presented. From the fig.4 it is evident that the regions of high counting rates are located chiefly on the sunside part of the orbit. In the region of the Earth's shadow the counting rate considerably decreases, approaching to the level compared with the cosmic rays background. Thus, the radiation recorded on the sunside part of the orbit can be regarded

Declassified in Part - Sanitized Copy Approved for Release 2011/12/08 : CIA-RDP80T00246A016600420001-1

Declassified in Part - Sanitized Copy Approved for Release 2011/12/08 : CIA-RDP80T00246A016600420001-1

as solar X-ray radiation. However, on some of the parts of the orbit located in the shadow ragion (mainly at the entry and exit from the shadow) the high counting rate is also observed. Theis radiation can be ascribed to the particles of the radiation belts.

The pick out of the parts of the orbit on wich interferences from the radiation belts are considerable can be made from the counter records on the shadow parts of the orbit where the exceeding of the counting rate above the cosmic rays background level is caused only by particles of the radiation belts. All these parts of the orbit turned to be concentrated in the latitude region hatched in fig.6, where numbers indicate the counting rate in pulses/sec.

Separated in this way parts of the records which are free from interference and belong to the sunside of the orbit can be mainly ascribed to solar X-ray radiation.[x] The interchange of the counting rate maxima and minima on these portions of the orbit is connected with the escape of the Sun from the viewing field of the counters due to rotation of the ship - the direct telemetrying records shown that in such memory device record minima the counting rate decreases to the cosmic rays background level /in the regions outside the radiation belts/.

---

x) It should be noted that at the transit from the sunlit to the shadow part of the orbit a sharp change of the counting rates is not recorded. It seems rather strange that solar X-ray radiation and the particles of the radiation belts give essentially the same counting rates. Apparently however this coincidence is a casual one.

Declassified in Part - Sanitized Copy Approved for Release 2011/12/08 : CIA-RDP80T00246A016600420001-1

Declassified in Part - Sanitized Copy Approved for Release 2011/12/08 : CIA-RDP80T00246A016600420001-1

During the time of the ship flight the intensity level of solar X-ray radiation remained approximately unchanged. A certain decrease of the intensity /approximately by 1.5 times/ was observed during the period from 20 to 23 h. on August 19. If we assume that the energy distribution in the spectrum is described by expression /1/ and if we assume Te $\sim 3 \cdot 10^{6}$° for the electron temperature value, then for the energy flux in the region shorter than 10A we get $7\text{-}8 \cdot 10^{-4}$ erg/cm^2 sec.

Days 19-20 August are characterized by the high solar activity. In the period of the registration of X-ray radiation several solar flares occurred, among them class 2 flare /15 h 40 min - 16 h 25 min/ and several class 1$^+$ and 1 flares /14h 32 min - 14 h 51 min., 15 h 33 min - 16 h 00 min., 17 h 07 min - 17 h 50 min. and others/. Ionospheric disturbances accompanied by fading of short radio waves were also observed /15 h 37 min. - 16 h 15 min., 21 h 22 min. - 22 h 01 min., 06 h 54 min., 10h 07 min. - 10 h 45 min. and others/. Some flares occurred when the ship was in the Earth's shadow; a number of flares took place when the ship was in the radiation belts region where the separation of the solar radiation component is difficult. However, several flares, among them the end of the flare 15 h 40 min. - 16 h 25 min. fell on the time moments when the ship was on the orbit part favourable for measurements of solar X-ray radiation. As fig.4 shows, a sharp increase of X-ray radiation in these moments was not observed. It should however be noted that the high average radiation level was close to the limit of the instrumentation measurement range. The considerable increase of the solar flux should have led to the over-

Declassified in Part - Sanitized Copy Approved for Release 2011/12/08 : CIA-RDP80T00246A016600420001-1

Declassified in Part - Sanitized Copy Approved for Release 2011/12/08 : CIA-RDP80T00246A016600420001-1

filling of the scalers and also to the overlod of the photon counters, accompanied by the decrease of the counting rate. Assuming that the counter worked in the decreasing region of the counting response the estimate of the radiation flux in the region 2-10Å during the flare on August 19, 15 h 40 min. when strong X-ray radiation and solar radio emission outburst took place, gives the value of the order of 10^{-2} erg/cm.sec. Apparently the increase of the radiation flux close to the off--scale readings was observed according to the direct telemetric records in the time moments 15 h 04 min. /August 19/, 06 h 02 min and 10 h 38 min. /August 20/. The last moment coincides with the class 2 ionospheric fading.

Into the instrumentation of spaceship III a number of considerable changes have been introduced. Two photon counters connected in parallel with a mica window /1.6 mg/cm^2/ covered by aluminium foil /2.7 mg/cm^2/ placed in a lead shield 1 mm thick were mounted on the selfpointing solar battery system and were constantly pointed to the Sun. On the same system two identical control counters were mounted, their axes were perpendicular to the direction to the Sun. In front of these counter windows was a tantalum plate inclined at the angle of 45° about the direction to the Sun and the counter axis. Apparently these counters did not practically register solar X-ray radiation which get into them only after reflection from the tantalum plate, i.e., considerably attenuated; with regard to the radiation belt particles these counters were equivalent to the wor-

Declassified in Part - Sanitized Copy Approved for Release 2011/12/08 : CIA-RDP80T00246A016600420001-1

Declassified in Part - Sanitized Copy Approved for Release 2011/12/08 : CIA-RDP80T00246A016600420001-1

king counters. This refers too to the particles with energies up to 40-50 kv, if there are such particles going towards the Sun, since they should cause approximately equal bremsstrahlung in the working counter windows and on the tantalum plate. On the ship itself the third detector block was placed containing two counters with the beryllium foil windows /15 mg/cm^2/ connected in parallel. The counters had magnetic shielding in front of the windows effective for electrons with energies up to 30-40 kw. and from the sides they were covered with lead shield 2 mm. thick. These counters made it possible to check the direction of the radiation input and also in combination with mica counters to estimate the energy distribution in the solar spectrum part under investigation.

The recording circuit was similar to that used on ship II. There were three independent registration channels and the state of the last eight binary stage in each channel were read out by the memory device every three minutes. By the end of the 24-hour of the ship flight the stored information was transmitted through the telemetry system to Earth.

The results of measurements — the counting rates of the counters read out from the memory device records are given in fig.7. From the graph /a/ is evident that the mica counters pointed towards the Sun registered the intense radiation shiefly on the sunside portion of the orbit. Graph /b/ which presents the control mica counters counting rates shows that considerable interferences produced by the radiation belt particles are observed not long before the entry to the shadow at high north

Declassified in Part - Sanitized Copy Approved for Release 2011/12/08 : CIA-RDP80T00246A016600420001-1

Declassified in Part - Sanitized Copy Approved for Release 2011/12/08 : CIA-RDP80T00246A016600420001-1

latitudes and also soon after the exit from the shadow at relatively high south latitudes.

The records of the beryllium window counter/graph e/ in general correspond to the records of the control mica counter differing only from them by the presence of individual narrow maxima when the ship is on the sunside of the orbit.

Comparison of the three graphs confirm that the records of mica counters pointed to the Sun in the middle and low latitudes are due to solar X-ray radiation and only to a less degree are distorted by radiation belt particles.

The counting rate of the mica counters pointed to the Sun retains approximately the constant value with the exception of several moments when it decreases almost up to the background level. In comparison with solar batteries current (where this data are aviable) data, show that those records correspond to the moments of the shadowing of the solar battery system and, therefore, of the counters located at this system, due to the ship rotation.

Analysis of the records of beryllium window counters has shown that the majprity of the maxima in fig.7 is due to the radiation belt particles. Maxima in the time moments 13 h 20 min and 17 h 38 min. on December I and also 01 h 07 min. and 02 h 34 min. on December 2 are due to the solar X-ray radiation. The origin of the maximum at 16 h 50 min. has not yet been established. Ratio of mica and beryllium counters records which have different spectral sensitivity gives the possibility of

Declassified in Part - Sanitized Copy Approved for Release 2011/12/08 : CIA-RDP80T00246A016600420001-1

Declassified in Part - Sanitized Copy Approved for Release 2011/12/08 : CIA-RDP80T00246A016600420001-1

evaluating roughly the energy distribution in the spectrum. Assuming as before that the radiation in the region 10Å is ~~Bremsstrahlung of the solar corona electrons~~ discussed by the expression (1) we get the value of about $2\text{-}10^6$°K for the electron temperature, and the energy flux in this region approximately $2.5 \cdot 10^{-4}$ erg.cm^{-2}.sec.$^{-1}$

The records shown also that during the time of observations the radiation intensity in the spectrum region below 10Å remained constant within the limits ± 20%. The fact that on December 1-2, 1960, the Sun was very quiet corresponds to this. During the time of observations one class 1$^+$ solar flare /14 h 24 min. - 15 h 15 min./ and several smaller flares took place. As it follows from fig.7, the increase of X-ray radiation flux during this and other flares was not revealed. This is in good agreement with the absence of ionospheric effects on the flight days connected with the flares.

The records of the control mica window counters made it possible to determine the enhanced radiation zones at the altitude of the spaceship flight. These zones are shown in fig.8.

The geophysical distribution of the enhanced radiation regions at these heights is in general similar to that given for the flight of ship II.

It should be noted that at the records of the counters on both spaceship II and III an anomaly is well observed in the region of the Atlantic Ocesn revealed in measurements carried out simultaneously at these spaceship, by V.L.Ginzburg, L.V.Kurnosova and others /10/ and by I.A.Savenko and others /11/.

Declassified in Part - Sanitized Copy Approved for Release 2011/12/08 : CIA-RDP80T00246A016600420001-1

Declassified in Part - Sanitized Copy Approved for Release 2011/12/08 : CIA-RDP80T00246A016600420001-1

4. Measurements during the total solar eclipse on February 15,1961

Measurements of X-ray solar radiation during the total solar eclipse and comparisons of the radiation flux during the eclipse with the radiation flux from the fully open Sun give the possibility to find out the corona regions in which generation of X-ray radiation takes place.

H.Fiedman and his collaborators have carried out corresponding measurements for the spectrum region 44-60A during the total eclipse of 1958 /12/. During the eclipse on February 15, 1961, we have made these measurements for the "Hotter" region of the spectrum - below IOA by vertical launching of a geophysical rocket /13/.

The radiation detector was the photon counter with the beryllium foil window /15 mg/cm^2/; a control counter was located with parallel axis. This counter was identical with the first one, but the window was additionally covered with silver and gold foil; this counter had the sensitivity by 10-20 times lower than that of the working counter to solar X-ray radiation and had approximately the same sensitivity for slow and fast corpuscul. The counter block was placed in the imstrumentation container and the counters where pointed to the Sun in the moment of the rocket launching. At the rocket ascent the instrumentation container separated from the rocket and retained its

Declassified in Part - Sanitized Copy Approved for Release 2011/12/08 : CIA-RDP80T00246A016600420001-1

Declassified in Part - Sanitized Copy Approved for Release 2011/12/08 : CIA-RDP80T00246A016600420001-1

orientation both on the remaining ascending portion of the trajectory and on the descending portion. The container reached a height of about 96 km. The moment of the rocket launching and the height of the trajectory were chosen so that the trajectory top approximately coincided with the axis of the shadow cone. The considerable increase of the counting rate of the working counter was recorded at the height of about 87 km. The control counter showed the absence of corpusculs. All the radiations recorded by the working counter can, consequently, be regarded as X-ray solar radiation.

Fig.9 shows the radiation energy distribution in the spectrum region 10-1.5A calculated from the results of the measurements; in this experiment the spectrum region below 5A made a very low contribution to the recorded counting rate. The obtained energy distribution is approximated well by expression /1/ at $T_e \sim 1.5 \cdot 10^6$°. The value 8.10^{-5} erg/cm^2 sec. was obtained for the energy flux in the region below 10A.

On the day of the eclipse the Sun was very quiet. Near the eastern and western edges of the disk small active regions were observed which were almost covered by the Moon during the eclipse. Apparently it can be considered that the measured radiation flux characterizes chiefly undisturbed regions of the corona. Having used Elwert's calculations /14/ we obtain the flux 4.10^{-4} erg/cm^2 sec. for the fully open undisturbed corona, in good agreement with the measurements indicated above.

Declassified in Part - Sanitized Copy Approved for Release 2011/12/08 : CIA-RDP80T00246A016600420001-1

Declassified in Part - Sanitized Copy Approved for Release 2011/12/08 : CIA-RDP80T00246A016600420001-1

5. Conclusion

The results of the measurements given above are listed in Table 1.

Table 1

Date	21.VIII.1959	19.VIII--20.VIII 1960	1.XII-9.XII 1960	15.II.1961
The radiation flux below 10A /erg/cm^2 sec./	7.2; 3.2·10^{-4}	7-8·10^{-4}	2.5·10^{-4}	4.10^{-4}
Radiation Te	4.5·10^{6}°	3.10^{6}°	2.10^{6}°	1.5·10^{6}°
The intensity of the Fe XIV line 5.303A	71	91 88	51 47	65

The absolute energy fluxes agree well with H.Friedman's measurements. A good correlation between the radiation flux and the green coronal line intensity is observed which was also observed by H.Friedman. This has made believe that solar shortwave radiation comes from all the corona regions in which the 5.303A line is excited.

Declassified in Part - Sanitized Copy Approved for Release 2011/12/08 : CIA-RDP80T00246A016600420001-1

Declassified in Part - Sanitized Copy Approved for Release 2011/12/08 : CIA-RDP80T00246A016600420001-1

Preliminary results of calculations shows that in the spectrum region below 10 Å the principal contributions to the coronal radiation is made by free-bond transitions of electrons in the field of "heavy" ions presented in the corona. It seems that the contributions of lines of this ions and free-free transitions and also free-free and free-bond transitions in the field of protons and Helium ions is relatively weak.

Our measurements have shown that in the region of interplanetary space in the vicinity to the Earth, at altitudes of 200-300 km in the latitude range approximately 35° N and 35°S solar X-ray radiation is the main hard radiation. In the region of higher latitudes radiation caused by the radiation belt particles is imposed on it.

Declassified in Part - Sanitized Copy Approved for Release 2011/12/08 : CIA-RDP80T00246A016600420001-1

Declassified in Part - Sanitized Copy Approved for Release 2011/12/08 : CIA-RDP80T00246A016600420001-1

References

1. I.S.Shklovsky, Uspekhi Fiz.Nauk,30,(1946),63; Izvestiya of the Crimean Astronomical Observatory,4,(1949),80.
2. G.Elwert, Zs.für Naturforschung,9a,(1954),637; J.Geophys.Res.,66,(1961),391.
3. C.de Jager, Ann.de Geophysique,11,(1955),1; Space Research,1,(1960),628.
4. T.V.Kazachevskaya and G.S.Ivanov-Kholodny, Astronomichesky Zhurnal,36,(1959),102.
5. H.Friedman, Space Research,1,(1960),695; Space Research, II,(1961),1021.
6. S.L.Mandelstam, B.N.Vasilyev, A.I.Shurygin, I.P.Tindo, Yu.K.Voronko, Iskusstvennye Sputniki Zemli /Artificial Earth Satellites/ in press
7. A.P.Lukirsky, M.A.Rumsh, L.A.Smirnov, Optika i Spectroscop., 9,(1960),505.
8. S.L.Mandelstam, I.P.Tindo, Yu.K.Voronko, A.I.Shurygin, B.N.Vasilyev, Iskusstv.Sputniki Zemli,10,(1961),12.
9. S.L.Mandelstam, I.P.Tindo, Yu.K.Voronko, B.N.Vasilyev, Iskusstv.Sputniki Zemli,II,(1961),3.
10. L.V.Kurnosova et al., Iskusstv.Sputniki Zemli,8,(1961),90. V.L.Ginzburg et al., Iskusstv.Sputniki Zemli, ,(1961),22.
11. I.A.Savenko et al., Iskusstv.Sputniki Zemli,9,(1961),71.
12. H.Friedman. Space Astrophys. Ed.by W.Liller,(1961),107.
13. S.L.Mandelstam, Yu.K.Voronko, I.P.Tindo, A.I.Shurygin, B.N.Vasilyev, Dokl.Akad.Nauk S.S.S.R.,142,(1962),77.
14. G.Elwert, J.Atm.Terr.Phys.,12,(1958),187.

Declassified in Part - Sanitized Copy Approved for Release 2011/12/08 : CIA-RDP80T00246A016600420001-1

Declassified in Part - Sanitized Copy Approved for Release 2011/12/08 : CIA-RDP80T00246A016600420001-1

Figures

Fig.1. The block diagram of the measuring channel.

Fig.2. The counting rate versus time in the evening launch on 21.VII.1959
a) The counting rate of the counter pointed to the Sun.
b) The counting rate of the control counter.

Fig.3. The distribution of the number of photons at the edge of the solar spectrum.
I -- the morning launching
II -- the evening launching
... -- the theoretical curve calculated according to the bremsstrahlung formula with Te $4.5 \cdot 10^{6}$°.

Fig.4. The counting rate of the counters during the flight of spaceship II on August 19-20,1960. /Moscow time/.

Fig.5. The samples of the records of the counting rates during the flight of spaceship II from the direct telemetric records /Moscow time/.

Fig.6. The corpuscular radiation enchanced intensity zone during spaceship II flight.

Declassified in Part - Sanitized Copy Approved for Release 2011/12/08 : CIA-RDP80T00246A016600420001-1

Declassified in Part - Sanitized Copy Approved for Release 2011/12/08 : CIA-RDP80T00246A016600420001-1

Fig.7. The counting rate of the counters during the flight of spaceship III on December 1-2,1960 /Moscow time/.
a) Counters pointed to the Sun
b) Control counters
c) Counters turning with the ship.

Fig.8. The corpuscular radiation enhanced intensity zone during spaceship III flight.

Fig.9. The distribution of the number of photons in the solar spectrum. The solid curve is calculated from the experimental values.
The dashed curves are calculated according to the bremsstrahlung formula.

Declassified in Part - Sanitized Copy Approved for Release 2011/12/08 : CIA-RDP80T00246A016600420001-1

Declassified in Part - Sanitized Copy Approved for Release 2011/12/08 : CIA-RDP80T00246A016600420001-1

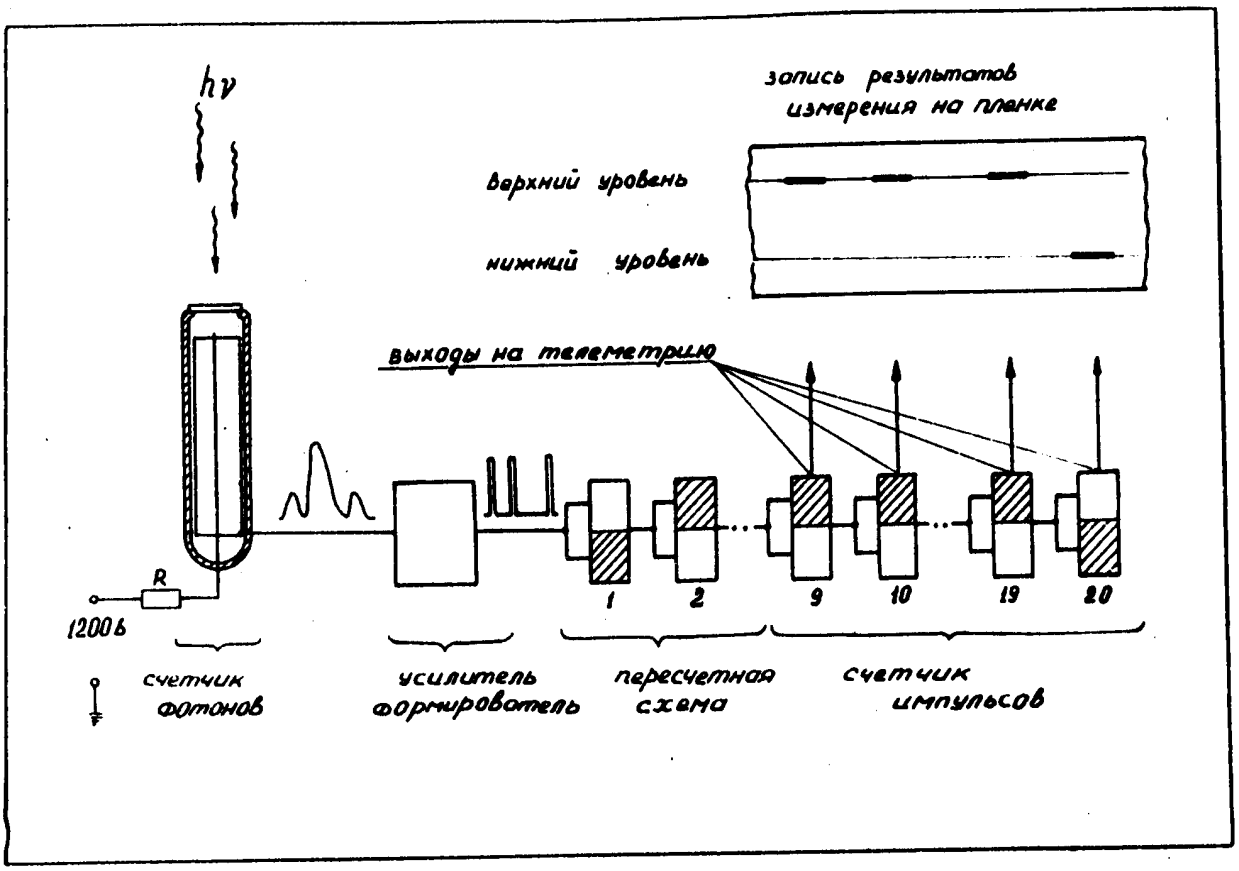

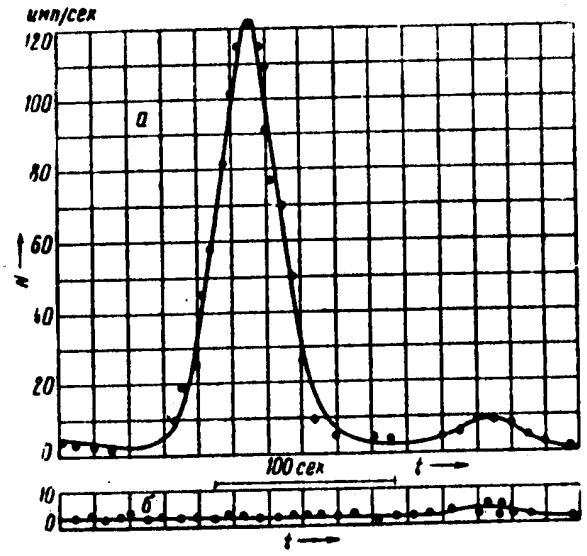

Declassified in Part - Sanitized Copy Approved for Release 2011/12/08 : CIA-RDP80T00246A016600420001-1

Declassified in Part - Sanitized Copy Approved for Release 2011/12/08 : CIA-RDP80T00246A016600420001-1

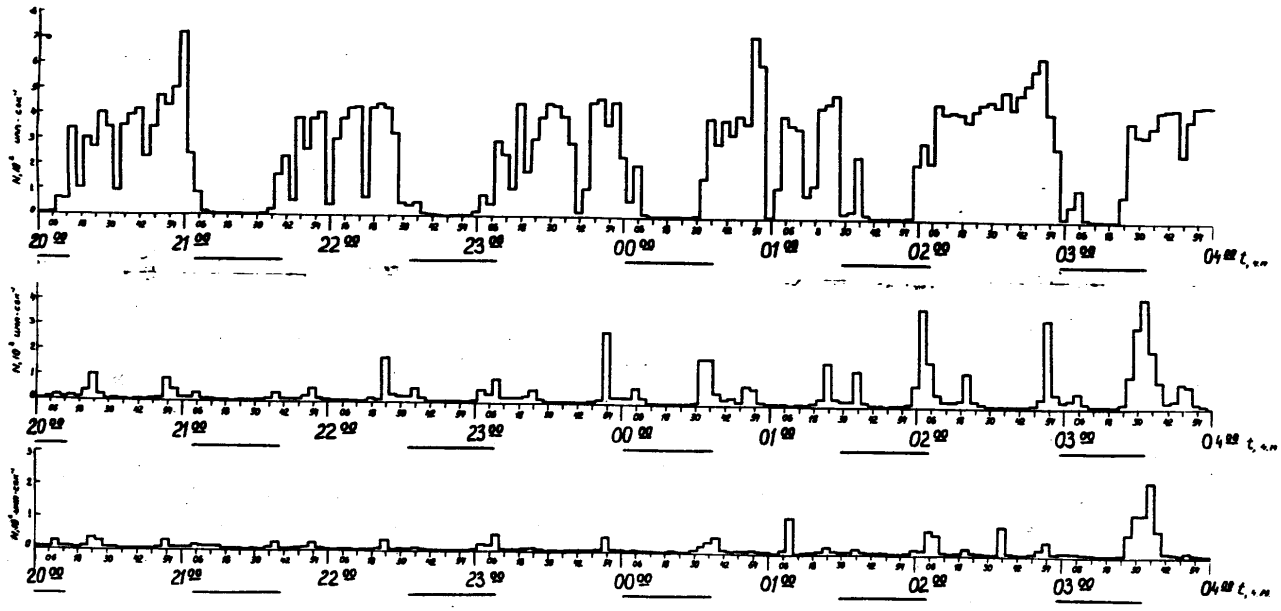

Declassified in Part - Sanitized Copy Approved for Release 2011/12/08 : CIA-RDP80T00246A016600420001-1

Declassified in Part - Sanitized Copy Approved for Release 2011/12/08 : CIA-RDP80T00246A016600420001-1

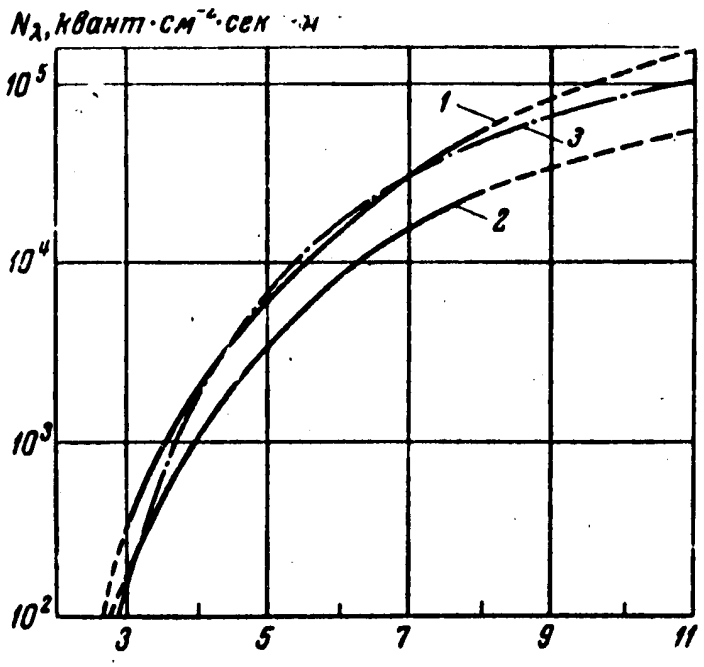

Declassified in Part - Sanitized Copy Approved for Release 2011/12/08 : CIA-RDP80T00246A016600420001-1

Declassified in Part - Sanitized Copy Approved for Release 2011/12/08 : CIA-RDP80T00246A016600420001-1

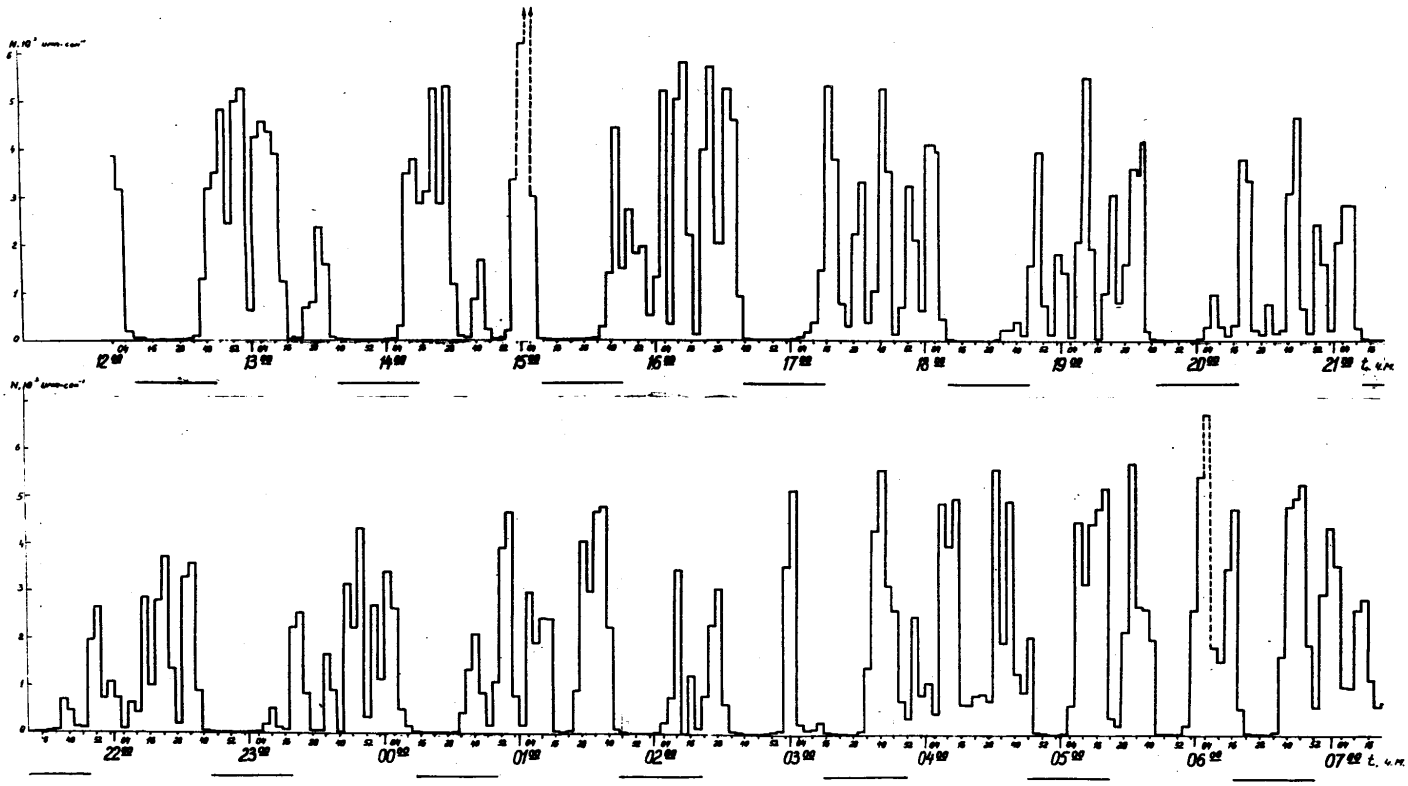

Declassified in Part - Sanitized Copy Approved for Release 2011/12/08 : CIA-RDP80T00246A016600420001-1

Declassified in Part - Sanitized Copy Approved for Release 2011/12/08 : CIA-RDP80T00246A016600420001-1

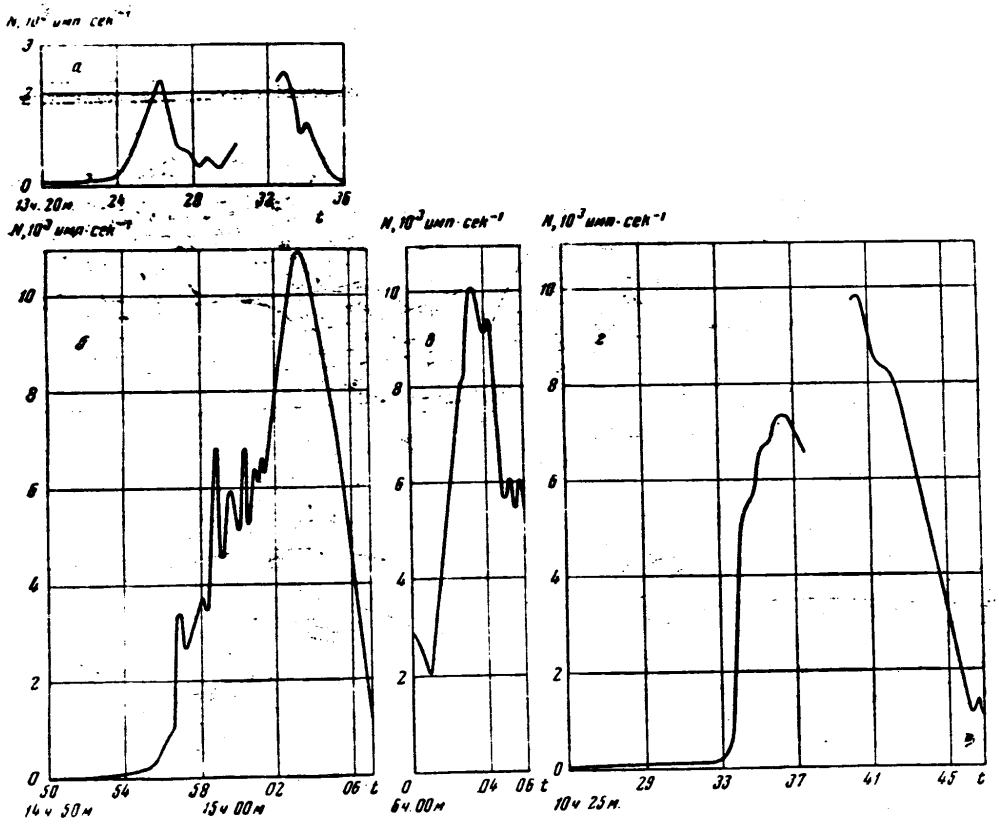

Declassified in Part - Sanitized Copy Approved for Release 2011/12/08 : CIA-RDP80T00246A016600420001-1

Declassified in Part - Sanitized Copy Approved for Release 2011/12/08 : CIA-RDP80T00246A016600420001-1

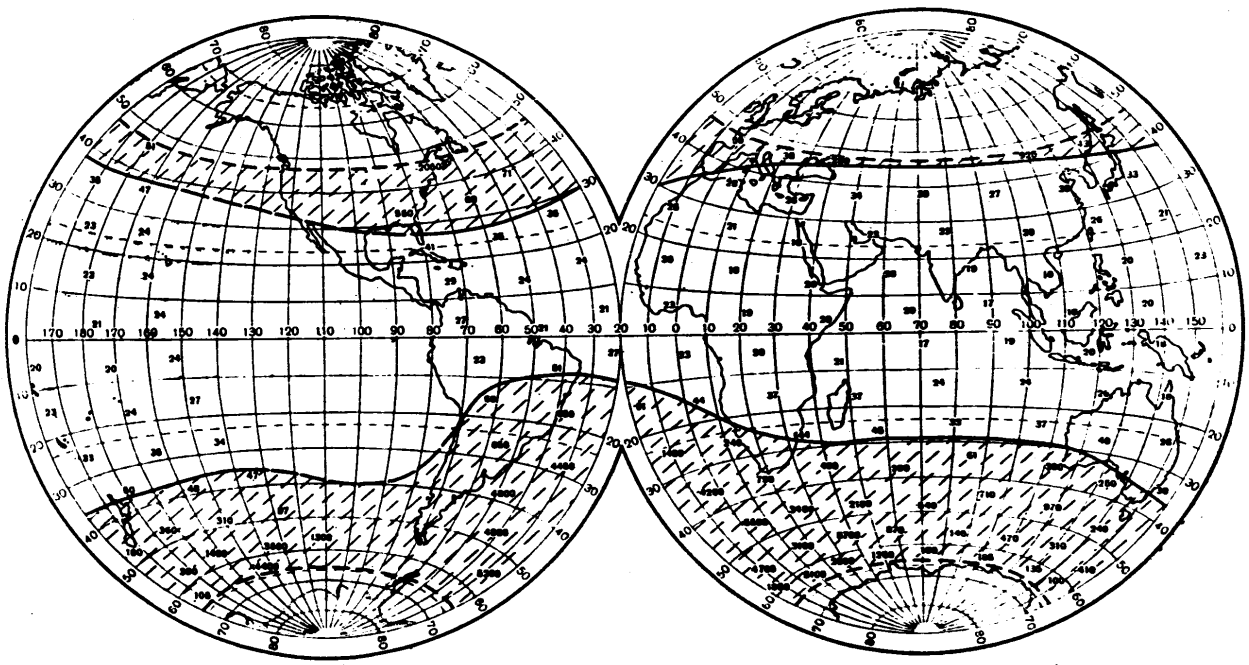

Declassified in Part - Sanitized Copy Approved for Release 2011/12/08 : CIA-RDP80T00246A016600420001-1

Declassified in Part - Sanitized Copy Approved for Release 2011/12/08 : CIA-RDP80T00246A016600420001-1

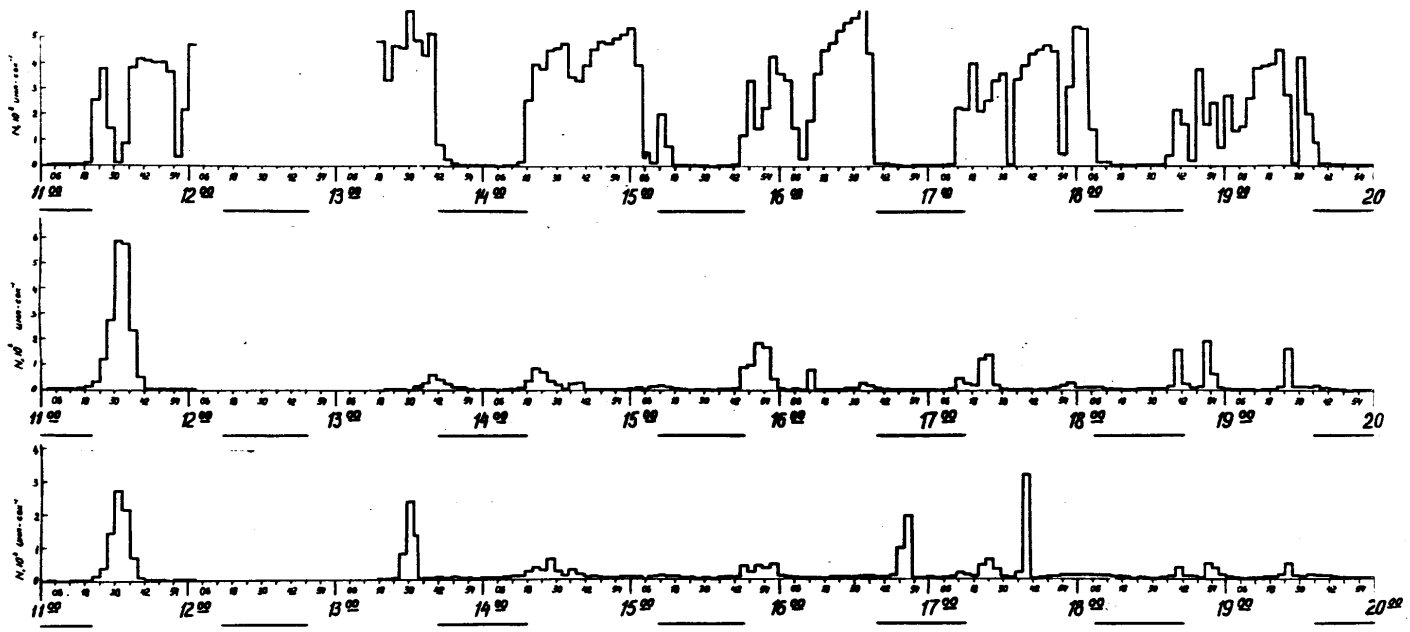

Declassified in Part - Sanitized Copy Approved for Release 2011/12/08 : CIA-RDP80T00246A016600420001-1

Declassified in Part - Sanitized Copy Approved for Release 2011/12/08 : CIA-RDP80T00246A016600420001-1

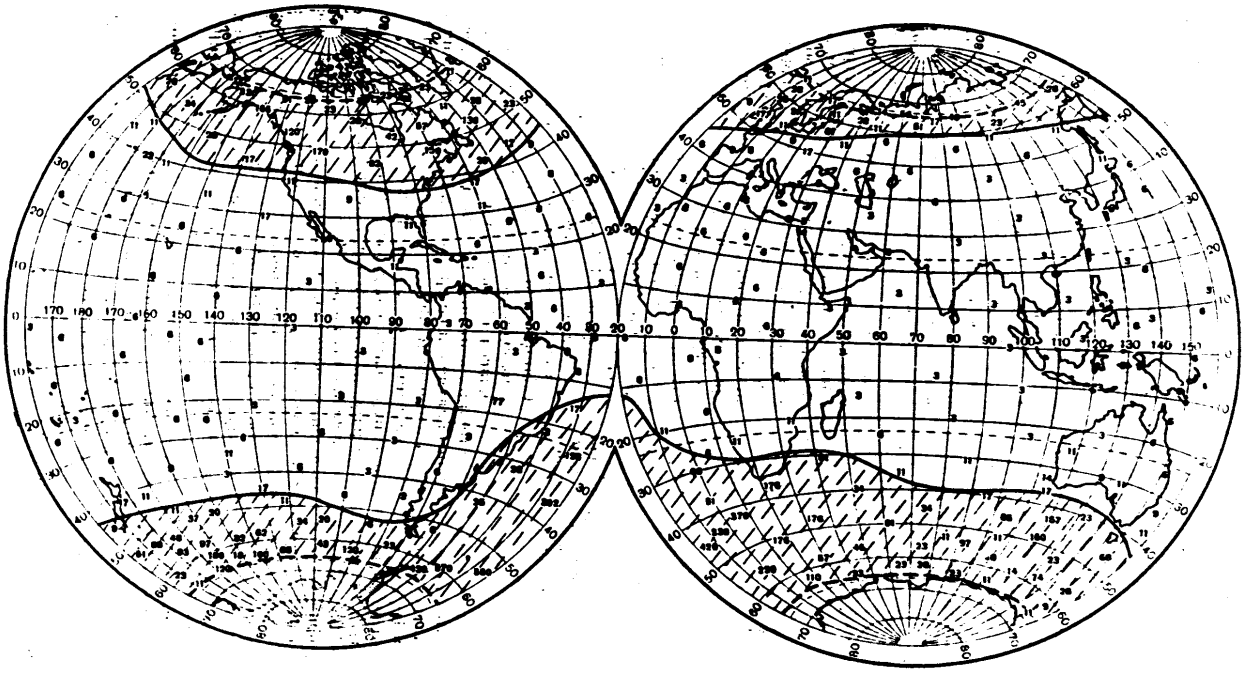

Declassified in Part - Sanitized Copy Approved for Release 2011/12/08 : CIA-RDP80T00246A016600420001-1

Declassified in Part - Sanitized Copy Approved for Release 2011/12/08 : CIA-RDP80T00246A016600420001-1

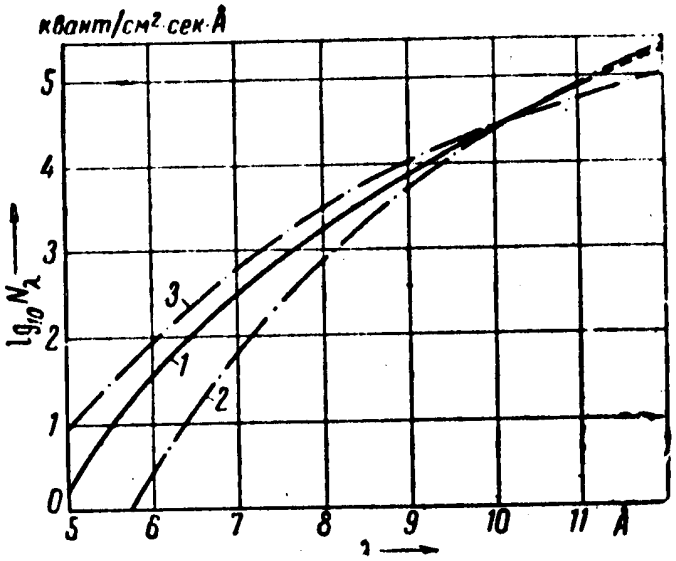

Declassified in Part - Sanitized Copy Approved for Release 2011/12/08 : CIA-RDP80T00246A016600420001-1

Declassified in Part - Sanitized Copy Approved for Release 2011/12/08 : CIA-RDP80T00246A016600420001-1

27. "THE ASTRONOMICAL UNIT OF LENGTH" by A. Mikhailov

The solar parallax and the distance of the Sun from the Earth are usually used as synonyms, this being the result of the historical development of determination of this important astronomical unit. The ultimate aim is to determine the mean distance of the Sun or the major semiaxis of the Earth's orbit in terrestrial measures such as kilometers. From the I7 century this was done by measuring the diurnal parallax of a suitable planet with a subsequent reduction to the parallax of the Sun. Thus this term came into use instead of the more exact concept of the astronomical unit (a.u.) of length.

In recent years owing to the development of interplanetary rockets the demand for a greater precision in the a.u. as expressed in Kilometers became urgent and the astronomical methods of determination of this important constant became insufficient. New methods were invented, founded on radio technique which give more directly and with more precision the length of the a.u. These methods are undergoing rapid development and have not as yet given a definitive result. They are liable, as all other methods, to systematic errors which are not sufficiently studied and elucidated.

At present there are four methods of determination of the a.u.: trigonometric - by angular measurement of the diurnal parallax of a suitable planet; spectroscopic - by determining on Doppler's principle the orbital velocity of the Earth or the radial velocity of a planet; gravitational or dynamic - by comparing the attractions of the Earth, Moon and Sun; and radar - by

Declassified in Part - Sanitized Copy Approved for Release 2011/12/08 : CIA-RDP80T00246A016600420001-1

Declassified in Part - Sanitized Copy Approved for Release 2011/12/08 : CIA-RDP80T00246A016600420001-1

measuring the distance of a planet by the time of propagation of radio signals. Moreover the solar parallax is connected with some other fundamental constants such as the constant of aberration.

Each of these methods consists of two parts: the necessary observations and the deduction from them of the final result. The first part is of a technical nature, depending on the mode of measurement, and its precision increases with the improvement of the instruments and methods used. The second part needs a minnte insight into the theory in order not to undermine the precision of the observations. When the measurements were comparatively rough there was no need to go into all the details of the theory in deducing the final results, but with the increasing precission of observations there came moments when the theoretical part became insufficient ~~enough~~ and therefore a revision and improvement of the theory was needed, which was not always done in time. It must be endeavoured that theory be in advance of observations in order not to loose the precision of the latter.

In this paper I do not intend to deduce a final value for the a.u. at present available, especially as the technique and accumulation of observations are evolving rapidly, so that such a value would have only a short duration. I cannot give also a full critical survey of the methods and results, as this task is too large for a short article, but I will try to draw attention to some principal items of the main methods hitherto used and point out some of their weak sides. In doing this the trigonometric method will be treated with more detail.

The first determination of the trigonometric parallax of a

Declassified in Part - Sanitized Copy Approved for Release 2011/12/08 : CIA-RDP80T00246A016600420001-1

Declassified in Part - Sanitized Copy Approved for Release 2011/12/08 : CIA-RDP80T00246A016600420001-1

planet was made in I672. Corresponding observations of Mars by Richer at Cayenne and Cassini in Paris gave the planet's parallax which was then transferred to the Sun by means of Kepler's third law.

Notwithstanding the low precision of observations at this time, which were accomplished by using telescopes, shortly before introduced into astrometric practice, the result of this determination was excellent: till the end of the I6 century Hipparchus' value of the solar parallax - 3' was adopted. Kepler lowered it down to I', but the observations of Mars at Cayenne together with those at Paris gave 9½", which is in error only by 8%.

Soon afterwards, according to a proposition by Halley, great attention was given to the transits of Venus across the Sun's disc. Of all the planets Venus can approach nearest to the Earth; its parallax can reach 33". The limb of the Sun's disk to which the planet is projected allows to fix the planet's position relative to the Sun. Although in this case the relative parallax of Venus is decreased to about 24", it still remains large enough for a good determination. The theory of this event was afterwards developed by a member of St.Petersbourg's academy Joseph Delisle.

The following transits of Venus took place in I76I and I769. During the first of these Lomonosov discovered the atmosphere of Venus.

For the observation of the transit of I76I many scientific institutions and learned societies sent expeditions to remote parts of Europe, Asia and islands of the Indian and Atlantic oceans. In all observations were made at 72 places. However the results

Declassified in Part - Sanitized Copy Approved for Release 2011/12/08 : CIA-RDP80T00246A016600420001-1

Declassified in Part - Sanitized Copy Approved for Release 2011/12/08 : CIA-RDP80T00246A016600420001-1

were hardly satisfactory.

The observations in I769 gave a better result, i.e. : 8".68I ± 0".052 , which differs only by I.4% from the true value. It is curious to note that a new discussion of these observations made afterwards by Encke gave a substantially worse value: 8".57II6, which was however in general use for more than twenty years, and of which Newcomb sarcastically remarked that the last figure may be true, but the first after the decimal point is undoubtedly wrong.

No fewer preparations were made for the observations of the transits of Venus in I874 and I882. In I882 there were 36 expeditions and besides visual micrometric measurements, photography was used for the first time. For the latter purpose special heliographs were constructed. However, notwithstanding a vast amount of care and labour involved, the result did not meet expectations owing to the interfering action of diffraction.

This ended the historic role of the transits of Venus for the determination of the solar parallax. The next transits will occur in 2004 and 20I2 and if they will be observed, then for quite different purposes, as the length of the a.u. will then be known with a precision to which the observations of the transits can not add anything.

After the discovery of minor planets it was found that some of them were much more suitable for a determination of the solar parallax than Mars and Venus as, owing to the large excentricity of their orbits together with an appropriate major axis, they can at times come much closer to the Earth. Moreover they can be observed with much greater precision than the major planets, as

Declassified in Part - Sanitized Copy Approved for Release 2011/12/08 : CIA-RDP80T00246A016600420001-1

Declassified in Part - Sanitized Copy Approved for Release 2011/12/08 : CIA-RDP80T00246A016600420001-1

they are seen as luminous points on a background of stars of about the same magnitude, this being especially convenient for photographic observations. Such minor planets were Flora, Iris, Victoria, Sappho and Eros. Later other planets were discovered which can approach even closer to the Earth, but either their orbits are not known well enough, or during their approach an insufficient number of observations were collected so that so far they cannot be used for our purpose. It must be remarked that the closer to the Earth a planet can approach, the better its orbit must be known and the greater will be the influence of perturbations from the Earth and the nearest major planets.

The advantage of observations of a near minor planet results from the large value of its parallax, so that the same absolute error of its determination makes the relative error proportionally smaller. On the other hand, however, the distance of the planet so found must be multiplied by a large factor in order to obtain the length of the a.u., which demands a more precise determination of the relative size of the orbits of the planet and the Earth.

The first three of the planets mentioned were observed with heliometers and filar micrometers with the following results:

Iris (I888)	$8''.825 \pm 0''.008$
Victoria (I889)	$8''.800 \pm 0.006$
Sappho (I889)	$8''.796 \pm 0.0I2$
mean	$8''.8036 \pm 0.0046$

In I898 Witt at the Urania in Berlin discovered the minor planet No.433 which was named Eros. Its orbit owing to a large excentricity and small inclination comes very near to the orbit of

Declassified in Part - Sanitized Copy Approved for Release 2011/12/08 : CIA-RDP80T00246A016600420001-1

Declassified in Part - Sanitized Copy Approved for Release 2011/12/08 : CIA-RDP80T00246A016600420001-1

Earth so that there are times of close approach to 0.I5 a.u.

A favourable opposition of Eros occured in I894 several years before its discovery. Somewhat less favourable was the opposition at the beginning of I90I - to 0.32 a.u. or 40 million kilometers. A large number of observations at many observatories were reduced by Hinks with the result $p = 8''.806 \pm 0''.003$.

For the observations of Eros during the next favourable opposition in I93I, when the minimum distance was 0.I74 a.u. = 26 million km. a large compaign was launched in which 23 observatories on 5 continents took part. The reduction and discussion of the observations, amounting to 2847, was undertaken at the Greenwich observatory by the Astronomer Royal Spencer Jones.

In order to deduce the parallactic displacement from the observations it was necessary to have very precise elements of the orbit and an excellent ephemeris of Eros taking into account all the perturbations. This was done by Witt and afterwards improved by Stracke at the Rechen-Institute in Berlin. The parallax of Eros amounting to 50" at its closest approach, could be determined in two ways: from the combination of nearly simultaneous observations made at separate observatories in different hour angles, using the displacement due to the diurnal rotation of the Earth, and employing mainly observations of right ascensions. In this last case the evening and morning observations had to be combined, but the number of the latter was small.

From the right ascensions of the planet the solar parallax was found to be $8''.7875 \pm 0''.0009$ and from the declinations $8''.7907 \pm 0''.00II$. As a final result Spencer Jones adopted $8''.790 \pm 0''.00I$. This unexpectedly low value of the parallax caused some amazement.

Declassified in Part - Sanitized Copy Approved for Release 2011/12/08 : CIA-RDP80T00246A016600420001-1

Declassified in Part - Sanitized Copy Approved for Release 2011/12/08 : CIA-RDP80T00246A016600420001-1

It was not only much smaller than the value obtained from observations of the same planet in I900 - I90I, but also smaller than the results derived by Gill from the observations of the minor planets Victoria, Iris and Sappho. Spencer Jones discussed his results in detail paying particular attention to a possible influence of atmospheric dispersion. It seemed that there was no possible cause which could have distorted the value of the parallax obtained.

Owing to the thoroughness of the deduction and discussion, the value of the solar parallax obtained by Spencer Jones became generally accepted.

Leaving at present the revealment of a possible cause of such a small value of the parallax, let us critically survey the method of determining the length of the a.u. by means of measuring the parallax. This unit a is connected with the parallax by the well known formula

$$a = \frac{\rho_e}{\sin p} = \frac{206264.806\ \rho_e}{p''} \qquad (I)$$

where ρ_e is the equatorial radius of the Earth. The relative error of determination of a is thus proportional to the error in ρ_e. For this constant the following values are used

International ellipsoid	6378388 m
Krassovsky	6378245
Zhongolovich (rounded)	6378I00

The difference in ρ_e amounts here to 288 m or I/52000 of the whole value of ρ_e. It must be considered, moreover, that the Earth's equator is better approximated by an ellipse with a dif-

Declassified in Part - Sanitized Copy Approved for Release 2011/12/08 : CIA-RDP80T00246A016600420001-1

Declassified in Part - Sanitized Copy Approved for Release 2011/12/08 : CIA-RDP80T00246A016600420001-1

ference of the two semiaxes of about 200m. According to Zhongolovich the mean square deviation of the equator from an exact circle equals ± 82m. This deviation must be added to the uncertainty of ϱ_e .

The flattening of the Earth does not enter explicitly into formula (I), however it is involved in the determination of ϱ_e . The observations for a trigonometric determination of the parallax are made at observatories at different latitudes and to calculate the displacement in RA and declination of the observed object due to the diurnal parallax the so-called parallactic factors must be known. These contain the radius of the local parallel $\varrho \cos\varphi$ and the distance of the observatory from the equatorial plane $\varrho \sin\varphi$ where ϱ is the local radius of Earth, and φ' the geocentric latitude, both depending on the adopted flattening α . Up to the first order of α the difference between the geographical latitude φ and φ' is

$$\varphi - \varphi' = \alpha \sin 2\varphi$$

and

$$\varrho = \varrho_e (1 - \alpha \sin^2 \varphi)$$

For a strict determination of the parallax the coordinates of the observer relative to the center of the Earth must be known. Thus the figure of Earth with all its irregularities is involved. Instead the problem is solved approximately by substituting for the real Earth an ellipsoid with a random center, which involves a double error due to disregarding the deviation of the plumb line and the elevation of the geoid above the ellipsoid. If there are many points of observation these errors are partly compensated. It will be possible to solve this problem only in the future, using data yielded by gravimetry and observations of the Moon and arti-

Declassified in Part - Sanitized Copy Approved for Release 2011/12/08 : CIA-RDP80T00246A016600420001-1

Declassified in Part - Sanitized Copy Approved for Release 2011/12/08 : CIA-RDP80T00246A016600420001-1

ficial satellites. So far, however, all trigonometric determinations of the solar parallax are subjected to this inexactitude.

Without any undue pessimism the uncertainty of the solar parallax caused by an error in the value of the radius of the equator and the irregularities of the geoid are evaluated to be about I:25000, or 0".00036 in the parallax, or 6000km in the length of the a.u. This error remains as yet beyond the precision of the trigonometric determination of parallax but is already near its limit.

A revision of the determination of the solar parallax from the observations of Eros in I930-3I was made by Rabe at Cincinnaty in I949. His calculations had two improvements as to the work of Spencer Jones: firstly, Rabe had at his disposal a larger number of normal places of observations of the planet inclusive to February I945, which gave a better determination of the planetary orbit; secondly, all the moments of observation were expressed in Ephemeris time thus eliminating errors caused by the irregularities of the Earth's rotation on the reckoning of time. It was also substantial that the equations of condition contained terms repreenting corrections of masses of the four principal perturbing major planets. These masses as determined by Rabe together with those of Newcomb, which were originally used by Witt, are as follows:

	I/m Rabe	I/m Newcomb
Mercury	6120000 ± 43000	6000000
Venus	408645 ± 208	408000
Earth + Moon	328452 ± 43	329390
Mars	3110000 ± 7700	3093500

A comparison of these numbers shows that the chief and (owing to the close approach to the Earth) decisive influence was that of

Declassified in Part - Sanitized Copy Approved for Release 2011/12/08 : CIA-RDP80T00246A016600420001-1

Declassified in Part - Sanitized Copy Approved for Release 2011/12/08 : CIA-RDP80T00246A016600420001-1

the combined mass of the Earth and Moon.

The subsequent deduction of the parallax was made by Rabe not trigonometrically, but dynamically; this was done probably because the former method would have been much more laborious, demanding a computation with the new elements and masses of a very detailed ephemeris of Eros, a comparison with it of all observations and solution of many equations of condition. On the contrary the dynamical method needed only a short computation by a well known and simple formula.

This formula can be obtained from elementary considerations. The centrifugal force of the Earth's orbital motion is in the mean equal to $\omega^2 a(m+\mu)$, where $\omega = 2\pi : S$ is the angular velocity of this motion, S=3I558I50 being the number of seconds in a sidereal year, $m+\mu$ the sum of masses of the Earth and Moon.

This centrifugal force is balanced by the Sun's attraction $\frac{fM}{a^2}(m+\mu)$, where f is the constant of gravitation, M - the mass of the Sun.

Equalling these two forces we obtain

$$\left(\frac{2\pi}{S}\right)^2 a (m+\mu) = \frac{fm}{a^2} M \left(1+\frac{\mu}{m}\right) \qquad (2)$$

In the theory of the figure of the Earth the Earth's mass is connected with the acceleration of gravity at the equator by the following formulas

$$\frac{fM}{\rho_e^2} = \frac{\gamma}{1+\sigma}$$

$$\sigma = \alpha + \frac{1}{2} q + \alpha^2 - \frac{2}{7} \alpha q + \frac{9}{4} q^2$$

q being the ratio of centrifugal acceleration at the equator, due

Declassified in Part - Sanitized Copy Approved for Release 2011/12/08 : CIA-RDP80T00246A016600420001-1

Declassified in Part - Sanitized Copy Approved for Release 2011/12/08 : CIA-RDP80T00246A016600420001-1

to the diurnal rotation of the Earth, to the acceleration of gravity:

$$q = \frac{\omega_e^2 \rho_e}{\gamma_e}$$

$\omega_e = \frac{2\pi}{86164}$ is the angular velocity of the Earth's rotation, the denominator is the number of seconds of mean time in a sidereal day.

Substituting $\rho_e \sin\varphi$ for a formula (2) gives

$$b^3 \sin 1'' = \sqrt[3]{\frac{2\pi^2 \rho_e (1+\sigma)}{S \gamma_e \left(1-\frac{q}{m}\right)}} \sqrt[3]{\frac{m+\mu}{M}} \qquad (3)$$

If, as usual, the masses m and μ are expressed in units of solar mass, M must be equalled to unity.

This formula contains two new constants: γ_e and $m+\mu$, all the other quantities are known with sufficient precision.

The determination of the absolute value of γ_e is a very difficult matter. An absolute determination of the acceleration of gravity was made in I898-I904 at the Potsdam Geodetic Institute. To reduce the value to the equator the flattening of the Earth's ellipsoid must be stipulated and to eliminate the influence of local anomalies many relative determinations of gravity in different parts of the Earth's surface are needed. In this way the international value for γ_e was found:

$$\gamma_e = 978.049 \ \text{cm}, \text{sec}^2.$$

During the last decades absolute determinations were made in Washington at the National Bureau of Standards, at the National Physical laboratory at Teddington and the Institute of Metrology in Leningrad. They all gave a smaller value by I3-I6 mgal, so that with an error not exceeding 3 mgal we can assume

$$\gamma_e = 978.034$$

Declassified in Part - Sanitized Copy Approved for Release 2011/12/08 : CIA-RDP80T00246A016600420001-1

Declassified in Part - Sanitized Copy Approved for Release 2011/12/08 : CIA-RDP80T00246A016600420001-1

The mass of the Moon is obtained as a by-product of a trigonometrical determination of the solar parallax. In fact, the center of mass of the system Earth-Moon moves along the earth's orbit, and the Earth rotates around this center with a period of one sidereal month. This center of mass lies on a line joining the centers of the Earth and Moon at a distance μ/m, on the average about 4670 from the former, i.e. still inside the body of the Earth. This produces also a kind of parallax which can be called the monthly parallax. For its determination a near planet must be observed for a sufficiently long time, during several periods i.e. months. The amplitude of these displacements gives the ratio of the masses of the Earth and Moon. From observations of Eros in I930 - 3I Spencer Jones determined μ/m = I:8I.276 ± 0.02I, whereas in I900 - 0I Hinks found using the same planet μ/m = I:8I.53 ± 0.047. However this is not the only method of determining the mass of the Moon, as the nutation of the Earth's axis due to the attraction of the Moon, also, together with the precessional motion, is connected with the Moon's parallax and mass, which was thus found by Spencer Jones to be I:8I.65. We see that this important constant still contains an uncertainty of about 0.5%.

The adopted value of μ only slightly influences the solar parallax as computed by formula (3). In fact it enters as a sum $I + \frac{\mu}{m}$ in the power of - I/3. Therefore an error ε in μ will produce an error of only $-I/3\varepsilon$. If ε is equalled to the difference of the values obtained by Hinks and Spencer Jones from Eros

$$\varepsilon = \frac{I}{81.27} - \frac{I}{81.53} = 0.000039$$

The resulting relative error in parallax will be 0.0000I3 or 0".000II5, which corresponds to about 2000 m in the a.u.

Declassified in Part - Sanitized Copy Approved for Release 2011/12/08 : CIA-RDP80T00246A016600420001-1

Declassified in Part - Sanitized Copy Approved for Release 2011/12/08 : CIA-RDP80T00246A016600420001-1

Computing the first radical in (3) for two different ellipsoids and assuming $\frac{m+\mu}{M}$ = I : 8I.375 according to Rabe, we obtain:

International ellipsoid $p = 607''.0428 \sqrt[3]{\frac{m+\mu}{M}}$

Krassovsky's " $p = 607.050I \sqrt[3]{\frac{m+\mu}{M}}$

Thus the difference between these ellipsoids is small, amounting to only 0.0000I2 = 0".000II in parallax. However the influence of the adopted value of $m+\mu$ is large. Taking Rabe's value $\frac{m+\mu}{M}$ = = I : 323452 as derived from the perturbation of Eros in I930-3I, we find for the

International ellipsoid $p = 8''.7983$, $a = I49532400$ km

Krassovsky " $p = 8''.79834$, $a = I49530900$ km

The value of p for the international ellipsoid is practically the same as that given by Rabe: 8".79835 ± 0."00039.

The susceptibility of the parallax to the value of $m+\mu$ is shown by putting $\frac{m+\mu}{M}$ = I : 329340 according to Spencer Jones, which gives $p = 8''.79044$, very close to his result. This is understandable, as we have here made a reverse calculation, by computing p from the derived masses, whereas Spencer Jones obtained his masses from the trigonometrically determined parallax.

The question remains open on the cause of such a discrepancy between the results obtained by Spencer Jones and Rabe, from the same observational material. It seems certain that the improvement of the orbit of Eros by Rabe could not influence the result by such a large amount, and this could only change the fourth decimal by I or 2 units; the influence of the introduction of ephemeris time is even less. It must be noted that the mass of the Earth and Moon used by Spencer Jones was also close to Rabe's value: Spencer Jones, when

Declassified in Part - Sanitized Copy Approved for Release 2011/12/08 : CIA-RDP80T00246A016600420001-1

Declassified in Part - Sanitized Copy Approved for Release 2011/12/08 : CIA-RDP80T00246A016600420001-1

calculating the perturbations of Eros, adopted the value of this mass according to Noteboom I : 328390, whereas Rabe found I:328452.

The thoroughness of Spencer Jones' work, in particular the discussion of a possible influence of atmospheric dispersion, makes his determination of the solar parallax very convincing, but his result deviates very appreciably from most of other determinations. Possibly the solution lies in the observations of several astronomers, who noted that Eros has an elongated and irregular shape: the planet is about 35 km long and some II - I6 km across and rotates about the axis of maximum moment of inertia with a period of $5^h I6^m$. In this case, depending upon the albedo of different parts of its surface, the image on the photographic plate could be displaced by several hundredths of a second of arc. Taking the amplitude of oscillations as I0 km, at a distance of 0.2 a.u. the shift of the image would amount to 0".07. Although the period is rather short, still this could mix with the parallactic displacement in such a manner, as to falsify the determination of parallax. It remains uncertain why this phenomenon did not influence, or even influence in the opposite direction the observations of Eros in I900--I90I.

An irregularity of the shape of Eros, which could distort the trigonometric determination of the parallax would not appreciably influence the determination of mass of the disturbing planets. In fact the action of perturbations changes slowly with the distance of the perturbing body. This process lasts many days, or even months during which Eros would make many revolutions and present to the observer its different aspects many times. Its apparent positions would be smoothed in such a complete manner as to give a true value for the masses of the perturbing planets. Therefore it

Declassified in Part - Sanitized Copy Approved for Release 2011/12/08 : CIA-RDP80T00246A016600420001-1

Declassified in Part - Sanitized Copy Approved for Release 2011/12/08 : CIA-RDP80T00246A016600420001-1

seems that Rabe's value of the parallax must be considered to be more reliable.

When comparing the trigonometric and dynamic methods of determination of the solar parallax the following consideration must be taken into account. In the trigonometric method some uncertainty is caused by the errors of the coordinates of the observed planet and the Earth as given by the ephemerides. A possible error in the positions of the major planets, in this case only Mars and Venus and , of course, the Earth or Sun, is of the order of I". It can be assumed that the error in the radius-vector is of the same order, i.e. about I/I00000. In the distance τ from the Earth this error is increased $\sqrt{2}$ times and the relative error $\frac{\sqrt{2}}{\tau}$ times, which can give approximately I/20000 or 0".0005 in the parallax (0".00I corresponds to I7000 km). In the case of a minor planet the error can be much larger in dependence on the character of the orbit, the number and quality of observations, the number of observed oppositions etc. The systematic errors of stellar catalogues may also have some influence, especially if during the observations used for the determination of parallax, the planet moved through a large arc on the celestial sphere.

In the dynamical method there seem to be less possible causes for error. The main are the error of determining the mass of the Earth and Moon and also of the absolute value of gravity. The latter depends on the determination of gravity at the base station and the elimination of gravity anomalies when deducing the equatorial constant $\sqrt{e}$. Observations of artificial sattelites will improve the knowlege of this constant and in this ~~regard~~ respect the investigations carried on by Zhongolovich at the Institute of Theoretical Astronomy in Leningrad are of great interest.

Declassified in Part - Sanitized Copy Approved for Release 2011/12/08 : CIA-RDP80T00246A016600420001-1

Declassified in Part - Sanitized Copy Approved for Release 2011/12/08 : CIA-RDP80T00246A016600420001-1

We have already considered the influence of the determination of the masses of the Earth and Moon in this method. Rabe evaluated the probable error of determination of $\frac{m+\mu}{M}$ as $\frac{43}{328\ 452}$, which gives a probable error of ± 0".00039 in the parallax. To this is added the error of γ_e. Not being very strict we can evaluate the probable error of parallax as ± 0".0005 or about ± I0000 km in the a.u.

We have just seen that an error of the same amount can be expected in the trigonometric method owing to the uncertainty in the size and shape of the planetary orbits and the position of the planet on them. Considering all arguments we can expect that the dynamical method has some advantages over the trigonometric.

It would seem that the dynamic method based on the determination of the parallactic inequality in the motion of the Moon has a large weight. The theory gives the principal term of this inequality in the form

$$\frac{m-\mu}{m+\mu}\left(\frac{15}{8}n+\frac{99}{8}n^2\gamma\ldots\right)\frac{a'}{a}\sin D$$

where n is the ratio of the length of a sidereal month to a sidereal year, known with great precision, and is 0,07480I33

$$\frac{a'}{a}=\frac{\sin p}{\sin p'}$$

is the ratio of mean distances of the Moon and Sun (about I/400), D - the mean angular distance of the Moon from the Sun, which has a period of one synodic month. According to Brown the coefficient at sin D equals I25".II9, which is I4 times larger than the solar parallax. Adopting p' = 3422".526 De Sitter obtained

$$\text{I4.2I32}\ p = \text{I25".II9}$$

Declassified in Part - Sanitized Copy Approved for Release 2011/12/08 : CIA-RDP80T00246A016600420001-1

Declassified in Part - Sanitized Copy Approved for Release 2011/12/08 : CIA-RDP80T00246A016600420001-1

and

$$\rho = 8''.8030$$

It would seem that this method is of advantage, as an error in determining the parallactic inequality is diminished I4 times. $a' = \frac{\varrho_e}{\sin \rho'}$ is known with an error not exceeding I/I.00000, the influence of an error in ϱ_e is eliminated in the ratio $\frac{a'}{a}$. Everything would be all right if not one circumstance: the length of the period coincides with the phases of the Moon. Thus for a determination of the amplitude of the parallactic inequality observations near the first quarter of the Moon must be combined with those near the last quarter. Here we meet with a difficult astrometrical problem. In meridian observations the transit of the illuminated limb is registered and for reducing to the center, the Moon's angular radius must be known. The latter however is influenced by irradiation and the irregularities of the profile of the limb. These influences give an error of the order of I". When observing the transits of the crater Moesting A the change of illumination affects the registered moment of time. Photographic observations, the technique of which has been well developed in the last years, and also heliometric observations have revealed a notable asymmetry in the Moon's figure, not yet sufficiently studied. All this appreciably diminishes the precision of this method of determination of the solar parallax but it can be hoped that at present the widely used photographic observations for investigations of the irregularities of the rotation of the Earth will give sufficient data for a reliable determination of the solar parallax.

A very close connection exists between the solar parallax and the constant of aberration of light κ. In a circular movement of the

Declassified in Part - Sanitized Copy Approved for Release 2011/12/08 : CIA-RDP80T00246A016600420001-1

Declassified in Part - Sanitized Copy Approved for Release 2011/12/08 : CIA-RDP80T00246A016600420001-1

Earth the latter would be equal to the ratio of the Earth's orbital velocity v to the velocity of light c :

$$k = \frac{v}{c}$$

If k is determined from astronomical observations we have

$$v = kc = \frac{2\pi a}{S}$$

where in the last part the velocity v is equalled to the length $2\pi a$ of the circular orbit divided by the length of the sidereal year in seconds. For an elliptical movement of the Earth this simple formula needs a correction, which depends on the determination of the constant of aberration k. This is done by taking the mean velocity of the Earth as the half sum of its greatest value at perihelion and its smallest value at aphelion. In this case the theory of elliptic motion gives the correcting divisor

$$\sqrt{1-e^2} = \cos\varphi$$

where φ is the excentricity angle defined by

$$\sin\varphi = e$$

Substituting $\frac{\varrho e}{\sin p}$ for a the exact relation is found

$$k'' p'' = \frac{2\pi \varrho_e \operatorname{cosec}^2 1''}{S \cos\varphi}$$

where $\operatorname{cosec}^2 1''$ is introduced in order to express both K and p in seconds of arc.

Here $\frac{2\pi \operatorname{cosec}^2 1''}{S \cos\varphi}$ is known with a high precision and equals 847I.875. Taking for the velocity of light, according to the best determinations, 299792.5 km/sec we obtain

International ellipsoid	K_p =	I80.2477
Krassovsky's	"	I80.2437
Zhongolovich	"	I80.2396

(a = 63678I00)

Declassified in Part - Sanitized Copy Approved for Release 2011/12/08 : CIA-RDP80T00246A016600420001-1

Declassified in Part - Sanitized Copy Approved for Release 2011/12/08 : CIA-RDP80T00246A016600420001-1

Without exagération of an unwarrented precision we will adopt

$$\kappa_1 = 180.24$$

which gives the following table:

κ	p
20".47	8".805I
20".48	8.8008
20".49	8.7965
20".50	8.7922
20".5I	8.7879

The International Conference on ephemerides in I896 adopted κ = 20".47 and p = 8".80. Thus we see that these values are not matched. Accoording to the latest determinations κ must be increased and I think that the best value at present is κ = 20".49, though some autorities incline to increase κ to 20".5I. It must be said that a great number of determinations of κ give a large scattering which proves the presence of considerable systematic errors. The problem of determining the constant of aberration is a difficult one owing to the circumstance that the aberrational displacement of the stars has an annual period and for the determination absolute methods are used. Therefore it is very difficult to exclude meteorological influences. We hope that the photographic polar tube of the Pulkovo observatory will help to improve the value of this important constant and thereby also the value of solar parallax.

We come now to the spectroscopic method of determination of the solar parallax or in a more direct way the length of the a.u. The Doppler's shift $\Delta\lambda$ of a spectral line with wavelength λ gives

Declassified in Part - Sanitized Copy Approved for Release 2011/12/08 : CIA-RDP80T00246A016600420001-1

Declassified in Part - Sanitized Copy Approved for Release 2011/12/08 : CIA-RDP80T00246A016600420001-1

the equation

$$\frac{\Delta\lambda}{\lambda} = \frac{v}{c}$$

which according to (4) is equal to the constant of aberration. In this way the latter can be determined spectroscopically without the knowlege of the velocity of light, as $\Delta\lambda$ is found by measuring spectrograms of a selected star. It is clear that such stars must be observed, which are situated near the prolongation of the tangent to the earth's orbit, and take the projection of the radial velocity on the tangent considered. To eliminate the peculiar velocity inherent to the star itself relative to the Sun, the same star must be observed after six months when the orbital velocity of the Earth is directed in the opposite direction. However if the star is a spectroscopic binary or has a variable radial velocity, due to some cause, this will unfavourably influence the result. It is necessary therefore to use many stars expecting that such influences will be mutually cancelled.

This method has so far not given sufficiently precise results, which could complete with the trigonometric or dynamic methods. The error of determination of the radial velocity of stars even having many well defined spectral lines is of the order of ±0.I km/ /sec. This is about I/300 of the quantity to be determined. At the Cape observatory Hough from seven bright stars obtained $p = 8''.802 \pm 0''.006$ m.e.

The French astronomer Guinot recently applied a similar method to the planet Venus during its most rapid approach and also recession relative to the Earth. Instead of a spectrograph a Fabry - Perrot interferometer was used. The radial velocity of Venus depends on the size of the orbits of Venus and Earth, thus being a function of the parallax. The determined

Declassified in Part - Sanitized Copy Approved for Release 2011/12/08 : CIA-RDP80T00246A016600420001-1

Declassified in Part - Sanitized Copy Approved for Release 2011/12/08 : CIA-RDP80T00246A016600420001-1

orbital velocity of the Earth gives directly the constant of aberration. The result could be distorted by an axial rotation of Venus, which is however very slow and besides acts in the opposite direction during the morning and evening observations of the planet. A large series of observations gave finally $K = 20''.514 \pm 0''.012$ whence $p = 8''.787 \pm 0''.005$

Summing up, it can be concluded that different methods give a large spread of values of the solar parallax, between 8".787 and 8".809, which owing to large systematic errors greatly exceeds the accidental errors of observation. It is difficult to evaluate the reliability of each result as the mean or probable errors given by the authors cannot serve as a true criterium of the precision. It is for this reason that the International colloquium on astronomical constants held in Paris in I950 could not choose a better value of the parallax and decided to keep the value adopted in I896 i.e. $p = 8''.800$.

Previous to I930 there was a tendency to consider that the parallax is several thousands of a second larger than 8".800. De Sitter in his critical survey of astronomical constants gave in I938 as the best value of the solar parallax 8".8030; the same ~~number~~ value is given in the text-book on Astronomy by Russell, Dugan and Stewart in I926. But under the influence of the observations of Eros in I930-3I and the determination by Spencer Jones, as well as radar determinations, there ~~are~~ is at present a strong tendency to a much smaller value such as 8".798 or even 8".794.

It must be noted that every 0".00I in parallax changes the astronomical unit in the opposite direction (i.e. a decrease in p increases the a.u.) by I7000 km.

Declassified in Part - Sanitized Copy Approved for Release 2011/12/08 : CIA-RDP80T00246A016600420001-1

Declassified in Part - Sanitized Copy Approved for Release 2011/12/08 : CIA-RDP80T00246A016600420001-1

In conclusion we will mention the results of published radar determinations. For this purpose the distance of a suitable major planet is measured by determining the time between the emitted radio impulse and its echo reflected by the planet. The only planet suitable used for this method has so far been Venus near its inferior conjunction with the Sun. Such determinations were made in England, the United States and the USSR. The advantageous side of this is that the a.u. is determined directly without involving intermediate quantities such as the size or mass of the Earth and Moon, by using the only datum - the velocity of propagation of the radiowaves, usually adopted equal to that of light.

Besides the radar method Doppler's principle was also used as applied to radiowaves.

Most of the measurements were made in March and April I96I with the following results.

Observations at Jodrell Bank, England, after transfer to parallax (presumably with the international ellipsoid of the Earth) yielded $p = 8''.7943 \pm 0''.0003$.

According to data published by Rechtin in the USA, as the mean of several determinations, a = I49598590 km, which corresponds to practically the same value $p = 8''.794I$.

V. A. Kotelnikov in the USSR obtained a = I4959900 km or $p = 8''.7940$.

All these determinations are in exceptionally good agreement between themselves, but they all give a smaller value of the parallax than expected. The question arises whether they are not subject to common systematic errors inherent to this method. It is

Declassified in Part - Sanitized Copy Approved for Release 2011/12/08 : CIA-RDP80T00246A016600420001-1

Declassified in Part - Sanitized Copy Approved for Release 2011/12/08 : CIA-RDP80T00246A016600420001-1

clear that it is unlikely to record the echo with any advance and only a retard seems possible in the detection of the first reflected signal. This would lead to an exageration of the distance. Secondly the existance of an interplanetery medium, especially in the direction towards the Sun and near the Earth, would decrease the velocity of propagation of the radiowaves and the computation of the distance with an unaltered full velocity would act in the same direction. Lastly an uncertainty is introduced by the dimensions of the planet itself, as it is not exactly known which part of its surface or atmosphere gives the first noticeable reflection.

It seems therefore that the radio observations so far are not totally devoid of a common bias and the true value of the solar parallax is somewhat larger than given by them. I would take $\rho = 8''.797$ as the most likely compromise of all determinations, the corresponding length of the a.u. being I49550000 km with a limiting error of 50000 km.

We must not wonder at the magnitude of this error, being I/3000 of the whole length. This corresponds to 0.3 mm in one meter - about the same error with which the length of a meter was initially determined as a I/40000000 part of the meridian of Paris. However this determination was made by measuring a net of triangles of favourable shape on the solid surface of the Earth with several not too short base lines. For a determination of the a.u. it is necessary to evaluate how many times the platinum rod representing the legal meter, kept at the International Bureau of weights and measures at Sèvres, Paris can be arrayed through outer space between the Earth and Sun in the void at a distance of I50 billion times greater where it is impossible to make the usual measurements by rods, wires or triangulation, disposing only of a base line

Declassified in Part - Sanitized Copy Approved for Release 2011/12/08 : CIA-RDP80T00246A016600420001-1

Declassified in Part - Sanitized Copy Approved for Release 2011/12/08 : CIA-RDP80T00246A016600420001-1

some 20 000 times shorter than the distance to be measured.

One more remark about the astronomical unit of length. Strictly speaking this unit, as calculated by Kepler's third law, does not equal to the mean (i.e. the halfsum of the greatest - at aphelion and smallest - at perihelion) distance of the Earth from the Sun. In this calculation the constant of gravitation as determined by Gauss is used. Since then the values of the length of the sidereal year and the ratio of the masses of the Earth and Moon to the Sun's mass have been improved so that Gauss' constant needs a small correction. It was decided, however, not to change this constant as this would lead to a re-calculation of many tables of theoretical astronomy and create confusion, and instead to adjust the major axes of the planetary orbits. As a result the major axis of the Earth's orbit became equal to 1.00000023, so that the mean distance of the Earth from the Sun is by 35 km greater, than the value obtained by means of Kepler's third law and using Gauss' constant. This correction is evidently so small that at present there is no need to take it into account.

What are the future perspectives in this complicated problem? It is difficult to be a prophet in the domain of science, where almost every year new unexpected vistas are opened. However I think that further progress can be expected in two directions. First in the development and perfection of radiotechnique

Declassified in Part - Sanitized Copy Approved for Release 2011/12/08 : CIA-RDP80T00246A016600420001-1

Declassified in Part - Sanitized Copy Approved for Release 2011/12/08 : CIA-RDP80T00246A016600420001-1

with a better reckoning of the influence of the interplanetary medium and knowledge of the reflecting properties of the pla - nets observed. Secondly in a direction which only a few years ago would have seemed perfectly fantastic: by measuring triang- les with the vertices: Earth, Sun and Moon, using the distance between the Earth and Moon as a base line. This would need the installation on the Moon of an observatory with an astrograph for determining the position of a chosen planet between the sur- rounding stars. Such a method would give a precision about a hundred times higher as the base line, known to about 1/100000 of its length, would be 60 times longer than those at present available on the Earth. The angular measurements on the Moon, owing to the absence of atmospheric disturbances and the Moon's slow rotation, could be made with more precision than on the Earth. The next few years will show what progress is to be expec- ted in this important problem.

Declassified in Part - Sanitized Copy Approved for Release 2011/12/08 : CIA-RDP80T00246A016600420001-1

Declassified in Part - Sanitized Copy Approved for Release 2011/12/08 : CIA-RDP80T00246A016600420001-1

3.17

by A.D.DANILOV

24.

"MODEL OF VENUS AND MARS IONOSPHERES"

On the basis of analysis of photochemical reactions proceeding in the Earth atmosphere there were constructed models of the Venus and Mars ionospheres, and the Venus ionosphere was adopted to be composed mainly of carbon dioxide and the Mars ionosphere - of molecular nitrogen. CO_2^+, CO^+ and O^+ ions are found in the Venus ionosphere, electron concentration maximum of the order of 10^6 electrons/cm^3 being situated at the altitude of about 100 km; and in the Mars ionosphere there were found N_2^+ and N^+ ions, electron concentration maximum of the order of 10^5 electrons/cm^3 being situated at about the 300 km altitude.

According to recent experimental data of electron and ion composition of the Earth upper atmosphere it became possible to reveal the main mechanisms of formation and disappearance of different ions, determining the ionosphere composition. It will be of interest to use these mechanisms to construct the ionosphere models of some other planets, and first of all, of Venus and Mars.

Declassified in Part - Sanitized Copy Approved for Release 2011/12/08 : CIA-RDP80T00246A016600420001-1

Declassified in Part - Sanitized Copy Approved for Release 2011/12/08 : CIA-RDP80T00246A016600420001-1

In order to build the ionosphere model of a planet it is necessary to assume distribution with height and neutral atmosphere composition. As for Venus, it is known from spectroscopic observations [1,2], that the main component of its atmosphere is carbon dioxide CO_2, the quantity of which in an atmosphere column above the cloud level is equivalent to the quantity of gas in the atmosphere column I km high under normal pressure. Supposing that the atmosphere density is distributed according to the barometric formulae:

$$\rho = \rho_0 e^{-\frac{h}{H}}, \text{ where}$$

$H = RT/\mu g$ scale height, T - temperature, μ - mean molecular weight, R - gas constant, g - acceleration of gravity, and assuming the temperature change with height one can compute CO_2 molecules concentration at any altitude. Temperature variation is taken on the basis of the following data: from the observation of occultation of Regulus by Venus for the altitude of the order of 100 km above the clouds layer the scale height - H - is found to be 6 km, [3] which, with $\mu = 44$ (CO_2) corresponds to 270°. At the same time radiometric estimates of the clouds layer temperature give the value of 235°. Assuming that according to both these values the temperature gradient is linear and equal to $0{,}35^{o}/_{km}$, one can compute temperature for greater altitudes. The assumed temperatures are listed in the second column of TableI, and obtained CO_2 concentrations versus height above the

Declassified in Part - Sanitized Copy Approved for Release 2011/12/08 : CIA-RDP80T00246A016600420001-1

Declassified in Part - Sanitized Copy Approved for Release 2011/12/08 : CIA-RDP80T00246A016600420001-1

clouds layer are shown in Fig.I (curve I).

Though recently there appeared some indications that in ionization processes proceeding in the Earth upper atmosphere besides solar ultraviolet radiation some other ionizing agents [4,5] can play an appreciable role; this paper deals with ions and electrons formation in the Venus atmosphere only as a result of solar ultraviolet, as the effect of other ionization sources is not yet known. According to the present data [6,7] the main part of ionizing solar radiation is concentrated in emission lines in spectrum region 100 - 800 Å; the total flux in these lines may be equal to 10^{12} qv/cm^2.sec.

Total ionization rate in the atmosphere at the given altitude is equal to:

$$V_{ion} = [M]\sigma_i n_{qv}$$

where $[M]$ - neutral particles concentration at the given altitude, σ_i - ionization cross-section, n_{qv} - ionizing radiation flux. The latter varies with height as a result of absorption:

$$n_{qv} = n^{\infty}_{qv}\, e^{-\tau}; \qquad \tau = N_M \sigma;$$

where N_M - the number of particles in an atmosphere column above the given level, σ - absorption cross-section. N_M value is estimated for the Venus atmosphere model in question, and V_{ion} value is given in the fifth column of Table I.

Declassified in Part - Sanitized Copy Approved for Release 2011/12/08 : CIA-RDP80T00246A016600420001-1

Declassified in Part - Sanitized Copy Approved for Release 2011/12/08 : CIA-RDP80T00246A016600420001-1

In computations the value of 3.10^{-17} cm is assumed for σ_i and σ [8].

According to experimental data /9/ under the action of ionizing radiation upon CO_2 molecule two kinds of ions are formed: CO_2^+ and O^+, the former being formed two times more than the latter.

$$CO_2 + h\nu \longrightarrow CO_2^+ + e \qquad (I)$$

$$CO_2 + h\nu \longrightarrow CO + O^+ + e$$

Based on the said the total ionization rate V_{ion} can be regarded as the sum

$$V_{ion} = V_{form}^{CO_2^+} + V_{form}^{O^+} \qquad (2)$$

where

$$V_{form}^{O^+} = \frac{1}{2} V_{form}^{CO_2^+}$$

Now, let us follow the fate of the formed ions CO_2^+ and O^+. As is known /10/ in the Earth ionosphere molecular ions quickly associate with electrons in dissociative recombination reactions, having a high rate coefficient about 10^{-6} cm^{3}sec^{-1}, measured experimentally. Hence, CO_2^+ ions, formed under ionisation will disappear as a result of the reaction.

$$CO_2^+ + e \longrightarrow CO + O \qquad (3)$$

Declassified in Part - Sanitized Copy Approved for Release 2011/12/08 : CIA-RDP80T00246A016600420001-1

Declassified in Part - Sanitized Copy Approved for Release 2011/12/08 : CIA-RDP80T00246A016600420001-1

As for atomic ions the quickest way of their disappearance is the charge transfer reaction with neutral molecules /IO/:

$$O^+ + CO_2 \longrightarrow CO^+ + O_2 \qquad (4)$$

with CO^+ ions disappearance in dissociative recombination reaction:

$$CO^+ + e \rightarrow C + O \qquad (5)$$

From conditions of equillibrium of O^+ formation and disappearance processes it follows:

$$V_{form}^{O^+} = V_{dis}^{O^+} = [O^+][CO_2]\gamma$$

where γ - rate coefficient of charge- transfer reaction (4) (4). Now it is not difficult to estimate O^+ concentration. γ is assumed to be equal to $IO^{-IO} cm^3 sec^{-I}$ the value much spoken about before /IO,II/. The obtained values of ions $/O^+/$ concentration versus height are listed in Fig.2, curve 2.

Let us define electron density n_e in the following way: the total rate of ions disappearance is defined by molecular ions disappearance in dissociative recombination reactions (3) and (5):

$$V_{rec} = \left\{[CO_2^+] + [CO^+]\right\} n_e \alpha$$

Declassified in Part - Sanitized Copy Approved for Release 2011/12/08 : CIA-RDP80T00246A016600420001-1

Declassified in Part - Sanitized Copy Approved for Release 2011/12/08 : CIA-RDP80T00246A016600420001-1

Table I.

H km	T_o K°	$[CO_2]$ cm^{-3}	V_{ion} $cm^{-3}sec^{-1}$	V_{form} $cm^{-3}sec^{-1}$	$[O_2^+]$ cm^{-3}	n_e cm^{-3}	$[CO^+]$ cm^{-3}	$[CO_2^+]$ cm^{-3}
90	-	$1,0.10^{12}$	$5,7.10^{-2}$	$1,9.10^{-2}$	$\sim 10^1$	$2,4.10^2$	$8,0.10^1$	$1,6.10^2$
100	270	$2,4.10^{11}$	$6,9.10^3$	$2,3.10^3$	$1,9.10^2$	$8,3.10^4$	$2,8.10^4$	$5,6.10^4$
120	-	$7,9.10^9$	$2,4.10^5$	$8,0.10^4$	$1,0.10^5$	$5,4.10^5$	$1,5.10^5$	$3,0.10^5$
140		$2,5.10^8$	$1,0.10^4$	$3,3.10^3$	$1,3.10^5$	$1,8.10^5$	$1,8.10^4$	$3,6.10^4$
160		$1,2.10^7$	$4,8.10^2$	$1,6.10^2$	$1,3.10^5$	$1,3.10^5$	$1,2.10^3$	$2,4.10^3$
180		$5,0.10^5$	$1,9.10^1$	6,7	$1,3.10^5$	$1,3.10^5$	$5,1.10^1$	$1,0.10^2$
200	305	$3,2.10^4$	1,3	$4,3.10^{-4}$	$1,3.10^5$	$1,3.10^5$	$<10^1$	$<10^1$
250	-	$2,0.10^1$	$7,8.10^{-4}$	$2,6.10^{-4}$	$1,6.10^4$	$1,6.10^4$		
300	340	$2,3.10^{-2}$	$9,0.10^{-7}$	$3,0.10^{-7}$	$5,5.10^2$	$5,5.10^2$		

Declassified in Part - Sanitized Copy Approved for Release 2011/12/08 : CIA-RDP80T00246A016600420001-1

Declassified in Part - Sanitized Copy Approved for Release 2011/12/08 : CIA-RDP80T00246A016600420001-1

From the condition of equillibrium of the number of acts of ions formation, V_{ion}, and the number of ions disappearances V_{dis} at each altitude we find:

$$V_{ion} = \left\{[CO_2^+] + [CO^+]\right\} n_e \alpha \qquad (6)$$

Taking into consideration that

$$\left\{[CO_2^+] + [CO^+]\right\} = n_e - [O^+]$$

(the number of negative ions is supposed to be negligibly small as is the case with the Earth atmosphere) we write (6) as:

$$n_e^2 - [O^+] n_e - \frac{V_{ion}}{\alpha} = 0$$

By solving this equation relative to n_e one can receive the electron concentration, shown in Fig.2, curve I. Concentrations of $[CO_2^+]$ and $[CO^+]$ are easily found from the following formulaes, based on corresponding ions formation and disappearance rates equillibrium:

$$[CO_2^+] n_e \alpha = V_{form}^{CO_2^+}$$

$$[CO^+] n_e \alpha = V_{form}^{CO^+}$$

The results of $[CO_2^+]$ and $[CO^+]$ concentrations computations are listed in Table I and Fig.2, curve 3.

Hence, electrons and ions in the Venus atmosphere are distributed as a layer with the maximum concentration of the order of 10^6 electrons/cm^3 at about the 100 km altitude. The lower part of ionosphere, up to about 150 km, is formed

Declassified in Part - Sanitized Copy Approved for Release 2011/12/08 : CIA-RDP80T00246A016600420001-1

Declassified in Part - Sanitized Copy Approved for Release 2011/12/08 : CIA-RDP80T00246A016600420001-1

by CO_2^+ and CO^+ molecular ions, and the upper part - by O^+ atomic ions. Sharp fall of electron density at 200-300 km is provided by the fact that neutral particles density at these altitudes falls so much, that the rate of O^+ ions disappearance in (4) becomes very low and radiative recombination reaction becomes the basic mechanism of ions disappearance:

$$O^+ + e \rightarrow O + h\nu \qquad (7)$$

It is necessary to point out, that an ionosphere model is directly connected with neutral particles distribution, therefore while discussing the reliability of the obtained results the first thing to consider is the correctness of the adopted atmosphere model. The main things here are: the correctness of the assumed composition and temperature gradient, determining neutral concentrations distribution with height. As was stated above, we consider the Venus atmosphere to be composed totally of CO_2.

Alongside with this we suppose that other compounds of the Venus atmosphere, spectroscopically detected in small, compared with CO_2, quantities, such as N_2O and CO, are distributed with height like CO_2 and, hence, at all the altitudes their concentration is as negligibly small relative to CO_2 concentration as in the whole atmosphere. It this is not true for one of the mentioned

Declassified in Part - Sanitized Copy Approved for Release 2011/12/08 : CIA-RDP80T00246A016600420001-1

Declassified in Part - Sanitized Copy Approved for Release 2011/12/08 : CIA-RDP80T00246A016600420001-1

gases and it is concentrated in a narrow layer or exists only at very high considerable altitudes its concentration at these altitudes may make up a considerable part of the total concentration, but the total number of molecules of this gas in an atmosphere column, estimated spectroscopically, will remain small. However to consider the possibilities of this kind is very difficult.

As to the assumed distribution of neutral particles density with height, it can be compared with the Venus atmosphere model, discussed in Vaucouleurs' work [12] (Fig.I, curve 2). The comparison of curves I and 2 in Fig.I shows no appeciable difference in the density variation with height between the two models, 25-30 km shear along the abscis may be connected with different reading of altitudes: from the Venus surface and from the clouds layer. There is however a possibility of existence in the Venus atmosphere of a higher temperature gradient and, hence, density distribution with height can be different. Therefore to speak about the connection of the obtained electron density with the assumed neutral concentration (lower scale along the abscis in Fig.2). seems to be correct. If the given neutral atmosphere model is in error and the density falls slower, electron layer in Fig.2 will stretch along the altitudes axis, preserving its form.

The ionosphere model in question agrees with the fact, that according to [12], Urey and Brewer identified 2 absorption bands. 4210 and 4372 Å, detected by N.A.Kosyrev [13] in the spectra of the illuminated part with CO^+ absorption bands. This model, however, as it was built on the spectroscopic basis data, not pointing out to N_2 presence

Declassified in Part - Sanitized Copy Approved for Release 2011/12/08 : CIA-RDP80T00246A016600420001-1

Declassified in Part - Sanitized Copy Approved for Release 2011/12/08 : CIA-RDP80T00246A016600420001-1

in the Venus atmosphere, does not show possible presence in this planet ionosphere of N_2^+ ions, the luminescence of which in the spectrum of the Venus night side was revealed by N.A.Kosyrev [14] and further backed by Newkirk [15].

Besides, the altitudes of these ions existence and their quantities in the Venus atmosphere are not yet clear. In the recent work Weinberg and Newkirk [19] consider that both previous observations of N_2^+ emission were in error.

It is necessary to poit out that the given model prevents from explanation of the observed Venus 10cm radio emission by the planet ionosphere emission. At present the question of the layers generating this emission is agurable. This emission can be of ionosphere origin only if electron concentrations in it are very high. And such concentrations may exist only if radiative recombination reaction is the main recombination process in the ionosphere. In [20] this question is treated in detail.

The Mars ionosphere model was constructed analogous to the Venus ionosphere. Its neutral atmosphere is assumed to be composed totally of N_2(according to Vaucouleurs [12] the part of other compounds does not prevail 2% of the volume), the quantity of which in an atmosphere column is equal to $1{,}6\cdot10^5$cm under normal conditions.

As there are no data of temperature distribution with height in the Mars atmosphere, while the atmosphere model construction the average equillibrium temperature value was assumed to be 230°K [16]. The distribution of the obtained concentrations with height is given in Table 2. The following reactions are assumed as the basic reactions of ions formation: ionisation reaction

$$N_2 + h\nu \rightarrow N_2^+ + e \qquad (7)$$

and dissociative recombination reaction

$$N_2^+ + h\nu \rightarrow N^+ + N + e \qquad (8)$$

Declassified in Part - Sanitized Copy Approved for Release 2011/12/08 : CIA-RDP80T00246A016600420001-1

Declassified in Part - Sanitized Copy Approved for Release 2011/12/08 : CIA-RDP80T00246A016600420001-1

which goes under the action of radiation with wave length less than 400 Å at a nitrogen molecule.

Table 2.

H km	$[N_2]$, cm^{-3}	V_{ion} cm^{-3} sek^{-1}	V_{form} $cm^{-3}sek^{-1}$	$[N^+]$ cm^{-3}	n_e, cm^{-3}	$[N_2^+]$, cm^{-3}
260	$1,2.10^{12}$	$4,0.10^{-2}$	$1,0.10^{-2}$	< 1	$2,0.10^{2}$	$2,0.10^{2}$
270	$7,1.10^{11}$	$3,5.10^{1}$	9,0	< 1	$5,9.10^{3}$	$5,9.10^{3}$
280	$4,0.10^{11}$	$1,4.10^{3}$	$3,5.10^{2}$	8,7	$5,7.10^{3}$	$5,7.10^{4}$
290	$2,2.10^{11}$	$7,9.10^{3}$	$2,0.10^{3}$	$9,1.10^{1}$	$8,9.10^{4}$	$8,9.10^{4}$
300	$1,3.10^{11}$	$1,7.10^{4}$	$4,2.10^{3}$	$3,2.10^{2}$	$1,3.10^{5}$	$1,3.10^{5}$
350	$7,9.10^{9}$	$1,3.10^{4}$	$3,2.10^{3}$	$4,2.10^{3}$	$1,1.10^{5}$	$1,1.10^{5}$
400	$5,0.10^{8}$	$1,0.10^{3}$	$2,5.10^{2}$	$5,0.10^{3}$	$3,4.10^{4}$	$2,9.10^{4}$
450	$3,2.10^{7}$	$6,4.10^{1}$	$1,6.10^{1}$	$5,0.10^{3}$	$1,1.10^{4}$	$5,8.10^{3}$
500	$2,0.10^{6}$	4,0	1,0	$5,0.10^{3}$	$5,7.10^{3}$	$7,0.10^{2}$
600	$7,9.10^{3}$	$1,6.10^{-2}$	$4,0.10^{-3}$	$5,0.10^{3}$	$5,0.10^{3}$	3,2
700	$3,2.10^{1}$	$6,4.10^{-5}$	$1,6.10^{-5}$	$4,0.10^{3}$	$4,0.10^{3}$	< 1

And N_2^+ and N^+ ions, formed as a result of (7) and (8), disappear /IO/ accordingly:

$$N_2^+ + e \longrightarrow N + N \qquad (9)$$

and

$$N^+ + N_2 \longrightarrow N_2^+ + N \qquad (10)$$

N_2 and N^+ electrons and ions concentrations, obtained while considering reactions (7 -IO) are listed in Table 2 and Fig.3. Besides, on the basis of data (7) estimation, the quantity of radiation with $\lambda < 400$ Å is assumed to make up one forth of the whole solar ionising radiation flux.

Declassified in Part - Sanitized Copy Approved for Release 2011/12/08 : CIA-RDP80T00246A016600420001-1

Declassified in Part - Sanitized Copy Approved for Release 2011/12/08 : CIA-RDP80T00246A016600420001-1

As is clear from Fig.3 and Table 2 electron concentration maximum (of the order of 10^5 electrons/cm^3) is situated at the 300 km altitude in the Mars atmosphere. Below this level concentration sharply decreases due to ionizing radiation absorption; at the 400-600 km altitudes the electron density decreases slowly due to small density gradient of the Mars neutral atmosphere, stipulated by slight acceleration of the planet gravity.

According to this ionosphere model the latter is made up mainly of molecular nitrogen ions at the 250-400 km altitudes. From the 500 km altitude and higher the main compound of the Mars ionosphere is N^+ ions.

As dissociative recombination reaction of N_2^+ ions (9) is, probably, responsible for luminiscence of atomic nitrogen lines 5200,3466,10400 Å in the night glow spectrum of the Earth atmosphere [17], one can expect the existence of the lines in question in the Mars atmosphere night glow, their intensity being about an order of magnitude higher than in the Earth night glow. As line 10400 intensity in the Earth night glow and auroras can be of the order of 10^4 relays, the question of this line presence in the Mars night side spectrum is of great interest. Especially as due to absence of appreciable quantities of water in this planet, the existence of strong hydroxile radiation, hampering line 10400 observation in the Earth atmosphere, is hardly possible. As is shown in works [4] the Earth atmosphere at the 200-400 km altitudes can hardly be explained only by solar ultraviolet radiation. Apparently, ionizing agent with higher absorption cross section plays an appreciable role at these altitudes. According to

Declassified in Part - Sanitized Copy Approved for Release 2011/12/08 : CIA-RDP80T00246A016600420001-1

Declassified in Part - Sanitized Copy Approved for Release 2011/12/08 : CIA-RDP80T00246A016600420001-1

G.S.Ivanov-Kholodny and L.A.Antonova /5/ soft electron flux is a possible agent, causing ionization in the F-layer.

Therefore the obtained values for the Mars and Venus ionospheres are to be considered the lower boundary of possible electron concentration, taking into consideration the possibility of the existence of other ionization sources, besides solar ultraviolet radiation in these planets atmospheres. The soft electrons can have the most appreciable effect in the Mars atmosphere, where like in the Earth atmosphere, molecular nitrogen is the main component.

Declassified in Part - Sanitized Copy Approved for Release 2011/12/08 : CIA-RDP80T00246A016600420001-1

Declassified in Part - Sanitized Copy Approved for Release 2011/12/08 : CIA-RDP80T00246A016600420001-1

References

I.G.P.Kuiper Atmospheres of the Earth and Planets, Chicago, I952,p.370

2.G.P.Kuiper The threshold of Space,Pergamon press, I957

3.G. de Vaucouleurs. Nature, I959, No.3295, 478

4. A.D.Danilov Dokl. AN SSSR, I96I,I37,N5

5.G.S.Ivanov-Kholodny, L.A.Antonova "Geomagnetizm i aeronomija" I96I,I,N2

6.G.S.Ivanov-Kholodny, G.M.Nikolsky Astron.j.,I96I,38,NI

7.G.S.Ivanov-Kholodny Dokl. AN SSSR, I96I,I37,N2

8.H.Sun,G.L. Weissler J.Chem.Phys, I955,23(9),I926

9.G.L.Weissler, J.A.Samson, M.Ogawa, J.R.Cook, J.Opt.Soc. America, I960,49(4),342

I0.A.D.Danilov Iskusstvennye sputniki Zemli, I960,v.8

II.A.D.Danilov Iskusstvennye sputniki Zemli, I960,v.5,60

I2.G. de Vaucouleurs J.Geophys,Res.,I959, 64(II),I739

I3. N.A.Kozyrev Izv. Krymsk. astrofiz. observ., I954, I2,I77

I4.N.A.Kozyrev Izv. Krymsk. Astrofiz. observ., I954,I2,I69.

I5.G.Newkirk Planet Space Sci., I959,I(I),32

I6.C.W.Allen Astrophysical quantities London, I955

I7.A.D.Danilov Geomagnetizm i aeronomija, I96I,I,NI

I8.M.S.Bhalla, J.D.Craggs Proc.Phys.Soc., I960, 76(3), 374

I9.J.L.Weinberg, G.Newkirk Pl.Space Sci. 5(2) I63,I96I

20. A.D.Danilov, S.P.Jatchenko "Geomagnetizm i aeronomija" 2(2), I962.

Declassified in Part - Sanitized Copy Approved for Release 2011/12/08 : CIA-RDP80T00246A016600420001-1

Declassified in Part - Sanitized Copy Approved for Release 2011/12/08 : CIA-RDP80T00246A016600420001-1

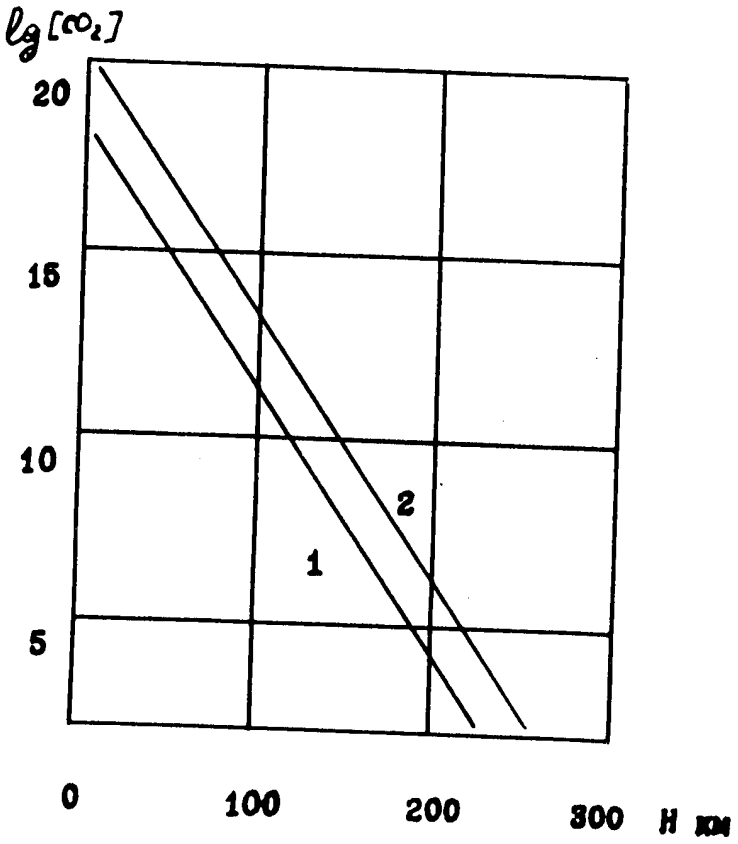

Declassified in Part - Sanitized Copy Approved for Release 2011/12/08 : CIA-RDP80T00246A016600420001-1

Declassified in Part - Sanitized Copy Approved for Release 2011/12/08 : CIA-RDP80T00246A016600420001-1

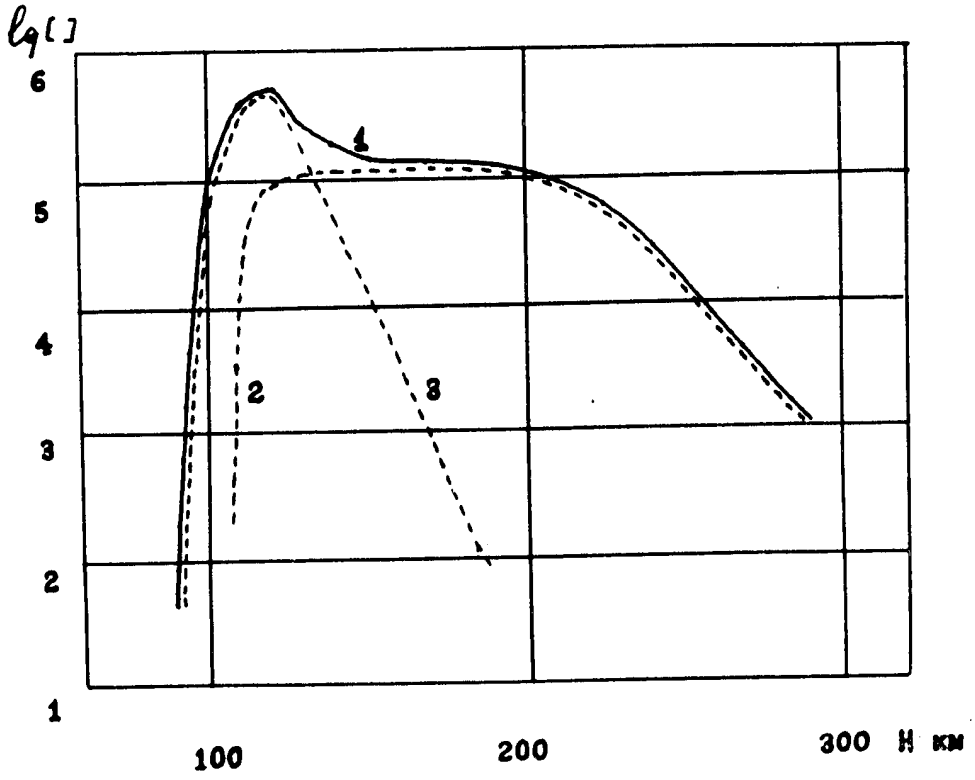

Declassified in Part - Sanitized Copy Approved for Release 2011/12/08 : CIA-RDP80T00246A016600420001-1

Declassified in Part - Sanitized Copy Approved for Release 2011/12/08 : CIA-RDP80T00246A016600420001-1

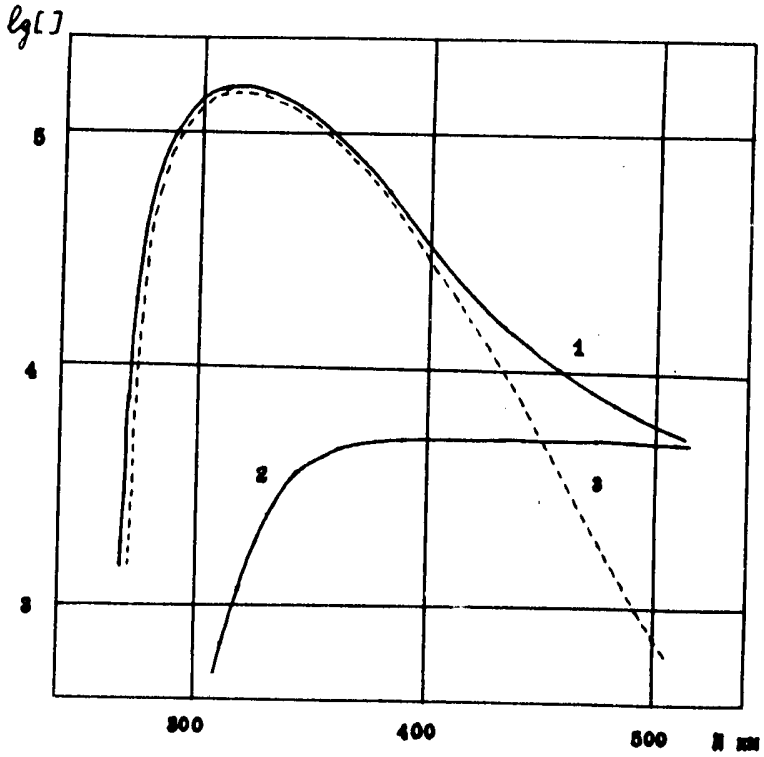

Рис 16. Распределение с высотой ионов и электронов в ионосфере Марса.

1 - $[e]$; 2 - $[N^+]$; 3 - $[N_2^+]$.

Declassified in Part - Sanitized Copy Approved for Release 2011/12/08 : CIA-RDP80T00246A016600420001-1

Declassified in Part - Sanitized Copy Approved for Release 2011/12/08 : CIA-RDP80T00246A016600420001-1

25- "THE RESULTS OF THE VENUS RADIO ASTRONOMICAL OBSERVATIONS CARRIED OUT AT THE P.N.LEBEDEV PHYSICAL INSTITUTE"

by A.D.Kuzmin, A.E.Salomonovich(x)

ABSTRACT

The observations by means of the 22 m radio telescope started at 0.8 cm near the 1959 inferior conjunction detected a phase variation of the Venus brightness temperature which indicated to the difference in brightness temperatures of the illuminated and unilluminated hemisphere. The value of the brightness temperature (315 ± 70°K) lower than at 3 and 10 cm was interpreted as a result of the radiation absorption in the colder planetary atmosphere. In the period near the 1961 inferior conjunction the observations were continued at 0.4, 0.8, 3.3 and 9.6 cm. At the first two wavelengths a regular rise in the brightness temperature with the increase of the relative area of the illuminated part of the disk (K) was detected. The minimum temperatures obtained at 0.4 cm and 0.8 cm are equal to 390 ± 120°K and 374± 75°K, respectively. At 3.3 cm the measurements were made in range K = 0.33 to K = 0.6. The average brightness temperature in this range was equal to 542°K. The linear extrapolation of the brightness temperature variations measured at 3.3 cm to K=0 gives the brightness temperature of unilluminated hemisphere equal to 372± 75°K. The mean value of the brightness temperature measured at 9.6 cm is 680°K.

The conclusions are drawn that the radiation at 0.4-3.3.cm is mainly the thermal one and it comes from the surface and

(x) P.N.Lebedev Physical Institute of the USSR Academy of Sciences.

Declassified in Part - Sanitized Copy Approved for Release 2011/12/08 : CIA-RDP80T00246A016600420001-1

Declassified in Part - Sanitized Copy Approved for Release 2011/12/08 : CIA-RDP80T00246A016600420001-1

~~is mainly the~~ thermal ~~one and it comes from the surface and~~ from the lower layers of the Venus atmosphere, the temperature of which is about 400°K at the unilluminated hemisphere. The brightness temperature of the illuminated hemisphere is estimated as not exceeding 750°K.

The pressure on the dark side surface not exceeding 5 atm. is estimated and the argument is put forward against the high concentration of water vapour. The argument is given in favour of a direct sense of rotation of the planet.

From the results of measurements at 9.6 cm the suppositions are made about the existence of the component connected possibly with the ionosphere radiation.

---

1. Investigations of the radio emission of Venus can give a number of important data on the temperature regime of the planet, on the character of its surface, on the composition of its atmosphere and on the elements of rotation. Therefore after the creation of large radio telescopes and sensitive instrumentation such investigations have been conducted for a number of years at radioastronomical stations of the USSR and the USA.

At the P.N.Lebedev Physical Institute of the USSR Academy of Sciences first observations of the radio emission of Venus (1) were made at 0.8 cm near the 1959 inferior conjunction by means of the 22 m radiotelescope (2). In 17 days after the inferior conjunction the Venusian brightness temperature turned out to be 315 $\pm$ 70°K. For the next two months a systematic increase in the brightness temperature

Declassified in Part - Sanitized Copy Approved for Release 2011/12/08 : CIA-RDP80T00246A016600420001-1

Declassified in Part - Sanitized Copy Approved for Release 2011/12/08 : CIA-RDP80T00246A016600420001-1

was observed with the increase of the portion of the planet disk illuminated by the Sun.

The variations with phase angle were interpreted as a result of the difference of the brightness temperatures of the illuminated and unilluminated sides of the planet which in its turn indicated to a relatively large period of its rotation. The difference of the 8 mm brightness temperature from the higher temperatures obtained at 3 and 10 cm by Mayer, McCullough and Sloanaker (3) was interpreted as a result of the absorption of the radiation coming from the surface by the cytherean atmosphere which is colder and semitransparent in the millimetre region.

A method was also suggested for determining the direction of the planet's rotation from the difference of its brightness temperatures at eastern and western elongations symmetrical with respect to the inferior conjunction.

Later Mayor, McCullough and Sloanaker (4) also reported about the existence of the phase variations of the brightness temperature of Venus at 3 and 10 cm. For quantitative explanationn of the measured difference of the brightness temperatures at 8 mm, on the one hand, and at 3 and 10 cm, on the other, Barrett (5) assumed the presence of the considerable pressure (up to 30 atm.) at the surface of the planet, or (with the lower pressure of 20-10 atm) the presence of the considerable water vapour content (1-3%) in in the atmosphere According to the opinion of Sagan (6) the attenuation of the millimeter radiation may be explained by absorption in the water cloud layer, and the high

Declassified in Part - Sanitized Copy Approved for Release 2011/12/08 : CIA-RDP80T00246A016600420001-1

Declassified in Part - Sanitized Copy Approved for Release 2011/12/08 : CIA-RDP80T00246A016600420001-1

temperature at the surface may be due to a considerable greenhouse effect.

Jones (7) has proposed another mechanism of the radio emission of Venus, according to which the optically thick (up to 3 cm) ionosphere of the planet is responsible for the radio emission at 20- 3 cm.

Both the first and the second models and also the "aeolosphere model" proposed by Öpik (8) are based on the above-mentioned results, the main of which is the considerable difference of the brightness temperatures at 3 and 10 cm on the one hand, and at 8 mm on the other.

2. During the period near the 1961 inferior conjunction, the observations of the radio emission of Venus at the P.N.Lebedev Physical Institute of the USSR Academy of Sciences were continued on a larger scale. From the middle of March up to the beginning of June observations were carried out at 4 mm[x] 8 mm and 9.6 cm. From May 26 to July 10 observations werealso made at 3.3 cm. The preliminary results of these observations were published (9, 10, 11).

At 4 and 8 mm a regular increase of the brightness temperature $T_{b\varphi}$ averaged over the visible planet's disk was revealed with an increase of the relative area of the illuminated portion of the planet's disk K. With the accuracy of errors in measurements the $T_{b\varphi}$ variations at 4 mm are close to the corresponding variations at 8 mm. Minimum $T_{b\varphi}$ values obtained at 4 and 8 mm are equal to $390 \pm 120^{\circ}$ K and

x) Observations at 4 mm were performed together with A.G.Kislyakov (Gorky Radiophysical Institute).

Declassified in Part - Sanitized Copy Approved for Release 2011/12/08 : CIA-RDP80T00246A016600420001-1

Declassified in Part - Sanitized Copy Approved for Release 2011/12/08 : CIA-RDP80T00246A016600420001-1

374 ± 75°K, respectively. What attracts one's attention is that the minimum at 8 mm, as well as at 4 mm, takes place not when K=0, but somewhat earlier than the inferior conjunction is observed. However, taking into account the fact that the parameters of the radio telescope changed in the process of observations and these changes could be estimated only approximately, this fact requires additional verification.

At 3.3 cm measurements were made between K= 0.33 ± 0.6. The average brightness temperature in this range was equal to 542° K. A tendency was revealed to a systematic increase of T_{bQ} with the growth of K .

At 9.6 cm the mean value of the brightness temperature in the period March 20 - June 1 was 690°K- The statistical treatment of the observational results has shown that due to large relative r.m.s. errors it is not possible to conclude if the variations of Venus brightness temperature observed at this wavelength (10,11) are actual or they are due to observational errors. However, several cases have been noted when the drift curves of Venus showed the anomalously high (1000-1500°K) brightness temperatures, which we could not explain by observational errors. To clear up this very important problem it is necessary to conduct additional observations.

3. The results of our measurements at 3.3 cm may be compared with the latest results of similar measurements, published by Mayor, McCullough and Sloanaker (4). Unfortunately both series of measurements were carried out during

Declassified in Part - Sanitized Copy Approved for Release 2011/12/08 : CIA-RDP80T00246A016600420001-1

Declassified in Part - Sanitized Copy Approved for Release 2011/12/08 : CIA-RDP80T00246A016600420001-1

different spans of Venus phase variations. Therefore, the comparison may be made only by extrapolation of one of the two series of the results. Assuming that to a first approximation the brightness temperatures are constant within illuminated and unilluminated hemispheres, we may consider the dependence of Venus brightness temperature $T_{\ell\varphi}$ upon K as linear one. The linear extrapolation of Mayer, MacCullough and Sloanaker's data (4) to K = 0.47 (the middle of our observation interval in 1961) gives $T_{\ell\varphi} = 763^{\circ}K$. Our results in the same phase is $T_{\ell\varphi} = 544^{\circ}K$. On the other hand, the linear extrapolation of temperatures measured by us in the interval K = 0.33 + 0.6 to K = 0 gives $T_{\ell\varphi} = 372 \pm 75^{\circ}K$. A similar extrapolation of the data (4) gives $T_{\ell\varphi} = 473^{\circ}K$.

Thus near the dihotomy the Venus brightness temperature at 3.3 cm measured by us is considerably lower than in (4). But the night brightness temperatures of the planet defined from our data or from (4), are close to each other ($\sim 400 \div 450^{\circ}K$). Consequently, it may be concluded that the brightness temperature phase dependence is considerably less steep than it was indicated in (4).

However it is necessary to note that the above results of extrapolation are not quite reliable due to large relative measurements errors. It is necessary to confirm them by direct measurements.

The confirmation of our results would have proved that the brightness temperature at 9.6 cm ($\sim 690^{\circ}K$) was essantially higher than at 3.3 cm. In this case, one can

Declassified in Part - Sanitized Copy Approved for Release 2011/12/08 : CIA-RDP80T00246A016600420001-1

Declassified in Part - Sanitized Copy Approved for Release 2011/12/08 : CIA-RDP80T00246A016600420001-1

assume that at the wave which is longer than those two at least for the part of radiation responsible is a medium above the planet's surface, while the radiation of Venus at 3.3 cm and also at 4 and 8 mm is in the main a thermal one of the surface itself and the layers of the atmosphere near the surface whose temperatureis close to 400°K.

Extrapolation of the results of our observations at 4 mm - 3 cm to K = 1 gives $T_{\ell_{\varphi}} \leq 750°K$. However, in addition to the thermal component connected with the surface of the planet, generally speaking a contribution can be made to this radiation due to the ionosphere (7) which apparently has a higher concentration on the day side of Venus than on the night side.

The question on the separation of the component due to the thermal radiation of the surface can be solved only after some additional investigations. At present it can be believed that the temperature of the surface of the day side of Venus hardly exceeds 750°K.

4. Since from the data obtained by us one cannot draw the conclusion about the considerable difference between brightness temperatures measured at 4 and 8 mm and at 3.3 cm it is not necessary for their explanation to have the high pressure or the presence of water vapour in the Venus atmosphere in considerable quantities, as it is necessary, for instance, in Barrett's models (5). Moreover, if the Venus atmosphere consists in the main of CO_2, then in order to satisfy the closeness of brightness temperatures obtained at 4 and 8 mm and 3.3 cm the pressure near the surface apparently should not exceed five earth's atmospheres.

Declassified in Part - Sanitized Copy Approved for Release 2011/12/08 : CIA-RDP80T00246A016600420001-1

Declassified in Part - Sanitized Copy Approved for Release 2011/12/08 : CIA-RDP80T00246A016600420001-1

5. As we have indicated earlier (I), the shift of the brightness temperature minimum of the planet relative to the point of the inferior conjunction provides an opportunity of determining the direction of its rotation. The shift of this minimum towards eastern elongations indicates a direct sense of rotation of Venus about its own axis, i.e. it coincides with the direction of its revolution about the Sun.

The shift of the $T_{\varphi\varphi}(k)$ minimum allows also to point out that though the period of the rotation of Venus is greater than that of the Earth, it cannot be equal to the period of revolution, as it was considered by a number of investigators (12).

6. As was pointed out above, it is possible that at least, the part of the radiation of Venus at 10 cm is generated in a medium above the surface of the planet. The ionosphere of Venus can become such a medium, if its optical thickness at 10 cm is close to unity.

With the decrease of the wavelength the ionosphere will become transparent and the observed radiation will be due to the thermal radiation of the surface of the planet. With the increase in the wavelength up to 10 cm the ionosphere turns to be optically thick and the brightness temperature of its radiation will be close to the kinetic temperature of electrons in the ionosphere.

The serious difficulty in this model is the mechanism of the production and the maintenance of the extremely high

Declassified in Part - Sanitized Copy Approved for Release 2011/12/08 : CIA-RDP80T00246A016600420001-1

Declassified in Part - Sanitized Copy Approved for Release 2011/12/08 : CIA-RDP80T00246A016600420001-1

26.

"New Details in the Infrared Spectrum of Venus (1-25 μ)"

by V.I. Moroz

Abstract

Some new details in the infrared spectrum of Venus are detected. Upper boundaries of N_2O, CO and CH_4 equivalent paths are estimated anew. Some remarks are given on the nature of the cloud layer and absorption in the 9-13 μ region.

In 1961 the author began investigations of the infrared spectrum of Venus. Preliminary results are given below. The spectrum of Venus was recorded in the 1-25 μ region by means of photoresistance PbS cooled by solid carbonic acid, of a 50" reflector and a diffraction spectrometer at a spectral width of slits 20 Å. Noises and inaccuracy of guiding to a certain degree deteriorated the actual resolving power, but, nevertheless, some new details were found: strong CO_2 bands in the 1.5-1.7 μ interval revealed, as it should be expected, doublet splitting. The edge of planetary absorption near 2.1 μ showed band structure. The sharpest detail of this structure- the absorption near 2.11 μ - coincides in the wavelength with the N_2O band which is observed in the Earth's atmosphere when air masses are very large.

Declassified in Part - Sanitized Copy Approved for Release 2011/12/08 : CIA-RDP80T00246A016600420001-1

Declassified in Part - Sanitized Copy Approved for Release 2011/12/08 : CIA-RDP80T00246A016600420001-1

The identification of the 2.11 μ planetary band with N_2O can be considered only as a hypothetical, since there are no definite indications to planetary absorption near 2.26 μ, where the second N_2O band should exist. Other possible identification is $C^{13}O_2^{16}$. The upper boundary of the N_2O equivalent path is about 10 cm for the 2.11 μ band. Upper boundaries are found for these gases from the absence of 2.35 μ CO and 2.37 μ CH_4 bands. They are 20 and 2 cm, respectively. Laboratory measurements were carried out at the atmospheric pressure.

If clouds consist of ice crystals, in 1.5 - 1.8 and 2.0 - 2.5 μ intervals smooth depressions should be observed in the direction short waves, as in the reflection spectrum of hoarfrost,,where these depressions are very strong. A rough comparison with hoarfrost has not shown such depressions in the spectrum of Venus. However, at the reflection from clouds which consist of smaller crystals, depressions can be weaker and it is necessary to conduct an additional investigation to solve the problem finally. Judging from the 2 - 2.5 μ region the C_3O_2 abundance hardly can be sufficient to ensure longwave absorption which was suggested as an explanation for the low intensity of CO_2 bands in the 8 - 13 μ interval.

Declassified in Part - Sanitized Copy Approved for Release 2011/12/08 : CIA-RDP80T00246A016600420001-1

Declassified in Part - Sanitized Copy Approved for Release 2011/12/08 : CIA-RDP80T00246A016600420001-1

Fig.1.

a) The spectrum of Venus (avaraging from four records).

b) The solar spectrum (higher resolving power).

c) The spectrum of Venus from Kuiper's publications.

Declassified in Part - Sanitized Copy Approved for Release 2011/12/08 : CIA-RDP80T00246A016600420001-1

Declassified in Part - Sanitized Copy Approved for Release 2011/12/08 : CIA-RDP80T00246A016600420001-1

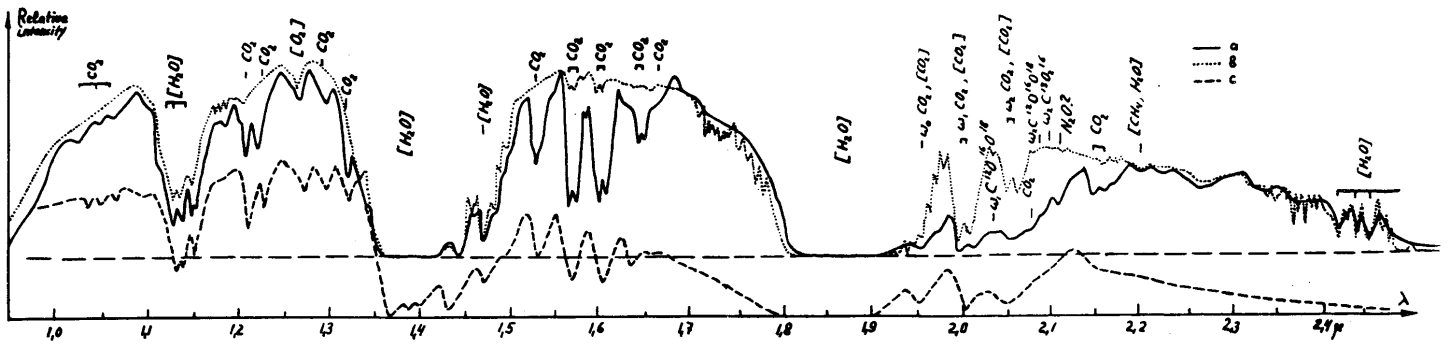

Declassified in Part - Sanitized Copy Approved for Release 2011/12/08 : CIA-RDP80T00246A016600420001-1

Declassified in Part - Sanitized Copy Approved for Release 2011/12/08 : CIA-RDP80T00246A016600420001-1

REPORT

to the International Space Science Symposium

to be held in Washington

27.

" SOME RESULTS OF THE MOON EXPLORATION BY RADIOPHYSICAL METHODS "

by V.S.Troitski

In the present paper I communicate some new results about the nature, thermal regime and the structure of lunar surface obtained by means of the investigation of the lunar radio emission which has been carried out by the group of the associates such as V.D.Krotikov, A.G.Kislyakov, M.R.Zelinskaya, L.I.Fedoseev, K.M. Strezhneva and oth. including myself at Radiophysical Research Institute of N.I.Lobachevsky Gorky State University.

Here, I introduce the main data of the year 1961. However, I briefly remind you of our earlier studies reported at the International Symposium "The Moon" in Pulkovo, because all the following results will be based on them.

I. Structure of lunar outer surface layer. Homogeneous or two-layer models.

It is known that the first observations of lunar radio emission carried out by I.H.Piddington and H.S.Minnett at I,25 cm[I] as well as the optical measurements showed that the physical conditions of a lunar surface layer are not uniform. The solid lunar rocks with

$$\gamma = (k\rho c)^{-1/2} = 100$$

Declassified in Part - Sanitized Copy Approved for Release 2011/12/08 : CIA-RDP80T00246A016600420001-1

Declassified in Part - Sanitized Copy Approved for Release 2011/12/08 : CIA-RDP80T00246A016600420001-1

are covered with a thin (several milimeters) layer of friable dust which has $\varepsilon = 1000$ and is transparent for radio waves. It represents the so-called two-layer model. Our investigations were directed in the first place to reveal if there is such a strong nonuniformity of the surface layer. It has been found out by the measurements at the 3,2 cm in 1952-1955 years that the thickness of radiating layer is practically proportional to the received wavelength.

Hence, carrying out the measurements of radiation in a large wave band one can explore the upper layer at different depths and determine if there is a sharp change of layer properties by comparison of the character of radiation change at the different exploring waves [3].

Following this aim the investigations of lunar radio emission have been carried out at very spaced wavelengths 0,4 cm, 1,6 cm and 3,2 cm that corresponds to the radiating layer thickness of about 12 cm, 50 cm and 100 cm. The basic characteristic of lunar radio emission is the ratio of a constant component to an amplitude of the first harmonic of radiation intensity variation [4]. The dependence of this ratio on a wavelength definitely points out the absence of any visible nonuniformity from the surface up to the depth of several meters. The comparison of the experimental data with the radiation theory of homogeneous or two-layer models are shown in figures 1 and 2. For the homogeneous model of a layer structure in this wave region the fact obtained ealier [3,5] is confirmed that the thickness of radiating layer increases proportionally with a wavelength. The dependence with a more precise proportional coefficient [4] equals

$$l_e = 2\lambda l_T \qquad (1)$$

Declassified in Part - Sanitized Copy Approved for Release 2011/12/08 : CIA-RDP80T00246A016600420001-1

Declassified in Part - Sanitized Copy Approved for Release 2011/12/08 : CIA-RDP80T00246A016600420001-1

where l_T is the penetration depth of a thermal wave. The dependence l_e on λ and l_e itself is analogous to those which take plase for earth's dry rocks. If a lunar material contained an essential quantity of powdery metal, for instance iron, the dependence l_e on λ would not be a linear one but according to the laboratory analysis would have a much higher degree of λ . The other interesting result of these measurements was an experimental determination of the ratio of a constant component to the first harmonic of a lunar surface temperature which turned out :

$$T_0/T_1 = 15 \qquad (2)$$

It must be noted that all the previous conclusions have been made using only the relative radiation intensity data (the ratio of radiation amplitudes of a constant component to a variable one, the dependence of this ratio on a wavelength and so on.)

2. Precise measurements of lunar radio temperatures. The method. The results.

The measurement accuracy of absolute values of lunar radio temperatures was not higher than ± I5 % up to the present day and therefore they cannot be used for obtaining the definite conclusions. Many attempts [I,6,7] always gave too large intervals of parameter magnitudes. For example, inaccuracy of ± I2 % of the lunar temperature in night-time led to a spread of parameter γ within the interval of 200-I000 [7]. Thus, one of the essential canals of the information of the physical and thermal conditions of the lunar surface could not be used up to nowadays. The optical measurements on which all the hopes were laid to determine accurately the surface temperature regime have not yet solved this problem. There appeared an ur-

Declassified in Part - Sanitized Copy Approved for Release 2011/12/08 : CIA-RDP80T00246A016600420001-1

Declassified in Part - Sanitized Copy Approved for Release 2011/12/08 : CIA-RDP80T00246A016600420001-1

gent task of precise measurements of temperature regime by radio methods. After the search over the long period of time the method of lunar radio temperature measurement at VHF was worked out and based which provides an extremely high unprecedented in radio astronomy absolute measurement accuracy with an error not more than I-2 % [8]. This accuracy is higher more than an order than the present one. The method is the comparison of a source radiation with a standard radio emission from an absolutely black disk placed freely or into a screen covered the main lobe of telescope pattern. In this case the disk size and the hole are selected in such a way that when placed in Frauhofer diffraction region with a distance from the D-diameter radio telescope not less than D^2/λ they have the same visible angle as the Moon. Both standard disks are set at a sufficient elevation angle. A standard signal is an average one of signals from a freely black disk and that placed in the hole of the screen. Considerable errors arise when a single standard signal is used, because of earth radiation owing to diffraction on the disk or hole. In the first case the standard signal from the disk increases on an unknown value due to earth radiation and in the second case it decreases on the same magnitude. The equality of these additions is explaned under some conditions by Babine's principle. The disks are shown in figure 3.

During the measurements of lunar integral radiation at 3,2 cm in February and August of the year I96I [8,9] following results were obtained for a constant component of radio temperature : 210 ± 5°K and 213 ± 4°K.

The precise measurements at I,62 cm [I0] and 9,6 [II] were also carried out at the latter first discovering pha-

Declassified in Part - Sanitized Copy Approved for Release 2011/12/08 : CIA-RDP80T00246A016600420001-1

Declassified in Part - Sanitized Copy Approved for Release 2011/12/08 : CIA-RDP80T00246A016600420001-1

se dependence of radiation. So, for the constant component the following data are obtained :

$$\lambda = 1{,}6 \qquad \tilde{\bar{T}}_M = 208 \pm 6^{\circ}K$$
$$\lambda = 3{,}2 \qquad \tilde{\bar{T}}_M = 211 \pm 3^{\circ}K \qquad (3)$$
$$\lambda = 9{,}6 \qquad \tilde{\bar{T}}_M = 218 \pm 4^{\circ}K$$

3. Mean-spherical emissivity of the Moon, dielectric constant and material density of the surface layer.

Some physical characteristics of the surface layer material may be determined by means of these accurate data. The thermal regime at the given solar radiation [12] has been calculated with the help of an electronic digital computer as it has been done by Jager [7]. The calculations showed that the average over the disk constant component of the real temperature is about $T_{M\ black} = 218^{\circ}$ K [13]. Since $T_{radio} = T_{M\ black} \cdot I$, where $\tilde{I} = 1 - \bar{R}$ is the mean spherical emissivity, we can conclude from (3) taking into account measurement errors that the magnitude of I is within

$$0{,}93 \leq \bar{I} \leq 0{,}97 \qquad (4)$$

Assuming that Fresnel reflection formulas are true to the lunar surface one can show the reflection coefficient at the normal incidence and under (4) must be within

$$0{,}001 \leq R \leq 0{,}02 \qquad (5)$$

Hence, according to $R_{\perp} = \left(\frac{\sqrt{\varepsilon}-1}{\sqrt{\varepsilon}+1}\right)^2$ we have immediately that the dielectric constant of surface rocks at VHF equals

$$\varepsilon = 1{,}5 \pm 0{,}3 \qquad (6)$$

As an average chemical composition of lunar rocks is like earth's ones [4] for which at density ρ_0 of the crystal state the dielectric constant at VHF is about 4,5 then it follows from (6) a high porosity of the lunar rocks. Yet,

Declassified in Part - Sanitized Copy Approved for Release 2011/12/08 : CIA-RDP80T00246A016600420001-1

Declassified in Part - Sanitized Copy Approved for Release 2011/12/08 : CIA-RDP80T00246A016600420001-1

it is not the only possible conclusion. A low magnitude of ε being determined according to the surface effect (emissivity) may be connected with a strong surface roughness in comparison with a wavelength while the material is sufficiently dense. However, radar reflection data pointing out the specular reflection testify to the first assumption. In this case using the theoretical data for a dielectric constant of porous media according to the formula

$$\varepsilon = \varepsilon_0 \cdot \left(1 - \frac{3p}{\frac{2\varepsilon_0 + 1}{\varepsilon_0 - 1} + p}\right),$$

where $p = 1 - \rho/\rho_0$, it is possible to find that the lunar surface rock density equals

$$\rho = 0{,}5 \pm 0{,}3 \qquad (8)$$

4. Determination of surface layer thermal parameters from radiation data.

An accurate value of the constant component of radio temperature revealed the possibility taking into account the probable values of R_1 according to radar reflection and radio emission data to determine the constant component of a real temperature T_0 in the centre of the lunar disk with an accuracy not less than $\pm$ 5 %. At the same time from the calculation of the moon surface thermal regime the functions $T_0(\gamma)$, $T_1(\gamma)$, T_0/T_1, T might have been found when γ changes within 20 ÷ I200. Then the comparison of the experimental magnitudes of T_0 and T_0/T_1 and the calculated ones showed that the latters are well in agreement at the $\gamma = (k\rho c)^{-1/2}$ which equals in absolute units [I4]

Declassified in Part - Sanitized Copy Approved for Release 2011/12/08 : CIA-RDP80T00246A016600420001-1

Declassified in Part - Sanitized Copy Approved for Release 2011/12/08 : CIA-RDP80T00246A016600420001-1

$$\gamma = 350 \pm 75 \qquad (9)$$

From (8) and considering that $c = 0,2$ we obtained according to (9) the thermal conductivity of layer rocks

$$\kappa \sim (1 \pm 0,5) \cdot 10^{-4} \text{ cal.grad.}^{-1}\text{cm}^{-1}\text{sec}^{-1}$$

This value is nearly two orders more than the accepted before. Apparently such a high thermal conductivity does not correspond to the dust in vacuo as it was suggested earlier but rather to a porous material like a pumice.

5. Density and structure determination of upper layer rocks from thermal parameters.

It has been shown above that γ itself reveals the possibility to discover the lunar rock density. The new method [15] of determining the lunar outer layer rocks density is based on using the dependence of the thermal conductivity $\kappa(\rho)$ on the density which is a universal function for earth rocks or at least a group of them. Thus it appears that $\gamma = (\kappa\rho c)^{-1/2} = [\kappa(\rho)\rho c]^{-1/2}$ depends only on ρ and is a known function for earth rocks. Since lunar rock chemical composition is like an earth's one then having γ for lunar rocks we can find ρ Yet it seems that the functions $\kappa(\rho)$ are different for foamy and dry substances. For the foamy ones we obtain

$$\rho = 0,4 \text{ g.cm}^{-3}$$

For dry ones

$$\rho = 0,9 \text{ g.cm}^{-3}$$

The Ist ρ corresponds to dielectric constant $\varepsilon = 1,5$ and the 2d to $\varepsilon = 2$. The Ist value is nearer to the

Declassified in Part - Sanitized Copy Approved for Release 2011/12/08 : CIA-RDP80T00246A016600420001-1

Declassified in Part - Sanitized Copy Approved for Release 2011/12/08 : CIA-RDP80T00246A016600420001-1

obtained by the radio emission data , hence a foamy structure is more corresponding to the reality.

6. Dielectric properties of surface layer material. Mineralogical structure.

In correspondance with the known thermal parameters from the expression (I) an effective electrical conductivity or a loss-angle tangent can be determined for a given wave - length. The determining of the loss-angle tangent is of a special interest for identifying lunar rocks with earth's ones.[4] It is known that it characterizes the kind of a rock, its chemical composition. But it also depends on the density, è.i. material porosity. The comparison must be carried out with an electrical parameter invariable of the density. Such a parameter is a ratio of a loss-angle tangent to the density $tg\Delta/\rho$. This magnetude at VHF is determined by only a chemical composition or a type of rock material. According to (I) the invariant for lunar rock [4] is

$$\frac{tg\Delta}{\rho} = \frac{88}{\sqrt{\varepsilon}} \cdot 10^{-6}\ c\gamma = \frac{88}{1{,}25} \cdot 10^{-6} \cdot 0{,}2 \cdot 350 = 5 \cdot 10^{-3}\ \text{г}^{-1}\text{см}^3$$

For searching the earth rocks similar to lunar ones by the value of this parameter a numerous laboratory measurements of the invariant at VHF have been carried out for different earth rocks [16] . It turned out that $tg\Delta/\rho = 5{,}10^{-3}$ is inherent in such rocks as gabbro, iolite, diabase (basic rocks), syenite, diorite (middle rocks) and granite (an acid rock). It is necessary to note that quartz sand has the least invariant 10^{-3} . Basalt, volcanic ashes have $tg\Delta/\rho = 20.\ 10^{-3}$ that is in four times more than of

Declassified in Part - Sanitized Copy Approved for Release 2011/12/08 : CIA-RDP80T00246A016600420001-1

Declassified in Part - Sanitized Copy Approved for Release 2011/12/08 : CIA-RDP80T00246A016600420001-1

lunar rocks; therefore they do not correspond to them. However, the value $tg\,\Delta/\rho$ obtained can be explained by a mixture of 80 % quartz sand with 20 % of these rocks.

7. Thermal flux out from the moon entrails.

The obtained accurate data of the moon temperatures at different wavelengths point out the possible thermal flux from underneath of lunar surface and the temperature increasing into the moon center. This way, for a thermal flux we have from the expression:

$$Q = \frac{T_{\lambda 2}\ T_{\lambda 1}\ \sqrt{\Omega_2}}{(1-R_1)2(\lambda_2-\lambda_1)\gamma}$$

$$0 \leq Q \leq 4 \cdot 10^{-6}\ cal\ /\ cm \cdot sec$$

And for a temperature gradient with l_T = 30 cm we have

$$0 \leq \text{grad } T \leq \text{grad/m}$$

It must be noted, that analogous estimations have been made in [18] , basing on the lunar radio temperature value $233^\circ \pm 8^\circ$ K which has been found at I,5 m wavelength. In our opinion thease measurements have not a high accuracy because of using the absolute magnitude of back-ground radiation, the accurate determination of which cannot be provided with an accuracy more than $\pm$ 7 - I0 % that gives an error $\pm$ 20 - 25° K. Furthemore, the electrical penetration depth l_e is not known at such a wave, and it may be much more than it follows from the proportional dependence on wavelength as it has accepted in [18] .

Declassified in Part - Sanitized Copy Approved for Release 2011/12/08 : CIA-RDP80T00246A016600420001-1

Declassified in Part - Sanitized Copy Approved for Release 2011/12/08 : CIA-RDP80T00246A016600420001-1

The reported results show that the developed methods of moon exploration by its radiation measurements jontly with laboratory investigations of rocks became more effective than any other ones devoted to determination of thermal regime, structure and outer surface nature of the Moon. We also believe, that these "passive" methods are effective in determination of statistical characteristics of surface geometry.

11/3 62

Declassified in Part - Sanitized Copy Approved for Release 2011/12/08 : CIA-RDP80T00246A016600420001-1

Declassified in Part - Sanitized Copy Approved for Release 2011/12/08 : CIA-RDP80T00246A016600420001-1

REFERENCES.

I. I.H.Piddington, H.C.Minnet, Astr.J.Sci.Res. 2A, 63, I949.

2. V.S.Troitski, M.R.Zelinskaya, Astron.Zh., 32, 550, I955.

3. V.S.Troitski, Transactions of the Fifth Conference on Cosmogonical Questions, p.325, (Acad.Sci.USSR Press) I956.

4. V.S.Troitski, Proceedings of Commission on planetary physics, № 3, I96I.

5. M.R.Zelinskaya, V.S.Troitski, L.I.Fedoseev, Astron.Zh., 3I, 4, 643, I959.

6. V.S.Troitski, Astron.Zh, 3I, 5II, I954.

7. J.C.Jaeger, Proc.Comb.Phys.Soc., 49, 355, I953.

8. V.D.Krotikov, V.A.Porfir'ev, V.S.Troitski, Izv.Vuz.MVSSO "Radiofizika", № 6, I96I.

9. L.I.Bondar', V.A.Porfir'ev, M.R.Zelinskaya, K.M.Strezhneva, Izv.Vuz.MVSSO "Radiofizika", I96I.

I0. S.A.Kamenskaya, B.I.Semenov, V.S.Troitski, Izv.Vuz.MVSSO "Radiofizika", I962. (in press).

II. V.D.Krotikov, Izv.Vuz.MVSSO "Radiofizika", I962. (in press).

I2. V.D.Krotikov, O.Shchuko, Astron.Zh., I962. (in press).

I3. V.D.Krotikov, V.S.Troitski, Astron.Zh., I962 (in press).

I4. V.D.Krotikov, V.S.Troitski, Astron.Zh., I962 (in press).

I5. V.S.Troitski, Izv.Vuz.MVSSO "Radiofizika", I962 (in press).

I6. V.D.Krotikov, Izv.Vuz.MVSSO "Radiofizika", I962 (in press).

I7. V.S.Troitski, Izv.Vuz.MVSSO "Radiofizika", I962 (in press).

Declassified in Part - Sanitized Copy Approved for Release 2011/12/08 : CIA-RDP80T00246A016600420001-1

Declassified in Part - Sanitized Copy Approved for Release 2011/12/08 : CIA-RDP80T00246A016600420001-1

NOTES TO THE FIGURES

Figure I - Theoretical dependence of the first harmonic phase drop on the ratio of a constant component to the first harmonic of radiation over a whole cycle.

I - homogeneous surface structure,

2,3- two-layer dusty one.

Black points - theoretical ones at λ =0,4; 0,8; I,25; I,63; 3,2cm; light points - experemental ones.

Rectangulars - the same points with phase correction.

Figure 2 - Dependence of the ratio of the constant component to the first harmonic of radiation on a wavelength.

Dotted curve - theoretical one for a one-layer model.

Points - experimental data.

Figure 3 - Standard outward appearance in operation.

Declassified in Part - Sanitized Copy Approved for Release 2011/12/08 : CIA-RDP80T00246A016600420001-1

Declassified in Part - Sanitized Copy Approved for Release 2011/12/08 : CIA-RDP80T00246A016600420001-1

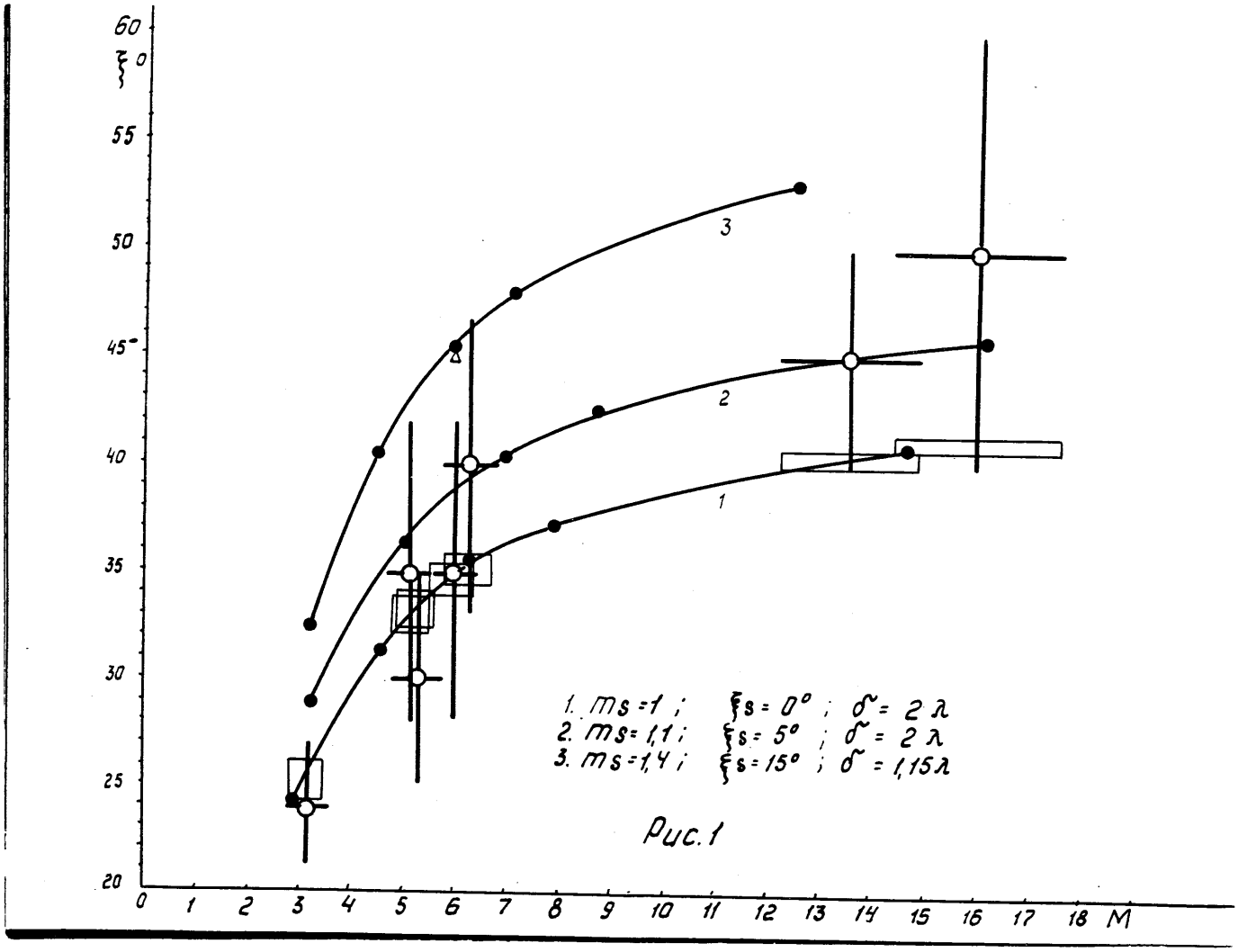

Рис. 1

Declassified in Part - Sanitized Copy Approved for Release 2011/12/08 : CIA-RDP80T00246A016600420001-1

Declassified in Part - Sanitized Copy Approved for Release 2011/12/08 : CIA-RDP80T00246A016600420001-1

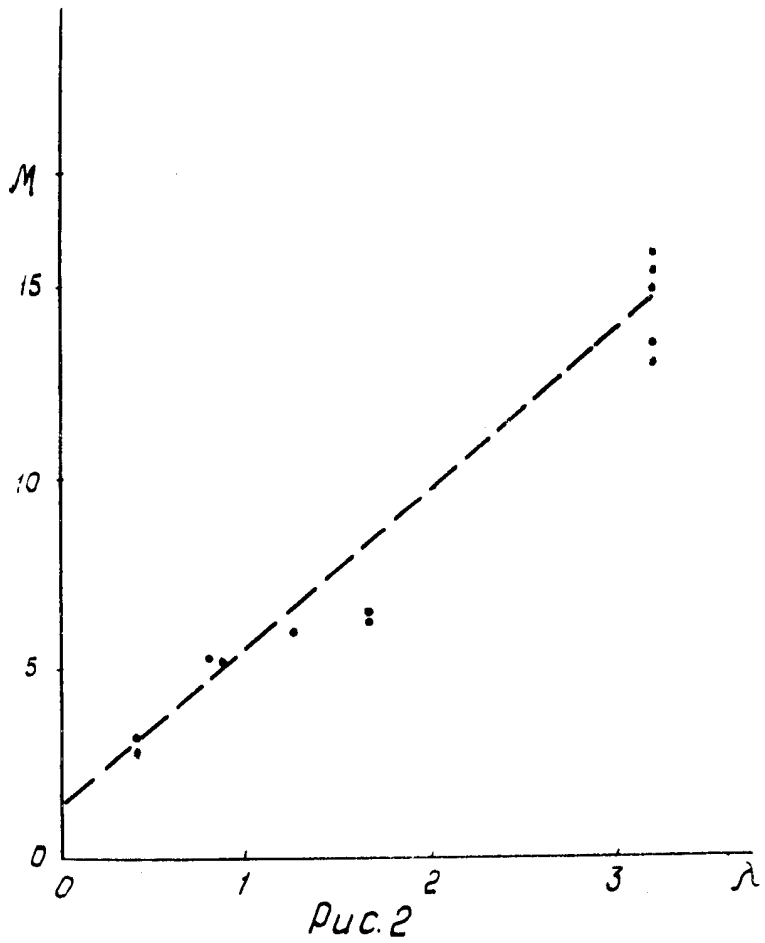

Рис. 2

Declassified in Part - Sanitized Copy Approved for Release 2011/12/08 : CIA-RDP80T00246A016600420001-1

Declassified in Part - Sanitized Copy Approved for Release 2011/12/08 : CIA-RDP80T00246A016600420001-1

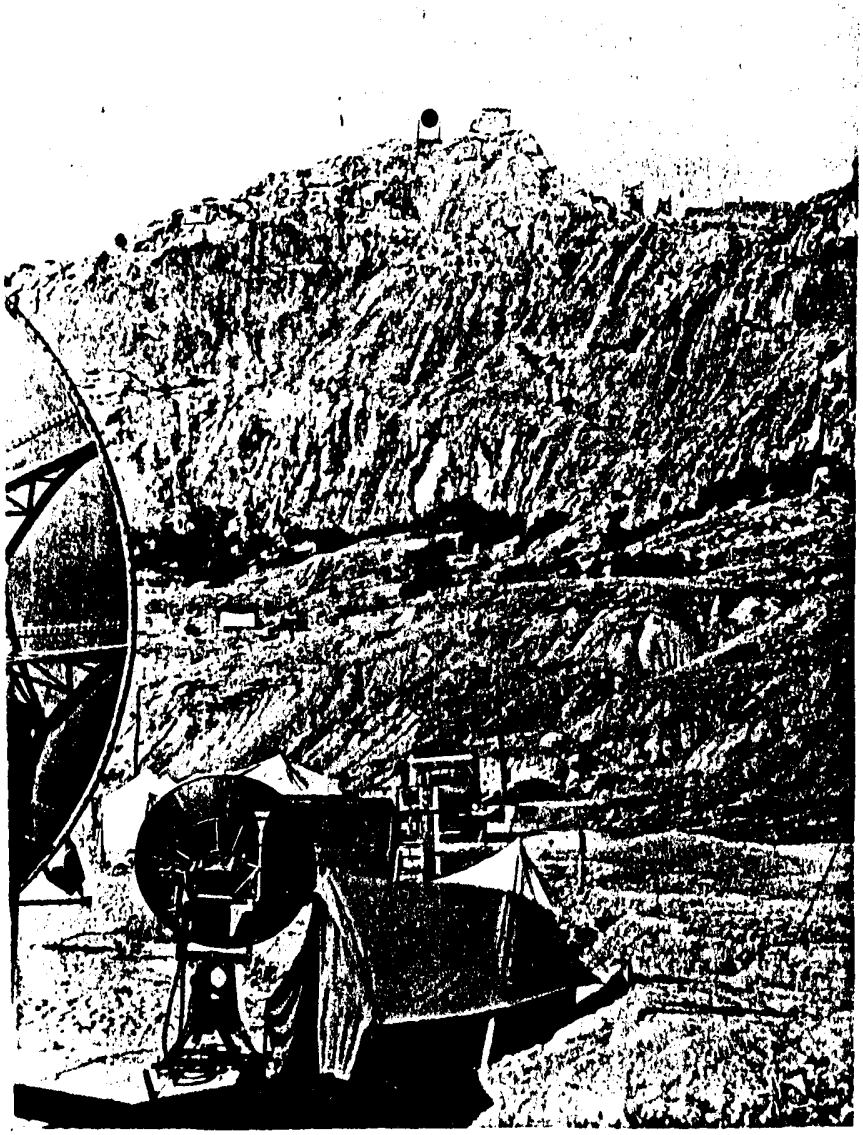

Declassified in Part - Sanitized Copy Approved for Release 2011/12/08 : CIA-RDP80T00246A016600420001-1

Declassified in Part - Sanitized Copy Approved for Release 2011/12/08 : CIA-RDP80T00246A016600420001-1

28 - "SOVIET EXPERIMENTS AIMED AT INVESTIGATING THE INFLUENCE OF THE SPACE FLIGHT FACTORS ON THE ORGANISM OF ANIMALS AND MAN"

by V.V. Parin and O.G. Gazenko

The USSR Academy of Sciences, Moscow, USSR.

Abstract

Results are given of biological experiments on space ships-satellites II, III, IY and Y and of scientific investigations made during Gagarin and Titov's flights aboard space ships Vostok I and Vostok II.

It is emphasized that physiological reactions to the action of the flight stress-factors are not of pathological character. In the period of afteraction no changes in health conditions of either cosmonauts, or animals were observed.

At the same time some peculiarities which were revealed while analysing physiological reactions and a number of biological indices require further investigations.

The most important tasks are to study the influence of protracted weightlessness, of the biological action of space radiation, of the action of overloads after stay under zero-gravity and also to analise the influence on the organism of the whole combination of spaceflight factors-including emotional strain.

Declassified in Part - Sanitized Copy Approved for Release 2011/12/08 : CIA-RDP80T00246A016600420001-1

Declassified in Part - Sanitized Copy Approved for Release 2011/12/08 : CIA-RDP80T00246A016600420001-1

In the Soviet Union a great number of biological experiments were made with a view to elucidating the action of space flight factors on living organisms and design of systems which are necessary to ensure life activity during flight aboard rocket space vehicles.

The first flight experiments with animals were conducted by means of geophysical rockets (1, 2).

The next step in this direction was made by the launching of Sputnik II in 1957 (3) and by experiments on space ships satellites in 1960-1961 (4).

The main purpose of flight and laboratory investigations was to obtain objective scientific materials necessary to ensure the safety of manned space flight.

In the present report the results are briefly summed up of biological experiments on Soviet space ships-satellites II, III, IV and V and also of some medical results of experimental flights realized by the first Soviet cosmonauts Gagarin and Titov on space ships Vostok I and Vostok 2.

1. Biological Experiments Aboard Space Ships - Satellites

Medico-biological investigations aboard space ships-satellites were designed to solve the following main tasks:

a) to study the biological action and afteraction of the combination of space flight factors on different living organisms;

b) to investigate the peculiarities of the work and efficiency of the life sustaining systems.

Declassified in Part - Sanitized Copy Approved for Release 2011/12/08 : CIA-RDP80T00246A016600420001-1

Declassified in Part - Sanitized Copy Approved for Release 2011/12/08 : CIA-RDP80T00246A016600420001-1

c) to study the functioning and reliability of the work of the systems ensuring descent and landing conditions safe for living organisms and also the methods of detection and delivery of the apparatus with biological objects to controlled conditions.

1. The technique and conditions of conducting the experiments had some peculiarities.

A program of preliminary preparation preceded flight experiments. This program included the selection of experimental animals, the determination of their individual resistance to the action of flight factors, the registration of the initial functional condition, the training for the supposed conditions of the flight experiment. Two control groups corresponded to each test animal group. One of these groups was located and examined under laboratory conditions for the whole time of preparing and conducting the flight experiment. The other group was subjected to the same effects as the test group with the exception of the space flight aboard the ship-satellite.

Female dogs weighing 5-6 kg, laboratory rats, white and black mice (C57 line), guinea pigs, frogs, fruit flies, higher plants (tradescance), dry seeds (wheat, peas, onion, maize, nygella) and sprouts of plants at different stages of development, snail's spawn, unicellular algae (chlorella), human and rabbit tissue cultures, cutaneous transplantates, bacterial cultures, viruses, phages, preparations of cellular nuclei and cellular cytoplasma, ferments and biochemical structures (desoxy ribonucleic acid) served as biological

Declassified in Part - Sanitized Copy Approved for Release 2011/12/08 : CIA-RDP80T00246A016600420001-1

Declassified in Part - Sanitized Copy Approved for Release 2011/12/08 : CIA-RDP80T00246A016600420001-1

objects.

During the whole flight normal barometrical pressure (760 ± 10 mm Hg) was maintained in the sealed cabin of the ship, the oxygen content was about 21-24%, relative humidity was from 35 to 50% and temperature amounted to 18 ± 3° Centigrade.

Biological objects which needed rigid temperature regime were placed in themorstats. Dogs, by means of the automatic device were fed by special jelly-like food, small laboratory animals had access to food and water if necessary. Microscopic objects developed on most favourable for them liquid or solid feeding media. To increase the radiosensitivity some objects were kept in the atmosphere enriched by oxygen.

By means of biotelemetry systems the registration of hygiene and physiological indices was made in flight and the functioning of some executive mechanisms checked up.

In particular, the following indices of the test dogs were recorded: electrocardiogram, arterial pressure, pneumogram, phonocardiogram, sphygmogram, seismocardiogram, electromyogram, the temperature of the body, motory activity, behaviour (by the television observation method) and some other indices.

Before and then after flight biological objects were subjected to physiological, biochemical, immunological, cytological, genetic and microbiological investigations.

2. Physiological studies were carried out on six dogs, four of which made a 24-hour flight and two orbited the

Declassified in Part - Sanitized Copy Approved for Release 2011/12/08 : CIA-RDP80T00246A016600420001-1

Declassified in Part - Sanitized Copy Approved for Release 2011/12/08 : CIA-RDP80T00246A016600420001-1

Earth one time. The behaviour, the condition of cardiovascular, respiration and muscular systems were investigated at different stages of flight: at the boost stage before placing the ship in orbit, in orbital stage (weightlessness), at the descent and landing stages, and also in the period of afteraction.

Reactions of the cardiovascular system and respiration of the majority of animals turned to be of one type (4) For the boost stage typical were changes which characterized the state of some functional strain of these systems.

Under weightlessness in 8-10 hours of flight functional changes of vegetative functions (relative decrease of the systolic index, changes in the shape of the wave T, etc.) were observed.

An attempt was made to investigate the character of the motor activity of dogs under zero-gravity. The animals within certain limits were given the opportunity of free motion, which was recorded by special monitors and devices. Besides, the motion of dogs in the cabin was controlled by means of two television cameras of side and frontal viewing fields.

The analysis of motions was made by comparison of close-ups of television films with the corresponding portions of the actogram recorded by means of telemetry systems. The actogram ensured the possibility of objective evaluation of motions visible on the television film according to amplitude and force. Let us give by way of example a short description of the behaviour of the animal on two character-

Declassified in Part - Sanitized Copy Approved for Release 2011/12/08 : CIA-RDP80T00246A016600420001-1

Declassified in Part - Sanitized Copy Approved for Release 2011/12/08 : CIA-RDP80T00246A016600420001-1

istic portions of ~~the flight of~~ space ship II flight. So, at the beginning of weightlessness the dog hanged in the air and made an attempt to touch the floor by its paws. As the paws touched the floor the dog strained all its muscles. The hind paws after one short-time impulse developed constant static stress which firmly fixed the dog's position. All this shows the complete retention of rapid and adequate reactions of the animal to such an unusual stimulant as weightlessness is.

Analysis of television close-ups and of telemetry information approximately in 12 hours of flight under weightlessness did not reveal any significant disorders of the coordination of the dog's motions. The absence of the support made the dog's motions not always rapid, since the paws sometimes slid on the floor. It is natural that for a short time interval it is difficult to expect total automatization of various motions caused by different situations.

However, a definite tendency was observed to automatization of some repeated simple motions, for instance, motions at the fixations of the body position.

Analysis of stresses developed by the animal under weightlessness for fixation of the body has shown that after several hundreds of exercises the animal begins to solve this problem with minimum waste of energy (Zhuravlev).

It should be added that the definite spontaneous pulsation of the muscles of the back extremities of the guinea pig which had been aboard space ship IV was observed during the first ten days after recovery to Earth. These changes turned to be little expressed in control animals and were observed only

Declassified in Part - Sanitized Copy Approved for Release 2011/12/08 : CIA-RDP80T00246A016600420001-1

Declassified in Part - Sanitized Copy Approved for Release 2011/12/08 : CIA-RDP80T00246A016600420001-1

during the first days after recovery to laboratory.

The state of the high nervous activity of two laboratory rats which made their flight aboard space ship II was investigated. The motor-food technique did not reveal changes as compared to the control animals. The conditioned reflexes of the above-mentioned guinea pig did not change too.

The data obtained made it possible to suppose that functional changes in the central nervous system apparently were limited to the sphere of the motor apparatus (Lifshits N.)

Prolonged investigations of test animals after flight and observation of their behaviour did not reveal any pathological disorders or changes of physiological functions. One of the test animals (Strelka) brought posterity twice which turned to be healthy and develops normally.

1.3. Biochemical investigations. A combination of biochemical tests considerably varying under the action of stress-factors and ionizing irradiation was used to study biological action of space radiation and other factors of flight.

The albumine composition of the blood, its non-specific cholinesterase activity, the content of 21-oxy-20 ketosteroids and intermediate products of the metabolism of nucleic acids (desoxycytidin and other substances) in urine.

Biochemical changes of different intensity were revealed (5) when dogs were tested and also before and after flight in geophysical rockets and ships-satellites.

Declassified in Part - Sanitized Copy Approved for Release 2011/12/08 : CIA-RDP80T00246A016600420001-1

Declassified in Part - Sanitized Copy Approved for Release 2011/12/08 : CIA-RDP80T00246A016600420001-1

So, after one effect under laboratory conditions (6-9 units, 1.5 min) or vibrations (70 Hz, amplitude 0.4 mm, 5-12 min.) during 1-6 days an increase of non-specific activity of cholinesterase and a decrease of the concentration of serum mucoids in the blood were observed. These changes testify to activatinn of the function of the liver and other systems of the organism.

In contrast to this at multiple actions of the above mentioned factors in a number of cases the dystrophic condition was revealed for which a stable increase of the concentration of serum mucoid and alpha-2- globulins in the blood was typical and also a decrease of the total quantity of protein at the expense of albumin fraction. Such changes were observed after a series of flights made by animals aboard high-altitude geophysical rockets.

Examination of two dogs, which made short-term (one circuit) flights aboard ships-satellites IV and V, did not reveal any disorders in the metabolism as compared to the control (reference) group of animals.

Analysis of the blood and urine of the tested dogs, rats and mice which made a 24-hour orbital flight revealed changes due to the stress reaction in two-six days after recovery. Analysis of the dogs revealed an increase of alpha-globulin serum mucoid and general protein of the blood and a decrease of cholinesterase activity. At the same time no considerable disorders in the metabolism of nucleic acids were revealed.

Declassified in Part - Sanitized Copy Approved for Release 2011/12/08 : CIA-RDP80T00246A016600420001-1

Declassified in Part - Sanitized Copy Approved for Release 2011/12/08 : CIA-RDP80T00246A016600420001-1

Examination of animals during the year after flight showed retention of the above indices within the limits of the norm.

Apparently single short-term space flights of animals do not cause irreversible changes of metabolism characteristic of stress-reactions.

Analysis of peripheral blood of test dogs, rats and mice did not show any pathological changes of white and red elements of the blood and the content of hemoglobine. In a number of cases after flight rapidly disappearing variations of the number of leucocytes were revealed.

1.4. Immunological investigations (O.Alexeyeva) have shown that one-time action of accelerations and vibrations effect chiefly the absorbing function of neutrophils. For instance, acceleration of 2 units leads to activation of the phagocytic ability, and acceleration of 6-12 units reduces not only absorbing, but also digesting ability of neutrophils. Bactericide properties of the skin relative to *E.coli* increase as a result of accelerations and vibrations.

No change of the natural cutaneous microflora and bacterocide properties of the plasma at the said actions was observed.

After flight aboard space ship II wave-like variations of the indices of the immunobiological reactiveness of both dogs were observed when the periods of depression of antimicrobe functions alterated with their activation.

The decrease of the number of microbes on the skin, the increase of bactericide property of the skin and the

Declassified in Part - Sanitized Copy Approved for Release 2011/12/08 : CIA-RDP80T00246A016600420001-1

Declassified in Part - Sanitized Copy Approved for Release 2011/12/08 : CIA-RDP80T00246A016600420001-1

activation of the phagocytic function of neutrophils should be considered as the most significant change of the dog's reactiveness.

In one-two months immunological reactiveness reached the level of average indices. The wave-like, but less expressed change of the reactiveness is revealed in dogs which made flights aboard space ships satellites IV and V. Remarkable is the fact of decreasing the immunological reactiveness of the animals at repeated effects after training.

1.5. Cytological and histological investigations (6) were conducted at sexually ripe mices of both sexes (breedless and of pure C57 line). Blood-forming organs, the central nervous system, the heart, respiration organs, etc., were analysed.

In the cells of the marrow of the mice which were aboard space ship-satellite II an increase of chromosome violations was revealed at the stage of the anaphase of mitotic division as compared to the control. For instance, the chromosome violations of the test party of animals amounted to 7-10% of the number of the cells investigated versus 3% revealed in control animals.

Considerable was also the difference in the chromosome violations of the cells of the marrow of the mice which made space flight and were irradiated by gamma-rays and neutrons of the total dose of 50 röntgens.

In the cells of the marrow of the mice which returned from flight fragmentation was almost completely absent at

Declassified in Part - Sanitized Copy Approved for Release 2011/12/08 : CIA-RDP80T00246A016600420001-1

Declassified in Part - Sanitized Copy Approved for Release 2011/12/08 : CIA-RDP80T00246A016600420001-1

the chromosome reconstructions and the chromosome violations were apparently not the result of the rupture of chromosomes, but of their sticking and consequent incorrect divergence.

Besides, the morphological analysis of the mice' marrow revealed an increase of mielopoese with the appearance of young forms and also the depression of eritropoese. No deviations from the norm were detected as far as the peripheral blood of these animals was concerned.

Histological investigations of the spleen of mice showed the depression with the consequent recovery of the blood-forming function of this organ.

At the same tine cytological, histological and morphological investigations of the marrow of mice which made short-time flights aboard space ships - satellites IV and V did not reveal expressed changes as compared to the control group.

The results of experiments specially set for elucidation of the influence of accelerations and vibrations on blood-forming organs have shown that such mechanical factor as vibrations is capable of causing the chromosome sticking and also changes in the morphological picture of the marrow.

In investigating of cutateous transplantates exposed on space ships-satellites (7) and then reimplanted to donors the degree of vitality is revealed identical to control specimens.

Declassified in Part - Sanitized Copy Approved for Release 2011/12/08 : CIA-RDP80T00246A016600420001-1

Declassified in Part - Sanitized Copy Approved for Release 2011/12/08 : CIA-RDP80T00246A016600420001-1

The expositions of oil-acid bacteria in automatic devices-bioelements in space ships made it possible to evaluate the suitability of this method for characterizing the action of space flight factors in long-term flights.

The investigation of the cultures of E.coli K-12,B and aerogenes has shown that the number of vital specimens in experimental cultures is practically equal to the control. No significant changes of biological and hereditary peculiarities were revealed in other microorganisms exposed in space ships in short-term and 24-hour flights.

1.6 Genetic investigations were made aboard all ships-satellites and revealed some hereditary changes in different organisms. For instance, dry seeds of onion and nygella differing in radio-sensitivity more rapid growing of the seeds of the test group is established as compared to the control one which remained at the Earth. The stimulating effect turned to be more expressed in radio stable nygella. It is obvious that the reason of the effect observed should be sought not in radiation, but in some other factors acting in space flight which are very unusual for the life of seeds on the Earth (8).

A significant acceleration of the processes of cellar division was revealed in sprouts of the pea, maize and wheat seeds which made a flight aboard ships-satellites. But especially considerable changes in the development were observed in radiant fungi cultures exposed in the cosmos. The vitality of the radiostable stamm (the number of out-

Declassified in Part - Sanitized Copy Approved for Release 2011/12/08 : CIA-RDP80T00246A016600420001-1

Declassified in Part - Sanitized Copy Approved for Release 2011/12/08 : CIA-RDP80T00246A016600420001-1

lived spores and developed colonies) increased by six times as compared to the control while the vitality of the radiosensitive stamm on the contrary decreased by 12 times (9).

The influence of the flight aboard space ships-satellites on the heredity of fruit-flies was investigated (10) with the use of three tests: 1) the frequency of the recessive lethal mutations in X-chromosome; 2) the frequency of the dominant lethal mutations leading to the death at the early stage; 3) primary indivergence of chromosomes.

Under conditions of flight two lines of the fruit-fly (Domodedovo-12 and Domodedovo - 18) were exposed whose mutageneous effect after flight was characterised by statistically reliable increase of the frequency recessive lethal mutations coupled with sex. The flies of the D-18 line turned to be more sensitive to mutageneous effect. The point character of the induced mutations and the increased frequency of the mutation of spermatides as compared with spermias apparently indicate the possible influence of space radiation.

As can be judged by the results of several series of experiments, the maximum genetic changes as compared to the control turned to be the following: the indivergence of chromosomes by four times, chromosome reconstructions by 3.5 times, gene mutations by about 10 times.

Analysis of these phenomena on the basis of additional laboratory experiments gives reasons to believe that the increase of genetic changes of the chromosome reconstructions type can be connected with dynamic factors of

Declassified in Part - Sanitized Copy Approved for Release 2011/12/08 : CIA-RDP80T00246A016600420001-1

Declassified in Part - Sanitized Copy Approved for Release 2011/12/08 : CIA-RDP80T00246A016600420001-1

flight. As far as chromosome indivergence is concerned, suppositions are expressed on the connection of this phenomenon with the state of weightlessness. However, the considerable increase of gene mutations not in all cases is correlated strictly with the duration of space ship flight. Due to this the genetic changes cannot be at present definitely ascribed to any single factor. Apparently a more ~~careful~~ modest conclusion should be drawn, namely, the changes of the heredity of ~~the~~ organisms can occur under the influence of the complex of flight factors.

Considering the material obtained on ships-satellites and processed at present it is possible to come to the conclusion that we have no convincing data at our disposal about ~~h~~unfavourable biological action of space flight. However, it should be borne in mind that these data should be considered as preliminary and referring to the used biological objects, indices and methods of investigations. Further work is in store to conduct a complete analysis of the whole material obtained. Besides, it should be remarked that present conclusions are valid only for concrete conditions of the conducted flight experiments since the orbits of space ships-satellites were below the Earth's radiation belts, and the duration of flight was relatively short.

As a result of flight experiments with animals aboard space ships-satellites scientific data were obtained which made it possible to draw the conclusion about the possibility of manned space flight.

Declassified in Part - Sanitized Copy Approved for Release 2011/12/08 : CIA-RDP80T00246A016600420001-1

Declassified in Part - Sanitized Copy Approved for Release 2011/12/08 : CIA-RDP80T00246A016600420001-1

A program of the selecting and training of cosmonauts was carried out simultaneously with the medico-biological experiments with animals.

Pilots Y.A.Gagarin and H.S.Titov were chosen for the realization of the first flights.

2. Medical Investigations During Experimental Flights of Space Ships Vostok.

The first flights of the astronauts were made in paths already tested in launchings of space ships with animals aboard. Animals in this case were specific indicators of danger. Close investigation of animals during flight and after recovery to Earth enabled us to conclude that there are no considerable changes dangerous for life and health of cosmonauts.

Thus, the first manned space flights were realised in the order of the logical succession when each step is the natural consequence of the previous one.

The life-sustaining systems of ships-satellites "Vostok" were tested in numerous laboratory experiments and then tested practically in a series of flight biological experiments with animals.

A combination of physiological methods and the corresponding medical research apparatus was used in order to make studies of the influence of space flight factors on the cosmonaut's organism. The information was telemetered to Earth, processed rapidly and closely analyzed. In choosing the methods of investigations and the telemetry

Declassified in Part - Sanitized Copy Approved for Release 2011/12/08 : CIA-RDP80T00246A016600420001-1

Declassified in Part - Sanitized Copy Approved for Release 2011/12/08 : CIA-RDP80T00246A016600420001-1

measur ements program specific conditions of flight experiments should be taken into account.

During Gagarin and Titov's flights physiological methods were used chiefly for the purposes of physician's control. Methods of electrocardiography and pneumography were slected. Special medical apparatus on semiconductors worked out for these flights was at first tested in flight experiments aboard ships-satellites IV and V.

Gagarin's Flight

Before the launch, at all the portions of the flight trajectory and after it the astronaut's health was satisfactory. Exceptional self-control, calmness and adequacy of reactions attracted the attention of those who observed him. It is very characteristic that 30 minutes before the lift-off the heart rate was amounted to 66 beats per minute, the respiration rate was 24 per minute. Three minutes before the launching Gagarin was calm and concentrated; however, some emotional strain was revealed in the pulse increase to 109 beats per minute, the respiration was smooth and calm. After lift-off during the gradual increase of velocity of the ship the heart rate increased to 140-158 beats per minute, the respiration rate was 20-26.

The changes of physiological indices at the boost stage were within permissible limits. No pathological symptoms were revealed. The powered portion of the flight was

Declassified in Part - Sanitized Copy Approved for Release 2011/12/08 : CIA-RDP80T00246A016600420001-1

Declassified in Part - Sanitized Copy Approved for Release 2011/12/08 : CIA-RDP80T00246A016600420001-1

endursed by the spaceman satisfactorily. He maintained radio communications with the Earth, successfully fulfilling the flight program. By the end of this period the heart rate decreased to 109 beats and the respiration rate reduced to 18 per minute.

In the transition to weightlessness and during the flight in this state the indices of cardiovascular system and of respiration gradually approached the initial values.

Y.Gagarin pointed out some unusual sensations under conditions of zero-gravity, though no disorders of functions were observed, he felt and performed his program well.

At the present stage at the retardation of the vehicle when, as at the boost stage of the flight, overloads again took place, short-term, rapidly disappearing periods of the respiration rate were observed. However, when he approached the Earth his respiration became not frequent, smooth and calm. In three hours after landing indices were fixed characteristic of the normal, calm condition of the space pilot.

While analysing physiological data some changes of individual indices were observed characteristic of each of the stages of the flight. All these changes do not go out of the limits of the variations of indices observed in the course of the trainings of the astronaut and cannot be considered pathological. It is rational, however, to conduct more detailed analysis of the revealed changes which can be useful for elucidating the influence of the mechanisms of physiological reactions on the action of

Declassified in Part - Sanitized Copy Approved for Release 2011/12/08 : CIA-RDP80T00246A016600420001-1

Declassified in Part - Sanitized Copy Approved for Release 2011/12/08 : CIA-RDP80T00246A016600420001-1

space flight factors.

Attention should be focussed on the most expressed changes of individual physiological indices, such as:

a) At the prelaunching stage — the pulse increase, the decrease of PQ, QRS and QT intervals , the increase of the systolic index.

b) At the beginning of the boost stage - the pulse increase, the decrease of intervals PQ, QRS, QT, the increase of the wave P_2, the decrease of the wave R, the decrease of respiration, the increase of the amplitude of the pneumogram.

c) At the end of the boost stage — the decrease of the pulse and respiration, the increase of the interval, the decrease of waves P2 and T2, the increase of the wave R2, the decrease of the amplitude of the pneumogram.

d) At the beginning of the orbital flight - the gradual decrease of the pulse, the lengthening of the intervals PQ, QRS,QT, the increase of T, the increase of P2, the gradual increase of the respiration amplitude.

e) At the end of the orbital flight - the decrease of PQ, the decrease of P2 and T2.

f) At the beginning of the descent portion-the increase of the pulse, the lengthening of PQ, QRS and QT intervals, the increase of the systolic index. Changes of the pulse rate of the respiration frequency and amplitude, changes of the amplitude of the waves of the electrocardiogram are the most essantial. The dynamics of the time intervals of the electrocardiogram apparently is connected with the dynamics

Declassified in Part - Sanitized Copy Approved for Release 2011/12/08 : CIA-RDP80T00246A016600420001-1

Declassified in Part - Sanitized Copy Approved for Release 2011/12/08 : CIA-RDP80T00246A016600420001-1

of the pulse frequency and is determined by extracardiac nervous-reflex effects. The lengthening of the time intervals of the electrocardiogram at the beginning of the descent draws one's attention.

Scientific results of the first manned space flight were as follows:

1. The orbital space flight which lasted for 108 minutes (including the portions of the boost stage and descent) did not cause any physiological deviations harmful to the cosmonaut's health and life.

2. All physiological changes are connected with the direct action of the combination of factors and with nervous emotional strain. They had in the main the character of adaptation reactions. Similar, though less definitely expressed reactions were observed during training in the centrifuge and other stands.

3. At all stages of the flight no disturbances of the space pilot's working capacity and health conditions were observed.

2.2 Titov's Flight

Since the program of the flight experiment was designed for 24 hours it was necessary to increase the number of objective methods for investigating the cosmonaut's condition in flight. The use was made of a number of methods to estimate the reactions of the vestibular apparatus, some psycho-physiological tests were conducted, and also the technique was used for investigating the mechanical

Declassified in Part - Sanitized Copy Approved for Release 2011/12/08 : CIA-RDP80T00246A016600420001-1

Declassified in Part - Sanitized Copy Approved for Release 2011/12/08 : CIA-RDP80T00246A016600420001-1

function of the heart-the cynetocardiogram.

The dynamics of the pulse frequency and the respiration rate at the boost and descent stages did not differ considerably from the data obtained during training.

Under conditions of orbital flight the indices of the pulse and respiration frequencies in average approached the initial pre-launching values, but were characterized by greater variability. Some changes of the mechanical function of the heart were observed, however, these data require further analysis.

The space pilot in general felt well. He fulfilled the flight program fully, maintained communication with the Earth, performed operations connected with the ship orientation, carried out cinema shooting and other kinds of activity. No noticeable disorders in the coordination of motions were observed. At the same time after the active portion of the flight ended and at the transition to the state of weightlessness, Titov marked a short time illusion of turning "the head down" position. Then when the flight continued under weightlessness unpleasant sensations appeared and then increased. These sensations resembled the motion sickness (giddiness, nausea). These phenomena increased at sharp movements of the head.

The sleep was at first restless, the appetite decreased. The paste-like food and water by means of special tube were taken without any difficulties. Urination was free, the technical devices functioned normally.

There are reasons to believe that giddiness, nausea,

Declassified in Part - Sanitized Copy Approved for Release 2011/12/08 : CIA-RDP80T00246A016600420001-1

Declassified in Part - Sanitized Copy Approved for Release 2011/12/08 : CIA-RDP80T00246A016600420001-1

the decrease of the appetite were the results of the change of the activity of nervous regulatory mechanisms which appeared under zero-gravity due to the interaction of a number of afferent systems.

At present a special theoretical and experimental studies of this problem are being made.

When Titov limited head movements and took an initial concentrated position, these phenomena decreased and almost disappeared. They reduced considerably after sleep and disappeared completely after the beginning of the action of overloads while recovering to the Earth.

The main scientific outcome of Titov's flight is the establishment of practical possibility of the stay in outer space during 24 hours without disturbances of the working capacity and the state of the main physiological functions.

2.3. The flight experiments with animals and the first manned space flights have made it possible to conclude that the general direction of scientific investigations aimed at utilization of outer space was correct. At present the following problems should be investigated in the first place: the effect of long-term radiation, the action of overloads after the stay under zero-gravity and the influence of the whole combination of factors on the organism including the state of emotional strain.

It should be pointed out that new space paths should be chosen on the basis of scientific data stored to the present time as a result of flight experiments with animals and first manned space flights.

Declassified in Part - Sanitized Copy Approved for Release 2011/12/08 : CIA-RDP80T00246A016600420001-1

Declassified in Part - Sanitized Copy Approved for Release 2011/12/08 : CIA-RDP80T00246A016600420001-1

Different biological objects should be used as indicators of possible harmful actions in outer space.

While interpreting the biological and genetic data obtained aboard satellites and space ships ~~and genetic data~~ it should be kept in mind that the organisms and the environment present the inseparable unity. Therefore, it is necessary to try to reveal hereditary changes, and adaptive phenomena which always accompany the evolution process wherever it takes place.

Further biological investigations of outer space, the collection of new materials and correct theoretical analysis of them will be the important condition of successful solution of numerous problems of space biology and medicine.

Declassified in Part - Sanitized Copy Approved for Release 2011/12/08 : CIA-RDP80T00246A016600420001-1

Declassified in Part - Sanitized Copy Approved for Release 2011/12/08 : CIA-RDP80T00246A016600420001-1

References

1. Bugrov B.G., Gorlov O.G., Petrov A.V., Serov A.D., Yugov E.M., Yakovlev V.I., Preliminary Results of Scientific Investigations by Means of the First Soviet Artificial Earth Satellites and Rockets, 1958, p.130.

2. Galkin A.M., Gorlov O.G., Kotova A.R., Kosov I.I., Petrov A.V, Serov A.D., Chernov V.N., Yakovlev V.I., Preliminary Results of Scientific Investigations by Means of the First Soviet Artificial Earth Satellites and Rockets, 1958, p.112.

3. Chernov V.N., Yakovlev V.I., Artificial Earth Satellites, 1959, Vol.7, p.80.

4. Gazenko, O.G., Space Research II, 1961, 656.

5. Gyurdzhian A.A., Demin N.N., Korneyeva N.V., Lvova T.S., Tutochkina L.T., Uspenskaya M.S., Fyodorova T.A., Artificial Earth Satellites, 11, 78, 1961.

6. Arsenyeva M.A., Antipov V.V., Retrukhin V.G., Lvova T.S., Orlova N.N. Ilyina S.S., Artificial Earth Satellites, Vol.10, p.82, 1961.

7. Zhukov-Verezhnikov, N.N., Maisky I.N., Yazdovsky V.I., Pekhov A.P., Gyurdzhian A.A., Artificial Earth Satellites, Vol. 11, p.42, 1961.

8. Sidorov B.N., Sokolov N.N., Artificial Earth Satellites, Vol.10, p.93, 1961.

9. Glembotsky, Ya.L.Prokofyeva-Belgkovskaya, A.A. Shamina Z.B., Goldat S.Yu., Khvostova V.V., Valeva S.A., Eiges N.S., Nevzgodina L.V., Artificial Earth Satellites, Vol.10,p.72,1961

Declassified in Part - Sanitized Copy Approved for Release 2011/12/08 : CIA-RDP80T00246A016600420001-1

Declassified in Part - Sanitized Copy Approved for Release 2011/12/08 : CIA-RDP80T00246A016600420001-1

10. Glembotsky, Ya.L., Abeleva E.A., Lapkin Yu.A., Parfyonov G.P., Artificial Earth Satellites, Vol.10, p.61, 1961.

Declassified in Part - Sanitized Copy Approved for Release 2011/12/08 : CIA-RDP80T00246A016600420001-1

Declassified in Part - Sanitized Copy Approved for Release 2011/12/08 : CIA-RDP80T00246A016600420001-1

27.

"ON PERSPECTIVES OF DEVELOPMENT OF EXOBIOLOGY"

By A.A.IMSHENETSKY

Advances in physics, mathematics and engineering have made exploration of space a reality. This resulted in emergence of several new scientific branches, among which an important place belongs to exobiology - a science studying existance and spread of life beyond the Earth, its characteristics, as well as effects of space factors on living creatures.

Exobiology has attracted attention of biologists working in various fields: genetics, general biology, microbiology, biochemistry, virology. In periodic press appear articles dealing with various problems of exobiology, but most of them are purely theoretic and contemplative in character. An obvious disbalance is felt between all-over biological generalizations and consideration of possible methodic approaches and experiments in this field. It is because of this feeling that present report is directed completely to discussion of items connected with experimentation in exobiology at present or in the nearest future. This seems more appropriate also since theoretical analysis of contemporary state of the problem has already been given in several publications (by Lederberg, Sagan, Briggs, Beckerel, Vishniak) as well as in Dr.Florkin's report which we have heard at this conference.

I. DETECTION OF EXTRATERRESTRIAL LIFE

Initial statements. Until first experimental evidence on existence of extraterrestrial life and metabolism of cosmobiontes is obtained, we have to proceed from theoretic premisses, analogies and present knowledge about temperature and other conditions on planets or in space.

Declassified in Part - Sanitized Copy Approved for Release 2011/12/08 : CIA-RDP80T00246A016600420001-1

Declassified in Part - Sanitized Copy Approved for Release 2011/12/08 : CIA-RDP80T00246A016600420001-1

We believe however that, whatever the direction of studies, the experimenter must use at first, the conceptions of life and criteria of living and non-living, which we use when studying living objects on earth. It is sometimes pointed out in articles that cosmobionts are feasible which contain no carbon, that biological systems may exist based on silicium or germanium compounds, that water may be replaced by other solvents such as glycols, etc. It would be utterly unwise to make no attempts to detect living forms analogous to terrestrial creatures in structure and way of life, the more so, since it is not excluded that life phenomena are possibly not so multiple as it is sometimes suggested. In any case, it is only when our efforts to find living forms similar to terrestrial ones fail, that we should change radically programs and methods of study and search for living forms principally different from those existing on earth. Undoubtedly, chemical analysis data on atmosphere and ground composition of planets as well as accurate data on environment, which will be obtained by that time, will greatly help us in planning new directions of study.

2. Biochemical analysis. Of no less interest, than the detection of living creatures, is the possibility of discovery in cosmos of chemical substances characteristic of living organisms. It may be supposed that such substances originate from simpler chemical compounds under the influence of physical factors, and that their appearence corresponds to the "organic substance evolution" which was discussed in detail at the Symposium on the origin of life held in Moscow in 1959. Detection of such substances on a planet bearing no life could throw light on that aspect of origin of "living matter" which at present is most difficult to explain.

Declassified in Part - Sanitized Copy Approved for Release 2011/12/08 : CIA-RDP80T00246A016600420001-1

Declassified in Part - Sanitized Copy Approved for Release 2011/12/08 : CIA-RDP80T00246A016600420001-1

It may be argued very much what compounds are most characteristic of life and what should be looked for in the first place. It seems to us that most founded would be attempts to detect organic phosphorus compounds, porphyrins and amino-nitrogen. It is quite likely however that some explorers will consider it more demonstrative to detect other compounds. In any case, prime attention should be paid to construction of instruments, small in size and capable of analysing planets' surface for possible presence of various organic substances and of transmitting the analytical data to the earth. Naturally, this will require a preliminary comparative examination of a number of analytical methods suitable for particular environment.

3. Methodic difficulties. A most obvious hazard in the search for living creatures in space and on planets is the possibility that as a result of technical failure the explorer will isolate terrestrial microorganisms which penetrated and multiplied in the nutrient media used. There are microbiological studies very similar in character to those connected with detection of life in cosmos. I mean microbiological analysis of rocks, meteorites, soil samples from areas of eternal congelation, large stone-salt pieces, etc. In literature there is no lack of reports claiming isolation from such samples of organisms supposed to have been in anabiotic state for hundreds thousand and millions of years. Unfortunately, all such reports do not stand criticism from technical point of view. When reports were published that living bacteria, algae and other forms were revealed upon thawing of soil samples taken in Siberia in areas of eternal congelation, the Institute of Microbiology of the Academy of Sciences organized a special expedition.

Declassified in Part - Sanitized Copy Approved for Release 2011/12/08 : CIA-RDP80T00246A016600420001-1

Declassified in Part - Sanitized Copy Approved for Release 2011/12/08 : CIA-RDP80T00246A016600420001-1

The expedition took monoliths from eternal frost levels using an electric saw in such a way that contamination with organisms penetrating from upper layers with filtering water was excluded, and transported samples by planes. Inoculation with such samples of numerous different nutrient media failed to reveal any living organisms.

All this goes to show that microbiological analysis of cosmic samples should be made with irreproachable technic so as to avoid completely contamination with terrestrial forms during taking a sample or its analysis.

4. Microbiological studies of meteorites.

The importance of technic may be further illustrated by results of microbiological analysis of meteorites. The possibility of transport of living germs to the earth with meteorites was admitted by such prominent scientists as Helmholtz, Van Tieghem, Sir Kelvin, Richter. But it should not be overlooked that with few exceptions meteorites remain lying in the ground for more or less long periodes before they are taken for examination. During that time various organisms penetrate inside the meteorites together with soil water. Subsequent thorough washing of samples with antiseptics or flaming them kill only cells remaining on the surface. Inoculations with powdered meteorites give rise to growth of various coccal, spore-forming and non-spore-forming bacteria, which had been without any foundation considered by Lipman as "inhabitants of meteorites". This equally applies to positive results obtained in other similar studies. It should be reminded here that Pasteur used a specially constructed probe for obtaining samples from a carbon meteorite which fell in I864 in d'Orgueil. He failed to isolate living organisms upon inoculation.

Thus, the question of possible presence of viable cells in meteorites remains open. Isolations free of technical fault would be, therefore, of great scientific interest.

Declassified in Part - Sanitized Copy Approved for Release 2011/12/08 : CIA-RDP80T00246A016600420001-1

Declassified in Part - Sanitized Copy Approved for Release 2011/12/08 : CIA-RDP80T00246A016600420001-1

5. Physiology of possible cosmobiontes.

Despite the microbiological studies with stratostats carried out to-date, the upper limit of earth's biosphere has not been established. It may be assumed theoretically that terrestrial microorganisms are, possibly, carried up to altitudes of dozens of kilometers. Investigations in that direction are immediately related to the problem of life export and import, that is the problem of interplanetary transport of germs. In such studies, however, the experimenter deals only with terrestrial forms. Of much greater interest for general biology is the problem of physiology of microorganisms inhabiting other planets.

At present the overwhelming majority of biologists are inclined to support the idea that chemo- and photo-autotrophs evolved as a result of specialization of function and have more recent origin than heterotrophs. Formation by purely chemical ways of various organic substances made existence of heterotrophs possible. Search for the latter organisms will comprise, therefore, the first task, and physiological distinctions of heterotrophs will determine methods of their detection. It is quite possible that simultaneously with that group can exist forms utilizing oxygen of nitrates or sulphates, that is denitrifying and desulphurating bacteria. Their detection should also be planned following experiments on detection of heterotrophs. The absence of oxygen in atmosphere of Mars suggests that there may exist exactly photosynthetic bacteria, which, in distinction to higher plants, evolve no oxygen.

Conditions for life on planets may be quite different and sharply distinct from those existing on earth. Discussing possible bearing of such environments one should set more hopes on creative role of selection, rather than resort to particular examples of resistance among terrestrial microorganisms.

Declassified in Part - Sanitized Copy Approved for Release 2011/12/08 : CIA-RDP80T00246A016600420001-1

Declassified in Part - Sanitized Copy Approved for Release 2011/12/08 : CIA-RDP80T00246A016600420001-1

Since among thermophile bacteria existing on earth are known cell species, which tolerate a hundred-hour boiling, there is ground to suppose as real an adaptation to even higher temperatures, than the maximal growth temperature of terrestrial thermophiles. Similarly, higher resistance to various kinds of radiation may be supposed. Some time ago we have shown a protective role of carotenoids, since pigmented forms of bacteria proved to be more resistant to ultraviolet radiation. It is not excluded that even more effective protection mechanisms have been developed as a result of adaptation by living forms unknown to us. It is well known to microbiologists that deserts are inhabited by xerophile actinomycetes and fungi which proliferate in substrate with very low water content. There is no reason to deny the possibility of existence of organisms with still lower water requirements. Ecology of cosmobiontes is a science of the future, but we have sufficient reason to admit the possibility that cosmobiontes can be adapted to even more extreme environments than terrestrial forms.

6. Methods of detection of cosmobiontes.

Whatever method may be used for detection of microorganisms beyond the earth some requirements of general character should be observed. An instrument selected must be sensitive enough to detect presence of populations relatively small in cell number. On the other hand, sending positive information not connected with presence or development of microorganisms should be excluded. The device must be small in size, not exceed certain weight and capable to detect possibly larger number of species with different physiology. For detecting viable microorganisms a number of methods can be used. Let us consider some of them.

Declassified in Part - Sanitized Copy Approved for Release 2011/12/08 : CIA-RDP80T00246A016600420001-1

Declassified in Part - Sanitized Copy Approved for Release 2011/12/08 : CIA-RDP80T00246A016600420001-1

I. A direct microscopy method, in particular that proposed by Lederberg, is undoubtedly interesting, but it is complicated and will not allow to detect the presence of small numbers of germs.

2. A method consisting in inoculation of a liquid nutrient medium with samples of atmosphere or surface of a planet, and tracing prolipheration with nephelometric means. Among undesirable aspects of such a method is possible development of turbidity in the medium from reasons not connected with multiplication of microbs. For instance, mineral particles may be introduced, or composition of the medium may change with formation of precipitate from action of some physical or chemical factors, and so on.

3. Methods of inoculation of samples obtained and automatic registration of pH changes resulting in the medium from multiplication of organisms.

4. Inoculation of atmosphere or surface samples of a planet in a liquid medium and manometric determination of pressure differences developed by respiration or fermentation of multiplying organisms.

5. Similar inoculation of samples in a liquid medium containing carbon-labelled compounds. Dissimilation of the latter will produce labelled carbon dioxide which is registered with a counter.

6. A method based on inoculation of samples obtained onto the surface of solid nutrient media and subsequent development of colonies. The images of colonies and, possibly, microscopic picture of cells comprising a colony can be transmitted to earth.

Naturally, other methods of detecting microorganisms are possible, but we should bear in mind that a better-founded choise of media composition and cultivation regime can be made only with gaining of more accurate and reliable data on conditions existing on a particular planet.

Declassified in Part - Sanitized Copy Approved for Release 2011/12/08 : CIA-RDP80T00246A016600420001-1

Declassified in Part - Sanitized Copy Approved for Release 2011/12/08 : CIA-RDP80T00246A016600420001-1

II. EFFECTS OF COSMIC FACTORS ON MICROORGANISMS

Most accessible for exobiology remain studies in which effects of cosmic conditions on living cells are determined experimentally. Such modelling on earth is much easier to do than to carry out repeated launchings of microb or tissue cultures into space.

It may be considered established that bacterial spore is most resistant to action of various physical and chemical factors, though the degree of resistance in different species varies greatly. Let us consider briefly those factors which are likely to act upon cells in space or on planets.

Low temperature. It has long been known that microorganisms remain viable after exposure to liquid helium, that is to temperatures close to absolute zero (0,0075°K). It was found later that even higher plants can survive freezing to minus 253° (Toomanoff). Thus, low temperatures do not kill microorganisms, although in the studies mentioned there was no investigation of influence of such low temperatures on subsequent metabolism and genetic properties of the organisms. The question of minimal temperature at which proliferation of living organisms is possible cannot be solved by analogies. In arctic seas and in refrigerators bacteria are found which slowly multiply at -7° to -9°. However, we have no ground to deny categorically the possibility of microorganism growth on other planets at still lower temperature in non-freezing natural media.

High temperature. Terrestrial microorganisms possess protection mechanisms enabling thermophiles to proliferate at 80 - 90°. With sufficiently high salt concentration in hot springs, the boiling point of their water is raised, and this equally applies to mud volcanoes.

Declassified in Part - Sanitized Copy Approved for Release 2011/12/08 : CIA-RDP80T00246A016600420001-1

Declassified in Part - Sanitized Copy Approved for Release 2011/12/08 : CIA-RDP80T00246A016600420001-1

Theoretically it is quite probable that unicellulate organisms are capable of adaptation to still greater temperatures than those at which life is observed in terrestrial conditions.

Vacuum. Experiments connected with influence of vacuum on unicellulate organisms are complicated by our inability so far to reproduce on earth the degree of vacuum existing in space. In biological publications there is plenty information on the effect of vacuum associated with lyophilization of microorganism cultures, the operation so widely used in institutions maintaining collections of type cultures. As regards deep vacuum, the problem remains almost unstudied. According to Portner et al., B. subtilis, Mycobact. smegmatis, and Asp. fumigatus survive exposure for 5 days to a vacuum of $3.6 \cdot 10^{-10}$ mm Hg. Thus, with considerable degree of certainty we may assume that vacuum cannot cause death of microbs in cosmos.

Radiation. The question of the effect of ionizing radiation can be answered comparatively easily, since doses which are likely to act upon organisms in space are below those which were found tolerable in experiments carried out on earth. Without going into detail it may be mentioned that complete sterilization (including killing of spores) requires hundreds of thousand Rentgens, i.e. doses which are not found in cosmos. Ultraviolet radiation is, on the contrary, a most serious sterilizing agent in cosmic conditions. Judging from data of Newell and Naugle on levels of radiation in space, we have to conclude that ultraviolet radiation will cause rather quick death of all known microorganisms, including spores. There remains, however, one possibility uninvestigated. Can a particle of cosmic dust, if it contains a microorganism cell, afford it adequate protection against ultraviolet radiation?

Declassified in Part - Sanitized Copy Approved for Release 2011/12/08 : CIA-RDP80T00246A016600420001-1

Declassified in Part - Sanitized Copy Approved for Release 2011/12/08 : CIA-RDP80T00246A016600420001-1

Size, shape, and composition of cosmic dust collected, for instance, from snow surface in the Arctic make quite probable the suggestion that such particles can serve an effective screen for protecting cells. Unfortunately, we have no experimental evidence bearing directly to this important problem.

Investigation of effects of separate cosmic factors should be supplemented with experiments where all known physical factors of cosmos act simultaneously. Such combined experiments will help to reproduce ecological conditions existing in space. Speaking of physical and chemical factors active in cosmos we proceed only from evidence available at present. It would be bold to state that we know all such factors well. It is not excluded that living cells acting as biological indicators, whose sensitivity quite often exceeds that of physical and chemical analytical methods, will facilitate discovery of still unknown factors harmful to living creatures.

III. STERILIZATION OF COSMIC ROCKETS AND SPACE SHIPS.

At meetings like this one it is unnecessary to emphasize the importance of absolute sterilization of space ships, especially those directed to other planets. Principal considerations bearing to this problem have already been set forth in the several statements worked out and published by the CETEX.

I shall, however, permit myself to mention some details of the problem because common point of view seems to be lacking.

I should like to object, first, to suggestions that transport of single viable germs to other planets may be permitted. Such reduction of requirements can lead to quite unexpected and undesireable consequences. It is too well known to microbiologist that there is no principal difference between transport of dozens or thousands of cells.

Declassified in Part - Sanitized Copy Approved for Release 2011/12/08 : CIA-RDP80T00246A016600420001-1

Declassified in Part - Sanitized Copy Approved for Release 2011/12/08 : CIA-RDP80T00246A016600420001-1

All depends on the ecological conditions where the germs will be transported. If the environment appears favourable for proliferation the hazard of introduction of even insignificant number of cells can be very great. Sterilization, therefore, must be complete and irreproachable.

Secondly, one cannot agree with suggestions that infection of the Moon with terrestrial microorganisms does not constitute a hazard, as they will not multiply on the Moon.

Next, it should be pointed out that it is impossible to sterilize rockets and space ships in such a way that they contained no dead bodies of microorganisms. Thus, the demands that microb "carcasses" were not carried to other planets is practically unrealizable. It may be supposed that introduction of killed bacteria on other planets will not constitute a hazard. The chance of these bodies being revealed in the ground of a planet by direct microscopy methods is not high. Also,it is unlikely that introduction of microb "carcasses" on planets possessing no life of their own will influence the cource of "chemical evolution" and lead to "reproduction" of organic substances characteristic of the Earth and not of the particular planet. There is ground to suppose that negligible amounts of dead protoplasma which can be carried with a space ship to a planet will not impede obtaining accurate information in subsequent analysis.

Fourth, it should be definitely emphasized that cosmic factors, that is radiation, vacuum, and low temperature, will not kill microorgamisms on the surface of cosmic rockets and space ships. The only logical conclusion is, therefore, to accomplish thorough sterilisation of outer surface of ships which theoretically cannot be sufficiently smooth to provide no shelter for bacterial spores against ultraviolet radiation.

Declassified in Part - Sanitized Copy Approved for Release 2011/12/08 : CIA-RDP80T00246A016600420001-1

Declassified in Part - Sanitized Copy Approved for Release 2011/12/08 : CIA-RDP80T00246A016600420001-1

As regards methods of actual sterilization, naturally, there is not only one way to free a cosmic ship from microorganisms, Sterilization itself presents some new technical problems: effects of desinfectants or radiation on various materials and instruments inside the ship; elimination of microbs which can get on the ship's surface during flight through the earth atmosphere; determination of optimal conditions for application of a particular sterilizing agent, etc. All these questions are of more practical character and I shall not discuss them.

In conclusion, I would like to make a few further remarks. When Arrhenius put forward his panspermia hypothesis he could not, of course, suppose that most probable means for transferring germs from one planet to another will be cosmic vehicles constructed by man. Reality always surpasses hypothesis. With wonderful advances of science, of which we are witnesses, scientific forecasts have become difficult. But it is certain that exobiological studies bring us nearer to solution of the main problem of biology - that of origin and evolution of life. There are no biologists at present who would dispute the thesis, that microorganisms are not firstlings of life, but specialized forms with complex organization, developed as a result of long evolution. Knowing no other more primitive living forms we direct our exploration of other planets towards detection of microorganisms. We should be prepared,however,to approach a task, much more difficult methodically, namely - to detect living creatures with less complex organization than microorganisms. For the sake of solving such a task one may at the beginning run the risk of some failures and disappointments.

Declassified in Part - Sanitized Copy Approved for Release 2011/12/08 : CIA-RDP80T00246A016600420001-1

Declassified in Part - Sanitized Copy Approved for Release 2011/12/08 : CIA-RDP80T00246A016600420001-1

A.G. Masevitch
Astronomical Council
USSR Academy of ...

31

"OPTICAL OBSERVATION TECHNIQUES" by A G Masevitch

Till quite recently the main base for determinations of the parameters of the gravitational potential of the Earth was given by geodetical and gravimetrical works done on the surface of the Earth. Several limited data could be obtained also from investigating the equations of the motion of the Moon. The launching of artificial satellites opened quite new possibilities for the study of the gravitational potential of our planet. Measurements of angles determining the direction on the satellite from an observing point, direct measurements of distances between the observer and the satellite with radio-technical devices, allow to connect the geocentric (relative to the mass-centrum of the Earth) coordinates of the observer, the mass of the Earth and the parameter of its gravitational potential with momentous (osculating) orbital elements of the satellite and various disturbances of these elements. The appropriate equations connecting all these values form the base of a new method for determination of the absolute coordinates of the Earth's surface, the mass of the Earth and the parameters of its gravitational potential. Depending on the way of the solution of this problem dynamical and geometrical (or "orbital")methods are used. All these methods are now very intensively under de - velopment in different countries. This development is possible along two lines: an improvement of the theorie of the motion of artificial cosmic bodies and the possible increase of the accu -

Declassified in Part - Sanitized Copy Approved for Release 2011/12/08 : CIA-RDP80T00246A016600420001-1

Declassified in Part - Sanitized Copy Approved for Release 2011/12/08 : CIA-RDP80T00246A016600420001-1

racy of observational data obtained.

In this paper I shall discuss the present state of the problem how to obtain precise tracking data of satellites. Although contemporary radio techniques allow in principle to obtain radar tracking data with an accuracy comparable to tracking data obtained with good optical systems [1], best results till now have been achieved by means of photographical tracking. The highest precision has been at present obtained by measuring a photograph of the satellite taken simultaneously with the background stars. Optical observational techniques and some related problems will be therefore the main subject of the present review.

2. TECHNIQUES OF PHOTOGRAPHICAL TRACKING.

When photographs of stars (point sources) are taken the effective power of a telescope depends on the area of the objective lens, on the area of the image (the circle of dispersion) and does not depend on the focal ratio of the objective lens. The effective power is proportional to the ratio D^2/d^2, where D is the diameter of the objective lens and d - the diameter of the image. When photographs of a satellite are taken (a moving body) the effective power of the telescope is determined by the ratio D^2/dF, as the satellite's image moves along the plate with a velocity which is inversely proportional to the focal ratio F of the camera. The relatively fast motion of the satellite shortens its effective exposure time (within parts of a

Declassified in Part - Sanitized Copy Approved for Release 2011/12/08 : CIA-RDP80T00246A016600420001-1

Declassified in Part - Sanitized Copy Approved for Release 2011/12/08 : CIA-RDP80T00246A016600420001-1

second). In order to increase this time the telescope or the plate should be following the satellite. It is also because of the great apparent angular velocity, that satellite tracking data require a very precise fixation of the moment of exposure within $0^{s}.001$. In fact the precision of satellite observations is determined rather by the precision of timing than by precision of coordinate measurements. For satellite tracking new systems of shutters for astronomical telescopes have to be evaluated and sometimes rather substantial modifications of the existing telescopes are needed.

Special cameras for tracking of artificial satellites, designed in the U.S.A., the Baker-Nunn cameras which account for all the mentioned above characteristic features of the satellites, are by now the best available optical techniques for tracking artificial cosmic bodies. With those cameras much valuable informa- has already been achieved. We shall have during this session a special report referring to the satellite service in the U.S.A. I shall, therefore review work done in other countries, with special emphasise to the U.S.S.R., concerning possibilities to use existing astronomical telescopes for precise photographic tracking of satellites with all the necessary auxiliary devices needed for this purpose.

As experience shows, the following photographic technics of satellite observations proves to be most effective.

The mounting of the camera should allow to turn the ca - mera freely round the axis and point it rapidly on a satellite.

Declassified in Part - Sanitized Copy Approved for Release 2011/12/08 : CIA-RDP80T00246A016600420001-1

Declassified in Part - Sanitized Copy Approved for Release 2011/12/08 : CIA-RDP80T00246A016600420001-1

The support must be massive, and clamping screws must be safe for an exclusion of vibrations during photographing. Vibrations (which lead to the appearance of zigzags on a satellite track and widening of star images) distort the results markedly.

Vibration is especially dangerous in the direction of a satellite track because then the zigzags are not detectable by eye, but the result is distorted as before. The opening and closing of a shutter must be done with the equal duration and quickly enough in order that the beginnings and ends of satellite tracks should be equivalent. Inobservance of this condition leads to a considerable systematic error which can not be accounted for during the reduction.

It is desirable to have the possibility to operate the shutter both by hand (at a given moment of time) and regularly by a chronometer or a clock. It is necessary to foresee the determination of the geometric centre of each frame of the film. The simplest way to achieve it is to put with luminous paint marks on the corners of the glass plate of the camera. When the film is pressed to the plate the marks leave an image on the corners of the frame. It is necessary also to know the position of the optical centre relative to the geometric one with the precision of 1-2 mm.

The expositions made should be short and frequent. The most favourable exposure time is 0,08; for in this case it is usually possible to measure directly the middles of the traces,

Declassified in Part - Sanitized Copy Approved for Release 2011/12/08 : CIA-RDP80T00246A016600420001-1

Declassified in Part - Sanitized Copy Approved for Release 2011/12/08 : CIA-RDP80T00246A016600420001-1

instead of their ends. The most favourable intervals between successive expositions for a satellite, which changes its brightness slowly, are $0^{s}.5$ - $1^{s}.0$. Short exposure times are especially necessary when we are photographing satellites, which change their brightness quickly, as the different density of the ends of the traces may lead otherwise to an unaccountable systematic error. Each time when the brightness increases it is expedient to make a number of short expositions symmetrically relative to the maximum of brightness.

When tracking an artificial satellite photographically it should be aimed to receive during one passage several photographs along the longest possible arc of the trajectory. Such observations allow to calculate a momentary orbit using data of one station only. Most valuable are those photographs that are made when the height of the satellite above the horizon is maximal. It is desirable that the satellite track should cross the centre of the plate. Tracks on the edges of the field of sight complicate the reduction enormously and reduce the accuracy.

While photographing objects, that ~~periodically~~ suddenly increase their brightness for a short time, it is necessary to follow the object with a guide and make one or several short expositions by hand at the moment of increasing brightness.

Besides short expositions ~~it is necessary in any case~~ should be made to make additional longer expositions for the stars. When pho-

Declassified in Part - Sanitized Copy Approved for Release 2011/12/08 : CIA-RDP80T00246A016600420001-1

Declassified in Part - Sanitized Copy Approved for Release 2011/12/08 : CIA-RDP80T00246A016600420001-1

tographs are taken with cameras on asimuthal mountings it is expedient to make 2-3 or more expositions with a duration of about 2^s-5^s (depending on the declination of the satellite ($2.^s$ sec), which should be divided by an interval not less than 1' in order to receive the star images in the form of a chain of pints. The long traces of the satellites' track make in this case help to identify it on the film on the tape of the chronographs.

When photographs are taken with cameras on parallactic mounting with clock-work, attention should be paid to the correct work of the clock-mechanism, as even a hardly visible distortion of the star images may be a source of considerable errors.

When photographing bright satellites it is desirable to use a yellow filter in order to improve the image.

While photographing a bright satellite at the background of a bright sky or through clouds it is possible to photograph stars on the same plate afterwards with a fixed camera.

Declassified in Part - Sanitized Copy Approved for Release 2011/12/08 : CIA-RDP80T00246A016600420001-1

Declassified in Part - Sanitized Copy Approved for Release 2011/12/08 : CIA-RDP80T00246A016600420001-1

5. PRECISE DETERMINATION OF COORDINATES.

The method used for reduction of each separate negative depends on the character of the satellite and stars images.

On negatives obtained with fixed cameras the satellite track crosses sometimes the star images.

In this case it is useful to apply a method used in meteor astronomy 4 which consists in measuring the coordinates of the crossing point. The declination of this point equal exactly declination of the star; the moment of the satellite's passage through this point can be determined by means of an interpolation along the track and the right ascention of the star plus the difference of passage times of the satellite and the star through the crossing point.

In cases, when this method cannot be used, but the number of touches on the satellite's track is large enough for an interpolation of the time to be made (that is if there are no less than four touches on an aeria about five degrees), it is appropriate to carry out the reduction with two reper stars. In this case the coordinates of the satellite in a nodal point (the crossing point of the track with the line connecting the reper stars) is determined.

The reduction and the evaluation of equatorial coordinates is carried out in the USSR according to an interpolation method given by A.A.Kiseley 5 ; which provides the necessary precision irrespective the declination of the satellite.

For an declination less than 60° a method given by A.N. Deutsch 6 is more convenient as it implies less calculations to provide the necessary accuracy. When the declination exceeds 60°, terms of the 3^{d} order should be taken into account in this method.

Declassified in Part - Sanitized Copy Approved for Release 2011/12/08 : CIA-RDP80T00246A016600420001-1

Declassified in Part - Sanitized Copy Approved for Release 2011/12/08 : CIA-RDP80T00246A016600420001-1

If it is possible to select four stars and to determine the coordinates of two neighbour nodal points, then one "normal" place can be given as a result. In this case a new nodal point is determined with the help of two stars referring to different couples of reper stars and then its coordinates are found repeatedly in the system of the nodal points obtained before. So nearly 6 touches take part in the creation of the final result, accidental errors are smoothed out and a control of the obtained results is achieved. (the so called N. control") (see 2 ,appendix 3).

If the satellite track is given by a number of separate touches situated far from each other or by groups consisting of 2-3 touches, the above mentioned methods are not suitable chiefly because of the unreliability of time interpolation. In this case the coordinates of the middle of one short touch should be determined. It is even better to join several touches into one. In this case the problem in general does not differ from the usual problem of the determination of the position of a celestial body and the reduction may be done with any of the well_known methods of photographic astrometry applying 3,4 or more reper stars. It must be noted however that the increase of the number of reper stars (above the necessary minimum) for a wide-angle short-focal rate camera does not give considerable advantages in accuracy as precision of photographic positions in these conditions depends mainly on systematic errors of measurements and proection and not on accidental errors. It is in gearal more favourable to take two or three reper stars close to the satellite track, than 5 - 6 reper stars distributed more or less evenly on an two or three times larger area.

It must be taken into account that in the case when the coordinates of a single touch are determined all accidental errors of its given image are completely included and cannot be excluded irrespective of the method used.

Declassified in Part - Sanitized Copy Approved for Release 2011/12/08 : CIA-RDP80T00246A016600420001-1

Declassified in Part - Sanitized Copy Approved for Release 2011/12/08 : CIA-RDP80T00246A016600420001-1

It is most favourable to have the touches as short as possible to be able to measure directly their control points. Otherwise their beginnings as well as the ends should be measured.

The moments of the beginnings and ends of all measured details (satellite and stars) should be marked on the chronograph.

The right ascention of the satellite determined on photographs obtained with fixed cameras should be corrected for the diurnal motion of the sky with the help of the following formulae;

$$+ 0{,}0027$$

where t_{star} is the moment during which the measured part of the star image was photographed, t - the moment of the satellite's passage through the normal point; the correction $0{,}0027 \cdot (t - t_{star})$ is taken into account when the chronograph works according to the mean time if $(t - t_{star})$ 20^s, when $(t - t_{star})$ 1^m the diurnal term in the coordinates and requires additional small corrections, in order to take into account the lack of coincidence (due to precession) of the equator of the time of observation and the equator 1950.0, to which satellite positions refer.

When astrophotographs are are reduced systematical errors appear:

a) because of inevitable deviations of the real photographic proection from its mathematical ideal - the central proection;

b) due to distortions (caused by refraction and aberration) of the apparent positions respectively to their real positions, taken from the reference catalogue.

c) because of errors in determination of the optical centre of the photograph.

Declassified in Part - Sanitized Copy Approved for Release 2011/12/08 : CIA-RDP80T00246A016600420001-1

Declassified in Part - Sanitized Copy Approved for Release 2011/12/08 : CIA-RDP80T00246A016600420001-1

For the Soviet standard cameras NAFA most essential are errors depending on the distortion of the objective lens and errors in determination of the optical centre δ . The correction for distortion should be taken into account if the distance between two reper stars $S \quad 4^{\circ}$, while the distance from the optical centre $r \quad 3^{\circ}$ (or $S \quad 2^{\circ}$ when $r \quad 10^{\circ}$) (see app.6,7) An inaccuracy in the determination of the optical centre for $\delta \quad 3^{\circ}$ equaling 4 mm leads to a noticeable error in the results. The differential refraction term is in most cases ($Z \quad 60^{\circ}$, $S \quad 5^{\circ}$) smaller than 1" and can be neglected.

As the refraction terms are different for a near by satellite and stars at an "infinite" distance a correction for "refractional parallax " depending on Z satellite has to be introduced. It is direct proportional to the refraction term and and inverse proportional to the distance to the satellite. For a satellite at a distance H = 400 km it becomes noticiable at $Z \quad 60^{\circ}$; for H = 1000km at $Z \quad 70^{\circ}$.

It is usually not necessary to take into account the annual aberration and aberrational time.

Declassified in Part - Sanitized Copy Approved for Release 2011/12/08 : CIA-RDP80T00246A016600420001-1

Declassified in Part - Sanitized Copy Approved for Release 2011/12/08 : CIA-RDP80T00246A016600420001-1

4. PRECISE DETERMINATION OF THE MOMENT OF THE SATELLITE'S PASSAGE THROUGH A NORMAL POINT IN THE SYSTEM OF A CHRONOGRAPH

The observational data for determination of the exact moment of the satellite's passage through a normal point consist of moments of opening (t_H) and closing (t_K) of the shutter read from the tape of a chronograph and measured on the negative; abscissae of the beginnings (X_n) and ends (X_k) of the touches of the satellite track. These data determine an empirical dependence relation t (x) - a function that allows to calculate the exact moment of the passage of the satellite's image through any given point M of his track on a negative (t_M).

However because of accidental and especially systematic errors in general not a single observed t corresponds to the measured x and vice versa.

The main task of the reduction therefore consists in a very thourough estimate of all systematic error. The accidental errors may be excluded by an usual "smoothing "procedure by using a sufficient number of observations.

The systematic errors enter both in determinations of the coordinate x and of the time t. The error of each observation "x" consists of the personal error when measuring the begin - nings (ends) of a touch and the "photographic" error depending on the place where an image of a moving bright spot appears. The personal error depend mainly on the density of the photographic track and on the quickness of the shutter. This error may reache a value of 20-50 micron. If the densities at the

Declassified in Part - Sanitized Copy Approved for Release 2011/12/08 : CIA-RDP80T00246A016600420001-1

Declassified in Part - Sanitized Copy Approved for Release 2011/12/08 : CIA-RDP80T00246A016600420001-1

ends of a touch do not differ and the velocity of the shutter during opening and closing is equal, the result of this error is a displacement of the measured "x" symmetrically relative to the central point of a touch.

The "photographic" component of the error is determined mainly by the inertia of the developing of the photographical image. It depends on the velocity of the passage of the satellite along the plate, on the brightness and the diameter of its image, also on the kind and the sensibleness of the photoemulsion and on the quickness of the shutter. This error causes a symmetrical displacement of the measured ends of each touch (interval) relative to its central if there are no noticable discontinuities in the velocity or the brightness of the satellite in the points compared.

The errors in the time coordinate t depend on the delays of contacts in the shutter and the chronograph. Delays of contacts in the shutter (generally speaking they are different when a shutter is being opened and closed) display in a different way the observed t_H and t_K relatively to their correct values corresponding to the time of the opening and the shutting. In the same way works the delay of a chronograph (since it is different at "the beginning" and at "the end" of the impulses) introducing an additional systematic error in the observed moments. This error is different for t_H and t_K.

Declassified in Part - Sanitized Copy Approved for Release 2011/12/08 : CIA-RDP80T00246A016600420001-1

Declassified in Part - Sanitized Copy Approved for Release 2011/12/08 : CIA-RDP80T00246A016600420001-1

It is important to note that these errors may be considered constant at least during one passage of a satellite.

Among the accidental errors the following ones are of the greatest importance:

a)The accidental errors of pointing when a negative is being measured. They are always larger along the track than in the transversal direction. The average value is about 3-5 and never surpasses 10 .

b)Displaces of a track as a result of vibrations of the camera. Vibrations become apparent in the form of typical short-periodical fading waves on the track if such displays occur in the transversal direction and may be undetectable if they occur along the track.

Those undetectable displays may reach 20 and compared with readings of a chronograph may lead to an error about $0^s.010 - 0^s.050$ depending on the apparent velocity of the satellite.

c)Accidental dispersions of the readings of the chronograph. An accidental error of one reading attains usually $0^s.08 - 0^s.005$, but may be decreased till $0^s.001$ by means of an appropriate regulation of the chronograph.

The errors of the observed x and t both "spoil" the functional relation t (x).

A division and independent exclusion of all these errors are not necessary in order to obtain the correct time coordinate, as there is no difference whatever which kinds of those errors

Declassified in Part - Sanitized Copy Approved for Release 2011/12/08 : CIA-RDP80T00246A016600420001-1

Declassified in Part - Sanitized Copy Approved for Release 2011/12/08 : CIA-RDP80T00246A016600420001-1

(errors in "x" or errors in "t") have led to the wrong result.

Bearing this in mind, the reduction of data should be made in a way to exclude completely all "symmetrical" systematic errors of the observed "x" and "t" and all accidental errors should be smoothed.

Then it remains only to introduce a correction for asymmetrical systematic errors, mainly errors in "t" depending on contacts in the shutter and the recording scheme. We call the resulting effect of all symmetrical errors of the observed x and t (expressed in time) the error which can be expressed in the following way

$$t_H + \quad = t\,(x_H)$$
$$t_K - \quad = t\,(x_K)$$

Those equations are true for two close adjacent observations (x_H, t_H) and (x_K, t_K) without any accidental errors.

The central points of touches (or intervals) and the corresponding to central times should be used for the elimination of , because

$$\bar{x} = \frac{x_H + x_K}{2}$$

$$\bar{t} = \frac{t_H + t_K}{2} = \frac{t\,(x_H) + t(x_K)}{2}$$

As a result of the irregularity of the apparent motion of the satellite

$$\frac{t(x_H) + t\,(x_K)}{2} = t\,\frac{x_H + x_K}{2} + \quad t$$

Declassified in Part - Sanitized Copy Approved for Release 2011/12/08 : CIA-RDP80T00246A016600420001-1

Declassified in Part - Sanitized Copy Approved for Release 2011/12/08 : CIA-RDP80T00246A016600420001-1

where the small value is determined by the observed function t (x). The best way is to use very short touches for which t practically equals zero, and coordinates of the central points may be measured directly.

The function t (x) can be expressed by a quadratic polynom $t(x) = B_0 + B_1 x + B_2 x^2$

For determination of the coefficients of this polynom a large amount of observations (x,t) should be used in order to smooth out the accidental errors.

For those cameras for which the times of opening and closing of the shutter differ and also in the case of different density of the ends of the touch, the exclusion of (as mentioned above) does not lead to the complete deliverence of the result t_M from the influence of assymetrical systematic errors of the x-coordinate. The error in this case may be rather large and has to be investigated specially.

When time interpolation is impossible and the coordinates of the centre of one short touch of the satellite track is determined then the calculation of the corresponding time coordinate is simplified extremely, the arithmetical mean of the times of the beginning and the end should be taken. However in this case all the accidental errors are included completely, the control is omitted and the accuracy reduced.

I should like to stress that the accuracy of photographic tracking data may be improved if appropriate methods of

Declassified in Part - Sanitized Copy Approved for Release 2011/12/08 : CIA-RDP80T00246A016600420001-1

Declassified in Part - Sanitized Copy Approved for Release 2011/12/08 : CIA-RDP80T00246A016600420001-1

photographing and reduction of photographs are applied. For example, the standard cameras NAFA 3s (D - 100mm, 250mm) used at the U.S.S.R. photographic stations were aimed to give an accuracy (according to first estimates) in position about 1 minute of arc. The application of A.A.Kiselev's 5 interpolation method and a thorough investigation both of systematical and accidental errors, made it possible to raise the accuracy nearly up to one order. At present all Soviet photographic stations obtain photographic data coordinates 4"-6" and $0^s.005$ in timing (registration of moment).

Declassified in Part - Sanitized Copy Approved for Release 2011/12/08 : CIA-RDP80T00246A016600420001-1

Declassified in Part - Sanitized Copy Approved for Release 2011/12/08 : CIA-RDP80T00246A016600420001-1

5. CAMERAS USED FOR PHOTOGRAPHIC TRACKING OF SATELLITES.

As has been mentioned earlier, for obtaining a track of the satellite on a photographic emulsion wide angle cameras with rather high apertures and optical qualities are needed.

The first attempt in most countries after the launch of the first satellites was to use existing aerial photocameras for this purpose.

The photographic tracking stations in the USSR (30 stations mostly attached to astronomical observatories and universities) are equipped with rather small aerial photocameras "NAFA 3s/25" which have been slightly modified.

The camera supplied with an objective lens "Uran-9" ($F = 25$ cm, $D = 10$ cm, field of sight $30^\circ \times 50^\circ$) was provided with a special shutter.

In order to obtain sharp ends of the satellite track the time of opening and closing of the shutter was decreased as much as possible and reduced to 0.0002 - 0.0003 sec by strengthening the springs.

A specially developed electro-scheme allows to open and to close the shutter by hand with the aid of a button in two regimes; the first regime-opening of the shutter at the start of the impulse and closing at the end; the second regime-opening at the start of the impulse and closing when the impulse is repeated.

A special contact allows to record with the help of the chronograph the moments of opening and closing of the shutter. The half-time moment of the exposure can be made coincident (with the precision of $0^s.002$) with the arithmetic mean of the moments of opening and closing of the shutter by regulating this contact with the help of a device supplied with a photocell. This excludes

Declassified in Part - Sanitized Copy Approved for Release 2011/12/08 : CIA-RDP80T00246A016600420001-1

Declassified in Part - Sanitized Copy Approved for Release 2011/12/08 : CIA-RDP80T00246A016600420001-1

the influence of the delay between the moments of contract and the moments of complete opening and closing of the shutter. Such a recording of the time has the advantage of excluding a number of systematic errors arising in measuring the ends of a satellite track during the reduction of the negative.

To obtain several exposures on one frame automatic reeling of the film after every exposure was eliminated. For better use the camera is supplied with a frame view-finder, and a special support, which makes it possible to turn the camera round the horizontal axis into the necessary position and to fasten it afterwards. If several short exposures (about $0^s.5$) are made during the time of the satellite's passage through the field of sight of the camera, the image of the satellite will consist of several tracks of 2 mm length, while the star images will be in the form of extremely short touches, practically like points.

At the stations which have no regular time service a printing chronograph with a quartz generator, which receives time signals before and after the observation of the satellite, is used as a time preserving device. In this case the error of the comparison of the printing chronograph with the precise time signals should not exceed 0.005 sec. For this purpose a special device is added to the receiver, which allows to mark the time signals directly on the tape of the chronograph. The delay of a signal in the receiver and in the additional device is accurately measured [10]. It is also possible to measure the delay of the signals in the additional device directly at the time when radio signals are received.

Similar cameras are under operation at several tracking stations in Roumania, Bulgaria, China, Thechoslovakia and Poland. With those cameras one can obtain an accuracy of 4" - 6" in position measuring and $0^s.005$ in timing, provided an appropriate way of photographing and reducing the plate is used.

Declassified in Part - Sanitized Copy Approved for Release 2011/12/08 : CIA-RDP80T00246A016600420001-1

Declassified in Part - Sanitized Copy Approved for Release 2011/12/08 : CIA-RDP80T00246A016600420001-1

In Germany at the Potsdam Observatory and at the tracking Station in Rodewisch Zeiss cameras with an objective lens "Tachar" (F = 25 cm, aperture 1:1,5) are used 11 . The accuracy obtained corresponds to 15" in position and about $0^s.01$ in time.

Photographic observations in France (Observatories in Meudon and Strassbourg) are carried out by means of an aerial camera K-37 (F = 305 mm, aperture 1:2,5) 12,13 . Brief Shifts in declination are given to the camera as a whole, while it follows the diurnal motion, to break up the track of the satellite. The mean error in the determination of the coordinates for a field of 20 for star images amounts to 2" (Meudon) and 1" (Strassbourg). The accuracy in timing is 0^s003.

A similar camera K - 37 with a triplet Dodak aero-Ektar lens is applied at the Asiago Observatory (Italy) 14 . Some radical modifications of the shutter trip control had to be made. The shutter was electrically connected with a tape recorder and with a recording chronograph controlled by a precision clock. Timing accuracy obtained amounts to 0^s01. At present tests are proceeding to record faint satellites by moving the film with such a velocity that for a 7 degrees arc the image of the satellite remains on the same point of the emulsion in the centre of the field of the camera.

A similar modification of an aerial camera has been proposed earlier by L.A.Panaiotov 18 (see also 8). Several cameras of this type are under operation at the Russian tracking stations. The film moves with the same speed and in the same direction as the image of the satellite in the focal plane.

It is possible to obtain photographs of satellites up to the 6^{th} - 7^{th} magnitude with such cameras (compared to 3-3,5 magnitude for a fixed camera). However, as experience

Declassified in Part - Sanitized Copy Approved for Release 2011/12/08 : CIA-RDP80T00246A016600420001-1

Declassified in Part - Sanitized Copy Approved for Release 2011/12/08 : CIA-RDP80T00246A016600420001-1

shows, the obtained accuracy is lower than for photographs obtained with a fixed camera. In Ujgorod simultaneous tracking of Echo I with a fixed camera and with a camera with moving film was carried out. Each negative was reduced separately. Then for t obtained for the moving film image α and δ for the "fixed" image were evaluated. A comparison shows that the difference may be as large as 15" - 20". Also the needed reduction time of the photographs obtained with the moving film camera is about 3 times larger than for a fixed camera.

Among new and very promising methods of precise photographic observations the work by H.Sotter and J.Streletsky (Pulkovo Observatory) [1] should be mentioned.

In order to compensate the motion of a weak satellite image relatively to the photographic plate a rotating plane-parallel glass plate is used similar to the Markowitz Moon cameras for compensation of the Moon motion relatively to stars. In a camera with the field of sight $5^0 \times 5^0$, an obturator with a plane-parallel plate is placed. (See fig. 1). The plane parallel plate displaces the satellite image in the focal plane for

where Z is the inclination of the plate to the falling rays; d - the thickness of the plate; n - the index of its refraction.

If /Z/ 20^0 then the formula becomes symplified

$$x' = d\,\frac{n-1}{n}\,Z$$

where x and d are given in mm, and Z - in radians.

3/2

Declassified in Part - Sanitized Copy Approved for Release 2011/12/08 : CIA-RDP80T00246A016600420001-1

Declassified in Part - Sanitized Copy Approved for Release 2011/12/08 : CIA-RDP80T00246A016600420001-1

The filter works in such a way that the energy distributed along a cigar like touch is concentrated into one point.

The width of the obturator is about $0^{\circ}5$ in the focal plane of the astrograph. The remaining part of the field is free for expositions of star images. In order to compensate the lengthening of the focal rate by the rotating plate a plane parallel fixed plate of the thickness is placed before the focal plane of the free part of the field. The time coordinate to which a satellite image on the background of stars refers can be obtained with the help of a contact mechanism, which gives a signals to a chronograph at the moment when the rotating and fixed filters are parallel. The angular velocity of the obturator is proportional to the topocentrical angular velocity of the satellite along the sky.

A number of images is obtained on the plate during one passage of the satellite.

When 5 images symmetrical relative to the optical centrm are measured, it is possible to obtain α and δ with an accuracy about 0"3 (for a certain reference time system). For geodetical purposes - to connect several distant places - the error in the absolute time system is not so significant as all the observations are close in time and may be referred to the same reference time signals.

This proposed device allows to obtain tracking data with a great precision comparable to the precision of observations of star-like bodies. With an astrograph (D = +230 mm F = 2300 mm) it is possible to obtain good positions for satellites rotating around the Earth at a height of 3000 m and having a brightness of 9^{m}.

Declassified in Part - Sanitized Copy Approved for Release 2011/12/08 : CIA-RDP80T00246A016600420001-1

Declassified in Part - Sanitized Copy Approved for Release 2011/12/08 : CIA-RDP80T00246A016600420001-1

It must be noted that a similar method is used also by W.Markovitz in his camera for satellite observations at the Naval Observatory in the USA (D = 178 mm, F = 1015 mm) 17 . The precision obtained is +5" in position and $\pm 0^{s}.002$ in time.

For geodetic purposes simultaneous photographing of satellites with similar cameras at different stations is most interesting.

At the Pulkovo Observatory (D.E.Shchegolev) synchronous satellite tracking for geodetic purposes on standard NAFA-3c/25c cameras is on work. Four observatories (Pulkovo, Nikolaev, Kharkov and Tashkent), which have good time services, take part in this work.

The satellitem is tracked photographically according to a fixed program: each two minutes during the satellite passage (from zero to thirtie seconds of odd minutes) short exposures are made every second. Moments of time are connected to the impulses of cristall clock, which in their turn are connected to London radio signals on 10^{h}.

Simultaneous "Threes" and "fours" are selected from a great number of obtained negatives taken at the same time at three or four stations. Up to 15 points of the track and 4 - 6 peper stars are measured at each negative. For reduction Kiselev's method 5 is used. Dependences and are evaluated, where t - is the time in the reference system of London time. Topocentrical and for definite moments are determined using interpolation.

Declassified in Part - Sanitized Copy Approved for Release 2011/12/08 : CIA-RDP80T00246A016600420001-1

Declassified in Part - Sanitized Copy Approved for Release 2011/12/08 : CIA-RDP80T00246A016600420001-1

If the position of two reference stations in any system of coordinates is known, it is possible to obtain satellite positions and with their help - coordinates of a third station in the same system.

At present 90 negatives obtained on May 7 and 9 1961 during 6 passages of the satellite "Echo-I" have been selected. Each passage was observed jointly from 6 to 18 minutes (that is from 400 to 7000 km. along the orbit). Measurements are being carried out.

The expected error in the determination of the coordinates of the third station from one series of observations is ± 50 m (the error in the determination of time - $\pm 0^{s}.0004$; in position - ± 4").

If the satellite is high enough then it is possible to draw an ellips through certain points of its orbit and to determine the focus (that is the centre of gravity of the Earth. If the beginning of the coordinates is displaced into this point then it is possible to obtain coordinates of stations in a system with a centre in the centre of gravity of the Earth.

If there are many stations and they are evenly distributed over the globe then the mentioned method may be used as a purely geometrical way for determinations of the figure of the Earth.

Declassified in Part - Sanitized Copy Approved for Release 2011/12/08 : CIA-RDP80T00246A016600420001-1

Declassified in Part - Sanitized Copy Approved for Release 2011/12/08 : CIA-RDP80T00246A016600420001-1

6. UTILIZATION OF EXISTING ASTRONOMICAL TELESCOPES

In general there are several difficulties in using existing astronomical telescopes for precise photographic tracking of satellites notwithstanding their rather high optical qualities. Existing astrographs are not provided with special timing devices allowing more exact measurements than within 1 sec. For satellite tracking new systems of shutters have to be evaluated as the existing shutters are usually operated by hand. Moreover, it is necessary to take into account that quick- working shutters for large apertures do not exist at all, and their construction is very complicated.

Nevertheless, a number of observatories have tried to apply the existing telescopes for satellite observations by introducing some modifications to the plate holder or designing some additional devices for timing purposes. A description of several such devices used at the U.S.S.R. observatories is given in [ ].

An interesting method for photographing faint artificial Earth satellites with long-focus astrographs was proposed by Abele [ ] (Riga University). Due to a special plate-holder it is possible to shift the plate uniformly for some millimeters in the direction of the motion of the satellite image with a velocity which is equal to that of the image passage

Declassified in Part - Sanitized Copy Approved for Release 2011/12/08 : CIA-RDP80T00246A016600420001-1

Declassified in Part - Sanitized Copy Approved for Release 2011/12/08 : CIA-RDP80T00246A016600420001-1

in the focal plane of the camera. During this time the image of the satellite influences practically the same part of the photographic emulsion. Then the plate remains for some time motionless and then quickly returns into the initial position. Then again it remains motionless foe some time. After that the cycle is repeated. When the plate-holder does not move the satellite image passes quickly along the plate and if the satellite is faint it does not influence the emulsion. But during this time faint background stars, the images of which were shifted while the plate-holder was moving, are exposed.

To move the plate-holder a template of special form is used. The template is set into rotation by a synchronous motor, which is fed with alternating current from a sound generator. The same template sends signals to the chronograph, at the moments when the plate - holder changes its motion. This results in 10-15 separate photographs of the satellite on the plate. The image of each star has the form of two parallel lines of spots, and the satellite's position has the form of separate spots. The time corresponding to the position of the satellite on the plate is obtained from the time of the beginning and the end of the uniform shift of the plate-holder in the direction of the movement of the satellite image. The position of each star at this time is equal to the mean position between two corresponding spots from two lines of its images if the template is such that $t_b - t_a = t_d - t_c$. With a good

Declassified in Part - Sanitized Copy Approved for Release 2011/12/08 : CIA-RDP80T00246A016600420001-1

Declassified in Part - Sanitized Copy Approved for Release 2011/12/08 : CIA-RDP80T00246A016600420001-1
50X1-HUM

Page Denied

Next 13 Page(s) In Document Denied

Declassified in Part - Sanitized Copy Approved for Release 2011/12/08 : CIA-RDP80T00246A016600420001-1